UNIVERSITY OF CALIFORNIA

SANTA CRUZ

INTERNAL PLASTICIZATION OF POLY(VINYL CHLORIDE) USING THERMAL AZIDE-ALKYNE HUISGEN CYCLOADDITION AND COPPER-MEDIATED ATOM TRANSFER RADICAL POLYMERIZATION

A dissertation submitted in partial satisfaction
of the requirements for the degree of

DOCTOR OF PHILOSOPHY

in

CHEMISTRY

by

Longbo Li

September 2020

The Dissertation of Longbo Li is approved:

Professor Rebecca Braslau, Advisor

Professor Scott Lokey, Chair

Assistant Professor Jevgenij Raskatov

Quentin Williams
Interim Vice Provost and Dean of Graduate Studies

Table of Contents

List of Figures

List of Tables

List of Schemes

Abstract

Internal Plasticization of Poly(Vinyl Chloride) using Thermal Azide-Alkyne Huisgen Cycloaddition and Copper-Mediated Atom Transfer Radical Polymerization

Longbo Li

Poly(vinyl chloride) (PVC) is one of the most widely used thermoplastics; uses range from building materials, medical devices, toys, and sports equipment. Pure PVC is rigid and brittle. Typically, small molecule plasticizers are added to modify the flexibility and durability of PVC. The most common external plasticizers are phthalate esters. These small molecules leach out of the PVC matrix into the environment; when inhaled, absorbed, or ingested into the human body, phthalates and their metabolites pose a significant risk to human health. The most efficient way to prevent leaching of plasticizers is to covalently attach them to PVC. This is referred to as "internal plasticization."

Two strategies have been used to achieve internal plasticization of PVC in this thesis. In the first strategy, thermal azide-alkyne Huisgen cycloaddition was utilized to attach electron-poor acetylenediamides using a branched glutamic acid linker to azidized PVC, incorporating four plasticizing moieties per attachment point. A systematic study incorporating either alkyl or triethylene glycol esters provided materials with varying degrees of plasticization, with depressed glass transition temperature (T_g) values ranging from −1 °C to 62 °C. T_g values of these internally plasticized PVC samples were shown to decrease with increasing chain length of the plasticizing ester. A branched internal plasticizer bearing a triethylene glycol ester had lower T_g values compared to that with a same length linear alkyl ester. Thermogravimetric analysis of PVC bearing internal plasticizers revealed that these branched internal plasticizers bearing alkyl ester chains are more thermally stable than similarity branched plasticizers bearing ethylene glycol esters. These internal tetra-plasticizers were synthesized and attached to PVC-azide in three simple synthetic steps.

In the second strategy, internal plasticization of PVC was achieved in one step using copper-mediated atom transfer radical polymerization (ATRP) to graft random *n*-butyl acrylate (BA) and 2-2-(2-ethoxyethoxy)ethyl acrylate (2EEA) copolymers from defect sites on the PVC chain. Five graft copolymers were made with different ratios of PBA and P2EEA; T_g values of these functionalized PVC polymers ranged from -28 °C to -50 °C. Single T_g values were observed for all polymers, indicating good compatibility between PVC and the grafted chains, with no evidence of microphase separation. Plasticization efficiency is higher for polyether P2EEA moieties compared with PBA components. The resultant PVC graft copolymers were thermally more stable compared to unmodified PVC. Increasing the reaction scale from 2 g to 14 g produced consistent and reproducible results, suggesting this method could be applicable on an industrial scale. Further optimizations of the ATRP conditions were carried out shortening the reaction time and varying the acrylate monomer to VC unit ratios. Nine different internally plasticized PVC graft copolymers with different weight percents of plasticizer spanning from 24% to 75% were prepared. A wide range of T_g values (-54 °C to 54 °C) were achieved, with T_g values below zero for samples with weight percent of plasticizer more than 50%. In summary, highly effective internal plasticization of PVC was accomplished by Cu-mediated ATRP in only one step. Whereas the azide-alkyne approach may be suffered from the potential danger in handling azides on large scale, the ATRP graft copolymerization approach is expected to be very attractive to industry, to afford internally plasticized PVC products with reliable and durable physical properties.

Acknowledgements

First, I would like to thank my advisor professor Rebecca Braslau. Thanks for accepting me to your lab five years ago. I hope you think you made a right decision. These five years have been such a great experience for me. You are such a wonderful PI. None of this work would be possible without your help and guidance. You are the nicest and sweetest person I have ever met. When there were good things happened, you were always there to celebrate. When there were failures and troubles, you were always there to cheer me up and to support. Thanks for being such a caring advisor and an inspiring scientist.

I also want to thank my thesis committee: Professor Scott Lokey and Professor Jevgenji Raskatov. Thanks for your advice in the past years. I have learned a lot from you. I could not have gotten this far without your help.

I want to thank our collaborators Dr. Rudy Wojtecki and Andy Tek at IBM. Many thanks for your help on the Glutamic acid project. I would like to thank my collaborators at EAG Laboratories: Dr. Yanika Schneider and Dr. Adrienne Hoeglund. It has been a great experience working with you. Thank you so much for your contributions to the ATRP project.

I would like to thank everyone in the Braslau group: Dr. Aruna Earla, Dr. Chad Higa, Jen Petraitis, Wiley Schultz-Simonton, Jerin Tasmin, Patrick Skelly, Greg Pitch (Ayzner Lab), Avery Baerlin, Chayo Fuentes, Ana Paula Kitos Vasconcelos, Rosa Rocha. Special thanks to Dr. Aruna Earla and Dr. Chad Higa, my projects would not go as smoothly without your work as a foundation. Dr. Aruna Earla, thanks for training me during my first year. I have learned how to be an efficient and dedicated chemist from you. Thanks to Dr. Chad Higa, your thorough attitude about research has had a big impact on me. You have been such a great friend. It is hard to study abroad with language barrier and different culture. Thanks for your friendship and company. You made Santa Cruz as home. I would like to give many thanks to Patrick Skelly. Pat, thanks for your help and company. I hope everyone can see how wonderful you are.

Please never change. Rosa, thanks for your help with the photo-ATRP project. You brought me so much joy. I wish you could always be around.

I also want to thank people in the MacMillan lab: Dr. Aswad Khadilkar, Dr. Rahul Shingare, Scott La, Anam Shaikh, Victor Aniebok, Duy Vo, Jocelyn Macho, David Delgadillo, and Alex Smith. Thanks for letting me borrow stuff from you and taking me to eat good Chinese food. I also would like to thank Dr. Jia Lu for your help measuring AFM. I want to thank Bingzhang Lu and Dr. Bin Yao, congratulations for all the achievements you have accomplished. I would like thank Gabriella Amberchan, Alejandro Rodriguez, A'Lester Allen, and Dr. Evan Vickers, I enjoyed the first year when we studied together. I had a lot of fun.

I want to thank Professor Bakthan Singaram, thanks for your caring and your good advice over the years. I wish I could be as inspiring as you are one day. I also want to thank Professor Yat Li. I would like to give my special thanks to Janet Jones. Thanks for helping me with all my questions in the early graduate school and helping me in every aspect in life. I also want to thank Dr. Jack Lee for helping with NMR and Li Zhang for helping with MS. I also want to thank Karen for being very helpful and approachable.

Last but not the least, I would like to thank my friends and family. My husband Andrew Meng, you have taught me so much in the past 6 years. Thanks for your advice on how to be a good scientist. Thanks for bringing so much fun and happiness to my life. I would like to thank my family: my parents, my brother, my sister-in-law, my nephews for being very supportive. I love you all.

1 Introduction: Internal Plasticization of PVC

Poly(vinyl chloride) (PVC) (**Figure 1.1**) is one of the most commonly used thermoplastics in the world. In 2018, PVC encompassed 17% of global plastic production.[1] The global market demand has been continuously increasing from 38.3 million tons in 2013 to 41.3 million tons in 2016.[2]

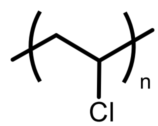

PVC

Figure 1.1 Structure of PVC

1.1 Synthesis of PVC

PVC was first discovered by Eugen Baumann in 1872.[3] Baumann found that a white solid (PVC) was formed after vinyl chloride was left exposed to sunlight. Currently, PVC is synthesized by free radical polymerization of vinyl chloride monomer (VC). This polymerization occurs through three distinct steps: initiation, propagation, and termination. The choice of initiator affects the polymerization rate and the molecular weight. Common initiators include azobisisobutyronitrile (AIBN) and various peroxides. In the propagation step, there are two ways that VC can add: head-to-tail and head-to-head (**Scheme 1.1**). Normally, head-to-tail addition occurs, however, head-to-head addition can happen, yielding an unstable primary radical which rearranges to form an allylic chloride, terminating chain growth (**Scheme 1.1**).[4] Head-to-tail addition is controlled by the polymerization temperature, which plays an important role in the resulting molecular weight and molecular weight distribution. Also, PVC is an atactic polymer, which means the repeating units do not have consistent stereochemistry. However, polymerization conducted under lower temperatures do favor formation of syndiotactic polymer because lower temperatures slow down the rotation of VC significantly.[4] The polymerization is terminated by a radical-radical disproportionation or dimerization reaction (**Scheme 1.2**).[5]

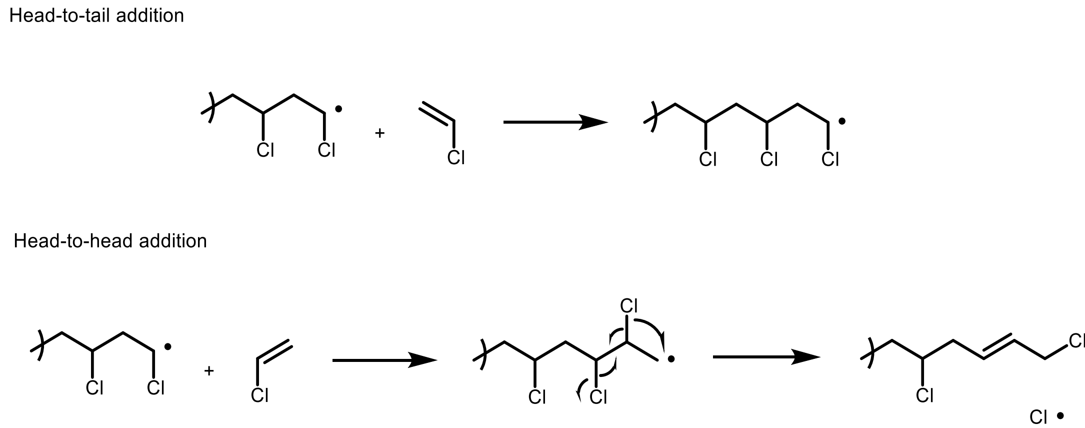

Scheme 1.1 Two Types of Addition Patterns of VC during Growth of PVC

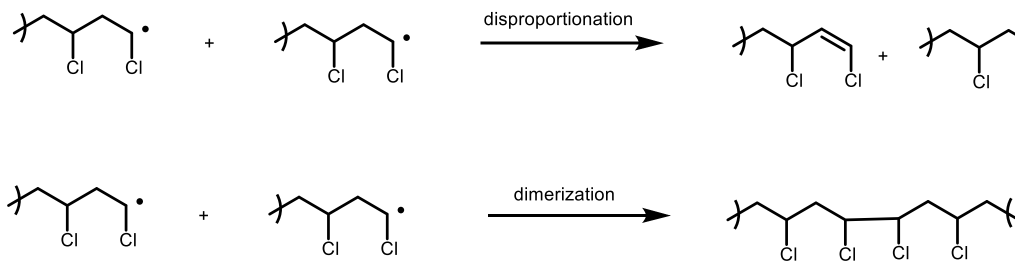

Scheme 1.2 Two types of termination

There are three main polymerization methods: suspension polymerization (dominant type), emulsion polymerization, and bulk polymerization.[4,5] The molecular weight and polydispersity of commercial PVC synthesized via different polymerization methods are summarized in **Table 1.1**.[6–8]

Table 1.1 Molecular Weights and Polydispersity Ranges for Commercial PVC

Polymerization method	M_n (Da)	M_w (Da)	M_w/M_n (PDI)
Suspension	20,32-69141	38,611-179,123	1.90-2.59
Emulsion	27,173-49,540	61,650-131,191	2.14-2.65
Bulk	26,351-37,772	52,683-77,829	2.00-2.06

1.2 Plasticizers

PVC was not widely used immediately after its discovery in 1872, because the polymer is inherently rigid and brittle.[3] In 1926, Waldo Semon at B.F. Goodrich Company made PVC flexible and practical by blending additives to PVC.[9] The additives used to make PVC flexible are also known collectively as “plasticizers”. Plasticizers are used to provide durability, elasticity, and flexibility in PVC, allowing it to be used in applications from toys, clothing, packing materials,

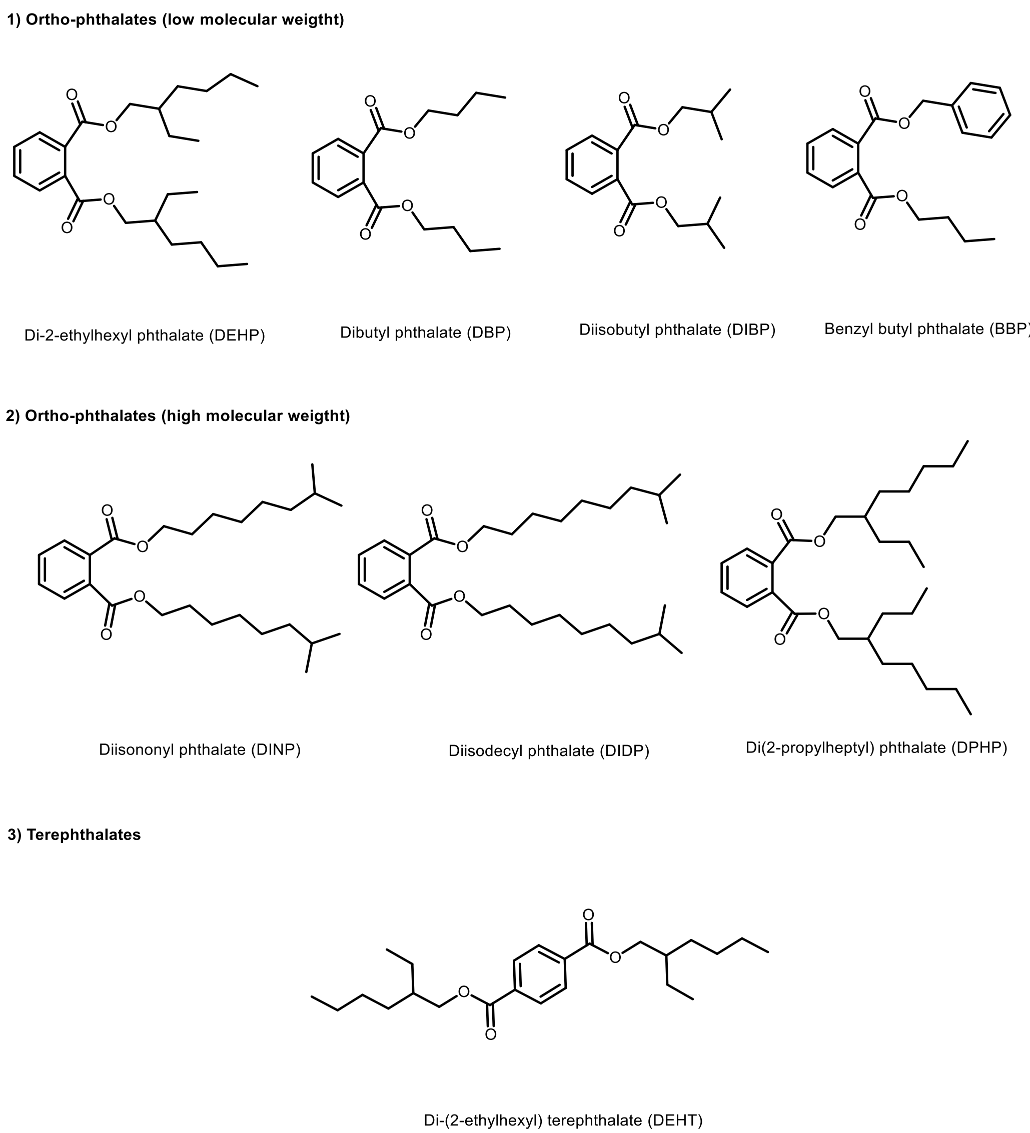

Figure 1.2 Examples of Common Phthalate Plasticizers

medical devices, electrical cable jacketing, auto interiors, and construction (wall covering and flooring).[2,10] Plasticizers that have been used in the PVC market are mostly esters: including phthalates (**Figure 1.2**), cyclohexane diesters, trimellitates, citrates, adipates, azalates, sebacates, and others (**Figure 1.3**).[4,11] Phthalates are the most common plasticizers, making up 65% of the global plasticizer market in 2017.This percentage is decreasing slowly, but phthalates will continue to account for the largest global consumption in the near future.[10]

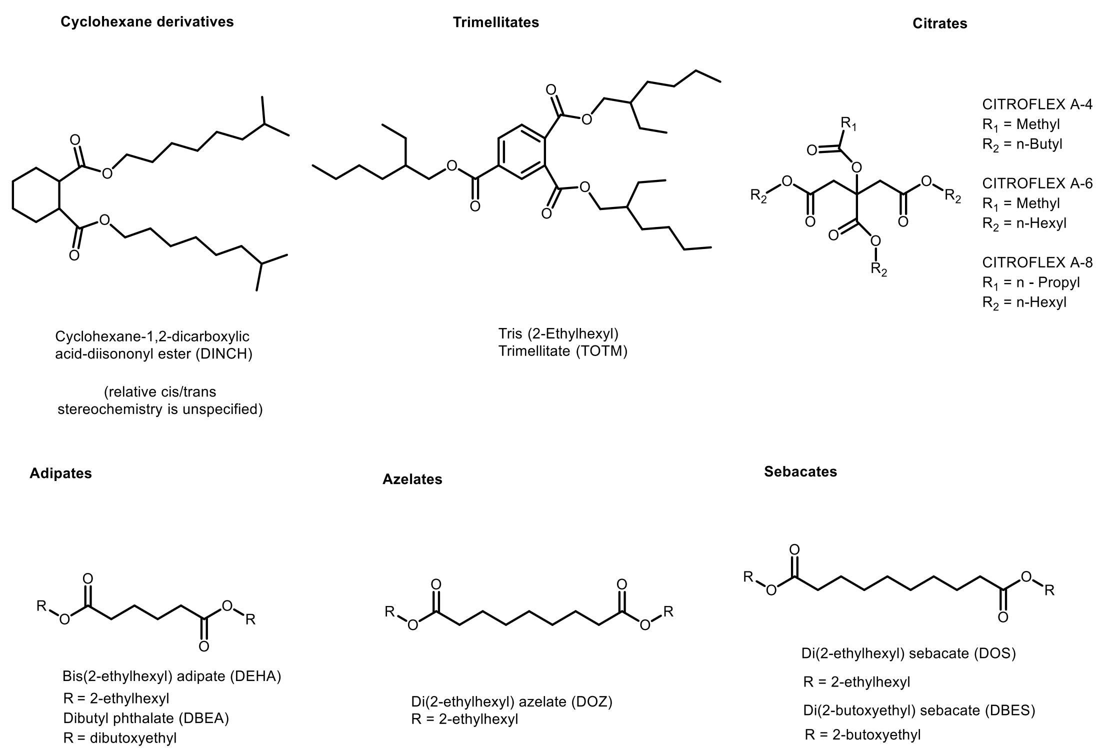

Figure 1.3 Examples of Commercial Phthalate Alternatives

1.3 Mechanisms of Plasticization

Several theories, include lubricity theory, gel theory, Moorshead's empirical approach, and the free volume theory have been used to explain plasticization.[12] In lubricity theory, plasticizers act like lubricants to reduce the intermolecular forces between the polymer chains. The resistance to polymer chains sliding past each other in the presence of the lubricants is reduced, resulting in more flexible materials.[12] Kirkpatrick,[13] Cark,[14] and Houwink[15] contributed to lubricity theory. In Kirkpatrick's proposal, in which the polymer structure was treated as a plastic micelle, part of the plasticizer molecule coordinates to the polymer molecule (acting as a solvent); the other part of the plasticizer molecule acts as a lubricant between the polymer chains.[13] Clark believed plasticizers, working as lubricants, fill in between the network of polymer molecules. The lubricants lie between parallel layers of polymer molecules, allowing the polymer chains to glide past one another.[14] In the gel theory, the polymer chains form a honeycomb network causing rigidity in the polymer. Plasticization is caused by plasticizers interacting with polymer chains in a solvation-desolvation equilibrium. This continuous dynamic equilibrium causes the polymer chains to aggregate and deaggregatate, resulting in a less rigid structure.[12] Moorshead designed an empirical approach to summarize certain requirements for being good plasticizers.[16] In this method, plasticizers need to be compatible with the polymers. The cohesive forces between plasticizer and polymer should be same as the cohesive forces between individual polymer chains. Otherwise, plasticizers and polymer chains will prefer to self-aggregate. For PVC, good plasticizers require both polar and nonpolar functional groups. In the PVC structure, chlorine atoms form dipole-dipole interactions with hydrogen atoms. Polar groups like esters show good compatibility with PVC because the polar groups break the dipole-dipole interactions between PVC chains, replacing them with new dipole-dipole interactions between plasticizer and the polymer chain. Polar groups also help reduce plasticizer migration from the PVC matrix, due to their polar interactions with PVC chains. Apolar aliphatic groups can sit in between polymer chains without introducing significant additional cohesive forces, increasing polymer flexibility.

The free volume theory was hypothesized by Fox and Flory[17] in 1950, multiple contributions have been added by others since that time.[12] This theory states that there is nothing but free volume between polymer chains. The only factor in plasticization is increasing the free volume, to give a more flexible material. One important concept in the free volume theory is the glass transition temperature (T_g): the temperature at which a polymer undergoes a phase change from a glassy to a rubbery state. Fox and Flory defined the free volume at temperatures above the transition temperature as the specific volume above the T_g minus the solid volume extrapolated to the same temperature.[17] This definition has a problem, because the free volume is always zero below the T_g when defined in this way. Another definition by Kanig[18] gives the free volume as the difference between the volume observed at absolute zero temperature and the volume of the real crystal, glass, or liquid, although the volume at absolute zero has to be obtained by extrapolation. Some other models have also been proposed, such as the Wlliiam-Landel-Ferry approach.[19] In this system, free volume can be measured by obtaining the specific volume of a polymer as a function of temperature through dilatometry. The free volume theory suggests that 1) longer chain substituents typically introduce more free volume more compared to short chains; 2) with the same weight fraction of plasticizer, small molecules create more free volume per mass added, thus they are more efficient than large molecule plasticizers; 3) branched structures increase free volume more than linear structures with the same number of carbon atoms.

Several mathematical models have been established based on the free volume theory to calculate the T_g of the plasticized polymer using the T_g of the pure polymer and the T_g of the plasticizer.[20–22] For example, one of the earliest is the Fox equation (**Equation 1.1**).[20]

$$\frac{1}{T_g} = \frac{w_1}{T_{g,1}} + \frac{w_2}{T_{g2}}$$ **Equation 1.1**

T_g: The glass transition temperature of the plasticized polymer

$T_{g,1}$: The glass transition temperature of the pure polymer

$T_{g,2}$: The glass transition temperature of the pure plasticizer

w_1 : The weight fraction of the polymer

w_2 : The weight fraction of the plasticizer.

None of the theories explains the observed effects of plasticization on their own. Instead, some combination of these theories is required to provide a general explanation of plasticization.[12]

1.4 Migration of Traditional Plasticizers from PVC

Small molecule plasticizers migrate out from the PVC matrix[23–28] due to relatively weak non-covalent interactions (**Figure 1.4**). Plasticizers can escape as a gas to the surrounding environment, be removed due to bulk mechanical abrasion, be leached into a solvent, or be removed from the polymer by direct diffusion into dust particles on the polymer surface.[29] Migration of plasticizers causes deterioration of the properties of the PVC material. But even worse, phthalate plasticizers contaminate the environment[26,30–37] and pose a significant risk to human health when ingested, absorbed or inhaled into the body, due to the toxicity of the parent phthalate itself and the subsequent metabolites.[38–43]

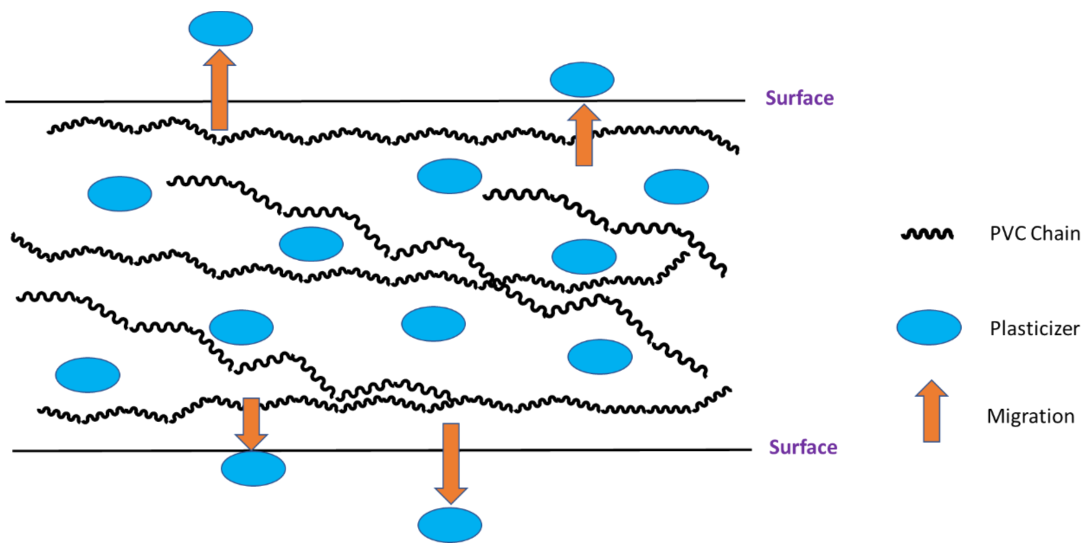

Figure 1.4 Schematic of Migration of Plasticizers from the PVC Matrix into the Environment, based on Guo[44]

1.5 DEHP and Its Toxicity

Di-2-ethylhexyl phthalate (DEHP) is the most utilized phthalate plasticizer. When DEHP enters the human body, it is metabolized through different stages (**Figure 1.5**). First, DEHP is hydrolyzed to form mono-2-ethylhexyl phthalate (MEHP). Then, various methyl/methylene carbons on MEHP are oxidized into alcohols. These alcohols can be further oxidized to the corresponding ketones or carboxylic acids.[45]

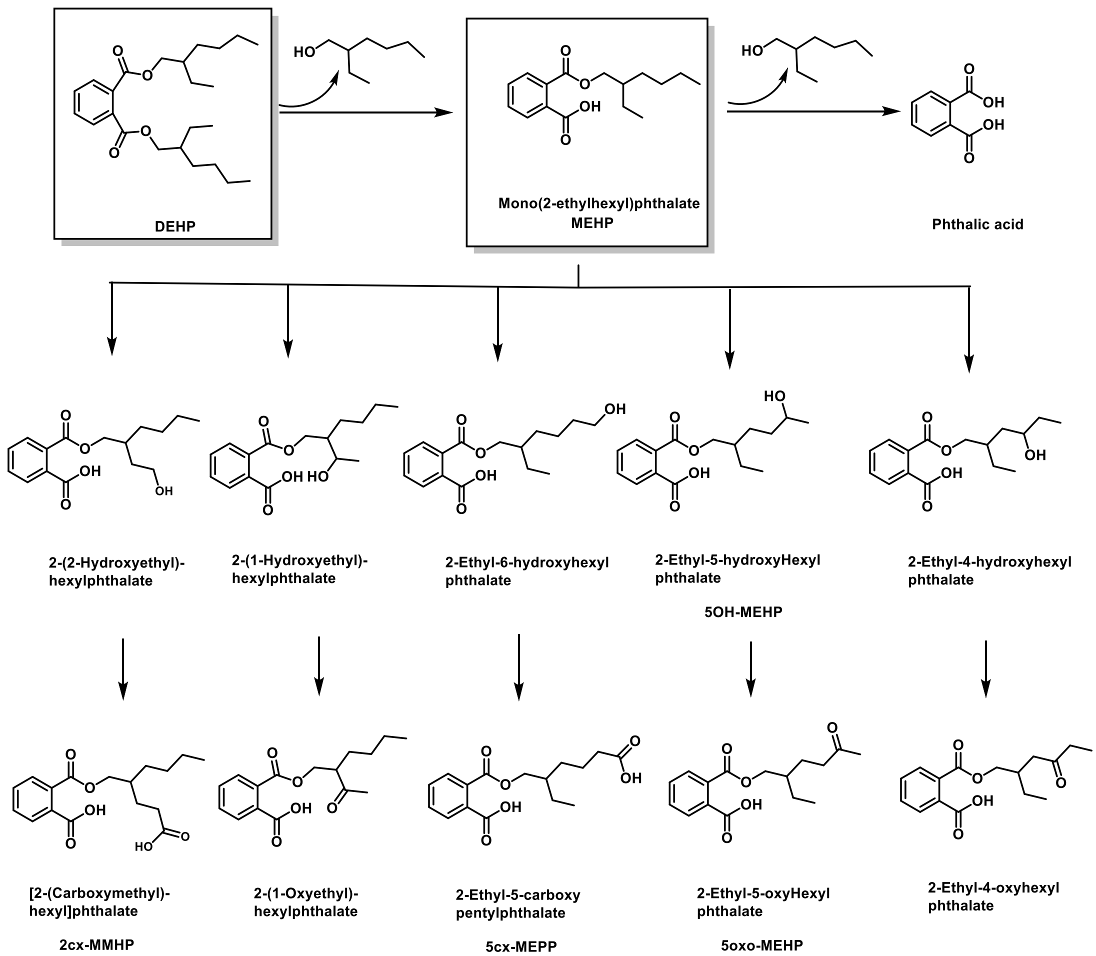

Figure 1.5 Metabolites of DEHP in Human Body[45]

The toxicities of DEHP and its metabolites (mainly MEHP) have been studied by scientists over decades. The toxicities include the following:[46]

1) Endocrine toxicity. The effects of DEHP metabolites on the endocrine system are well documented. For example, studies show that after male rats were exposed to DEHP, their aldosterone and testosterone concentrations decreased.[47,48] DEHP can also enhance

estrogenic activity in zebrafish, suggesting potential effects on humans.[49] DEHP and MEHP can change the level of thyroid hormones and impact the synthesis, regulation, and action of these hormones in zebrafish larvae.[50,51] Data also suggest that DEHP and its metabolites have a positive association with body mass index (BMI) of children.[52]

2) Testicular toxicity. Testicular toxicity was observed in male rats treated with MEHP.[53] DEHP can potentially affect male genital development. Studies also show that the anogenital distance of human newborn boys decreases when the mom was exposed to DEHP in the first-trimester. No effect was observed on the anogenital distance of newborn girls.[54] Newborn male genital anomalies have also been correlated to DEHP.[55]

3) Ovarian toxicity. Ovarian toxicity has been mainly associated with MEHP.[56,57] All studies were done in mice or *in vitro*. No human data is available.

4) Renal toxicity. Renal toxicity was observed in rats and mice.[58–60] However, studies show DEHP had no negative effect on the kidney of male monkeys.[61] No human data is available.

5) Other possible toxicities: neurotoxicity, hepatotoxicity, cardiotoxicity.[46]

6) Studies also found high plasma concentrations of DEHP or MEHP were detected in women with endometriosis, indicating endometriosis may be caused by DEHP and its metabolites.[62–65]

1.6 Approaches to Solve Migration of Plasticizers

One approach to solving the plasticizer migration problem is to use polymeric plasticizers. These are mainly polyesters, and they show significant improvement in migration resistance compared to small molecule plasticizers. In general, polymeric plasticizers have molecular weights greater than 500 g/mol. Polyadipates (**Figure 1.6**) are the only polymeric plasticizers used in PVC medical devices.[11] In general, polyesters show good compatibility with PVC;[66] a leaching study showed that the polyadipate migration rate is 100 times lower than DEHP in gastric juices.[67]

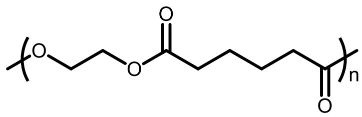

Poly(ethylene adipate)

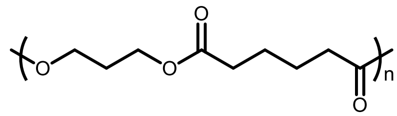

Poly(propylene adipate)

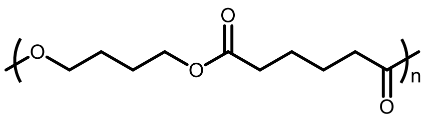

Poly(butylene adipate)

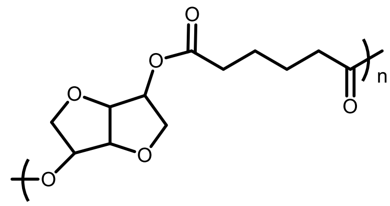

Poly(isosorbide adipate)

Figure 1.6 Examples of Polyadipate Plasticizers

Other polymeric plasticizers have been developed for PVC, including poly(ε-caprolactone) (PCL) and its copolymers (**Figure 1.7**).[11,68] No migration was observed for branched PCL from volatility, extractability, and exudation tests.[69] Other polyesters have been

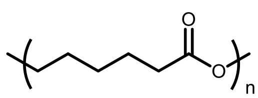

PCL

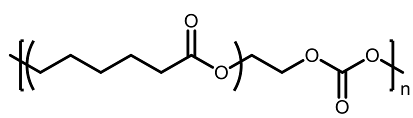

PCL-*co*-Polycarbonate

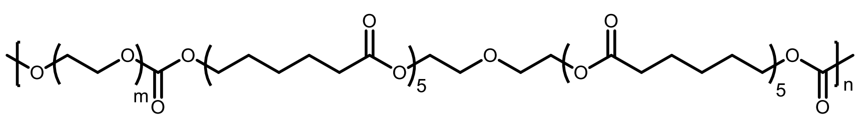

PCL-*co*-PEG

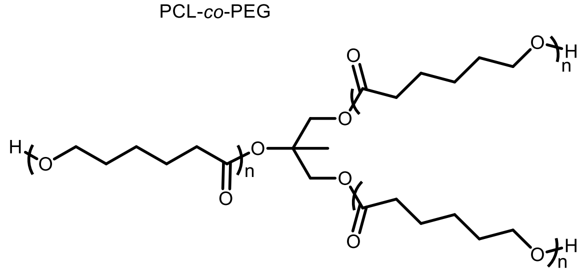

Branched PCL

Figure 1.7 Examples of Polyadipates

investigated, showing desirable plasticization properties (**Figure 1.8**).[70–72]

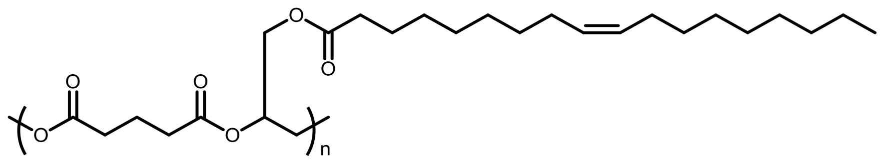

Poly(glutaric acid-glyceryl monooleate)

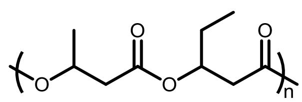

Poly(3-hydroxybutyrate-*co*-3-hydroxyvalerate)

Figure 1.8 Other Polyester Polymeric Plasticizers[70–72]

The major drawbacks of polymeric plasticizers are their lack of homogeneous mixing with the PVC resin, and lower plasticization efficiency compared to low molecular weight traditional plasticizers. Toxicity has yet to be studied for the majority of polymeric plasticizers.

Surface treatment is another approach to reduce plasticizer migration. Various surface treatment procedures for PVC are possible, including surface crosslinking,[73–79] surface grafting,[74,80,81] and surface coating.[82,83] However, surface treatment may compromise the flexibility and mechanical properties of the polymer.

1.7 Internal Plasticization: Covalent Attachment of Plasticizers to PVC

Covalently attaching plasticizers to PVC is one of the most effective ways to prevent plasticizer migration. Multiple different approaches have been utilized, including nucleophilic substitution and methods involving polymerization.

1.7.1 Covalent Attachment of Plasticizers via Nucleophilic Substitution to PVC

1.7.1.1 Sulfide Linkages

The first example of internal plasticization of PVC was reported by Michel *et al.*[84] in 1986 using sodium thiolates to covalently bond the 2-ethylhexyl ester of *o*-mercaptobenzoic **1.1** acid and of the similar ester of thioglycolic acid **1.3** to PVC (**Scheme 1.3**). The T_g values of the polymer decreased with increasing amounts of sulfide substitution. As mentioned in the Free Volume Theory, T_g is the glass transition temperature. For a polymer, this is the temperature at which a polymer changes from a glassy state to a rubbery state. As a result, materials with lower T_g value will be more flexible. T_g of commercially available PVC is around 81 °C.[85] The 2-ethylhexyl ester of thioglycolic acid **1.3** showed better plasticization efficiency compared to 2-ethylhexyl ester of *o*-mercaptobenzoic acid **1.1**. The lowest T_g achieved in this work was 56 °C with 15 mol% of covalently linked 2-ethylhexyl ester of thioglycolic acid.

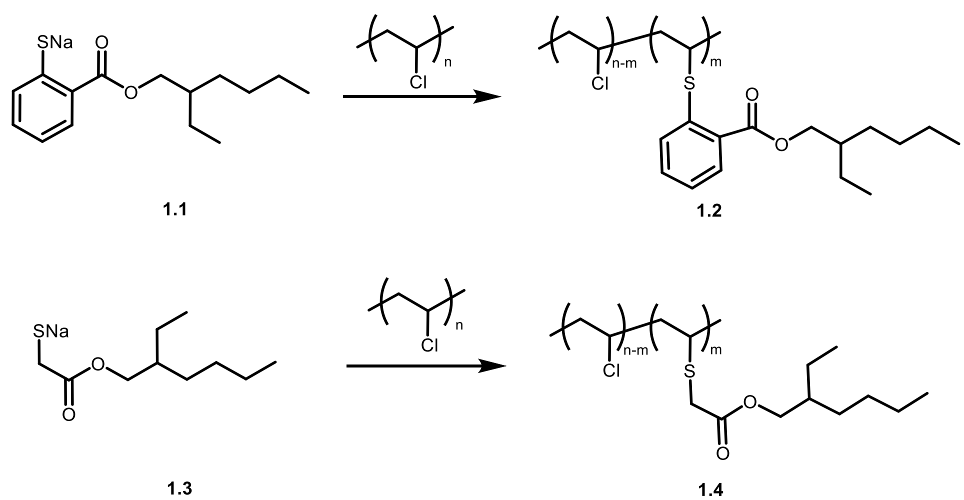

Scheme 1.3 Covalently Bonding the 2-Ethylhexyl Ester of *o*-Mercaptobenzoic Acid and Thioglycolic Acid to PVC using a Sulfide Linkage

In 2010, the Reinecke group[86] synthesized several regioisomers of 2-ethylhexyl thiol-phthalates in three steps, and covalently linked them to PVC by nucleophilic substitution (**Scheme 1.4**). The lowest T_g in obtained was 0 °C for 23 mol% substitution. This is the first example of directly attaching the phthalate motif to PVC. Extraction studies were done at room temperature using heptane as solvent, which showed no migration at all.

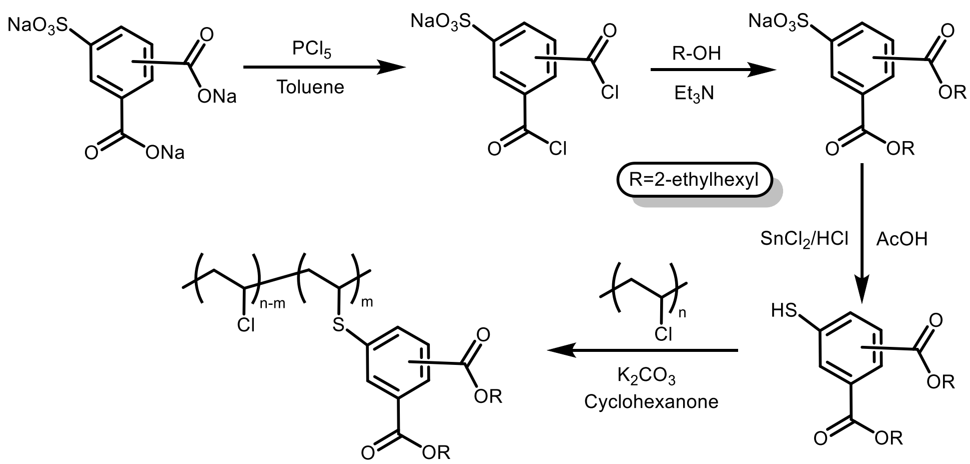

Scheme 1.4 Covalent Attachment of 2-Ethylhexyl Thiol-Phthalate Regioisomers to PVC

In 2016, the Reinecke group developed two strategies to attach plasticizers via aromatic (**Scheme 1.5**).or hetero-aromatic thiols (**Scheme 1.6**).[87] Both strategies required 4-5 synthetic steps. For the first strategy, T_g values for PVC bearing 40 wt% plasticizer range from 28 to 37 °C (**Scheme 1.5**). The second strategy used trichlorotriazine (TCTA) as the starting material (**Scheme 1.6**). Two chlorines on TCTA were replaced either by amines or alcohols. Then the third chlorine was converted to the sodium thiolate using thiourea followed by NaOH, and then attached to the PVC backbone at 85 °C for 2 hours. For PVC bearing 40 wt% thiol-based plasticizer, T_g values range from 35 to 55 °C.

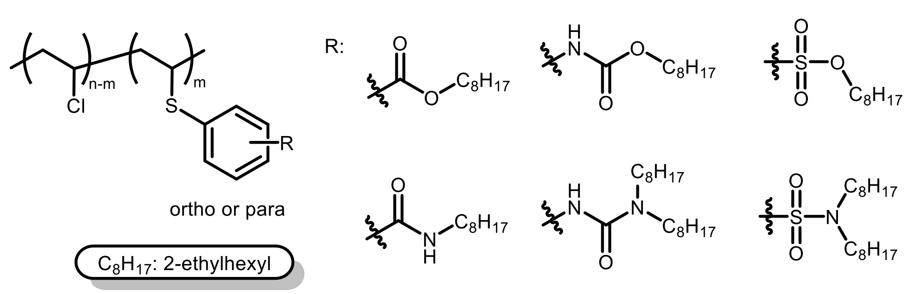

Scheme 1.5 Covalent Attachment of Aromatic Thiol Plasticizers to PVC

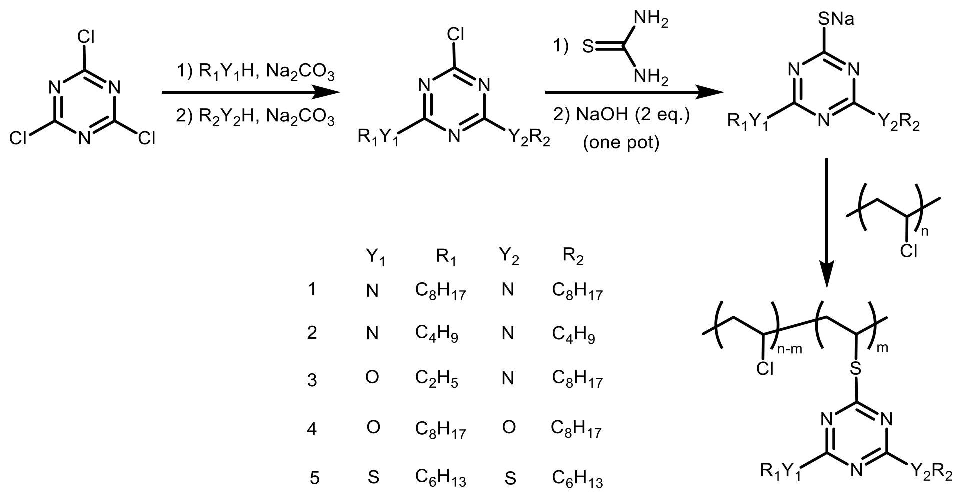

Scheme 1.6 Covalent Attachment of Hetero-Aromatic Thiol Plasticizers to PVC

In 2016 and 2017, the Reinecke group[88,89] used high molecular weight plasticizers to achieve plasticization with less chlorine substitution (**Scheme 1.7**). They also explored the influence of the compatibility of the covalently attached plasticizers on T_g by changing the ratio

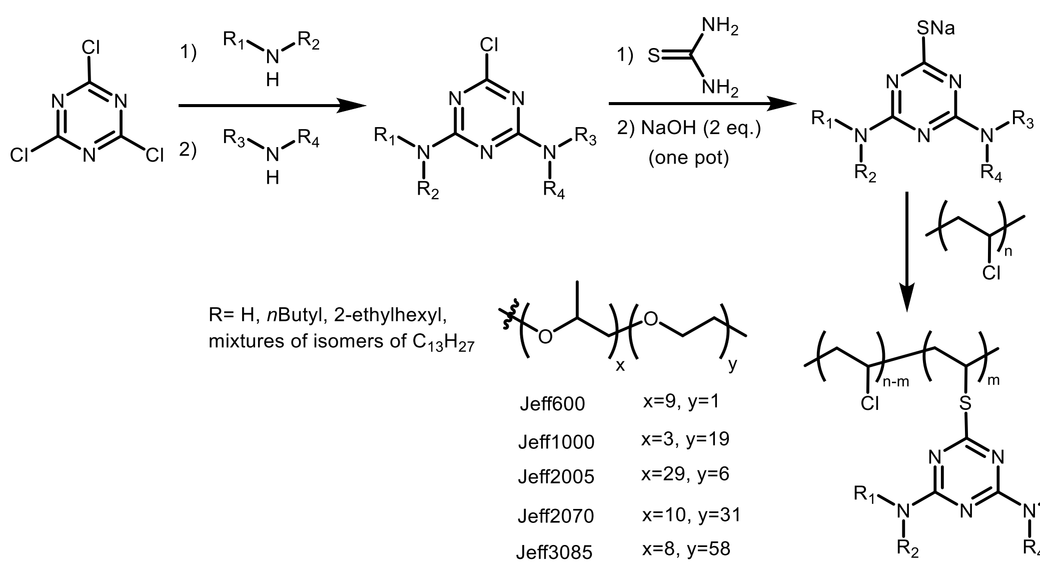

Scheme 1.7 Covalent Attachment of PEG-PPO TCTA Plasticizers to PVC

of PVC-miscible polyethylene glycol (PEG) and PVC-immiscible polypropylene oxide (PPO) made using commercially available Jeffamines® in the designed plasticizers. Compared to previous studies, these new PEG-PPO trichlorotriazine (TCTA) derivatives exhibited low T_g values. For example, when R_1=$(PO)_3(EG)_{19}$, R_2=H, R_3=$(PO)_3(EG)_{19}$, R_4=H (with M_w=2100 g/mol), the T_g value was -18 °C for 45 wt% plasticizer, and the T_g was -41 °C for 73 wt% plasticizer. Comparing traditional non-covalently attached DEHP/PVC mixtures at 45 wt%, the PEG-PPO TCTA system plasticizes at an equivalent efficiency. Amines containing more EG repeat units have higher plasticization efficiency compare to amines with more PO repeat units. Interestingly, several polymers showed an additional T_s peak at T_m = 24 °C. The authors explain this as the fusion of crystallized EO segments.

In 2019, Zhou *et al.*[90] reported a method to attach epoxidized biomass-based plasticizers, including cardanol glycidyl ether, epoxidized acetylated castor oil methyl ester, and epoxidized soybean oil to PVC using thiosalicylic acid (**Scheme 1.8** & **1.9**). Three biomass-based plasticizers were attached with the same mol amount by carboxylate nucleophilic addition to epoxides. The lowest T_g value obtained was 38 °C with epoxided soybean oil. T_g values for the grafted epoxidized acetylated castor oil methyl ester and cardanol glycidyl ether were 44 °C and 42 °C, respectively. From these sulfide linked plasticizer studies, one can conclude: 1) at a constant weight percent of incorporation, large molecular weight plasticizers efficiently decrease the T_g value because large plasticizers introduce fewer anchor points to the PVC backbone. The anchor points, which are considered anti-plasticizing, reduce the free movement of the PVC backbone. 2) miscibility of the plasticizer with PVC is important. One can use these results to further improve internal plasticizer design. There are several drawbacks to sulfides: 1) Sulfides are susceptible to oxidation;[91] 2) the resulting oxidation products (sulfoxides, sulfones, etc.) can undergo elimination, leading to degradation of the polymer; 3) sulfides and thiols can release foul odors upon degradation, as well as potential odors from residual thiols in the material. Sulfides and other sulfur compounds can lead to discoloration of the PVC products.

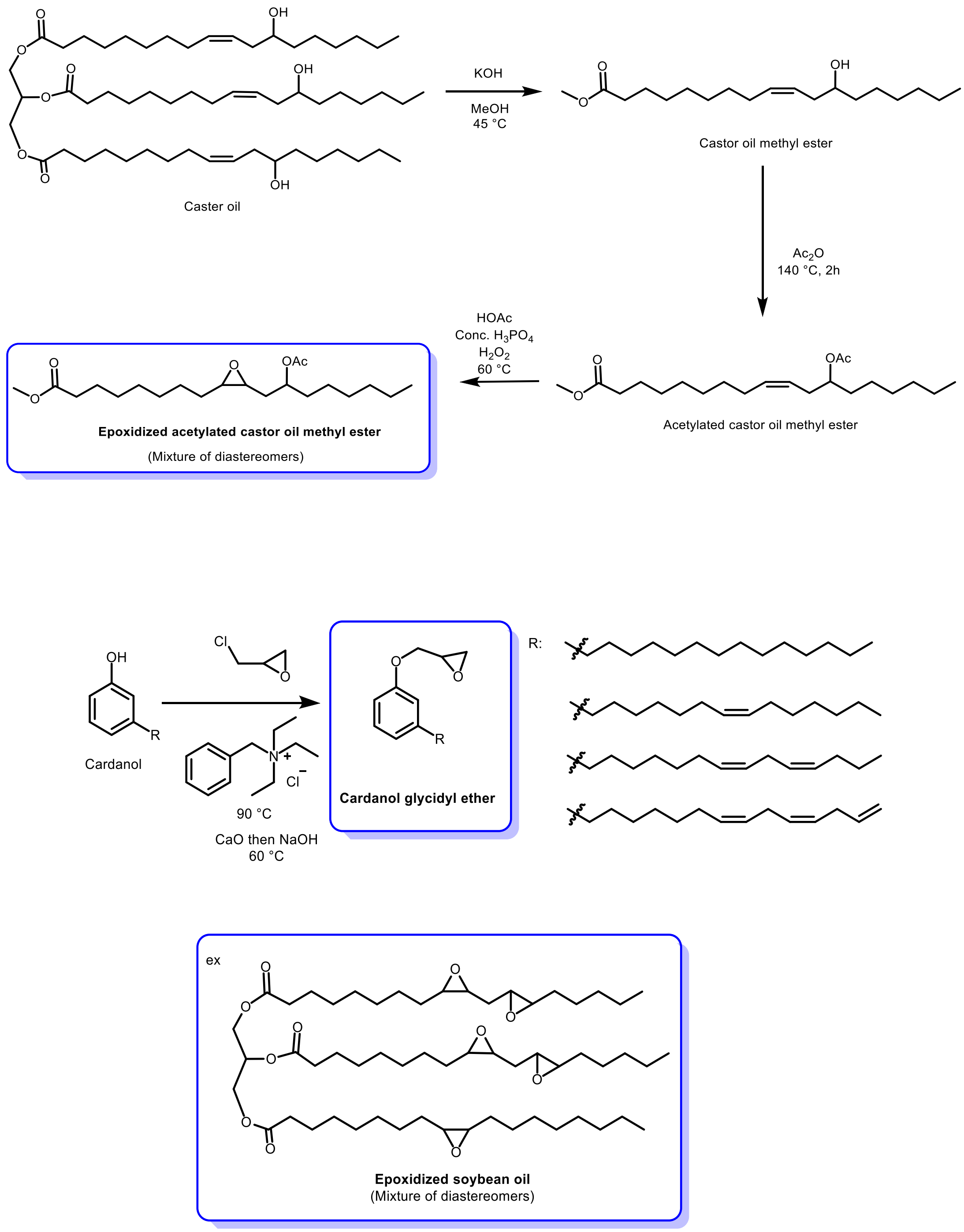

Scheme 1.8 Synthesis of Biomass-Based Epoxides from Cardanol and Soybean Oil

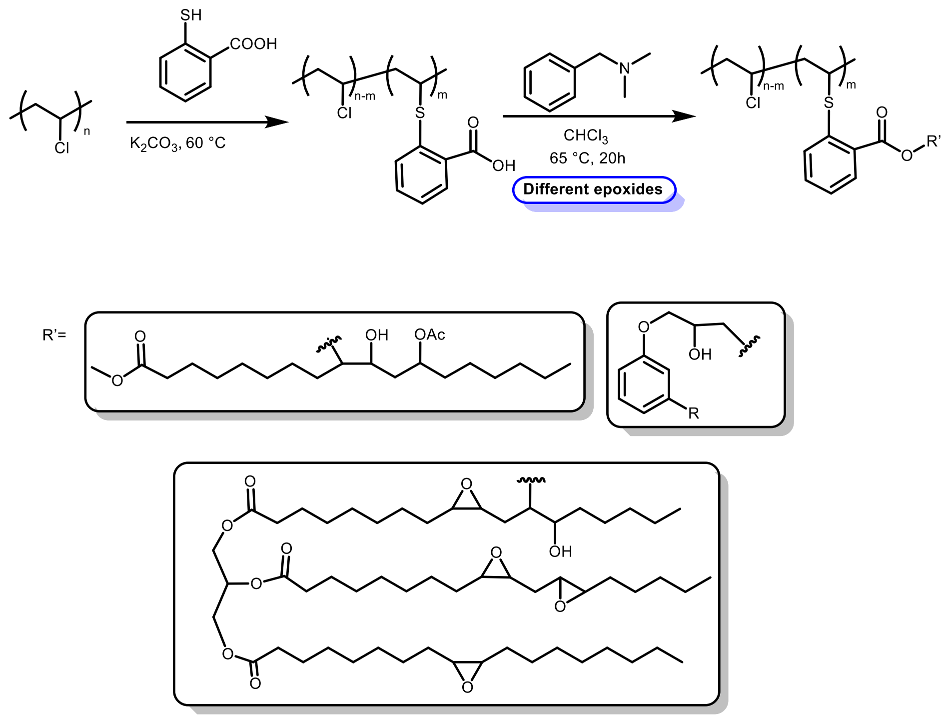

Scheme 1.9 Covalent Attachment of Epoxidized Biomass-Based Plasticizers to PVC Modified with Thiosalicylic Acid

1.7.1.2 Amine Linkages

Zhou *et al.* published two papers using inexpensive and environmentally-friendly compounds: tung oil[92] and cardanol[93] as sources of internal plasticizers. In particular, cardanol is a waste byproduct of the cashew industry: it is the oil from the cashew shells, which can cause dermatitis upon contact for sensitive individuals. These plasticizers were covalently bonded to PVC by nucleophilic substitution, using an amine as the nucleophile. To prepare the amine-terminated plasticizing group, tung oil was transesterified with methanol to give the methyl ester (**Scheme 1.10**). Amidolysis with propylenediamine formed an amide with a terminal amine. This aminated tung oil was attached to PVC by substitution of chlorine under heat. Interestingly, there was no mention if competitive HCl elimination by the primary amine. The lowest T_g value achieved was 44 °C for 37 wt%. Tensile modulus and tensile strength decreased while elongation at break increased.

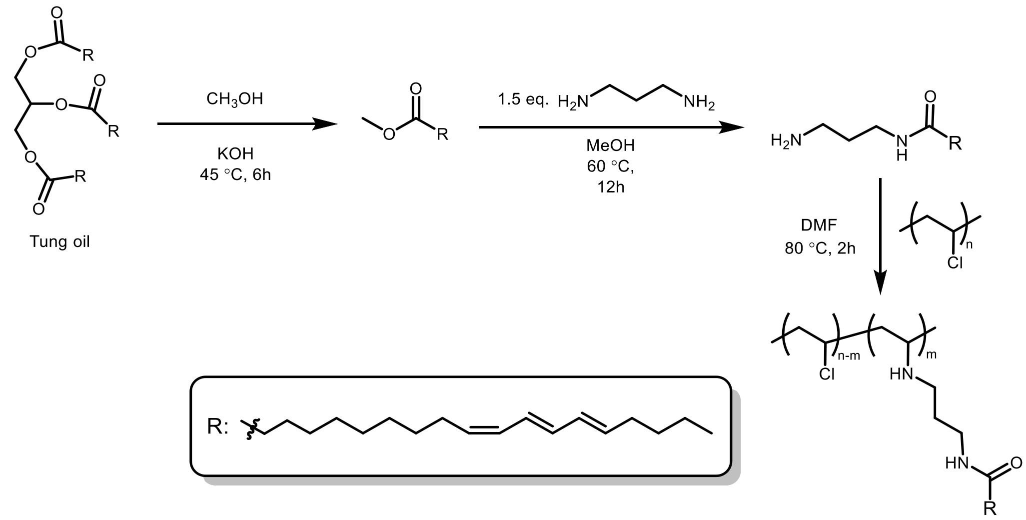

Scheme 1.10 Covalent Attachment of Aminated Tung Oil Plasticizers to PVC

Using cardanol, Jia et al. synthesized the Mannich base of cardanol butyl ether in 2 steps (**Scheme 1.11**). In the first step, cardanol was treated with butyl chloride and base under

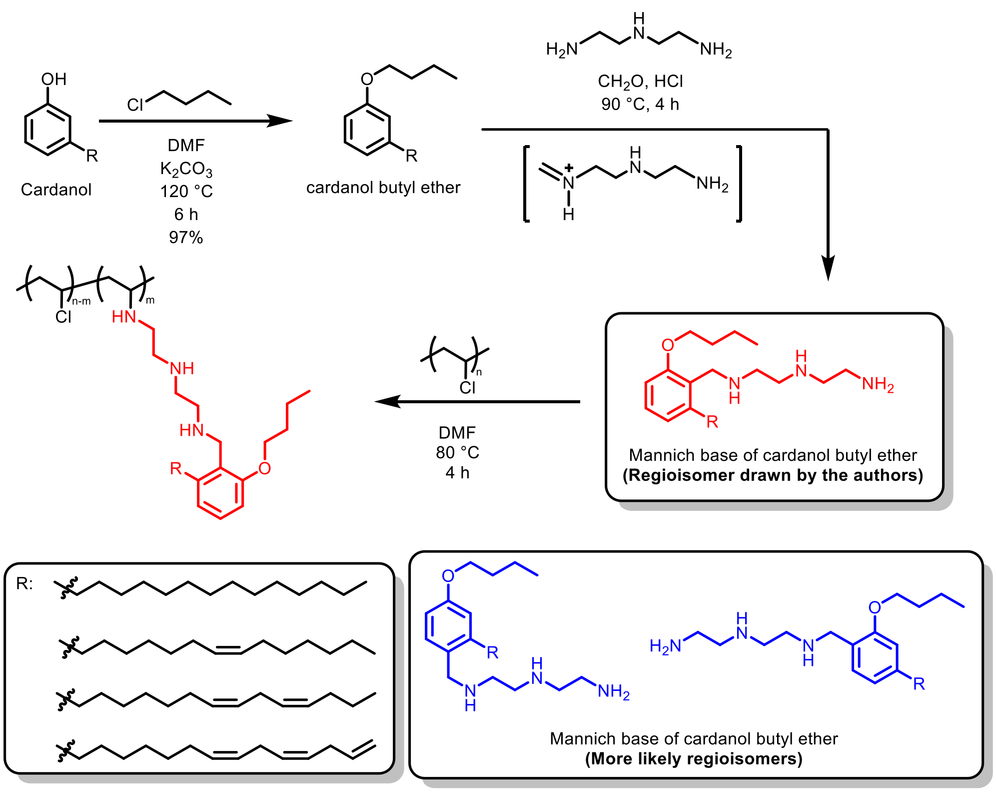

Scheme 1.11 Covalent Attachment of Aminated Cardanol Butyl Ether Plasticizers to PVC

heat to give cardanol butyl ether. In the second step, the reactive iminium ion was formed under acidic conditions to further react with cardanol butyl ether through aromatic electrophilic substitution to give the Mannich base of cardanol butyl ether. However, the authors proposed formation of a regioisomer that is least likely to be formed due to steric hindrance. The Mannich base of cardanol butyl ether was then attached to PVC as a plasticizer by amine nucleophilic solution. Possible competing base mediated elimination on PVC was not discussed, and the lowest T_g value obtained was 49 °C for 38.4 wt% of cardanol plasticizer.

1.7.2 Covalent Attachment of Plasticizers to PVC via 3+2 Azide-Alkyne Cycloaddition

1.7.2.1 Copper-Free 3+2 Thermal Azide-Alkyne Cycloaddition

The Braslau group has focused on covalently attaching phthalate or phthalate mimics to PVC via thermal azide-alkyne cycloaddition (TAAC), as the triazole diester resembles the phthalate structure consisting of a flat, aromatic ring bearing two ortho esters (**Figure 1.9**). Thermal 3+2 Azide/Alkyne was first discovered by A. Michael[94] in 1893, and then popularized and developed by Huisgen[95] 70 years later (**Scheme 1.12**).

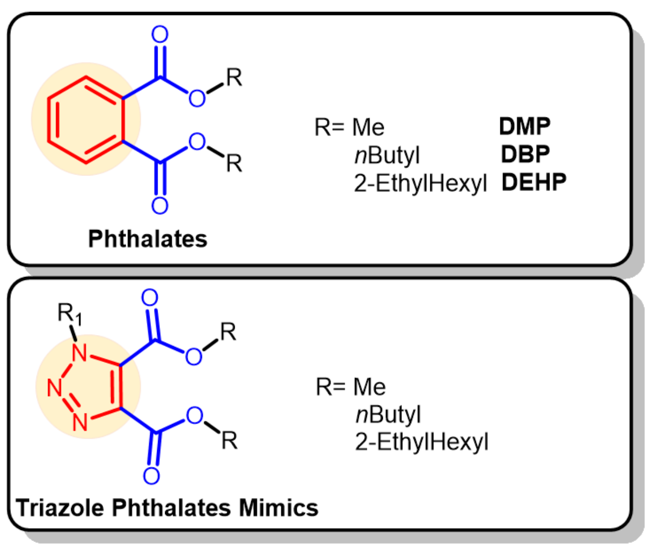

Figure 1.9 Phthalates or Triazole Phthalate Mimics

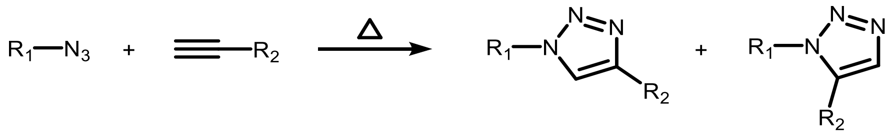

Scheme 1.12 Thermal Azide-Alkyne Dipolar Huisgen Cycloaddition

The ease of the thermal azide-alkyne cycloaddition (TAAC) is primarily a function of the HOMO-LUMO gap of the azide/alkyne pair.[96] A low energy gap between the azide HOMO and the alkyne LUMO increases the rate of cyclization. For example, Brook[97] investigated a series of alkynes with differing electronic structures, measuring the TAAC reaction onset temperatures by differential scanning calorimetry (DSC) (**Table 1.2**). The conclusion from this study is that increasing the number of electron withdrawing R-groups on the alkyne increases the reaction rate for the TAAC reaction. The most reactive alkyne was diethyl acetylenedicarboxylate, because it has two electron withdrawing groups connected to the alkyne to lower the energy of

Table 1.2 Onset Temperatures of Different Alkynes for TACC[97]

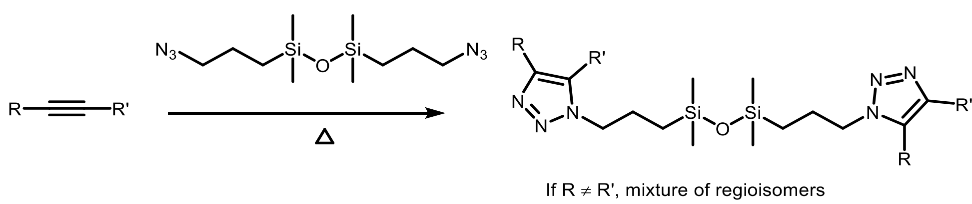

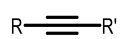	Onset Temp.(°C)	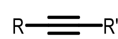	Onset Temp.(°C)
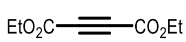	37	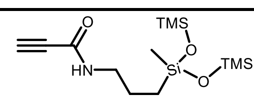	74
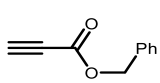	51	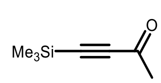	90
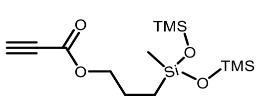	64	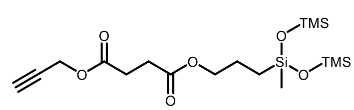	101
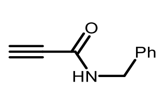	72		

the alkyne LUMO, resulting in a cycloaddition onset temperature of 37 °C.[97] Electron poor alkynes, particularly diesters, are attractive for thermal attachment to azide.

In 2019, Patrick Skelly in the Braslau lab also studied the effect of electron withdrawing groups on the rate of the TAAC reaction with a wider scope of alkynes (**Table 1.3**) both experimentally and by DFT calculations.[98] The most reactive alkyne studied contained a sulfone group and an ester group, to make it the most electron poor alkyne of the series.

Table 1.3 Relative Reaction Rates of Different Alkynes for TACC[98]

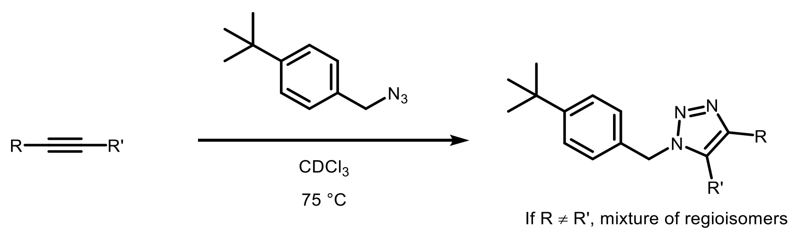

R—≡—R'	Relative Rate	R—≡—R'	Relative Rate
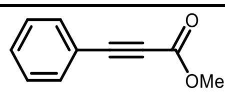	1.0	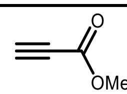	25
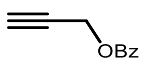	1.4	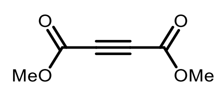	130
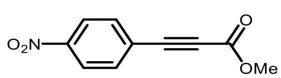	3.7	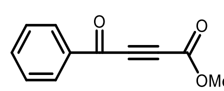	150
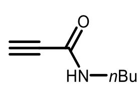	8.8	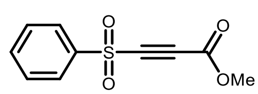	2400
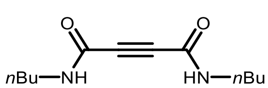	15		

In 2014, Aruna Earla and Braslau[99] demonstrated covalent attachment of phthalate mimics to PVC via TAAC (**Scheme 1.13**). In 2018, Chad Higa in the Braslau lab expanded the scope to polyethylene glycol methyl ethers.[85] The lowest T_g value obtained was -29 °C for $PEG_{550}Me$ at 15 mol% plasticizer. Interestingly, the T_g value for the dimethyl ester phthalate mimic (R=Me) was 96 °C, which was higher than the T_g of unmodified PVC (81 °C). This indicates that the rigidity of triazole ring is inherently anti-plasticizing.

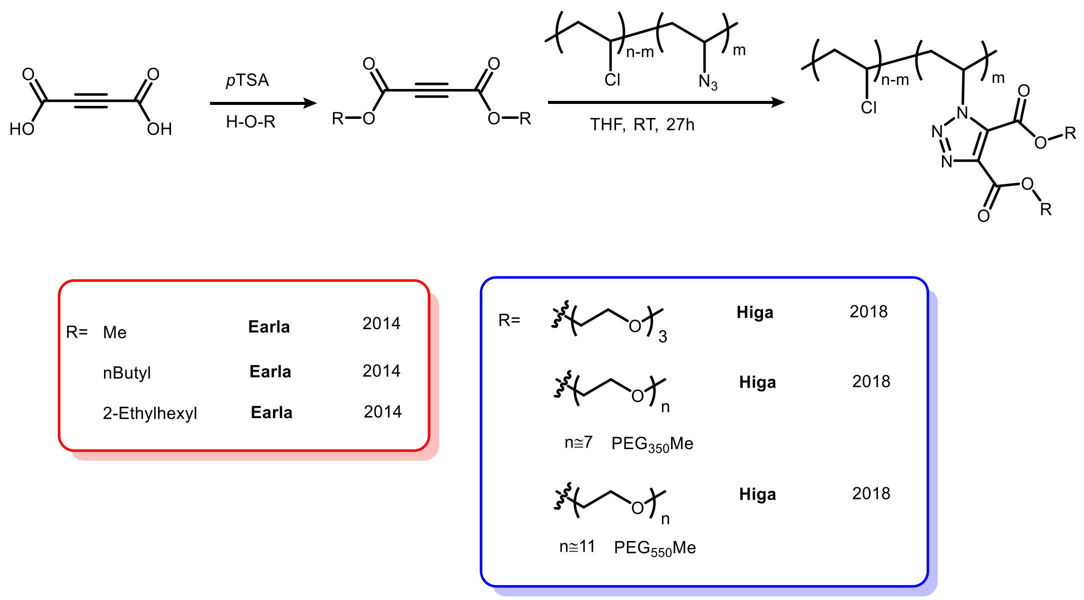

Scheme 1.13 Covalent Attachment of Phthalate Mimics onto PVC via TAAC

In 2017, Earla[100] made a propargylated DEHP derivative and covalently attached it with a tether to PVC via TAAC. The ester linker was used to 1) increase the rotational degree of freedom of DEHP to increase the efficiency of plasticization and 2) increase the activity of the alkyne by lowering the LUMO with an electron withdrawing group to achieve TAAC (**Scheme 1.14**). PVC substituted with 15 mol% of covalently linked DEHP resulted in a material with a T_g of 60 °C. This synthetic route from commercially available starting material to the tethered DEHP modified PVC product was four steps. Interestingly, acetylenedicarboxylic acid was chosen to obtain a diester bearing two DEHP groups to increase the plasticization. However, only the monoester was obtained since decarboxylation occurred under basic conditions and heat, as shown in the box of **Scheme 1.15**.[100]

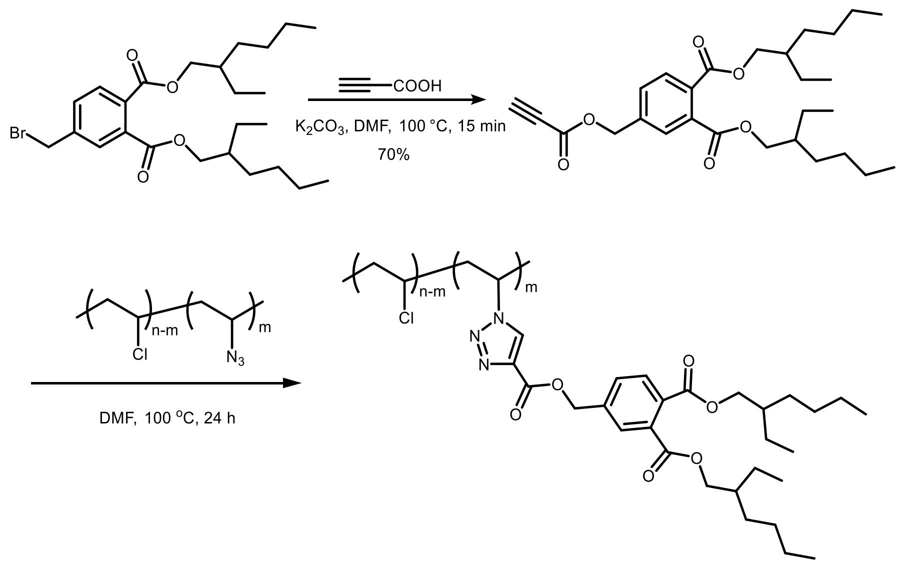

Scheme 1.14 Covalent Attachment of Tethered DEHP to PVC via TAAC

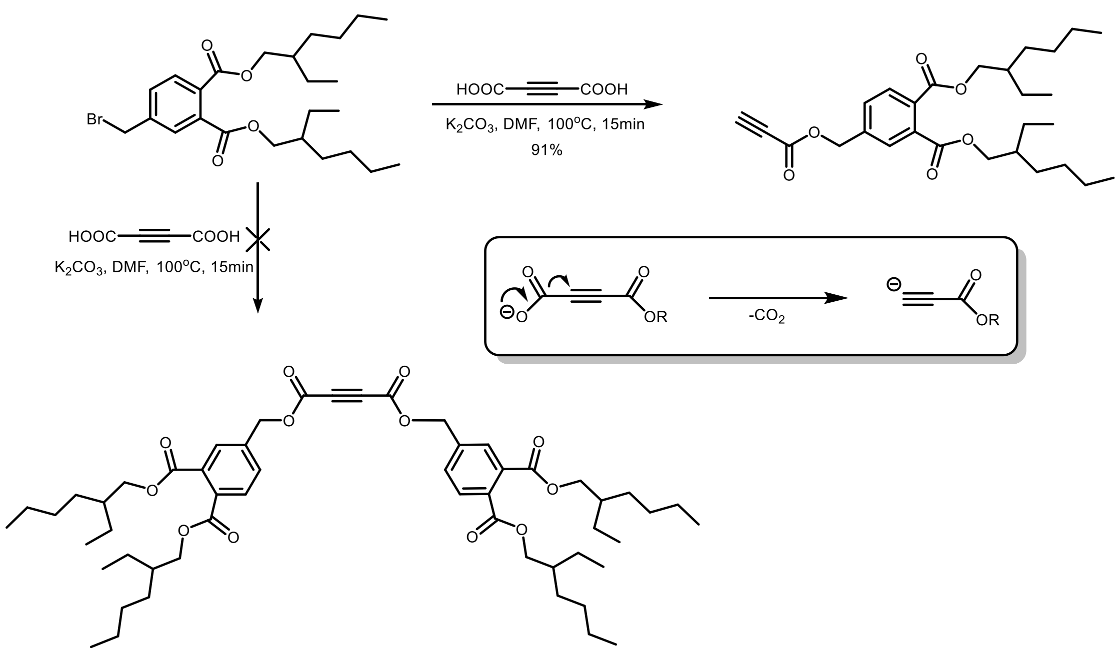

Scheme 1.15 Decarboxylation of Acetylenedicarboxylic Acid upon Reaction with Benzyl Bromide under Basic Conditions

Higa continued work in the Braslau lab on thermal azide-alkyne attachment of plasticizers to PVC (**Scheme 1.16**).[85] A six-carbon linker, chosen for the low-cost and easy to synthesize, was added in between the linking triazole to reduce the rigidity caused by the aromatic ring. The T_g values for internal plasticization with this six-carbon linker are lower than the analogues PVC samples where the triazole diester is directly attached to the PVC chain. The lowest T_g obtained in this series was 18 °C, where R = TEGMe at 15 mol% azidation.

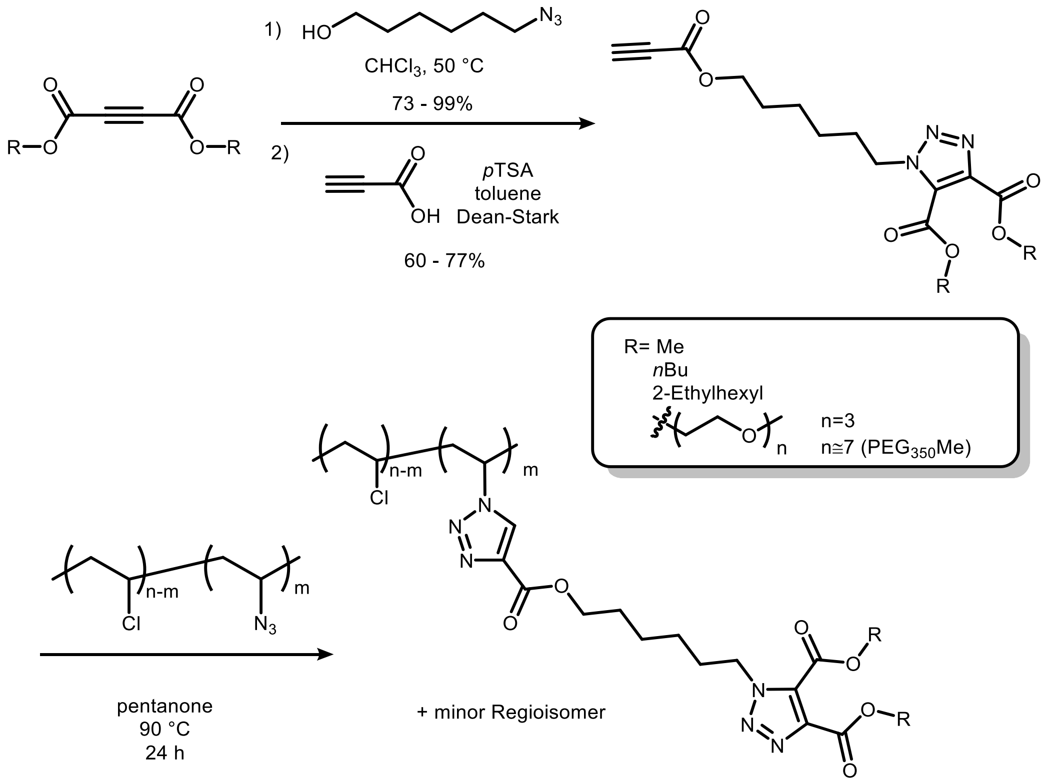

Scheme 1.16 Covalent Attachment of Rotationally Labile Phthalate Mimics with a Six Carbon Tether to PVC

Higa then developed a branched internal plasticizer bearing two tethered triazole mimics with a larger molecular weight (**Scheme 1.17**).[85] Because acetylene dicarboxylates are excellent Michael acceptors, one can not use traditional coupling agents nor make the corresponding diacid chloride. Thus one must protect the alkyne as the 1,2-dibromide, make the diacid chloride, esterify, and then restore the alkyne. Following this protocol, the synthesis of the plasticizer required four steps. Acetylene dicarboxylic acid was converted to dibromofumaryl chloride in two steps. Esterification followed by deprotection of the alkyne was carried using Zn and a catalytic amount of iodine to give double-sided hexyl tethered alkynes.

The lowest T_g value was -17 °C for the sample bearing two TEGMe polyether esters (**Figure 1.10**). Even though the T_g value is higher than that of non-covalent DEHP at the same weight percentage, this internal plasticizer illustrates the efficacy of this approach.

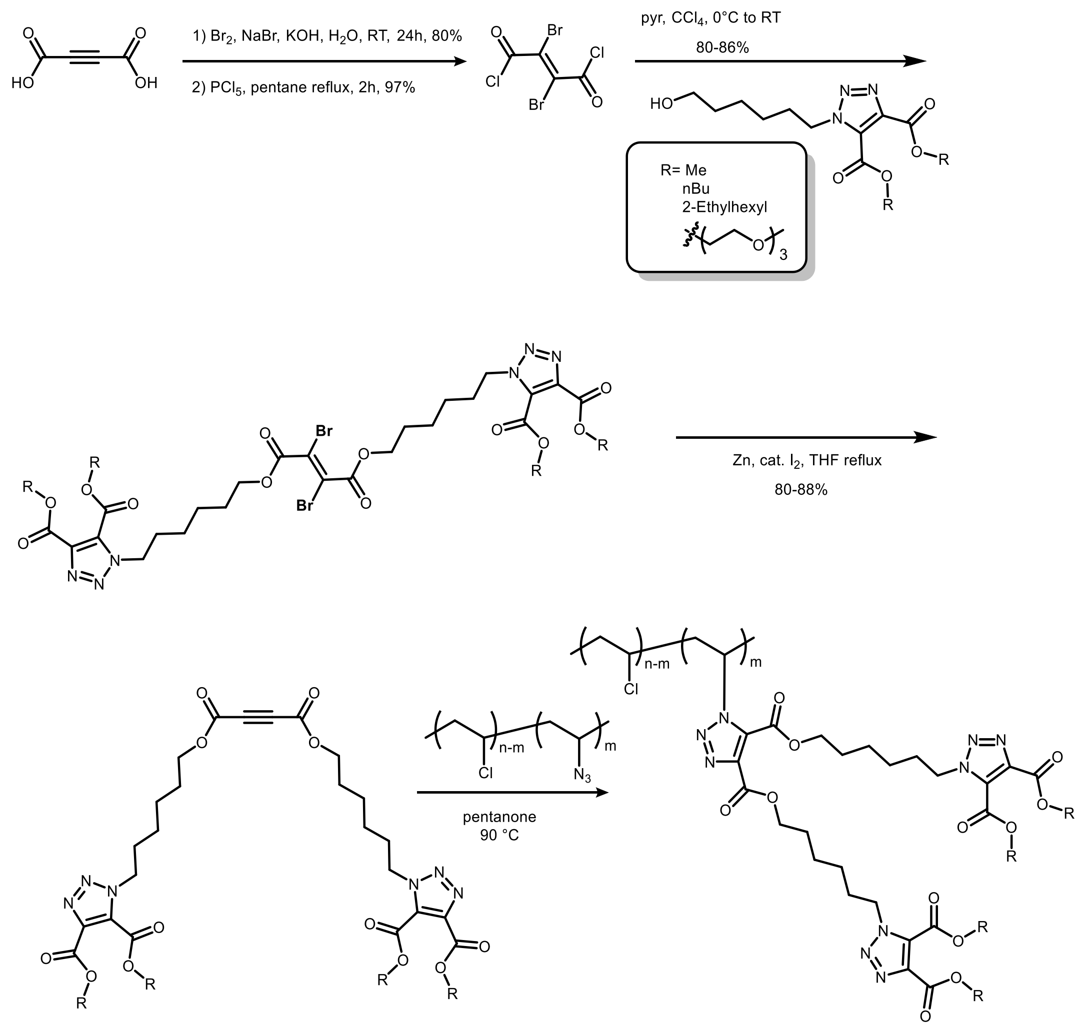

Scheme 1.17 Covalent Attachment of an Internal Plasticizer with Two Tethered Triazole Mimics to PVC

Higa then developed the most impressive internal plasticizers of this series with high plasticization efficiencies from propionic acid single sided alkynes with $PEG_{1000}Me$, and $PEG_{2000}Me$ ester in only two synthetic steps (**Scheme 1.18**). A low T_g value of -42 °C was obtained with $PEG_{2000}Me$ at 15% azidation.

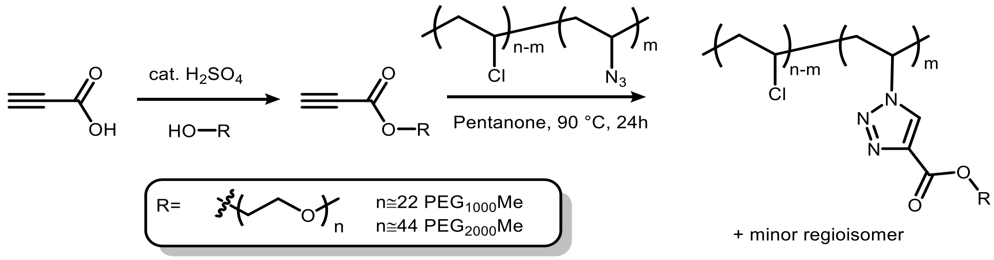

Scheme 1.18 Covalent Attachment of Polyether Propionic Esters made in Two Steps to PVC

Overall, Higa developed four generations of triazole plasticizers (**Figure 1.10**). The T_g values for all generations at 15 mol% plasticizer are summarized in **Figure 1.11**. The T_g value decreases with the increasing length of the R ester groups within the same generation. Generations one and four, which required the fewest number of reaction steps, gave the lowest T_g values, due to the attachment of very long polyether chains as the ester moiety.

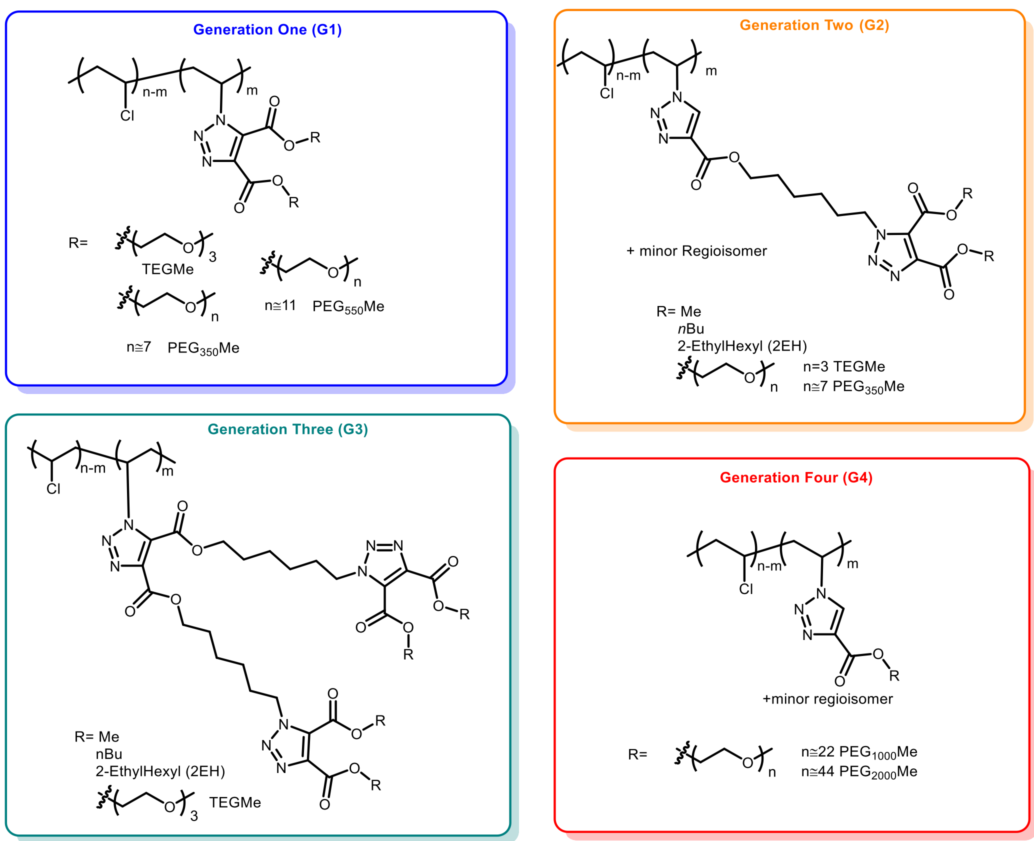

Figure 1.10 Higa's Four Generations of Triazole Plasticizers[85]

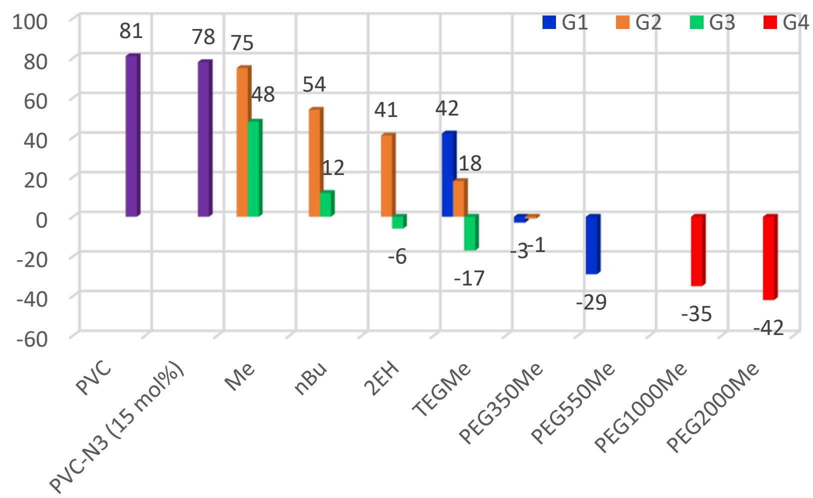

Figure 1.11 T_g Values for Four Generations at 15 mol% Plasticizer (Higa)[85]

1.7.2.2 Copper-Catalyzed 3+2 Azide-Alkyne Cycloadditions

Following the publication of the attachment of phthalate mimics to PVC by thermal azide/alkyne cycloaddition in the Braslau lab[99], in 2015 the Shi group[101] used cardanol as starting material to make propargyl ether cardanol using S_N2 reaction with propargyl bromide,

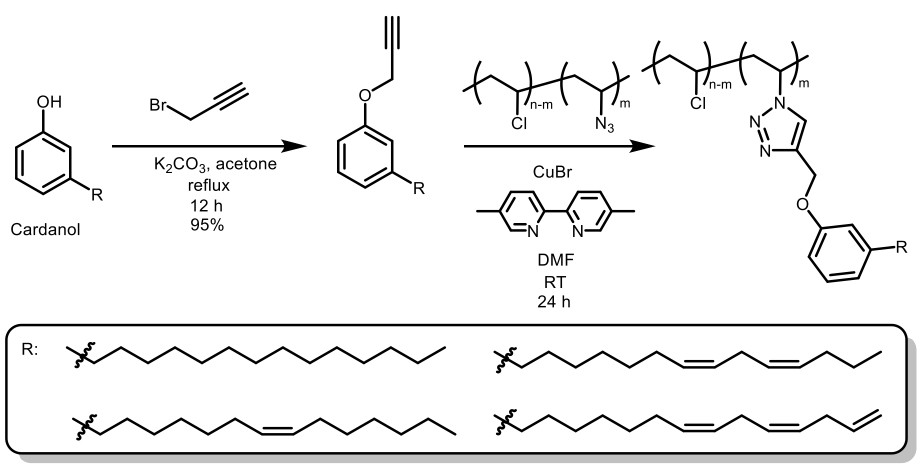

Scheme 1.19 Covalent Attachment of Cardanol to PVC via CuAAC[101]

followed by copper-catalyzed 3+2 azide-alkyne cycloaddition (CuAAC)[102–104] to attach 10 mol% cardanol to PVC (**Scheme 1.19**). The lowest T_g value was 51 °C. In this chapter, approximately one equivalent of copper catalyst was utilized for CuAAC, a fair amount of which remained in the polymer.

In 2015, Demirci and Tasdelen[105] utilized photoinduced copper-catalyzed 3+2 azide-alkyne cycloaddition to attach alkyne-terminated poly(epsilon-caprolactone) (PECL) to azide-functionalized PVC. Alkyne-terminated PECL was synthesized from propargyl alcohol by ring opening polymerization using $Sn(Oct)_2$ as the catalyst. Cycloaddition was conducted under UV light with catalytic $Cu(II)Br_2$ and PMDETA as the ligand, using 2, 2-dimethoxy-2-phenyl acetophenone as photoinitiator in DMF (**Scheme 1.20**).

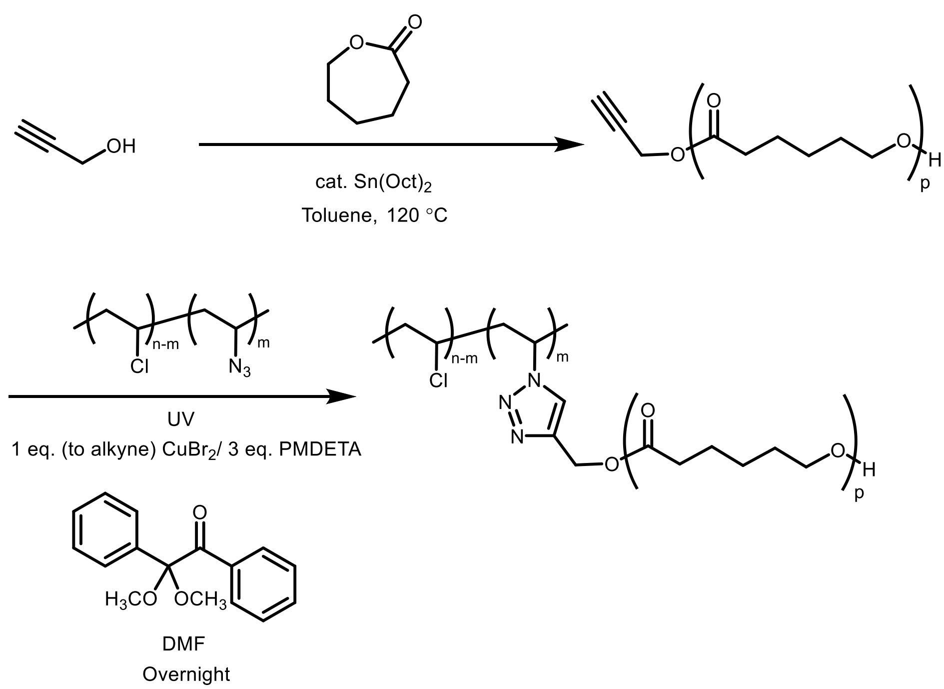

Scheme 1.20 Covalent Attachment of PVC-*g*-PECL PECL to PVC via CuAAC[105]

In 2016, the Kwak group[106] developed a hyperbranched polyglycerol (HPG) plasticizer, which was grafted onto PVC utilizing CuAAC. The HPG was synthesized by a one-pot ring opening polymerization (**Scheme 1.21**). Although gel permeation chromatography (GPC) data was obtained, the exact structure of this plasticizer is not known (M_n 1606 g/mol). Excellent low

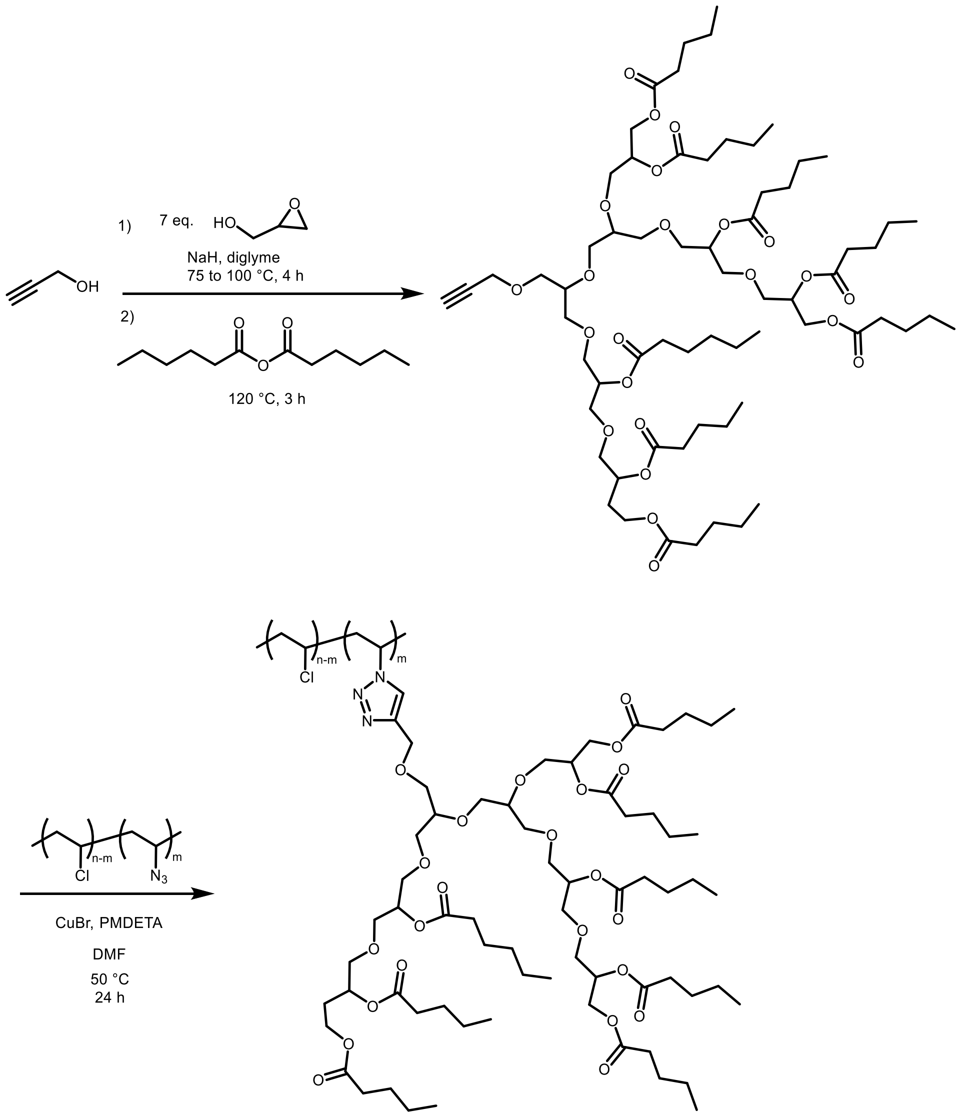

Scheme 1.21 Covalent Attachment of Alkyne-Terminated HPG to PVC via CuAAC[106]

T_g values were achieved: T_g of 16 °C, -5 ºC, and -29 °C were found for 3.6 mol%, 5.8 mol%, and 9.0 mol% plasticizer, respectively. The storage modulus data indicate this covalent plasticizer promotes segmental motion in the system and improves the softness of the HPG linked PVC at room temperature. The HPG modified PVC was softer and more flexible than PVC/DEHP for the same T_g values. Several mechanical properties of these grafted polymers were tested. The most interesting result is that the elongation at break of HPG linked PVC increased with increasing amounts of incorporated plasticizer, and reached 912% at 9 mol% of HPG whereas noncovalent HPG plasticized PVC reached its maximum value of 153% at 1.7 mol% of added HPG, then decreased with increasing mol% of HPG. The CuAAC is a simple one-pot covalent attachment of HPG to PVC, and demonstrates several important points: 1) covalent plasticizers can decrease T_g to levels achieved by conventional plasticizers; 2) covalent plasticizers can increase the elongation at break of a polymer; 3) attachment of a hyperbranched plasticizer allowed PVC to maintain its structure under tensile testing. These results using semi-dendritic covalently linked HPG plasticizer points to possible further developments of internal plasticizers.

In 2017, the Zhou group[107] covalently attached a triethyl citrate based plasticizer to PVC via CuAAC to give a material with a T_g value of 36 °C at 34 wt% plasticizer (**Scheme 1.22**).

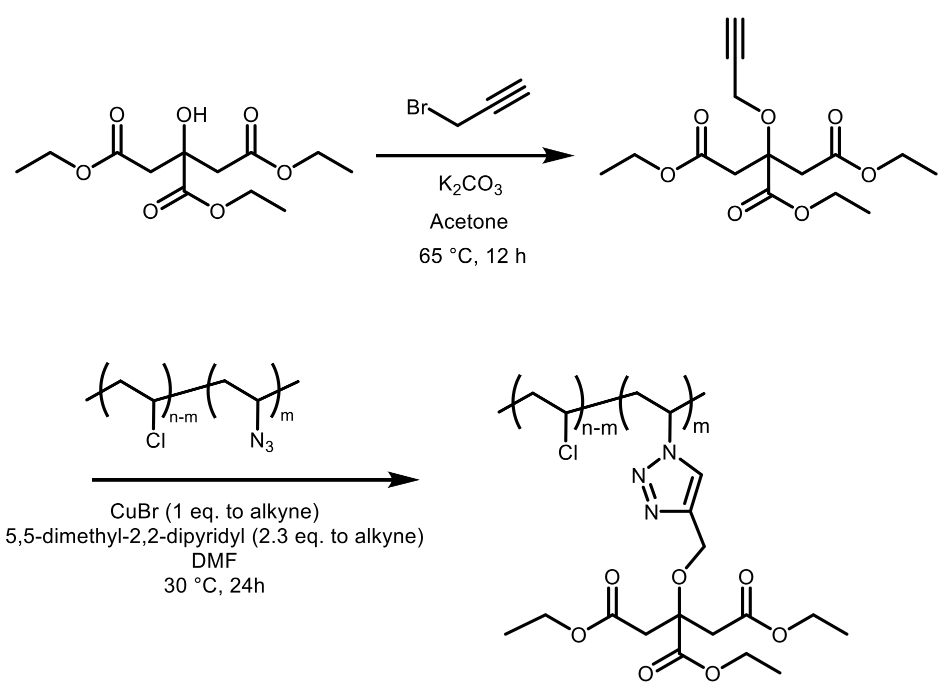

Scheme 1.22 Covalent Attachment of Alkyne-Terminated Triethyl Citrate Based Plasticizer to PVC via CuAAC[107]

Based on TGA data, this modified PVC is thermally more stable compared to unmodified PVC. Migration tests showed no leaching in distilled water, 10% aq. ethanol, 30% aq. acetic acid, and petroleum ether, confirming the covalent attachment.

Also in 2017, the Zhou group[108] covalently attached monooctyl phthalate derivatives to PVC to achieve a T_g value of 66 °C (**Scheme 1.23**). TGA data showed this modified PVC was less stable than unmodified PVC. No migration was observed in different solvents including distilled water, 10% aq. ethanol, 30% aq. acetic acid and petroleum ether.

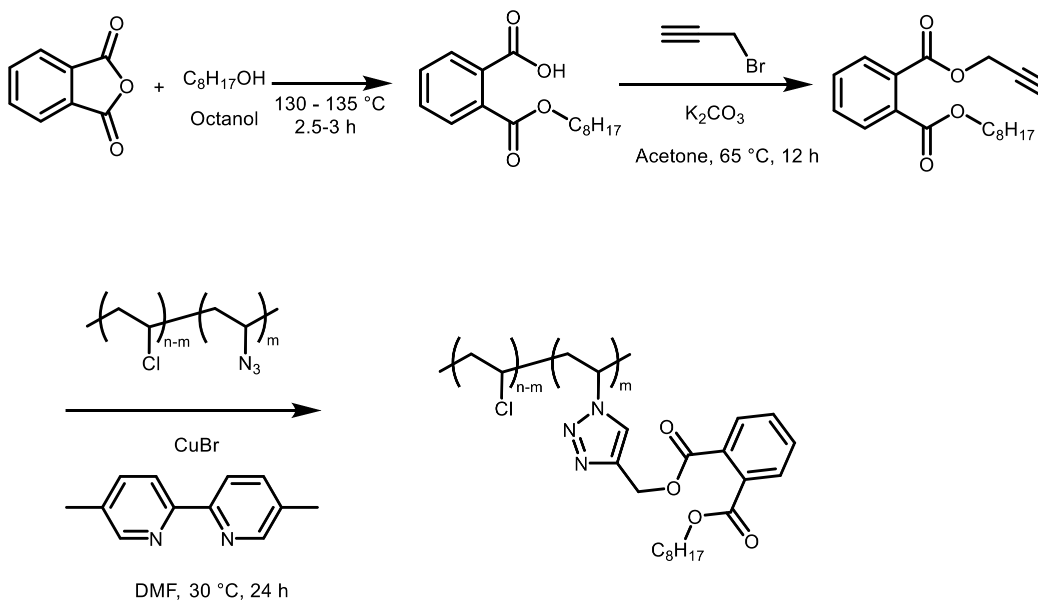

Scheme 1.23 Covalent Attachment of Alkyne-Terminated Monooctyl Phthalate Derivatives to PVC by CuAAC[108]

In 2017, Earla made a DEHP derivative by Diels-Alder cycloaddition, benzylic bromination and propargylation, and covalently attached it to PVC via CuAAC (**Scheme 1.24**).[100] An ether linker rather than an ester linker was used to enhanced the rotational degrees of freedom of the attached plasticizer. PVC with 15 mol% of covalently linked DEHP resulted in a T_g of 55 °C. This synthetic route from commercially available starting materials to this DEHP-modified PVC product required four steps.

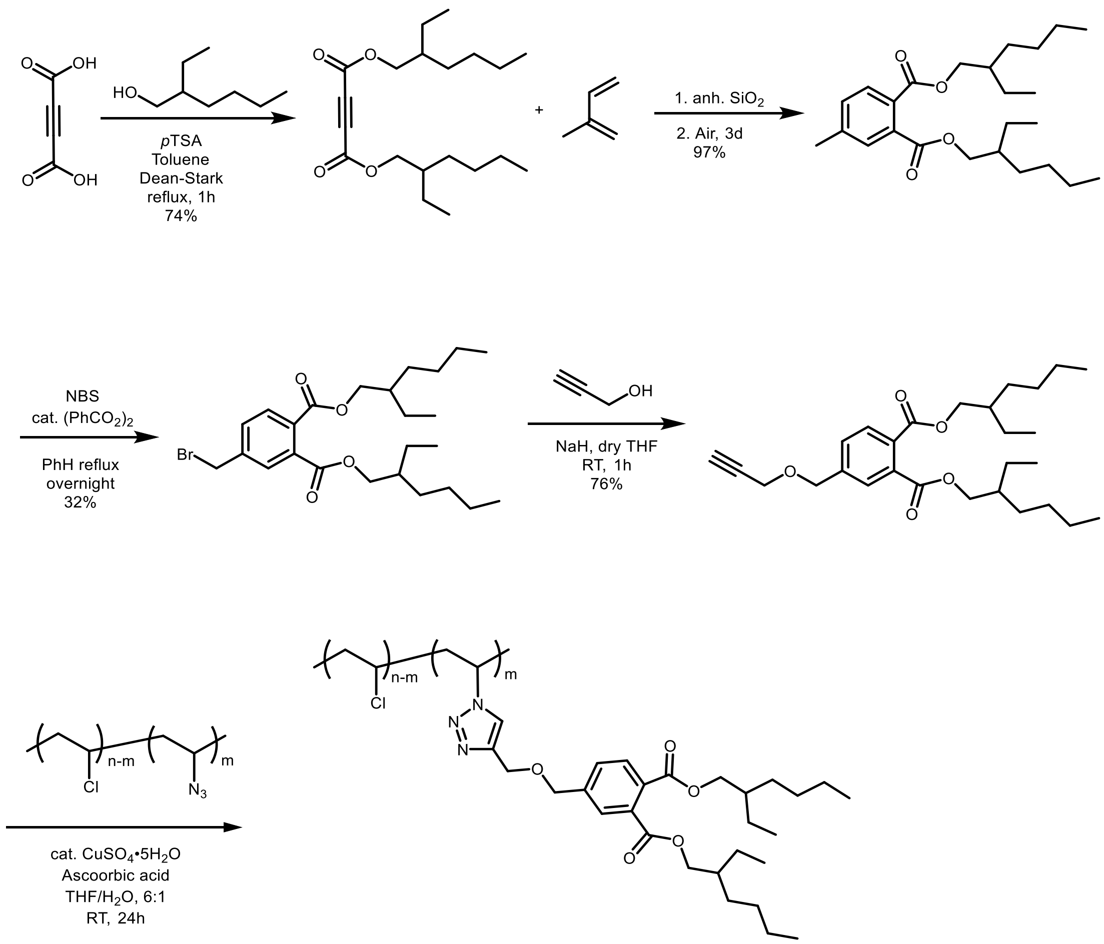

Scheme 1.24 Covalent Attachment of Alkyne-Terminated DEHP with an Ether Linker to PVC by CuAAC[100]

In 2018, Chu and Ma[109] applied CuAAC to attach a propargylated castor oil based derivative to PVC-azide. (**Scheme 1.25**) The T_g value achieved for modified PVC was 41.6 °C. TGA indicates that direct attachment of the triazole group decreases the thermal stability of modified PVC.

The Zhou group[110] used biomass-sourced dehydroabietic acid, a common diterpene from conifer trees, as a plasticizer to be covalently attach to PVC-azide (**Scheme 1.26**). Among three materials, the lowest T_g value achieved was 37 °C with about 23 wt% of plasticizer. The paper claims modified PVC materials were less thermally stable at 150-300 °C than unmodified

PVC due to the triazole group. This instability of the triazole has also been noted by other researchers.[85]

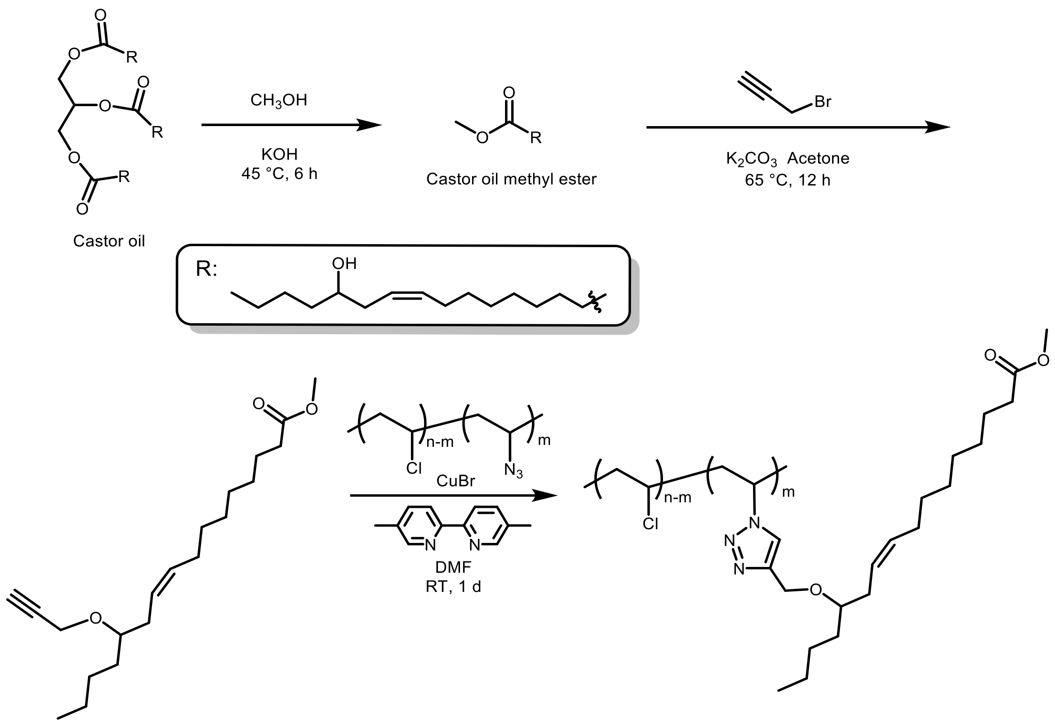

Scheme 1.25 Covalent Attachment of Alkyne-Terminated Propargylated Castor Oil Methyl Ester with an Ether Linker to PVC by CuAAc[109]

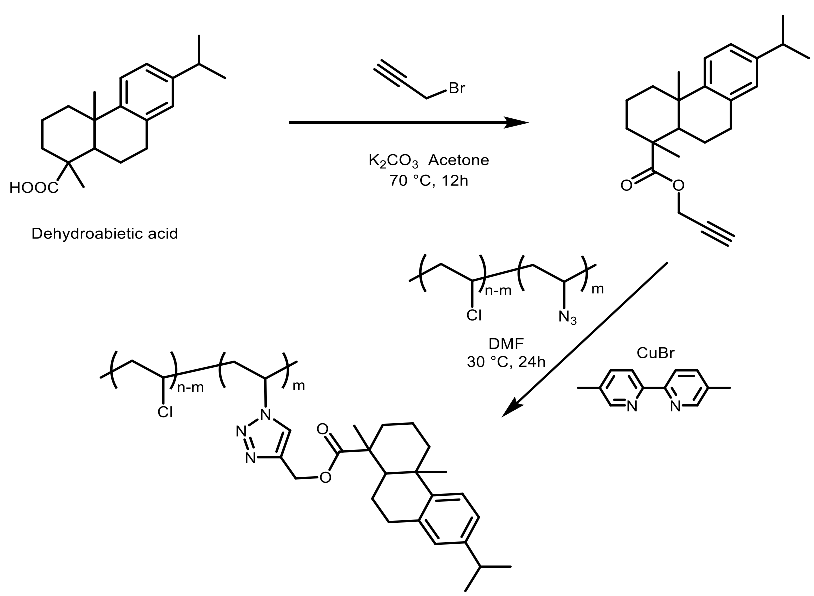

Scheme 1.26 Covalent Attachment of Alkyne-Terminated Dehydroabietic Acid with an Ether Linker to PVC by CuAAC[110]

1.7.3 Covalent Attachment of Plasticizers to PVC via Polymerization

1.7.3.1 Grafting Internal Plasticizers to PVC by Atom Transfer Radical Polymerization (ATRP)

Atom transfer radical polymerization (ATRP),[111–113] has been utilized to grow graft copolymers off of PVC from defect sites in the PVC chain.[114–125] ATRP is a reversible – deactivation radical polymerization,[126] also known as a controlled radical polymerization (CRP). The general reaction scheme of transition-metal-catalyzed ATRP is shown below (**Scheme 1.27**).[111]

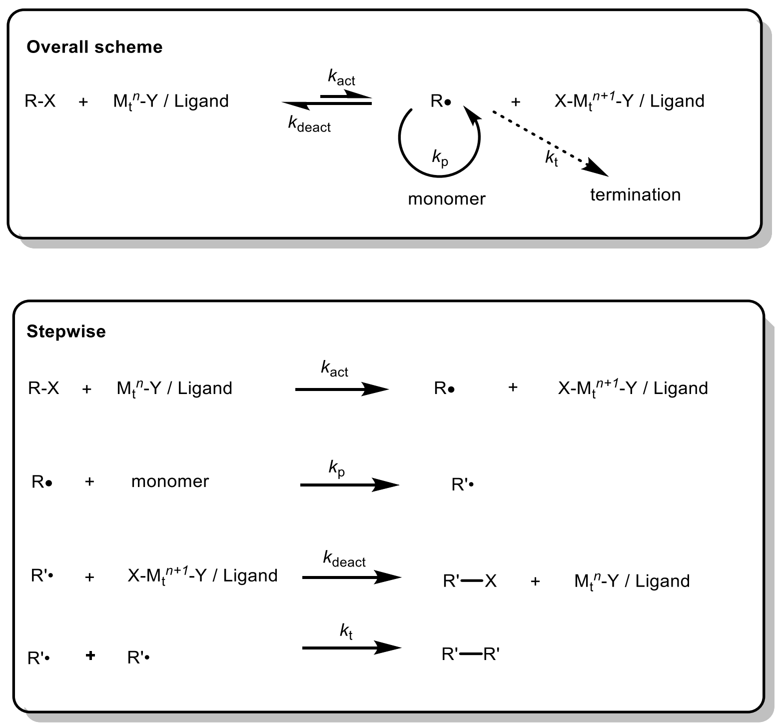

Scheme 1.27 General Scheme of Transition-Metal-Catalyzed ATRP[111]

In ATRP, at any one time, there are a large amount of dormant species, usually alkyl halides, and a tiny fraction of active alkyl radicals species. Alkyl radicals are generated from alkyl halides by a metal complex (M_t^n–Y), with an activation via rate constant k_{act} though single electron transfer concurrently with halogen atom abstraction. The alkyl radical reacts with a monomer to perpetuate polymer chain growth with a propagation rate k_p, before being deactivated by halogen transfer with a rate constant k_{deact} back to the dormant alkyl halides. Radical-radical termination reactions occur very rarely due to the low concentration of reactive radicals at any one time.

The key to successful ATRP is fast initiation and quick reversible deactivation.[111] Also, a small k_p/k_{deact} will result in lower polydispersity (PDI), meaning well-controlled polymerization.[127] If the interconversion of active alkyl radicals and dormant alkyl halides is faster than propagation, polymer chains will grow statistically at the same rate.[126] For typical alkyl chlorides, due to the relatively strong carbon-chlorine bond (compared to bromides and iodides), the initiation rate is slow, resulting in uncontrolled polymerization by CuX-initiated ATRP.[127]

1.7.3.2 Internal PVC Plasticization via ATRP

In 1998, Matyjaszewski *et al*.[114] used a PVC random copolymer containing 1 mol% poly(vinyl chloroacetate) (PVCA) as a macroinitiator to form a series of graft copolymers, including PVC-*g*-poly(*n*-butyl acrylate) (PBA), an internally plasticized form of PVC (**Scheme 1.28**).

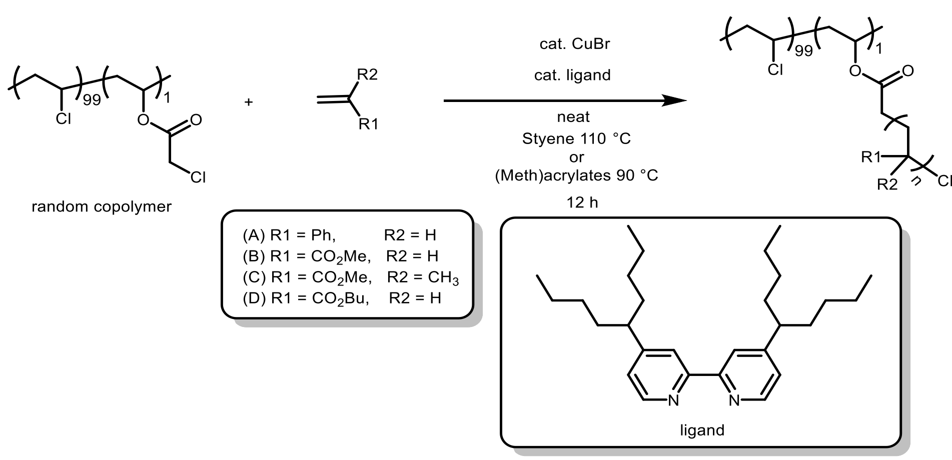

Scheme 1.28 Matyjaszewski's ATRP graft Polymerization using PVC-*co*-PVCA as a Macroinitiator[114]

The best performer had a T_g value of -19 °C, achieved with 65 mol% of PBA. The chlorines on the poly(vinyl chloroacetate) residues were considered to be the active chlorines initiating ATRP graft growth. Matyjaszewski stated that chlorines on the PVC backbone do not initiated ATRP because the secondary chloride-carbon bond is too strong to undergo dissociation.

Commercially, PVC is formed by uncontrolled, conventional free radical polymerization. This results in defect sites on the PVC backbone consisting of both allylic and tertiary chlorides (**Figure 1.12**).[8] In 2001, Percec and Asgarzadeh[115] applied copper catalyzed ATRP from these active sites in commercial PVC as initiators for graft polymerization (**Scheme 1.29**). There is at least one defect site in each PVC chain: allylic chlorides have been estimated to occur about 0.0-0.6/molecule;[128] and tertiary chlorides about 0.7-2.1/1000 monomer units.[129] They carried out a systematic study of Cu-catalyzed ATRP from the defects on PVC using a variety of vinylic monomers and Cu catalysts. The authors chose several small model compounds to study the efficiency of secondary chlorides, tertiary chlorides, and allylic chlorides as initiators (**Figure 1.13**). The results reveal a scale of initiator efficiencies from most to least reactive: allylic chlorides > tertiary chlorides >> secondary chlorides. Polymerization from the secondary chloride model compound does occur, but the initiation rate is about three orders of magnitude slower compared to allylic and tertiary chlorides. Based on these results, they concluded that ATRP grows grafts from defect sites on PVC rather than from the ubiquitous secondary chlorides. The T_g value of PVC-*g*-PBA was -4 °C at 53 mol%. A monomodal distribution was seen using GPC, indicating no detectable free homopolymer.

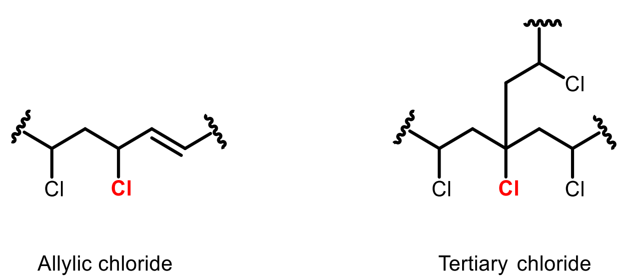

Figure 1.12 Structural defects of commercial PVC: allylic and tertiary chlorides[8]

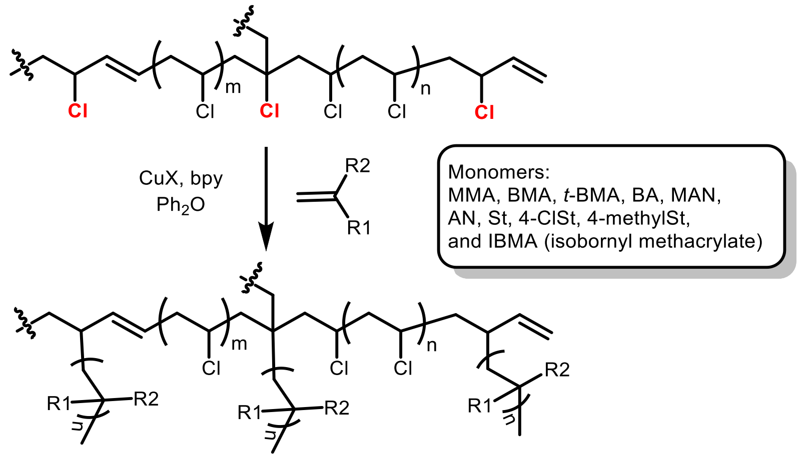

Scheme 1.29 Grafting of Various Polymers to Defect Sites on PVC via Cu-Catalyzed ATRP[115]

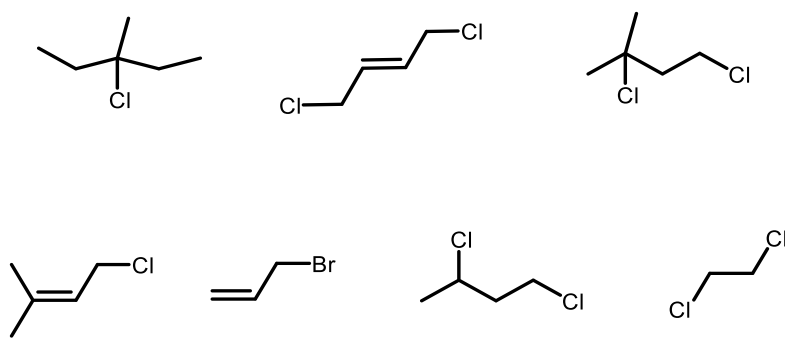

Figure 1.13 Model Compounds used in Percec's Study[115]

In 2003, Bicak and Ozlem[130] applied ATRP to graft PBA and poly(2-ethylhexyl acrylate) (P2EHA) from defect sites onto PVC (**Scheme 1.30**). The polymerizations were carried out in 1,2-dichlorobenzene. However, no T_g values were measured for these graft copolymers. The authors claimed that no homo-polymerization was observed, based on the following procedure. Following polymerization, the reaction mixture was precipitated in butanol because PBA is soluble in butanol and PVC is not. The butanol solution was then poured into MeOH. The authors stated that because there was no precipitate observed in methanol, no non-grafted PBA had formed. This is not very convincing because PBA is a viscous oil at room temperature, so one would not expect to see any precipitate to be formed in MeOH upon mixing with PBA dissolved in dilute butanol solution. In 2006, *Bicak et al* carried out ATRP of 2-ethylhexyl acrylate (2EHA) from defects sites on PVC in an aqueous suspension using 0.25% α-methylcellulose as a suspension stabilizer (**Scheme 1.31**).[118] Interestingly, these authors stated that there might be up to 4% of defect sites on PVC. A T_g value of 58 °C was obtained for one graft copolymer made of 2-ethylhexyl acrylate.

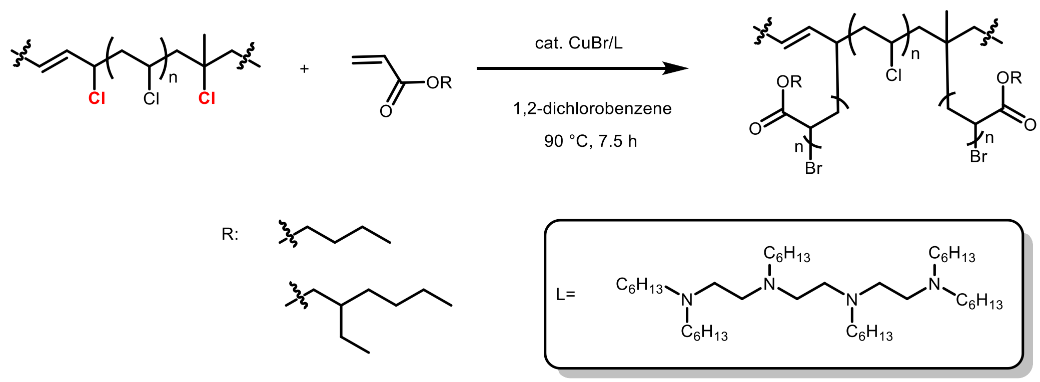

Scheme 1.30 Grafting of PBA and P2EHA from Defect Sites on PVC via ATRP[130]

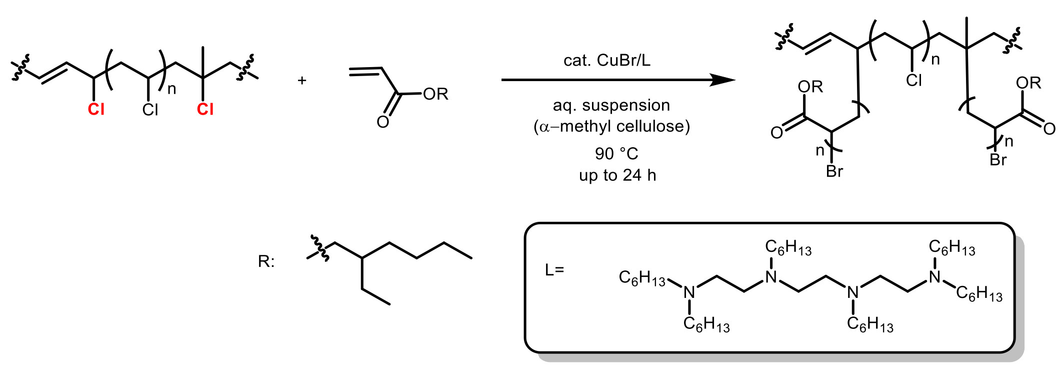

Scheme 1.31 Grafting of P2EHA from Defect Sites on PVC via ATRP in Aqueous Solution[118]

PVC-*g*-poly(oxyethylene methacrylate) (POEM) prepared by Hong in 2009, also using Cu catalyzed ATRP, gave material with two T_g values (-68 °C and 32 °C), which indicates micro-phase separation (**Scheme 1.32**).[120] All polymers discussed so far are homogeneous materials if not specified.

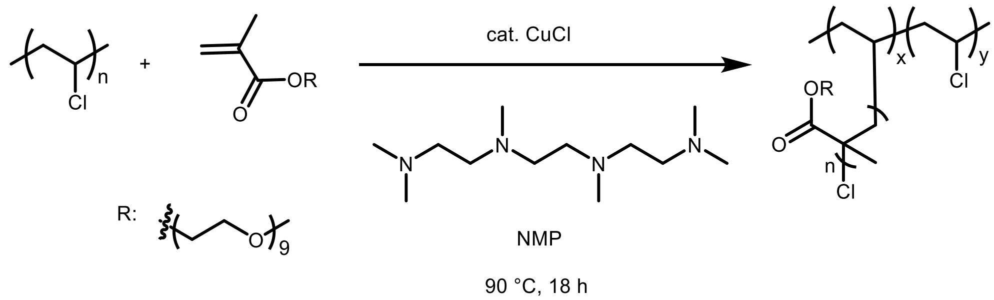

Scheme 1.32 Grafting of POEM from Defect Sites on PVC via ATRP[120]

1.7.3.3 Internal Plasticization via Other Polymerization Methods

PVC-*b*-PBA-*b*-PVC was prepared by Coelho *et al*.[131,132] in a two-step process utilizing single electron transfer – degenerative chain transfer living radical polymerization (SET-DTLRP). The first step makes the macroinitiator α,ω-di(iodo)poly(butyl acrylate) [α,ω-di(iodo)PBA][133] using $Na_2S_2O_4$ as an initiator via SET-DTLRP with iodoform and butyl acrylate (**Scheme 1.33**). In the second step, α,ω-di(iodo)PBA acts as a macroinitiator for vinyl chloride polymerization to form PVC-*b*-PBA-*b*-PVC via SET-DTLRP (**Scheme 1.34**). T_g values for these internally plasticized ABA triblock copolymers as low as -16 °C were obtained.[131]

In 2020, Coelho and Braslau *et al*.[134] prepared copolymers of VC and an acrylate bearing the pendant phthalate mimic DEHT. Specifically, poly(vinyl chloride)-*co*-poly(4,5-bis(2-ethylhexyl)-1-[6-prop-2-enoyloxy) hexyl]-1H-1,2,3-triazole-4,5-dicarboxylate) (PVC-*co*-P(DEHT-HA)) was prepared using conventional free radical polymerization. Optimization of polymerization conditions was investigated by applying different solvents, reaction temperatures, monomer ratios, and initiators. The optimized condition is shown in **Scheme 1.35**. T_g values as low as -27 °C were achieved with 74 wt% of P(DEHT-HA). The single T_g value indicates that PVC and P(DEHT-HA) are miscible. The monomer DEHT-HA, which is a mimic of DEHP, was synthesized in four steps.

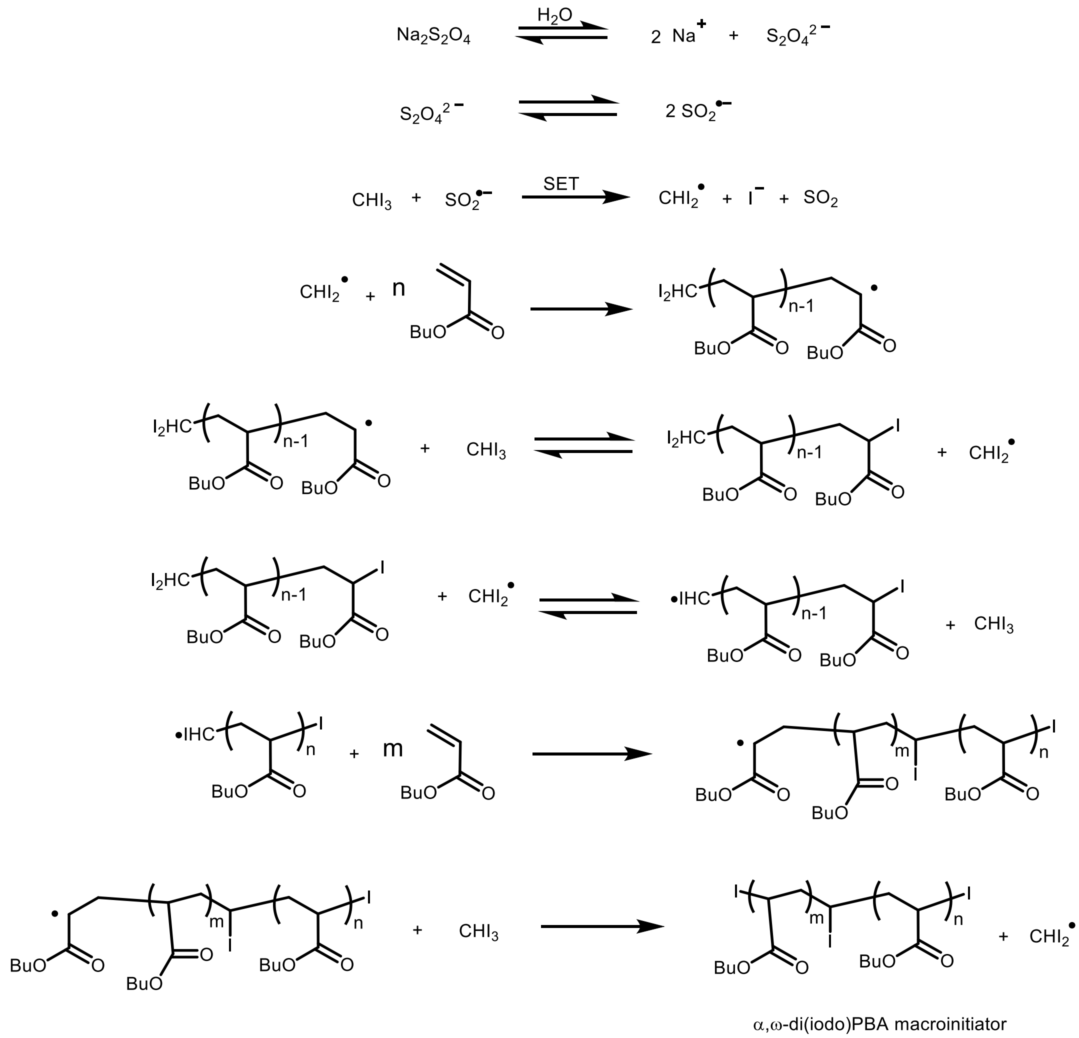

Scheme 1.33 Formation of Macroinitiator α,ω-di(iodo)PBA in SET-DTLRP [133]

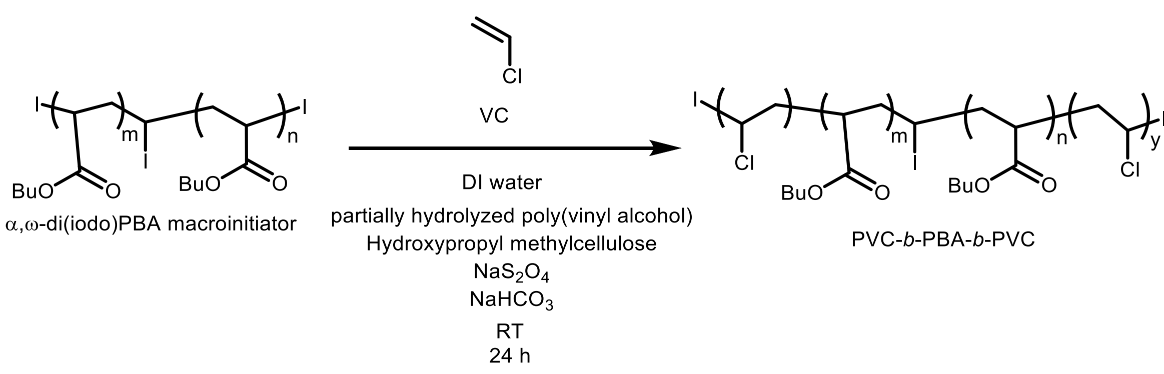

Scheme 1.34 Synthesis of internally plasticized PVC-*b*-PBA-*b*-PVC via SET-DTLRP[131]

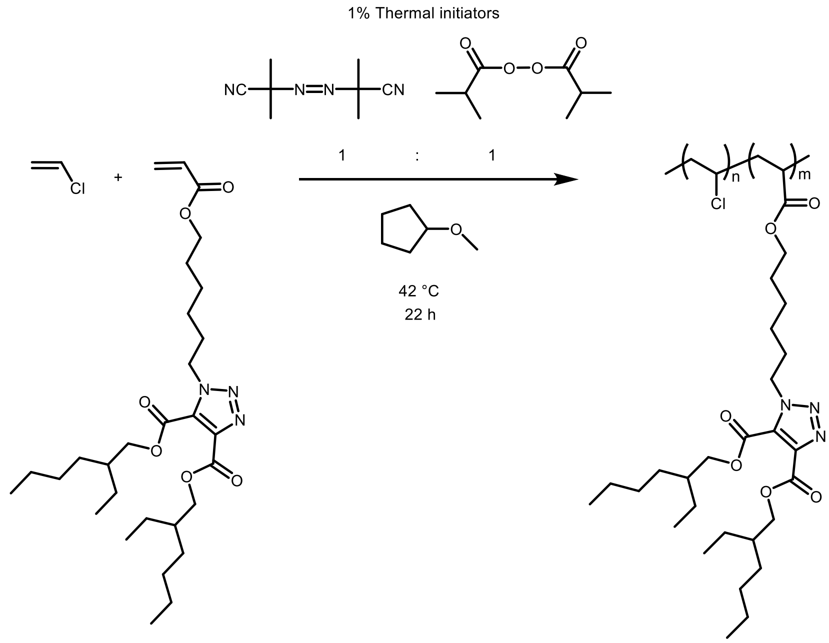

Scheme 1.35 Synthesis of internally plasticized PVC-*co*-P(DEHT-HA)[134]

Mood and Thang *et al.*[135] prepared an A-*b*-B block copolymer: PVC-*b*-PCL in a sequential polymerization process using reversible addition−fragmentation chain transfer polymerization (RAFT) followed by ring-opening polymerization (ROP) (**Scheme 1.36**). T_g values as low as -35 °C were achieved using 90 wt % of PCL.

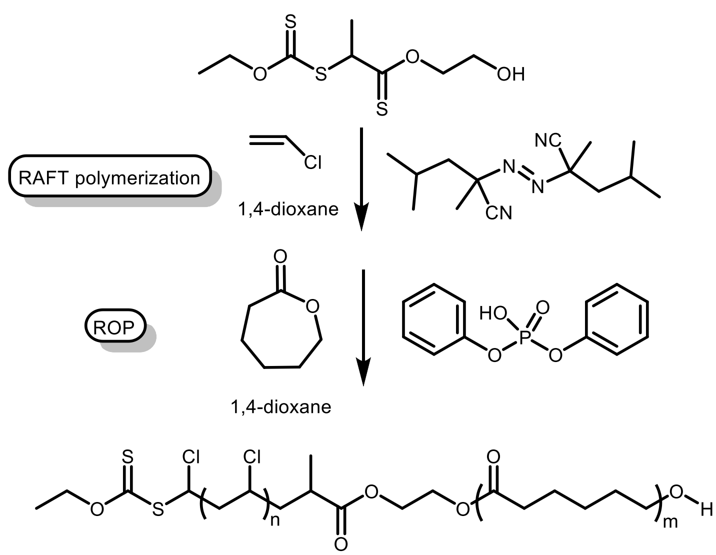

Scheme 1.36 Preparation Internally Plasticized PVC-*b*-PCL via RAFT Followed by ROP[135]

Although not technically an internal plasticizer, the Z.-M. Li[136] group synthesized flexible latex particles made of crosslinked, swollen PBA/PVC composites, and then grafted PBA through a multistage emulsion polymerization method. In stage one: PBA was synthesized by a seeded emulsion polymerization using a large amount of BA and small amount of 1,4-butylene glycol diacrylate (BDDA) as an insoluble crosslinker and $K_2S_2O_8$ as the initiator in water, to form a PBA crosslinked latex. In stage two: 3-(trimethoxysilyl) propyl methacrylate (MPS) was hydrolyzed to a diacrylate, triacrylate or tetraacrylate, a star-like crosslinker. MPS and allyl methacrylate (AMA) and vinyl chloride were used to grow a crosslinked PVC shell around the PBA particles to form a “PBA/PVC latex”. In stage three: the PBA/PVC latex was first soaked in BA to allow it to penetrate into the PBA/PVC colloidal particles. Unreacted AMA ends were the grafting sites. Emulsion polymerization at 75 °C was initiated by $K_2S_2O_8$, forming the final composite particles of PBA/PVC-*sg*-PBA. Small amounts of these compatibilized latex composites were then blended with commercial PVC and traditional phthalate DEHP. However, two T_g values were observed by DMA for all samples including the PVC/DEHP mix.

Moad and Thang[137] and co-workers have prepared a 3-armed star-[(PVC-*b*-PBA);(PBA)2] by sequential RAFT polymerization. One of the uses is as a macroplasticizer when mixed with PVC. No migration of the star macroplasticizer was observed when blended with PVC, and extracted with *n*-hexane.

1.8 Conclusion

PVC is one of the most popular thermoplastics, with applications ranging from packing materials, medical devices, toys to construction pipes. Plasticizers are used to provide durability, elasticity, and flexibility in PVC. However, small molecule plasticizers leach out from the PVC matrix over time, resulting in significant health problems for humans, as well as in damage to the environment. Covalent attachment of plasticizers to PVC chains, “internal plasticization,” is one of the most effective ways to avoid migration of plasticizers from PVC. Several different internal plasticization strategies are explored in this thesis.

1.9 References

(1) IHS Markit. Population Growth and Materials Demand Study Prepared for: American Chemistry Council Https://Plastics.Americanchemistry.Com/IHS-Economic-Growth-and-Materials-Demand-Executive-Summary.Pdf Accessed 04/24/2020.

(2) Polyvinyl Chloride (PVC) Properties, Production, Price, Market, and Uses Https://Www.Plasticsinsight.Com/Resin-Intelligence/Resin-Prices/Pvc/#production Accessed 04/25/2020.

(3) Baumann, E. Ueber Einige Vinylverbindungen. *Ann. Chem. Pharm.* **1872**, *163*, 308–322. https://doi.org/10.1002/jlac.18721630303

(4) Carroll, W. F.; Johnson, R. W.; Moore, S. S.; Paradis, R. A. 4 - Poly(Vinyl Chloride). In *Applied Plastics Engineering Handbook (Second Edition)*; Kutz, M., Ed.; William Andrew Publishing, 2017; pp 73–89. https://doi.org/10.1016/B978-0-323-39040-8.00004-3.

(5) Wypych, G. 2 - PVC MANUFACTURE TECHNOLOGY. In *PVC Degradation and Stabilization (Third Edition)*; Wypych, G., Ed.; ChemTec Publishing: Boston, 2015; pp 25–45. https://doi.org/10.1016/B978-1-895198-85-0.50004-2.

(6) Pepperl, G. Molecular Weight Distribution of Commercial PVC. *J. Vinyl Addit. Technol.* **2000**, *6* (2), 88–92. https://doi.org/10.1002/vnl.10229.

(7) Pepperl, G. Molecular Weight Distribution of Commercial Emulsion Grade PVC. *J. Vinyl Addit. Technol.* **2002**, *8* (3), 209–213. https://doi.org/10.1002/vnl.10364.

(8) Wypych, G. 1 - CHEMICAL STRUCTURE OF PVC. In *PVC Degradation and Stabilization (Third Edition)*; Wypych, G., Ed.; ChemTec Publishing: Boston, 2015; pp 1–23. https://doi.org/10.1016/B978-1-895198-85-0.50003-0.

(9) Waldo Semon Https://Ohiohistorycentral.Org/w/Waldo_Semon Accessed 04/25/2020.

(10) IHS Markit. Plasticizers Https://Ihsmarkit.Com/Products/Plasticizers-Chemical-Economics-Handbook.Html Accessed 04/26/2020.

(11) Chiellini, F.; Ferri, M.; Morelli, A.; Dipaola, L.; Latini, G. Perspectives on Alternatives to Phthalate Plasticized Poly(Vinyl Chloride) in Medical Devices Applications. *Prog. Polym. Sci.* **2013**, *38* (7), 1067–1088. https://doi.org/10.1016/j.progpolymsci.2013.03.001.

(12) Marcilla, A.; Beltrán, M. 5 – MECHANISMS OF PLASTICIZERS ACTION. In *Handbook of Plasticizers (Second Edition)*; Wypych, G., Ed.; William Andrew Publishing: Boston, 2012; pp 119–133. https://doi.org/10.1016/B978-1-895198-50-8.50007-2.

(13) Kirkpatrick, A. Some Relations Between Molecular Structure and Plasticizing Effect. *J. Appl. Phys.* **1940**, *11* (4), 255–261. https://doi.org/10.1063/1.1712768.

(14) Clark, F. W. Plasticizers. *Chemistry and Industry(London. U K)* **1941**, 228–230.

(15) Houwink, R. *Proc. XIth Int. Congr. Pure Appl. Chem. Lond. 17th-24th July 1947* **1947**.

(16) Moorshead T C. Advances in PVC Compounding and Processing; London, 1962; p Ch. 2.

(17) Fox, T. G.; Flory, P. J. Second-Order Transition Temperatures and Related Properties of Polystyrene. I. Influence of Molecular Weight. *J. Appl. Phys.* **1950**, *21* (6), 581–591. https://doi.org/10.1063/1.1699711.

(18) Ueberreiter, K.; Kanig, G. **1952**, *7*, 569.

(19) Williams, M. L.; Landel, R. F.; Ferry, J. D. The Temperature Dependence of Relaxation Mechanisms in Amorphous Polymers and Other Glass-Forming Liquids. *J. Am. Chem. Soc.* **1955**, *77* (14), 3701–3707. https://doi.org/10.1021/ja01619a008.

(20) Fox, T. G. Influence of Diluent and of Copolymer Composition on the Glass Temperature of a Polymer System. *Bull Am Phs Soc* **1956**, *1*, 123.

(21) Kelley, F. N.; Bueche, F. Viscosity and Glass Temperature Relations for Polymer-Diluent Systems. *J. Polym. Sci.* **1961**, *50* (154), 549–556. https://doi.org/10.1002/pol.1961.1205015421.

(22) Dimarzio, E. A.; Gibbs, J. H. Molecular Interpretation of Glass Temperature Depression by Plasticizers. *J. Polym. Sci. A* **1963**, *1* (4), 1417–1428. https://doi.org/10.1002/pol.1963.100010428.

(23) Zhang, X.; Li, Y.; Hankett, J. M.; Chen, Z. The Molecular Interfacial Structure and Plasticizer Migration Behavior of “Green” Plasticized Poly(Vinyl Chloride). *Phys. Chem. Chem. Phys.* **2015**, *17* (6), 4472–4482. https://doi.org/10.1039/C4CP05287K.

(24) Marcilla, A.; García, S.; García-Quesada, J. C. Study of the Migration of PVC Plasticizers. *J. Anal. Appl. Pyrolysis* **2004**, *71* (2), 457–463. https://doi.org/10.1016/S0165-2370(03)00131-1.

(25) Marcilla, A.; Garcia, S.; Garcia-Quesada, J. C. Migrability of PVC Plasticizers. *Polym. Test.* **2008**, *27* (2), 221–233. https://doi.org/10.1016/j.polymertesting.2007.10.007.

(26) Tüzüm Demir, A. P.; Ulutan, S. Migration of Phthalate and Non-Phthalate Plasticizers out of Plasticized PVC Films into Air. *J. Appl. Polym. Sci.* **2013**, *128* (3), 1948–1961. https://doi.org/10.1002/app.38291.

(27) Hakkarainen, M. Migration of Monomeric and Polymeric PVC Plasticizers. In *Chromatography for Sustainable Polymeric Materials: Renewable, Degradable and Recyclable*; Albertsson, A.-C., Hakkarainen, M., Eds.; Springer Berlin Heidelberg: Berlin, Heidelberg, 2008; pp 159–185. https://doi.org/10.1007/12_2008_140.

(28) Wang, Q.; Storm, B. K. Migration of Additives from Poly(Vinyl Chloride) (PVC) Tubes into Aqueous Media. *Macromol. Symp.* **2005**, *225* (1), 191–204. https://doi.org/10.1002/masy.200550715.

(29) Bui, T. T.; Giovanoulis, G.; Cousins, A. P.; Magnér, J.; Cousins, I. T.; de Wit, C. A. Human Exposure, Hazard and Risk of Alternative Plasticizers to Phthalate Esters. *Sci. Total Environ.* **2016**, *541* (Supplement C), 451–467. https://doi.org/10.1016/j.scitotenv.2015.09.036.

(30) Hwang, H.-M.; Park, E.-K.; Young, T. M.; Hammock, B. D. Occurrence of Endocrine-Disrupting Chemicals in Indoor Dust. *Sci. Total Environ.* **2008**, *404* (1), 26–35. https://doi.org/10.1016/j.scitotenv.2008.05.031.

(31) Wang, J.; Chen, G.; Christie, P.; Zhang, M.; Luo, Y.; Teng, Y. Occurrence and Risk Assessment of Phthalate Esters (PAEs) in Vegetables and Soils of Suburban Plastic Film Greenhouses. *Sci. Total Environ.* **2015**, *523* (Supplement C), 129–137. https://doi.org/10.1016/j.scitotenv.2015.02.101.

(32) Zhang, X.; Chen, Z. Observing Phthalate Leaching from Plasticized Polymer Films at the Molecular Level. *Langmuir* **2014**, *30* (17), 4933–4944. https://doi.org/10.1021/la500476u.

(33) Fierens, T.; Van Holderbeke, M.; Willems, H.; De Henauw, S.; Sioen, I. Transfer of Eight Phthalates through the Milk Chain — A Case Study. *Environ. Int.* **2013**, *51* (Supplement C), 1–7. https://doi.org/10.1016/j.envint.2012.10.002.

(34) Ji, L.; Liao, Q.; Wu, L.; Lv, W.; Yang, M.; Wan, L. Migration of 16 Phthalic Acid Esters from Plastic Drug Packaging to Drugs by GC-MS. *Anal. Methods* **2013**, *5* (11), 2827–2834. https://doi.org/10.1039/C3AY40234G.

(35) Fromme, H.; Gruber, L.; Seckin, E.; Raab, U.; Zimmermann, S.; Kiranoglu, M.; Schlummer, M.; Schwegler, U.; Smolic, S.; Völkel, W. Phthalates and Their Metabolites in Breast Milk — Results from the Bavarian Monitoring of Breast Milk (BAMBI). *Environ. Int.* **2011**, *37* (4), 715–722. https://doi.org/10.1016/j.envint.2011.02.008.

(36) Bernard, L.; Cueff, R.; Breysse, C.; Décaudin, B.; Sautou, V. Migrability of PVC Plasticizers from Medical Devices into a Simulant of Infused Solutions. *Int. J. Pharm.* **2015**, *485* (1), 341–347. https://doi.org/10.1016/j.ijpharm.2015.03.030.

(37) Net, S.; Delmont, A.; Sempéré, R.; Paluselli, A.; Ouddane, B. Reliable Quantification of Phthalates in Environmental Matrices (Air, Water, Sludge, Sediment and Soil): A Review. *Sci. Total Environ.* **2015**, *515–516*, 162–180. https://doi.org/10.1016/j.scitotenv.2015.02.013.

(38) Shapiro, G. D.; Dodds, L.; Arbuckle, T. E.; Ashley-Martin, J.; Fraser, W.; Fisher, M.; Taback, S.; Keely, E.; Bouchard, M. F.; Monnier, P.; Dallaire, R.; Morisset, AS.; Ettinger, A. S. Exposure to Phthalates, Bisphenol A and Metals in Pregnancy and the Association with Impaired Glucose Tolerance and Gestational Diabetes Mellitus: The MIREC Study. *Environ. Int.* **2015**, *83* (Supplement C), 63–71. https://doi.org/10.1016/j.envint.2015.05.016.

(39) Schaedlich, K.; Schmidt, J.-S.; Kwong, W. Y.; Sinclair, K. D.; Kurz, R.; Jahnke, H.-G.; Fischer, B. Impact of Di-Ethylhexylphthalate Exposure on Metabolic Programming in P19 ECC-Derived Cardiomyocytes. *J. Appl. Toxicol.* **2015**, *35* (7), 861–869. https://doi.org/10.1002/jat.3085.

(40) Golshan, M.; Hatef, A.; Socha, M.; Milla, S.; Butts, I. A. E.; Carnevali, O.; Rodina, M.; Sokołowska-Mikołajczyk, M.; Fontaine, P.; Linhart, O.; Alavi, S. M. H. Di-(2-Ethylhexyl)-Phthalate Disrupts Pituitary and Testicular Hormonal Functions to Reduce Sperm Quality in Mature Goldfish. *Aquat. Toxicol.* **2015**, *163* (Supplement C), 16–26. https://doi.org/10.1016/j.aquatox.2015.03.017.

(41) Liu, T.; Li, N.; Zhu, J.; Yu, G.; Guo, K.; Zhou, L.; Zheng, D.; Qu, X.; Huang, J.; Chen, X.; Wang, S.; Ye, L. Effects of Di-(2-Ethylhexyl) Phthalate on the Hypothalamus-Pituitary-Ovarian Axis in Adult Female Rats. *Reprod. Toxicol.* **2014**, *46* (Supplement C), 141–147. https://doi.org/10.1016/j.reprotox.2014.03.006.

(42) Weiss, B. Endocrine Disruptors as a Threat to Neurological Function. *J. Neurol. Sci.* **2011**, *305* (1), 11–21. https://doi.org/10.1016/j.jns.2011.03.014.

(43) North, M. L.; Takaro, T. K.; Diamond, M. L.; Ellis, A. K. Effects of Phthalates on the Development and Expression of Allergic Disease and Asthma. *Ann. Allergy. Asthma. Immunol.* **2014**, *112* (6), 496–502. https://doi.org/10.1016/j.anai.2014.03.013.

(44) Xu, Y.; Xiong, Y.; Guo, S. Issues Caused by Migration of Plasticizers from Flexible PVC and Its Countermeasures. *Prog. Chem.* **2015**, *27*, 286–296. https://doi.org/DOI: 10.7536/PC140826.

(45) Koch, H. M.; Preuss, R.; Angerer, J. Di(2-Ethylhexyl)Phthalate (DEHP): Human Metabolism and Internal Exposure – an Update and Latest Results1. *Int. J. Androl.* **2006**, *29* (1), 155–165. https://doi.org/10.1111/j.1365-2605.2005.00607.x.

(46) Rowdhwal, S. S. S.; Chen, J. Toxic Effects of Di-2-Ethylhexyl Phthalate: An Overview. *BioMed Res. Int.* **2018**, *2018*, 1750368. https://doi.org/10.1155/2018/1750368.

(47) Martinez-Arguelles, D. B.; Culty, M.; Zirkin, B. R.; Papadopoulos, V. In Utero Exposure to Di-(2-Ethylhexyl) Phthalate Decreases Mineralocorticoid Receptor Expression in the Adult Testis. *Endocrinology* **2009**, *150* (12), 5575–5585. https://doi.org/10.1210/en.2009-0847.

(48) Martinez-Arguelles, D. B.; Guichard, T.; Culty, M.; Zirkin, B. R.; Papadopoulos, V. In Utero Exposure to the Antiandrogen Di-(2-Ethylhexyl) Phthalate Decreases Adrenal Aldosterone Production in the Adult Rat1. *Biol. Reprod.* **2011**, *85* (1), 51–61. https://doi.org/10.1095/biolreprod.110.089920.

(49) Chen, X.; Xu, S.; Tan, T.; Lee, S. T.; Cheng, S. H.; Lee, F. W. F.; Xu, S. J. L.; Ho, K. C. Toxicity and Estrogenic Endocrine Disrupting Activity of Phthalates and Their Mixtures. *Int. J. Environ. Res. Public. Health* **2014**, *11* (3), 3156–3168.

(50) Jia, P.-P.; Ma, Y.-B.; Lu, C.-J.; Mirza, Z.; Zhang, W.; Jia, Y.-F.; Li, W.-G.; Pei, D.-S. The Effects of Disturbance on Hypothalamus-Pituitary-Thyroid (HPT) Axis in Zebrafish Larvae after Exposure to DEHP. *PLOS ONE* **2016**, *11* (5), e0155762. https://doi.org/10.1371/journal.pone.0155762.

(51) Zhai, W.; Huang, Z.; Chen, L.; Feng, C.; Li, B.; Li, T. Thyroid Endocrine Disruption in Zebrafish Larvae after Exposure to Mono-(2-Ethylhexyl) Phthalate (MEHP). *PLOS ONE* **2014**, *9* (3), e92465. https://doi.org/10.1371/journal.pone.0092465.

(52) Wang, H.; Zhou, Y.; Tang, C.; He, Y.; Wu, J.; Chen, Y.; Jiang, Q. Urinary Phthalate Metabolites Are Associated with Body Mass Index and Waist Circumference in Chinese School Children. *PLOS ONE* **2013**, *8* (2), e56800. https://doi.org/10.1371/journal.pone.0056800.

(53) Dalgaard, M.; Nellemann, C.; Lam, H. R.; Sørensen, I. K.; Ladefoged, O. The Acute Effects of Mono(2-Ethylhexyl)Phthalate (MEHP) on Testes of Prepubertal Wistar Rats. *Toxicol. Lett.* **2001**, *122* (1), 69–79. https://doi.org/10.1016/S0378-4274(01)00348-4.

(54) Swan, S. H.; Sathyanarayana, S.; Barrett, E. S.; Janssen, S.; Liu, F.; Nguyen, R. H. N.; Redmon, J. B.; the TIDES Study Team. First Trimester Phthalate Exposure and Anogenital Distance in Newborns. *Hum. Reprod.* **2015**, *30* (4), 963–972. https://doi.org/10.1093/humrep/deu363.

(55) Sathyanarayana, S.; Grady, R.; Barrett, E. S.; Redmon, B.; Nguyen, R. H. N.; Barthold, J. S.; Bush, N. R.; Swan, S. H. First Trimester Phthalate Exposure and Male Newborn Genital Anomalies. *Environ. Res.* **2016**, *151*, 777–782. https://doi.org/10.1016/j.envres.2016.07.043.

(56) Hannon, P. R.; Brannick, K. E.; Wang, W.; Flaws, J. A. Mono(2-Ethylhexyl) Phthalate Accelerates Early Folliculogenesis and Inhibits Steroidogenesis in Cultured Mouse Whole Ovaries and Antral Follicles1. *Biol. Reprod.* **2015**, *92* (120, 1–11). https://doi.org/10.1095/biolreprod.115.129148.

(57) Gupta, R. K.; Singh, J. M.; Leslie, T. C.; Meachum, S.; Flaws, J. A.; Yao, H. H.-C. Di-(2-Ethylhexyl) Phthalate and Mono-(2-Ethylhexyl) Phthalate Inhibit Growth and Reduce Estradiol Levels of Antral Follicles in Vitro. *Toxicol. Appl. Pharmacol.* **2010**, *242* (2), 224–230. https://doi.org/10.1016/j.taap.2009.10.011.

(58) David, R. M.; Moore, M. R.; Finney, D. C.; Guest, D. Chronic Toxicity of Di(2-Ethylhexyl)Phthalate in Mice. *Toxicol. Sci.* **2000**, *58* (2), 377–385. https://doi.org/10.1093/toxsci/58.2.377.

(59) David, R. M.; Moore, M. R.; Finney, D. C.; Guest, D. Chronic Toxicity of Di(2-Ethylhexyl)Phthalate in Rats. *Toxicol. Sci.* **2000**, *55* (2), 433–443. https://doi.org/10.1093/toxsci/55.2.433.

(60) Crocker, J. F. S.; Safe, S. H.; Acott, P. Effects of Chronic Phthalate Exposure on the Kidney. *J. Toxicol. Environ. Health* **1988**, *23* (4), 433–444. https://doi.org/10.1080/15287398809531126.

(61) Pugh, G., Jr.; Isenberg, J. S.; Kamendulis, L. M.; Ackley, D. C.; Clare, L. J.; Brown, R.; Lington, A. W.; Smith, J. H.; Klaunig, J. E. Effects of Di-Isononyl Phthalate, Di-2-Ethylhexyl Phthalate, and Clofibrate in Cynomolgus Monkeys. *Toxicol. Sci.* **2000**, *56* (1), 181–188. https://doi.org/10.1093/toxsci/56.1.181.

(62) Cobellis, L.; Latini, G.; Felice, C. D.; Razzi, S.; Paris, I.; Ruggieri, F.; Mazzeo, P.; Petraglia, F. High Plasma Concentrations of Di-(2-ethylhexyl)-phthalate in Women with Endometriosis. *Hum. Reprod.* **2003**, *18* (7), 1512–1515. https://doi.org/10.1093/humrep/deg254.

(63) Kim, S. H.; Chun, S.; Jang, J. Y.; Chae, H. D.; Kim, C.-H.; Kang, B. M. Increased Plasma Levels of Phthalate Esters in Women with Advanced-Stage Endometriosis: A Prospective Case-Control Study. *Fertil. Steril.* **2011**, *95* (1), 357–359. https://doi.org/10.1016/j.fertnstert.2010.07.1059.

(64) Kim, S. H.; Cho, S.; Ihm, H. J.; Oh, Y. S.; Heo, S.-H.; Chun, S.; Im, H.; Chae, H. D.; Kim, C.-H.; Kang, B. M. Possible Role of Phthalate in the Pathogenesis of Endometriosis: In

Vitro, Animal, and Human Data. *J. Clin. Endocrinol. Metab.* **2015**, *100* (12), E1502–E1511. https://doi.org/10.1210/jc.2015-2478.

(65) Reddy, B.; Rozati, R.; Reddy, B.; Raman, N. General Gynaecology: Association of Phthalate Esters with Endometriosis in Indian Women. *BJOG Int. J. Obstet. Gynaecol.* **2006**, *113* (5), 515–520. https://doi.org/10.1111/j.1471-0528.2006.00925.x.

(66) Ziska, J. J.; Barlow, J. W.; Paul, D. R. Miscibility in PVC-Polyester Blends. *Polymer* **1981**, *22* (7), 918–923. https://doi.org/10.1016/0032-3861(81)90268-8.

(67) Subotic, U.; Hannmann, T.; Kiss, M.; Brade, J.; Breitkopf, K.; Loff, S. Extraction of the Plasticizers Diethylhexylphthalate and Polyadipate From Polyvinylchloride Nasogastric Tubes Through Gastric Juice and Feeding Solution. *J. Pediatr. Gastroenterol. Nutr.* **2007**, *44* (1), 71-76. https://doi.org/10.1097/01.mpg.0000237939.50791.4b

(68) Penco, M.; Sartore, L.; Bignotti, F.; Rossini, M.; D'Amore, A.; Fassio, F. Binary Blends Based on Poly(Vinyl Chloride) and Multi-Block Copolymers Containing Poly(ϵ-Caprolactone) and Poly(Ethylene Glycol) Segments. *Macromol. Symp.* **2002**, *180* (1), 9–22. https://doi.org/10.1002/1521-3900(200203)180:1<9::AID-MASY9>3.0.CO;2-1.

(69) Choi, J.; Kwak, S.-Y. Hyperbranched Poly(ε-Caprolactone) as a Nonmigrating Alternative Plasticizer for Phthalates in Flexible PVC. *Environ. Sci. Technol.* **2007**, *41* (10), 3763–3768. https://doi.org/10.1021/es062715t.

(70) Oriol-Hemmerlin, C.; Pham, Q. T. Poly 1,3-Butylene Adipate Reoplex® as High Molecular Weight Plasticizer for PVC-Based Cling Films—Microstructure and Number-Average Molecular Weight Studied by 1H and 13C NMR. *Polymer* **2000**, *41* (12), 4401–4407. https://doi.org/10.1016/S0032-3861(99)00662-X.

(71) Rivera-Briso, L. A.; Serrano-Aroca, Á. Poly(3-Hydroxybutyrate-Co-3-Hydroxyvalerate): Enhancement Strategies for Advanced Applications. *Polymers* **2018**, *10* (7). https://doi.org/10.3390/polym10070732.

(72) Jia, P.; Bo, C.; Hu, L.; Zhang, M.; Zhou, Y. Synthesis of a Novel Polyester Plasticizer Based on Glyceryl Monooleate and Its Application in Poly(Vinyl Chloride). *J. Vinyl Addit. Technol.* **2016**, *22* (4), 514–519. https://doi.org/10.1002/vnl.21468.

(73) Jayakrishnan, A.; Sunny, M. C. Phase Transfer Catalysed Surface Modification of Plasticized Poly(Vinyl Chloride) in Aqueous Media to Retard Plasticizer Migration. *Polymer* **1996**, *37* (23), 5213–5218. https://doi.org/10.1016/0032-3861(96)00501-0.

(74) Lakshmi; Jayakrishnan. Migration Resistant, Blood-Compatible Plasticized Polyvinyl Chloride for [Medical and Related Applications. *Artif. Organs* **1998**, *22* (3), 222–229. https://doi.org/10.1046/j.1525-1594.1998.06124.x.

(75) Lakshmi, S.; Jayakrishnan, A. Synthesis, Surface Properties and Performance of Thiosulphate-Substituted Plasticized Poly(Vinyl Chloride). *Biomaterials* **2002**, *23* (24), 4855–4862. https://doi.org/10.1016/S0142-9612(02)00243-0.

(76) Lakshmi, S.; Jayakrishnan, A. Properties and Performance of Sulfide-Substituted Plasticized Poly(Vinyl Chloride) as a Biomaterial. *J. Biomed. Mater. Res. B Appl. Biomater.* **2003**, *65B* (1), 204–210. https://doi.org/10.1002/jbm.b.10562.

(77) Ito, R.; Seshimo, F.; Haishima, Y.; Hasegawa, C.; Isama, K.; Yagami, T.; Nakahashi, K.; Yamazaki, H.; Inoue, K.; Yoshimura, Y.; Saito, K.; Tsuchiya, T.; Nakazawa, H. Reducing the Migration of Di-2-Ethylhexyl Phthalate from Polyvinyl Chloride Medical Devices. *Int. J. Pharm.* **2005**, *303* (1), 104–112. https://doi.org/10.1016/j.ijpharm.2005.07.009.

(78) X. Q. Wen; X. H. Liu; G. S. Liu. Prevention of Plasticizer Leaching From the Inner Surface of Narrow Polyvinyl Chloride Tube by DC Glow Discharge Plasma. *IEEE Trans. Plasma Sci.* **2010**, *38* (11), 3152–3155. https://doi.org/10.1109/TPS.2010.2074209.

(79) Reddy, N. N.; Mohan, Y. M.; Varaprasad, K.; Ravindra, S.; Vimala, K.; Raju, K. M. Surface Treatment of Plasticized Poly(Vinyl Chloride) to Prevent Plasticizer Migration. *J. Appl. Polym. Sci.* **2010**, *115* (3), 1589–1597. https://doi.org/10.1002/app.31157.

(80) McGinty, K. M.; Brittain, W. J. Hydrophilic Surface Modification of Poly(Vinyl Chloride) Film and Tubing Using Physisorbed Free Radical Grafting Technique. *Polymer* **2008**, *49* (20), 4350–4357. https://doi.org/10.1016/j.polymer.2008.07.063.

(81) Zhao, B.; Brittain, W. Polymer Brushes: Surface-Immobilized Macromolecules. *Prog. Polym. Sci.* **2000**, *25*, 677–710. https://doi.org/10.1016/S0079-6700(00)00012-5.

(82) Breme, F.; Buttstaedt, J.; Emig, G. Coating of Polymers with Titanium-Based Layers by a Novel Plasma-Assisted Chemical Vapor Deposition Process. *Int. Conf. Metall. Coat. Thin Films* **2000**, *377–378*, 755–759. https://doi.org/10.1016/S0040-6090(00)01329-8.

(83) Messori, M.; Toselli, M.; Pilati, F.; Fabbri, E.; Fabbri, P.; Pasquali, L.; Nannarone, S. Prevention of Plasticizer Leaching from PVC Medical Devices by Using Organic–Inorganic Hybrid Coatings. *Polymer* **2004**, *45* (3), 805–813. https://doi.org/10.1016/j.polymer.2003.12.006.

(84) Mijangos, C.; Martinez, A.; Michel, A. Fonctionnalisation Du Polychlorure de Vinyle: Greffage de Fonctions Plastifiantes (Type Ester d'éthyle-Hexyle). *Eur. Polym. J.* **1986**, *22* (5), 417–421. https://doi.org/10.1016/0014-3057(86)90139-4.

(85) Higa, C. M.; Tek, A. T.; Wojtecki, R. J.; Braslau, R. Nonmigratory Internal Plasticization of Poly(Vinyl Chloride) via Pendant Triazoles Bearing Alkyl or Polyether Esters. *J. Polym. Sci. Part Polym. Chem.* **2018**, *56* (21), 2397–2411. https://doi.org/10.1002/pola.29205.

(86) Navarro, R.; Pérez Perrino, M.; Gómez Tardajos, M.; Reinecke, H. Phthalate Plasticizers Covalently Bound to PVC: Plasticization with Suppressed Migration. *Macromolecules* **2010**, *43* (5), 2377–2381. https://doi.org/10.1021/ma902740t.

(87) Navarro, R.; Perrino, P. M.; García, C.; Elvira, C.; Gallardo, A.; Reinecke, H. Opening New Gates for the Modification of PVC or Other PVC Derivatives: Synthetic Strategies for the Covalent Binding of Molecules to PVC. *Polymers* **2016**, *8* (4). https://doi.org/10.3390/polym8040152.

(88) Navarro, R.; Pérez Perrino, M.; García, C.; Elvira, C.; Gallardo, A.; Reinecke, H. Highly Flexible PVC Materials without Plasticizer Migration As Obtained by Efficient One-Pot Procedure Using Trichlorotriazine Chemistry. *Macromolecules* **2016**, *49* (6), 2224–2227. https://doi.org/10.1021/acs.macromol.6b00214.

(89) Navarro, R.; Gacal, T.; Ocakoglu, M.; García, C.; Elvira, C.; Gallardo, A.; Reinecke, H. Nonmigrating Equivalent Substitutes for PVC/DOP Formulations as Shown by a TG

Study of PVC with Covalently Bound PEO–PPO Oligomers. *Macromol. Rapid Commun.* **2017**, *38* (6), 1600734-n/a. https://doi.org/10.1002/marc.201600734.

(90) Jia, P.; Ma, Y.; Kong, Q.; Xu, L.; Hu, Y.; Hu, L.; Zhou, Y. Graft Modification of Polyvinyl Chloride with Epoxidized Biomass-Based Monomers for Preparing Flexible Polyvinyl Chloride Materials without Plasticizer Migration. *Mater. Today Chem.* **2019**, *13*, 49–58. https://doi.org/10.1016/j.mtchem.2019.04.010.

(91) BARNARD, D.; BATEMAN, L.; CUNNEEN, J. I. CHAPTER 21 - OXIDATION OF ORGANIC SULFIDES A2 - KHARASCH, N. In *Organic Sulfur Compounds*; Pergamon, 1961; pp 229–247. https://doi.org/10.1016/B978-1-4831-9982-5.50024-5.

(92) Jia, P.; Hu, L.; Yang, X.; Zhang, M.; Shang, Q.; Zhou, Y. Internally Plasticized PVC Materials via Covalent Attachment of Aminated Tung Oil Methyl Ester. *RSC Adv.* **2017**, *7* (48), 30101–30108. https://doi.org/10.1039/C7RA04386D.

(93) Jia, P.; Hu, L.; Shang, Q.; Wang, R.; Zhang, M.; Zhou, Y. Self-Plasticization of PVC Materials via Chemical Modification of Mannich Base of Cardanol Butyl Ether. *ACS Sustain. Chem. Eng.* **2017**, *5* (8), 6665–6673. https://doi.org/10.1021/acssuschemeng.7b00900.

(94) Michael, A. Ueber Die Einwirkung von Diazobenzolimid Auf Acetylendicarbonsäuremethylester. *J. Für Prakt. Chem.* **1893**, *48* (1), 94–95. https://doi.org/10.1002/prac.18930480114.

(95) Huisgen, R.; Grashey, R.; Sauer, J. *Chemistry of Alkenes, Interscience*; New York. **1964**.

(96) Ess, D. H.; Houk, K. N. Theory of 1,3-Dipolar Cycloadditions: Distortion/Interaction and Frontier Molecular Orbital Models. *J. Am. Chem. Soc.* **2008**, *130* (31), 10187–10198. https://doi.org/10.1021/ja800009z.

(97) Pascoal, M.; Brook, M. A.; Gonzaga, F.; Zepeda-Velazquez, L. Thermally Controlled Silicone Functionalization Using Selective Huisgen Reactions. *Eur. Polym. J.* **2015**, *69* (Supplement C), 429–437. https://doi.org/10.1016/j.eurpolymj.2015.06.026.

(98) Skelly, P. W.; Sae-Jew, J.; Kitos Vasconcelos, A. P.; Tasnim, J.; Li, L.; Raskatov, J. A.; Braslau, R. Relative Rates of Metal-Free Azide–Alkyne Cycloadditions: Tunability over 3 Orders of Magnitude. *J. Org. Chem.* **2019**, *84* (21), 13615–13623. https://doi.org/10.1021/acs.joc.9b01887.

(99) Earla, A.; Braslau, R. Covalently Linked Plasticizers: Triazole Analogues of Phthalate Plasticizers Prepared by Mild Copper-Free “Click” Reactions with Azide-Functionalized PVC. *Macromol. Rapid Commun*. **2014**, *35* (6), 666–671. https://doi.org/10.1002/marc.201300865.

(100) Earla, A.; Li, L.; Costanzo, P.; Braslau, R. Phthalate Plasticizers Covalently Linked to PVC via Copper-Free or Copper Catalyzed Azide-Alkyne Cycloadditions. *Polymer* **2017**, *109* (Supplement C), 1–12. https://doi.org/10.1016/j.polymer.2016.12.014.

(101) Yang, P.; Yan, J.; Sun, H.; Fan, H.; Chen, Y.; Wang, F.; Shi, B. Novel Environmentally Sustainable Cardanol-Based Plasticizer Covalently Bound to PVC via Click Chemistry: Synthesis and Properties. *RSC Adv.* **2015**, *5* (22), 16980–16985. https://doi.org/10.1039/C4RA15527K.

(102) Rostovtsev, V. V.; Green, L. G.; Fokin, V. V.; Sharpless, K. B. A Stepwise Huisgen Cycloaddition Process: Copper(I)-Catalyzed Regioselective “Ligation” of Azides and Terminal Alkynes. *Angew. Chem. Int. Ed.* **2002**, *41* (14), 2596–2599. https://doi.org/10.1002/1521-3773(20020715)41:14<2596::AID-ANIE2596>3.0.CO;2-4.

(103) Hein, J. E.; Fokin, V. V. Copper-Catalyzed Azide–Alkyne Cycloaddition (CuAAC) and beyond: New Reactivity of Copper(i) Acetylides. *Chem. Soc. Rev.* **2010**, *39* (4), 1302–1315. https://doi.org/10.1039/B904091A.

(104) Tornøe, C. W.; Christensen, C.; Meldal, M. Peptidotriazoles on Solid Phase: [1,2,3]-Triazoles by Regiospecific Copper(I)-Catalyzed 1,3-Dipolar Cycloadditions of Terminal Alkynes to Azides. *J. Org. Chem.* **2002**, *67* (9), 3057–3064. https://doi.org/10.1021/jo011148j.

(105) Demirci, G.; Tasdelen, M. A. Synthesis and Characterization of Graft Copolymers by Photoinduced CuAAC Click Chemistry. *Eur. Polym. J.* **2015**, *66* (Supplement C), 282–289. https://doi.org/10.1016/j.eurpolymj.2015.02.029.

(106) Lee, K. W.; Chung, J. W.; Kwak, S.-Y. Structurally Enhanced Self-Plasticization of Poly(Vinyl Chloride) via Click Grafting of Hyperbranched Polyglycerol. *Macromol. Rapid Commun.* **2016**, *37* (24), 2045–2051. https://doi.org/10.1002/marc.201600533.

(107) Jia, P.; Hu, L.; Feng, G.; Bo, C.; Zhang, M.; Zhou, Y. PVC Materials without Migration Obtained by Chemical Modification of Azide-Functionalized PVC and Triethyl Citrate Plasticizer. *Mater. Chem. Phys.* **2017**, *190*, 25–30. https://doi.org/10.1016/j.matchemphys.2016.12.072.

(108) Puyou Jia; Rui Wang; Lihong Hu; Meng Zhang; Yonghong Zhou. Self-Plasticization of PVC via Click Reaction of a Monooctyl Phthalate Derivative. *Pol. J. Chem. Technol.* **2017**, *19* (3), 16–19. https://doi.org/10.1515/pjct-2017-0042.

(109) Chu, H.; Ma, J. A Strategy to Prepare Internally Plasticized PVC Using a Castor Oil Based Derivative. *Korean J. Chem. Eng.* **2018**, *35* (11), 2296–2302. https://doi.org/10.1007/s11814-018-0118-5.

(110) Jia, P.; Ma, Y.; Feng, G.; Hu, L.; Zhou, Y. High-Value Utilization of Forest Resources: Dehydroabietic Acid as a Chemical Platform for Producing Non-Toxic and Environment-Friendly Polymer Materials. *J. Clean. Prod.* **2019**, *227*, 662–674. https://doi.org/10.1016/j.jclepro.2019.04.220.

(111) Matyjaszewski, K.; Xia, J. Atom Transfer Radical Polymerization. *Chem. Rev.* **2001**, *101* (9), 2921–2990. https://doi.org/10.1021/cr940534g.

(111) Matyjaszewski, K. Atom Transfer Radical Polymerization (ATRP): Current Status and Future Perspectives. *Macromolecules* **2012**, *45* (10), 4015–4039. https://doi.org/10.1021/ma3001719.

(113) Matyjaszewski, K.; Tsarevsky, N. V. Macromolecular Engineering by Atom Transfer Radical Polymerization. *J. Am. Chem. Soc.* **2014**, *136* (18), 6513–6533. https://doi.org/10.1021/ja408069v.

(112) Paik, H.; Gaynor, S. G.; Matyjaszewski, K. Synthesis and Characterization of Graft Copolymers of Poly(Vinyl Chloride) with Styrene and (Meth)Acrylates by Atom Transfer Radical Polymerization. *Macromol. Rapid Commun.* **1998**, *19* (1), 47–52. https://doi.org/10.1002/(SICI)1521-3927(19980101)19:1<47::AID-MARC47>3.0.CO;2-Q.

(115) Percec, V.; Asgarzadeh, F. Metal-Catalyzed Living Radical Graft Copolymerization of Olefins Initiated from the Structural Defects of Poly(Vinyl Chloride). *J. Polym. Sci. Part Polym. Chem.* **2001**, *39* (7), 1120–1135. https://doi.org/10.1002/1099-0518(20010401)39:7<1120::AID-POLA1089>3.0.CO;2-Z.

(113) Percec, V.; Cappotto, A.; Barboiu, B. Metal-Catalyzed Living Radical Graft Copolymerization of Butyl Methacrylate and Styrene Initiated from the Structural Defects of Narrow Molecular Weight Distribution Poly(Vinyl Chloride). *Macromol. Chem. Phys.* **2002**, *203* (10-11), 1674–1683. https://doi.org/10.1002/1521-3935(200207)203:10/11<1674::AID-MACP1674>3.0.CO;2-N.

(117) Bicak, N.; Ozlem, M. Graft Copolymerization of Butyl Acrylate and 2-Ethyl Hexyl Acrylate from Labile Chlorines of Poly(Vinyl Chloride) by Atom Transfer Radical Polymerization. *J. Polym. Sci. Part Polym. Chem.* **2003**, *41* (21), 3457–3462. https://doi.org/10.1002/pola.10944.

(114) Bicak, N.; Karagoz, B.; Emre, D. Atom Transfer Graft Copolymerization of 2-Ethyl Hexylacrylate from Labile Chlorines of Poly(Vinyl Chloride) in an Aqueous Suspension. *J. Polym. Sci. Part Polym. Chem.* **2006**, *44* (6), 1900–1907. https://doi.org/10.1002/pola.21298.

(119) Coşkun, M.; Barim, G.; Demirelli, K. A Grafting Study on Partially Dehydrochlorinated Poly(Vinyl Chloride) by Atom Transfer Radical Polymerization. *J. Macromol. Sci. Part A* **2007**, *44* (5), 475–481. https://doi.org/10.1080/10601320701229068.

(115) Ahn, S. H.; Seo, J. A.; Kim, J. H.; Ko, Y.; Hong, S. U. Synthesis and Gas Permeation Properties of Amphiphilic Graft Copolymer Membranes. *J. Membr. Sci.* **2009**, *345* (1), 128–133. https://doi.org/10.1016/j.memsci.2009.08.037.

(121) Patel, R.; Patel, M.; Ahn, S. H.; Sung, Y. K.; Lee, H.-K.; Kim, J. H.; Sung, J.-S. Bioinert Membranes Prepared from Amphiphilic Poly(Vinyl Chloride)-g-Poly(Oxyethylene Methacrylate) Graft Copolymers. *Mater. Sci. Eng. C* **2013**, *33* (3), 1662–1670. https://doi.org/10.1016/j.msec.2012.12.097.

(122) Fang, L.-F.; Matsuyama, H.; Zhu, B.-K.; Zhao, S. Development of Antifouling Poly(Vinyl Chloride) Blend Membranes by Atom Transfer Radical Polymerization. *J. Appl. Polym. Sci.* **2018**, *135* (6), 45832. https://doi.org/10.1002/app.45832.

(123) Lanzalaco, S.; Galia, A.; Lazzano, F.; Mauro, R. R.; Scialdone, O. Utilization of Poly(Vinylchloride) and Poly(Vinylidenefluoride) as Macroinitiators for ATRP Polymerization of Hydroxyethyl Methacrylate: Electroanalytical and Graft-Copolymerization Studies. *J. Polym. Sci. Part Polym. Chem.* **2015**, *53* (21), 2524–2536. https://doi.org/10.1002/pola.27717.

(124) Huang, Z.; Feng, C.; Guo, H.; Huang, X. Direct Functionalization of Poly(Vinyl Chloride) by Photo-Mediated ATRP without a Deoxygenation Procedure. *Polym. Chem.* **2016**, *7* (17), 3034–3045. https://doi.org/10.1039/C6PY00483K.

(125) Liu, K.; Pan, P.; Bao, Y. Synthesis, Micellization, and Thermally-Induced Macroscopic Micelle Aggregation of Poly(Vinyl Chloride)-g-Poly(N-Isopropylacrylamide) Amphiphilic Copolymer. *RSC Adv.* **2015**, *5* (115), 94582–94590. https://doi.org/10.1039/C5RA16726D.

(126) Aubrey D. Jenkins; Richard G. Jones; Graeme Moad. Terminology for Reversible-Deactivation Radical Polymerization Previously Called “Controlled” Radical or “Living” Radical Polymerization (IUPAC Recommendations 2010). *Pure Appl. Chem.* **2009**, *82* (2), 483–491. https://doi.org/10.1351/PAC-REP-08-04-03.

(127) Matyjaszewski, K. The Importance of Exchange Reactions in Controlled/Living Radical Polymerization in the Presence of Alkoxyamines and Transition Metals. *Macromol. Symp.* **1996**, *111* (1), 47–61. https://doi.org/10.1002/masy.19961110107.

(128) Van Cauter, K.; Van Den Bossche, B. J.; Van Speybroeck, V.; Waroquier, M. Ab Initio Study of Free-Radical Polymerization: Defect Structures in Poly(Vinyl Chloride). *Macromolecules* **2007**, *40* (4), 1321–1331. https://doi.org/10.1021/ma062174s.

(129) Rogestedt, M.; Hjertberg, T. Structure and Degradation of Commercial Poly(Vinyl Chloride) Obtained at Different Temperatures. *Macromolecules* **1993**, *26* (1), 60–64. https://doi.org/10.1021/ma00053a009.

(130) Bicak, N.; Ozlem, M. Graft Copolymerization of Butyl Acrylate and 2-Ethyl Hexyl Acrylate from Labile Chlorines of Poly(Vinyl Chloride) by Atom Transfer Radical Polymerization. *J. Polym. Sci. Part Polym. Chem.* **2003**, *41* (21), 3457–3462. https://doi.org/10.1002/pola.10944.

(131) Coelho, J. F. J.; Carreira, M.; Popov, A. V.; Gonçalves, P. M. O. F.; Gil, M. H. Thermal and Mechanical Characterization of Poly(Vinyl Chloride)-b-Poly(Butyl Acrylate)-b-Poly(Vinyl Chloride) Obtained by Single Electron Transfer – Degenerative Chain Transfer Living Radical Polymerization in Water. *Eur. Polym. J.* **2006**, *42* (10), 2313–2319. https://doi.org/10.1016/j.eurpolymj.2006.05.023.

(132) Coelho, J. F. J.; Carreira, M.; Gonçalves, P. M. O. F.; Popov, A. V.; Gil, M. H. Processability and Characterization of Poly(Vinyl Chloride)-b-Poly(n-Butyl Acrylate)-b-Poly(Vinyl Chloride) Prepared by Living Radical Polymerization of Vinyl Chloride. Comparison with a Flexible Commercial Resin Formulation Prepared with PVC and Dioctyl Phthalate. *J. Vinyl Addit. Technol.* **2006**, *12* (4), 156–165. https://doi.org/10.1002/vnl.20088.

(133) Coelho, J. F. J.; Silva, A. M. F. P.; Popov, A. V.; Percec, V.; Abreu, M. V.; Gonçalves, P. M. O. F.; Gil, M. H. Single Electron Transfer–Degenerative Chain Transfer Living Radical Polymerization of N-Butyl Acrylate Catalyzed by $Na_2S_2O_4$ in Water Media. *J. Polym. Sci. Part Polym. Chem.* **2006**, *44* (9), 2809–2825. https://doi.org/10.1002/pola.21389.

(134) Rezende, T. C.; Abreu, C. M. R.; Fonseca, A. C.; Higa, C. M.; Li, L.; Serra, A. C.; Braslau, R.; Coelho, J. F. J. Efficient Internal Plasticization of Poly(Vinyl Chloride) via Free Radical Copolymerization of Vinyl Chloride with an Acrylate Bearing a Triazole Phthalate Mimic. *Polymer* **2020**, *196*, 122473. https://doi.org/10.1016/j.polymer.2020.122473.

(135) Sun, Z.; Choi, B.; Feng, A.; Moad, G.; Thang, S. H. Nonmigratory Poly(Vinyl Chloride)-Block-Polycaprolactone Plasticizers and Compatibilizers Prepared by Sequential RAFT and Ring-Opening Polymerization (RAFT-T-ROP). *Macromolecules* **2019**, *52* (4), 1746–1756. https://doi.org/10.1021/acs.macromol.8b02146.

(136) Chang, Y.; Pan, M.; Yuan, J.; Liu, Y.; Wang, X.; Jiang, P.; Wang, Y.; Zhong, G.-J.; Li, Z.-M. Morphology and Film Performance of Phthalate-Free Plasticized Poly(Vinyl Chloride) Composite Particles via the Graft Copolymerization of Acrylate Swelling Flower-like Latex Particles. *RSC Adv.* **2015**, *5* (50), 40076–40087. https://doi.org/10.1039/C5RA04747A.

(137) Sun, Z.; Wang, M.; Li, Z.; Choi, B.; Mulder, R. J.; Feng, A.; Moad, G.; Thang, S. H. Versatile Approach for Preparing PVC-Based Mikto-Arm Star Additives Based on RAFT Polymerization. *Macromolecules* **2020**. https://doi.org/10.1021/acs.macromol.0c00125.

2 Internal Plasticization of Poly(vinyl) Chloride using Glutamic Acid as a Branched Linker to Incorporate Four Plasticizers per Anchor Point

2.1 Background

Covalent attachment of plasticizers to PVC chains, internal plasticization, is an effective way to avoid migration of plasticizers from PVC. Previous work in the Braslau laboratory on preparing plasticizers covalently linked to PVC has utilized efficient metal-free Huisgen thermal azide-alkyne dipolar cycloadditions (TAAC).[1–3] Post-polymerization functionalization involving azide displacement of chlorine atoms on PVC via a facile S_N2 reaction occurs with no detectable competitive elimination. Reaction of the pendant azides with electron-poor alkynes under mild heat gives substituted triazoles. With the goal of increasing the number of internal plasticizing moieties per azide group, the use of electron-poor alkynes bearing branched linkers displaying multiple plasticizing species was explored (**Figure 2.1**). This work has been published: Li, L.; Tek, A. T.; Wojtecki, R. J.; Braslau, R. *J. Polym. Sci. Part A; Polym. Chem.* **2019**, *57*, 1821–1835.

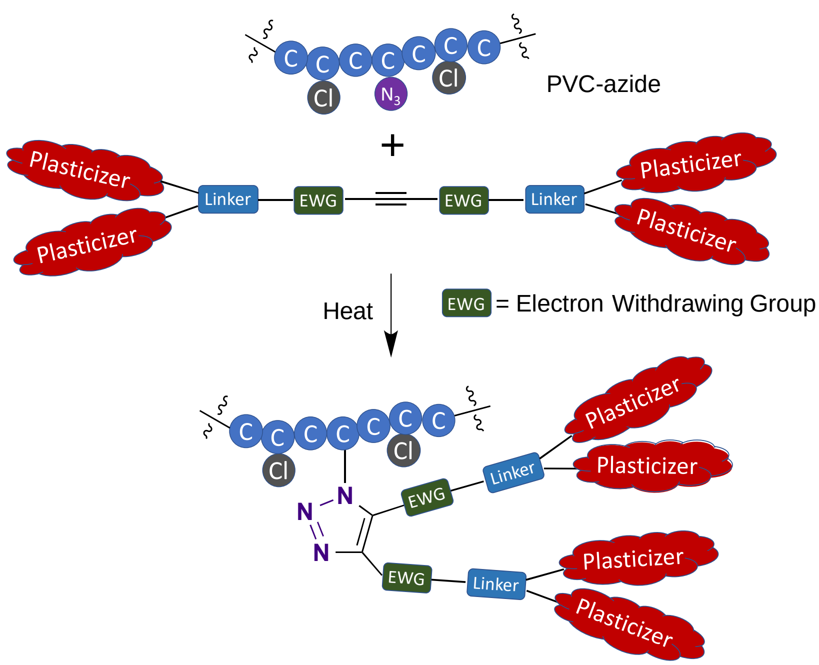

Figure 2.1 Overview: Cycloaddition of a Disubstituted Alkyne Bearing Branched Linkers Introduces Four Plasticizers Per Azide on PVC

Glutamic acid was selected as the branched linker, as it is inexpensive, and can be incorporated in only two synthetic steps (esterification and amidification) to form the requisite electron-poor alkyne (**Scheme 2.1**). The use of L-glutamic acid, as opposed to racemic material, was selected solely due to its natural abundance, and thus the low cost of the L-enantiomer.

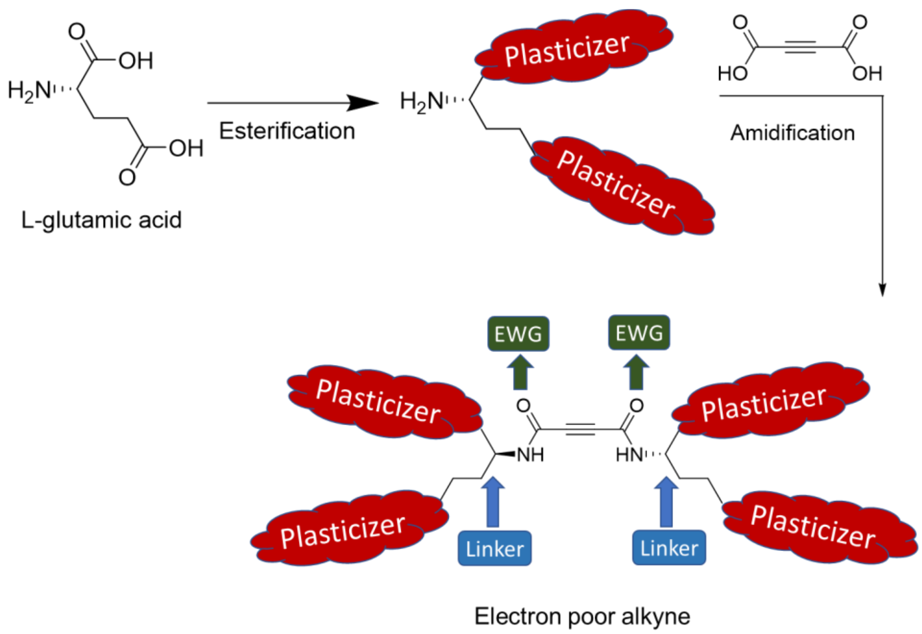

Scheme 2.1 Use of Glutamic Acid as a Branched Linker for Making an Electron-Poor Alkyne Bearing Four Plasticizing Species

2.2 Synthesis of an Electron-Poor Alkyne Bearing Branched Linkers Displaying Four Plasticizing Species

The first example of an electron-poor alkyne, **2.2a,** bearing four *n*-butyl esters, was prepared in two steps (**Scheme 2.2**). Glutamate ester **2.1a** was synthesized by reaction of L-glutamic acid with *n*-butanol via Fischer esterification.[4] Esterification and amidification of acetylenedicarboxylic acid can be particularly difficult, due to competing Michael addition, especially when employing traditional coupling agents. For example, use of the conventional coupling reagent dicyclohexylcarbodiimide (DCC) results only in an undesired intramolecular Michael addition to form the 1,3,5-trisubstituted hydantoin (**Scheme 2.3**).[5,6] Heyl and Fessner developed the coupling reagent DMTMM (4-(4,6-dimethoxy-1,3,5-triazin-2-yl)-4-methylmorpholinium chloride), which allows direct amidification of acetylenedicarboxylic acid with amines.[7] DMTMM in *N*-methyl-2-pyrrolidone (NMP) as solvent provides the acetylenediamide **2.2a** with amine **2.1a** in 82% yield. The disadvantage of this route is that a full equivalent of DMTMM is needed for each amide bond formation.

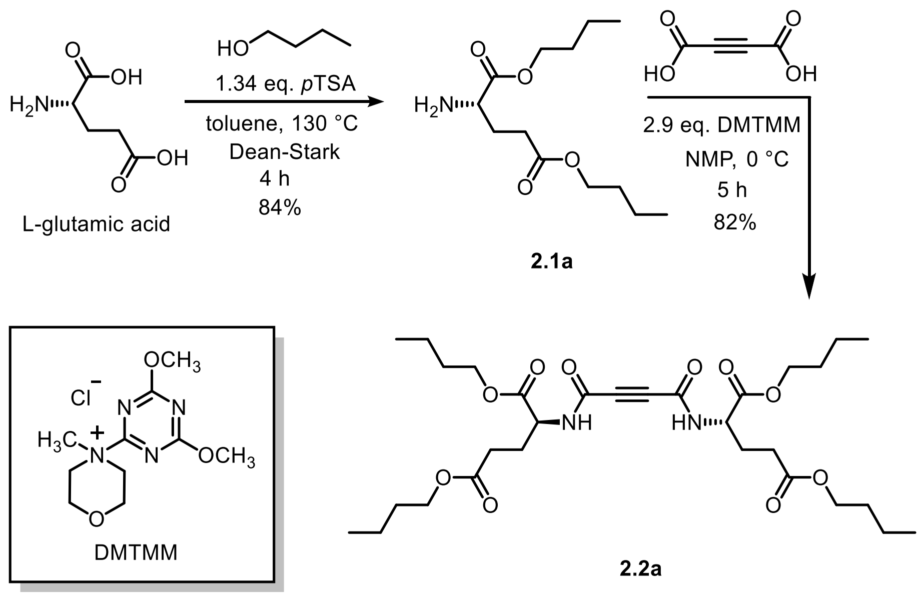

Scheme 2.2 Synthesis of Acetylenediamide Tetraester **2.2a** Based on Glutamic Acid as a Branched Linker.

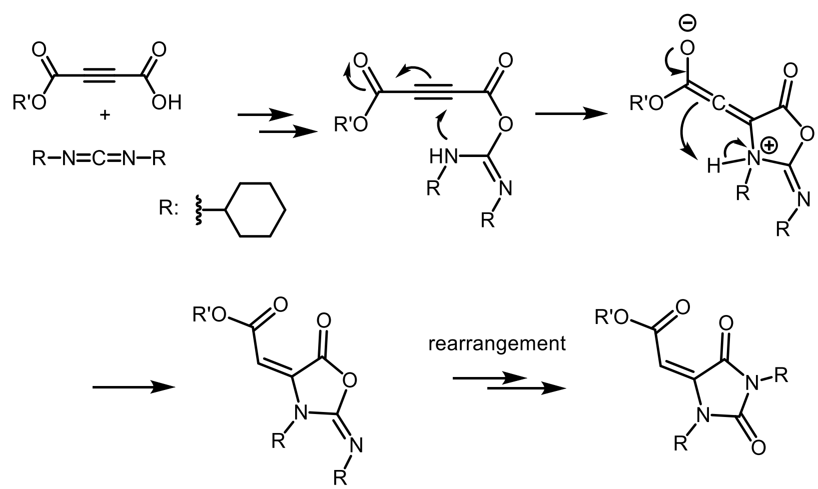

Scheme 2.3 Undesired Intramolecular Michael Addition when Trying to activate the carboxylic acid with DCC

2.3 Model Reaction

A model reaction was carried out prior to applying the cycloaddition to azidized PVC. There were two reasons for conducting this small molecule model reaction: 1) test the thermal reactivity of the alkyne diamide **2.2a** with an organoazide for which the reaction could be monitored by NMR; 2) the structural information of the model triazole product could be determined by HRMS, IR, and NMR, which would help identify the structural information of functionalized PVC triazole samples with the same structure motif. Therefore, a small organoazide molecule, benzylic azide **2.3** was synthesized from 1-bromomethyl-4-*tert*-butylbenzene using Amberlite IRA-400 ion-exchange resin pre-charged with aqueous NaN_3.[8] Reaction of alkyne **2.2a** with the model azide **2.3** gave triazole **2.4** as a well-defined molecule following chromatographic purification in 74% yield (**Scheme 2.4**).

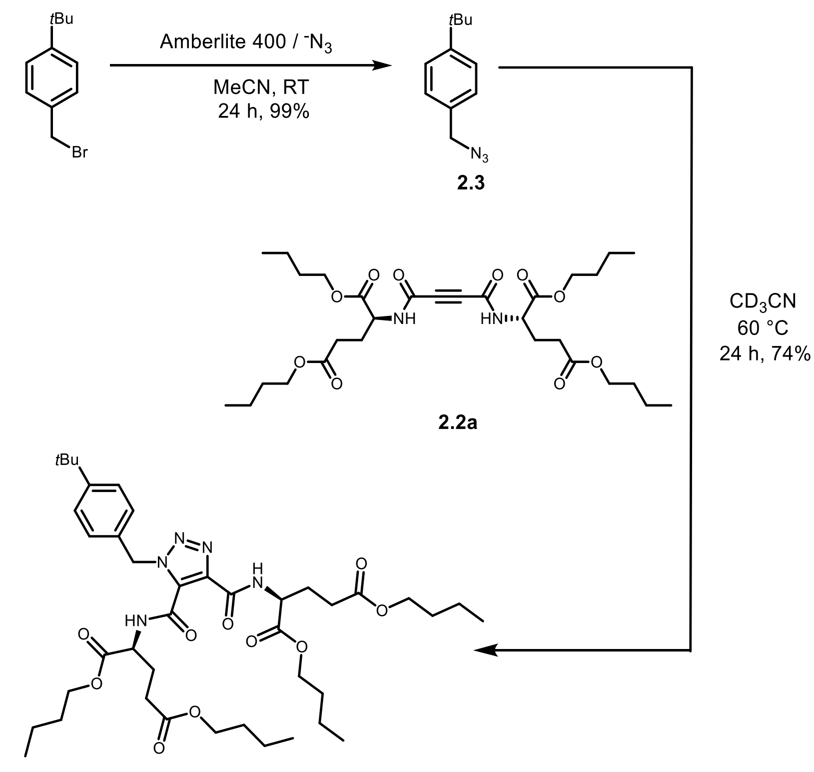

Scheme 2.4 Model Reaction: Cycloaddition of Small Molecule Azide with Acetylenediamide Tetraester **2.2a**

2.4 Characterization of Small Model 2.4

The stuctural information for compound **2.4** was confirmed by HRMS, IR, ^{1}H NMR, ^{13}C NMR, DEPT, and NOESY. IR was used to confirm the functional groups of triazole tetraester **2.4**. In the IR spectrum (**Figure 2.2**), the broad amide N-H stretch is found near 3350 cm^{-1}. The ester C=O stretch is seen at 1739 cm^{-1} for model triazole **2.4**. The amide C=O stretch and N-H bend are observed at 1678 cm^{-1} (C=O stretching, amide I band) and at 1552 cm^{-1} (NH bending, amide II band), respectively.

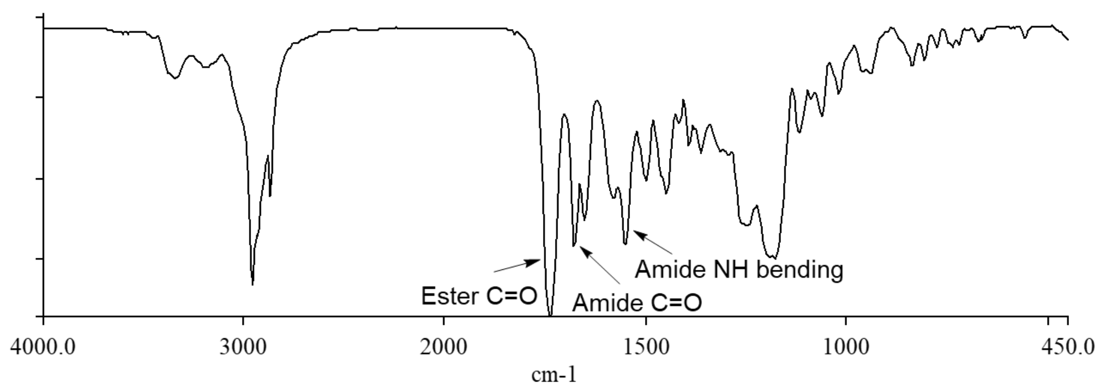

Figure 2.2 IR Spectrum of Small Model Molecule **2.4**

In the ^{1}H NMR spectrum, the proton peaks of compound **2.4** at δ 1.6, 1.4, and 0.9 ppm (labeled **g**, **h**, and **i** in **Figure 2.3**) come from the *n*-butyl chains of the diglutamate tetraester. Interestingly, the benzylic hydrogens for peak **a** is an AB quartet instead of a singlet, as the two methylene hydrogens are diastereotopic. The ^{1}H NMR spectrum also shows there are two types of amide proton peaks, appearing at δ 11.3 and 8.3 ppm. Conjugation of the carbonyl amides to the triazole aromatic group[9] results in downfield shifts of the amide protons. The differences between the ^{1}H chemical shifts of the two amides likely arises from intramolecular H-bonding[10] of the more downfield amide proton at δ 11.3 ppm. However, the positions of j and k can not be distinguished by 1D NOESY (Nuclear Overhauser Effect Spectroscopy) NMR (**Figure 2.4**). Irradiation of the methylene **a** at δ 6.1 ppm results in NOE enhancement of only phenyl hydrogen **m** at δ 7.3 ppm. Note that the ortho and meta aryl hydrogens happen to both appear at δ 7.3 ppm.

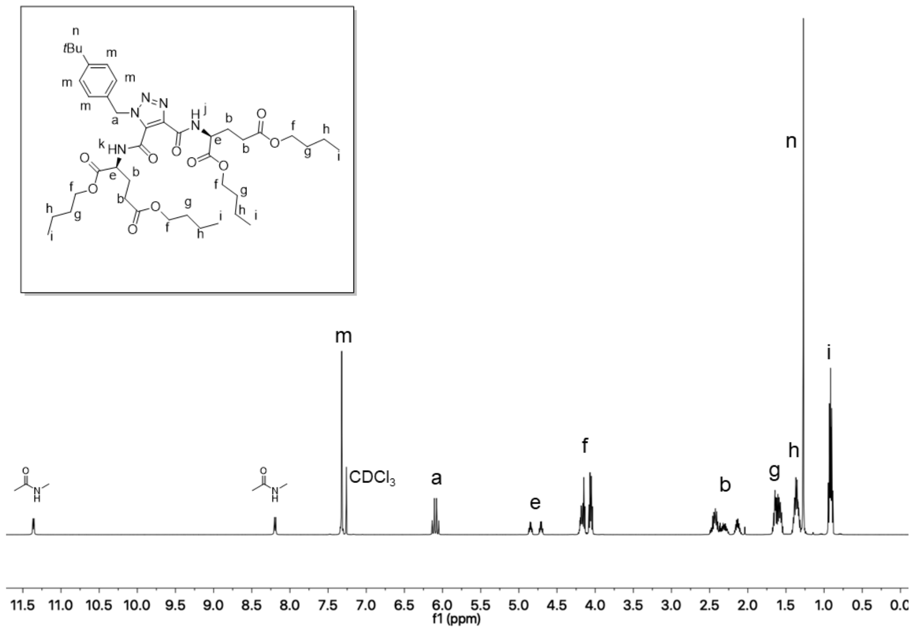

Figure 2.3 [1]H NMR of Small Model Molecule **2.4.** Note: Peak **a** is an AB Quartet.

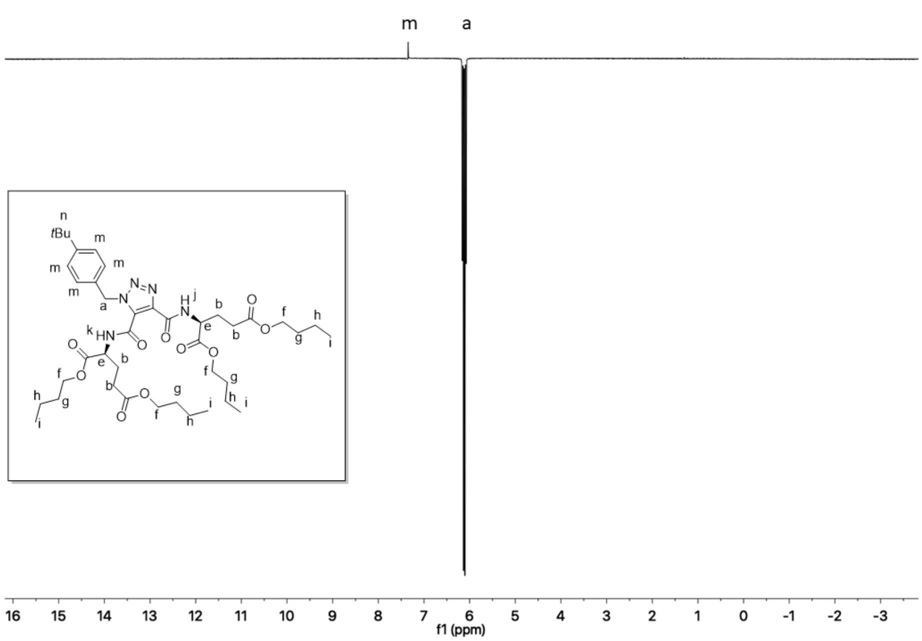

Figure 2.4 1D Selective NOESY Spectra of Small Model Molecule **2.4**

2.5 Determination of Percentage of Azidation on PVC

PVC-azides with 4.4% azidation **2.5** and 12.0% azidation **2.5'** were prepared using NaN_3 in an S_N2 displacement of chlorine atoms on PVC in DMF at 62 °C for 0.5 h and 2.0 h, respectively (**Scheme 2.5**).[2,3] The percentage of azidation was calculated based on elemental analysis (**Table 2.1**) using the equation developed by Higa (**Equation 2.1 – 2.5**).[11]

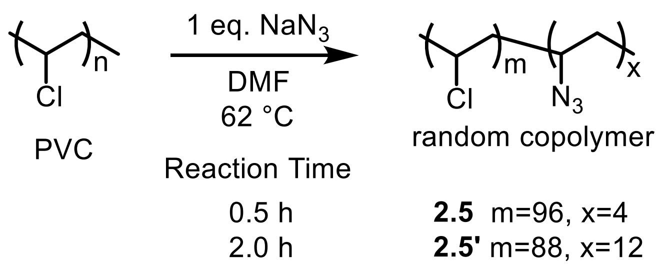

Scheme 2.5 Preparation of PVC-Azide **2.5** and **2.5'**

Table 2.1 Elemental Analysis of PVC-Azide **2.5** and **2.5'**

Polymer	wt% of carbon	wt% of hydrogen	wt% of nitrogen
2.5	39.23	5.12	3.02
2.5'	38.69	5.22	8.17

Given the elemental analysis results, if there are 100 grams of PVC-azide **2.5**, the mass of nitrogen is 3.02 grams (3.02 wt% of nitrogen). The moles of nitrogen atoms are therefore 0.216 mol (**Equation 2.1**).

$$The\ moles\ of\ nitrogen\ atoms = \frac{The\ mass\ of\ nitrogen}{Atomic\ weight\ of\ nitrogen} = \frac{3.02\ g}{14.01\ g/mol} = 0.216\ mols$$ **Equation 2.1**

The moles of azide group are one third of that: 0.072 mol (**Equation 2.2**).

$$The\ moles\ of\ azide\ group = \frac{The\ moles\ of\ nitrogen\ atoms}{3} = \frac{0.216\ mols}{3} = 0.072\ mols$$ **Equation 2.2**

The mass of carbon is 39.23 grams (39.23 wt% of carbon) for 100 grams of PVC-azide **2.5**. The moles of carbon is 3.27 mols (**Equation 2.3**).

$$The\ moles\ of\ carbon\ atom = \frac{The\ mass\ of\ carbon}{Atomic\ weight\ of\ carbon} = \frac{39.23\ g}{12.01\ g/mol} = 3.27\ mols$$ **Equation 2.3**

The total moles of vinyl chloride and vinyl azide are 1.64 mols (**Equation 2.4**).

$$The\ total\ moles\ of\ vinyl\ chloride\ and\ vinyl\ azide = \frac{The\ moles\ of\ carbon\ atoms}{2}$$

$$= \frac{3.27\ mols}{2} = 1.64\ mols$$ **Equation 2.4**

Therefore, the azidation percentage of PVC-azide **2.5** is 4.39% (**Equation 2.5**).

$$The\ azidation\ percentage = \frac{The\ moles\ of\ azide\ group}{The\ total\ moles\ of\ vinyl\ chloride\ and\ vinyl\ azide} \times 100\%$$

$$= \frac{0.072\ mols}{1.64\ mols} \times 100\% = 4.39\ \%$$ **Equation 2.5**

The same calculation method was applied to polymer **2.5'** giving percentage of the of 12.04%.

2.6 Preparation of Tetraester Alkynes and Introduction to PVC via Thermal Azide/Alkyne Cycloaddition

A series of glutamate ester diamide alkynes **2.2b-f** bearing a variety of terminal ester groups were synthesized (**Scheme 2.6**) using analogous reactions to that of **2.2a** (**Scheme 2.6**). Thermal azide-alkyne dipolar cycloaddition was then carried out to form the triazole attachments bearing tetraesters at 90 °C for 48 h or 72 h, to give PVC functionalized at 4% of the original chlorine sites (polymer **2.6a-f**), and at 12% (polymers **2.6'a-f**). The reaction time for cycloaddition of PVC-azide and diamide alkynes to go to completion is longer compared to diester alkynes due to the less electron-poor nature of the diamide alkynes compared to diester alkynes.[3,12]

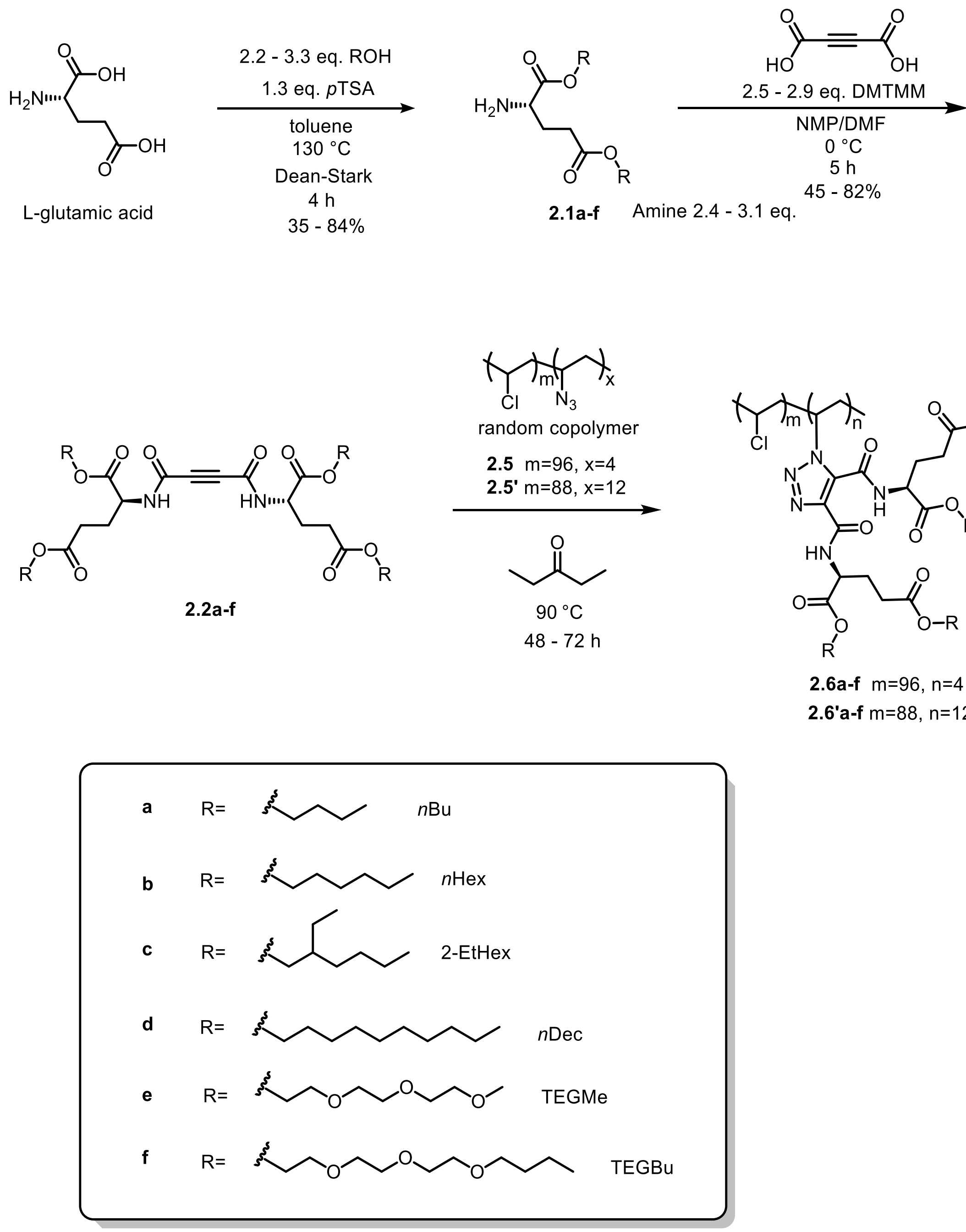

Scheme 2.6 Preparation of Tetraester Alkynes and Introduction onto PVC via Azide-Alkyne Cycloaddition.

2.7 Characterization of Functionalized PVC

IR spectroscopy was effective at evaluating triazole formation on the polymer by monitoring the disappearance of the distinct azide peak at 2114 cm^{-1} (**Figure 2.5a**).

Comparison of the IR spectra of diglutamate ester functionalized PVC **2.6'a** and small molecule triazole **2.4** (**Figures 2.5b** and **2.5c**) revealed very similar peaks. For both the model compound **2.4** and the diglutamate ester triazole functionalized PVC **2.6'a**, the broad amide N-H stretch was found near 3350 cm^{-1}. Similarly, the ester C=O stretch was seen at 1737 cm^{-1} for functionalized PVC **2.6'a** and at 1739 cm^{-1} for model **2.4**. The amide C=O stretch and N-H bend were observed for both the internally plasticized PVC **2.6'a** and model **2.4** at 1677 and 1678 cm^{-1} (amide C=O stretching, amide I band) and at 1551 and 1552 cm^{-1} (amide NH bending, amide II band), respectively.

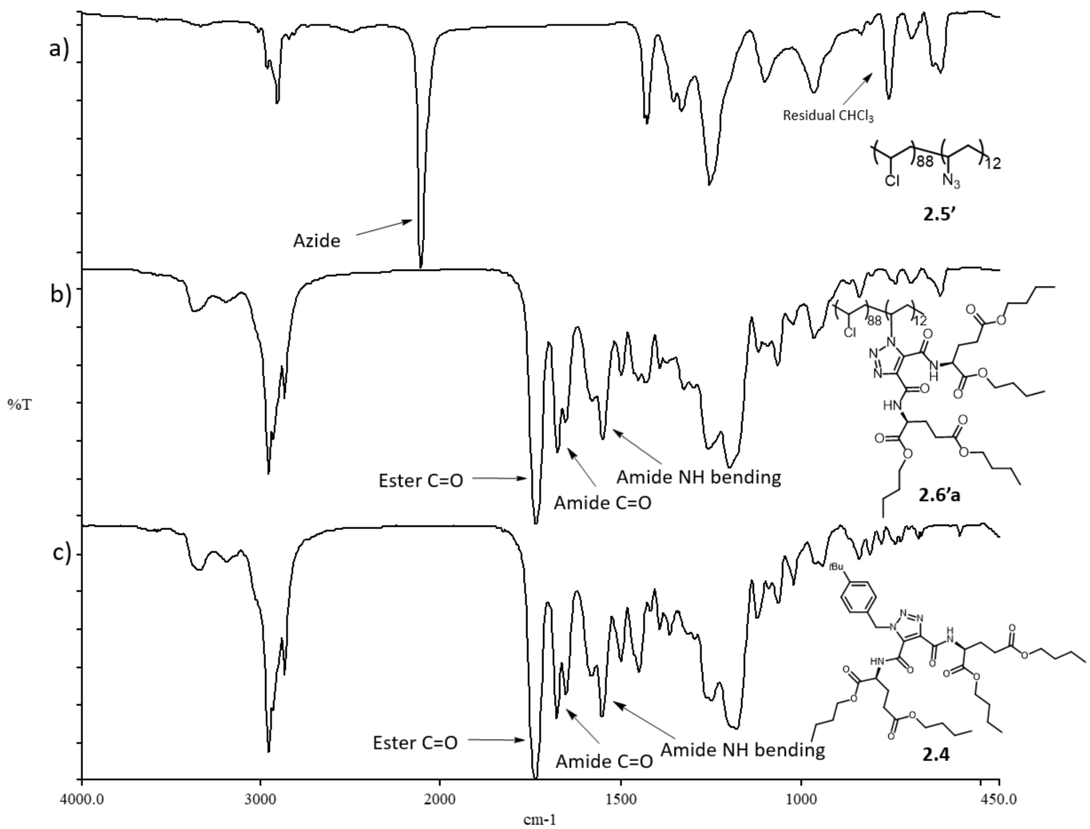

Figure 2.5 IR Spectra Comparing a) PVC-12%-azide **2.5'**, b) PVC-12%-*n*Bu **2.6'a**, and c) Model Triazole **2.4**

Internally plasticized 12% *n*Bu tetraester PVC **2.6'a** was further characterized by comparing the ^{1}H NMR spectrum of the polymer **2.6'a** to spectra of PVC-12%-azide **2.5'** and model triazole **2.4** (**Figure 2.6**). Comparing the [1]H NMR spectra of PVC-12%-azide **2.5'** (**Figure 2.6a**) with that of polymer **2.6'a** (**Figure 2.6b**), it is clear that both feature protons from the PVC backbone: CH-Cl methine protons of the PVC backbone have a chemical shift of δ 4.7-4.2 ppm; $-CH_2-$ methylene protons from the PVC have a chemical shift of δ 2.5-1.6 ppm. Peaks from the tetraester triazole polymer **2.6'a** were corelated to model triazole **2.4**. For both, there are again two types of amide proton peaks, appearing at δ 11.3 and 8.3 ppm. Comparison of the [13]C NMR spectra PVC-12%-N_3 **2.5'**, PVC-12%-*n*Bu **2.6'a**, and model compound **2.4** (**Figure 2.7**) also supports the structure of **2.6'a**, which contains both PVC backbone carbons (**2.5'**) and *n*Bu tetraester (**2.4**).

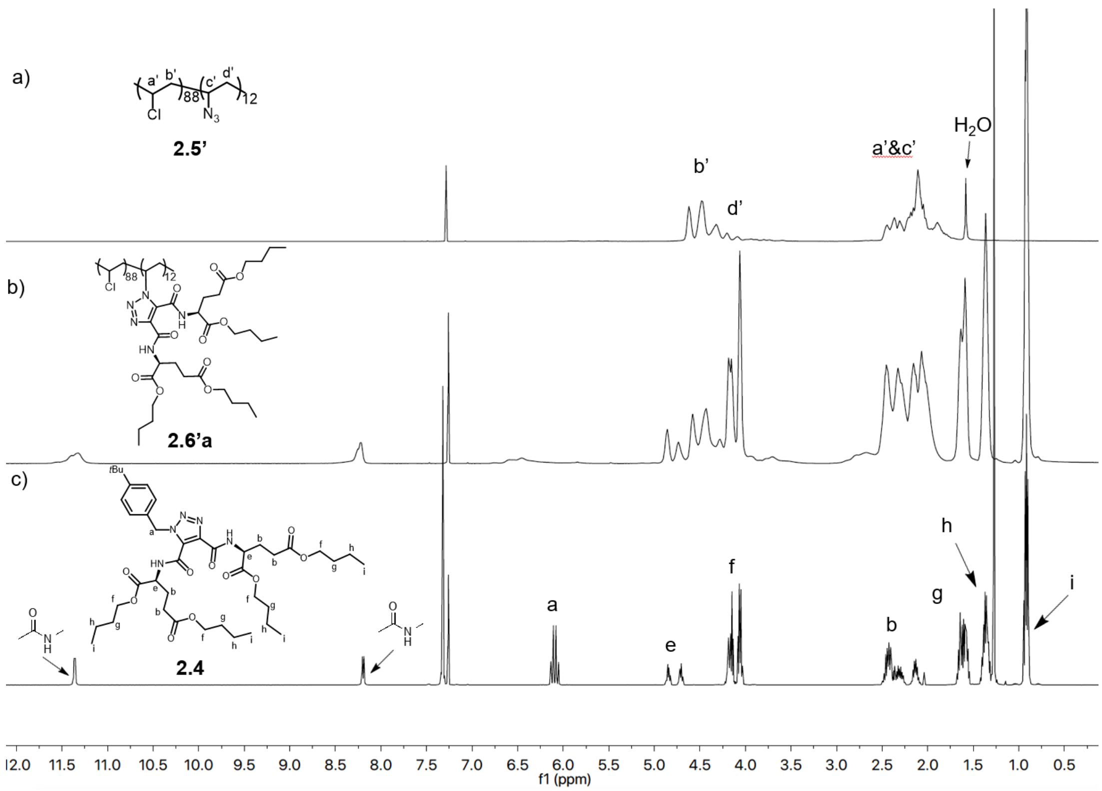

Figure 2.6 [1]H NMR Spectra (in $CDCl_3$) of a) PVC-12%-N_3 **2.5'**, b) PVC-12%-*n*Bu **2.6'a**, and c) Model Compound **2.4**

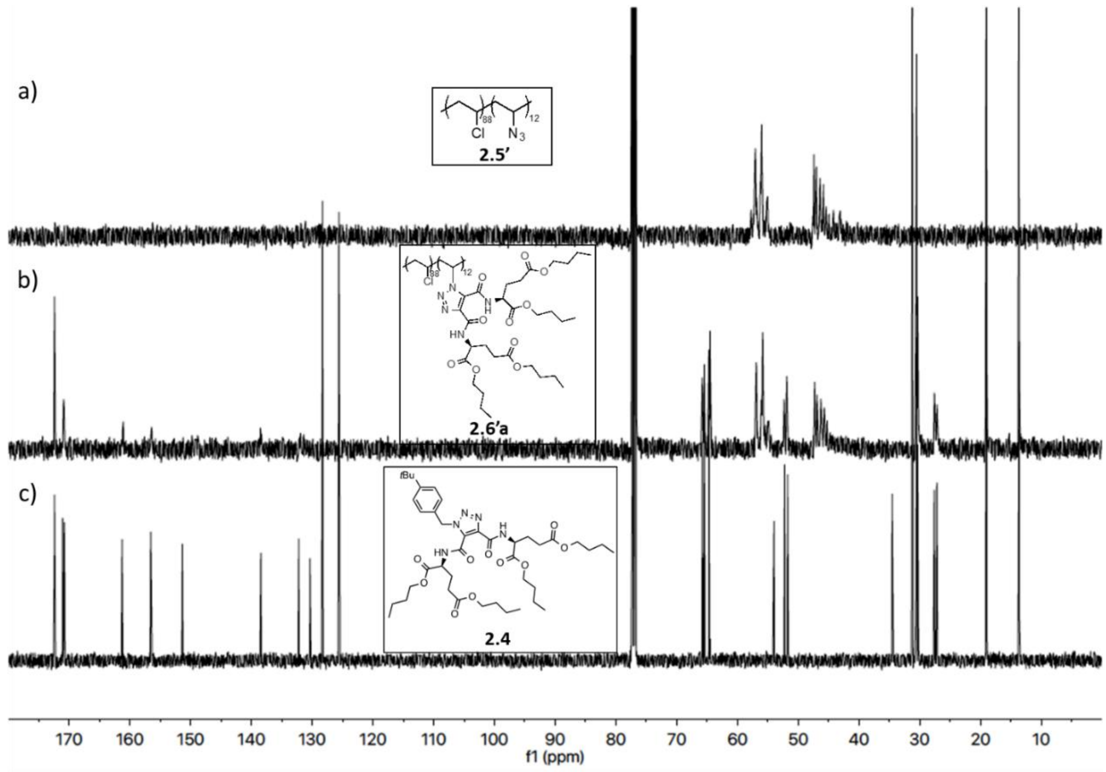

Figure 2.7 ^{13}C NMR Spectra (in $CDCl_3$) of a) PVC-12%-N_3 **2.5'**, b) PVC-12%-*n*Bu **2.6'a**, and c) model compound **2.4**

2.8 Glass transition temperature of functionalized PVC

The glass transition temperature (T_g) is the temperature at which a polymer undergoes a phase change from a glassy state to a rubbery state (**Figure 2.8**). The T_g value reflects the flexibility of a polymer; the lower the T_g, the more flexible the material. T_g values in this chapter were measured at IBM by Andy Tek with the collaboration of Dr. Rudy Wojtecki, using a differential scanning calorimetry (DSC) Q2000 with a heat-cool-heat protocol, and a scanning range of −90 to 200 °C at a heating rate of 10 °C min^{-1}. The T_g was collected during the second heating cycle because the first heating cycle was used to erase the thermal history of the polymer and remove residual solvents.

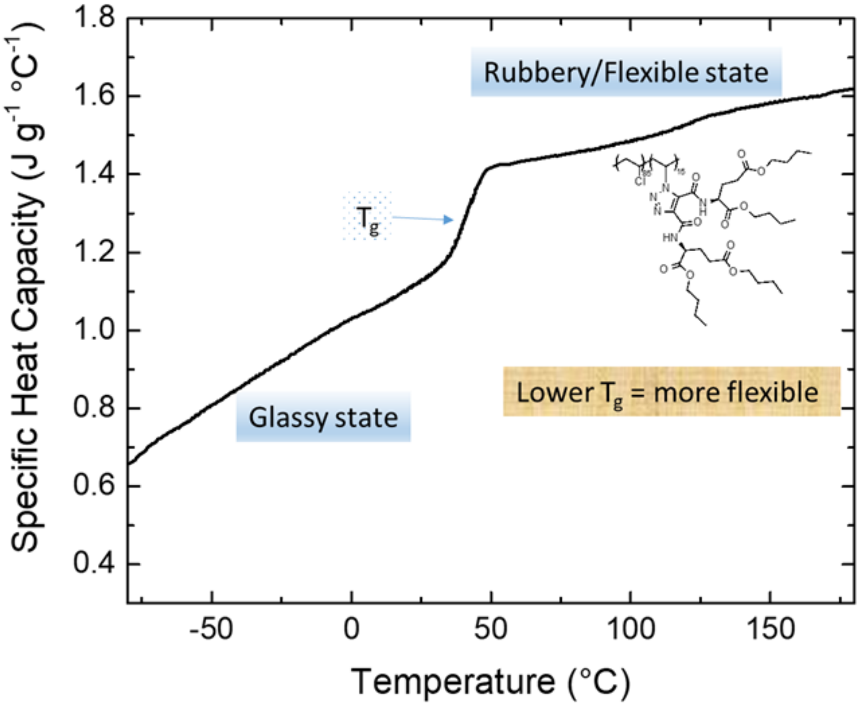

Figure 2.8 DSC (Second Heat Cycle) of Internally Plasticized PVC **2.6'a**

The DSC data of diglutamate tetraester functionalized PVC samples show specific heat capacities during the second heating cycle for both 4 and 12 mol % samples. The T_g value of unmodified PVC is 81 °C, showing PVC is in its glassy state at room temperature. For PVC bearing 4 mol % internal plasticizer, T_g values range from 62 °C to 39 °C (**Figure 2.9**). The highest T_g value (62 °C) was obtained for PVC-4%-*n*Bu **2.6a**. T_g values decrease with increasing ester *O*-alkyl chain length. The T_g value of PVC-4%-*n*Hex **2.6b** is 53 °C, and T_g value of PVC-4%-2-EtHex **2.6c** is 47 °C. Collected T_g values of the second heating cycle are given in **Table 2.2**.

For PVC bearing 12 mol % of internal plasticizer, the lowest T_g value obtained is -1 °C for the tetra(TEGBu) ester diglutamate triazole PVC-12%-TEGBu **2.6'f** , indicating excellent internal plasticization. The T_g values of the *O*-alkyl esters are all higher than those of the *O*-

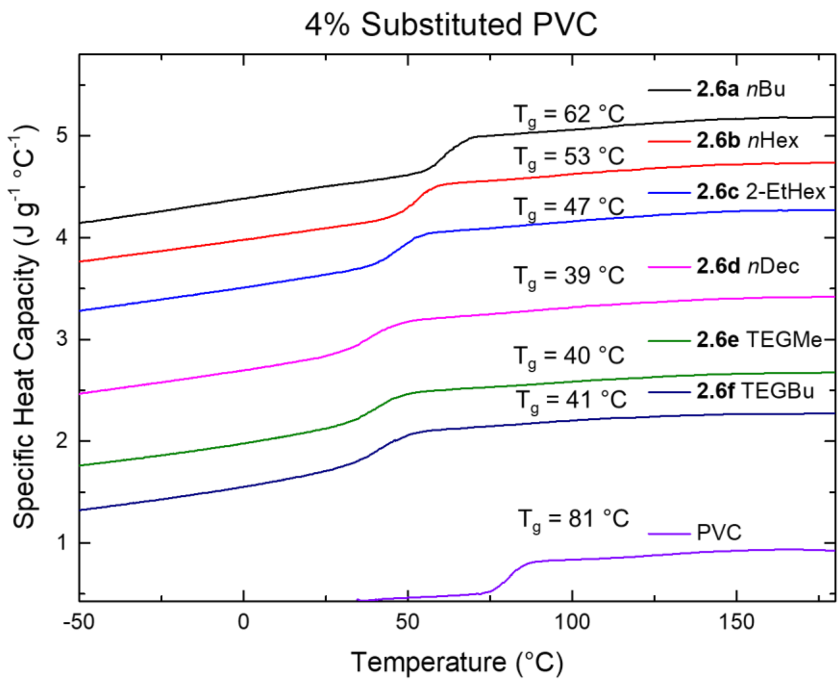

Figure 2.9 DSC (2nd Heat Cycle) of 4 mol% Internally Plasticized PVC

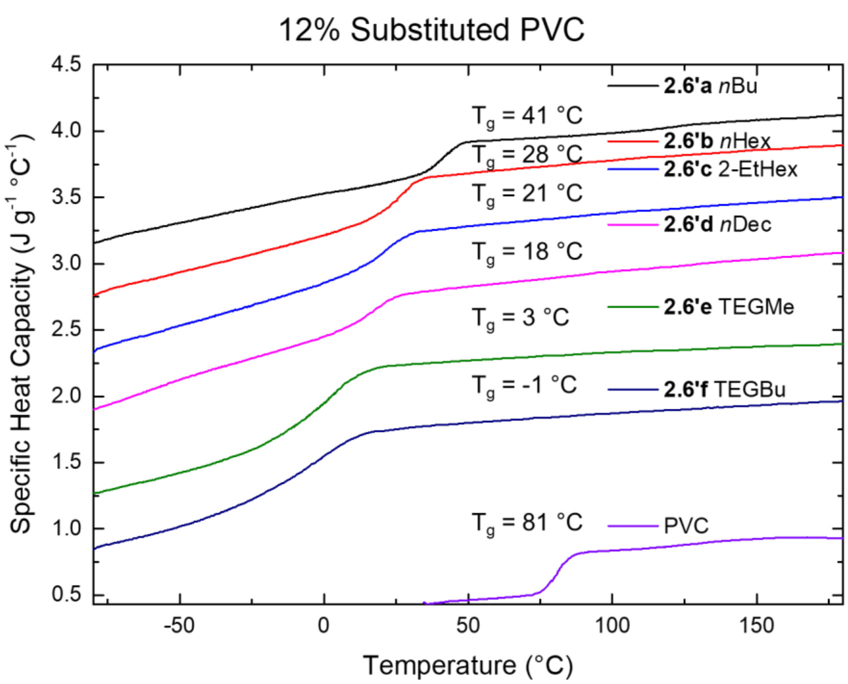

Figure 2.10 DSC (2nd Heat Cycle) for Samples of 12 mol% Internally Plasticized PVC

PEG esters, even though the alkyl *n*Dec (T_g = 18 °C) and polyether TEGMe (T_g = 3 °C) esters are the same length (**Figure 2.10**). Within the alkyl esters, longer alkyl ester chains result in lower T_g values than shorter chains. Adding an *n*-butyl group to the end of the PEG ester in place of the methyl group makes very little difference, giving only a slight depression of the T_g value at 12% substitution, and was indistinguishable at 4 mol%. Collected T_g values of the second heating cycle are given in Table **2.2**.

Table 2.2 DSC T_g Values for PVC Bearing 4 mol % and 12 mol % Glutamic Ester-Derived Branched Internal Plasticizers

Polymer	T_g (°C)[a]	Polymer	T_g (°C)[a]
PVC	81		
2.6a 4% *n*Bu	62	**2.6'a** 12% *n*Bu	41
2.6b 4% *n*Hex	53	**2.6'b** 12% *n*Hex	28
2.6c 4% 2EtHex	47	**2.6'c** 12% 2EtHex	21
2.6d 4% *n*Dec	39	**2.6'd** 12% *n*Dec	18
2.6e 4% TEGMe	40	**2.6'e** 12% TEGMe	3
2.6f 4% TEGBu	41	**2.6'f** 12% TEGBu	-1

[a] T_g is from the 2nd heating cycle

2.9 Plasticization Efficiency of Branched Internal Plasticizers Compared to Previous Internal Plasticizers Developed in Braslau Lab

To examine the effect of doubling the density of ester plasticizing moieties using this branched linker, a comparison with TEGMe diester internal plasticizers **2.7** and **2.7'** from the previous work of Higa in the Braslau lab[3] is useful (**Figure 2.11**). For 4 mol % PVC samples, the T_g value of diester **2.7** = 61 °C, whereas for the tetraester **2.6e** the T_g = 40 °C. Even more pronounced, for the more densely substituted PVC sample **2.7'**, the diester plasticizer showed a T_g = 42 °C compared to the tetraester **2.6'e** at T_g = 3 °C. Thus doubling the number of esters from two to four for each triazole linkage gives significantly enhanced plasticization. Thus the concept of multivalent attachment per azide linker does seem to enhance plasticization.

However, the diesters functionalized PVC samples **2.7** and **2.7'** were synthesized in three steps: one step less compared to the synthesis of the diglutamate tetraester functionalized PVC samples **2.6e** and **2.6'e** in this work.

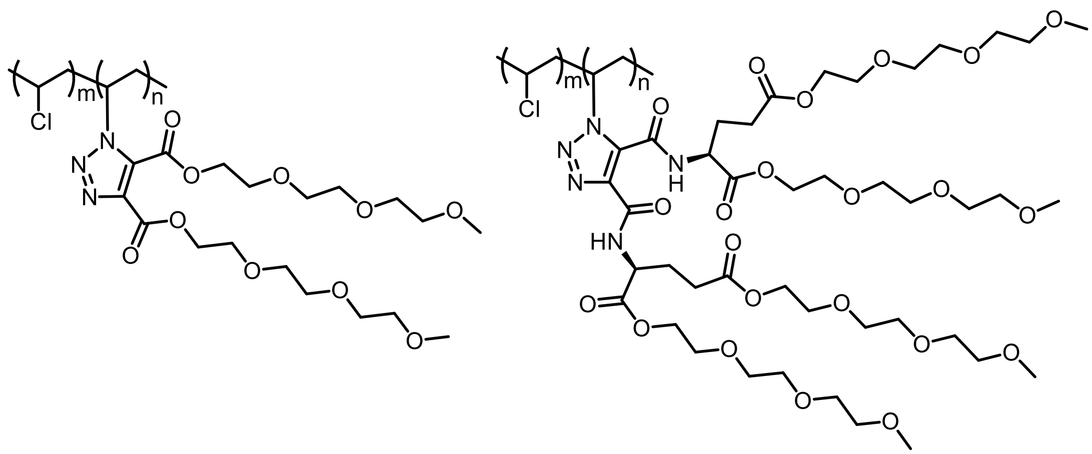

2.7 m=96, n=4
2.7' m=88, n=12

2.6e m=96, n=4
2.6'e m=88, n=12

		T_g(°C)		T_g(°C)
4%	**2.7**	61	**2.6e**	40
12%	**2.7'**	42	**2.6'e**	3

Figure 2.11 Comparison of Glass Transition Temperatures between Previous TEGMe Diesters and Branched TEGMe Tetraesters

2.10 Plasticization Efficiencies of Branched Internal Plasticizers

The weight percent of internal plasticizer was calculated using **Equation 2.6**.[11]

$$Weight\ percent\ plasticizer\ (\%) = \frac{Mass_{Triazole\ plasticizer}}{Mass_{Triazole\ plasticizer} + Mass_{Polymeric\ main\ chain}} \times 100$$

Equation 2.6

Calculations of $Mass_{Triazole\ plasticizer}$ and $Mass_{Polymeric\ main\ chain}$ are based on **Figure 2.12,** using PVC-4%-*n*Bu **2.6a** as an example (note: the radical on each fragment is a formalism):

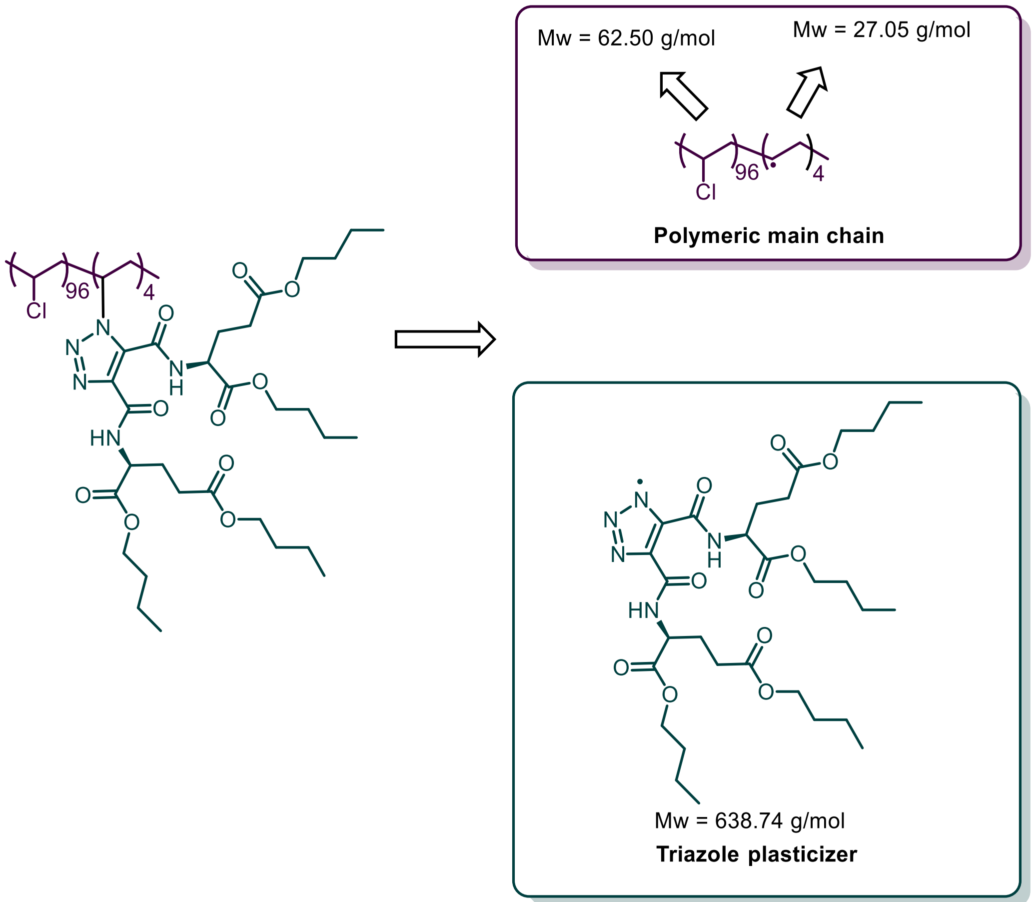

Figure 2.12 Molecular Weight of Polymeric Main Chain and Triazole Plasticizer

Therefore, the weight percent of internal plasticizer for PVC-4%-*n*Bu **2.6a** is 31.56%, as in **Equation 2.7**.

$$Weight\ percent\ plasticizer = \frac{638.74 \times 4.4}{638.74 \times 4.4 + 62.50 \times 95.6 + 27.05 \times 4.4} \times 100\%$$

$$= 31.6\% \qquad \textbf{Equation 2.7}$$

The weight percent plasticizer for each of the modified PVC polymers are summarized in **Table 2.3**, calculated using **Equation 2.7** and **Figure 2.12**.

Table 2.3 Weight Percent (wt%) of Internal Plasticizers

R Group	Triazole plasticizer Mw (g/mol)	4.4 mol% Functionalized PVC (wt%)	12.0 mol% functionalized PVC (wt%)
*n*Bu	638.74	31.6	56.9
*n*Hex	750.96	35.2	60.8
2-EtHex	863.17	38.4	64.1
*n*Dec	975.39	41.3	66.9
TEGMe	999.05	41.9	67.4
TEGBu	1167.38	45.7	70.7

In order to evaluate the efficacy of plasticization, the T_g values of these branched internally plasticized PVC samples were compared to that of externally plasticized DEHP-PVC[3] as a function of plasticizer content by weight percent (**Figure 2.13**). The trend shows that use

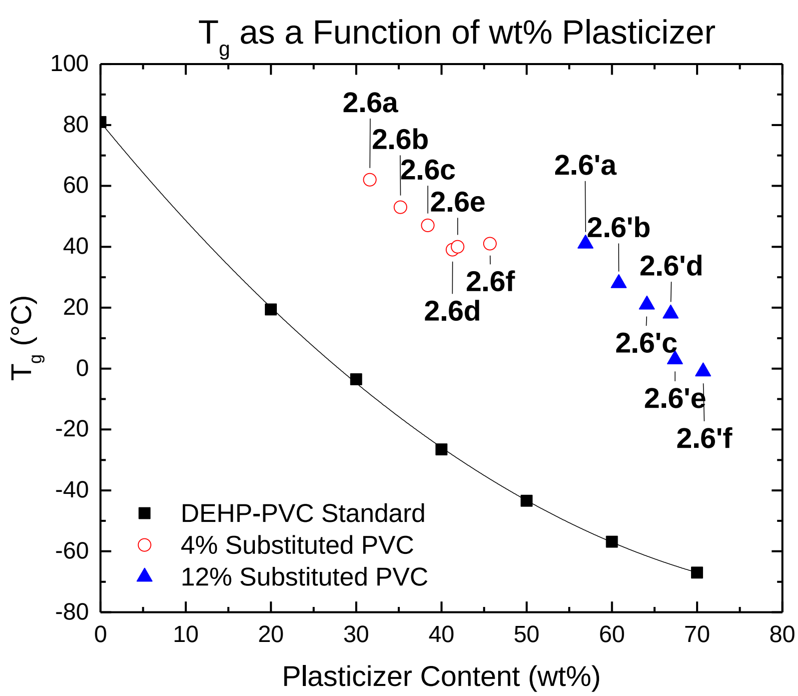

Figure 2.13 Plot of T_g versus Plasticizer Content of DEHP-PVC Standard (black square), 4% Substituted PVC **2.6a-2.6f** (Red Circles), and 12% Substituted PVC **2.6'a-2.6'f** (Blue Triangles)

of traditional DEHP plasticizer is more effective than these tetraester triazole internally plasticized samples. This makes sense if one considers the mechanism of plasticization. Large internal plasticizers reduce the rotation of the polymer backbone compared to unattached small molecule plasticizers. In terms of free volume theory, for the same weight percent of plasticizers, smaller molecule plasticizers introduce more free volume, leading to more flexible materials.[13] Among these internally plasticized samples, the T_g values are correlated with the degree of PVC substitution; T_g values below 0 °C can be achieved by 12% TEGBu substituted PVC.

Plasticization efficiency ($E_{\Delta T_g}$) for each internal plasticizer was calculated based on the following equations (**Equation 2.8 – 2.12 and Equation 2.6**).[3,14] **Equation 2.11** was developed by Higa based on his experiment data.[3]

$$E_{\Delta T_g} = \frac{\Delta T_{g,plasticizer}}{\Delta T_{g,DEHP}} \times 100\%$$ **Equation 2.8**

$$\Delta T_{g,plasticizer} = T_{g,unmodified\ PVC} - T_{g,modified\ PVC}$$ **Equation 2.9**

$$\Delta T_{g,DEHP} = T_{g,unmodified\ PVC} - T_{g,DEHP}$$ **Equation 2.10**

$$T_{g,DEHP} = 0.0186x^2 - 3.4124x + 80.898$$ **Equation 2.11**

$$x\ (\%) = weight\ percent\ plasticizer$$ **Equation 2.12**

$$Weight\ percent\ plasticizer = \frac{Mass_{Triazole\ plasticizer}}{Mass_{Triazole\ plasticizer} + Mass_{Polymeric\ main\ chain}} \times 100\%$$

Equation 2.6

Plasticization efficiency increases with increasing plasticizer weight percent (**Figure 2.14**). There is also a subtle dependence of plasticization efficiency on the ester functional group: polyether esters lead to higher plasticization efficiencies than alkyl esters at a similar plasticizer weight percent (**2.6'd** = *n*Dec, 66.9 wt% of plasticizer, T_g = 18 °C; **2.6'e** = TEGMe, 67.4 wt% of plasticizer, T_g = 3 °C). Also, 4% TEGBu substituted PVC **2.6f** gives a higher plasticization efficiency (34%) than 12% *n*Bu substituted PVC **2.6'a** (29%), thus the use of polyethers overrides the lower degree of substitution on PVC. Although DEHP-PVC is more effective as a plasticizer, the migratory issue makes the traditional phthalate approach less satisfactory considering the durability of the compromised PVC products following loss of plasticizer due to migration, and the health issues ensuing from phthalate contamination. However, the price of the coupling reagent DMTMM ($80/100g) is a drawback of this method.

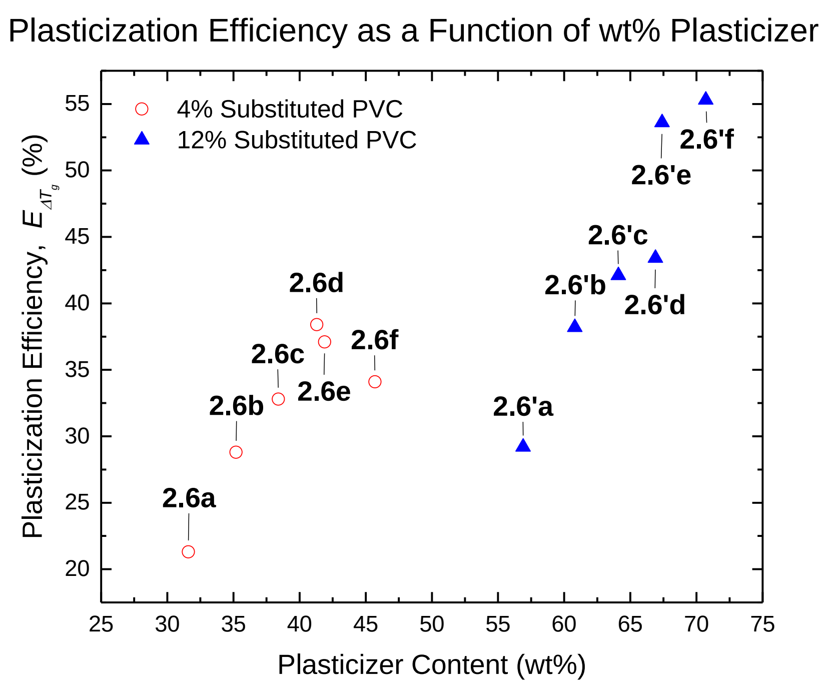

Figure 2.14 Plot of Plasticization Efficiency of 4% Substituted PVC **2.6a-2.6f** (Red Circles) and 12% Substituted PVC **2.6'a-2.6'f** (Blue Triangles)

2.11 Thermogravimetric analysis of functionalized PVC

Thermogravimetric analysis (TGA) was performed in order to evaluate the thermal stability of these functionalized polymers (**Figure 2.15** and **2.16**). TGA in this chapter were measured at IBM by Andy Tek with the collaboration of Dr. Rudy Wojtecki. For the alkyl chain tetraester diglutamates, the sample weight stays relatively unchanged until an onset temperature is reached. For most of the polymers tested, the temperature at 5% weight loss is

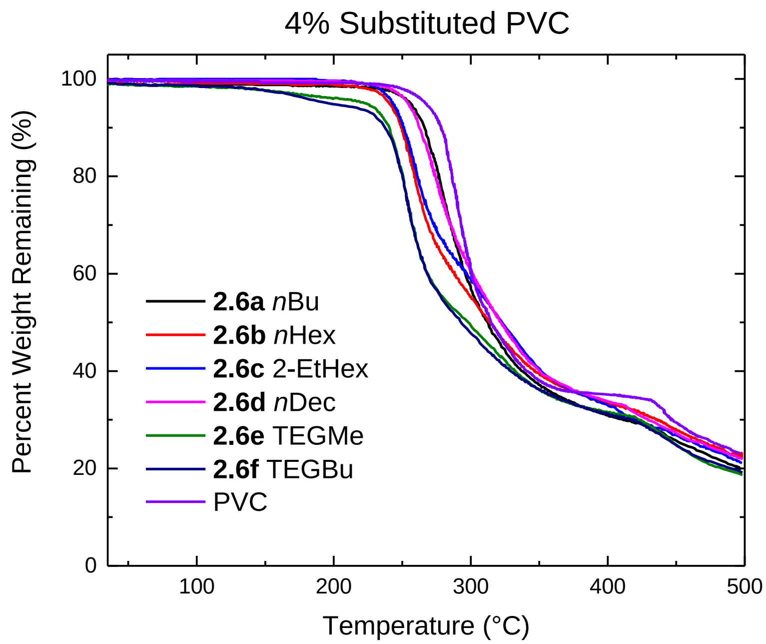

Figure 2.15 TGA data (open to air) illustrating percent weight remaining versus temperature for 4 mol% functionalized and unfunctionalized PVC

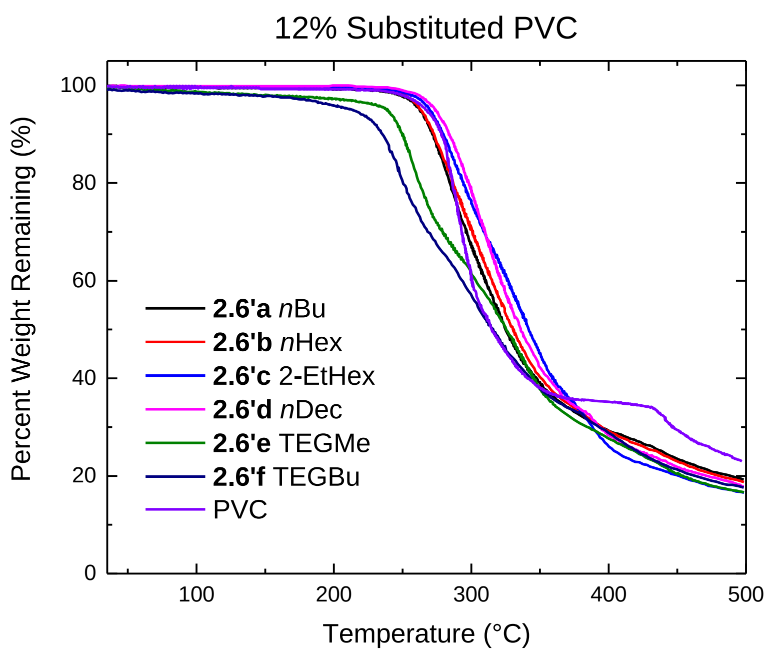

Figure 2.16 TGA data (open to air) illustrating percent weight remaining versus temperature for 12 mol% functionalized and unfunctionalized PVC

greater than 200 °C, and is directly correlated with the alkyl ester chain length (**Table 2.4**). Focusing on the 12 mol % polymers, a successive increase in temperature for 5% weight loss is observed from *n*Bu to *n*Hex to *n*Dec diglutamate functionalized PVC. The temperatures at 5% weight loss are higher for the 12 mol % substituted series compared to the 4 mol % polymers. Compared to pure PVC, the temperatures at 5% weight loss for the alkyl tetraester diglutamate functionalized PVC samples are similar, suggesting that this type of internal plasticizer is relatively stable, even under significant thermal stress. Examining the triethylene glycol ester diglutamate esters (TEGMe and TEGBu), the sample weights decrease at moderate temperatures, starting at approximately 150 °C. The observed temperatures of thermal decomposition for the triethylene glycol esters are consistent with previous reports of thermal degradation for typical poly(ethylene glycol).[15–17] The slope of the initial decrease is small, followed by a sharper decline. This suggests that the polyethers initially undergo a slow decomposition process under thermal stress before undergoing rapid decomposition at higher temperatures. TGA data measured under nitrogen show higher onset temperatures in comparison with data measured under air; otherwise, no significant differences were observed.

Table 2.4 TGA temperatures at 5% weight loss

Polymer	T_5 (°C)[a]	Polymer	T_5 (°C)[a]
PVC	267		
2.6a 4% *n*Bu	256	**2.6’a** 12% *n*Bu	262
2.6b 4% *n*Hex	240	**2.6’b** 12% *n*Hex	263
2.6c 4% 2EtHex	243	**2.6’c** 12% 2EtHex	270
2.6d 4% *n*Dec	254	**2.6’d** 12% *n*Dec	274
2.6e 4% TEGMe	224	**2.6’e** 12% TEGMe	239
2.6f 4% TEGBu	197	**2.6’f** 12% TEGBu	214

[a] T_5 = temperature at 5% weight loss, TGA measured open to air

2.12 Conclusion

Internal plasticization of PVC bearing triazoles with branched glutamic acid linkers displaying four ester groups per triazole has been investigated. A facile 3-step synthesis involving Fischer esterification, DMTMM amide coupling, and thermal 3+2 azide-alkyne cycloaddition was employed. By varying the ester substituents and examining the effects on the glass transition temperatures, longer length substituents correlate with lower T_g values for both alkyl and polyether esters. Polyether esters are more effective at depressing the T_g values compared to alkyl esters. By TGA, the triethylene glycol esters degrade at lower temperatures than the alkyl esters. In summary, non-migratory plasticization was successfully achieved, with impressive T_g values and plasticizing efficiencies greater than 50% for tetra(polyether) esters at 12% substitution of the chlorine atoms on the PVC chain.

2.13 References

(1) Earla, A.; Braslau, R. Covalently Linked Plasticizers: Triazole Analogues of Phthalate Plasticizers Prepared by Mild Copper-Free “Click” Reactions with Azide-Functionalized PVC. *Macromol. Rapid Commun.* **2014**, *35* (6), 666–671. https://doi.org/10.1002/marc.201300865.

(2) Earla, A.; Li, L.; Costanzo, P.; Braslau, R. Phthalate Plasticizers Covalently Linked to PVC via Copper-Free or Copper Catalyzed Azide-Alkyne Cycloadditions. *Polymer* **2017**, *109* (Supplement C), 1–12. https://doi.org/10.1016/j.polymer.2016.12.014.

(3) Higa, C. M.; Tek, A. T.; Wojtecki, R. J.; Braslau, R. Nonmigratory Internal Plasticization of Poly (Vinyl Chloride) via Pendant Triazoles Bearing Alkyl or Polyether Esters. *J. Polym. Sci. Part Polym. Chem.* **2018**, *56* (21), 2397–2411. https://doi.org/10.1002/pola.29205

(4) Niikura, K.; Nambara, K.; Okajima, T.; Matsuo, Y.; Ijiro, K. Influence of Hydrophobic Structures on the Plasma Membrane Permeability of Lipidlike Molecules. *Langmuir* **2010**, *26* (12), 9170–9175. https://doi.org/10.1021/la101039w

(5) Bellucci, M. C.; Marcelli, T.; Scaglioni, L.; Volonterio, A. Synthesis of Diverse Spiroisoxazolidinohydantoins by Totally Regio-and Diasteroselective 1, 3-Dipolar Cycloadditions. *RSC Adv.* **2011**, *1* (7), 1250–1264. https://doi.org/10.1039/C1RA00573A

(6) Marcelli, T.; Olimpieri, F.; Volonterio, A. Domino Synthesis of 1, 3, 5-Trisubstituted Hydantoins: A DFT Study. *Org. Biomol. Chem.* **2011**, *9* (14), 5156–5161. https://doi.org/10.1039/C1OB05242J

(7) Heyl, D.; Fessner, W.-D. Facile Direct Synthesis of Acetylenedicarboxamides. *Synthesis* **2014**, 1463–1468. https://doi.org/10.1055/s-0033-1341101

(8) Hassner, A.; Stern, M. Synthesis of Alkyl Azides with a Polymeric Reagent. *Angew. Chem. Int. Ed. Engl.* **1986**, *25* (5), 478–479. https://doi.org/10.1002/anie.198604781

(9) Henen, A. M.; Hamdi, A.; Farahat, A. A.; Massoud, A. M. Understanding Chemistry and Unique NMR Characters of Novel Amide and Ester Leflunomide Analogues. *Magnetochemistry* **2017**, *3* (4). https://doi.org/10.3390/magnetochemistry3040041.

(10) Gorobets, N. Yu.; Yermolayev, S. A.; Gurley, T.; Gurinov, A. A.; Tolstoy, P. M.; Shenderovich, I. G.; Leadbeater, N. E. Difference between 1H NMR Signals of Primary Amide Protons as a Simple Spectral Index of the Amide Intramolecular Hydrogen Bond Strength. *J. Phys. Org. Chem.* **2012**, *25* (4), 287–295. https://doi.org/10.1002/poc.1910.

(11) Higa, C. M. Non-Migratory Internal Plasticization of Poly(Vinyl Chloride) via Pendant Triazoles Bearling Alkyl or Polyether Esters. Ph.D. Dissertation, University of California, Santa Cruz, CA, 2018.

(12) Pascoal, M.; Brook, M. A.; Gonzaga, F.; Zepeda-Velazquez, L. Thermally Controlled Silicone Functionalization Using Selective Huisgen Reactions. *Eur. Polym. J.* **2015**, *69* (Supplement C), 429–437. https://doi.org/10.1016/j.eurpolymj.2015.06.026.

(13) Marcilla, A.; Beltrán, M. 5 – Mechanisms of Plasticizers Action. In *Handbook of Plasticizers (Second Edition)*; Wypych, G., Ed.; William Andrew Publishing: Boston, 2012; pp 119–133. https://doi.org/10.1016/B978-1-895198-50-8.50007-2.

(14) Lee, K. W.; Chung, J. W.; Kwak, S.-Y. Synthesis and Characterization of Bio-Based Alkyl Terminal Hyperbranched Polyglycerols: A Detailed Study of Their Plasticization Effect and Migration Resistance. *Green Chem.* **2016**, *18* (4), 999–1009. https://doi.org/10.1039/C5GC02402A.

(15) Han, S.; Kim, C.; Kwon, D. Thermal/Oxidative Degradation and Stabilization of Polyethylene Glycol. *Polymer* **1997**, *38* (2), 317–323. https://doi.org/10.1016/S0032-3861(97)88175-X.

(16) P. Lattimer, R. Mass Spectral Analysis of Low-Temperature Pyrolysis Products from Poly(Ethylene Glycol). *J. Anal. Appl. Pyrolysis* **2000**, *56* (1), 61–78. https://doi.org/10.1016/S0165-2370(00)00074-7.

(17) de Sainte Claire, P. Degradation of PEO in the Solid State: A Theoretical Kinetic Model. *Macromolecules* **2009**, *42* (10), 3469–3482. https://doi.org/10.1021/ma802469u.

3 Internal Plasticization of Poly(Vinyl Chloride) by Grafting Copolymers of Butyl Acrylate and 2-(2-Ethoxyethoxy)Ethyl Acrylate via Copper-Mediated Atom Transfer Radical Polymerization

3.1 Background

Many methods of chemically attaching plasticizers to PVC require three or more synthetic steps. The key attachments traditionally include sulfide linkages,[1–6] amine linkages,[7,8] and triazole linkages.[9–18] The lowest T_g (-42 °C) by internal plasticization previously achieved required three steps using 84 wt % of an attached plasticizer with a triazole linkage by Chad Higa in the Braslau group.[17] Another strategy involves the formation of copolymers of vinyl chloride with other monomers. For example, Coelho and Braslau[19] made random copolymers of vinyl chloride with an acrylate bearing a triazole phthalate mimic DEHT-HA using free radical polymerization. However, preparation of the monomer DEHT-HA required four synthetic steps. Feng, Moad and Thang[20] prepared highly plasticized PVC-*b*-PCL in two steps using reversible addition−fragmentation chain transfer polymerization followed by ring-opening polymerization.

Atom transfer radical polymerization (ATRP),[22–24] a reversible–deactivation radical polymerization,[25] has been used to grow graft copolymers from defect sites off of PVC chains to achieve internally plasticized PVC in a single reaction.[26–37] This type of graft copolymerization can be nucleated from defect sites on PVC, including both allylic and tertiary chlorides (**Figure 3.1**).[38] As mentioned in **Chapter 1**, estimates of allylic chlorides range from 0.05-0.72/1000 vinyl chloride units,[39,40] and tertiary chlorides from 0.7-2.1/1000 vinyl chloride units.[41] Although these estimates vary, there is usually at least one defect site in each PVC chain.[27] One pathway to the formation of allylic chlorides is head-to-head addition, followed by rearrangement during propagation (**Scheme 3.2**).[42] Tertiary chlorides in PVC are generated by backbiting through a six member ring hydrogen abstraction transition state (**Scheme 3.3**).[43,44]

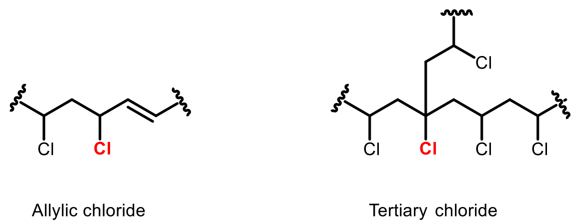

Figure 3.1 Structural Defects in Commercial PVC

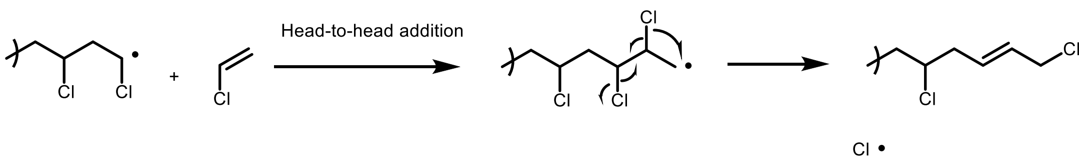

Scheme 3.1 Formation of a Terminal Allylic Chloride Caused by Head-to-Head Addition, Followed by Radical Fragmentative Rearrangement

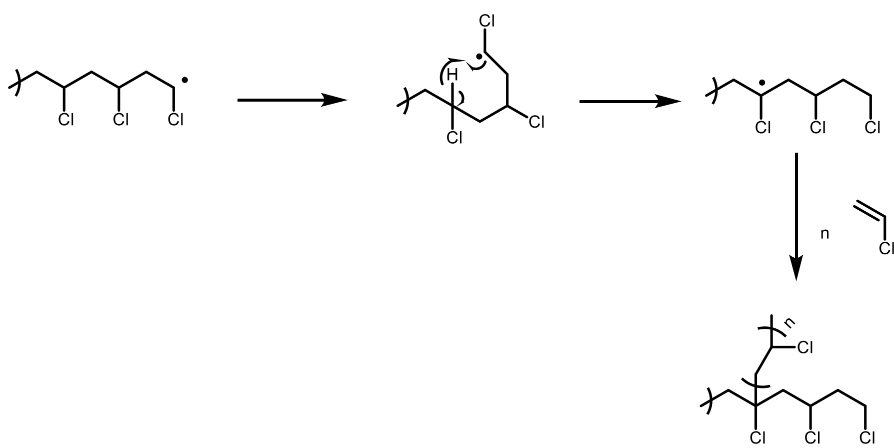

Scheme 3.2 Generation of Tertiary Chloride by Backbiting

Percec and Asgarzadeh[27] carried out a systematic study of Cu-catalyzed ATRP directly from defects sites on PVC, achieving functionalized PVC materials in a single step. The lowest T_g value obtained was -4 °C for PVC-*g*-PBA. Multiple researchers have demonstrated good compatibility between PVC and PBA segments in graft copolymers.[26,27,30]

Polyethers have been utilized as highly effective internal plasticizers for PVC by a number of researchers[5,6,17,18] including the work of Chad Higa[17] in the Braslau group and my own work discussed in **Chapter 2** and summarized in **Figure 3.2**.[18] Polyether chains tend to be more effective compared to analogous materials with straight-chain or branched alkyl groups. In **chapter 2**, the T_g value of functionalized PVC **2.6'd** with *n*Dec is 18 °C which is significantly higher than the T_g value of 3 °C for **2.6'e** with TEGMe (**Figure 3.2**). However, PVC-*g*-poly(oxyethylene methacrylate) (POEM) prepared by Hong *et al.*[32] using Cu-catalyzed ATRP resulted in a material with two T_g values (-68 °C and 32 °C), indicating micro-phase separation.

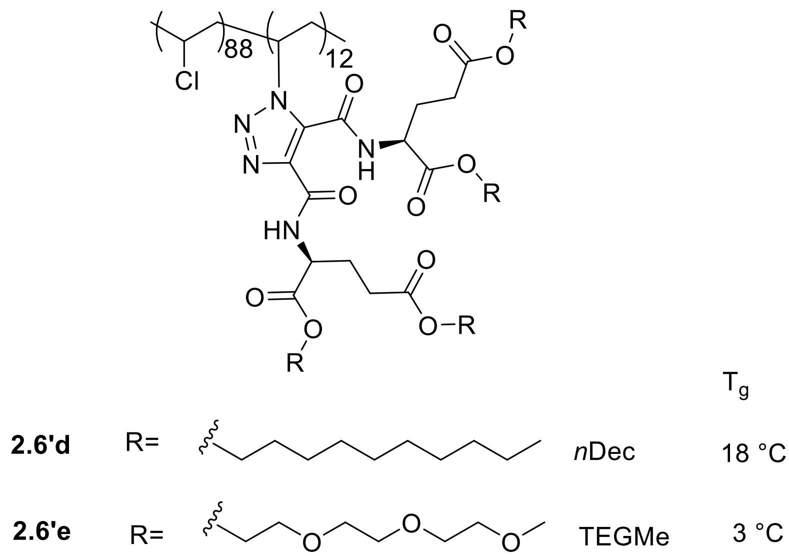

Figure 3.2 Structure and T_g Values of **2.6'd** and **2.6'e**

In this chapter, the compatibility of PBA combined with the plasticization efficiency of polyethers was investigated. Although Cu-ATRP is generally more effective with methacrylates than acrylates, the rigidity imposed on the graft chains by the quaternary carbons bearing the methacrylate methyl group makes polyacrylates better plasticizers than polymethacrylates. Thus, graft polymerization of different ratios of PBA-*co*-P(2-(2-ethoxyethoxy)ethyl acrylate) (PBA-*co*-P2EEA) were investigated to achieve effective plasticizing efficiency while avoiding microphase separation (**Scheme 3.3**). For this work, we collaborated with Dr. Yanika Schneider and Dr. Adrienne Hoeglund at EAG Laboratories. FTIR was measured by Yanika Schneider. DSC, TGA, and GPC were measured by Adrienne Hoeglund.

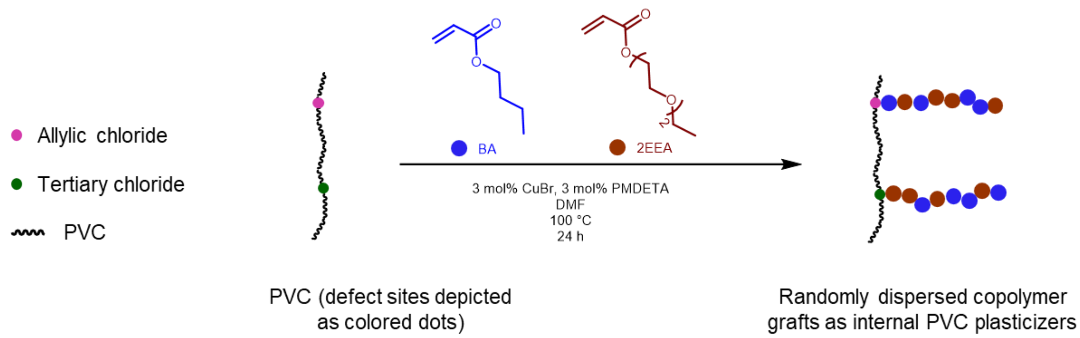

Scheme 3.3 General Scheme: Preparation of Graft PBA-*co*-P2EEA via ATRP

3.2 Synthesis of PVC-*g*-(PBA-*co*-P2EEA)

Commercially available PVC was purified before use through three cycles of dissolution in THF and precipitation in MeOH. PVC graft copolymers were prepared by ATRP initiated from defect sites using 3 mol% CuBr, 3 mol% PMDETA as the ligand, and DMF as the solvent. The initial reaction mixture was deoxygenated using the freeze-pump-thaw method, followed by heating at 100 °C for 24 h. Five different ratios of *n*-butyl acrylate (BA) and 2-(2-ethoxyethoxy)ethyl acrylate (2EEA) were investigated, ranging from homopolymer grafts of each monomer, to 3 : 1 to 1 : 1 to 1 : 3 ratios, resulting in a series of PVC-*g*-(PBA-*co*-P2EEA) variants (**Table 3.1**).

Table 3.1 Polymerization Conditions and Percent Conversions[a]

Entry	[PVC]/[BA]/[2EEA]/[CuBr]/[PMDETA][b]	Initial molar ratio of [BA]/[2EEA]	$\%Conv_{NMR}$[c] (2 g scale)	$\%Conv_{NMR}$[c] (14 g scale)
1	1 : 2.5 : 0 : 0.03 : 0.03	BA only	81%	88%
2	1 : 1.9 : 0.6 : 0.03 : 0.03	3 : 1	73%	88%
3	1 : 1.3 : 1.3 : 0.03 : 0.03	1 : 1	84%	86%
4	1 : 0.6 : 1.9 : 0.03 : 0.03	1 : 3	80%	72%
5	1 : 0 : 2.5 : 0.03 : 0.03	2EEA only	80%	80%
6	0 : 1.3 : 1.3 : 0.03 : 0.03[d]	1 : 1	23% [e]	-

[a]All polymerizations were conducted at 100 °C in DMF for 24 h; [b]Ratios were calculated in mol; [c]Conversion of total monomers; polymers were not completely soluble in the $CDCl_3$ NMR solvent; [d]Control without PVC; [e]Sample was completely soluble in the $CDCl_3$ NMR solvent.

These ATRP graft polymerizations were initially conducted using 0.5 g of PVC, yielding around 2 g of the PVC graft copolymers. To test the consistency and reproducibility of this ATRP method, all ratios were scaled up starting with 3.0 g of PVC, yielding approximately 14 g of PVC graft copolymer.

The conversion of total monomers was calculated based on crude ^{1}H NMR spectra. The NMR of PVC-*g*-(50%PBA-*co*-50%P2EEA) is used as an example to demonstrate how percent conversion of total monomer was calculated (**Figure 3.3**). Proton **a** of BA and **a'** of 2EEA both appear at 5.8 ppm, the integration of which was set to 1. Protons **b** of BA and **b'** of PBA appear at 0.9 ppm and integrate to 9.21. Protons **c** of 2EEA and **c'** of P2EEA were seen at 1.2 ppm integrate to 9.36. The percent conversion was calculated using **Equation 3.1**. Based on NMR, the percent conversion ranges from 72%-87%. As the samples were not completely soluble in the $CDCl_3$ solvent, it is likely that the percent conversion obtained by NMR is not accurate.

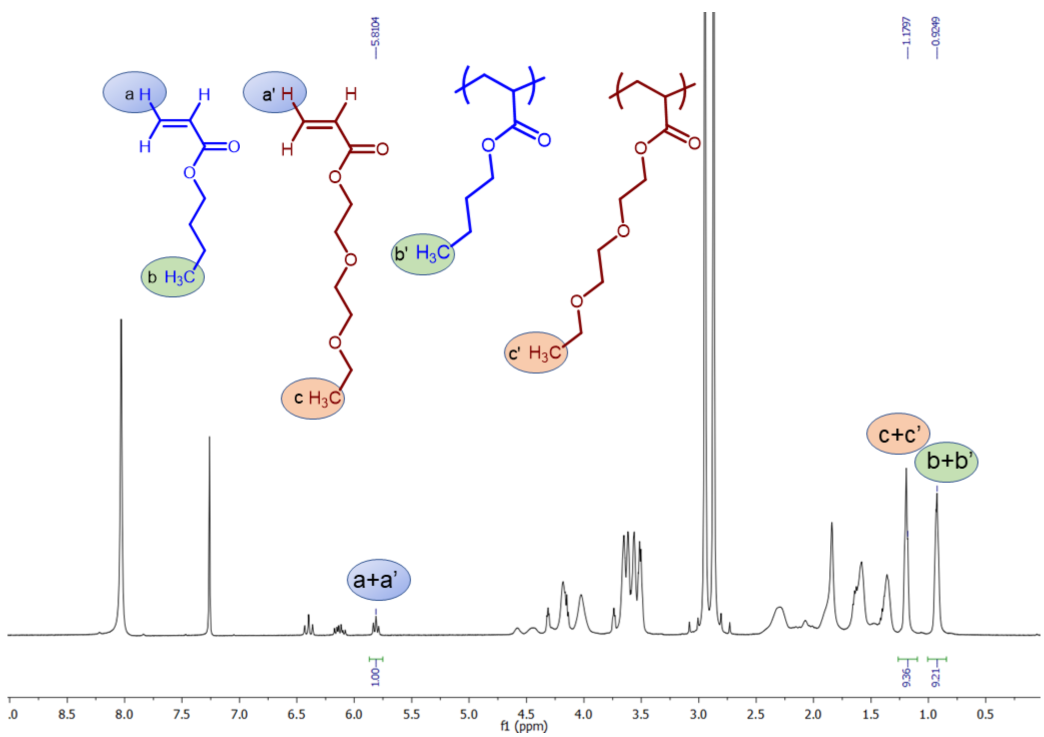

Figure 3.3 Crude NMR of PVC-*g*-(50%PBA-*co*-50%P2EEA) (2 g Scale)

$$Conv.\%_{total\ monomers} = \frac{Intergration_{all\ CH_3} - Intergration_{CH_3\ of\ monomers}}{Intergration_{all\ CH_3}} \times 100\%$$
$$= \frac{(Intergration_{c+c'} + Intergration_{b+b'}) - Intergration_{a+a'} \times 3}{Intergration_{c+c'} + Intergration_{b+b'}} \times 100\%$$
$$= \frac{9.36 + 9.21 - 1.00 \times 3}{9.36 + 9.21} \times 100\% = 84\%$$

Equation 3.1 Calculation of Percent Conversion of Total Monomer of PVC-*g*-(50%PBA-*co*-50%P2EEA)

3.3 Spontaneous Thermal Homopolymerization of Acrylates

Defect sites (allylic chloride and tertiary chloride) on PVC were assumed at first to be the only initiating species for ATRP. However, a control experiment without PVC resulted in 23% of polymer (**Table 3.1**, Entry 6). This is likely from self-initiation of BA or 2EEA at 100 °C.[45,46] One mechanism for spontaneous thermal homopolymerization of acrylates was postulated by Soroush (**Scheme 3.4**),[45,47] in which two monomers form a diradical species upon heating. These radical species then react with monomer in two ways to form monoradical species, which then initiate polymerization. The percent conversion and molecular weight of the polymer varies with the solvent used. The control reaction in the absence of PVC indicates that there is likely some unattached polymer contaminating the PVC-*g*-PBA, PVC-*g*-(PBA-*co*-P2EEA), and PVC-*g*-P2EEA samples. However, this does not diminish the overall usefulness of this approach towards nonmigratory plasticization of PVC.

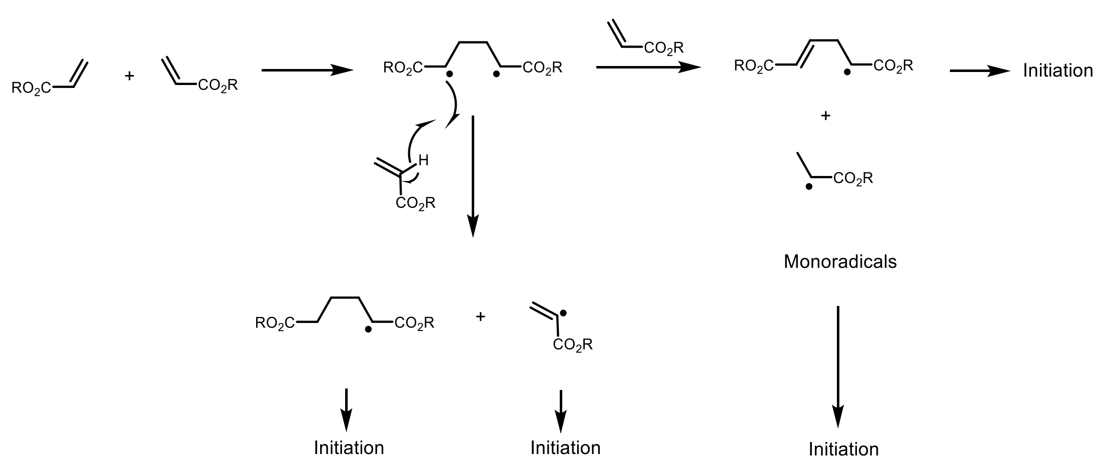

Scheme 3.4 Mechanism for Radical Auto-Initiation of Acrylates as Postulated by Soroush[45]

3.4 Characterization of PVC Copolymers

Characterization by Fourier Transform Infrared (FTIR), and [1]H Nuclear Magnetic Resonance (NMR) spectroscopies, and Gel Permeation Chromatography (GPC) of the functionalized PVC graft copolymers provided important structural information. All five modified polymers show a distinctive ester carbonyl peak around 1740 cm^{-1} in the FTIR (**Figure 3.4**), confirming the incorporation of acrylates into these modified PVC samples.

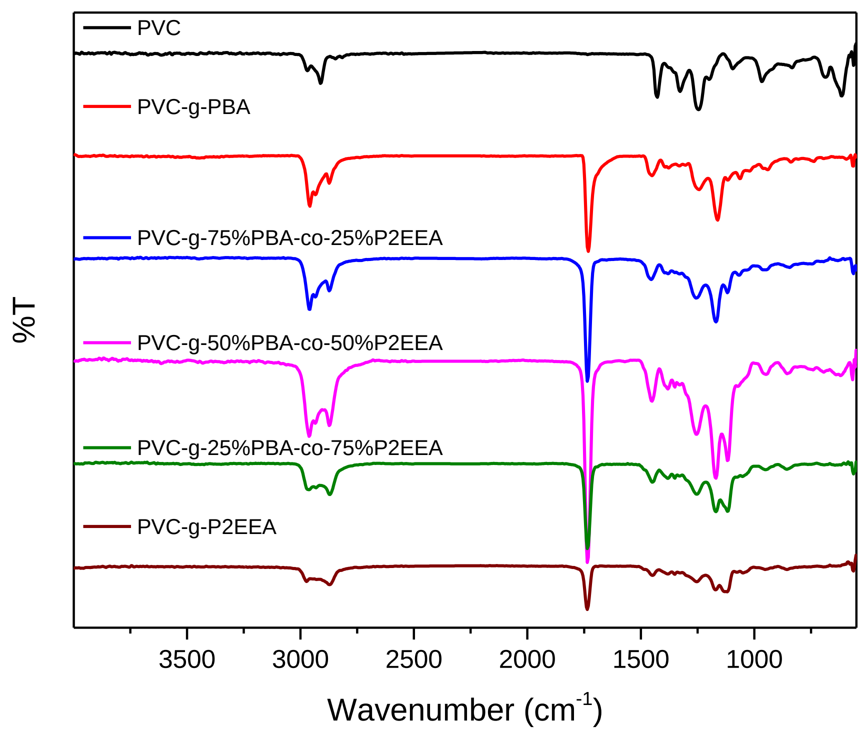

Figure 3.4 FTIR of PVC-*g*-PBA, PVC-*g*-(PBA-*co*-P2EEA), and PVC-*g*-P2EEA Graft Polymers

In the [1]H NMR spectrum (**Figure 3.5**), the CH-Cl methine protons **a** of PVC appear at 4.6-4.2 ppm, the -CH_2-O-C=O methylene protons **c'** of PBA are seen at 4.0 ppm. The -CH_3 methyl protons **f'** are seen at 0.93 ppm. The NMR data clearly demonstrate the presence of PVC and PBA in the graft copolymers.

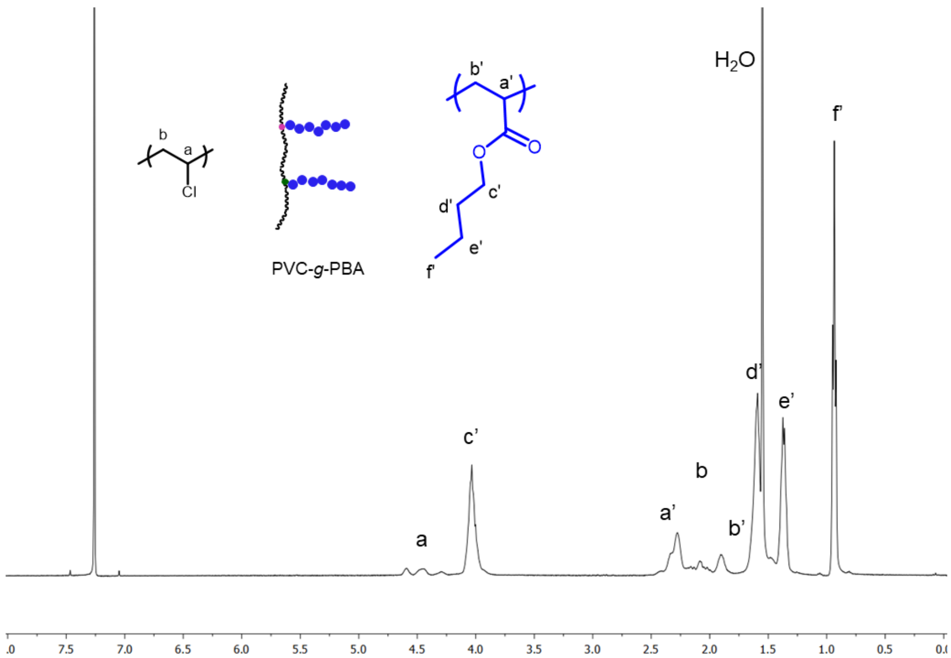

Figure 3.5 ^{1}H NMR Spectrum of PVC-*g*-PBA

The ^{1}H NMR spectrum of PVC-*g*-P2EEA is shown in **Figure 3.6**. The -CH$_2$-O-C=O methylene protons of P2EEA have a chemical shift of 4.2 ppm. The -CH$_3$ methyl protons are

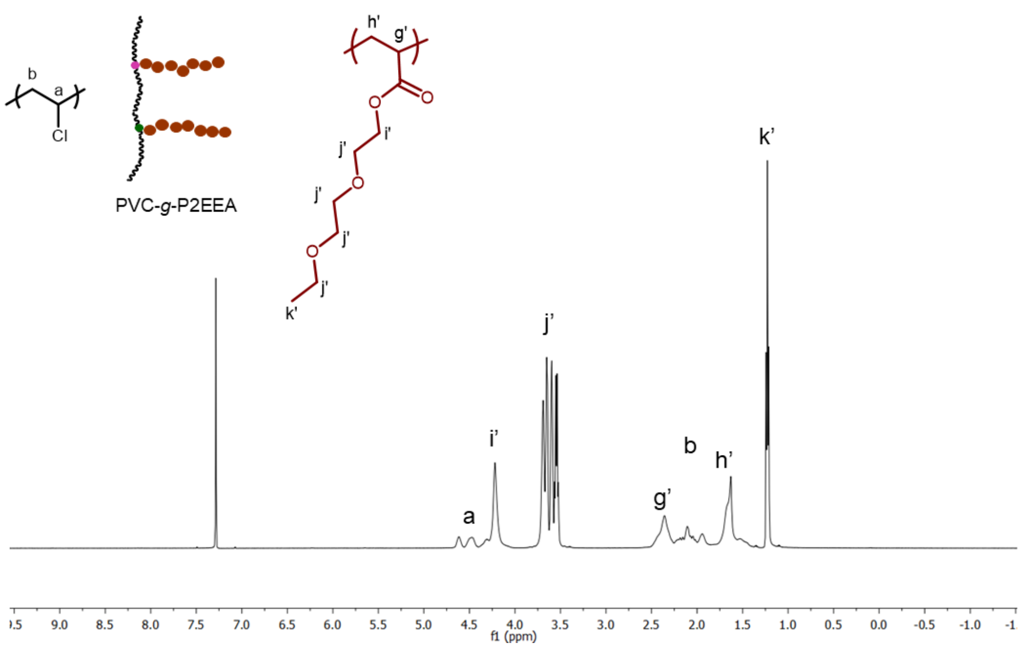

Figure 3.6 ^{1}H NMR Spectrum of PVC-*g*-P2EEA

seen at 1.20 ppm. The presence of both PVC and P2EEA in the graft copolymers is clearly supported by this ^{1}H NMR spectrum. The ^{1}H NMR spectra of all five polymers (made on a 2 g scale) are shown in **Figure 3.7**.

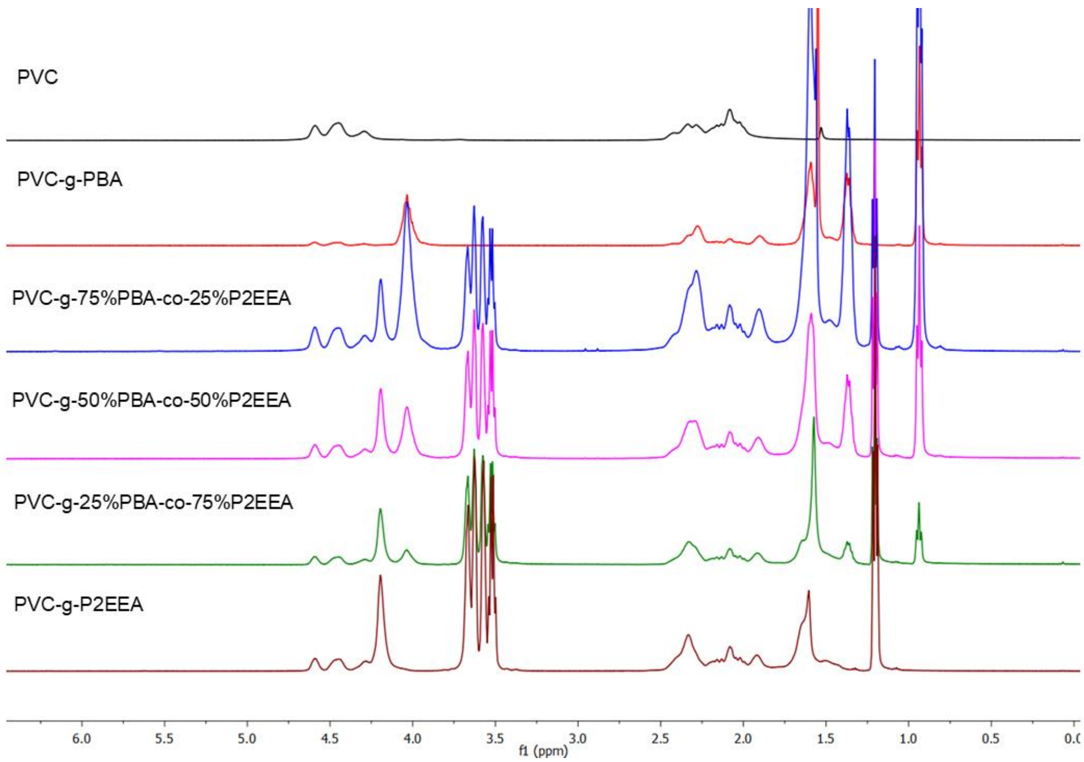

Figure 3.7 ^{1}H NMR Spectra of PVC-*g*-PBA, PVC-*g*-(PBA-*co*-P2EEA), PVC-*g*-P2EEA

3.5 Composition and Relative Size of the New Grafts

Information on the composition and relative size of the new grafts as determined by ^{1}H NMR is summarized in **Table 3.2**. The integration of the CH-Cl methine protons (**Figure 3.8**, proton **a**) of PVC, of the -CH_2-O-C=O methylene protons (**Figure 3.8**, proton **b**) of PBA, and of the -CH_2-O-C=O methylene protons (**Figure 3.8**, proton **b'**) of P2EEA were used to determine the ratio of PVC to total polyacrylate in the functionalized polymers (**Equation 3.2**).

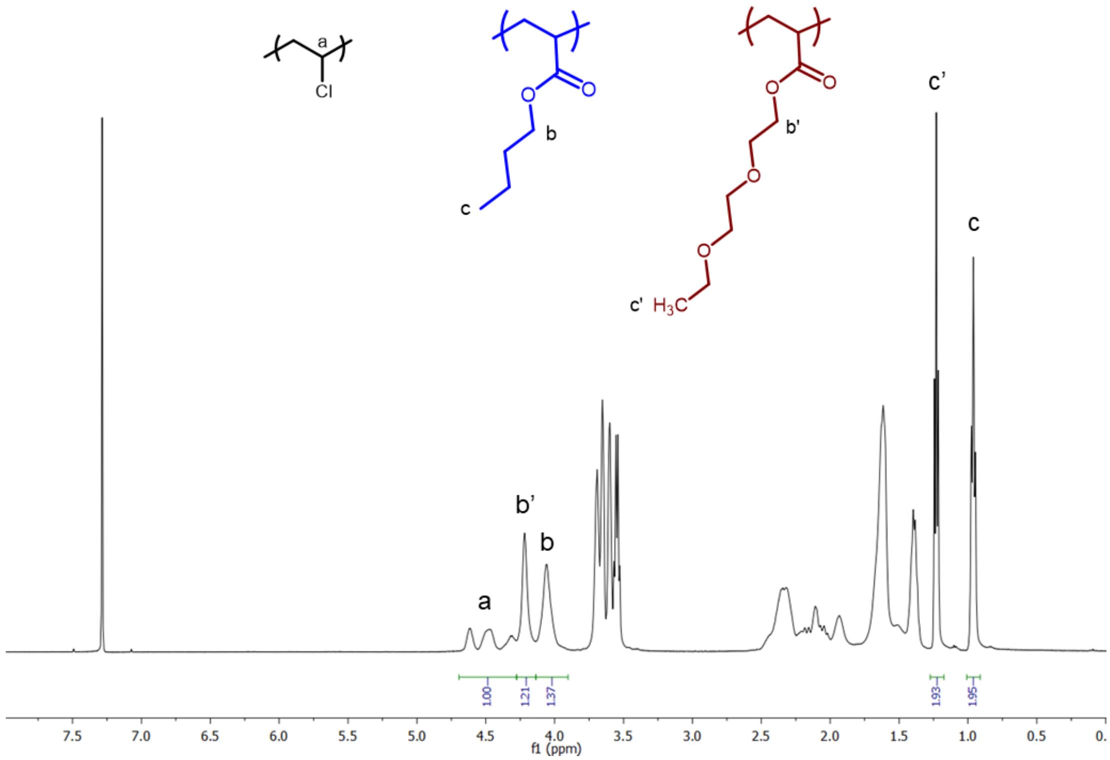

Figure 3.8 ^{1}H NMR Spectrum of PVC-*g*-(50%PBA-*co*-50%P2EEA) as an Example

$$PVC : Polyacrylate$$
$$= Intergration_{CH-Cl\ methine,PVC} : \frac{Intergration_{\text{-CH}_2\text{–O–C=O methylene, PBA+P2EEA}}}{2}$$
$$= Intergration_a : \frac{Intergration_{b+b'}}{2}$$

Equation 3.2

The ratio of PBA to P2EEA was calculated (**Equation 3.3**) based on the integration of the methyl protons of PBA at 0.9 ppm (**Figure 3.8**, proton **c**) and the methyl protons of P2EEA at 1.2 ppm (**Figure 3.8**, proton **c'**). The ratios of incorporated acrylate monomers were very close to the initial monomer ratios, indicating the two monomers have similar addition rates in ATRP.

$$PBA : P2EEA = Intergration_{-CH_3,\ PBA} : Intergration_{\text{-CH}_3,\ \text{P2EEA}}$$
$$= Intergration_{c} : Intergration_{c'} \qquad \textbf{Equation 3.3}$$

Interestingly, the relative length of the polyacrylate graft (a combination of PBA and polyether) decreases with increasing amounts of 2EEA monomer, from PBA : PVC = 1.6 : 1.0 (for 100% BA) to P2EEA : PVC = 1.0 : 1.0 (for 100% 2EEA). This may be an artifact of the work-up procedure, in which MeOH was used to precipitate the polymer, preferentially dissolving the P2EEA-rich copolymers. The PVC graft copolymer samples were not completely soluble in the $CDCl_3$ solvent, thus it is likely that the ratios obtained by integration are not accurate.

Table 3.2 Composition of Graft Copolymers based on ^{1}H NMR Analysis

Monomer Ratio used BA : 2EEA	Polymer P(BA) : P(2EEA)[a] (2 g and 14 g scale)	Graft (PBA+P2EEA) : PVC[a] (2 g scale)	Graft (PBA+P2EEA) : PVC[a] (14 g scale)
BA only	PBA only	1.6 : 1.0	1.4 : 1.0
75% : 25%	3.0 : 1.0	1.4 : 1.0	1.3 : 1.0
50% : 50%	1.0: 1.0	1.3 : 1.0	1.0 : 1.0
25% : 75%	1.0 : 2.9	1.1 : 1.0	1.2 : 1.0
2EEA only	P2EEA only	1.0 : 1.0	0.8 : 1.0

[a] By ^{1}H NMR integration; samples were not completely soluble in the $CDCl_3$ NMR solvent. The dissolved sample was assumed to represent the same composition as the bulk sample.

The weight percent of total plasticizer was calculated by gravimetry (**Equation 3.4**). There was 73 – 80% plasticizer for all samples (**Table 3.3**). The very similar results on both 2 g and 14 g scales demonstrates the reproducibility and easy scale-up of this simple ATRP modification of PVC. When scaled up to 14 g, the results were even better than the initial 2 g batch, indicating that this one step self-plasticization method can be industrially relevant.

$$Weight\ percent\ plasticizer = \frac{Weight_{resulting\ PVC\ copolymer} - Weight_{initial\ PVC}}{Weight_{resulting\ PVC\ copolymer}} \times 100\%$$

Equation 3.4

Table 3.3 Weight Percent Plasticizer

Samples	Wt% plasticizer (grav.) (2 g scale)	Wt% plasticizer (grav.) (14 g scale)
PVC-*g*-PBA	80%	80%
PVC-*g*-75%PBA-*co*-25%P2EEA	75%	79%
PVC-*g*-50%PBA-*co*-50%P2EEA	75%	77%
PVC-*g*-25%PBA-*co*-75%P2EEA	73%	78%
PVC-*g*-P2EEA	73%	78%

3.6 Glass Transition Temperatures of PVC Graft Copolymers

The glass transition temperatures (T_g) of the internally plasticized PVC samples were probed by differential scanning calorimetry (DSC). The DSC data show only a single T_g value for each sample, indicating no phase separation (**Table 3.4** and **Figure 3.9**). For both 2 g and 14 g scale samples, the T_g decreased with increasing amounts of P2EEA. All functionalized polymers physically displayed great flexibility at room temperature, and exhibited T_g values lower than 0 °C. The lowest T_g value achieved was for PVC-*g*-P2EEA (2 g scale) and PVC-*g*-25%PBA-*co*-75%P2EEA (14 g scale). The PVC-*g*-PBA samples displayed slightly higher T_g values of -30.0 °C (2 g scale) and -25.3 °C (14 g scale). Comparing the samples prepared on the 2 g and 14 g scale, the T_g values are very close, consistently showing a decrease in the T_g value with increasing P2EEA content, attesting to the efficiency of the polyether functionality as a PVC plasticizer.[5,6,17,18]

Table 3.4 T_g data for Grafted PVC Copolymers

Samples	T_g (°C) (2 g scale)	T_g (°C) (14 g scale)
PVC	83.6	-
PVC-*g*-PBA	-30.0	-25.3
PVC-*g*-75%PBA-*co*-25%P2EEA	-41.4	-38.4
PVC-*g*-50%PBA-*co*-50%P2EEA	-47.9	-44.7
PVC-*g*-25%PBA-*co*-75%P2EEA	-48.5	-49.6
PVC-*g*-P2EEA	-50.3	-48.9

1) 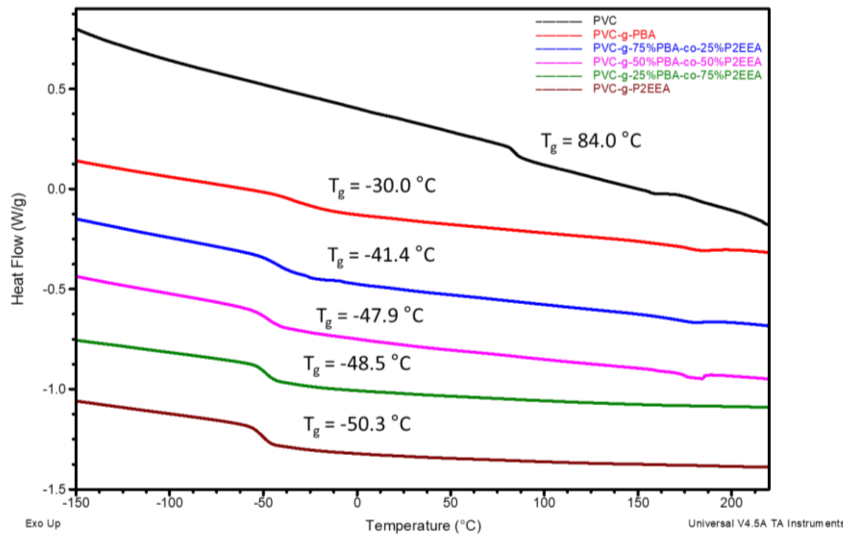

2) 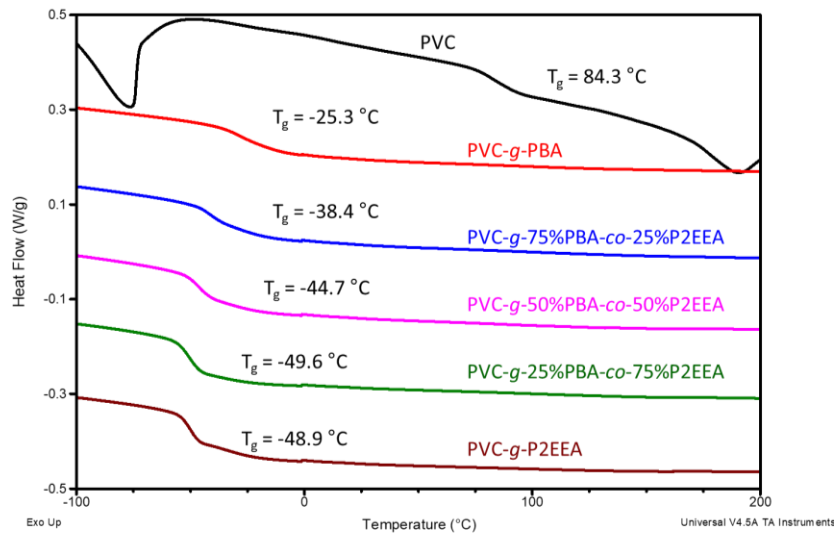

Figure 3.9 DSC (2nd heat cycle) of Grafted PVC Polymers: 1) 2 g Scale and 2) 14 g Scale

There are several conclusions from the T_g data: 1) there is no microphase separation appears in these PVC graft copolymers, as only a single T_g value is observed; 2) T_g values for all PVC graft polymers are lower than -25 °C, indicating great flexibility; 3) T_g values are very similar for both reaction scales, showing that the ATRP process is easy to scale up, which bodes well for industrial applications; 4) the flexibility (T_g value) of the polymer can be tuned by altering the ratio of BA and 2EEA; 5) P2EEA (the polyether chain) is more efficient as a plasticizer compared to PBA (polyalkyl chain). In particular, comparison of PVC-*g*-25%PBA-*co*-75%P2EEA with PVC-*g*-PBA shows that addition of 25% P2EEA leads to a significant decrease of T_g from -25 °C to -38 °C. Further increasing the amount of P2EEA successively lowers the T_g values decrease. PVC-*g*-25%PBA-*co*-75%P2EEA and PVC-*g*-P2EEA have very similar T_g values. Considering that monomer 2EEA is more expensive (2EEA: $0.20/g; BA: $0.04/g), BA : 2EEA = 3 : 1 yielding PVC-*g*-75%PBA-*co*-25%P2EEA is an attractive ratio when taking both price and plasticizing efficiency into account.

In comparing Hong's[32] work, which showed two T_g values for PVC-*g*-POEM (**Scheme 1.32**), there are several differences to this new ATRP work. Both the monomer and the reaction conditions are different. The observed phase separation observed by Hong may be due to the use of a methacrylate monomer (poly(oxyethylene methacrylate)): the methacrylate installs a quarternary center every two carbons of the graft, making a big difference in the flexibility of the pendant graft chains.

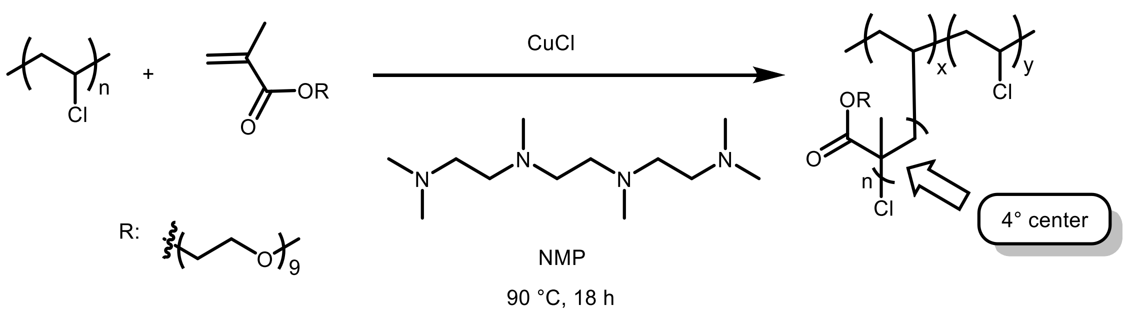

Scheme 1.32 Hong's Covalent Attachment of POEM to PVC via ATRP[32]

3.7 Plasticization Efficiencies of Polyacrylates Grafts

Plasticization efficiencies were calculated based on **Equation 2.8 - 2.12** (**Chapter 2**). The weight percent plasticizer of the graft copolymers was based on gravimetry (**Table 3.3)**. **Equation 2.11** using the conventional phthalate plasticizer DEHP was developed in the thesis of Chad Higa in the Braslau group based on his experimental results.[48] The plasticization efficiencies for all grafts are higher than 70% (**Table 3.5**). The highest plasticization efficiency is shown by the P2EEA graft homopolymer (2 g scale). The lowest plasticization efficiency is for the PBA graft homopolymer. The efficiency increases with increasing percentage of P2EEA, which is consistent with the conclusion that the polyether functionality is more efficient than alkyl chains as a PVC plasticizer.[5,6,17,18] In conclusion, the plasticization efficiencies are very high (71 – 87%). Even though the graft plasticizers are not as good as DEHP in terms of plasticization efficiencies, there is no migration of plasticizers from the PVC matrix using this graft copolymer strategy.

$$E_{\Delta T_g} = \frac{\Delta T_{g,plasticizer}}{\Delta T_{g,DEHP}} \times 100\%$$ **Equation 2.8**

$$\Delta T_{g,plasticizer} = T_{g,unmodified\ PVC} - T_{g,modified\ PVC}$$ **Equation 2.9**

$$\Delta T_{g,DEHP} = T_{g,unmodified\ PVC} - T_{g,DEHP}$$ **Equation 2.10**

$$T_{g,DEHP} = 0.0186x^2 - 3.4124x + 80.898$$ **Equation 2.11**

$$x\ (\%) = weight\ percent\ plasticizer$$ **Equation 2.12**

Table 3.5 Plasticization Efficiency of Polyacrylates Grafts

	$\Delta T_{g,plasticizer}$ (2 g)	$\Delta T_{g,DEHP}$ (2 g)	$E_{\Delta T_g}$ (2 g)	$\Delta T_{g,plasticizer}$ (14 g)	$\Delta T_{g,DEHP}$ (14 g)	$E_{\Delta T_g}$ (14 g)
PVC-*g*-PBA	114	156.7	73%	109.6	157.4	70%
PVC-*g*-75%PBA-*co*-25%P2EEA	125.4	154.0	81%	122.7	156.9	78%
PVC-*g*-50%PBA-*co*-50%P2EEA	131.9	154.0	86%	129.0	155.9	83%
PVC-*g*-25%PBA-*co*-75%P2EEA	132.5	152.7	87%	133.9	156.4	86%
PVC-*g*-P2EEA	134.3	152.7	88%	133.2	156.4	85%

3.8 Thermal Stability of PVC and Its Copolymers

Thermogravimetric analysis (TGA) and Derivative Thermogravimetry (DTG) were measured to examine the thermal stabilities of PVC and these new PVC graft copolymers.

3.8.1 Thermal Stability of PVC

PVC has a two-stage degradation below 500 °C (**Figure 3.10**).[49] The first stage occurs at ~200 °C due to dehydrochlorination, with the formation of HCl and benzene as major byproducts. The second stage starts at ~360 °C, resulting in the formation of other aromatics.[50,51]

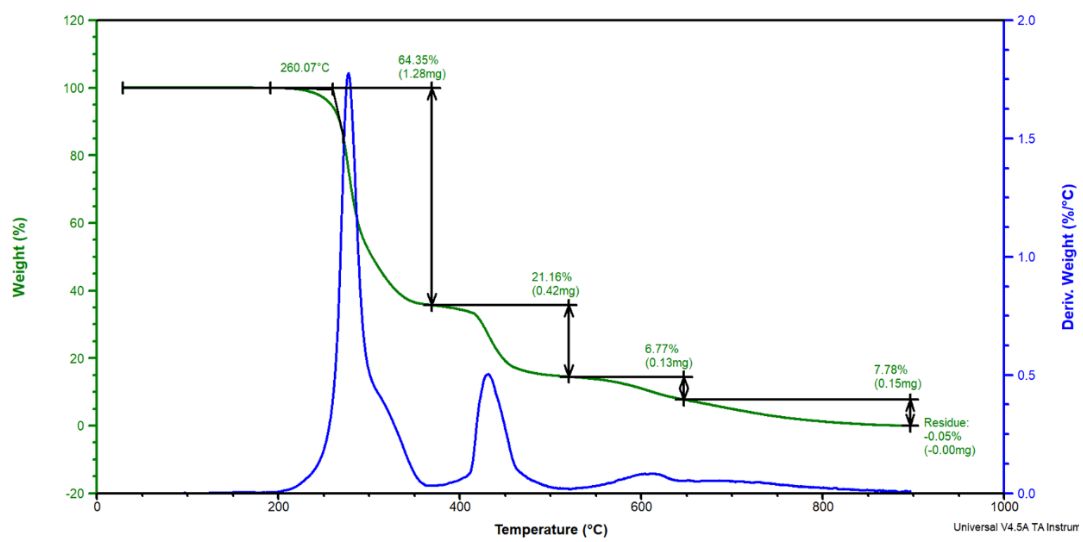

Figure 3.10 TGA (Green) and DTG (Blue) Curves of PVC

The reactive tertiary and allylic chlorine atoms at defect sites are expected to be the most reactive to dehydrochlorination. As mentioned before, allylic chlorides range from 0.05-0.72/1000 vinyl chloride units,[39,40] and tertiary chlorides from 0.7-2.1/1000 vinyl chloride units.[41] Rate constants for dehydrochlorination of tertiary chlorine, allylic chlorine, and secondary chlorine have been calculated to be 1.75×10^{-3}, 1.17×10^{-3}, and 5.00×10^{-7} s^{-1}, respectively.[52] The relative rate constants for dehydrochlorination for different types of chlorines are as follows: tertiary chlorine > allylic chlorine >> secondary chlorine. There is a higher amount of tertiary chlorides, which contributes to their function as the most important initiation sites.[40,51,53] A mathematical model was established by Hjertberg and Sörvik (**Equation 3.5**).[52,54]

$$V_{Hcl} = 0.0105 \times Cl_{tertiary} + 0.0067 \times Cl_{allylic} + 0.0030$$ **Equation 3.5**

V_{Hcl}: initial rate constant of PVC degradation in % moles per minute

$Cl_{tertiary}$: the concentration of tertiary chlorine in mol per 1000 VC unit

$Cl_{allylic}$: the concentration of allylic chlorine in mol per 1000 VC unit

A four-center mechanism for HCl elimination was postulated by Bacaloglu *et al*. based on a series of small molecule models (**Figure 3.11**).[52,55,56] Formation of the new alkene further accelerates the speed of subsequent dehydrochlorination. The rate constants of dehydrochlorination for different types of chlorines in PVC are shown in **Table 3.6**.[57]

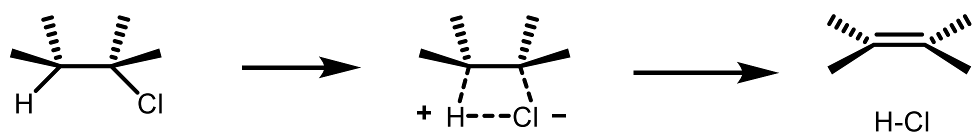

Figure 3.11 Fisch's Four-Center Mechanism of HCl Elimination[56]

Table 3.6. Rate Constants of Dehydrochlorination for Different Types Chlorines in PVC[57]

Types of chlorines	Rate constant, s^{-1}
~CHCl-CH_2~	7.4×10^{-8},[a]
	2.1×10^{-7},[b]
~CH=CH-CHCl-CH_2~	4.0×10^{-4}
~CH=CH-CH=CH-CHCl-CH_2~	1.1×10^{-1}

[a]Turcsányi[58]. [b]Troitskaya[59]

HCl catalyzes the dehydrochlorination of unsaturated PVC; one possible mechanism has been postulated by Wypych[50] (**Figure 3.12**). Overall, labile chlorines initiate a chain reaction of dehydrochlorination of PVC, leading to thermal degradation.

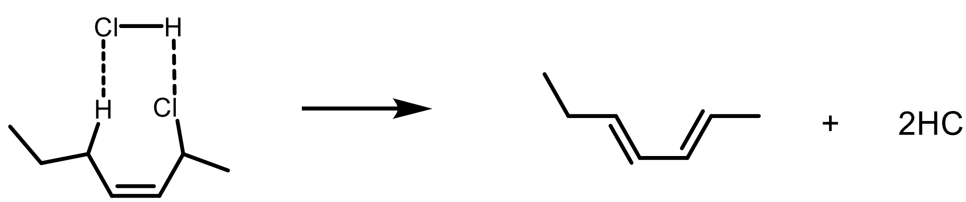

Figure 3.12 Possible Mechanism for HCl Catalyzed Dehydrochlorination[50]

3.8.2 Thermal Stabilities of PVC Graft Copolymers

The TGA and DTG curves of PVC graft copolymers are shown in **Figure 3.13** and **Figure 3.14**, respectively. The data are summarized in **Table 3.7** for 2 g and 14 g scales. The PVC graft copolymers have higher onset temperatures and higher temperatures at 5% weight loss compared to unmodified PVC. The onset temperatures for PVC graft copolymers are ~270 °C, which are about 10 °C higher than unmodified PVC is (~260 °C). The temperatures at 5% weight loss for PVC graft copolymers are ~280 °C, which are 20 °C higher than unmodified PVC. The reason can be explained by the thermal degradation mechanism of PVC. Since the reactive tertiary and allylic chlorine atoms at defect sites are expected to initiate dehydrochlorination, replacement of these chlorines with carbon grafts by ATRP results in enhanced thermal stability. Polyvinyl acrylates such as PBA degrade in a one-stage process starting at ~300 °C,[60] forming carbon dioxide, alkenes, and butyl alcohol. The grafted PVC copolymers predominantly display two main stages during the decomposition process (**Figure 3.13**). The first stage occurs from ~270 °C to ~320 °C, with a weight loss ranging from 16% to 24%. This is likely caused by dehydrochlorination of PVC. At ~320 °C, the degradation is dominated by the polyacrylate portion. The differences in the TGA curves between the PVC graft copolymers are very small. PVC-g-PBA has a slightly steeper slope for the second stage compared to other copolymers. There is no significant dependence of the TGA and DTG data on the scale of polymerization (**Table 3.7**), which is consistent with the conclusion that the ATRP reaction conditions are easily scalable. In summary, all of the graft polymers were more thermally stable materials compared to unmodified PVC, and the thermal stabilities of these novel internally plasticized materials remain consistent when the polymerizations are scaled up.

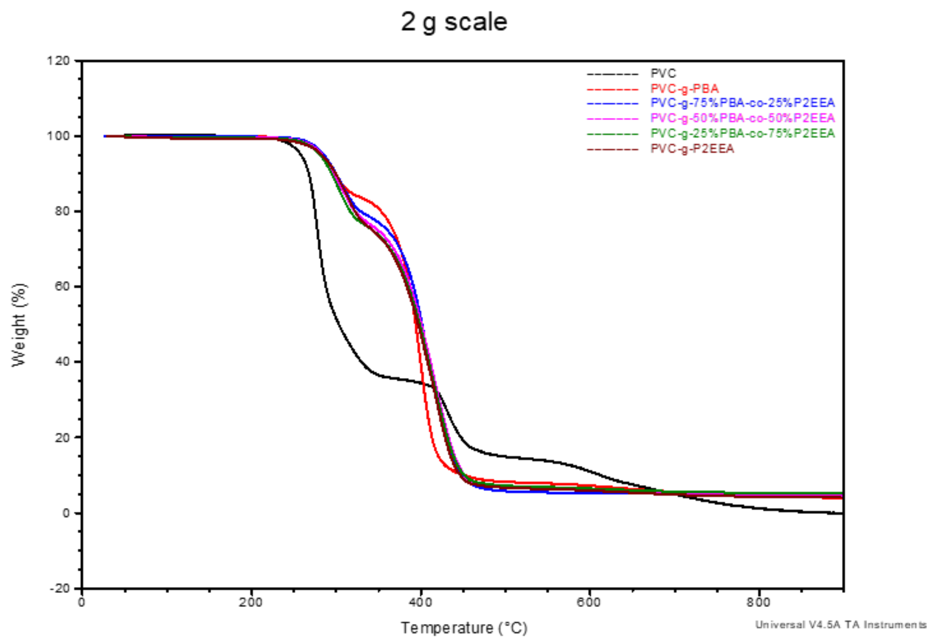

1)

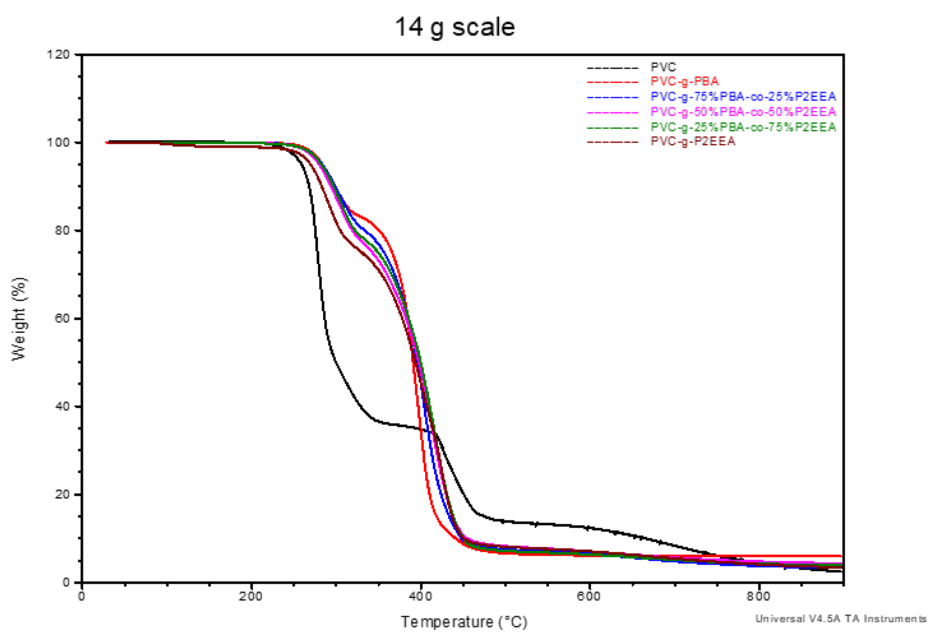

2)

Figure 3.13 TGA Curves of Samples Made on: 1) 2 g Scale and 2) 14 g Scale

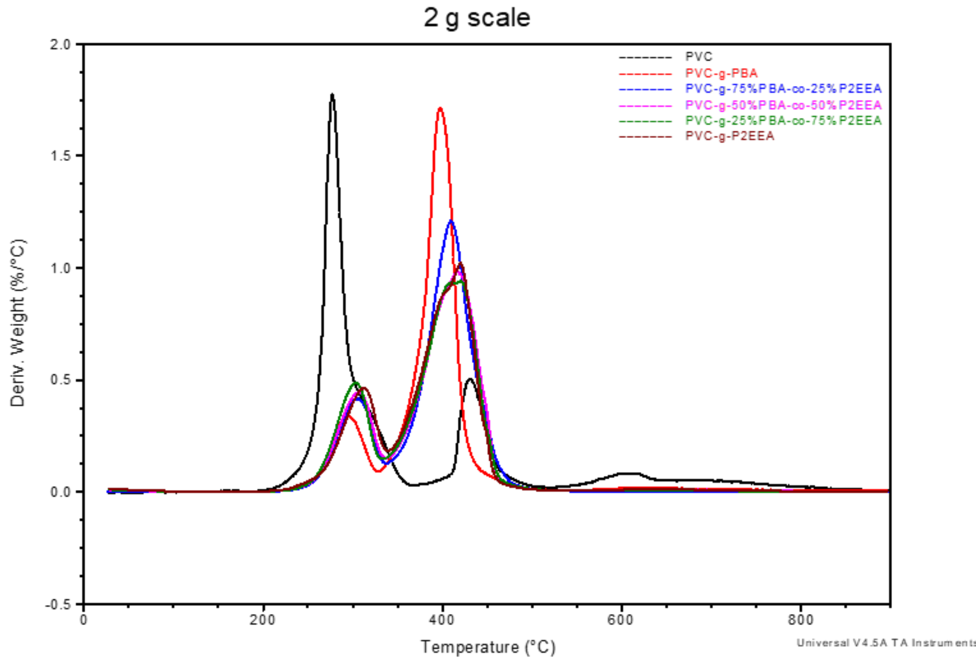

1)

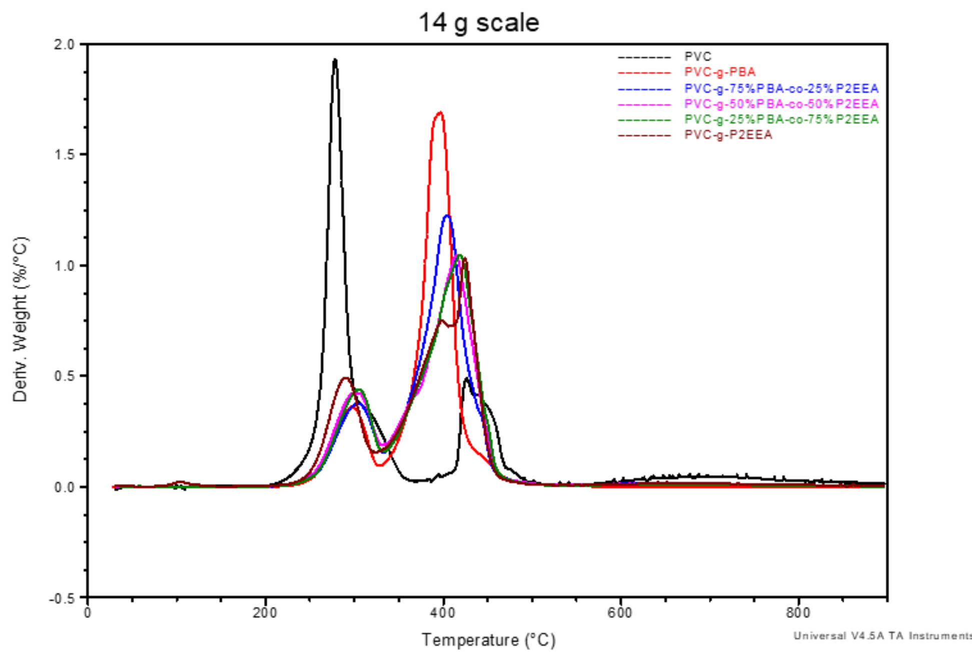

2)

Figure 3.14 DTG curves of Samples Made on: 1) 2 g Scale and 2) 14 g Scale

Table 3.7 TGA Data for PVC Graft Copolymers Prepared on the 2 g Scale (Yellow) and 14 g Scale (Blue)

Compounds	Temp.at 5% weight loss (°C)	Onset temp. (°C)	Residue (%) at 900 °C	Mass loss first stage(%)	Mass loss second stage(%)	Mass loss third stage(%)	Mass loss fourth stage(%)	$T_{d,1}$ (°C)	$T_{d,2}$ (°C)	$T_{d,3}$ (°C)
PVC	258.2	260.1	-0.1	64.4	21.2	6.8	7.8	277.2	-	431.1
PVC	258.7	261.4	2.5	54.5	9.7	22.3	11.0	278.2	-	426.6
PVC-*g*-PBA	282.5	269.1	4.0	16.2	75.9	4.0	-	293.2	397.4	-
PVC-*g*-PBA	283.4	271.0	6.0	16.9	71.8	5.3	-	297.3	397.1	-
PVC-*g*-75%PBA-*co*-25%P2EEA	285.1	273.2	5.2	21.2	73.6	-	-	305.3	409.4	-
PVC-*g*-75%PBA-*co*-25%P2EEA	283.3	269.4	3.4	20.0	72.8	3.8	-	303.4	404.1	-
PVC-*g*-50%PBA-*co*-50%P2EEA	283.1	273.6	4.6	23.1	72.3	-	-	305.9	416.1	-
PVC-*g*-50%PBA-*co*-50%P2EEA	279.6	269.6	4.4	23.0	69.3	3.4	-	303.0	414.1	-
PVC-*g*-25%PBA-*co*-75%P2EEA	280.6	273.2	5.2	23.6	71.2	-	-	303.6	420.4	-
PVC-*g*-25%PBA-*co*-75%P2EEA	282.3	272.7	3.9	21.9	71.4	2.9	-	304.9	418.9	-
PVC-*g*-P2EEA	282.9	274.3	4.1	24.3	69.4	-	2.2	312.1	420.0	-
PVC-*g*-P2EEA	269.4	265.0	3.5	23.2	37.2	30.8	4.4	290.1	398.8	424.4

3.9 GPC Results of PVC Graft Copolymers

Gel Permeation Chromatography (GPC) is a type of size exclusion chromatography (SEC) which separates polymers by their effective volume. GPC was used to analyze polymer molecular weight distributions. In GPC, polymer molecules elute from the column based on approximate size. Larger molecules come out first. To determine the unknown polymer molecular weight, a calibration curve is applied using molecular weight standards; linear polystyrene standards were used. M_p (peak molecular weight), M_n (number-average molecular weight, **Equation 3.6**), M_w (weight-average molecular weight, **Equation 3.7**), M_z (Z-average molecular weight, **Equation 3.8**) and PD (polydispersity, **Equation 3.9**) were determined by GPC for all PVC graft copolymers. For synthetic polymers: $M_n<M_w<M_z$.

$$M_n = \frac{\sum N_i M_i}{\sum N_i}$$ **Equation 3.6**

$$M_w = \frac{\sum N_i M_i^2}{\sum N_i M_i}$$ **Equation 3.7**

$$M_z = \frac{\sum N_i M_i^3}{\sum N_i M_i}$$ **Equation 3.8**

M_i: the molecular weight of a chain

N_i: the number of chains of that molecular weight

$$PD = \frac{M_w}{M_n}$$ **Equation 3.9**

The GPC traces of the PVC graft copolymers are shown in **Figure 3.15**. Compared to unmodified PVC, the retention times of all of the PVC graft copolymers are slightly decreased, reflecting their higher weights and volumes. The peak sizes of the PVC graft copolymers are significantly less than those of unmodified PVC. This may be due to the poor solubilities of the PVC graft copolymers in THF, indicative of possible crosslinking during the 24 h polymerization. These graft copolymers were also poorly soluble in common solvents including DMFand NMP.

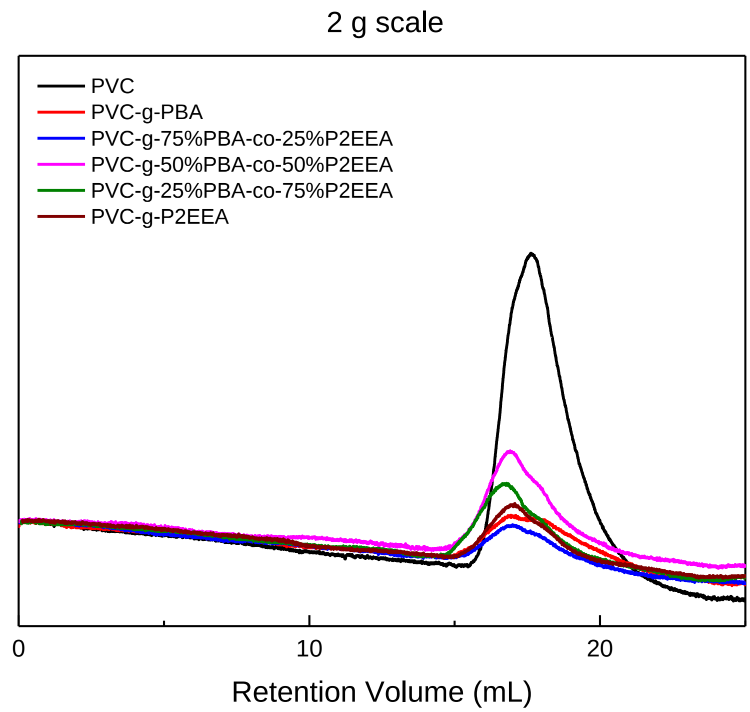

1)

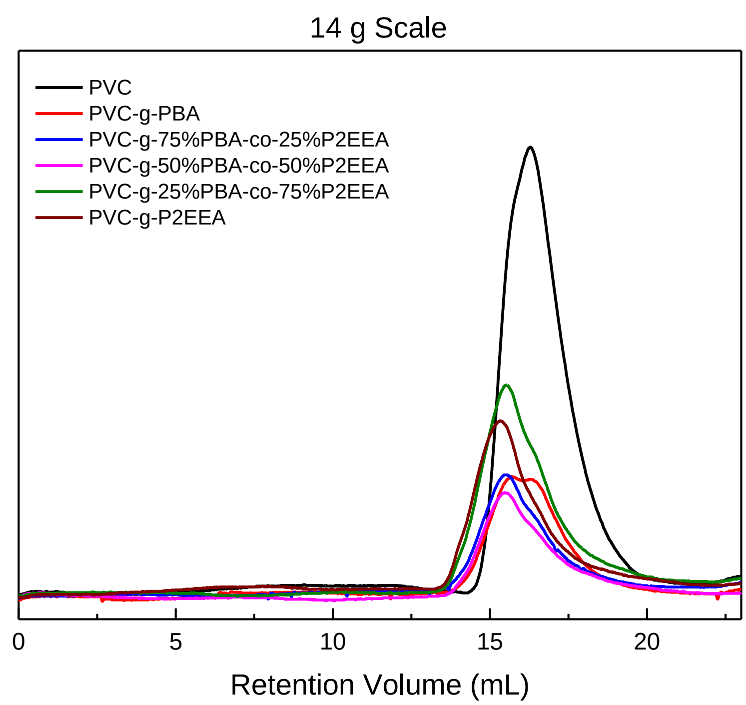

2)

Figure 3.15 GPC Traces of PVC Graft Copolymers: 1) 2 g Scale and 2) 14 g Scale

Interestingly, PVC-*g*-PBA shows a bimodal distribution. Some of these polymers show a shoulder corresponding to unmodified PVC, indicating that some unreacted PVC homopolymer remains.

The values of M_p, M_w, and M_z of the functionalized PVC samples are significantly larger compared to unmodified PVC (**Table 3.8**). The values of M_n for some of the 14 g scale graft copolymers with larger than 50% P2EEA are smaller than the apparent M_n values for unmodified PVC. This is likely due to: 1) the poor solubility of the larger molecular weight, possibly crosslinked polymers, leaving only the smaller members in solution; 2) the inaccuracy of using linear polystyrene as molecular weight standards for these polymer brushes. The graft copolymers are dense, structurally complex species that take up volume in a manner far different from a linear polymer chain.

Table 3.8 GPC of PVC and the Resulting Graft Copolymers on the 2 g Scale (Yellow) and 14 g Scale (Blue)

Samples	M_p	M_n	M_w	M_z	PD
PVC	74,292	38,818	79,916	130,585	2.1
PVC	68,869	36,411	73,053	114,440	2.0
PVC-*g*-PBA	127,483	39,700	113,565	284,191	2.9
PVC-*g*-PBA	112,543	34,034	108,192	244,293	3.2
PVC-*g*-75%PBA-*co*-25%P2EEA	128,227	46,457	126,394	247,734	2.7
PVC-*g*-75%PBA-*co*-25%P2EEA	137,340	44,642	140,454	286,532	3.2
PVC-*g*-50%PBA-*co*-50%P2EEA	145,078	46,010	145,214	296,674	3.2
PVC-*g*-50%PBA-*co*-50%P2EEA	140,688	30,775	132,957	277,584	4.3
PVC-*g*-25%PBA-*co*-75%P2EEA	173,590	47,486	187,444	419,274	3.9
PVC-*g*-25%PBA-*co*-75%P2EEA	135,636	29,958	136,902	289,786	4.6
PVC-*g*-P2EEA	140,902	49,093	148,200	300,457	3.0
PVC-*g*-P2EEA	163,642	34,337	165,613	342,201	4.8

3.10 Concerns with Using Copper

A big concern with using Cu-mediated ATRP is the residual copper in the resulting polymer. For example, on the 14 g scale, approximately 200 mg of CuBr was used. Although the graft co-polymer samples were washed with methanol several times to remove both catalyst and ligand, some polymers still had a faint green color, indicating residual copper. This contamination limits the applications of these polymers in medical devices and food packaging. Efforts aimed at reducing the amount of copper, for example following Matyjaszewski's work[24] with activated ligands, are ongoing in our lab.

3.11 Conclusion

A series of PVC-*g*-(PBA-*co*-P2EEA) polymers were prepared by ATRP in a single step, resulting in materials with T_g values as low as -50 °C. Several conclusions can be drawn from this systematic study. Most importantly, all of these internally plasticized PVC graft copolymers were homogeneous (non-phase separated) materials, as reflected by single T_g temperatures. Grafts made of pendent polyethers are more efficient plasticizers compared to pendant poly(*n*-butyl) esters, although mixtures of the two monomers can be used to tune the T_g value. This is the first time that polyether grafts have been attached to PVC via ATRP to achieve very low T_g values without phase separation. In addition to highly effective internal plasticization, these graft copolymers display enhanced thermal stability, as the ATRP process removes the particularly labile tertiary and allylic chlorine atoms at the defect sites. The graft polymerization was carried out initially on 0.5 g of PVC, forming about 2 g of derivatized PVC. This was easily scaled up to form 14 g of plasticized PVC: the properties of the resulting materials on both scales are very similar. This bodes well for the scalability of this process, which can be envisioned to be applicable on an industrial level. Overall, the internal plasticization of PVC has been successfully demonstrated using operationally simple ATRP to give flexible, homogeneous graft copolymers.

3.12 References

(1) X. Q. Wen; X. H. Liu; G. S. Liu. Prevention of Plasticizer Leaching From the Inner Surface of Narrow Polyvinyl Chloride Tube by DC Glow Discharge Plasma. *IEEE Trans. Plasma Sci.* **2010**, *38* (11), 3152–3155. https://doi.org/10.1109/TPS.2010.2074209.

(2) Reddy, N. N.; Mohan, Y. M.; Varaprasad, K.; Ravindra, S.; Vimala, K.; Raju, K. M. Surface Treatment of Plasticized Poly(Vinyl Chloride) to Prevent Plasticizer Migration. *J. Appl. Polym. Sci.* **2010**, *115* (3), 1589–1597. https://doi.org/10.1002/app.31157.

(3) Navarro, R.; Perrino, P. M.; García, C.; Elvira, C.; Gallardo, A.; Reinecke, H. Opening New Gates for the Modification of PVC or Other PVC Derivatives: Synthetic Strategies for the Covalent Binding of Molecules to PVC. *Polymers* **2016**, *8* (4). https://doi.org/10.3390/polym8040152.

(4) Navarro, R.; Pérez Perrino, M.; Gómez Tardajos, M.; Reinecke, H. Phthalate Plasticizers Covalently Bound to PVC: Plasticization with Suppressed Migration. *Macromolecules* **2010**, *43* (5), 2377–2381. https://doi.org/10.1021/ma902740t.

(5) Navarro, R.; Gacal, T.; Ocakoglu, M.; García, C.; Elvira, C.; Gallardo, A.; Reinecke, H. Nonmigrating Equivalent Substitutes for PVC/DOP Formulations as Shown by a TG Study of PVC with Covalently Bound PEO–PPO Oligomers. *Macromol. Rapid Commun.* **2017**, *38* (6), 1600734-n/a. https://doi.org/10.1002/marc.201600734.

(6) Navarro, R.; Pérez Perrino, M.; García, C.; Elvira, C.; Gallardo, A.; Reinecke, H. Highly Flexible PVC Materials without Plasticizer Migration As Obtained by Efficient One-Pot Procedure Using Trichlorotriazine Chemistry. *Macromolecules* **2016**, *49* (6), 2224–2227. https://doi.org/10.1021/acs.macromol.6b00214.

(7) Jia, P.; Hu, L.; Yang, X.; Zhang, M.; Shang, Q.; Zhou, Y. Internally Plasticized PVC Materials via Covalent Attachment of Aminated Tung Oil Methyl Ester. *RSC Adv.* **2017**, *7* (48), 30101–30108. https://doi.org/10.1039/C7RA04386D.

(8) Jia, P.; Hu, L.; Shang, Q.; Wang, R.; Zhang, M.; Zhou, Y. Self-Plasticization of PVC Materials via Chemical Modification of Mannich Base of Cardanol Butyl Ether. *ACS Sustain. Chem. Eng.* **2017**, *5* (8), 6665–6673. https://doi.org/10.1021/acssuschemeng.7b00900.

(9) Yang, P.; Yan, J.; Sun, H.; Fan, H.; Chen, Y.; Wang, F.; Shi, B. Novel Environmentally Sustainable Cardanol-Based Plasticizer Covalently Bound to PVC via Click Chemistry: Synthesis and Properties. *RSC Adv.* **2015**, *5* (22), 16980–16985. https://doi.org/10.1039/C4RA15527K.

(10) Demirci, G.; Tasdelen, M. A. Synthesis and Characterization of Graft Copolymers by Photoinduced CuAAC Click Chemistry. *Eur. Polym. J.* **2015**, *66*, 282–289. https://doi.org/10.1016/j.eurpolymj.2015.02.029.

(11) Lee, K. W.; Chung, J. W.; Kwak, S.-Y. Structurally Enhanced Self-Plasticization of Poly(Vinyl Chloride) via Click Grafting of Hyperbranched Polyglycerol. *Macromol. Rapid Commun.* **2016**, *37* (24), 2045–2051. https://doi.org/10.1002/marc.201600533.

(12) Jia, P.; Hu, L.; Feng, G.; Bo, C.; Zhang, M.; Zhou, Y. PVC Materials without Migration Obtained by Chemical Modification of Azide-Functionalized PVC and Triethyl Citrate Plasticizer. *Mater. Chem. Phys.* **2017**, *190*, 25–30. https://doi.org/10.1016/j.matchemphys.2016.12.072.

(13) Puyou Jia; Rui Wang; Lihong Hu; Meng Zhang; Yonghong Zhou. Self-Plasticization of PVC via Click Reaction of a Monooctyl Phthalate Derivative. *Pol. J. Chem. Technol.* **2017**, *19* (3), 16–19. https://doi.org/10.1515/pjct-2017-0042.

(14) Earla, A.; Li, L.; Costanzo, P.; Braslau, R. Phthalate Plasticizers Covalently Linked to PVC via Copper-Free or Copper Catalyzed Azide-Alkyne Cycloadditions. *Polymer* **2017**, *109* (Supplement C), 1–12. https://doi.org/10.1016/j.polymer.2016.12.014.

(15) Chu, H.; Ma, J. A Strategy to Prepare Internally Plasticized PVC Using a Castor Oil Based Derivative. *Korean J. Chem. Eng.* **2018**, *35* (11), 2296–2302. https://doi.org/10.1007/s11814-018-0118-5.

(16) Jia, P.; Ma, Y.; Feng, G.; Hu, L.; Zhou, Y. High-Value Utilization of Forest Resources: Dehydroabietic Acid as a Chemical Platform for Producing Non-Toxic and Environment-Friendly Polymer Materials. *J. Clean. Prod.* **2019**, *227*, 662–674. https://doi.org/10.1016/j.jclepro.2019.04.220.

(17) Higa, C. M.; Tek, A. T.; Wojtecki, R. J.; Braslau, R. Nonmigratory Internal Plasticization of Poly (Vinyl Chloride) via Pendant Triazoles Bearing Alkyl or Polyether Esters. *J. Polym. Sci. Part Polym. Chem.* **2018**, *56* (21), 2397–2411.

(18) Li, L.; Tek, A. T.; Wojtecki, R. J.; Braslau, R. Internal Plasticization of Poly(Vinyl) Chloride Using Glutamic Acid as a Branched Linker to Incorporate Four Plasticizers per Anchor Point. *J. Polym. Sci. Part Polym. Chem.* **2019**, *57* (17), 1821–1835. https://doi.org/10.1002/pola.29455.

(19) Rezende, T. C.; Abreu, C. M. R.; Fonseca, A. C.; Higa, C. M.; Li, L.; Serra, A. C.; Braslau, R.; Coelho, J. F. J. Efficient Internal Plasticization of Poly(Vinyl Chloride) via Free Radical Copolymerization of Vinyl Chloride with an Acrylate Bearing a Triazole Phthalate Mimic. *Polymer* **2020**, *196*, 122473. https://doi.org/10.1016/j.polymer.2020.122473.

(20) Sun, Z.; Choi, B.; Feng, A.; Moad, G.; Thang, S. H. Nonmigratory Poly(Vinyl Chloride)-Block-Polycaprolactone Plasticizers and Compatibilizers Prepared by Sequential RAFT and Ring-Opening Polymerization (RAFT-T-ROP). *Macromolecules* **2019**, *52* (4), 1746–1756. https://doi.org/10.1021/acs.macromol.8b02146.

(21) Chang, Y.; Pan, M.; Yuan, J.; Liu, Y.; Wang, X.; Jiang, P.; Wang, Y.; Zhong, G.-J.; Li, Z.-M. Morphology and Film Performance of Phthalate-Free Plasticized Poly(Vinyl Chloride) Composite Particles via the Graft Copolymerization of Acrylate Swelling Flower-like Latex Particles. *RSC Adv.* **2015**, *5* (50), 40076–40087. https://doi.org/10.1039/C5RA04747A.

(22) Matyjaszewski, K.; Xia, J. Atom Transfer Radical Polymerization. *Chem. Rev.* **2001**, *101* (9), 2921–2990. https://doi.org/10.1021/cr940534g.

(23) Matyjaszewski, K. Atom Transfer Radical Polymerization (ATRP): Current Status and Future Perspectives. *Macromolecules* **2012**, *45* (10), 4015–4039. https://doi.org/10.1021/ma3001719.

(24) Matyjaszewski, K.; Tsarevsky, N. V. Macromolecular Engineering by Atom Transfer Radical Polymerization. *J. Am. Chem. Soc.* **2014**, *136* (18), 6513–6533. https://doi.org/10.1021/ja408069v.

(25) Aubrey D. Jenkins; Richard G. Jones; Graeme Moad. Terminology for Reversible-Deactivation Radical Polymerization Previously Called “Controlled” Radical or “Living” Radical Polymerization (IUPAC Recommendations 2010). *Pure Appl. Chem.* **2009**, *82* (2), 483–491. https://doi.org/10.1351/PAC-REP-08-04-03.

(26) Paik, H.; Gaynor, S. G.; Matyjaszewski, K. Synthesis and Characterization of Graft Copolymers of Poly(Vinyl Chloride) with Styrene and (Meth)Acrylates by Atom Transfer Radical Polymerization. *Macromol. Rapid Commun.* **1998**, *19* (1), 47–52. https://doi.org/10.1002/(SICI)1521-3927(19980101)19:1<47::AID-MARC47>3.0.CO;2-Q.

(27) Percec, V.; Asgarzadeh, F. Metal-Catalyzed Living Radical Graft Copolymerization of Olefins Initiated from the Structural Defects of Poly(Vinyl Chloride). *J. Polym. Sci. Part Polym. Chem.* **2001**, *39* (7), 1120–1135. https://doi.org/10.1002/1099-0518(20010401)39:7<1120::AID-POLA1089>3.0.CO;2-Z.

(28) Percec, V.; Cappotto, A.; Barboiu, B. Metal-Catalyzed Living Radical Graft Copolymerization of Butyl Methacrylate and Styrene Initiated from the Structural Defects of Narrow Molecular Weight Distribution Poly(Vinyl Chloride). *Macromol. Chem. Phys.* **2002**, *203* (10-11), 1674–1683. https://doi.org/10.1002/1521-3935(200207)203:10/11<1674::AID-MACP1674>3.0.CO;2-N.

(29) Bicak, N.; Ozlem, M. Graft Copolymerization of Butyl Acrylate and 2-Ethyl Hexyl Acrylate from Labile Chlorines of Poly(Vinyl Chloride) by Atom Transfer Radical Polymerization. *J. Polym. Sci. Part Polym. Chem.* **2003**, *41* (21), 3457–3462. https://doi.org/10.1002/pola.10944.

(30) Bicak, N.; Karagoz, B.; Emre, D. Atom Transfer Graft Copolymerization of 2-Ethyl Hexylacrylate from Labile Chlorines of Poly(Vinyl Chloride) in an Aqueous Suspension. *J. Polym. Sci. Part Polym. Chem.* **2006**, *44* (6), 1900–1907. https://doi.org/10.1002/pola.21298.

(31) Coşkun, M.; Barim, G.; Demirelli, K. A Grafting Study on Partially Dehydrochlorinated Poly(Vinyl Chloride) by Atom Transfer Radical Polymerization. *J. Macromol. Sci. Part A* **2007**, *44* (5), 475–481. https://doi.org/10.1080/10601320701229068.

(32) Ahn, S. H.; Seo, J. A.; Kim, J. H.; Ko, Y.; Hong, S. U. Synthesis and Gas Permeation Properties of Amphiphilic Graft Copolymer Membranes. *J. Membr. Sci.* **2009**, *345* (1), 128–133. https://doi.org/10.1016/j.memsci.2009.08.037.

(33) Patel, R.; Patel, M.; Ahn, S. H.; Sung, Y. K.; Lee, H.-K.; Kim, J. H.; Sung, J.-S. Bioinert Membranes Prepared from Amphiphilic Poly(Vinyl Chloride)-g-Poly(Oxyethylene Methacrylate) Graft Copolymers. *Mater. Sci. Eng. C* **2013**, *33* (3), 1662–1670. https://doi.org/10.1016/j.msec.2012.12.097.

(34) Fang, L.-F.; Matsuyama, H.; Zhu, B.-K.; Zhao, S. Development of Antifouling Poly(Vinyl Chloride) Blend Membranes by Atom Transfer Radical Polymerization. *J. Appl. Polym. Sci.* **2018**, *135* (6), 45832. https://doi.org/10.1002/app.45832.

(35) Lanzalaco, S.; Galia, A.; Lazzano, F.; Mauro, R. R.; Scialdone, O. Utilization of Poly(Vinylchloride) and Poly(Vinylidenefluoride) as Macroinitiators for ATRP Polymerization of Hydroxyethyl Methacrylate: Electroanalytical and Graft-Copolymerization Studies. *J. Polym. Sci. Part Polym. Chem.* **2015**, *53* (21), 2524–2536. https://doi.org/10.1002/pola.27717.

(36) Huang, Z.; Feng, C.; Guo, H.; Huang, X. Direct Functionalization of Poly(Vinyl Chloride) by Photo-Mediated ATRP without a Deoxygenation Procedure. *Polym. Chem.* **2016**, *7* (17), 3034–3045. https://doi.org/10.1039/C6PY00483K.

(37) Liu, K.; Pan, P.; Bao, Y. Synthesis, Micellization, and Thermally-Induced Macroscopic Micelle Aggregation of Poly(Vinyl Chloride)-g-Poly(N-Isopropylacrylamide) Amphiphilic Copolymer. *RSC Adv.* **2015**, *5* (115), 94582–94590. https://doi.org/10.1039/C5RA16726D.

(38) Wypych, G. 1 - CHEMICAL STRUCTURE OF PVC. In *PVC Degradation and Stabilization (Third Edition)*; Wypych, G., Ed.; ChemTec Publishing: Boston, 2015; pp 1–23. https://doi.org/10.1016/B978-1-895198-85-0.50003-0.

(39) Dean, L.; Dafei, Z.; Deren, Z. Mechanism and Kinetics of Thermo-Dehydrochlorination of Poly(Vinyl Chloride). *Polym. Degrad. Stab.* **1988**, *22* (1), 31–41. https://doi.org/10.1016/0141-3910(88)90054-7.

(40) Xie, T. Y.; Hamielec, A. E.; Rogestedt, M.; Hjertberg, T. Experimental Investigation of Vinyl Chloride Polymerization at High Conversion: Polymer Microstructure and Thermal Stability and Their Relationship to Polymerization Conditions. *Polymer* **1994**, *35* (7), 1526–1534. https://doi.org/10.1016/0032-3861(94)90354-9.

(41) Rogestedt, M.; Hjertberg, T. Structure and Degradation of Commercial Poly(Vinyl Chloride) Obtained at Different Temperatures. *Macromolecules* **1993**, *26* (1), 60–64. https://doi.org/10.1021/ma00053a009.

(42) Carroll, W. F.; Johnson, R. W.; Moore, S. S.; Paradis, R. A. 4 - Poly(Vinyl Chloride). In *Applied Plastics Engineering Handbook (Second Edition)*; Kutz, M., Ed.; William Andrew Publishing, 2017; pp 73–89. https://doi.org/10.1016/B978-0-323-39040-8.00004-3.

(43) Starnes, W. H.; Schilling, F. C.; Plitz, I. M.; Cais, R. E.; Freed, D. J.; Hartless, R. L.; Bovey, F. A. Branch Structures in Poly(Vinyl Chloride) and the Mechanism of Chain Transfer to Monomer during Vinyl Chloride Polymerization. *Macromolecules* **1983**, *16* (5), 790–807. https://doi.org/10.1021/ma00239a016.

(44) Starnes, W. H. Structural and Mechanistic Aspects of the Thermal Degradation of Poly(Vinyl Chloride). *Prog. Polym. Sci.* **2002**, *27* (10), 2133–2170. https://doi.org/10.1016/S0079-6700(02)00063-1.

(45) Srinivasan, S.; Kalfas, G.; Petkovska, V. I.; Bruni, C.; Grady, M. C.; Soroush, M. Experimental Study of the Spontaneous Thermal Homopolymerization of Methyl and N-Butyl Acrylate. *J. Appl. Polym. Sci.* **2010**, *118* (4), 1898–1909. https://doi.org/10.1002/app.32313.

(46) Moghadam, N.; Liu, S.; Srinivasan, S.; Grady, M. C.; Soroush, M.; Rappe, A. M. Computational Study of Chain Transfer to Monomer Reactions in High-Temperature Polymerization of Alkyl Acrylates. *J. Phys. Chem. A* **2013**, *117* (12), 2605–2618. https://doi.org/10.1021/jp3100798.

(47) Srinivasan, S.; Lee, M. W.; Grady, M. C.; Soroush, M.; Rappe, A. M. Computational Study of the Self-Initiation Mechanism in Thermal Polymerization of Methyl Acrylate. *J. Phys. Chem. A* **2009**, *113* (40), 10787–10794. https://doi.org/10.1021/jp904036k.

(48) Higa, C. M. Non-Migratory Internal Plasticization of Poly(Vinyl Chloride) via Pendant Triazoles Bearling Alkyl or Polyether Esters, University of California, Santa Cruz, 2018.

(49) McNeill, I. C.; Memetea, L.; Cole, W. J. A Study of the Products of PVC Thermal Degradation. *Polym. Degrad. Stab.* **1995**, *49* (1), 181–191. https://doi.org/10.1016/0141-3910(95)00064-S.

(50) Wypych, G. 4 - PRINCIPLES OF THERMAL DEGRADATION. In *PVC Degradation and Stabilization (Third Edition)*; Wypych, G., Ed.; ChemTec Publishing: Boston, 2015; pp 79–165. https://doi.org/10.1016/B978-1-895198-85-0.50006-6.

(51) Van Cauter, K.; Van Den Bossche, B. J.; Van Speybroeck, V.; Waroquier, M. Ab Initio Study of Free-Radical Polymerization: Defect Structures in Poly(Vinyl Chloride). *Macromolecules* **2007**, *40* (4), 1321–1331. https://doi.org/10.1021/ma062174s.

(52) Bacaloglu, R.; Fisch, M. Degradation and Stabilization of Poly(Vinyl Chloride). II. Simulation of the Poly(Vinyl Chloride) Degradation Processes Initiated in the Polymer Backbone. *Polym. Degrad. Stab.* **1994**, *45* (3), 315–324. https://doi.org/10.1016/0141-3910(94)90201-1.

(53) Fisch, M. H.; Bacaloglu, R. Kinetics and Mechanism of the Thermal Degradation of Poly(Vinyl Chloride). *J. Vinyl Addit. Technol.* **1995**, *1* (4), 233–240. https://doi.org/10.1002/vnl.730010409.

(54) Hjertberg, T.; Sörvik, E. M. Formation of Anomalous Structures in PVC and Their Influence on the Thermal Stability: 3. Internal Chloroallylic Groups. *Polymer* **1983**, *24* (6), 685–692. https://doi.org/10.1016/0032-3861(83)90004-6.

(55) Bacaloglu, R.; Fisch, M. Degradation and Stabilization of Poly(Vinyl Chloride). I. Kinetics of the Thermal Degradation of Poly(Vinyl Chloride). *Polym. Degrad. Stab.* **1994**, *45* (3), 301–313. https://doi.org/10.1016/0141-3910(94)90200-3.

(56) Bacaloglu, R.; Fisch, M. Degradation and Stabilization of Poly(Vinyl Chloride). III. Correlation of Activation Enthalpies and Entropies for Dehydrochlorination of Chloroalkanes, Chloralkenes and Poly(Vinyl Chloride). *Polym. Degrad. Stab.* **1994**, *45* (3), 325–338. https://doi.org/10.1016/0141-3910(94)90202-X.

(57) Troitskii, B. B.; Troitskaya, L. S. Degenerated Branching of Chain in Poly(Vinyl Chloride) Thermal Degradation. *Eur. Polym. J.* **1999**, *35* (12), 2215–2224. https://doi.org/10.1016/S0014-3057(99)00002-6.

(58) Iván, B.; Kennedy, J. P.; Kelen, T.; Tüdõs, F.; Nagy, T. T.; Turcsányi, B. Degradation of PVCs Obtained by Controlled Chemical Dehydrochlorination. *J. Polym. Sci. Polym. Chem. Ed.* **1983**, *21* (8), 2177–2188. https://doi.org/10.1002/pol.1983.170210802.

(59) Troitskii, B. B.; Troitskaya, L. S. Mathematical Models of the Initial Stage of the Thermal Degradation of Poly(Vinyl Chloride). II. The Thermal Degradation of Poly(Vinyl Chloride) with Effective Removal of HCl. *J. Polym. Sci. Part Polym. Chem.* **1993**, *31* (1), 75–81. https://doi.org/10.1002/pola.1993.080310109.

(60) Grassie, N.; Speakman, J. G. Thermal Degradation of Poly(Alkyl Acrylates). I. Preliminary Investigations. *J. Polym. Sci. [A1]* **1971**, *9* (4), 919–929. https://doi.org/10.1002/pol.1971.150090408.

4 Optimization of Copper-Mediated ATRP for Internal Plasticization

4.1 Background

In **Chapter 3**, internally plasticized PVC graft copolymers were prepared in a single step via Cu-mediated ATRP initiated from defect sites on the PVC. However, a control experiment without PVC revealed 23% conversion, indicating the existence of some non-grafted polymer in the sample. Some of the graft copolymers obtained were not soluble or had poor solubility in common solvents including THF, DMF, and NMP. This low solubility might be caused by crosslinking during polymerization, due to the long reaction duration. Three aims in this chapter are: 1) decrease the competitive self-initiated non-grafted polymerization; 2) develop graft copolymers with high solubility in common solvents; 3) lower the monomer : VC unit ratio needed to achieve flexible polymers, with tunable flexibility that can be tailored to specific applications. Therefore, the ATRP reaction time was shortened from 24 h to 2 h (**Scheme 4.1**) in order to lower competing unattached polymer growth and possible crosslinking. Subsequently, variations in monomer to PVC stoichiometries were explored to optimize the ratios needed for achieving flexible PVC graft copolymers.

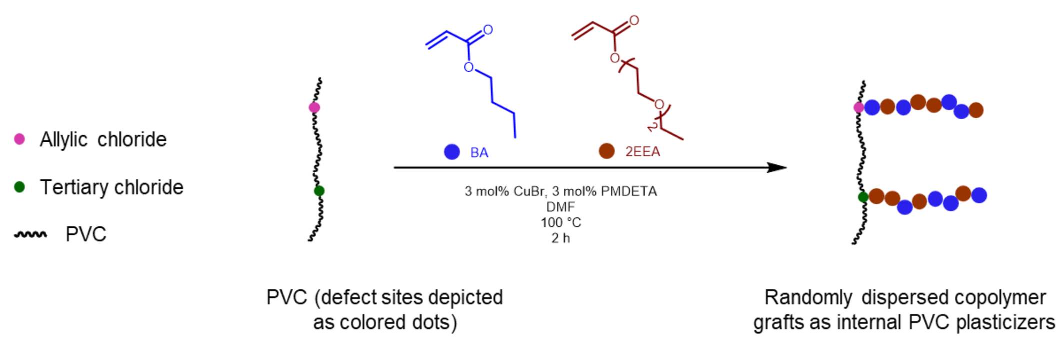

Scheme 4.1 General Reaction Scheme for 2 h ATRP

4.2 Preparation of PVC-g-(PBA-co-P2EEA) with a Two Hour Reaction Time

To determine an upper limit on background competitive non-grafted polymerization, control reactions were conducted without PVC for each monomer: *n*-butyl acrylate (BA) and 2-

(2-ethoxyethoxy)ethyl acrylate (2EEA) (**Table 4.1**, **Entries 1** and **2**). The reaction conditions were the same as in **Chapter 3**: 3 mol% of CuBr was used as catalyst, 3 mol% of PMDETA was used as ligand, and DMF was used as the solvent. The only difference was that the reaction time was shortened to 2 h from 24 h. Percent conversion of monomer was calculated based on ^{1}H NMR spectra of the reaction crude mixtures (**Figure 4.1** and **Figure 4.2**), using the equation in **Chapter 3** (**Equation 3.1**). The percent conversions for nongrafted homopolymer were 10% for BA and 6% for 2EEA (**Table 4.1**), significantly lower than the 23% obtained when the reaction ran for 24 h.

Table 4.1 Control Experiments without PVC: Polymerization Conditions and Percent Conversion[a]

Entry	[PVC]/[BA]/[2EEA]/[CuBr]/[PMDETA][b]	Initial molar ratio of [BA]/[2EEA]	%Conv.$_{NMR}$
1	0 : **2.5** : 0 : 0.03 : 0.03	BA only	10%
2	0 : 0 : **2.5** : 0.03 : 0.03	2EEA only	6%

[a]All polymerizations were conducted at 100 °C in DMF for 2 h; [b]Ratios were calculated in mol.

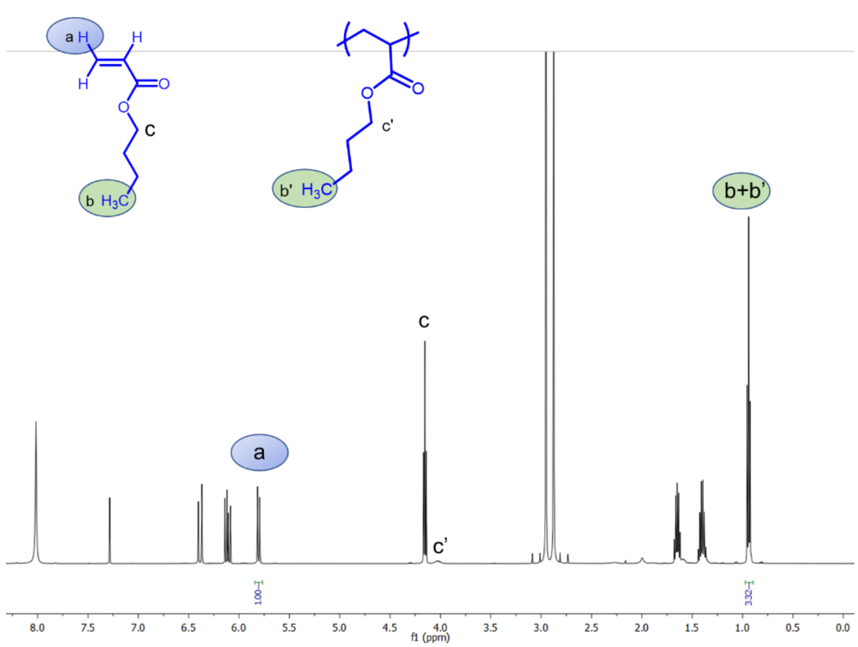

Figure 4.1 Crude ^{1}H NMR ($CDCl_3$) of Control Experiment with BA Only for 2 h

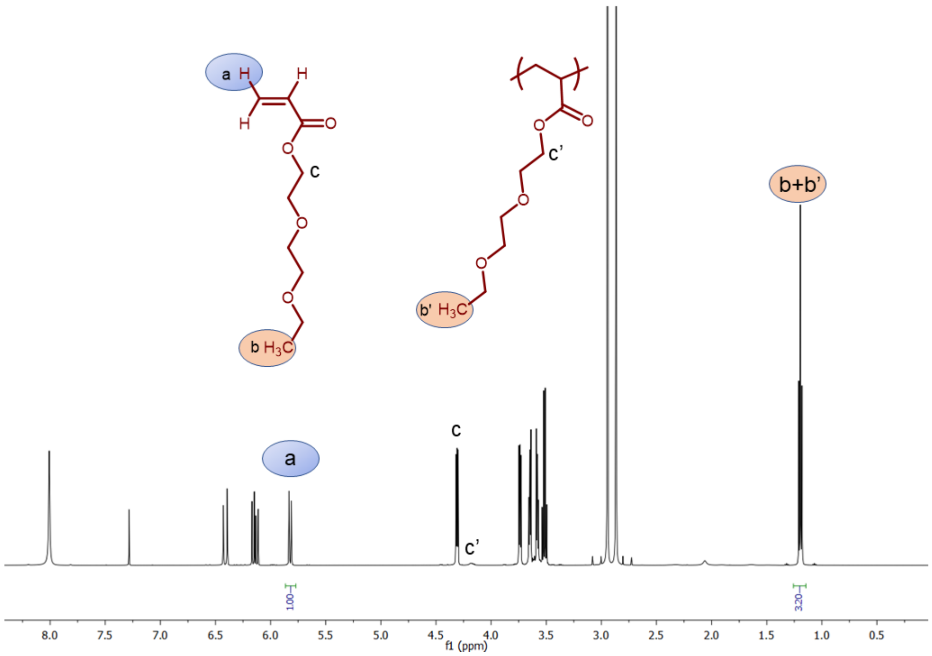

Figure 4.2 Crude ^{1}H NMR ($CDCl_3$) of Control Experiment with 2EEA Only for 2 h

Because the percent conversion of self-initiated polymerization[1] was low for both BA and 2EEA using a reaction time of 2 h, a series of graft copolymers were prepared under these same reaction conditions (**Table 4.2**). Five different monomer ratios (BA to 2EEA) were used in analogy to the graft polymerizations described in **Chapter 3**. The percent conversions ranged from 56% to 78% (**Table 4.2**, **Entry 1 - 5**).

Table 4.2 Graft Polymerizations after 2 Hours: Percent Conversion[a]

Entry	[PVC]/[BA]/[2EEA]/[CuBr]/[PMDETA][b]	Initial molar ratio of [BA]/[2EEA]	%Conv.$_{NMR}$[c]
1	1 : **2.5** : **0** : 0.03 : 0.03	BA only	78%
2	1 : **1.9** : **0.6** : 0.03 : 0.03	3 : 1	61%
3	1 : **1.3** : **1.3** : 0.03 : 0.03	1 : 1	60%
4	1 : **0.6** : **1.9** : 0.03 : 0.03	1 : 3	56%
5	1 : **0** : **2.5** : 0.03 : 0.03	2EEA only	60%

[a]All polymerizations were conducted at 100 °C in DMF for 2 h; [b]Ratios were calculated in mol; [c]Conversion of total monomers; all product polymers were completely soluble in the $CDCl_3$ NMR solvent

For comparison, the percent conversions for these ATRP grafting reactions conducted for 2 h and 24 h are shown in **Table 4.3**. The percent conversion using only BA after 2 h was 78% (**Table 4.2**, **Entry 1**): the highest among these 2 hours polymerizations. Surprisingly, the percent conversion for the corresponding 24 h reaction was 81%, which is not significantly different. The percent conversions for all other grafts polymerizations with added 2EEA were around 60%, which are 12 - 24% lower than the same reactions carried out for 24 h. As the samples obtained by 24 h reactions were not completely soluble in the $CDCl_3$ solvent, it is likely that the percent conversions calculated for the 24 h reactions by ^{1}H NMR are inaccurate. Overall, the 2 h ATRP graft polymerizations, which is more energy-efficient, were able to achieve high percent conversions, and the graft copolymers have better solubilities than those carried out for 24 h, indicating less crosslinking.

Table 4.3 Comparison of Percent Conversions for 2 h and 24 h Graft Polymerizations

Sample	$\%Conv._{NMR, 2 h}$[a]	$\%Conv._{NMR, 24 h}$[b]
PVC-*g*-PBA	78%	81%
PVC-*g*-75%PBA-*co*-25%P2EEA	61%	73%
PVC-*g*-50%PBA-*co*-50%P2EEA	60%	84%
PVC-*g*-25%PBA-*co*-75%P2EEA	56%	80%
PVC-*g*-P2EEA	60%	80%

[a]Conversion of total monomers; polymers were completely soluble in the $CDCl_3$ NMR solvent; [b]Conversion of total monomers made with 0.5 g PVC; not all of the sample was soluble in the $CDCl_3$ NMR solvent

4.3 Composition and Relative Size of the PVC-g-(PBA-co-P2EEA) Grafts Copolymers Made Using a Two Hour Reaction Time

^{1}H NMR was used to characterize the PVC grafts prepared under the 2 h duration (**Table 4.4**). The calculation method is the same as shown in Chapter 3. Two main trends were found to be consistent with the results in **Chapter 3**: 1) the PBA : P2EEA ratio in the grafts were very close to the initial BA : 2EEA monomer ratio; and 2) PVC-*g*-PBA gave the highest polyacrylate graft length (PBA : PVC = 1.4 : 1.0). Other graft copolymers showed about the same polyacrylate lengths. This is consistent with the percent conversions shown in **Table 4.2**.

Table 4.4 Composition of Graft Copolymers Formed after 2 Hours Based on ^{1}H NMR Integration

Samples	Initial molar ratio of [BA]/[2EEA]	Polymer PBA/P2EEA	Polymer (PBA + P2EEA)/PVC
PVC-*g*-PBA	BA only	PBA only	1.4 : 1.0
PVC-*g*-75%PBA-*co*-25%P2EEA	3 : 1	3.0 : 1.0	1.0 : 1.0
PVC-*g*-50%PBA-*co*-50%P2EEA	1 : 1	1.0 : 1.0	0.9 : 1.0
PVC-*g*-25%PBA-*co*-75%P2EEA	1 : 3	1.0 : 2.8	0.9 : 1.0
PVC-*g*-P2EEA	2EEA only	P2EEA only	0.9 : 1.0

PVC graft copolymers made by ATRP over 2 h had lower weight percent (wt%) grafts compared to polymers made by ATRP running for 24 h (**Table 4.5**), which is consistent with the higher percent conversions seen for these one day reactions (**Table 4.3**). Interestingly, for PVC copolymers with more than 50% P2EEA, the difference in plasticizer weight fraction for 2 and 24 h ATRP reactions (5 – 8%) was not as significant as the difference between percent conversion (20 – 24%). This might be caused by a difference in the selective loss of polyether-rich material during the workup procedure. For the 24 h samples, multiple methanol washes were performed, and the PVC graft copolymers were stirred overnight in methanol. Conversely, 2 h reaction samples were washed in methanol one time and then soaked in a different batch of methanol overnight without stirring. Homopolymer P2EEA is soluble in methanol, so performing multiple washes and stirring contributes to inadvertent enhanced removal of homopolymer P2EEA and P2EEA-rich PVC graft copolymers. A simplified work-up procedure was adopted, as stirring physically breaks the polymer sample into small pieces, making isolation by decantation challenging. Contamination by a small portion of non-grafted plasticizing polymer in the 2 h samples may contribute in a positive or negative manner to the T_g and other mechanical properties. The polymer samples made over 24 h remained in larger pieces after stirring, possibly because they exhibit a degree of crosslinking.

Table 4.5 Wt% Plasticizer for 2 h and 24 h Polymerizations

Samples	Wt% Plasticizer$_{grav.}$ 2 h	Wt% plasticizer$_{grav}$ 24 h
PVC-*g*-PBA	75%	80%
PVC-*g*-75%PBA-*co*-25%P2EEA	68%	75%
PVC-*g*-50%PBA-*co*-50%P2EEA	68%	75%
PVC-*g*-25%PBA-*co*-75%P2EEA	68%	73%
PVC-*g*-P2EEA	70%	73%

4.4 Preparation of PVC Graft Copolymers with Varying Monomer : VC Unit Ratios

All PVC graft copolymers discussed to this point were synthesized with a total acrylate monomer to PVC (VC unit) molar ratio of 2.5 : 1.0, resulting in PVC with a wt% of grafted plasticizer above 68%. These polymers were clearly flexible upon being handled in the lab. To test the effect of lowering the wt% of plasticizer on flexibility, the ratio of monomer to PVC was reduced. The purpose of lowering the ratio of monomer to PVC was three-fold: 1) to explore how little the grafts can be while still attaining plasticity, 2) to examine the flexibility of graft copolymers with different wt% plasticizer, and 3) to compare the plasticization efficiencies of PBA versus P2EEA.

Three BA : VC unit ratios (0.5 : 1.0, 1.0 : 1.0, and 2.5 : 1.0) were used to make a series of PVC-*g*-PBA copolymers (**Table 4.6**). The percent conversion ranged from 59% to 78%, increasing with larger BA to VC unit ratios, reflecting the higher available monomer during the polymerization.

Table 4.6 Polymerization Conversions for Making PVC-*g*-PBA Copolymers as a Function of BA to VC Unit Ratio[a]

Entry	Initial molar ratio BA : VC unit	%Conv.$_{NMR}$
1	0.5 : 1.0	59%
2	1.0 : 1.0	67%
3	2.5 : 1.0	78%

[a]All polymerizations were conducted at 100 °C in DMF for 2 h with [PVC]/[CuBr]/[PMDETA] = 1/0.03/0.03

Likewise the same three 2EEA : VC unit ratios were investigated for making PVC-*g*-P2EEA copolymers (**Table 4.7**). The percent conversions were lower: 40 – 60%, with the highest for 2EEA : VC unit = 2.5 : 1.0. In all cases, comparing PVC-*g*-PBA and PVC-*g*-P2EEA at the same monomer ratio, the butyl acrylate grafts were 7% - 19% longer. In conclusion, conversions were lower with the polyether monomer for the same monomer : VC unit ratio.

Table 4.7 Polymerization Conversions for Making PVC-*g*-P2EEA Copolymers as a Function of 2EEA to VC Unit Ratio[a]

Entry	Initial molar ratio 2EEA : VC unit	%Conv.$_{NMR}$
1	0.5 : 1.0	40%
2	1.0 : 1.0	59%
3	2.5 : 1.0	60%

[a]All polymerizations were conducted at 100 °C in DMF for 2 h with [PVC]/[CuBr]/[PMDETA] = 1/0.03/0.03

4.5 Relative Size of the New Grafts for PVC-*g*-PBA Copolymers and PVC-*g*-P2EEA Copolymers

The relative size of the new grafts for PVC-*g*-PBA copolymers (**Table 4.8**) was calculated based on ^{1}H NMR (**Equation 4.1**). Using PVC-*g*-PBA-0.5 as an example, the integration of PBA -C**H**$_2$-O-C=O- (**Figure 4.3**, proton **c**) is 0.52. the integration of PVC -C**H**-Cl-methylene (proton **a**) is 1. The molar ratio of PBA / PVC was 0.26 (**Equation 4.2**).

$$Molar\ ratio_{\frac{PBA}{PVC}NMR} = \frac{Intergration_{-CH_2-O-C=O\ methylene,PBA}}{2 \times Intergration_{CH-Cl\ methine,PVC}}$$

Equation 4.1

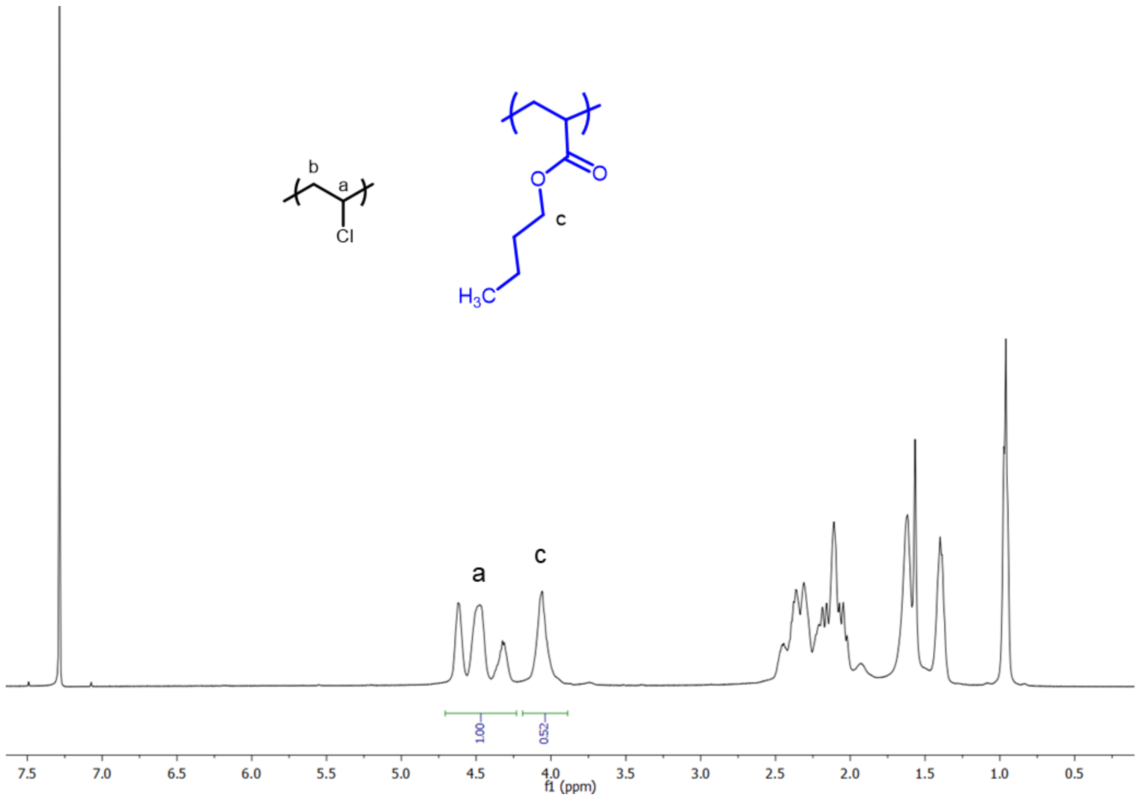

Figure 4.3 [1]H NMR of PVC-*g*-PBA-0.5

$$Molar\ ratio_{\frac{PBA}{PVC}NMR} = \frac{Intergration_{-CH_2-O-C=O\ methylene,PBA}}{2 \times Intergration_{CH-Cl\ methine,PVC}}$$

$$= \frac{Integration\ of\ proton\ \boldsymbol{c}}{2 \times Integration\ of\ proton\ \boldsymbol{a}} = \frac{0.52}{2} = 0.26$$

Equation 4.2

For PVC-*g*-PBA copolymers, the grafted PBA to PVC ratio increased with the increase of BA ratio (**Table 4.8**). As expected, the PBA : PVC ratio increases almost linearly with the initial [BA] : [VC unit] monomer ratios.

Table 4.8 Composition of PVC-*g*-PBA copolymers

Sample[a]	Initial molar ratio BA : VC	Polymer molar ratio PBA : PVC
PVC-*g*-PBA-0.5	0.5 : 1.0	0.3 : 1.0
PVC-*g*-PBA-1.0	1.0 : 1.0	0.6 : 1.0
PVC-*g*-PBA-2.5	2.5 : 1.0	1.4 : 1.0

[a]0.5, 1.0 and 2.5 in the sample name indicates the monomer ratio to VC unit

Similarly, for PVC-*g*-P2EEA copolymers, the molar ratio of P2EEA to PVC was calculated using **Equation 4.3**. The grafted P2EEA to PVC ratio also increased with higher amount of 2EEA monomer (**Table 4.9**). As expected, the P2EEA : PVC ratio increases linearly with the initial monomer [2EEA] : [VC unit] ratios, this trend is reflected in the PVC-*g*-PBA copolymers. Comparison of PVC-*g*-PBA and PVC-*g*-P2EEA copolymers at the same monomer : VC unit ratio, the length of PBA graft is longer than the length of P2EEA graft. This is consistent with the higher percent conversion of PBA discussed in **Section 4.4**.

$$Molar\ ratio_{\frac{P2EEA}{PVC}NMR} = \frac{Intergration_{\text{-}\boldsymbol{CH_2}-O-C=O\ methylene,P2EEA}}{2 \times Intergration_{\boldsymbol{CH}-Cl\ methine,PVC}}$$

Equation 4.3

Table 4.9 Composition of PVC-*g*-P2EEA copolymers

Sample[a]	Initial molar ratio 2EEA : VC unit	Polymer molar ratio P2EEA : PVC
PVC-*g*-P2EEA-0.5	0.5 : 1.0	0.2 : 1.0
PVC-*g*-P2EEA-1.0	1.0 : 1.0	0.4 : 1.0
PVC-*g*-P2EEA-2.5	2.5 : 1.0	0.9 : 1.0

[a]0.5, 1.0 and 2.5 in the sample name indicates the monomer ratio to VC unit

4.6 Wt% Plasticizer for PVC-*g*-PBA Copolymers and PVC-*g*-P2EEA Copolymers

Wt% plasticizer was calculated in two ways: gravimetry (**Chapter 3**, **Equation 3.4**) and ^{1}H NMR (**Equation 4.4**).

$$Wt\%\ plasticizer_{NMR} = \frac{Weight_{Polyacrylate}}{Weight_{PVC} + Weight_{Polyacrylate}} \times 100\%$$

$$= \frac{Molecular\ weight_{BA} \times molar\ ratio_{\frac{Polyacrylate}{PVC},NMR}}{Molecular\ weight_{VC} + Molecular\ weight_{BA} \times molar\ ratio_{\frac{Polyacrlate}{PVC},NMR}} \times 100\%$$

Equation 4.4

For the [1]H NMR method, using PVC-*g*-PBA-0.5 as an example, the molar ratio of PBA / PVC was 0.26 (**Figure 4.3**, **Equation 4.2**). The molecular weight of BA is 128.17 g/mol. The wt% plasticizer for PVC-*g*-PBA-0.5 is shown in **Equation 4.5**.

$$Wt\%\ plasticizer_{NMR} = \frac{128.17 \times 0.26}{62.50 + 128.17 \times 0.26} \times 100\% = 34.8\%$$

Equation 4.5

Wt% of plasticzer for PVC-*g*-PBA copolymers are shown in **Table 4.10**. Interestingly, for PVC-*g*-PBA-1.0 and PVC-*g*-PBA-2.5, the wt% plasticizer calculated by [1]H NMR and gravimetry were very close. However, for PVC-*g*-PBA-0.5, the wt% plasticizer calculated by [1]H NMR and gravimetry are not as closely matched.

Table 4.10 Wt% of Plasticizer for PVC-*g*-PBA Copolymers

Sample[a]	wt% $Plasticizer_{grav.}$	wt% $Plasticizer_{NMR}$
PVC-*g*-PBA-0.5	27%	35%
PVC-*g*-PBA-1.0	50%	53%
PVC-*g*-PBA-2.5	74%	75%

[a]0.5, 1.0 and 2.5 in the sample name indicates the monomer ratio to VC unit

For PVC-*g*-P2EEA copolymers, the difference between the wt% of plasticizer calculated by [1]H NMR and gravimetry decreases with increasing 2EEA ratio (**Table 4.11**). For the PVC-*g*-P2EEA-2.5 sample, the wt% plasticizer calculated by [1]H NMR and gravimetry are almost identical. Surprisingly, the wt% of plasticizer of PVC-*g*-PBA and PVC-*g*-P2EEA are very similar at the same initial monomer ratios in all cases. Overall, with three monomer : VC unit ratios, one can obtain polymers with plasticizer wt% around 30%, 50%, and 70%. The FTIR spectra for all nine samples discussed in this chapter are as expected are reported in the Experimental Section and included in the Supporting Information.

Table 4.11 Wt% Plasticzer of PVC-*g*-P2EEA Copolymers

Sample[a]	wt% $Plasticizer_{grav.}$	wt% $Plasticizer_{NMR}$
PVC-*g*-P2EEA-0.5	24%	38%
PVC-*g*-P2EEA-1.0	48%	55%
PVC-*g*-P2EEA-2.5	70%	72%

[a]0.5, 1.0, and 2.5 in the sample name indicates the monomer ratio to VC unit

4.7 Glass Transition Temperatures of PVC Copolymers made with Monomer to VC Unit Molar Ratio of 2.5 to 1.0 Using a Two Hour Reaction Time

The glass transition temperatures (T_g) of PVC graft copolymers were measured using differential scanning calorimetry (DSC). The second heating cycle of PVC copolymers made with monomer to VC unit molar ratio of 2.5 : 1.0 are shown in **Figure 4.4**. Only a single T_g was observed for all graft copolymers, indicating that there is no microphase separation. Compared to the T_g value of PVC (T_g = 84.3 °C), the graft copolymers have significantly lower T_g values. The highest T_g value achieved was for PVC-*g*-PBA (T_g = -25.5 °C). The lowest T_g value obtained was for PVC-*g*-25%PBA-*co*-75%P2EEA (T_g = -53.5 °C). This is consistent with the observation that P2EEA has a higher plasticization efficiency compared to PBA. The slightly lower T_g value of PVC-*g*-25%PBA-*co*-75%P2EEA (wt% $plasticizer_{grav}$. = 68%) compared to PVC-g-P2EEA (wt% $plasticizer_{grav}$. = 70%) might be an artifact of the workup procedure, which preferentially dissolves and washes away P2EEA-rich copolymers.

Comparing PVC copolymers made with 2 h and 24 h reaction times, the T_g values of PVC copolymers made over 2 h are for the most part slightly higher than those made over 24 h at the same PBA to P2EEA ratio (**Table 4.12**). This is consistent with the wt% plasticizer of 24 h reactions being slightly higher than for the corresponding 2h reactions. The only exception was for PVC-*g*-25%PBA-*co*-75%P2EEA, for which the 2 h reaction resulted in a lower T_g value than for the 24 h reaction.

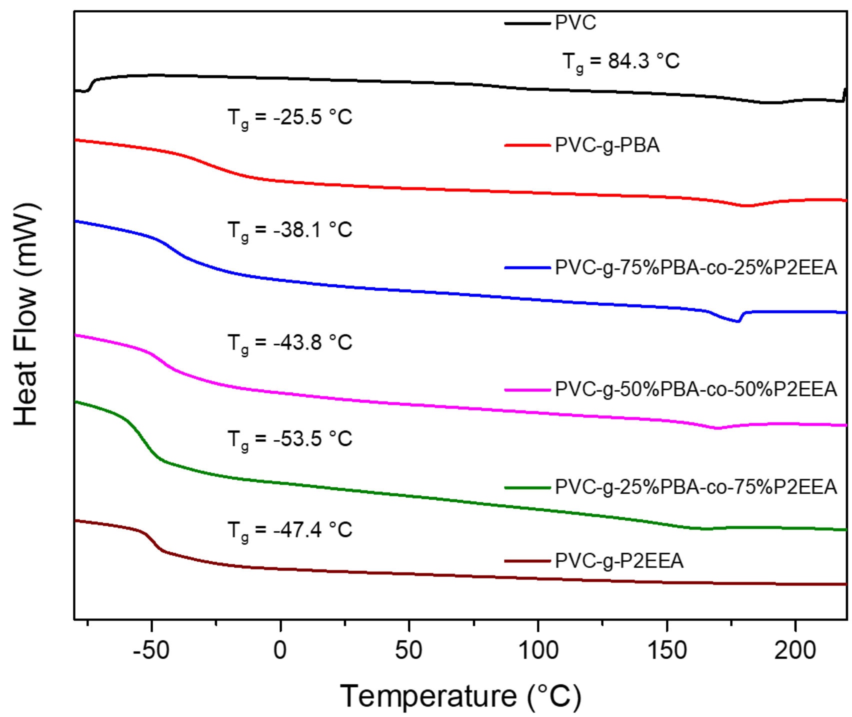

Figure 4.4 DSC (2nd heat cycle) of Grafted PVC Polymers made using 2 h Reaction Time (Monomer : VC Unit Ratio 2.5 to 1.0)

Table 4.12 T_g values of PVC Graft Copolymer made with 2 h and 24 h Reaction Times

Samples	T_g (°C) 2 h	Wt% Plasticizer$_{grav.}$ 2 h	T_g (°C) 24 h	Wt%[a] Plasticizer$_{grav}$ 24 h
PVC-*g*-PBA	-25.5	75%	-34.5	80%
PVC-*g*-75%PBA-*co*-25%P2EEA	-38.1	68%	-43.2	73%
PVC-*g*-50%PBA-*co*-50%P2EEA	-43.8	68%	-47.4	73%
PVC-*g*-25%PBA-*co*-75%P2EEA	-53.5	68%	-48.2	75%
PVC-*g*-P2EEA	-47.4	70%	-50.0	75%

[a]Both 2 h and 24 h reaction used 500 mg of PVC

4.8 Glass Transition Temperatures of PVC-g-PBA Copolymers

The T_g values of PVC-*g*-PBA copolymers synthesized with different BA to PVC monomer molar ratios are shown in **Figure 4.5**. The T_g transition was very wide for PVC-*g*-PBA-0.5, no distinct T_g value was detected in the second heating cycle. Comparison of PVC-*g*-PBA-1.0 (T_g = -14.2 °C) and PVC-*g*-PBA-2.5 (T_g = -25.5 °C) show that T_g values decrease with increasing length of the graft polymer chain. Single T_g values were observed for PVC-*g*-PBA-1.0 and PVC-*g*-PBA-2.5, indicating no microphase separation.

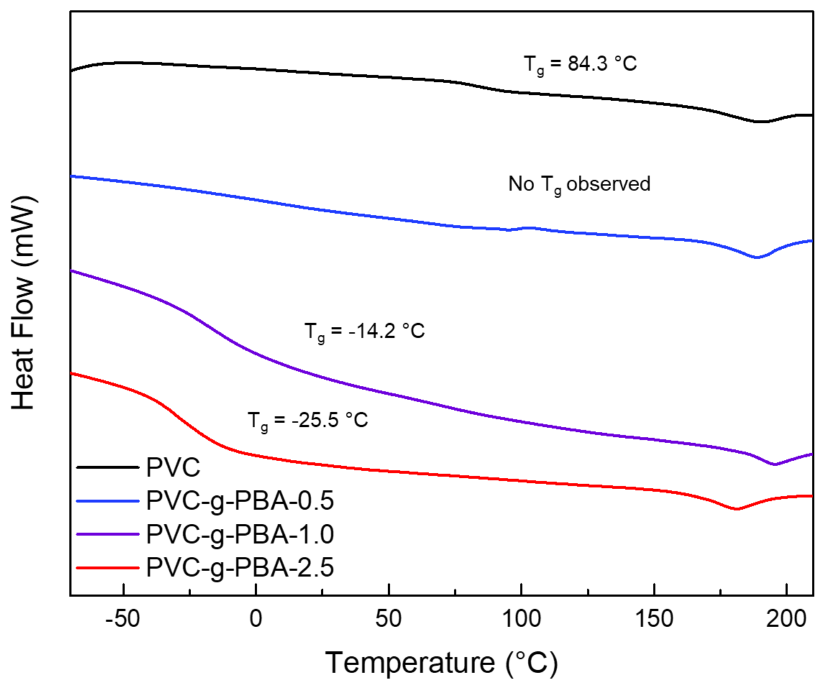

Figure 4.5 DSC (2nd heating cycle) of PVC-*g*-PBA Graft Copolymers

The purpose of this section is to explore how short the grafts can be while still attaining plasticity and to examine the flexibility, of graft copolymers with different wt% plasticizer (**Table 4.13**). Even though no T_g value was identified for PVC-*g*-PBA-0.5 with 27% plasticizer by DSC, this polymer sample was *not* flexible at room temperature upon handling the sample. PVC-*g*-

PBA-1.0 with 50% plasticizer had a T_g value below 0 °C, indicating good flexibility of the copolymer and it did feel flexible. In conclusion, flexible PVC-*g*-PBA material could be achieved with a monomer to VC unit molar ratio of 1.0 : 1.0, which is a much more efficient than the original ratio of 2.5 : 1.0.

Table 4.13 T_g Values of PVC-*g*-PBA Copolymers

Sample	T_g (°C)	wt% $Plasticizer_{grav.}$
PVC	84.3	0
PVC-*g*-PBA-0.5	-[a]	27%
PVC-*g*-PBA-1.0	-14.2	50%
PVC-*g*-PBA-2.5	-25.5	74%

[a]No T_g value observed in the second heating cycle

4.9 Glass Transition Temperatures of PVC-*g*-P2EEA Copolymers

The T_g values of PVC-*g*-P2EEA copolymers made with different 2EEA to VC unit molar ratios are shown in **Figure 4.6**. Again, the T_g values decrease with increasingly long grafts. No phase separation was indicated by the single T_g value for each polymer.

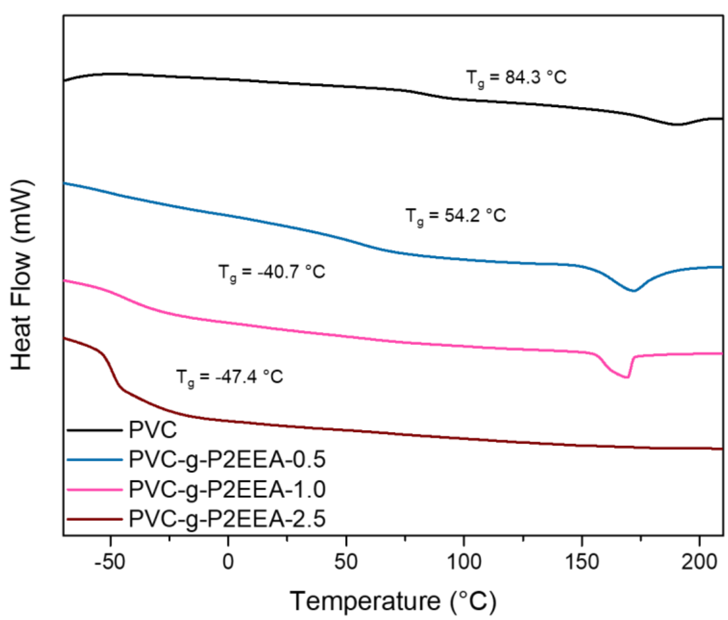

Figure 4.6 DSC (2nd heating cycle) of PVC-*g*-PBA Copolymers

For PVC-*g*-P2EEA graft copolymers, the lowest T_g achieved (-47 °C) was for PVC-*g*-P2EEA-2.5 with 70% plasticizer (**Table 4.14**). For PVC-*g*-P2EEA-0.5 with 24% plasticizer, a T_g value of 54.2 °C was determined, indicating that the material is rigid at room temperature. Surprisingly, for PVC-*g*-P2EEA-1.0, a T_g value of -40.7 °C was achieved with only 48% plasticizer. This illustrates that the most efficient monomer to VC unit molar ratio among these three examples is 1.0 : 1.0, similar to the results for the PVC-*g*-PBA copolymers. Comparison of PBA and P2EEA (**Table 4.13** and **Table 4.14**) at similar wt% plasticizer shows that PVC-*g*-P2EEA graft copolymers have significant lower T_g values than the PVC-*g*-PBA graft copolymers.

Table 4.14 T_g Values of PVC-*g*-PBA Graft Copolymers

Sample	T_g (°C)	wt% Plasticizer$_{grav}$.
PVC	84.3	0
PVC-*g*-P2EEA-0.5	54.2	24%
PVC-*g*-P2EEA-1.0	-40.7	48%
PVC-*g*-P2EEA-2.5	-47.4	70%

4.10 Thermal Stability of PVC Graft Copolymers made with a Monomer : VC Unit Ratio 2.5 to 1.0

Thermogravimetric analysis (TGA, **Figure 4.7**) and Derivative Thermogravimetry (DTG, **Figure 4.8**) of PVC graft copolymers were measured to examine their thermal stabilities. As shown in **Figure 4.7**, PVC and PVC grafted copolymers all have a three-stage degradation. The third stage (4 – 6% weight loss) for PVC grafted copolymers are not obvious compared to the first two stages. TGA data are summarized in **Table 4.15**. The onset temperatures of PVC grafted copolymers are higher than unmodified PVC because unstable defect sites are replaced with carbon grafts.[2] This is consistent with previous results in **Chapter 3**. Overall, PVC grafted copolymers were more thermally stable compared to unmodified PVC. The thermal stabilities of PBA and P2EEA grafts were similar. In the second degradation stage, the PBA rich copolymers, PVC-*g*-PBA and PVC-*g*-75%PBA-*co*-25%P2EEA, had a slightly steeper slope compared to other P2EEA rich graft copolymers.

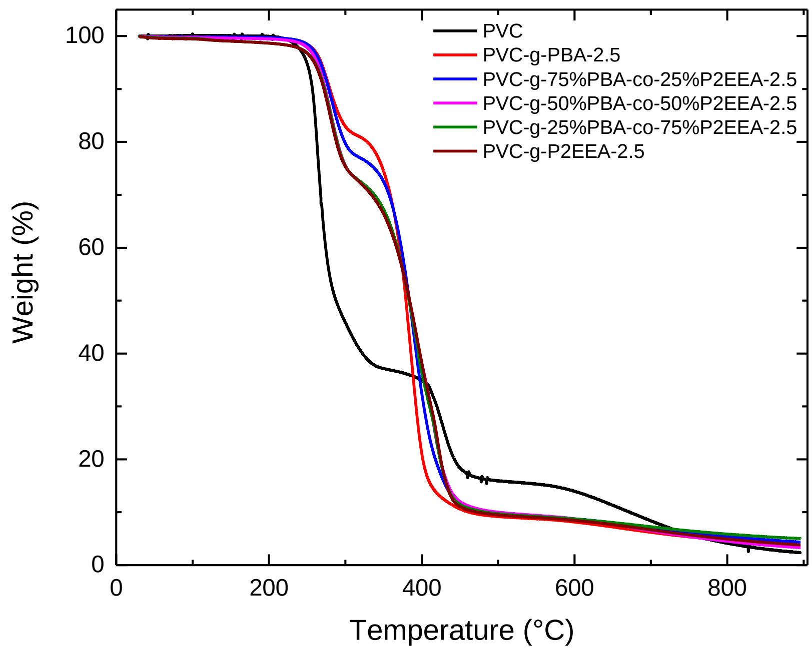

Figure 4.7 TGA Curves of Samples made with 2 h Reaction Time

Table 4.15 TGA Data for PVC Graft Copolymers made with a 2 h Reaction Time[a]

Sample	Onset temp. (°C)	Residue (%) at 900 °C	Mass loss first stage(%)	Mass loss second stage(%)	Mass loss third stage(%)
PVC	253.4	2.4	63.1	21.1	13.4
PVC-*g*-PBA	260.2	3.7	18.7	72.4	5.2
PVC-*g*-75%PBA-*co*-25%P2EEA	260.0	4.4	22.9	73.6	4.8
PVC-*g*-50%PBA-*co*-50%P2EEA	258.1	3.3	27.3	63.3	6.1
PVC-*g*-25%PBA-*co*-75%P2EEA	259.5	5.0	26.2	63.6	4.2
PVC-*g*-P2EEA	257.6	3.8	26.3	63.7	5.2

[a]Monomer : VC unit = 2.5 : 1.0

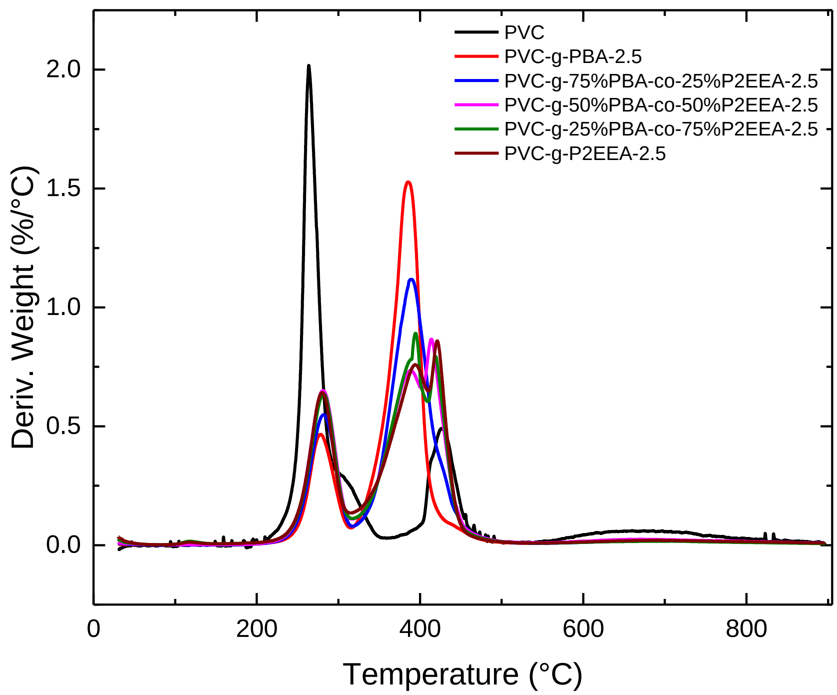

Figure 4.8 DTG Curves of Samples made with 2 h Reaction Time

4.11 Thermal Stabilities of PVC-g-PBA Copolymers and PVC-g-P2EEA Copolymers

PVC-*g*-PBA copolymers made with different monomer : VC unit ratios have a three-stage degradation (**Figure 4.9** and **Table 4.16**). For PVC-*g*-PBA copolymers, as shown in **Figure 4.9**, the thermal stabilities increase with increasing amount of BA monomer. Onset temperatures of PVC-*g*-PBA copolymers also have the same trend (**Table 4.16**). The slightly higher onset temperature for higher wt% PBA might be caused by increased replacement of defect sites with stable carbon grafts.

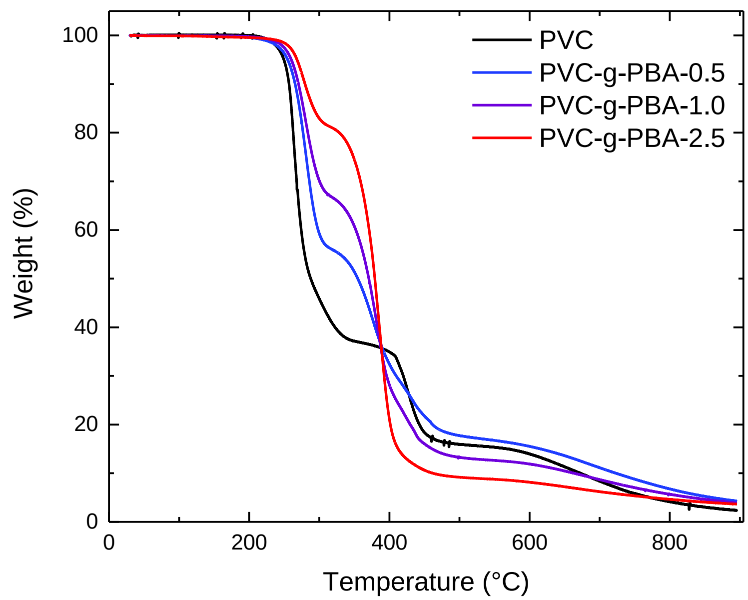

Figure 4.9 TGA Curves of PVC-*g*-PBA Copolymers

Table 4.16 TGA Data for PVC-*g*-PBA Copolymers

Compounds	Onset temp. (°C)	Residue (%) at 900 °C	Mass loss first stage(%)	Mass loss second stage(%)	Mass loss third stage(%)
PVC	253.4	2.4	63.1	21.1	13.4
PVC-*g*-PBA-0.5	257.2	4.3	44.1	38.8	12.8
PVC-*g*-PBA-1.0	258.7	3.9	33.3	54.0	8.8
PVC-*g*-PBA-2.5	260.2	3.7	18.7	72.4	5.2

For the PVC-*g*-P2EEA copolymers, both PVC-*g*-P2EEA-0.5 and PVC-*g*-P2EEA-2.5 exhibited a three-stage degradation; PVC-*g*-P2EEA-1.0 exhibited a two-stage degradation (**Figure 4.10** and **Table 4.17**). For PVC-*g*-P2EEA copolymers, as shown in **Figure 4.10**, the thermal stabilities increase with increasing amount of P2EEA. Onset temperatures of PVC-*g*-2EEA copolymers are higher than unmodified PVC (**Table 4.17**). PVC-*g*-P2EEA-1.0 showed a very small amount of weight loss at around 40 °C. The cause of residual solvent is excluded as no distinguishable solvent peaks was observed in ^{1}H NMR. In conclusion, the thermal stabilities of PVC-*g*-2EEA copolymers are higher than unmodified PVC.

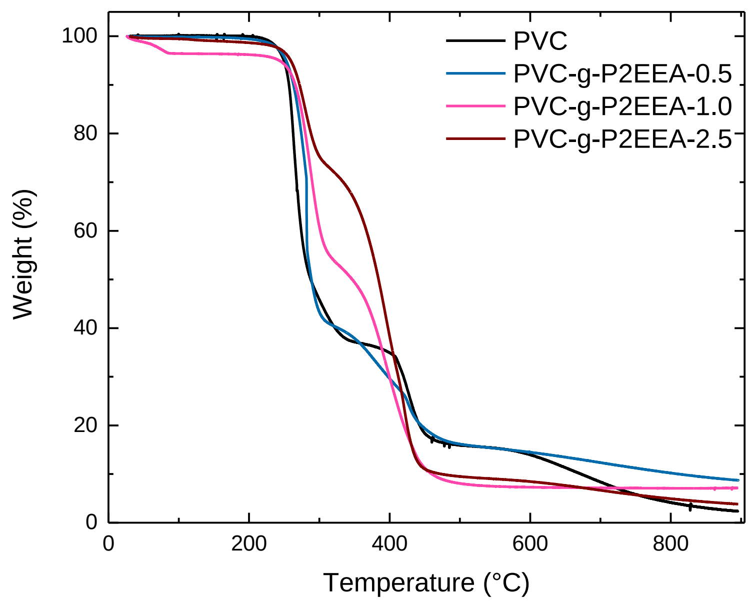

Figure 4.10 TGA Curves of PVC-*g*-P2EEA Copolymers

Table 4.17 TGA Data for PVC-*g*-P2EEA Copolymers

Compounds	Onset temp. (°C)	Residue (%) at 900 °C	Mass loss first stage(%)	Mass loss second stage(%)	Mass loss third stage(%)
PVC	253.4	2.4	63.1	21.1	13.4
PVC-*g*-P2EEA-0.5	259.7	8.7	59.7	25.1	6.5
PVC-*g*-P2EEA-0.5	264.3	7.1	43.7	45.5	-
PVC-*g*-P2EEA-2.5	257.6	3.8	26.3	63.7	5.2

4.12 GPC Results of PVC Graft Copolymers

The GPC traces of the PVC graft copolymers (monomer : VC = 2.5 : 1.0) are shown in **Figure 4.11**. Compared to unmodified PVC, the retention times of all of the PVC graft copolymers are shorter, reflecting their higher weights and effective volumes. This data indicates that the grafting polymerization was successful. The GPC peak sizes of the PVC graft copolymers are similar to those of unmodified PVC, unlike the copolymers made in **Chapter 3**. This supports the absence of significant crosslinking for the 2 h polymerizations. Most of these new polymers have a unimodal distribution. Interestingly, PVC-*g*-PBA shows a trimodal distribution. indicating that some unreacted PVC homopolymer remains. As expected, the values of M_p, M_n, M_w, and M_z of the functionalized PVC samples are significantly larger compared to unmodified PVC (**Table 4.18**).

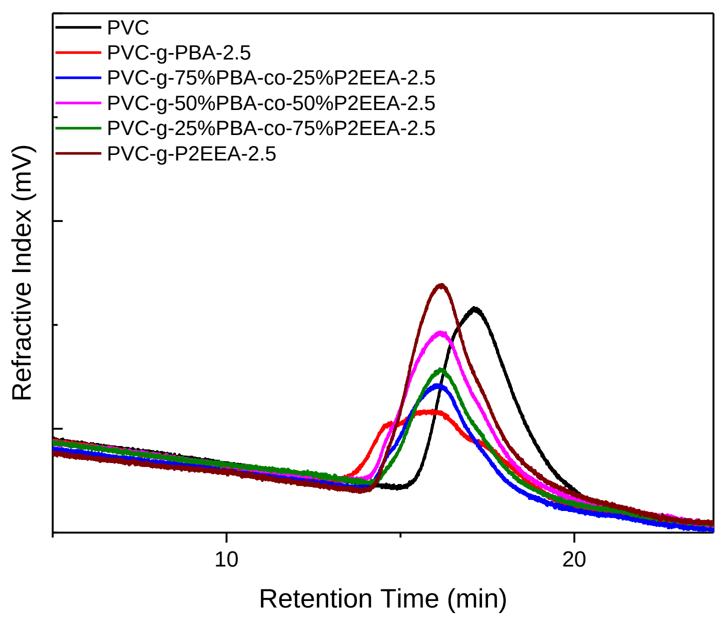

Figure 4.11 GPC Traces of PVC Graft Copolymers (2 h reaction time)

Table 4.18 GPC of Graft Copolymers made with 2 h Reaction[a]

Samples	M_p	M_n	M_w	M_z	PD
PVC	72,209	39,494	77,531	123,662	2.0
PVC-*g*-PBA	178,143	68,853	291,758	723,500	4.2
PVC-*g*-75%PBA-*co*-25%P2EEA	172,361	88,757	213,125	381,652	2.4
PVC-*g*-50%PBA-*co*-50%P2EEA	165,018	55,367	196,889	383,581	3.6
PVC-*g*-25%PBA-*co*-75%P2EEA	163,883	65,257	173,870	302,799	2.7
PVC-*g*-P2EEA	163,191	48,719	174,183	331,414	3.6

[a]Monomer to VC unit ratio = 2.5 : 1.0

The GPC traces of the PVC-*g*-PBA and PVC-*g*-P2EEA graft copolymers with different monomer to polymer ratios are shown in **Figure 4.12** and **Figure 4.13**, respectively. Compared to unmodified PVC, the retention times of all of the PVC graft copolymers are again shorter, reflecting their higher molecular weights and volumes. For the PBA grafts, bimodal and trimodal

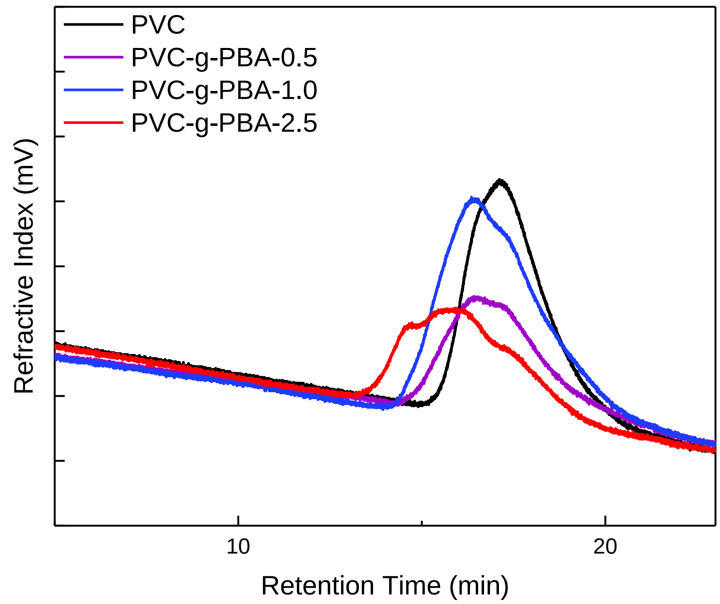

Figure 4.12 GPC Traces of PVC-*g*-PBA Copolymers

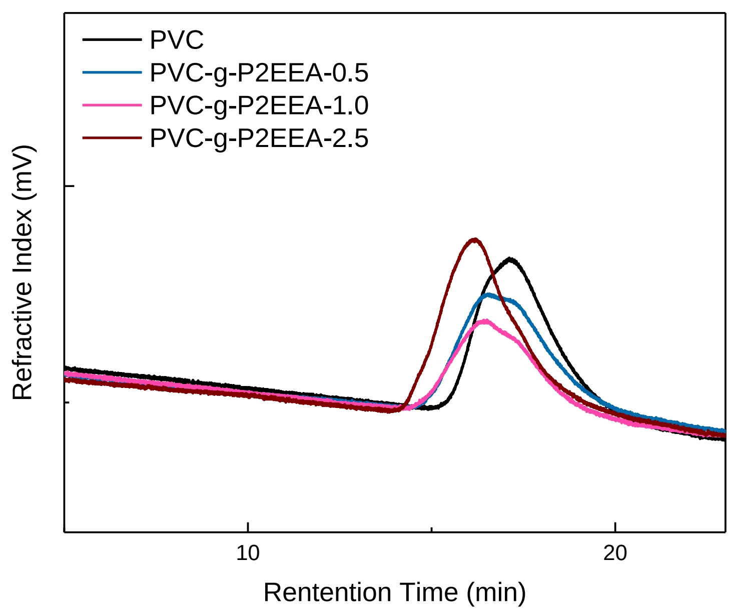

Figure 4.13 GPC Traces of PVC-*g*-PBA Copolymers

distribution are observed, indicating that some unreacted PVC homopolymer remains. For the P2EEA grafts PVC-*g*-P2EEA-0.5 and PVC-*g*-P2EEA-1.0, bimodal distributions are observed, implying that these polymer samples contain some unmodified PVC. For PVC-*g*-P2EEA-2.5, a unimodal distribution is observed, indicating little if any unreacted PVC remains. The values of M_p, M_w, and M_z of the functionalized PVC samples are significantly larger compared to unmodified PVC (**Table 4.19**). Furthermore, the polydispersity (PD) of the grafted polymers is observed to be significantly larger than that of unmodified PVC. This is consistent with the expectation that each PVC molecule may have a different number of defect sites for initiation of ATRP. Because there could be a large distribution of defect site density on the PVC chains, some PVC may have significantly more grafts than others, leading to a large variation in molecular weights and therefore polydispersity.

Table 4.19 GPC of PVC-*g*-PBA Copolymers and PVC-*g*-P2EEA Copolymers

Samples	M_p	M_n	M_w	M_z	PD
PVC	72,209	39,494	77,531	123,662	2.0
PVC-*g*-PBA-0.5	118,435	28,197	109,128	231,422	3.9
PVC-*g*-PBA-1.0	129,037	20,909	121,602	274,063	5.8
PVC-*g*-PBA-2.5	178,143	68,853	291,758	723,500	4.2
PVC-*g*-P2EEA-0.5	113,112	20,709	100,167	206,475	4.8
PVC-*g*-P2EEA-1.0	127,333	34,117	122,968	240,034	3.6
PVC-*g*-P2EEA-2.5	163,191	48,719	174,183	331,414	3.6

4.13 Conclusion

In this chapter, nine different internally plasticized PVC graft copolymers were prepared by ATRP with 2 h reaction times. Different wt% plasticizer (24% - 75%) with a very wide range of T_g values (-54 °C to +54 °C) were achieved. The most flexible graft copolymer is PVC-*g*-25%PBA-*co*-75%P2EEA made with a molar ratio of acrylate monomer : VC unit = 2.5 : 1.0. The least flexible copolymers are PVC-*g*-PBA-0.5 and PVC-*g*-P2EEA-0.5. Graft copolymers with 50 wt% plasticizer or more have T_g values below 0 °C, indicating that effective ratios of acrylate monomer : VC unit are 1.0 : 1.0 or higher. The lower T_g values of polyether compared to PBA graft copolymers further confirm the higher plasticization efficiency of the polyether compared to alkyl ester grafts. Observation of a single T_g value for all graft copolymers except the PVC-*g*-PBA-0.5 (which showed no distinct T_g) indicates complete miscibility of both PBA and P2EEA grafts with PVC. GPC reveals larger effective volumes for these graft polymers compared to the unmodified PVC. These PVC graft copolymers are more thermally stable compared to unmodified PVC, with thermal stability increasing with increasing amounts of wt% plasticizer.

4.14 Future Work

The work in this chapter shows very exciting results, in that a wide variation in flexible PVC samples can be prepared using ATRP graft polymerization, varying from materials that are rigid at room temperature to those with T_g values significantly below 0°C. Because the grafts initiate from defect sites on PVC, the resulting polymers exhibit improved thermal stabilities compared to PVC. Thus, PVC flexibility and thermal stability can be simultaneously achieved with internal plasticization, while avoiding plasticizer loss over time. There are a couple of drawbacks: 1) the freeze-pump-thaw method used to remove oxygen prior to the ATRP polymerization would be challenging on scale-up; 2) residual copper remains in the flexible PVC. **Table 4.20** lists some challenges to be addressed in the future. Most of these focus on making the internal plasticization process even more industrially relevant, and making the chemistry more environmentally friendly. The use of internally plasticized PVC might even allow PVC products to be recycled in the future.

Table 4.20 Possible Future Directions

	Future Work	Note/Reason
1	Apply activators regenerated by electron transfer (ARGET) ATRP	Lower residual catalyst to below the ppm level
2	Screen environmentally friendly catalysts (ex. Fe based catalysts)	Develop greener process
3	Screen environmentally friendly solvents	Develop greener process
4	Screen more efficient ligands	Decrease the amount of non-graft homopolymer
5	Lower reaction temperatures	Decrease the amount of non-graft Homopolymer, greener process
6	Utilize PVC without pre-treatment	Simplify potential industrial applications

4.15 Closing Remarks

Internal plasticization was accomplished by several approaches, starting with using thermal azide-alkyne cycloaddition to append branched plasticizers to the PVC chain. T_g values below room temperature were achieved in four synthetic steps from commercial PVC. Glutamic acid was used as a branched linker for plasticization moieties, which resulted in tetrester functionalized PVC. Although a highly branched internal plasticizer was developed, the lowest T_g value achieved using this method was only -1°C with short PEG functionalized tetraesters. Furthermore, thermal instability was observed in the materials, presumably associated with the key triazole attached to the PVC chain.

ATRP polymerization was then successfully used to make PVC graft copolymers in one step from PVC. No vigorous conditions or hazardous azide precursors are needed for this method, making it amenable to industrial scale-up. A systematic study of polyether ester vs *n*-butyl ester functionalities was performed, confirming that polyethers exhibit higher plasticization efficiency. By creating a series of polymers with different plasticizer to PVC ratios, graft copolymers with a wide range of T_g values can be obtained. It appears that a 1.0 : 1.0 ratio of acrylate graft monomers to vinyl chloride monomers is a good compromise between plasticizing efficiency and the cost and amount of added acrylate monomer contributing to graft length. These polymers are more thermally stable than PVC because the grafted segments were initiated from PVC defects, which play a role in the early stages of thermal degradation of PVC. Internally plasticized PVC materials are much better than materials using external plasticizers, as small molecules plasticizers can migrate out of the PVC matrix, resulting in deterioration of the properties of the PVC material over time, with concomitant environmental contamination, and health issues upon human exposure. Thus, these internally plasticized PVC materials are better than currently used externally plasticized PVC composites in terms of impacts on human health, product longevity, and caring for our environment.

4.16 References

(1) Srinivasan, S.; Kalfas, G.; Petkovska, V. I.; Bruni, C.; Grady, M. C.; Soroush, M. Experimental Study of the Spontaneous Thermal Homopolymerization of Methyl and N-Butyl Acrylate. *J. Appl. Polym. Sci.* **2010**, *118* (4), 1898–1909. https://doi.org/10.1002/app.32313.

(2) Wypych, G. 4 - Principles of Thermal Degradation. In *PVC Degradation and Stabilization (Third Edition)*; Wypych, G., Ed.; ChemTec Publishing: Boston, 2015; pp 79–165. https://doi.org/10.1016/B978-1-895198-85-0.50006-6.

5 Experimental Section

5.1 Experimental Section for Chapter 2

5.1.1 Materials

PVC (M_w = 43,000, M_n = 22,000) was purchased from Sigma-Aldrich. 3-Pentanone (≥99%), tri(ethylene glycol) monomethyl ether (95%), and silica gel (Grade 60, 230–400 mesh particle size, 40–63 μm particle size) were purchased from Sigma-Aldrich. L-glutamic acid (≥99%) was purchased from Alfa Aesar. *n*-Butanol Heysham, England (HPLC grade), toluene (HPLC grade), tetrahydrofuran (HPLC grade), acetonitrile (Optima™, LC/MS grade), dimethylformamide (DMF) (sequencing grade), *N*-methyl-2-pyrrolidone (NMP) (>99.8%), dichloromethane (DCM) (stabilized HPLC grade, submicron filtered), methanol, hexanes, ethyl acetate, and tetrahydrofuran (HPLC grade, submicron filtered, uninhibited) were purchased from Fisher Scientific. *n*-Hexanol (>98%), *n*-decanol (97%), 2-ethyl-1-hexanol (>99.5%), and tri(ethylene glycol) monobutyl ether (>97%) were supplied by Tokyo Chemical Industries (TCI). *p*-Tolenesulfonic acid monohydrate (*p*TSA)(99%, extra pure), sodium azide (99%, extra pure), and acetylenedicarboxylic acid (98%) were purchased from Acros Organics. 4-(4,6-Dimethoxy-1,3,5-triazin-2-yl)-4-methylmorpholinium chloride (DMTMM) (tech) was purchased from Oakwood Chemical. $CDCl_3$ (D 99.8%) was supplied by Cambridge Isotope Laboratories.

5.1.2 Measurements

Fourier transform infrared spectroscopy (FTIR) was recorded with a Perkin-Elmer Spectrum One Spectrometer. Liquid samples were measured neat. Soild samples (expect for polymers) were measured using the KBr pellet method. Polymers were measured by forming a thin film on a sodium chloride plate. Nuclear magnetic resonance (NMR) spectra were recorded with a Bruker Avance III HD 4 channel 500 MHz Oxford Magnet NMR Spectrometer with Automation or a Varian Unity Plus 500 MHz Oxford Magnet NMR Spectrometer at ambient temperature in $CDCl_3$ as solvent. The signal of residual $CHCl_3$ was used as an internal standard

(^{1}H NMR, δ 7.26 ppm; ^{13}C NMR, δ 77.16 ppm). High-resolution mass spectrometry (HRMS) was recorded with a Thermo Scientific LTQ Orbitrap Velos Pro HRMS using acetonitrile (CH_3CN) with 0.1% formic acid as solvent. Elemental analysis was performed by either MHW Laboratories or NuMega Resonance Labs. Glass-transition temperatures (T_gs)of polymers were measured using a TA Instruments differential scanning calorimetry (DSC) Q2000 with a heat-cool-heat protocol, and a scanning range of −90 to 200 °C at a heating rate of 10 °C min^{-1}. Derivative thermogravimetry (DTG) and thermal gravimetric analyses (TGA) were performed using a TA Instruments TGA Q500. TGA was performed within a scanning range of 30–500 °C at a heating rate of 10 °C min^{-1} in air or nitrogen, as specified.

5.1.3 Experimental Method

Preparation of 2-Aminopentanedioate (2.1a-f)

These esterifications were carried out following a modified procedure by Ijiro et al.[1]

Preparation of 1,5-Bisbutyl (2S)-2-Aminopentanedioate (2.1a)

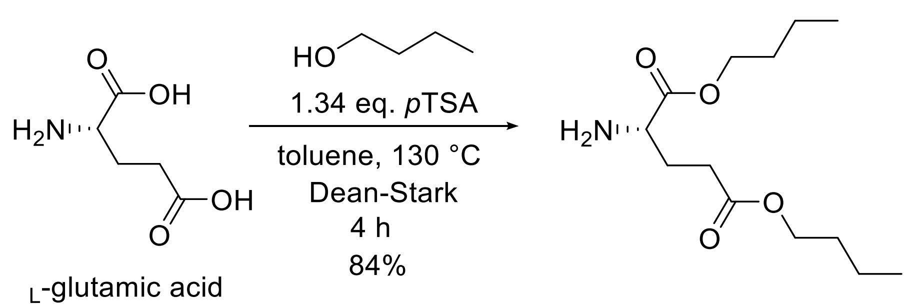

2.1a

To a 100 mL round-bottom flask was added L-glutamic acid (1.372 g, 9.325 mmol), 1-butanol (2.80 mL, 30.6 mmol), *p*TSA (2.377 g, 12.50 mmol), and toluene (40 mL). The solution was refluxed with a Dean-Stark apparatus for 4 h. The reaction mixture was then concentrated *in vacuo* and the residue neutralized using sat. $NaHCO_3$ (50 mL). The aqueous solution was extracted with EtOAc (50 mL). The organic layer was washed with sat.

$NaHCO_3$ (50 mL), brine (50 mL × 2), and then dried over $MgSO_4$ and concentrated *in vacuo* . The residue was purified by silica gel column chromatography using $MeOH/CH_2Cl_2$ (5/95) to give **2.1a** as a pale yellow liquid (2.041 g, 84.41%).

R_f: 0.48 (SiO_2, $MeOH/CH_2Cl_2$, 5/95).

^{1}H NMR (500 MHz, $CDCl_3$, δ, ppm): 4.13 (td, *J* = 6.7, 1.6 Hz, 2H), 4.08 (t, *J* = 6.7 Hz, 2H), 3.54–3.46 (m, 1H), 2.46 (t, *J* = 7.5 Hz, 2H), 2.15–2.03 (m, 1H), 1.85 (dq, *J* = 15.1, 7.7 Hz, 1H), 1.78–1.56 (m, 6H), 1.44–1.32 (m, 4H), 0.94 (t, *J* = 7.4 Hz, 3H), 0.93 (t, *J* = 7.4 Hz, 3H).

^{13}C NMR (126 MHz, $CDCl_3$, δ, ppm): 175.78 (C=O), 173.35 (C=O), 65.06 (O—CH_2), 64.54 (O—CH_2), 53.97 (NH_2—CH), 30.82 (CH_2), 30.79 (CH_2), 30.78 (CH_2), 29.95 (CH_2), 19.27 (CH_2), 19.25 (CH_2), 13.84 (CH_3), 13.82 (CH_3).

IR (NaCl, neat, cm^{-1}): 3387 (w, amine N—H), 3322 (w, amine N—H), 2961 (s, alkane C—H), 2936 (s, alkane C—H), 2875 (m, alkane C—H), 1735 (s, ester C=O), 1607 (w, amine N—H bending), 1183 (s, ester C—O).

HRMS (*m/z*): calcd for $C_{13}H_{26}NO_4$, 260.1856; found, 260.1836 $[M + H]^+$.

Preparation of 1,5-Bishexyl (2S)-2-Aminopentanedioate (2.1b)

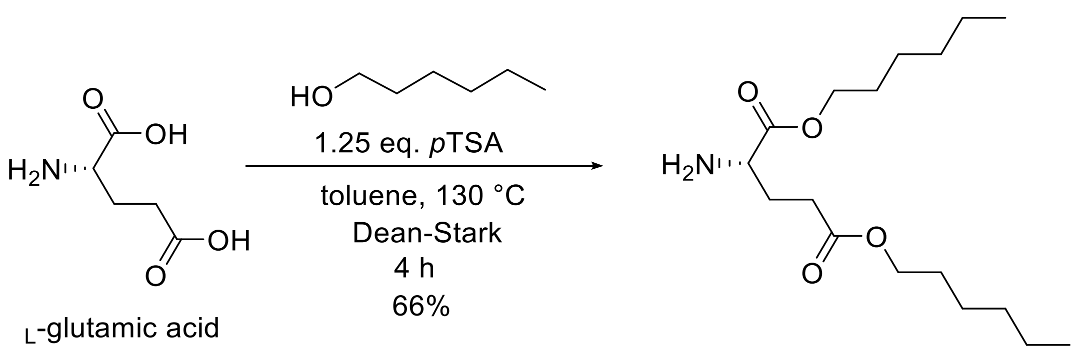

2.1b

To a 100 mL round-bottom flask was added L-glutamic acid (1.472 g, 10.00 mmol), 1-hexanol (2.248 g, 22.00 mmol), *p*TSA (2.378 g, 12.50 mmol), and toluene (40 mL). The solution was refluxed with a Dean–Stark apparatus for 4 h. The reaction mixture was concentrated *in vacuo* and then the residue was neutralized using sat. $NaHCO_3$ (50 mL). The aqueous solution was extracted with EtOAc (50 mL). The organic layer was washed with sat. $NaHCO_3$ (50 mL), brine (50 mL × 2), and then dried over $MgSO_4$ and concentrated *in vacuo* . The residue was purified by silica gel column chromatography using $MeOH/CH_2Cl_2$ (3/97) to give **2.1b** as a pale yellow liquid (2.077 g, 65.84%).

R_f: 0.33 (SiO_2, $MeOH/CH_2Cl_2$, 3/97).

^1H NMR (500 MHz, $CDCl_3$, δ, ppm): 4.12 (td, J = 6.8, 1.7 Hz, 2H), 4.07 (t, J = 6.8 Hz, 2H), 3.49 (dd, J = 8.3, 5.2 Hz, 1H), 2.47 (t, J = 7.5 Hz, 2H), 2.09 (dtd, J = 13.1, 7.7, 5.2 Hz, 1H), 1.86 (dq, J = 15.0, 7.6 Hz, 3H), 1.71–1.55 (m, 4H), 1.41–1.23 (m, 12H), 0.89 (t, J = 6.5 Hz, 6H).

^{13}C NMR (126 MHz, $CDCl_3$, δ, ppm): 175.78 (C=O), 173.35 (C=O), 65.36 (O—CH_2), 64.84 (O—CH_2), 53.97 (NH_2—CH), 31.57 (CH_2), 31.54 (CH_2), 30.83 (CH_2), 29.94 (CH_2), 28.72 (CH_2), 28.70 (CH_2), 25.72 (CH_2), 25.68 (CH_2), 22.67 (CH_2), 22.65 (CH_2), 14.13 (CH_3), 14.12 (CH_3).

IR (NaCl, neat, cm^{-1}): 3388 (w, amine N—H), 3324 (w, amine N—H), 2957 (s, alkane C—H), 2932 (s, alkane C—H), 2860 (m, alkane C—H), 1736 (s, ester C=O), 1607 (w, amine N—H bending), 1180 (s, ester C—O).

HRMS (*m/z*): calcd for $C_{17}H_{34}NO_4$, 316.2482; found, 316.2466 $[M + H]^+$.

Preparation of 1,5-Bis(2-Ethylhexyl) (2S)-2-Aminopentanedioate (2.1c)

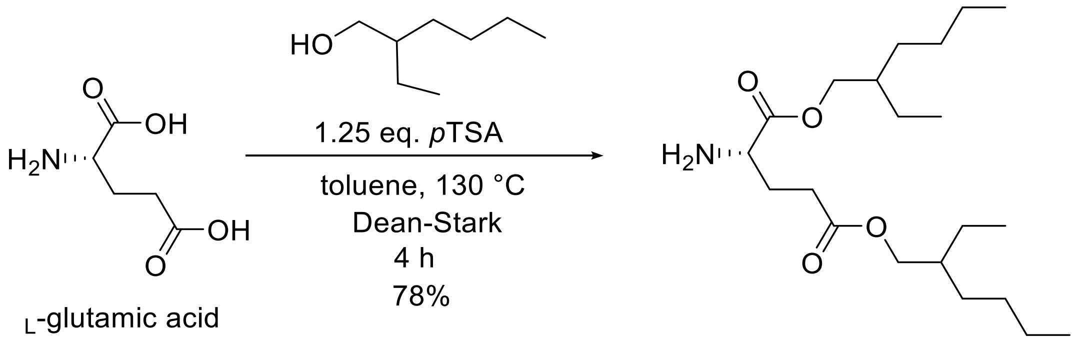

2.1c

To a 100 mL round-bottom flask was added L -glutamic acid (1.471 g, 10.00 mmol), 2-ethyl-1-hexanol (2.866 g, 22.01 mmol), *p*TSA (2.377 g, 12.50 mmol), and toluene (40 mL). The solution was refluxed with a Dean–Stark apparatus for 4 h. The reaction mixture was concentrated *in vacuo* and then the residue was neutralized using sat. $NaHCO_3$ (50 mL). The aqueous solution was extracted with EtOAc (50 mL). The organic layer was washed with sat. $NaHCO_3$ (50 mL), brine (50 mL × 2), and then dried over $MgSO_4$ and concentrated *in vacuo* . The residue was purified by silica gel column chromatography using MeOH/CH_2Cl_2 (3:97) to give **2.1c** as a pale yellow liquid (2.899 g, 78.02%).

R_f: 0.35 (SiO_2, MeOH/CH_2Cl_2, 3/97).

^{1}H NMR (500 MHz, $CDCl_3$, δ, ppm): 4.11–4.02 (m, 2H), 4.02–3.95 (m, 2H), 3.52 (s, 1H), 2.48 (t, J = 7.5 Hz, 2H), 2.16–2.04 (m, 1H), 2.04–1.68 (m, 3H), 1.66–1.51 (m, 2H), 1.41–1.33 (m, 4H), 1.33–1.20 (m, 12H), 1.04–0.74 (m, 12H).

^{13}C NMR (126 MHz, $CDCl_3$, δ, ppm): 175.87 (C=O), 173.43 (C=O), 67.57 (O—CH_2), 67.09 (O—CH_2), 54.02 (NH_2—CH), 38.93 (CH), 38.89 (CH), 30.87 (CH_2), 30.54 (CH_2), 30.48 (CH_2), 29.94 (CH_2), 29.07 (CH_2), 29.05 (CH_2), 23.93 (CH_2), 23.90 (CH_2), 23.11 (CH_2), 23.09 (CH_2), 14.18 (CH_3 × 2), 11.12 (CH_3), 11.09 (CH_3).

IR (NaCl, neat, cm^{-1}): 3389 (w, amine N—H), 3324 (w, amine N—H), 2959 (s, alkane C—H), 2931 (s, alkane C—H), 2874 (s, alkane C—H), 2861 (s, alkane C—H), 1736 (s, ester C=O), 1607 (w, amine N—H bending), 1180 (s, ester C—O).

HRMS (*m/z*): calcd for $C_{21}H_{42}NO_4$: 372.3108; found, 372.3094 $[M + H]^+$.

Preparation of 1,5-Bis(Decyl) (2S)-2-Aminopentanedioate (2.1d)

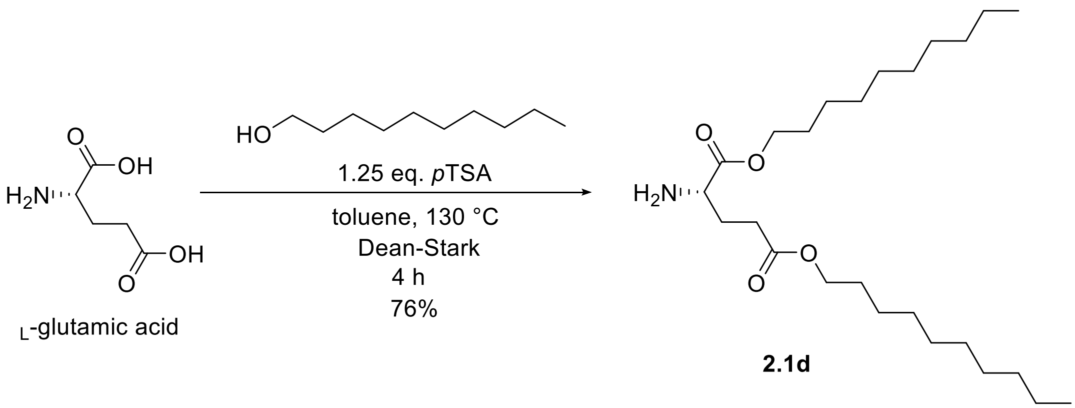

To a 100 mL round-bottom flask was added L-glutamic acid (1.472 g, 10.01 mmol), 1-n-decanol (4.28 ml, 22.4 mmol), *p*TSA (2.378 g, 12.50 mmol), and toluene (40 mL). The solution was refluxed with a Dean–Stark apparatus for 4 h. The reaction mixture was concentrated *in vacuo* and then the residue was neutralized using sat. $NaHCO_3$ (50 mL). The aqueous solution was extracted with EtOAc (50 mL). The organic layer was washed with sat. $NaHCO_3$ (50 mL), brine (50 mL × 2), and then dried over $MgSO_4$ and concentrated *in vacuo* and then the residue was purified by silica gel column chromatography using $MeOH/CH_2Cl_2$ (3/97) to give **2.1d** as a pale yellow liquid (3.268 g, 76.33%).

R_f: 0.43 (SiO_2, $MeOH/CH_2Cl_2$, 3/97).

^1H NMR (500 MHz, $CDCl_3$, δ, ppm): 4.11 (t, J = 6.8 Hz, 2H), 4.07 (t, J = 6.8 Hz, 2H), 3.47 (dd, J = 8.3, 5.2 Hz, 1H), 2.46 (t, J = 7.5 Hz, 2H), 2.14–2.03 (m, 1H), 1.90–1.79 (m, 1H), 1.70–1.55 (m, 6H), 1.41–1.16 (m, 28H), 0.88 (t, J = 6.8 Hz, 6H).

^{13}C NMR (126 MHz, $CDCl_3$, δ, ppm): 175.81 (C=O), 173.35 (C=O), 65.36 (CH_2), 64.84 (CH_2), 53.98 (NH_2—CH), 32.03 (CH_2 × 2), 30.83 (CH_2), 29.96 (CH_2), 29.67 (CH_2), 29.65 (CH_2), 29.44 (CH_2 × 2), 29.40 (CH_2), 29.37 (CH_2), 28.77 (CH_2), 28.75 (CH_2), 26.06 (CH_2), 26.02 (CH_2), 22.82 (CH_2 × 2), 14.24 (CH_3 × 2).

IR (NaCl, neat, cm^{-1}): 3389 (w, amine N—H), 3324.5 (w, amine N—H), 2954.9 (s, alkane C—H), 2925.7 (s, alkane C—H), 2855.4 (s, alkane C—H), 1736.1 (s, ester C=O), 1607.4 (w, amine N-H bending), 1179.5 (s, ester C—O).

HRMS (*m/z*): calcd for $C_{25}H_{50}NO_4$, 428.3734; found, 428.3714 $[M + H]^+$.

Preparation of 1,5-Bis({2-[2-(2-Methoxyethoxy)Ethoxy]Ethyl}) (2S)-2-Aminopentanedioate (2.1e)

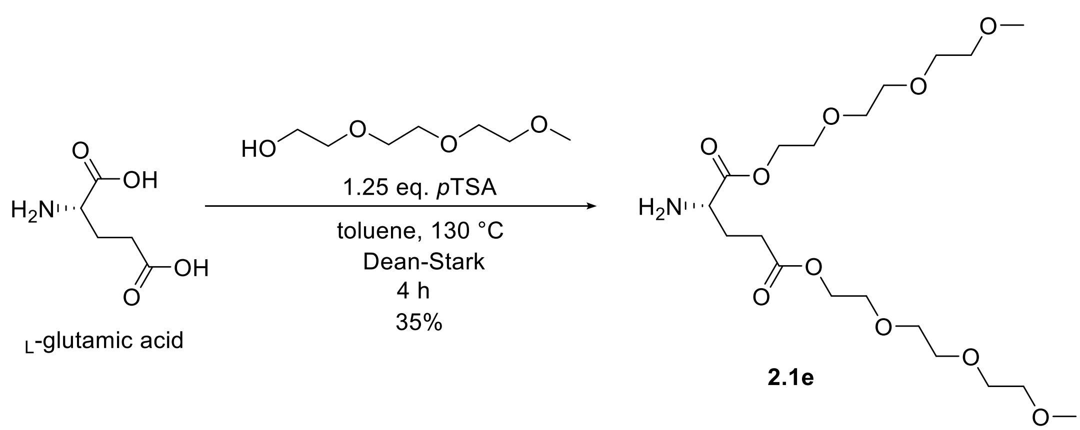

To a 100 mL round-bottom flask was added L-glutamic acid (1.472 g, 10.01 mmol), triethyleneglycol methyl ether (4.538 g, 27.64 mmol), *p*TSA (2.378 g, 12.50 mmol), and toluene (40 mL). The solution was refluxed with a Dean–Stark apparatus for 4 h. The reaction mixture was concentrated *in vacuo* and then the residue was neutralized using sat. $NaHCO_3$ (50 mL). The aqueous solution was extracted with DCM (50 mL). The organic layer was washed with sat. $NaHCO_3$ (50 mL), brine (50 mL × 2), and then dried over $MgSO_4$ and concentrated *in* *vacuo* . The residue was purified by silica gel column chromatography using MeOH/CH_2Cl_2 (5/95) to give **2.1e** as a yellow liquid (1.535 g, 34.90%).

R_f: 0.30 (SiO_2, MeOH/CH_2Cl_2, 5/95).

^{1}H NMR (500 MHz, $CDCl_3$, δ, ppm): 4.28 (t, *J* = 4.9 Hz, 2H), 4.23 (t, *J* = 4.9 Hz, 2H), 3.76–3.68 (m, 4H), 3.68–3.59 (m, 12H), 3.58–3.53 (m, 4H), 3.51 (dd, *J* = 8.4, 5.0 Hz, 1H), 3.38 (s, 6H), 2.51 (t, *J* = 7.5 Hz, 2H), 2.10 (dtd, *J* = 13.1, 7.4, 5.1 Hz, 1H), 1.93–1.81 (m, 1H), 1.68 (s, 2H).

^{13}C NMR (126 MHz, $CDCl_3$, δ, ppm): 175.66 (C=O), 173.21 (C=O), 72.08 (CH_2 × 2), 70.76 (CH_2 × 2), 70.74 (CH_2), 70.72 (CH_2 × 2), 69.24 (CH_2), 69.14 (CH_2), 64.15 (CH_2), 64.13 (CH_2), 63.75 (CH_2), 59.18 (CH_3 × 2), 53.90 (NH_2—CH), 30.68 (CH_2), 29.70 (CH_2).

IR (NaCl, neat, cm^{-1}): 3382 (w, amine N—H), 3315 (w, amine N—H), 2877 (s, alkane C—H), 1733 (s, ester C=O), 1607 (w, amine N—H bending), 1183 (s, ester C—O), 1112 (s, ether C—O).

HRMS (*m/z*): calcd for $C_{19}H_{38}NO_{10}$, 440.2490; found, 440.2479 $[M + H]^+$.

Preparation of 1,5-Bis({2-[2-(2-Butoxyethoxy)Ethoxy]Ethyl}) (2S)-2-Aminopentanedioate (2.1f)

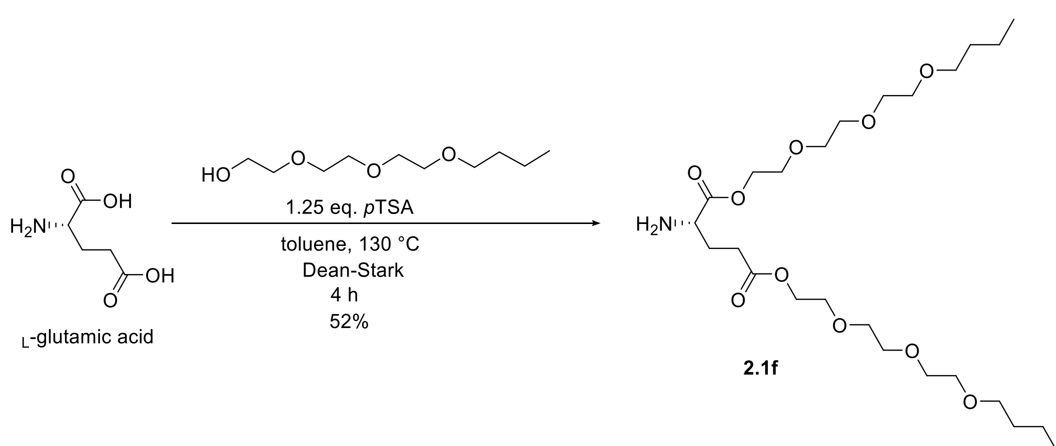

2.1f

To a 100 mL round-bottom flask was added L-glutamic acid (1.471 g, 9.998 mmol), triethyleneglycol butyl ether (4.553 g, 22.07 mmol), *p*TSA (2.378 g, 12.50 mmol), and toluene (40 mL). The solution was refluxed with a Dean–Stark apparatus for 4 h. The reaction mixture was concentrated *in vacuo* and then the residue was neutralized using sat. $NaHCO_3$ (50 mL). The aqueous solution was extracted with DCM (50 mL). The organic layer was washed with sat. $NaHCO_3$ (50 mL), brine (50 mL × 2), and then dried over $MgSO_4$ and concentrated *in vacuo*. The residue was purified by silica gel column chromatography using MeOH/CH_2Cl_2 (4/96) to give **2.1f** as a pale yellow liquid (2.721 g, 51.97%).

R_f: 0.47 (SiO_2, MeOH/CH_2Cl_2, 4/96).

^{1}H NMR (500 MHz, $CDCl_3$, δ, ppm): 4.27 (t, J = 4.9 Hz, 2H), 4.23 (t, J = 4.9 Hz, 2H), 3.74–3.67 (m, 4H), 3.67–3.61 (m, 12H), 3.60–3.54 (m, 4H), 3.50 (dd, J = 8.3, 5.1 Hz, 1H), 3.45 (t, J = 6.7 Hz, 4H), 2.50 (t, J = 7.6 Hz, 2H), 2.15–2.03 (m, 1H), 1.91–1.80 (m, 1H), 1.64 (s, 2H), 1.60–1.51 (m, 4H), 1.41–1.29 (m, 4H), 0.91 (t, J = 7.4 Hz, 6H).

^{13}C NMR (126 MHz, $CDCl_3$, δ, ppm): 175.64 (C=O), 173.20 (C=O), 71.33 (CH_2 × 2), 70.81 (CH_2), 70.74 (CH_2), 70.72 (CH_2), 70.19 (CH_2), 69.22 (CH_2), 69.12 (CH_2), 64.13 (CH_2), 63.75 (CH_2), 53.88 (NH_2—CH), 31.83 (CH_2 × 2), 30.66 (CH_2), 29.68 (CH_2), 19.40 (CH_2 × 2), 14.04 (CH_3 × 2).

IR (NaCl, neat, cm^{-1}): 3384 (w, amine N—H), 3318 (w, amine N—H), 2957 (s, alkane C—H), 2933 (s, alkane C—H), 2870 (s, alkane C—H), 1736 (s, ester C=O), 1607 (w, amine N—H bending), 1180 (s, ester C—O), 1115 (s, ether C—O).

HRMS (*m/z*): calcd for $C_{25}H_{50}NO_{10}$, 524.3429; found, 524.3406 $[M + H]^+$.

Preparation of 2.2a-f

These amidations were carried out following the general procedure by Heyl and Fessner.[2]

Preparation of 1,5-dibutyl (2S)-2-(3-{[(2S)-1,5-dibutoxy-1,5-dioxopentan-2-yl]carbamoyl }prop-2-ynamido)pentanedioate (2.2a)

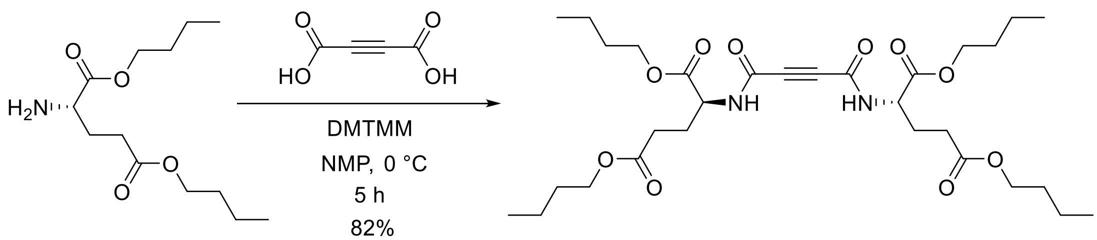

2.1a

2.2a

To a solution of acetylenedicarboxylic acid (286.2 mg, 2.509 mmol) in NMP (5 mL) at 0 °C was added a solution dropwise of amine **2.1a** (1.553 g, 5.988 mmol) in NMP (2.5 mL). After 10 min, DMTMM (2.006 g, 7.249 mmol) was added. The reaction mixture was stirred at 0 °C for 5 h. The mixture was partitioned between ethyl acetate (50 mL) and water (50 mL). The organic layer was washed with brine (50 mL), sat. $NaHCO_3$ (50 mL), 1 M HCl (50 mL), and brine (50 mL × 2). The organic layer was dried over $MgSO_4$ and concentrated *in vacuo* . The residue was dissolved in a minimum amount of refluxing THF, cooled to room temperature, and then stored at −20 °C overnight. The byproduct (6-dimethoxy-1,3,5-triazin-2(1H)-one) was crystallized from the THF solution and removed by filtration. The solution was concentrated *in vacuo* and further purified by column chromatography (SiO_2, hexanes/ethyl acetate, 7/3). The product was obtained as an amorphous white solid (1.220 g, 2.045 mmol, 81.51%).

R_f: 0.25 (SiO_2, hexanes/ethyl acetate, 7/3).

Melting point: 62–63 °C.

^{1}H NMR (500 MHz, $CDCl_3$, δ, ppm): 7.10 (d, *J* = 8.0 Hz, 2H), 4.68 (td, *J* = 7.9, 5.0 Hz, 2H), 4.17 (td, *J* = 6.7, 2.8 Hz, 4H), 4.09 (t, *J* = 6.7 Hz, 4H), 2.48–2.33 (m, 4H), 2.29–2.20 (m, 2H), 2.04 (dtd, *J* = 14.3, 8.1, 6.4 Hz, 2H), 1.69–1.57 (m, 8H), 1.44–1.33 (m, 8H), 0.94 (t, *J* = 7.5 Hz, 6H), 0.93 (t, *J* = 7.3 Hz, 6H).

^{13}C NMR (126 MHz, $CDCl_3$, δ, ppm): 172.71 (C=O), 171.01 (C=O), 151.13 (C=O), 76.84 (C-alkyne), 66.12 (CH_2), 64.94 (CH_2), 52.28 (CH), 30.74 (CH_2), 30.62 (CH_2), 30.25 (CH_2), 27.35 (CH_2), 19.25 (CH_2), 19.16 (CH_2), 13.83 (CH_3), 13.78 (CH_3).

IR (KBr pellet, cm^{-1}): 3279 (s, amine N—H), 2960 (s, alkane C—H), 2934 (s, alkane C—H), 2874 (s, alkane C—H), 1744 (s, ester C=O), 1728 (s, ester C=O), 1650 (s, amide C=O), 1538 (s, amide N—H bending), 1176 (s, ester C—O).

HRMS (*m/z*): Calcd for $C_{30}H_{49}N_2O_{10}$, 597.3382; found, 597.3384 $[M + H]^+$.

Preparation of 1,5-Bishexyl (2S)-2-(3-{[(2S)-1,5-Bis(Hexyloxy)-1,5-Dioxopentan-2-yl] Carbamoyl} Prop-2-Ynamido)Pentanedioate (2.2b)

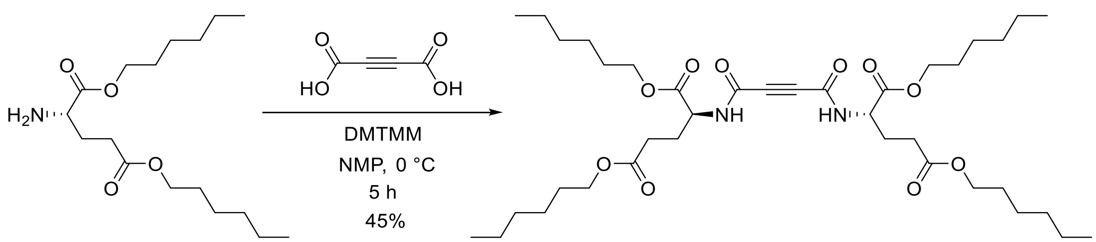

To a solution of acetylenedicarboxylic acid (1.134 g, 9.942 mmol) in NMP (20 mL) at 0 °C was added a solution dropwise of amine **2.1b** (9.677 g, 30.68 mmol) in NMP (10 mL). After 10 min, DMTMM (7.783 g, 28.13 mmol) was added. The reaction mixture was stirred at 0 °C for 5 h. The mixture was partitioned between ethyl acetate (150 mL) and water (150 mL). The organic layer was washed with brine (200 mL), sat. $NaHCO_3$(200 mL), 1 M HCl (200 mL), and brine (200 mL × 2). Then the organic layer was dried over $MgSO_4$ and concentrated *in vacuo* . The residue was dissolved in a minimum amount of refluxing THF, cooled to room temperature, and then stored at −20 °C overnight. The byproduct (6-dimethoxy-1,3,5-triazin-2(1H)-one) was crystallized from the THF solution and removed by filtration. The solution was concentrated *in* *vacuo* and further purified by column chromatography (SiO_2, hexanes/ethyl acetate, 75/25). The product was obtained as an amorphous white solid (3.160 g, 4.457 mmol, 44.83%).

R_f: 0.43 (SiO_2, hexanes/ethyl acetate, 75/25).

Melting point: 60–62 °C.

^{1}H NMR (500 MHz, $CDCl_3$, δ, ppm): 6.80 (d, J = 7.8 Hz, 2H), 4.66 (td, J = 7.6, 5.0 Hz, 2H), 4.17 (td, J = 6.8, 3.7 Hz, 4H), 4.08 (t, J = 6.8 Hz, 4H), 2.50–2.30 (m, 4H), 2.29–2.19 (m, 2H), 2.05 (dp, J = 14.4, 7.3, 6.7 Hz, 2H), 1.71–1.57 (m, 8H), 1.41–1.22 (m, 24H), 0.97–0.81 (m, 12H).

^{13}C NMR (126 MHz, $CDCl_3$, δ, ppm): 172.67 (C=O), 171.03 (C=O), 151.14 (C=O), 76.85 (C-alkyne), 66.41 (O—CH_2), 65.23 (O—CH_2), 52.26 (NH_2—CH), 31.56 (CH_2), 31.47 (CH_2), 30.24 (CH_2), 28.66 (CH_2), 28.55 (CH_2), 27.35 (CH_2), 25.69 (CH_2), 25.57 (CH_2), 22.66 (CH_2), 22.63 (CH_2), 14.13 (CH_3), 14.10 (CH_3).

IR (KBr pellet, cm^{-1}): 3269 (s, amine N—H), 2958 (s, alkane C—H), 2932 (s, alkane C—H), 2860 (s, alkane C—H), 1739 (s, ester C=O), 1646 (s, amide C=O), 1540 (s, amide N—H bending), 1190 (s, ester C—O).

HRMS (*m/z*): Calcd for $C_{38}H_{65}N_2O_{10}$, 709.4634; found, 709.4628 $[M + H]^+$.

Preparation of 1,5-Bis(2-Ethylhexyl) (2S)-2-(3-{[(2S)-1,5-Bis[(2-Ethylhexyl)Oxy]-1,5-Dioxopentan-2-yl]Carbamoyl}Prop-2-Ynamido)Pentanedioate (2.2c)

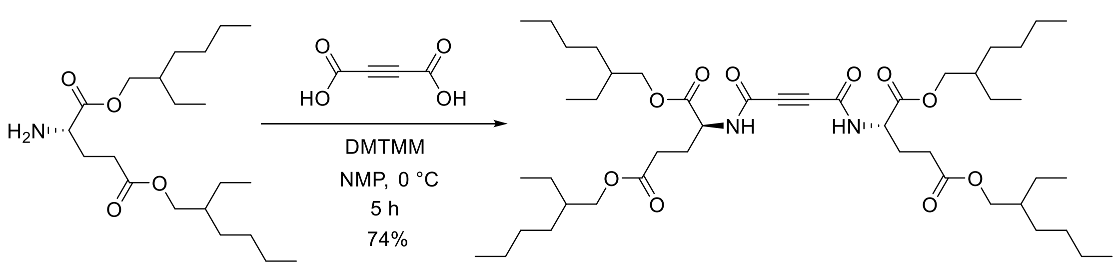

2.1c **2.2c**

To a solution of acetylenedicarboxylic acid (286.6 mg, 2.513 mmol) in NMP (5 mL) at 0 °C was added a solution dropwise of amine **2.1c** (2.538 g, 6.831 mmol) in NMP (2.5 mL). After 10 min, DMTMM (2.005 g, 7.246 mmol) was added. The reaction mixture was stirred at 0 °C for 5 h. The mixture was partitioned between ethyl acetate (50 mL) and water (50 mL). The organic layer was washed with brine (50 mL), sat. $NaHCO_3$ (50 mL), 1 M HCl (50 mL), and brine (50 mL × 2). Then the organic layer was dried over $MgSO_4$ and concentrated *in vacuo* . The residue was dissolved in a minimum amount of refluxing THF, cooled to room temperature, and then stored at −20 C overnight. The byproduct (6-dimethoxy-1,3,5-triazin-2(1H)-one) was crystallized from the THF solution and removed by filtration. The solution was concentrated *in vacuo* and further purified by column chromatography (SiO_2, hexanes/ethyl acetate, 80/20). The product was obtained as an amorphous white solid (1.528 g, 1.861 mmol, 74.05%).

R_f: 0.37 (SiO_2, hexanes/ethyl acetate, 80/20).

Melting point: 49–53 °C.

^1H NMR (500 MHz, $CDCl_3$, δ, ppm): 6.84 (d, J = 7.8 Hz, 2H), 4.68 (td, J = 7.6, 4.9 Hz, 2H), 4.15–4.05 (m, 4H), 4.05–3.96 (m, 4H), 2.49–2.31 (m, 4H), 2.29–2.21 (m, 2H), 2.09–2.01 (m, 2H), 1.66–1.55 (m, 4H), 1.43–1.18 (m, 32H), 1.04–0.74 (m, 24H).

^{13}C NMR (126 MHz, $CDCl_3$ δ, ppm): 172.72 (C=O), 171.10 (C=O), 151.09 (C=O), 76.81 (C-alkyne), 68.61 (O─CH_2), 68.58 (O─CH_2), 67.48 (O-CH_2), 52.28 (NH_2─CH), 38.83 (CH), 38.79 (CH), 30.47 (CH_2), 30.41 (CH_2), 30.37 (CH_2), 30.24 (CH_2), 29.05 (CH_2), 29.00 (CH_2), 28.98 (CH_2), 27.41 (CH_2), 23.86 (CH_2), 23.81 (CH_2), 23.79 (CH_2), 23.09 (CH_2), 23.06 (CH_2), 23.05 (CH_2), 14.18 (CH_3), 14.15 (CH_3), 11.09 (CH_3), 11.05 (CH_3), 11.02 (CH_3).

IR (KBr pellet, cm^{-1}): 3291 (s, amine N─H), 2959 (s, alkane C─H), 2931 (s, alkane C─H), 2874 (s, alkane C─H), 2860 (s, alkane C─H), 1742 (s, ester C=O), 1731 (s, ester C=O), 1651 (s, amide C=O), 1641 (s, amide C=O), 1533 (s, amide N─H bending), 1179 (s, ester C─O).

HRMS (*m/z*): Calcd for $C_{46}H_{81}N_2O_{10}$, 821.5886; found, 821.5890 $[M + H]^+$.

Preparation of 1,5-Bis(Decyl) (2S)-2-(3-{[(2S)-1,5-Bis(Decyloxy)-1,5-Dioxopentan-2-yl] Carbamoyll}Prop-2-Ynamido)Pentanedioate (2.2d)

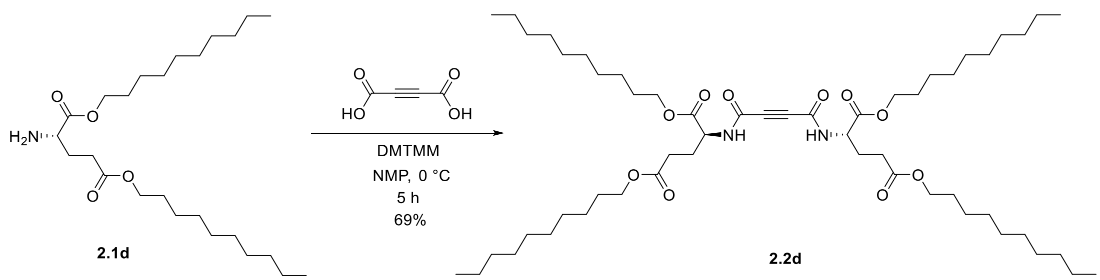

To a solution of acetylenedicarboxylic acid (1.378 g, 12.08 mmol) in NMP (24 mL) at 0 °C was added a solution dropwise of amine **2.1d** (12.74 g, 29.79 mmol) in NMP (12 mL). After 10 min, DMTMM (9.300 g, 33.61 mmol) was added. The reaction mixture was stirred at 0 °C for 5 h. The mixture was partitioned between ethyl acetate (200 mL) and water (200 mL). The organic layer was washed with brine (200 mL), sat. $NaHCO_3$ (200 mL), 1 M HCl (200 mL), and brine (200 mL × 2). The organic layer was then dried over $MgSO_4$ and concentrated *in vacuo* . The residue was dissolved in a minimum amount of refluxing THF, cooled to room temperature, and then stored at −20 °C overnight. The byproduct (6-dimethoxy-1,3,5-triazin-2(1H)-one) was crystallized from the THF solution and removed by filtration. The solution was concentrated *in vacuo* and further purified by column chromatography (SiO_2, hexanes/ethyl acetate, 80/20). The product was obtained as an amorphous white solid (7.818 g, 8.376 mmol, 69.34%).

R_f: 0.40 (SiO_2, hexanes/ethyl acetate, 80/20).

Melting point: 50–51 °C.

^{1}H NMR (500 MHz, $CDCl_3$, δ, ppm): 6.79 (d, *J* = 7.7 Hz, 2H), 4.66 (td, *J* = 7.6, 5.1 Hz, 2H), 4.21–4.11 (m, 4H), 4.08 (t, *J* = 6.8 Hz, 4H), 2.49–2.30 (m, 4H), 2.24 (dq, *J* = 13.5, 7.2 Hz, 2H), 2.04 (dq, *J* = 14.5, 7.5 Hz, 2H), 1.71–1.57 (m, 8H), 1.39–1.18 (m, 58H), 0.88 (t, *J* = 6.8 Hz, 12H).

^{13}C NMR (126 MHz, $CDCl_3$, δ, ppm): 172.67 (C=O), 171.02 (C=O), 151.13 (C=O), 76.80 (C-alkyne), 66.42 (O—CH_2), 65.24 (O—CH_2), 52.26 (NH_2—CH), 32.02 (CH_2 × 2), 30.23 (CH_2), 29.68 (CH_2), 29.67 (CH_2 × 2), 29.63 (CH_2), 29.44 (CH_2 × 2), 29.40 (CH_2), 29.34 (CH_2), 28.71 (CH_2), 28.60 (CH_2), 27.36 (CH_2), 26.03 (CH_2), 25.91 (CH_2), 22.81 (CH_2 × 2), 14.24 (CH_3 × 2).

IR (KBr pellet, cm^{-1}): 3307 (s, amine N—H), 2955 (s, alkane C—H), 2922 (s, alkane C—H), 2854 (s, alkane C—H), 1746 (s, ester C=O), 1733 (s, ester C=O), 1648 (s, amide C=O), 1643 (s, amide C=O), 1528 (s, amide N—H bending), 1199 (s, ester C—O).

HRMS (*m/z*): Calcd for $C_{54}H_{97}N_2O_{10}$, 933.7138; found, 933.7143 $[M + H]^+$.

Preparation of 1,5-Bis({2-[2-(2-MethoxyEthoxy)Ethoxy]Ethyl}) (2S)-2-(3-{[(2S)-1,5-Bis({2-[2-(2-MethoxyEthoxy)Ethoxy]Ethoxy})-1,5-Dioxopentan-2-yl]Carbamoyl}Prop-2-Ynamido)Pentanedioate (2.2e)

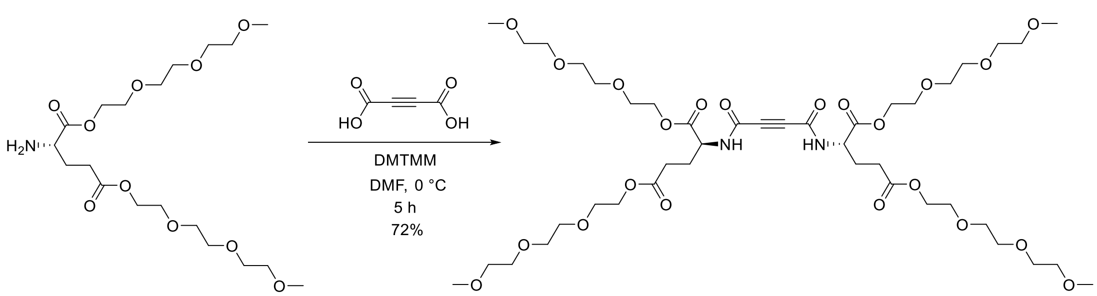

To a solution of acetylenedicarboxylic acid (0.8424 g, 7.386 mmol) in DMF (15 mL) at 0 °C was added a solution dropwise of amine **2.1e** (9.055 g, 20.60 mmol) in DMF (7.5 mL).

After 10 min, DMTMM (5.180 g, 18.72 mmol) was added. The reaction mixture was stirred at 0 °C for 5 h. The mixture was filtered. The filtrate was partitioned between DCM (150 mL) and water (150 mL). The organic layer was washed with brine (150 mL), sat. $NaHCO_3$ (150 mL), 1 M HCl (150 mL), and brine (150 mL × 2). The organic layer was dried over $MgSO_4$ and concentrated *in vacuo*. The residue was purified by column chromatography (SiO_2, CH_2CH_2/MeOH, 95/5). The product was obtained as a clear oil (5.104 g, 5.333 mmol, 72.20%).

R_f: 0.38 (SiO_2, CH_2CH_2/MeOH, 95/5).

^{1}H NMR (500 MHz, $CDCl_3$, δ, ppm): 7.54 (d, *J* = 8.1 Hz, 2H), 4.67 (td, *J* = 8.1, 5.1 Hz, 2H), 4.31 (dt, *J* = 10.9, 6.1 Hz, 4H), 4.28–4.18 (m, 4H), 3.70 (t, *J* = 4.9 Hz, 8H), 3.67 (s, 7H), 3.66–3.61 (m, 17H), 3.58–3.52 (m, 8H), 3.37 (d, *J* = 2.5 Hz, 12H), 2.53–2.36 (m, 4H), 2.24 (dtd, *J* = 14.6, 7.4, 5.1 Hz, 2H), 2.06 (dq, *J* = 14.8, 7.6 Hz, 2H).

^{13}C NMR (126 MHz, $CDCl_3$, δ, ppm): 172.54 (C=O), 170.64 (C=O), 151.25 (C=O), 76.78 (C-alkyne), 72.07 (CH_2), 72.03 (CH_2), 70.80 (CH_2), 70.71 (CH_2 × 2), 70.65 (CH_2), 70.63 (CH_2), 69.06 (CH_2), 68.86 (CH_2), 64.85 (CH_2), 64.00 (CH_2), 59.11 (CH_3 × 2), 52.22 (NH_2—CH), 30.38 (CH_2), 27.10 (CH_2).

IR (NaCl, neat, cm^{-1}): 3260 (s, amine N—H), 2878 (s, alkane C—H), 1736 (s, ester C=O), 1665 (s, amide C=O), 1535 (s, amide N—H bending), 1199 (s, ester C—O), 1104(s, ether C–O).

HRMS (*m/z*): Calcd for $C_{42}H_{73}N_2O_{22}$, 957.4649; found, 957.4652 $[M + H]^+$.

Preparation of 1,5-Bis({2-[2-(2-Butoxyethoxy) Ethoxy]Ethyl}) (2S)-2-(3-{[(2S)-1,5-Bis({2-[2-(2-Butoxyethoxy)Ethoxy]Ethoxy})-1,5-Dioxopentan-2-yl]Carbamoyl}Prop-2-Ynamido)Pentanedioate (2.2f)

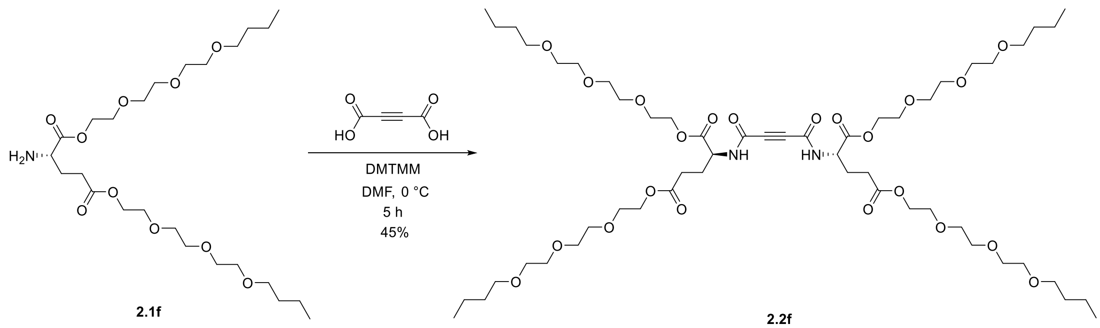

To a solution of acetylenedicarboxylic acid (0.7922 g, 6.945 mmol) in DMF (15 mL) at 0 °C was added a solution dropwise of amine **2.1f** (12.47 g, 23.81 mmol) in DMF (7.5 mL). After 10 min, DMTMM (5.430 g, 19.62 mmol) was added. The reaction mixture was stirred at 0 °C for 5 h. The mixture was filtered. The filtrate was partitioned between DCM (150 mL) and water (150 mL). The organic layer was washed with brine (150 mL), sat. $NaHCO_3$ (150 mL), 1 M HCl (150 mL), and brine (150 mL × 2). The organic layer was dried over $MgSO_4$ and concentrated *in vacuo* . The residue was purified by column chromatography (SiO_2, CH_2CH_2/MeOH, 96/4). The product was obtained as a clear oil (3.520 g, 3.128 mmol, 45.04%).

R_f: 0.28 (SiO_2, CH_2CH_2/MeOH, 96/4).

^{1}H NMR (500 MHz, $CDCl_3$, δ, ppm): 7.38 (d, J = 8.0 Hz, 2H), 4.68 (td, J = 7.9, 5.1 Hz, 2H), 4.37–4.29 (m, 4H), 4.29–4.18 (m, 4H), 3.75–3.69 (m, 8H), 3.67 (s, 7H), 3.66–3.61 (m, 17H), 3.61–3.55 (m, 8H), 3.46 (td, J = 6.7, 2.9 Hz, 8H), 2.55–2.36 (m, 4H), 2.25 (dtd, J = 14.7, 7.3, 5.2 Hz, 2H), 2.07 (dq, J = 14.7, 7.5 Hz, 2H), 1.61–1.51 (m, 8H), 1.41–1.30 (m, 8H), 0.91 (t, J = 7.4 Hz, 12H).

^{13}C NMR (126 MHz, $CDCl_3$, δ, ppm): 172.55 (C=O), 170.65 (C=O), 151.16 (C=O), 76.77 (C-alkyne), 71.35 (CH_2), 71.34 (CH_2), 70.81 (CH_2 × 2), 70.78 (CH_2 × 2), 70.74 (CH_2 × 2), 70.20 (CH_2), 70.17 (CH_2), 69.08 (CH_2), 68.87 (CH_2), 64.91 (CH_2), 64.04 (CH_2), 52.27 (NH_2—CH), 31.83 (CH_2 × 2), 30.34 (CH_2), 27.13 (CH_2), 19.41 (CH_2 × 2), 14.07 (CH_3 × 2).

IR (NaCl, neat, cm^{-1}): 3270 (m, amine N—H), 2975 (s, alkane C—H), 2933 (s, alkane C—H), 2871 (s, alkane C—H), 1740 (s, ester C=O), 1668 (s, amide C=O), 1534 (m, amide N—H bending), 1198 (s, ester C—O), 1119 (s, ether C—O).

HRMS (*m/z*): Calcd for $C_{54}H_{97}N_2O_{22}$, 1125.6527; found, 1125.6523 $[M + H]^+$.

Preparation of 1-Azidomethyl-4-Tert-Butylbenzene (2.3)

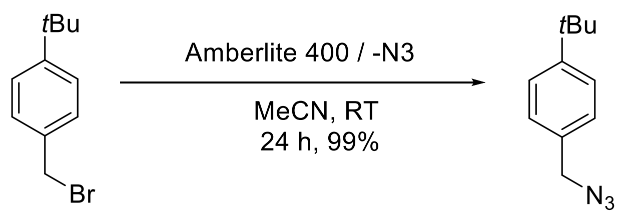

2.3

Caution

Sodium azide and organic azide can be toxic and explosive. Guidelines for safe organic azides should follow $(N_C + N_O)/N_N \geq 3$ and $N_C > N_N$ (N = number of atoms).[3] *t*-Butylbenzylic azide and PVC-azide (4.4% and 12.0%) were found safe to manipulate in the laboratory. Special care is still needed when handling organic azides.

Preparation of Amberlite-N_3

To a 250 mL beaker was added 40.00 g Amberlite IPA-400 and a solution of 15.00 g NaN_3 in 80 ml water.[4] The mixture was left to stir for 1 h. The mixture was filtered and washed with water (100 mL × 2). The charged Amberlite-N_3 was then charged a second time with a new solution of 15 g NaN_3 in 80 mL water for 1 h. After the second charge, Amberlite-N_3 was filtered and washed with water (100 mL × 3), followed by methanol (100 mL), ether (50 mL × 2), and then dried under vacuum for 20 mins.

To a 100 ml round bottom flask was added 1-bromomethyl-4-*tert* -butylbenzene (1.650 g, 7.264 mmol), acetonitrile (30 mL), and Amberlite-N_3 (12.83 g). The reaction was stirred at room temperature for 18 h. The reaction went to completion as monitored by TLC. The reaction mixture was filtered, then dried over $MgSO_4$, filtered again and concentrated. The product was obtained as a clear oil (1.356 g, 7.165 mmol, 98.64%).

R $_f$: 0.57 (SiO_2, hexanes/ethyl acetate, 95/5).

^{1}H NMR (500 MHz, $CDCl_3$, δ, ppm): δ 7.41 (d, *J* = 8.1 Hz, 2H), 7.25 (d, *J* = 7.8 Hz, 2H), 4.31 (s, 2H), 1.33 (s, 9H).

Preparation of 1,5-Dibutyl (2S)-2-({1-[(4-Tert-Butylphenyl)Methyl]-4-{[(2S)-1,5-Dibutoxy-1,5-Dioxopentan-2-yl]Carbamoyl}-1H-1,2,3-Triazol-5-Yl}Formamido)Pentanedioate (2.4)

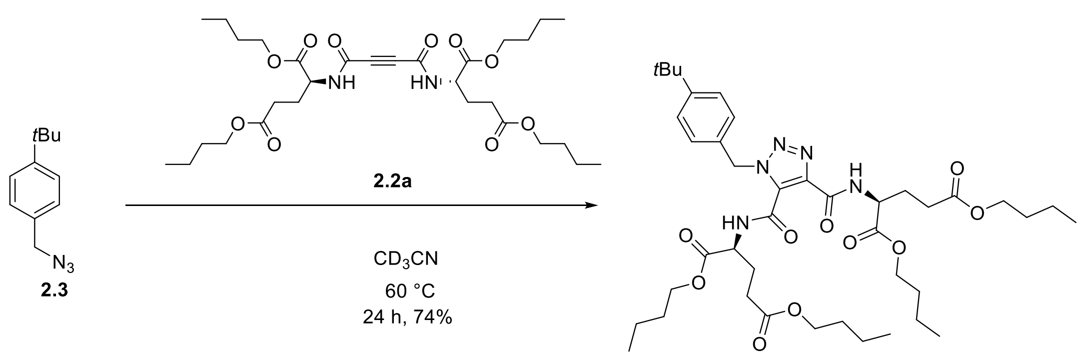

To a solution of benzylic azide **2.3** (94.3 mg, 0.498 mmol) in 2 mL acetonitrile-*d* $_6$ was added alkyne **2.2a** (282.4 mg, 0.4733 mmol). The reaction was heated to 60 °C for 22 h. The reaction mixture was concentrated *in vacuo* and further purified by column chromatography (SiO_2, hexanes/ethyl acetate, 8/2). The product was obtained as a clear oil (290.2 mg, 0.3692 mmol, 74.14%).

R $_f$: 0.41 (SiO_2, hexanes/ethyl acetate, 8/2).

^{1}H NMR (500 MHz, $CDCl_3$, δ, ppm): 11.36 (d, *J* = 7.3 Hz, 1H), 8.19 (d, J = 8.5 Hz, 1H), 7.32 (s, 4H), 6.12(AB, *J* = 13.9 Hz, 1H), 6.07 (AB, *J* = 13.9 Hz, 1H), 4.85 (td, J = 8.0, 5.0 Hz, 1H), 4.71 (td, J = 7.6, 5.4 Hz, 1H), 4.24–4.10 (m, 4H), 4.10–3.99 (m, 4H), 2.53–2.23 (m, 6H), 2.20–2.07 (m, 2H), 1.69–1.55 (m, 9H), 1.44–1.31 (m, 8H), 1.27 (s, 9H), 0.99–0.84 (m, 12H).

^{13}C NMR (126 MHz, $CDCl_3$, δ, ppm): 172.53 (C=O), 172.51 (C=O), 171.19 (C=O), 170.90 (C=O), 161.41 (C=O), 156.69 (C=O), 151.49 (triazole ring C=C), 138.57 (triazole ring C=C), 132.33 (benzene ring C), 130.48 (benzene ring C), 128.42 (benzene ring CH), 125.73 (benzene ring CH), 65.89 (CH_2), 65.53 (CH_2), 64.81 (CH_2), 64.64 (CH_2), 54.12 (CH_2), 52.37 (CH), 51.89 (CH), 34.68 (C), 31.37 (CH_3 × 3), 30.77 (CH_2), 30.71 (CH_2), 30.65 (CH_2), 30.64 (CH_2), 30.48 (CH_2), 30.37 (CH_2), 27.74 (CH_2), 27.33 (CH_2), 19.24 (CH_2), 19.22 (CH_2), 19.16 (CH_2 × 2), 13.83 (CH_3), 13.80 (CH_3), 13.78 (CH_3), 13.76 (CH_3).

IR (neat): 3346 (w, amide N─H), 2961 (s, alkane C─H), 2936 (s, alkane C─H), 2874 (m, alkane C─H), 1739 (s, ester C=O), 1678 (s, amide C=O), 1654 (m, amide C=O), 1582 (m, amide N─H bending), 1552 (s, amide N─H bending), 1180 (s, ester C─O).

HRMS (*m/z*): Calcd for $C_{41}H_{64}N_5O_{10}$, 786.4648; found, 786.4618 $[M + H]^+$.

Preparation of PVC-azide

Purification of PVC

PVC (25.00 g, 400 mmol) was dissolved in THF (250 mL).[5-7] The solution was precipitated in MeOH (1 L). The precipitates were filtered, dissolved in THF, precipitated in MeOH another two times. The precipitate was then dried over house vacuum for 3 days.

Preparation of 4.4 mol % PVC-N_3 (2.5)

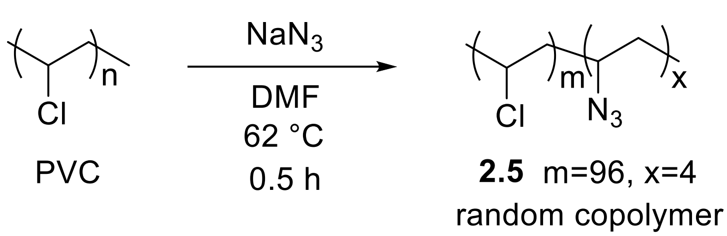

To a solution of purified PVC (12.03 g, 19.24 mmol) in DMF (120 mL) was slowly added sodium azide (11.95 g, 18.38 mmol). The reaction mixture was stirred at 62 °C for 30 min. After cooling to room temperature, the reaction mixture was filtered to remove insoluble salt. The filtrate was precipitated in 1.2 L of MeOH. The mixture was stirred with a stir bar for 10 min. The precipitates were filtered and dried under vacuum to remove the majority of MeOH. The precipitated was then dissolved in 120 mL of THF and precipitated in 600 mL of MeOH/water (3/1). Precipitates were filtered, washed with MeOH, and then dissolved in 120 mL of THF. The solution was then precipitated in MeOH (900 mL). Precipitates were filtered and dried under vacuum for 3 days. The 4.4 mol % PVC-N_3 was obtained as a white solid (8.153 g).

^{1}H NMR (500 MHz, $CDCl_3$, δ, ppm): δ 4.77–4.54 (br, s), 4.54–4.37 (br, s), 4.37–4.23 (br, s), 4.22–4.13 (br, s), 4.13–4.01 (br, s), 2.53–2.23 (br, m), 2.23–1.92 (br, m), 1.92–1.72 (br, m).

Elemental analysis: C, 39.23; H, 5.12; N, 3.02.

Preparation of 12.0 mol % PVC-N_3 (2.5′)

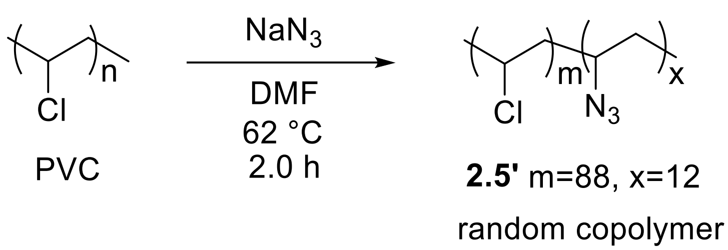

To a solution of PVC (20.00 g, 32.00 mmol) in DMF (200 mL) was slowly added sodium azide (20.00 g, 30.76 mmol). The reaction mixture was stirred to 62 °C for 2 h. The workup procedure was the same as for the 4.4 mol % PVC sample above. The 12.0 mol % PVC-N_3 was obtained as a white solid (12.61 g).

^{1}H NMR (500 MHz, $CDCl_3$, δ, ppm): δ 4.68–4.53 (br, s), 4.53–4.38 (br, s), 4.38–4.22 (br, s), 4.22–4.12 (br,s), 4.12–4.01 (br,s), 2.52–2.23 (br, m), 2.23–1.95 (br, m), 1.95–1.65 (br, m).

Elemental analysis: C, 38.69; H, 5.22; N, 8.17.

Preparation of Internally Plasticized PVC

Preparation of PVC-4.4%-nBu (2.6a)

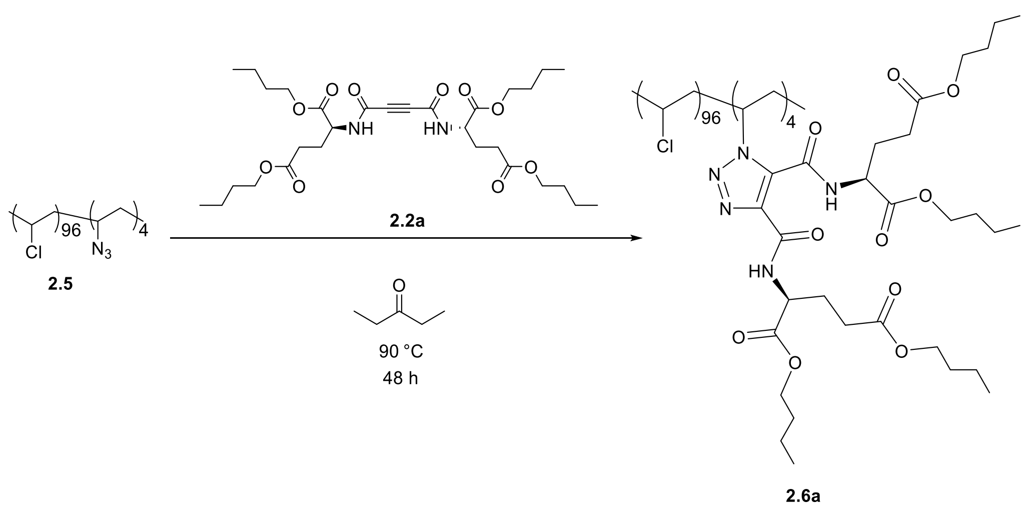

To a 50 mL round bottom flask was added PVC-4.4%-N_3 **2.5** (805.2 mg, 12.88 mmol), alkyne **2.2a** (384.3 mg, 0.6440 mmol), and 3-pentanone (8 mL).[6] The reaction mixture was heated to 90 °C for 48 h. The resulting polymer was purified via precipitation in 100 mL of MeOH three times. The polymer was filtered and dried to give a white solid (750.0 mg).

^{1}H NMR (500 MHz, $CDCl_3$, δ, ppm): δ 11.66–11.23 (br, m), 8.42–8.16 (br, m), 6.77–6.34 (br, m), 4.95–4.82 (br, s), 4.82–4.67 (br, s), 4.67–4.54 (br, m), 4.54–4.39 (br, m), 4.36–4.24 (br, m), 4.24–4.13 (br, m), 4.13–4.01 (br, m), 3.90–3.62 (br, m), 2.99–2.57 (br, m), 2.57–2.23 (br, m), 2.23–1.73 (br, m), 1.73–1.45 (br, m), 1.45–1.15 (br, m), 1.00–0.74 (br, m).

^{13}C NMR (126 MHz, $CDCl_3$, δ, ppm): 172.52 (C=O), 171.03 (C=O), 170.91 (C=O), 161.20 (C=O), 156.55 (C=O), 132.17 (triazole —C=C—), 65.93 ($—CH_2—O—$), 65.59 ($—CH_2—O—$), 64.84 ($—CH_2—O—$), 64.64 ($—CH_2—O—$), 57.11–55.02 (PVC —CH—Cl— and PVC —CH—triazole), 52.43 (˙NH—CH—), 52.01 (—NH—CH—), 47.40–44.94 (family of CH_2 PVC peaks), 30.75 (CH_2), 30.71(CH_2), 30.65 (CH_2), 30.62 (CH_2), 30.49 (CH_2), 30.40 (CH_2), 27.69 (CH_2), 27.31 (CH_2), 19.24 (CH_2), 19.17 (CH_2), 13.87 (CH_3), 13.84 (CH_3), 13.78 (CH_3).

IR (NaCl, thin film, cm^{-1}): 3384 (w, amide N—H), 2962 (s, alkane C—H), 2934 (s, alkane C—H), 2873 (m, alkane C—H), 1736 (s, ester C=O), 1677 (s, amide C=O), 1655 (m, amide C=O), 1579 (m, amide N—H bending), 1552 (m, amide N—H bending), 1255 (s, ester C—O), 1199 (s, ester C—O), 615 (m, C—Cl).

Preparation of PVC-12.0%-nBu (2.6′a)

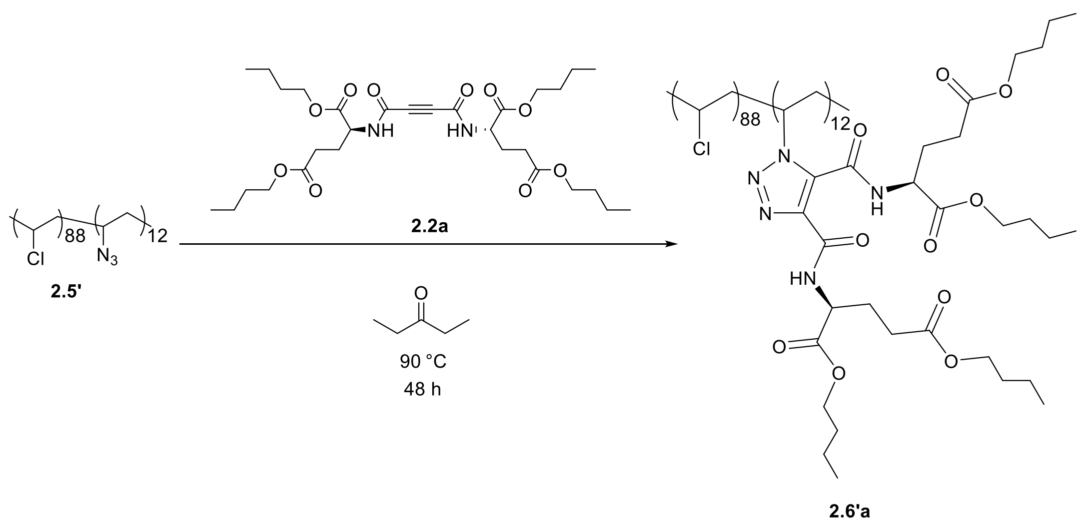

To a 15 mL round bottom flask was added PVC-12.0%-N_3 **2.5′** (217.5 mg, 3.480 mmol), alkyne **2.2a** (780.1 mg, 1.307 mmol), and 3-pentanone (3.5 mL). The reaction mixture was heated to 90 °C for 48 h. The resulting polymer was purified via precipitation in 40 mL of MeOH three times. The polymer was filtered and dried to give a pale yellow solid (297.4 mg).

^{1}H NMR (500 MHz, $CDCl_3$, δ, ppm): 11.69–11.07 (br, m), 8.59–8.10 (br, m), 6.73–6.11 (br, m), 4.94–4.80 (br, s), 4.80–4.66 (br, s), 4.66–4.52 (br, m), 4.52–4.33 (br, m), 4.33–4.24 (br, s), 4.24–4.09 (br, m), 4.09–3.98 (br, m), 3.89–3.50 (br, m), 3.08–2.58 (br, m), 2.57–2.22 (br, m), 2.22–1.81 (br, m), 1.73–1.50 (br, m), 1.49–1.09 (br, m), 1.04–0.70 (br, m).

^{13}C NMR (126 MHz, $CDCl_3$, δ, ppm): 172.52 (C=O), 170.98 (C=O), 161.19 (C=O), 156.52 (C=O), 138.62 (triazole ─C=C─), 132.03 (triazole ─C=C─), 65.91 (─CH_2─O─), 65.57 (─CH_2─O─), 64.82 (─CH_2─O─), 64.62 (─CH_2─O─˙), 57.04–54.95 (PVC ─CH─Cl─ and PVC ─CH─triazole), 52.43 (─NH─CH─), 52.01 (─NH─CH─), 47.40–45.37 (family of CH_2 PVC peaks), 30.75 (CH_2), 30.71 (CH_2), 30.64 (CH_2), 30.62 (CH_2), 30.47 (CH_2), 30.39 (CH_2), 27.69 (CH_2), 27.29 (CH_2), 19.23 (CH_2), 19.16 (CH_2), 13.86 (CH_2), 13.82 (CH_3), 13.77 (CH_3).

IR (NaCl, thin film, cm^{-1}): 3378 (w, amide N─H), 2961 (s, alkane C─H), 2935 (s, alkane C─H), 2874 (m, alkane C─H), 1737 (s, ester C=O), 1677 (s, amide C=O), 1655 (m, amide C=O), 1579 (m, amide N─H bending), 1551 (s, amide N─H bending), 1259 (s, ester C─O), 1199 (s, ester C─O), 616 (w, C─Cl).

Preparation of PVC-4.4%-nHex (2.6b)

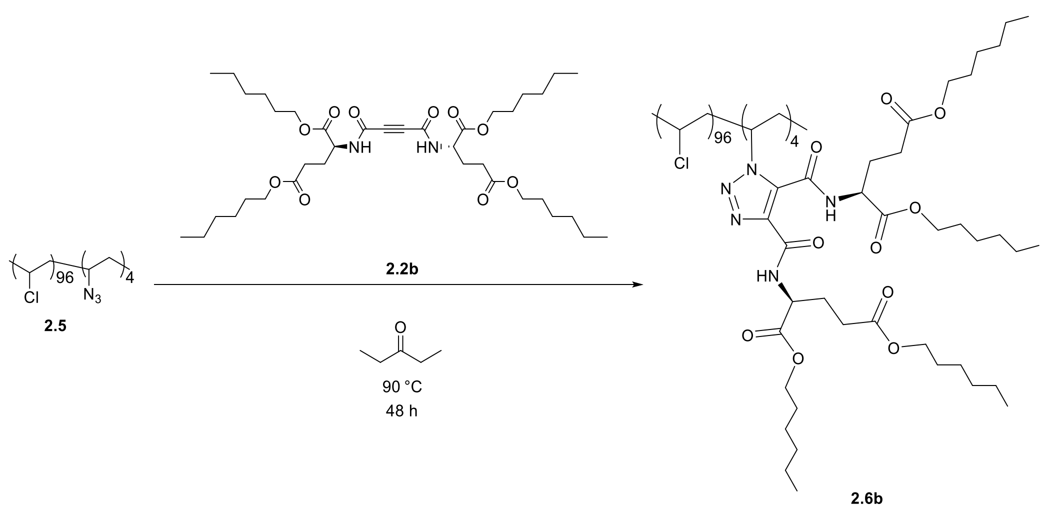

To a 25 mL round bottom flask was added PVC-4.4%-N_3 **2.5** (1.001 g, 16.02 mmol), alkyne **2.2b** (1.155 g, 1.629 mmol), and 3-pentanone (8 mL). The reaction mixture was heated to 90 °C for 48 h. The resulting polymer was purified via precipitation in 100 mL of MeOH three times. The polymer was filtered and dried to give a pale yellow solid (902.3 mg).

^{1}H NMR (500 MHz, $CDCl_3$, δ, ppm): 11.65–11.19 (br, m), 8.53–8.15 (br, m), 6.77–6.25 (br, m), 4.93–4.81 (br, m), 4.81–4.66 (br, s), 4.66–4.52 (br, m), 4.52–4.37 (br, m), 4.37–4.22 (br, m), 4.22–4.10 (br, m), 4.10–4.00 (br, m), 3.90–3.60 (br, m), 3.05–2.59 (br, m), 2.59–2.22 (br, m), 2.22–1.78 (br, m), 1.74–1.52 (br, m), 1.46–1.15 (br, m), 1.03–0.71 (br, m).

^{13}C NMR (126 MHz, $CDCl_3$, δ, ppm): 172.51 (C=O), 171.03 (C=O), 161.18 (C=O), 156.54 (C=O), 138.69 (triazole —C=C—), 132.18 (triazole —C=C—), 66.24 (—CH_2—O—), 65.89 (—CH_2—O—), 65.14 (—CH_2—O—), 64.95 (—CH_2—O—), 57.12–55.02 (PVC —CH—Cl— and PVC —CH—triazole), 52.44 (—NH—CH—), 51.99 (—NH—CH—), 47.41–44.94 (family of CH_2 PVC peaks), 31.54 (CH_2), 31.49 (CH_2), 31.46 (CH_2), 30.49 (CH_2), 30.38 (CH_2), 28.68 (CH_2), 28.65 (CH_2), 28.57 (CH_2), 27.74 (CH_2), 27.34 (CH_2), 25.68 (CH_2), 25.58 (CH_2), 22.66 (CH_2), 22.62 (CH_2), 14.15 (CH_3).

IR (NaCl, thin film, cm^{-1}): 3383 (w, amide N—H), 2957 (s, alkane C—H), 2931 (s, alkane C—H), 2859 (m, alkane C—H), 1736 (s, ester C=O), 1677 (m, amide C=O), 1654 (m, amide C=O), 1578 (m, amide N—H bending), 1551 (m, amide N—H bending), 1255 (s, ester C—O), 1196 (s, ester C—O), 615 (w, C—Cl).

Preparation of PVC-12.0%-nHex (2.6′b)

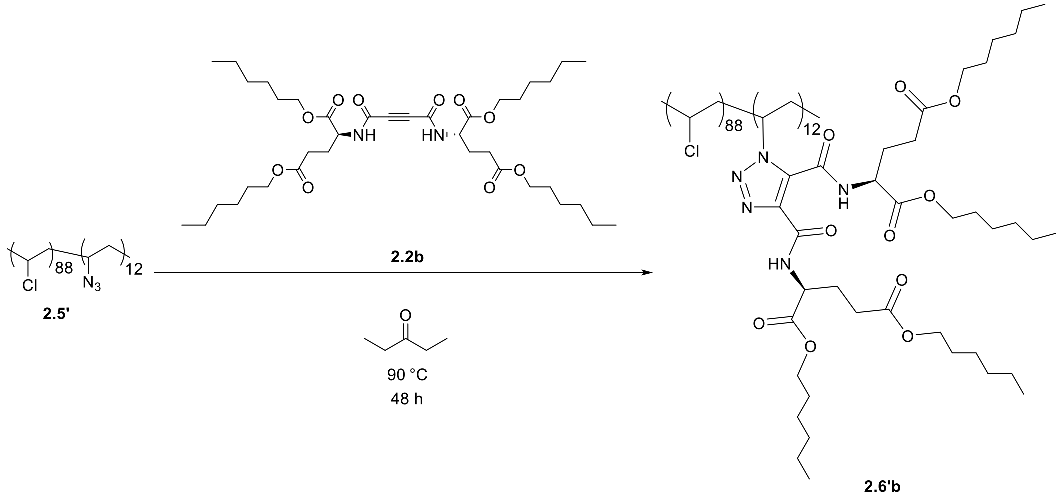

To a 25 mL round bottom flask was added PVC-12.0%-N_3 **2.5′** (399.1 mg, 6.386 mmol), alkyne **2.2b** (1.701 g, 2.399 mmol), and 3-pentanone (6.4 mL). The reaction mixture was heated to 90 °C for 48 h. The resulting polymer was purified via precipitation in 40 mL of MeOH three times. The polymer was filtered and dried to give a pale yellow solid (824.2 mg).

^{1}H NMR (500 MHz, $CDCl_3$, δ, ppm): 11.64–11.03 (br, m), 8.56–8.09 (br, m), 6.71–6.10 (br, m), 4.98–4.80 (br, m), 4.80–4.65 (br, m), 4.65–4.51 (br, m), 4.51–4.33 (br, m), 4.33–4.22 (br, m), 4.22–4.09 (br, m), 4.09–3.98 (br, m), 3.87–3.41 (br, m), 3.07–2.58 (br, m), 2.56–2.22 (br, m), 2.22–1.81 (br, m), 1.74–1.50 (br, m), 1.45–1.10 (br, m), 1.03–0.71 (br, m).

^{13}C NMR (126 MHz, $CDCl_3$, δ, ppm): 172.50 (C=O), 170.99 (C=O), 161.21 (C=O), 156.54 (C=O), 138.51 (triazole –C=C–), 132.14 (triazole –C=C–), 66.21 (–CH_2–O–), 65.86 (–CH_2–O–), 65.25 (–CH_2–O–), 65.12 (–CH_2–O–), 64.92 (–CH_2–O–), 57.07–55.00 (PVC –CH–Cl– and PVC –CH–triazole), 52.42 (–NH–CH–), 51.97 (–NH–CH–), 47.41–45.38 (family of CH_2 PVC peaks), 31.54 (CH_2), 31.52 (CH_2), 31.47 (CH_2), 31.44 (CH_2), 30.47 (CH_2), 30.36 (CH_2), 28.66 (CH_2), 28.63 (CH_2), 28.55 (CH_2), 27.72 (CH_2), 27.30 (CH_2), 25.66 (CH_2), 25.56 (CH_2), 22.63 (CH_2), 22.60 (CH_2), 14.12 (CH_3), 14.10 (CH_3).

IR (NaCl, thin film, cm^{-1}): 3378 (w, amide N—H), 2957 (s, alkane C—H), 2931 (s, alkane C—H), 2859 (m, alkane C—H), 1737 (s, ester C=O), 1676 (s, amide C=O), 1655 (s, amide C=O), 1579 (s, amide N—H bending), 1551 (s, amide N—H bending), 1255 (s, ester C—O), 1195 (s, ester C—O), 615 (w, C—Cl).

Preparation of PVC-4.4%-2EtHex (2.6c)

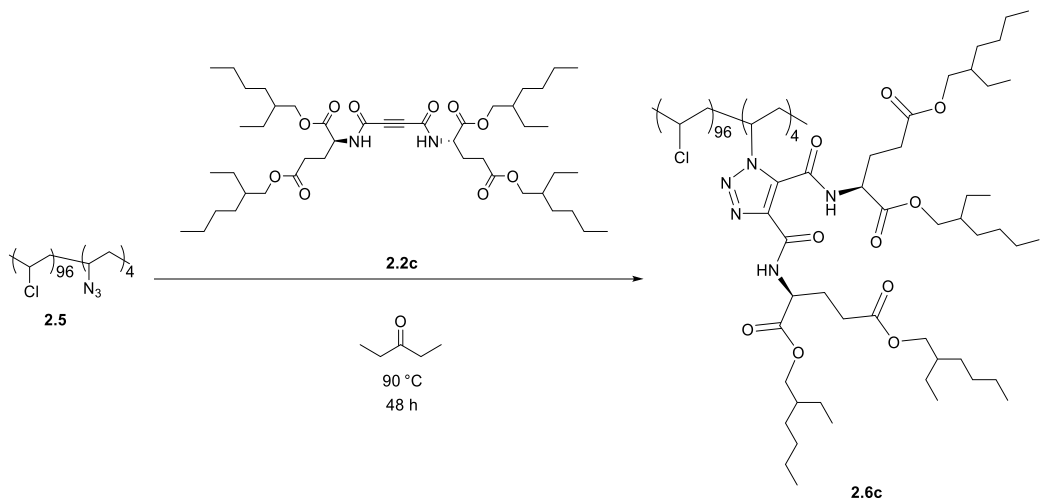

To a 15 mL round bottom flask was added PVC-4.4%-N_3 **2.5** (615.0 mg, 9.840 mmol), alkyne **2.2c** (1.037 g, 1.263 mmol), and 3-pentanone (10 mL). The reaction mixture was heated to 90 °C for 48 h. The resulting polymer was purified via precipitation in 100 mL of MeOH/hexanes (70/30) three times. The polymer was filtered and dried to give a pale yellow solid (786.9 mg).

^{1}H NMR (500 MHz, $CDCl_3$, δ, ppm): 11.65–11.15 (br, m), 8.38–8.14 (br, m), 6.72–6.16 (br, m), 4.93–4.83 (br, m), 4.83–4.67 (br, s), 4.67–4.53 (br, m), 4.53–4.37 (br, m), 4.37–4.16 (br, m), 4.16–4.04 (br, m), 4.04–3.89 (br, m), 3.89–3.49 (br, m), 3.00–2.59 (br, m), 2.59–2.23 (br, m), 2.23–1.73 (br, m), 1.73–1.45 (br, m), 1.45–1.07 (br, m), 1.07–0.69 (br, m).

^{13}C NMR (126 MHz, $CDCl_3$, δ, ppm): 172.53 (C=O), 171.10 (C=O), 170.96 (C=O), 161.13 (C=O), 156.58 (C=O), 138.60 (triazole —C=C—), 132.16 (triazole —C=C—), 68.39

(—CH_2—O—), 68.02 (—CH_2—O—), 67.40 (—CH_2—O—), 67.19 (—CH_2—O—), 57.11–55.02 (PVC —CH—Cl— and PVC —CH—triazole), 52.46 (—NH—CH—), 52.01 (—NH—CH—), 47.41–44.94 (family of CH_2 PVC peaks), 38.80 (CH), 38.75 (CH), 30.54 (CH_2), 30.45 (CH_2), 30.41 (CH_2), 30.36 (CH_2), 29.03 (CH_2), 28.99 (CH_2), 27.75 (CH_2), 27.42 (CH_2), 23.86 (CH_2), 23.84 (CH_2), 23.81 (CH_2), 23.09 (CH_2), 23.08 (CH_2), 23.05 (CH_2), 23.04 (CH_2), 14.21 (CH_3), 14.19 (CH_3), 11.11 (CH_3), 11.09 (CH_3), 11.07 (CH_3).

IR (neat): 3382 (w, amide N—H), 2960 (s, alkane C—H), 2930 (s, alkane C—H), 2873 (m, alkane C—H), 2861 (s, alkane C—H), 1736 (s, ester C=O), 1677 (s, amide C=O), 1655 (m, amide C=O), 1578 (m, amide N—H bending), 1551 (m, amide N—H bending), 1256 (s, ester C—O), 1199 (s, ester C—O), 615 (w, C—Cl).

Preparation of PVC-12.0%-2EtHex (2.6′c)

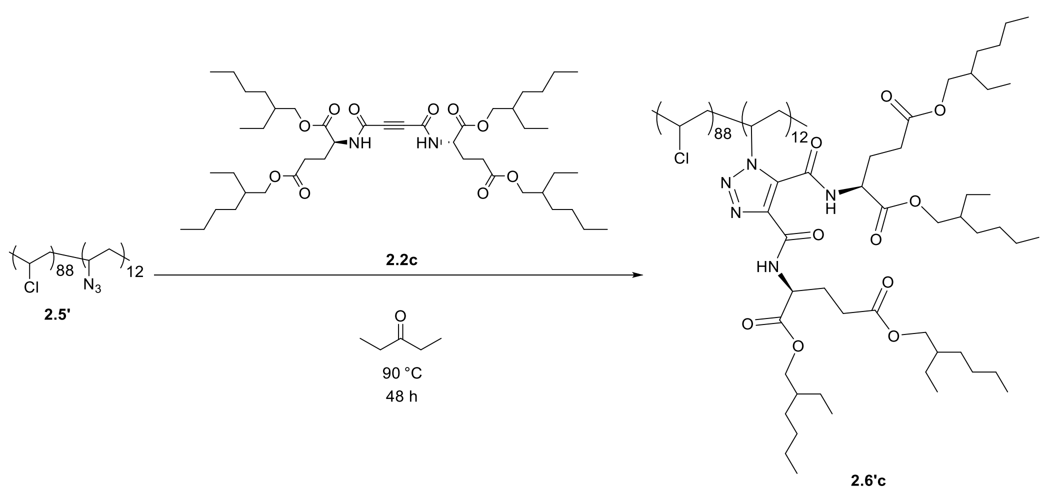

To a 15 mL round bottom flask was added PVC-12.0%-N_3 (**2.5′**) (198.3 mg, 3.173 mmol), alkyne **2.2c** (987.2 mg, 1.202 mmol), and 3-pentanone (3.2 mL). The reaction mixture was heated to 90 °C for 48 h. The resulting polymer was purified via precipitation in 100 mL of MeOH/hexanes (70/30) three times. The polymer was filtered and dried to give a pale yellow solid (115.8 mg).

^{1}H NMR (500 MHz, $CDCl_3$, δ, ppm): 11.69–11.16 (br, m), 8.54–8.11 (br, m), 6.75–6.08 (br, m), 4.98–4.83 (br, m), 4.83–4.68 (br, s), 4.68–4.52 (br, m), 4.52–4.33 (br, m), 4.33–4.19 (br, m), 4.19–4.04 (br, m), 4.04–3.86 (br, m), 3.86–3.44 (br, m), 3.00–2.60 (br, m), 2.60–2.23 (br, m), 2.23–1.77 (br, m), 1.71–1.46 (br, m), 1.46–1.07 (br, m), 1.06–0.66 (br, m).

^{13}C NMR (126 MHz, $CDCl_3$, δ, ppm): 172.53 (C=O), 170.98 (C=O), 161.18 (C=O), 156.57 (C=O), 138.68 (triazole —C=C—), 132.19 (triazole —C=C—), 68.37 (—CH_2—O—), 68.01 (—CH_2—O—), 67.38 (—CH_2—O—), 67.17 (—CH_2—O—), 57.05–55.00 (PVC —CH—Cl— and PVC —CH-triazole), 52.45 (—NH—CH—), 52.00 (—NH—CH—), 47.42–45.42 (family of CH_2 PVC peaks), 38.80 (CH), 30.45 (CH_2), 30.41 (CH_2), 29.02 (CH_2), 28.99 (CH_2), 27.75 (CH_2), 27.40 (CH_2), 23.86 (CH_2), 23.84 (CH_2), 23.07 (CH_2), 23.05 (CH_2), 14.18 (CH_3), 11.08 (CH_3), 11.05 (CH_3).

IR (neat): 3379 (w, amide N—H), 2960 (s, alkane C—H), 2931 (s, alkane C—H), 2873 (m, alkane C—H), 2861 (s, alkane C—H), 1737 (s, ester C=O), 1677 (s, amide C=O), 1655 (s, amide C=O), 1579 (s, amide N—H bending), 1551 (s, amide N—H bending), 1259 (s, ester C—O), 1198 (s, ester C—O), 616 (w, C—Cl).

Preparation of PVC-4.4%-nDec (2.6d)

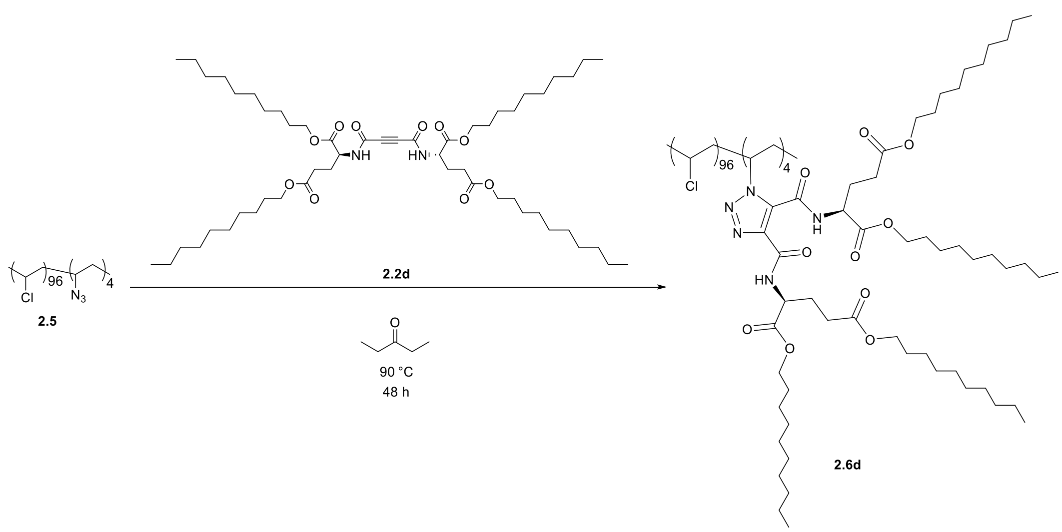

To a 50 mL round bottom flask was added PVC-4.4%-N_3 **2.5** (1.024 g, 16.38 mmol), alkyne **2.2d** (1.912 g, 2.048 mmol), and 3-pentanone (8 mL). The reaction mixture was heated to 90 °C for 48 h. The resulting polymer was purified via precipitation in 100 mL of MeOH/hexanes (70/30) three times. The polymer was filtered and dried to give a pale yellow solid (1.207 g).

^{1}H NMR (500 MHz, $CDCl_3$, δ, ppm): 11.54–11.21 (br, m), 8.42–8.14 (br, m), 6.70–6.25 (br, m), 4.95–4.81 (br, m), 4.81–4.67 (br, m), 4.67–4.53 (br, m), 4.53–4.37 (br, m), 4.37–4.22 (br, m), 4.22–4.10 (br, m), 4.10–3.89 (br, m), 3.89–3.43 (br, m), 3.17–2.60 (br, m), 2.60–2.23 (br, m), 2.23–1.80 (br, m), 1.80–1.48 (br, m), 1.48–1.06 (br, m), 1.04–0.71 (br, m).

^{13}C NMR (126 MHz, $CDCl_3$, δ, ppm): 172.48 (C=O), 171.03 (C=O), 170.91 (C=O), 161.13 (C=O), 156.54 (C=O), 138.51 (triazole —C=C—), 132.13 (triazole —C=C—), 66.23 (—CH_2—O—), 65.88 (—CH_2—O—), 65.12 (—CH_2—O—), 64.93 (—CH_2—O—), 57.11–55.01 (PVC —CH—Cl— and PVC —CH—triazole), 52.41 (—NH—CH—), 51.96 (—NH—CH—), 47.38–44.93 (family of CH_2 PVC peaks), 31.99 (CH_2), 30.46 (CH_2), 30.35 (CH_2), 29.67 (CH_2), 29.65 (CH_2), 29.63 (CH_2), 29.59 (CH_2), 29.41 (CH_2), 29.37 (CH_2), 29.34 (CH_2), 29.30 (CH_2), 28.72 (CH_2), 28.68 (CH_2), 28.60 (CH_2), 27.73 (CH_2), 27.31 (CH_2), 26.00 (CH_2), 25.90 (CH_2), 22.79 (CH_2), 14.25 (CH_3).

IR (neat): 3381 (w, amide N—H), 2954 (s, alkane C—H), 2926 (s, alkane C—H), 2855 (m, alkane C—H), 1737 (s, ester C=O), 1677 (m, amide C=O), 1657 (m, amide C=O), 1580 (m, amide N—H bending), 1551 (m, amide N—H bending), 1255 (s, ester C—O), 1199 (s, ester C—O), 616 (w, C—Cl).

Preparation of PVC-12.0%-nDec (2.6′d)

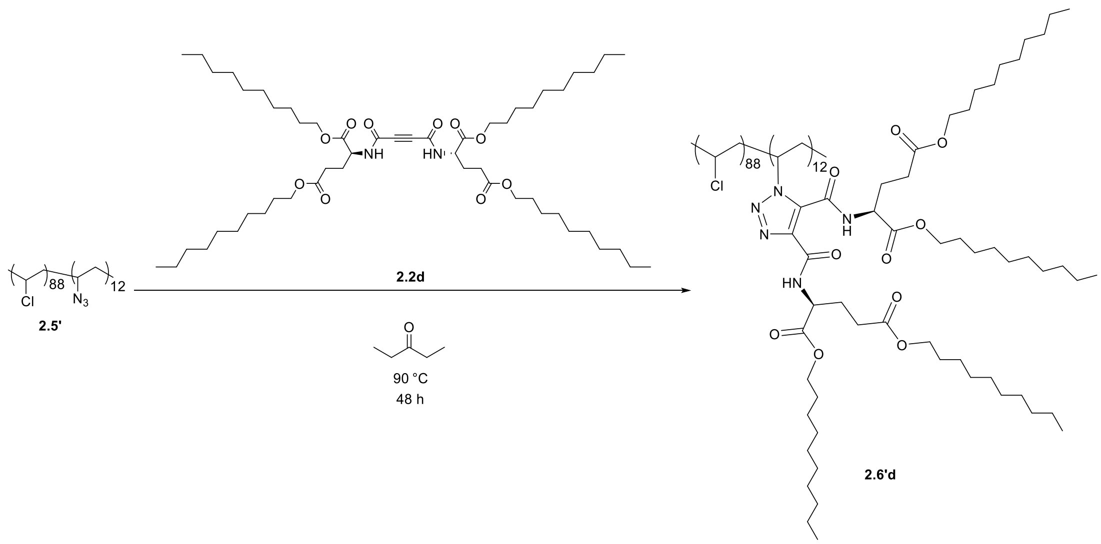

To a 50 mL round bottom flask was added PVC-12.0%-N_3 (**2.5′**) (919.1 mg, 14.71 mmol), alkyne **2.2d** (5.100 g, 5.464 mmol), and 3-pentanone (14.7 mL). The reaction mixture was heated to 90 °C for 48 h. The resulting polymer was purified via precipitation in 100 mL of MeOH/hexanes (70/30) three times. The polymer was filtered and dried to give a pale yellow solid (1.489 g).

^1H NMR (500 MHz, $CDCl_3$, δ, ppm): 11.63–11.05 (br, m), 8.57–8.06 (br, m), 6.83–6.07 (br, m), 4.97–4.80 (br, s), 4.80–4.66 (br, s), 4.66–4.52 (br, s), 4.52–4.33 (br, m), 4.33–4.23 (br, s), 4.23–4.08 (br, m), 4.08–3.86 (br, s), 3.86–3.34 (br, m), 3.16–2.59 (br, m), 2.59–2.21 (br, m), 2.21–1.83 (br, m), 1.81–1.50 (br, m), 1.50–1.03 (br, m), 1.03–0.60 (br, m).

^{13}C NMR (126 MHz, $CDCl_3$, δ, ppm): 172.48 (C=O), 170.97 (C=O), 161.15 (C=O), 156.55 (C=O), 138.57 (triazole ─C=C─), 132.03 (triazole ─C=C─), 66.21 (─CH_2─O─), 65.87 (─CH_2─O─), 65.12 (─CH_2─O─), 64.93 (─CH_2─O─), 57.02–54.99 (PVC ─CH─Cl─ and PVC ─CH─triazole), 52.42 (─NH─CH─), 51.96 (─NH─CH─), 47.42–45.41 (Family of CH_2 PVC peaks), 32.01 (CH_2), 30.46 (CH_2), 30.35 (CH_2), 29.67 (CH_2), 29.65 (CH_2), 29.61 (CH_2), 29.42 (CH_2), 29.38 (CH_2), 29.35 (CH_2), 29.31 (CH_2), 28.73 (CH_2), 28.70 (CH_2), 28.62 (CH_2), 27.75 (CH_2), 27.32 (CH_2), 26.01 (CH_2), 25.92 (CH_2), 22.80 (CH_2), 14.24 (CH_3).

IR (neat): 3379 (w, amide N─H), 2955 (s, alkane C─H), 2926 (s, alkane C─H), 2855 (m, alkane C─H), 1739 (s, ester C=O), 1676 (s, amide C=O), 1655 (m, amide C=O), 1579 (m, amide N─H bending), 1551 (s, amide N─H bending), 1259 (s, ester C─O), 1198 (s, ester C─O), 616 (w, C─Cl).

Preparation of PVC-4.4%-TEGMe (2.6e)

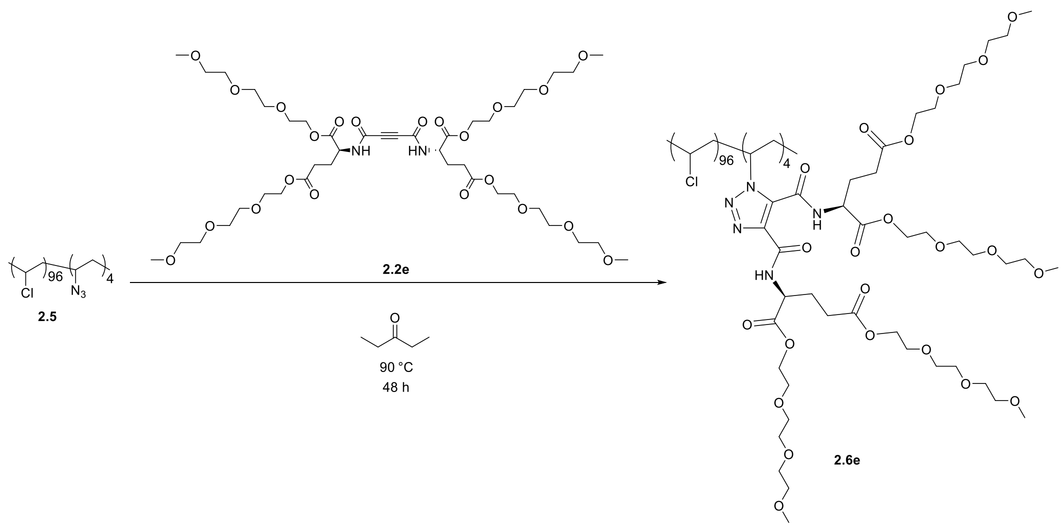

To a 50 mL round bottom flask was added PVC-4.4%-N_3 (**2.5**) (1.064 g, 17.02 mmol), alkyne **2.2e** (2.036 g, 2.127 mmol), and 3-pentanone (17 mL). The reaction mixture was heated to 90 °C for 48 h. The resulting polymer was purified via precipitation in 100 mL of MeOH four times. The polymer was filtered and dried to give a pale yellow solid (1.159 g).

^{1}H NMR (500 MHz, $CDCl_3$, δ, ppm): 11.71–11.14 (br, m), 8.44–8.19 (br, m), 6.70–6.29 (br, m), 4.98–4.82 (br, s), 4.82–4.67 (br, s), 4.67–4.52 (br, m), 4.52–4.37 (br, m), 4.37–4.09 (br, m), 3.85–3.58 (br, m), 3.58–3.45 (br, m), 3.36 (s), 2.95–2.61 (br, m), 2.61–2.46 (br, m), 2.46–2.22 (br, m), 2.22–1.68 (br, m).

^{13}C NMR (126 MHz, $CDCl_3$, δ, ppm): 172.47 (C=O), 172.37 (C=O), 170.95 (C=O), 170.77 (C=O), 162.32 (C=O), 161.19 (C=O), 156.53 (C=O), 138.63 (triazole ─C=C─), 132.02

(triazole —C=C-), 72.54 (—CH_2—O—), 72.00 (—CH_2—O—), 71.95 (—CH_2—O—), 70.70 (—CH_2—O—), 70.67 (—CH_2—O—), 70.63 (—CH_2—O—), 69.13 (—CH_2—O—), 69.09 (—CH_2—O—), 68.87 (—CH_2—O—), 64.88 (—CH_2—O—), 64.60 (—CH_2—O—), 63.97 (—CH_2—O—), 63.80 (—CH_2—O—), 61.81 (—CH_2—O—), 59.11 (CH_3), 57.10–55.00 (PVC —CH—Cl— and PVC —CH—triazole), 52.31 (—NH—CH—), 51.92 (—NH—CH—), 47.36–44.90 (family of CH_2 PVC peaks), 30.17 (CH_2), 27.35 (CH_2), 27.06 (CH_2).

IR (neat): 3380 (w, amide N—H), 2911 (s, alkane C—H), 2877 (s, alkane C—H), 1739 (s, ester C=O), 1676 (s, amide C=O), 1653 (m, amide C=O), 1579 (m, amide N—H bending), 1552 (s, amide N—H bending), 1254 (s, ester C—O), 1199 (s, ester C—O), 1105 (s, ether C—O), 615 (w, C—Cl).

Preparation of PVC-12.0%-TEGMe (2.6′e)

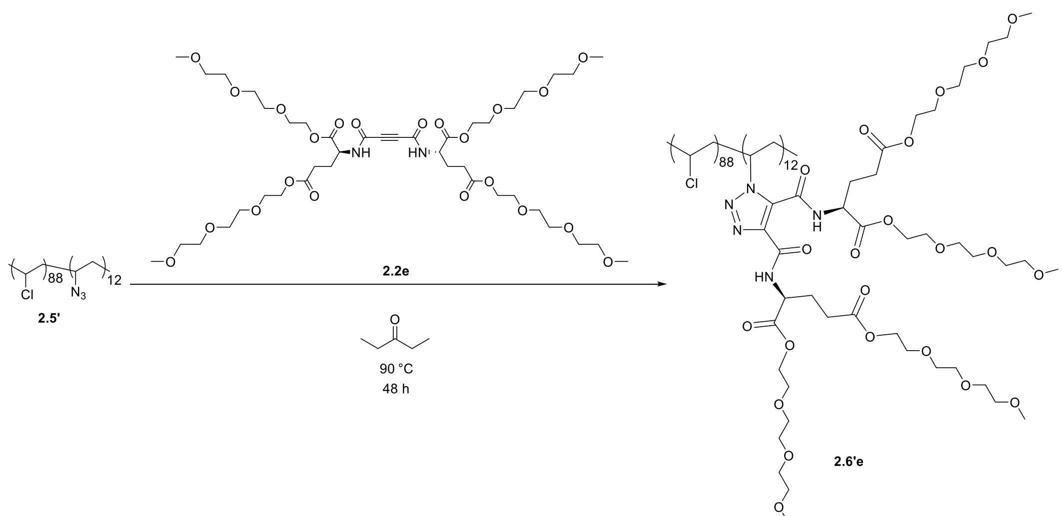

To a 25 mL round bottom flask was added PVC-12.0%-N_3 **2.5′** (285.1 mg, 4.562 mmol), alkyne **2.2e** (1.642 g, 1.716 mmol), and 3-pentanone (4.6 mL). The reaction mixture was heated to 90 °C for 48 h. The resulting polymer was purified via precipitation in 40 ml of MeOH four times. The polymer was filtered and dried to give a pale yellow solid (550.8 mg).

[1]H NMR (500 MHz, $CDCl_3$, δ, ppm): 11.71–11.13 (br, s), 8.59–8.20 (br, s), 6.70–6.13 (br, m), 5.02–4.81 (br, s), 4.81–4.67 (br, s), 4.67–4.51 (br, m), 4.51–4.09 (br, m), 3.92–3.55 (br, m), 3.57–3.43 (br, m), 3.42–3.27 (br, s), 2.95–2.42 (br, m), 2.44–1.70 (br, m).

[13]C NMR (126 MHz, $CDCl_3$, δ, ppm): 172.49 (C=O), 170.96 (C=O), 161.37 (C=O), 156.54 (C=O), 132.10 (triazole ─C=C─), 72.58 (─CH_2─O─), 72.04 (─CH_2─O─), 70.70 (─CH_2─O─), 70.66 (─CH_2─O─), 69.12 (─CH_2─O─), 68.88 (─CH_2─O─), 64.89 (─CH_2─O─), 64.62 (─CH_2─O─), 63.99 (─CH_2─O─), 63.82 (─CH_2─O─), 61.86 (─CH_2─O─), 59.14 (CH_3), 57.10–56.00 (PVC ─CH─Cl─ and PVC ─CH─triazole), 51.93 (─NH─CH─), 47.39–45.81 (family of CH_2 PVC peaks), 30.18 (CH_2), 27.10 (CH_2).

IR (neat): 3334 (m, amide N─H), 2881 (s, alkane C─H), 1736 (s, ester C=O), 1676 (s, amide C=O), 1542 (m, amide N─H bending), 1254 (s, ester C─O), 1199 (s, ester C─O), 1108 (s, ether C─O), 612 (w, C─Cl).

Preparation of PVC-4.4%-TEGBu (2.6f)

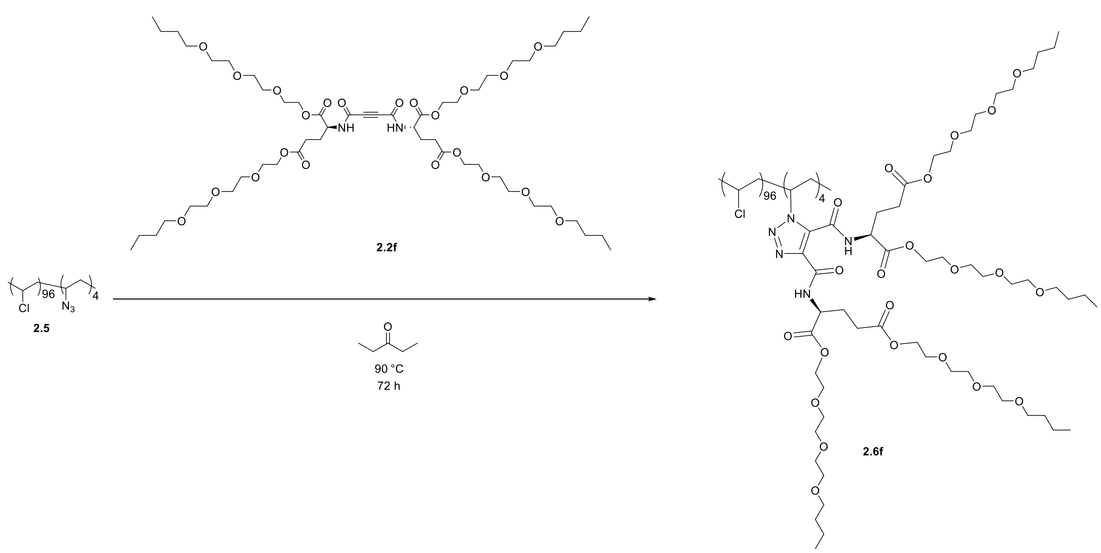

To a 50 mL round bottom flask was added PVC-4.4%-N_3 (**2.5**) (1.008 g, 16.13 mmol), alkyne **2.2f** (2.270 g, 2.017 mmol), and 3-pentanone (15 mL). The reaction mixture was heated to 90 °C for 72 h. The resulting polymer was purified via precipitation in 100 mL of MeOH four times. The polymer was filtered and dried to give a pale yellow solid (974.5 mg).

^{1}H NMR (500 MHz, $CDCl_3$, δ, ppm): 11.53–11.04 (br, s), 8.44–8.19 (br, s), 6.68–6.62 (br, m), 4.99–4.82 (br, s), 4.82–4.68 (br, s), 4.66–4.52 (br, m), 4.52–4.36 (br, m), 4.38–4.06 (br, m), 3.87–3.65 (br, m), 3.66–3.59 (br, m), 3.60–3.52 (br, m), 3.44 (t, *J* = 6.7 Hz), 2.97–2.62 (br, m), 2.62–2.47 (br, m), 2.48–2.22 (br, m), 2.22–1.81 (br, m), 1.61–1.48 (br, m), 1.44–1.29 (br, m), 0.90 (t, *J* = 7.4 Hz).

^{13}C NMR (126 MHz, $CDCl_3$, δ, ppm): 172.49 (C=O), 170.94 (C=O), 161.57 (C=O), 156.55 (C=O), 138.67 (triazole —C=C—), 71.30 (—CH_2—O—), 70.78 (—CH_2—O—), 70.71 (—CH_2—O—), 70.66 (—CH_2—O—), 70.16 (—CH_2—O—), 69.13 (—CH_2—O—), 68.90 (—CH_2—O—), 64.92 (—CH_2—O—), 64.62 (—CH_2—O—), 64.01 (—CH_2—O—), 63.84 (—CH_2—O—), 57.11–55.01 (PVC —CH—Cl— and PVC —CH—triazole), 52.35 (—NH—CH—), 51.94 (—NH—CH—), 47.38–44.93 (family of CH_2 PVC peaks), 31.82 (CH_2), 30.18 (CH_2), 27.02 (CH_2), 19.39 (CH_2), 14.07 (CH_3).

IR (neat): 3326 (m, amide N—H), 2958 (s, alkane C—H), 2934 (s, alkane C—H), 2872 (s, alkane C—H), 1739 (s, ester C=O), 1672 (s, amide C=O), 1536 (s, amide N—H bending), 1254 (s, ester C—O), 1195 (s, ester C—O), 1119 (s, ether C—O), 615 (w, C—Cl).

Preparation of PVC-12.0%-TEGBu (2.6′f)

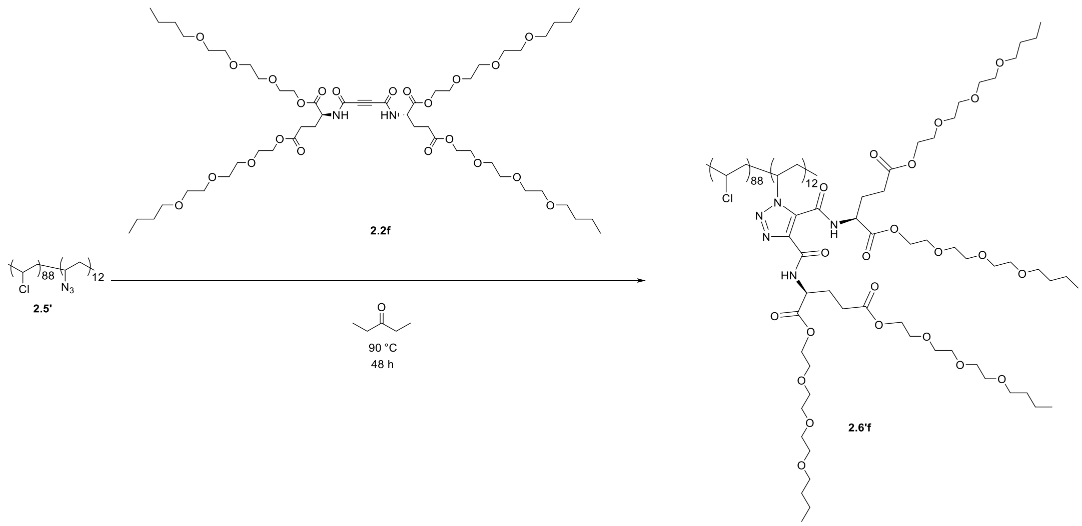

To a 25 mL round bottom flask was added PVC-12.0%-N_3 (**2.5′**) (294.0 mg, 4.704 mmol), alkyne **2.2f** (2.008 g, 1.784 mmol), and 3-pentanone (4.7 mL). The reaction mixture was heated to 90 °C for 48 h. The resulting polymer was purified via precipitation in 40 mL of MeOH four times. The polymer was filtered and dried to give a pale yellow solid (513.2 mg).

^{1}H NMR (500 MHz, $CDCl_3$, δ, ppm): 11.52–11.09 (br, s), 8.58–8.16 (br, s), 6.51 (br, m), 5.03–4.82 (br, s), 4.82–4.68 (br, s), 4.68–4.53 (br, m), 4.53–4.05 (br, m), 3.86–3.51 (br, s), 3.45 (s), 2.95–2.61 (br, m), 2.61–2.42 (br, m), 2.42–2.24 (br, m), 2.24–1.77 (br, m), 1.72–1.46 (br, m), 1.46–1.23 (br, m), 1.09–0.72 (br, m).

^{13}C NMR (126 MHz, $CDCl_3$, δ, ppm): 172.46 (C=O), 170.93 (C=O), 170.76 (C=O), 161.33 (C=O), 161.13 (C=O), 156.60 (C=O), 139.68 (Triazole —C=C—), 138.62 (triazole —C=C—), 77.41 (—CH_2—O—), 77.16 (—CH_2—O—), 76.91 (—CH_2—O—), 71.28 (—CH_2—O—), 70.77 (—CH_2—O—), 70.72 (—CH_2—O—), 70.70 (—CH_2—O—), 70.66 (—CH_2—O—), 70.15 (—CH_2—O—), 69.11 (—CH_2—O—), 68.88 (—CH_2—O—), 64.89 (—CH_2—O—), 64.60 (—CH_2—O—), 63.81 (—CH_2—O—), 61.72 (—CH_2—O—), 57.08–54.98 (PVC —CH—Cl— and PVC —CH—triazole), 52.31

(─NH─CH─), 51.91 (─NH─CH─), 47.37–44.92 (family of CH_2 PVC peaks), 31.81 (CH_2), 30.17 (CH_2), 27.41 (CH_2), 27.06 (CH_2), 19.38 (CH_2), 14.05 (CH_3).

IR (neat): 3380 (m, amide N─H), 2957 (s, alkane C─H), 2933 (s, alkane C─H), 2871 (s, alkane C─H), 1739 (s, ester C=O), 1677 (s, amide C=O), 1653 (m, amide C=O), 1579 (m, amide N─H bending), 1552 (s, amide N─H bending), 1254 (s, ester C─O), 1195 (s, ester C─O), 1116 (s, ether C─O), 614 (w, C─Cl).

5.2 Experimental Section for Chapter 3 and Chapter 4

5.2.1 Materials

Polyvinyl chloride (PVC) (Mw = 43,000, Mn = 22,000) was purchased from Sigma-Aldrich and was purified before use by the following method:[5-7] PVC (40.05 g, 640.8 mmol) was dissolved in 200 mL of THF. The polymer was precipitated by addition to 1 L of MeOH. The precipitate was filtered, dissolved in 230 mL of THF, and precipitated again in 1 L of MeOH. The precipitate was filtered, dissolved in 230 mL of THF, and finally precipitated in 2 L of MeOH. The precipitate was filtered and dried under vacuum. Copper bromide (CuBr) was purchased from Oakwood Chemical and was purified by the following method:[8] 7.08 g of CuBr was suspended in 20 mL of glacial acetic acid, and stirred under nitrogen at room temperature overnight. The solid was filtered using a Büchner funnel, washed with 200 mL of absolute ethanol, followed by 100 mL of anhydrous diethyl ether. The solid CuBr was then dried under vacuum, and stored under N_2 at -20 °C. *n*-Butyl acrylate (BA) (>99%) was purchased from Acros Organics. BA used in Chapter 3 was purified to remove the inhibitor by distillation under reduced vacuum. BA used in Chapter 4 was purified to remove inhibitor by passing it neat through basic Al_2O_3. 2-2-(2-ethoxyethoxy)ethyl acrylate (2EEA) was purchased from TCI America and was purified to remove inhibitor by passing it neat through basic aluminum oxide. *N, N, N′, N″, N″*-pentamethyldiethylenetriamine (PMDETA) (99%) was purchased from Sigma-Aldrich and was purified before use by distillation under reduced vacuum. DMF (extra dry, 99.8%) was purchased from Acros Organics, acetic acid (99.7%) and methanol (99.8%), tetrahydrofuran (99.9%) were purchased from Fisher Chemical. Activated basic aluminum oxide was purchased from Oakwood Chemical.

5.2.2 Measurements:

Nuclear magnetic resonance (NMR) spectra were recorded with a Bruker AVANCE III HD 4 channel 500 MHz Oxford Magnet NMR Spectrometer with Automation at ambient temperature in $CDCl_3$ as solvent. The signal of residual $CHCl_3$ was used as an internal standard (^1H NMR, δ 7.26 ppm). Fourier transform infrared spectroscopy (FTIR) was recorded with a Thermo-Nicolet 6700 Fourier Transform Infrared (FTIR) spectrometer equipped with a Continuum microscope in transmission mode. A small portion of each sample was transferred to an infrared transmitting substrate. The analytical spot size was approximately 100 microns x 100 microns. OMNIC 8.0 software was used to perform data analysis. Glass transition temperatures of polymers were measured using TA Instruments DSC Q2000 with a heat-cool-heat protocol. DSC was equilibrated at 180 °C. First heat cycle: a scanning range of −180 to 240 °C at a heating rate of 10 °C min^{-1}. First cool cycle: 240 °C to -175 °C at 5 ° C min^{-1}. Second heat cycle: -175 °C to 240 °C at 10 ° C min^{-1}. Derivative thermogravimetry (DTG) and thermal gravimetric analyses (TGA) were performed with TA Instrument TGA Q500. TGA was performed within a scanning range of ambient to 900 °C at a heating rate of 10 °C min^{-1} with nitrogen purge. GPC was recorded with a Malvern Viscotek TDA 305 Triple Detector. Sample was dissolved in THF with concentration 1 mg/mL. The column set used was PLgel 50A. The flow rate was 1 mL/min. Injection volume was 100 µL.

5.2.3 Preparation of PVC Graft Copolymers for Chapter 3

Preparation of PVC-*g*-PBA (2 g scale)

To a 10 mL Schlenk flask was added PVC (500.0 mg, 8.000 mmol) and 3 mL of DMF. The mixture was stirred and warmed slightly to fully dissolve the PVC. BA (2.87 mL, 20.0 mmol) was added to the solution. To a 2 mL vial was added CuBr (34.40 mg, 0.2398 mmol) and 0.75 mL of DMF to form a suspension. The CuBr suspension was transferred to the PVC solution by pipet. Residual CuBr was washed into the PVC solution using an additional 0.25 mL of DMF. PMDETA (50 µL, 0.24 mmol) was added, and the reaction mixture was degassed via four cycles of freeze-pump-thaw, and then heated to 100 °C while stirring under nitrogen. After 24 h, an aliquot was taken to analyze the crude reaction by ^{1}H NMR using $CDCl_3$ as solvent (%conv.$_{NMR}$ = 81%). The resulting polymer was precipitated by addition to 200 mL of MeOH, followed by stirring for 20 min. Then MeOH was decanted. The polymer was stirred overnight in an additional 200 mL of MeOH. The solution phase was decanted, the polymer was washed with stirring with two additional portions of MeOH (200 mL × 2). The polymer was filtered and dried under vacuum to yield 2.4810 g (wt% plasticizer$_{grav.}$ = 80%) of a pale green, pliable polymer.

^{1}H NMR (500 MHz, $CDCl_3$) δ 4.644.54 (br s), 4.53–4.37 (br m), 4.37–4.23 (br s), 4.17–3.85 (br s), 2.50–2.21 (br m), 2.20–1.98 (br m), 1.97–1.80 (br m), 1.75–1.56 (br m), 1.51–1.44 (br m), 1.43–1.29 (br m), 0.93 (t, J = 7.3 Hz). Based by ^{1}H NMR integration: PBA : PVC = 1.6 : 1.0.

FT-IR: 2960 (s, alkane C─H), 2935 (s, alkane C─H), 2873 (s, alkane C─H), 1733 (s, ester C=O), 1163 (s, ester C─O).

Preparation of PVC-*g*-75%PBA-*co*-25%P2EEA (2 g scale)

To a 10 mL Schlenk flask was added PVC (500.0 mg, 8.000 mmol) and 3 mL of DMF. The mixture was stirred and warmed slightly to fully dissolve the PVC. BA (2.15 mL, 15.0 mmol) and 2EEA (0.93 mL, 5.0 mmol) were added to the solution. To a 2 mL vial was added CuBr (34.32 mg, 0.2392 mmol) and 0.75 mL of DMF to form a suspension. The CuBr suspension was transferred to the PVC solution by pipet. Residual CuBr was washed into the PVC solution using an additional 0.25 mL of DMF. PMDETA (50 µL, 0.24 mmol) was added, and the reaction mixture was degassed via four cycles of freeze-pump-thaw, and then heated to 100 °C while stirring under nitrogen. After 24 h, an aliquot was taken to analyze the crude reaction by ^1H NMR using $CDCl_3$ as solvent (%$conv._{NMR}$ = 73%). The resulting polymer was precipitated by addition to 200 mL of MeOH, followed by stirring for 20 min. Then MeOH was decanted. The polymer was stirred in an additional 200 mL of MeOH overnight. The solution phase was decanted. The polymer was washed with stirring with two additional portions of MeOH (200 mL × 2). The polymer was filtered and dried under vacuum to yield 2.0065 g (wt% $plasticizer_{grav.}$ = 75%) of a pale yellow, pliable polymer.

^1H NMR (500 MHz, $CDCl_3$) δ 4.71–4.53 (br m), 4.53–4.37 (br m), 4.37–4.25 (br m), 4.25–4.12 (br s), 4.12–3.85 (br s), 3.75–3.65 (br m), 3.65–3.60 (br m), 3.57 (br m), 3.52 (q, J = 7.0 Hz), 2.53–2.22 (br m), 2.22–1.97 (br m), 1.97–1.80 (br s), 1.80–1.57 (br m), 1.43–1.29 (br m), 1.21 (t, J = 7.0 Hz), 0.93 (t, J = 7.4 Hz). Based by ^1H NMR integration: (PBA + P2EEA) : PVC = 1.4 : 1.0; PBA : P2EEA = 3.0 : 1.0.

FT-IR: 2960 (s, alkane C─H), 2873 (s, alkane C─H), 1736 (s, ester C=O), 1169 (s, ester C─O). 1116 (s, ether C─O)

Preparation of PVC-*g*-50%PBA-*co*-50%P2EEA (2 g scale)

To a 10 mL Schlenk flask was added PVC (500.0 mg, 8.000 mmol) and DMF (3 mL). The mixture was stirred and warmed slightly to fully dissolve the PVC. BA (1.43 mL, 9.97 mmol) and 2EEA (1.85 mL, 9.99 mmol) were added to the solution. To a 2 mL vial was added CuBr (34.22 mg, 0.2386 mmol) and 0.75 mL of DMF to form a suspension. The CuBr suspension was transferred to the PVC solution by pipet. Residual CuBr was washed into the PVC solution using an additional 0.25 mL of DMF. PMDETA (50 µL, 0.24 mmol) was added, and the reaction mixture was degassed via four cycles of freeze-pump-thaw, and then heated to 100 °C while stirring under nitrogen. After 24 h, an aliquot was taken to analyze the crude reaction by ^1H NMR using $CDCl_3$ as solvent (%$conv._{NMR}$ = 84%). The resulting polymer was precipitated by addition to 200 mL of MeOH, followed by stirring for 20 min. Then MeOH was decanted. The polymer was stirred in an additional 200 mL of MeOH overnight. The solution phase was decanted. The polymer was washed with stirring with two additional portions of MeOH (200 mL × 2). The polymer was filtered and dried under vacuum to yield 1.9994 g (wt% plasticizer$_{grav.}$ = 75%) of a pale yellow, pliable polymer.

^{1}H NMR (500 MHz, $CDCl_3$) δ 4.66–4.53 (br m), 4.53–4.38 (br m), 4.38–4.25 (br m), 4.25–4.11 (br s), 4.11–3.89 (br m), 3.73–3.65 (br m), 3.65–3.60 (br m), 3.60–3.55 (br m), 3.52 (q, J = 7.0 Hz), 2.51–2.22 (br m), 2.22–1.97 (br m), 1.97–1.80 (br m), 1.76–1.52 (br m), 1.51–1.43 (br m), 1.43–1.28 (br m), 1.20 (t, J = 7.0 Hz), 0.94 (t, J = 7.3 Hz). Based by ^{1}H NMR integration: (PBA + P2EEA) : PVC = 1.3 : 1.0; PBA : P2EEA = 1.0 : 1.0.

FT-IR: 2962 (s, alkane C–H), 2873 (s, alkane C–H), 1735 (s, ester C=O), 1170 (s, ester C–O). 1116 (s, ether C–O)

Preparation of PVC-*g*-25%PBA-*co*-75%P2EEA (2 g scale)

To a 10 mL Schlenk flask was added PVC (500.0 mg, 8.000 mmol) and DMF (3 mL). The mixture was stirred and warmed slightly to fully dissolve the PVC. BA (0.72 mL, 5.02 mmol) and 2EEA (2.78 mL, 15.0 mmol) were added to the solution. To a 2 mL vial was added CuBr (34.38 mg, 0.2397 mmol) and 0.75 mL of DMF to form a suspension. The CuBr suspension was transferred to the PVC solution by pipet. Residual CuBr was washed into the PVC solution using an additional 0.25 mL of DMF. PMDETA (50 µL, 0.24 mmol) was added, and the reaction mixture was degassed via four cycles of freeze-pump-thaw, and then heated to 100 °C while stirring under nitrogen. After 24 h, an aliquot was taken to analyze the crude reaction by ^{1}H NMR using $CDCl_3$ as solvent (%conv.$_{NMR}$ = 80%). The resulting polymer was precipitated by addition to 200 mL of MeOH, followed by stirring for 20 min. The majority of MeOH was decanted. The polymer was stirred in an additional 200 mL of MeOH overnight. The solution phase was decanted. The polymer was washed with stirring with two additional portions of

MeOH (200 mL × 2). The polymer was filtered and dried under vacuum to yield 1.8376 g (wt% $plasticizer_{grav.}$ = 73%) of a pale yellow, pliable polymer.

^{1}H NMR (500 MHz, $CDCl_3$) δ 4.65–4.53 (br m), 4.53–4.38 (br m), 4.38–4.26 (br m), 4.26–4.10 (br s), 4.10–3.91 (br m), 3.74–3.65 (br m), 3.65–3.60 (br m), 3.60–3.55 (br m), 3.52 (q, *J* = 7.0 Hz), 2.52–2.23 (br m), 2.23–1.97 (br m), 1.97–1.82 (br s), 1.73–1.45 (br m), 1.42–1.30 (br m), 1.20 (t, *J* = 7.0 Hz), 0.94 (t, *J* = 7.3 Hz). Based by ^{1}H NMR integration: (PBA + P2EEA) : PVC = 1.1 : 1.0; PBA : P2EEA = 1.0 : 2.9.

FT-IR: 2962 (s, alkane C─H), 2873 (s, alkane C─H), 1736 (s, ester C=O), 1169 (s, ester C─O). 1116 (s, ether C─O)

Preparation of PVC-*g*-P2EEA (2 g scale)

To a 10 mL Schlenk flask was added PVC (500.7 mg, 8.011 mmol) and DMF (3 mL). The mixture was stirred and warmed slightly to fully dissolve the PVC. 2EEA (3.70 mL, 20.0 mmol) were added to the solution. To a 2 mL vial was added CuBr (34.37 mg, 0.2396 mmol) and 0.75 mL of DMF to form a suspension. The CuBr suspension was transferred to the PVC solution by pipet. Residual CuBr was washed into the PVC solution using an additional 0.25 mL of DMF. PMDETA (50 µL, 0.24 mmol) was added, and the reaction mixture was degassed via four cycles of freeze-pump-thaw, and then heated to 100 °C while stirring under nitrogen. After 24 h, an aliquot was taken to analyze the crude reaction by ^{1}H NMR using $CDCl_3$ as solvent ($\%conv._{NMR}$ = 80%). The resulting polymer was precipitated by addition to 200 mL of MeOH, followed by stirring for 20 min. The majority of MeOH was decanted. The polymer was stirred in an additional 200 mL of MeOH overnight. The solution phase was decanted. The polymer was washed with stirring with two additional portions of MeOH (200 mL × 2). The polymer was filtered and dried under vacuum to yield 1.8646 g (wt% $plasticizer_{grav.}$ = 73%) of a pale green, pliable polymer.

^{1}H NMR (500 MHz, $CDCl_3$) δ 4.64–4.53 (br m), 4.53–4.38 (br m), 4.38–4.26 (br m), 4.26–4.02 (br s), 3.74–3.64 (br m), 3.64–3.60 (br m), 3.60–3.55 (br m), 3.52 (q, J = 7.1 Hz), 2.51–2.23 (br m), 2.23–1.97 (br m), 1.97–1.83 (br m), 1.73–1.56 (br m), 1.55–1.39 (br m), 1.20 (t, J = 7.0 Hz). Based by ^{1}H NMR integration: P2EEA : PVC = 1.0 : 1.0.

FT-IR: 2973 (s, alkane C─H), 2872 (s, alkane C─H), 1736 (s, ester C=O), 1171 (s, ester C─O). 1120 (s, ether C─O)

Control experiment without PVC

To a 10 mL Schlenk flask was added a suspension of CuBr (34.56 mg, 0.2409 mmol) and 4 mL of DMF. PMDETA (50 µL, 0.24 mmol), BA (1.43 mL, 9.97 mmol), and 2EEA (1.85 mL, 9.99 mmol) were added to the suspension. The reaction mixture was degassed via four cycles of freeze-pump-thaw, and then heated to 100 °C while stirring under nitrogen for 24 h. An aliquot was taken to analyze the crude reaction by ^{1}H NMR using $CDCl_3$ as solvent (%$conv._{NMR}$ = 23%).

Preparation of PVC-*g*-PBA (14 g scale)

To a 50 mL Schlenk flask was added PVC (3.00 g, 48.0 mmol) and DMF (18 mL). The mixture was stirred and warmed slightly to fully dissolve the PVC. BA (17.2 mL, 120 mmol) was added to the solution. To a 20 mL vial was added CuBr (206.50 mg, 1.4395 mmol) and 6 mL of DMF was used to transfer CuBr to the PVC solution by pipet. PMDETA (0.30 mL, 1.43 mmol) was added, and the reaction mixture was degassed via four cycles of freeze-pump-thaw, and then heated to 100 °C while stirring under nitrogen. After 24 h, an aliquot was taken to analyze the crude reaction by ^{1}H NMR using $CDCl_3$ as solvent (%$conv._{NMR}$ = 87%). The resulting polymer was diluted in 20 mL of THF and precipitated by addition to 400 mL of MeOH. The polymer was washed with stirring with two additional portions of MeOH (400 mL × 2) and gently stirred in MeOH overnight. Then MeOH was decanted. The polymer was dissolved in 30 mL of THF and then stirred in 400 mL of MeOH overnight. The polymer was washed with stirring with two additional portions of MeOH (400 mL × 2). The polymer was filtered and dried under vacuum to yield 14.98 g (wt% plasticizer$_{grav.}$ = 80%) of a pale green, pliable polymer.

^{1}H NMR (500 MHz, $CDCl_3$) δ 4.65–4.54 (br m), 4.54–4.38 (br m), 4.38–4.23 (br m), 4.15–3.85 (br m), 2.50–2.22 (br m), 2.22–1.97 (br m), 1.97–1.79 (br m), 1.77–1.56 (br m), 1.51–1.43 (br m), 1.43–1.29 (br m), 0.94 (t, J = 7.3 Hz). Based by ^{1}H NMR integration: PBA : PVC = 1.4 : 1.0.

Preparation of PVC-*g*-75%PBA-*co*-25%P2EEA (14 g scale)

To a 50 mL Schlenk flask was added PVC (3.00 g, 48.0 mmol) and DMF (18 mL). The mixture was stirred and warmed slightly to fully dissolve the PVC. BA (12.9 mL, 90.0 mmol) and 2EEA (5.56 mL, 30.0 mmol) were added to the solution. To a 20 mL vial was added CuBr (206.36 mg, 1.4386 mmol) and 6 mL of DMF was used to transfer CuBr to the PVC solution by pipet. PMDETA (0.30 mL, 1.43 mmol) was added, and the reaction mixture was degassed via four cycles of freeze-pump-thaw, and then heated to 100 °C while stirring under nitrogen. After 24 h, an aliquot was taken to analyze the crude reaction by ^{1}H NMR using $CDCl_3$ as solvent (%conv.$_{NMR}$ = 88%). The resulting polymer was diluted in 20 mL of THF and precipitated by addition to 400 mL of MeOH. The polymer was washed with stirring with two additional portions of MeOH (400 mL × 2) and gently stirred in MeOH overnight. The polymer was then washed with stirring with additional portion of 400 mL of MeOH). The polymer was filtered and dried under vacuum to yield 13.99 g (wt% plasticizer$_{grav.}$ = 79%) of a pale yellow, pliable polymer.

^{1}H NMR (500 MHz, $CDCl_3$) δ 4.69–4.54 (br s), 4.54–4.38 (br m), 4.38–4.25 (br m), 4.25–4.12 (br s), 4.12–3.87 (br m), 3.74–3.65 (br m), 3.65–3.60 (br m), 3.60–3.55 (br m), 3.52 (q, *J* = 7.0 Hz), 2.54–2.22 (br m), 2.22–1.97 (br m), 1.97–1.79 (br m), 1.72–1.56 (br m), 1.52–1.43 (br m), 1.43–1.29 (br m), 1.21 (t, *J* = 7.0 Hz), 0.94 (t, *J* = 7.4 Hz). Based by ^{1}H NMR integration: (PBA + P2EEA) : PVC = 1.3 : 1.0; PBA : P2EEA = 3.0 : 1.0.

Preparation of PVC-*g*-50%PBA-*co*-50%P2EEA (14 g scale)

To a 50 mL Schlenk flask was added PVC (3.00 g, 48.0 mmol) and DMF (18 mL). The mixture was stirred and warmed slightly to fully dissolve the PVC. BA (8.60 mL, 60.0 mmol) and 2EEA (11.12 mL, 60.03 mmol) were added to the solution. To a 20 mL vial was added CuBr (206.18 mg, 1.4373 mmol) and 6 mL of DMF was used to transfer CuBr to the PVC solution by pipet. PMDETA (0.30 mL, 1.43 mmol) was added, and the reaction mixture was degassed via four cycles of freeze-pump-thaw, and then heated to 100 °C while stirring under nitrogen. After 24 h, an aliquot was taken to analyze the crude reaction by ^{1}H NMR using $CDCl_3$ as solvent (%conv.$_{NMR}$ = 86%). The resulting polymer was diluted in 20 mL of THF and precipitated by addition to 400 mL of MeOH. The polymer was washed with stirring with two additional portions of MeOH (400 mL × 2) and gently stirred in MeOH overnight. The polymer was then washed with stirring with additional portion of 400 mL). The polymer was filtered and dried under vacuum of MeOH to yield 13.14 g (wt% plasticizer$_{grav.}$ = 77%) of a pale yellow, pliable polymer.

^{1}H NMR (500 MHz, $CDCl_3$) δ 4.68–4.54 (br s), 4.54–4.38 (br s), 4.38–4.25 (br m), 4.25–4.12 (br s), 4.12–3.90 (br s), 3.72–3.65 (br m), 3.65–3.60 (br m), 3.60–3.55 (br m), 3.52 (q, *J* = 7.0 Hz), 2.50–2.23 (br m), 2.23–1.98 (br m), 1.98–1.82 (br m), 1.72–1.57 (br m), 1.51–1.44 (br m), 1.44–1.29 (br m), 1.21 (t, *J* = 7.0 Hz), 0.94 (t, *J* = 7.3 Hz). Based by ^{1}H NMR integration: (PBA + P2EEA) : PVC = 1.0 : 1.0; PBA : P2EEA = 1.0 : 1.0.

Preparation of PVC-*g*-25%PBA-*co*-75%P2EEA (14 g scale)

To a 50 mL Schlenk flask was added PVC (3.00 g, 48.0 mmol) and DMF (18 mL). The mixture was stirred and warmed slightly to fully dissolve the PVC. BA acrylate (4.30 mL, 30.0 mmol) and 2EEA (16.67 mL, 89.98 mmol) were added to the solution. To a 20 mL vial was added CuBr (206.22 mg, 1.4376 mmol) and 6 mL of DMF was used to transfer CuBr to the PVC solution by pipet. PMDETA (0.30 mL, 1.43 mmol) was added, and the reaction mixture was degassed via four cycles of freeze-pump-thaw, and then heated to 100 °C while stirring under nitrogen. After 24 h, an aliquot was taken to analyze the crude reaction by ^{1}H NMR using

$CDCl_3$ as solvent (%conv.$_{NMR}$ = 72%). The resulting polymer was diluted in 20 mL of THF and precipitated by addition to 400 mL of MeOH. The polymer was washed with stirring with two additional portions of MeOH (400 mL × 2) and gently stirred in MeOH overnight. The polymer was then washed with stirring with additional portion of 400 mL of MeOH). The polymer was filtered and dried under vacuum to yield 13.66 g (wt% plasticizer$_{grav.}$ = 78%) of a pale yellow, pliable polymer.

^{1}H NMR (500 MHz, $CDCl_3$) δ 4.59 (br s), 4.54–4.38 (br s), 4.38–4.26 (br m), 4.26–4.11 (br s), 4.04 (br s), 3.73–3.65 (br m), 3.63 (br s), 3.57 (br m), 3.52 (q, *J* = 7.0 Hz), 2.53–2.23 (br m), 2.23–1.98 (br m), 1.98–1.81 (br s), 1.75–1.59 (br m), 1.55–1.43 (br m), 1.37 (br m), 1.20 (t, *J* = 7.0 Hz), 0.94 (t, *J* = 7.2 Hz). Based by ^{1}H NMR integration: (PBA + P2EEA) : PVC = 1.0 : 2.9; PBA : P2EEA = 1.2 : 1.0.

Preparation of PVC-*g*-P2EEA (14 g scale)

To a 50 mL Schlenk flask was added PVC (3.00 g, 48.0 mmol) and DMF (18 mL). The mixture was stirred and warmed slightly to fully dissolve the PVC. 2EEA (22.23 mL, 120.0 mmol) was added to the solution. To a 20 mL vial was added CuBr (206.89 mg, 1.4422 mmol) and 6 mL of DMF was used to transfer CuBr to the PVC solution by pipet. PMDETA (0.30 mL, 1.43 mmol) was added, and the reaction mixture was degassed via four cycles of freeze-pump-thaw, and then heated to 100 °C while stirring under nitrogen. After 24 h, an aliquot was taken to analyze the crude reaction by ^{1}H NMR using $CDCl_3$ as solvent (%conv.$_{NMR}$ = 78%). The resulting polymer was diluted in 20 mL of THF and precipitated by addition to 400 mL of MeOH. The polymer was washed with stirring with two additional portions of MeOH (400 mL × 2) and gently stirred in MeOH overnight. The polymer was then washed with stirring with additional portion of 400 mL of MeOH). The polymer was filtered and dried under vacuum to yield 13.34 g (wt% plasticizer$_{grav.}$ = 78%) of a pale yellow, pliable polymer.

^{1}H NMR (500 MHz, $CDCl_3$) δ 4.64–4.54 (br s), 4.54–4.38 (br s), 4.38–4.26 (br m), 4.26–4.02 (br s), 3.73–3.65 (br m), 3.65–3.60 (br m), 3.60–3.55 (br m), 3.52 (q, J = 7.0 Hz), 2.51–2.23 (br s), 2.23–1.98 (br m), 1.98–1.84 (br s), 1.77–1.60 (br s), 1.50–1.38 (br m), 1.20 (t, J = 7.0 Hz). Based by ^{1}H NMR integration: P2EEA : PVC = 0.8 : 1.0.

5.2.4 Preparation of PVC Graft Copolymers for Chapter 4

Control Experiment: Polymerization without PVC as macroinitiator (PBA, 2 h)

To a 10 mL Schlenk flask was added DMF (3 mL) and BA (2.87 mL, 20.0 mmol). To a 2 mL vial was added CuBr (34.43 mg, 0.2400 mmol) and 0.75 mL of DMF to form a suspension. The CuBr suspension was transferred to the PVC solution by pipet. Residual CuBr was washed into the PVC solution using 0.25 mL of DMF. PMDETA (50 µL, 0.24 mmol) was added, and the reaction mixture was degassed via four cycles of freeze-pump-thaw, and then heated to 100 °C and stirred under nitrogen. After 2 h, an aliquot was taken to analyze the crude reaction by ^{1}H NMR using $CDCl_3$ as solvent ($\%conv._{NMR}$ = 10%).

Control Experiment: Polymerization without PVC as macroinitiator (P2EEA, 2 h)

To a 10 mL Schlenk flask was added DMF (3 mL) and 2EEA (3.70 mL, 20.0 mmol). To a 2 mL vial was added CuBr (34.34 mg, 0.2394 mmol) and 0.75 mL of DMF to form a suspension. The CuBr suspension was transferred to the PVC solution by pipet. Residual CuBr was washed into the PVC solution using 0.25 mL of DMF. PMDETA (50 µL, 0.24 mmol) was added, and the reaction mixture was degassed via four cycles of freeze-pump-thaw, and then heated to 100 °C and stirred under nitrogen. After 2 h, an aliquot was taken to analyze the crude reaction by ^{1}H NMR using $CDCl_3$ as solvent ($\%conv._{NMR}$ = 6%).

Preparation of PVC-*g*-PBA-2.5 (2 h)

To a 10 mL Schlenk flask was added PVC (500.6 mg, 8.010 mmol) and DMF (3 mL). The mixture was stirred and slightly warmed to fully dissolve the PVC in the DMF. BA (2.87 mL, 20.0 mmol) was added to the solution. To a 2 mL vial was added CuBr (34.43 mg, 0.2400 mmol) and 0.75 mL of DMF to form a suspension. The CuBr suspension was transferred to the PVC solution by pipet. Residual CuBr was washed into the PVC solution using 0.25 mL of DMF. PMDETA (50 µL, 0.24 mmol) was added, and the reaction mixture was degassed via four cycles of freeze-pump-thaw, and then heated to 100 °C and stirred under nitrogen. After 2 h, an aliquot was taken to analyze the crude reaction by ^{1}H NMR using $CDCl_3$ as solvent (%$conv._{NMR}$ = 78%). The resulting polymer was diluted in 1 mL of THF and precipitated by addition to 200 mL of MeOH, followed by stirring for 20 min. Then MeOH was decanted. The polymer was gently stirred in an additional 100 mL of MeOH overnight. The solution phase was decanted. The product was rinsed with 100 mL of MeOH. The solution phase was decanted. The product was dried under vacuum to yield 1.9721 g (wt% $plasticizer_{grav.}$ = 75%) of a pale green, pliable polymer.

^{1}H NMR (500 MHz, $CDCl_3$) δ 4.65–4.54 (br m), 4.54–4.38 (br m), 4.38–4.22 (br m), 4.16–3.86 (br m), 2.49–2.22 (br m), 2.22–1.97 (br m), 1.97–1.80 (br m), 1.70–1.57 (br m), 1.51–1.43 (br m), 1.43–1.29 (br m), 0.93 (t, J = 7.4 Hz). Based by ^{1}H NMR integration: PBA : PVC = 1.4 : 1.0; wt% $plasticizer_{NMR}$ = 78%.

FTIR: 2962 (m, alkane C─H), 2935 (m, alkane C─H), 2873 (m, alkane C─H), 1736 (s, ester C=O), 1165 (s, ester C─O).

Preparation of PVC-*g*-75%PBA-*co*-25%P2EEA-2.5 (2 h)

To a 10 mL Schlenk flask was added PVC (498.2 mg, 7.971 mmol) and 3 mL of DMF. The mixture was stirred and slightly warmed to fully dissolve the PVC in the DMF. BA (2.15 mL, 15.0 mmol) and 2EEA (0.93 mL, 5.0 mmol) were added to the solution. To a 2 mL vial was added CuBr (34.37 mg, 0.2396 mmol) and 0.75 mL of DMF to form a suspension. The CuBr suspension was transferred to the PVC solution by pipet. Residual CuBr was washed into the PVC solution using 0.25 mL of DMF. PMDETA (50 µL, 0.24 mmol) was added, and the reaction mixture was degassed via four cycles of freeze-pump-thaw, and then heated to 100 °C and stirred under nitrogen. After 2 h, an aliquot was taken to analyze the crude reaction by ^{1}H NMR using $CDCl_3$ as solvent (%conv.$_{NMR}$ = 61%). The resulting polymer was precipitated by addition to 200 mL of MeOH, followed by stirring for 30 min. Then MeOH was decanted. The polymer was soaked in an additional 100 mL of MeOH overnight without stirring. The solution phase was decanted. The product was rinsed with 100 mL of MeOH. The solution phase was decanted. The polymer was dried under vacuum to yield 1.5463 g (wt% plasticizer$_{grav.}$ = 68%) of a pale green, pliable polymer.

^{1}H NMR (500 MHz, $CDCl_3$) δ 4.66–4.54 (br s), 4.54–4.38 (br m), 4.38–4.24 (br m), 4.24–4.12 (br s), 4.12–3.89 (br m), 3.72–3.65 (br m), 3.65–3.60 (br m), 3.60–3.55 (br m), 3.52 (q, *J* = 7.0 Hz), 2.55–2.22 (br m), 2.22–1.97 (br m), 1.97–1.81 (br m), 1.70–1.57 (br m), 1.52–1.44 (br m), 1.43–1.29 (br m), 1.21 (t, *J* = 7.0 Hz), 0.94 (t, *J* = 7.3 Hz). Based by ^{1}H NMR integration: (PBA + P2EEA) : PVC = 1.0 : 1.0; PBA : P2EEA = 3.0 : 1.0; wt% plasticizer$_{NMR}$ = 61%.

FTIR: 2958 (m, alkane C─H), 2935 (m, alkane C─H), 2873 (m, alkane C─H), 1732 (s, ester C=O), 1165 (s, ester C─O), 1115 (m, ether C─O).

Preparation of PVC-*g*-50%PBA-*co*-50%P2EEA-2.5 (2 h)

To a 10 mL Schlenk flask was added PVC (500.7 mg, 8.011 mmol) and DMF (3 mL). The mixture was stirred and slightly warmed to fully dissolve the PVC in DMF. BA (1.43 mL, 9.97 mmol) and 2EEA (1.85 mL, 9.99 mmol) were added to the solution. To a 2 mL vial was added CuBr (34.22 mg, 0.2386 mmol) and 0.75 mL of DMF to form a suspension. The CuBr suspension was transferred to the PVC solution by pipet. Residual CuBr was washed into the PVC solution using 0.25 mL of DMF. PMDETA (50 µL, 0.24 mmol) was added, and the reaction mixture was degassed via four cycles of freeze-pump-thaw, and then heated to 100 °C and stirred under nitrogen. After 2 h, an aliquot was taken to analyze the crude reaction by ^{1}H NMR using $CDCl_3$ as solvent (%conv.$_{NMR}$ = 60%). The resulting polymer was precipitated by addition to 200 mL of MeOH, followed by stirring for 30 min. Then MeOH was decanted. The polymer was left in an additional 100 mL of MeOH overnight without stirring. The solution phase was decanted. The polymer was dried under mild house vacuum. The polymer (still containing residual solvent) was washed with an additional 5 mL of MeOH, and the solvent decanted. The product was thoroughly dried under vacuum to yield 1.5567 g (wt% $plasticizer_{grav.}$ = 68%) of a pale green, pliable polymer.

^{1}H NMR (500 MHz, $CDCl_3$) δ 4.65–4.54 (br m), 4.54–4.38 (br m), 4.38–4.25 (br m), 4.25–4.12 (br m), 4.12–3.93 (br m), 3.72–3.65 (br m), 3.65–3.60 (br m), 3.60–3.55 (br m), 3.52 (q, *J* = 7.0 Hz), 2.49–2.23 (br m), 2.23–1.97 (br m), 1.97–1.81 (br m), 1.74–1.57 (br m), 1.51–1.43 (br m), 1.43–1.29 (br m), 1.21 (t, *J* = 7.0 Hz), 0.94 (t, *J* = 7.3 Hz). Based by ^{1}H NMR integration: (PBA + P2EEA) : PVC = 0.9 : 1.0; PBA : P2EEA = 1.0 : 1.0; wt% $plasticizer_{NMR}$ = 60%.

FTIR: 2974 (m, alkane C─H), 2931 (m, alkane C─H), 2873 (m, alkane C─H), 1736 (s, ester C=O), 1169 (s, ester C─O), 1119 (m, ether C─O).

Preparation of PVC-*g*-25%PBA-*co*-75%P2EEA-2.5 (2 h)

To a 10 mL Schlenk flask was added PVC (500.6 mg, 8.010 mmol) and DMF (3 mL). The mixture was stirred and slightly warmed to fully dissolve the PVC in DMF. BA (0.72 mL, 5.02 mmol) and 2EEA (2.78 mL, 15.0 mmol) were added to the solution. To a 2 mL vial was added CuBr (34.43 mg, 0.2400 mmol) and 0.75 mL of DMF to form a suspension. The CuBr suspension was transferred to the PVC solution by pipet. Residual CuBr was washed into the PVC solution using 0.25 mL of DMF. PMDETA (50 µL, 0.24 mmol) was added, and the reaction mixture was degassed via four cycles of freeze-pump-thaw, and then heated to 100 °C and stirred under nitrogen. After 2 h, an aliquot was taken to analyze the crude reaction by ^{1}H NMR using $CDCl_3$ as solvent (%$conv._{NMR}$ = 56%). The resulting polymer was precipitated by addition to 200 mL of MeOH, followed by stirring for 30 min. Then majority of MeOH was decanted. An additional 50 mL of MeOH was added, and the polymer was allowed to sit overnight without stirring. The solution phase was decanted. The polymer was washed with an additional 50 mL of MeOH. The solution phase was decanted. The Polymer was dried under house vacuum. The polymer still containing residual solvent was washed with 10 mL of MeOH. The product was thoroughly dried under vacuum to yield 1.5532 g (wt% $plasticizer_{grav.}$ = 68%) of a pale green, pliable polymer.

^{1}H NMR (500 MHz, $CDCl_3$) δ 4.65–4.54 (br m), 4.54–4.39 (br m), 4.39–4.25 (br m), 4.25–4.12 (br s), 4.12–3.91 (br m), 3.72–3.65 (br m), 3.65–3.60 (br m), 3.60–3.55 (br m), 3.52 (q, *J* = 7.0 Hz), 2.52–2.23 (br m), 2.23–1.97 (br m), 1.97–1.83 (br m), 1.75–1.55 (br m), 1.52–1.42 (br m), 1.42–1.28 (br m), 1.20 (t, *J* = 7.0 Hz), 0.94 (t, *J* = 7.3 Hz). Based by ^{1}H NMR integration: (PBA + P2EEA) : PVC = 0.9 : 1.0; PBA : P2EEA = 1.0 : 2.8; wt% $plasticizer_{NMR}$ = 56%.

FTIR: 2962 (m, alkane C─H), 2931 (m, alkane C─H), 2873 (m, alkane C─H), 1736 (s, ester C=O), 1169 (s, ester C─O), 1119 (m, ether C─O).

Preparation of PVC-*g*-P2EEA-2.5 (2 h)

To a 10 mL Schlenk flask was added PVC (500.7 mg, 8.011 mmol) and DMF (3 mL). The mixture was stirred and slightly warmed to fully dissolve the PVC in DMF. 2EEA (3.70 mL, 20.0 mmol) was added to the solution. To a 2 mL vial was added CuBr (34.37 mg, 0.2396 mmol) and 0.75 mL of DMF to form a suspension. The CuBr suspension was transferred to the PVC solution by pipet. Residual CuBr was washed into the PVC solution using 0.25 mL of DMF. PMDETA (50 µL, 0.24 mmol) was added, and the reaction mixture was degassed via four cycles of freeze-pump-thaw, and then heated to 100 °C and stirred under nitrogen. After 2 h, an aliquot was taken to analyze the crude reaction by ^{1}H NMR using $CDCl_3$ as solvent ($\%conv._{NMR}$ = 60%). The resulting polymer was precipitated by addition to 200 mL of MeOH, followed by stirring for 30 min. The majority of MeOH was decanted. An additional 100 mL of

MeOH was added, and the polymer was allowed to sit overnight without stirring. The majority of the solution phase was decanted. The polymer was dried under house vacuum. The polymer (still containing residual solvent) was washed with 20 mL of MeOH, and then the solvent was decanted. The product was dried under vacuum to yield 1.6420 g (wt% $Plasticizer_{grav.}$ = 70%) of a pale green, pliable polymer.

^1H NMR (500 MHz, $CDCl_3$) δ 4.64–4.54 (br m), 4.54–4.38 (br m), 4.38–4.25 (br m), 4.25–4.05 (br m), 3.73–3.65 (br m), 3.65–3.60 (br m), 3.60–3.55 (br m), 3.52 (q, *J* = 7.0 Hz), 2.49–2.23 (br m), 2.23–1.97 (br m), 1.97–1.81 (br m), 1.73–1.62 (br m), 1.54–1.39 (br m), 1.20 (t, *J* = 7.0 Hz). Based by ^1H NMR integration: P2EEA : PVC = 0.9 : 1.0; wt% $plasticizer_{NMR}$ = 60%.

FTIR: 2958 (m, alkane C─H), 2931 (m, alkane C─H), 2873 (m, alkane C─H), 1736 (s, ester C=O), 1169 (s, ester C─O), 1115 (m, ether C─O).

Preparation of PVC-*g*-PBA-0.5 (2 h)

To a 10 mL Schlenk flask was added PVC (500.2 mg, 8.003 mmol) and DMF (3 mL). The mixture was stirred and slightly warmed to fully dissolve the PVC in DMF. BA (0.57 mL, 3.98 mmol) was added to the solution. To a 2 mL vial was added CuBr (34.32 mg, 0.2392 mmol) and 0.75 mL of DMF to form a suspension. The CuBr suspension was transferred to the PVC solution by pipet. Residual CuBr was washed into the PVC solution using 0.25 mL of DMF. PMDETA (50 µL, 0.24 mmol) was added, and the reaction mixture was degassed via four cycles of freeze-pump-thaw, and then heated to 100 °C and stirred under nitrogen. After 2 h, an aliquot was taken to analyze the crude reaction by ^1H NMR using $CDCl_3$ as solvent (%$conv._{NMR}$ = 59%). The resulting polymer was precipitated by addition to 200 mL of MeOH and left in MeOH overnight. The MeOH was decanted. The polymer was washed with 100 mL of MeOH. The solution phase was decanted. The product was dried under vacuum to yield 681.4 mg (wt% $plasticizer_{grav.}$ = 27%) of a pale green polymer.

^{1}H NMR (500 MHz, $CDCl_3$) δ 4.67–4.54 (br m), 4.54–4.38 (br m), 4.38–4.22 (br m), 4.14–3.89 (br m), 2.51–2.40 (br m), 2.40–2.23 (br m), 2.23–1.97 (br m), 1.97–1.77 (br m), 1.70–1.49 (br m), 1.44–1.30 (br m), 0.94 (t, *J* = 7.3 Hz). Based by ^{1}H NMR integration: PBA : PVC = 0.3 : 1.0; wt% $plasticizer_{NMR}$ = 35%

FTIR: 2958 (m, alkane C–H), 2931 (m, alkane C–H), 2873 (m, alkane C–H), 1732 (s, ester C=O), 1169 (s, ester C–O)

Preparation of PVC-*g*-PBA-1.0 (2 h)

To a 10 mL Schlenk flask was added PVC (501.0 mg, 8.016 mmol) and DMF (3 mL). The mixture was stirred and slightly warmed to fully dissolve the PVC in DMF. BA (1.15 mL, 8.02 mmol) was added to the solution. To a 2 mL vial was added CuBr (34.45 mg, 0.2402 mmol) and 0.75 mL of DMF to form a suspension. The CuBr suspension was transferred to the PVC solution by pipet. Residual CuBr was washed into the PVC solution using 0.25 mL of DMF. PMDETA (50 µL, 0.24 mmol) was added, and the reaction mixture was degassed via four cycles of freeze-pump-thaw, and then heated to 100 °C and stirred under nitrogen. After 2 h, an aliquot was taken to analyze the crude reaction by ^{1}H NMR using $CDCl_3$ as solvent (%$conv._{NMR}$ = 67%). The resulting polymer was precipitated by addition to 200 mL of MeOH, followed by stirring for 30 min. The MeOH was decanted. The polymer was allowed to sit in another 100 mL of MeOH without stirring overnight. The solution phase was decanted. The product was rinsed with 100 mL of MeOH. The solution phase was decanted. The polymer was thoroughly dried under vacuum to yield 1.0109 g (wt% $plasticizer_{grav.}$ = 50%) of a pale green, pliable polymer.

^{1}H NMR (500 MHz, $CDCl_3$) δ 4.66–4.54 (br m), 4.54–4.38 (br m), 4.38–4.23 (br m), 4.13–3.89 (br m), 2.51–2.23 (br m), 2.23–1.97 (br m), 1.97–1.79 (br m), 1.72–1.56 (br m), 1.51–1.44 (br m), 1.44–1.30 (br m), 0.93 (t, *J* = 7.3 Hz). Based by ^{1}H NMR integration: PBA : PVC = 0.6 : 1.0; wt% $plasticizer_{NMR}$ = 53%.

FTIR: 2958 (m, alkane C─H), 2935 (m, alkane C─H), 2873 (m, alkane C─H), 1728 (s, ester C=O), 1157 (s, ester C─O).

Preparation of PVC-*g*-P2EEA-0.5 (2 h)

To a 10 mL Schlenk flask was added PVC (500.8 mg, 8.013 mmol) and DMF (3 mL). The mixture was stirred and slightly warmed to fully dissolve the PVC in DMF. 2EEA (0.74 mL, 20.0 mmol) was added to the solution. To a 2 mL vial was added CuBr (34.48 mg, 0.2396 mmol) and 0.75 mL of DMF to form a suspension. The CuBr suspension was transferred to the PVC solution by pipet. Residual CuBr was washed into the PVC solution using 0.25 mL of DMF. PMDETA (50 µL, 0.24 mmol) was added, and the reaction mixture was degassed via four cycles of freeze-pump-thaw, and then heated to 100 °C and stirred under nitrogen. After 2 h, an aliquot was taken to analyze the crude reaction by ^{1}H NMR using $CDCl_3$ as solvent ($\%conv._{NMR}$ = 40%). The resulting polymer was precipitated by addition to 200 mL of MeOH, followed by stirring for 20 min. Then MeOH was decanted. The polymer was allowed to sit in another 100 mL of MeOH without stirring overnight. The solution phase was decanted. The product was rinsed with 100 mL of MeOH. The solution phase was decanted. The polymer was dried under vacuum to yield 657.7 mg (wt% $plasticizer_{grav.}$ = 24%) of a pale green polymer.

^{1}H NMR (500 MHz, $CDCl_3$) δ 4.67–4.54 (br m), 4.54–4.38 (br m), 4.38–4.25 (br m), 4.25–4.06 (br s), 3.73–3.65 (br m), 3.65–3.60 (br m), 3.60–3.55 (br m), 3.52 (q, J = 7.0 Hz), 2.51–2.23 (br m), 2.23–1.96 (br m), 1.96–1.87 (br s), 1.74–1.61 (br m), 1.20 (t, J = 7.0 Hz). Based by ^{1}H NMR integration: P2EEA : PVC = 0.2 : 1.0; wt% $plasticizer_{NMR}$ = 38%.

FTIR: 2974 (m, alkane C─H), 2908 (m, alkane C─H), 2866 (m, alkane C─H), 1732 (s, ester C=O), 1169 (m, ester C─O) 1111 (s, ether C─O).

Preparation of PVC-*g*-P2EEA-1.0 (2 h)

To a 10 mL Schlenk flask was added PVC (500.8 mg, 8.013 mmol) and DMF (3 mL). The mixture was stirred and slightly warmed to fully dissolve the PVC in DMF. 2EEA (0.74 mL, 20.0 mmol) was added to the solution. To a 2 mL vial was added CuBr (34.45 mg, 0.2402 mmol) and 0.75 mL of DMF to form a suspension. The CuBr suspension was transferred to the PVC solution by pipet. Residual CuBr was washed into the PVC solution using 0.25 mL of DMF. PMDETA (50 µL, 0.24 mmol) was added, and the reaction mixture was degassed via four cycles of freeze-pump-thaw, and then heated to 100 °C and stirred under nitrogen. After 2 h, an aliquot was taken to analyze the crude reaction by ^{1}H NMR using $CDCl_3$ as solvent ($\%conv._{NMR}$ = 59%). The resulting polymer was precipitated by addition to 200 mL of MeOH, followed by stirring for 30 min. The MeOH was decanted. The polymer was allowed to sit in another 100 mL of MeOH without stirring. The solution phase was decanted. The product was rinsed with 100 mL of MeOH. The solution phase was decanted. The polymer was dried under vacuum to yield 954.2 mg (wt% $plasticizer_{grav.}$ = 48%) of a pale yellow, pliable polymer.

^{1}H NMR (500 MHz, $CDCl_3$) δ 4.66–4.54 (br m), 4.54–4.38 (br m), 4.38–4.25 (br m), 4.25–4.03 (br m), 3.74–3.65 (br m), 3.65–3.60 (br m), 3.60–3.55 (br m), 3.52 (q, *J* = 7.1 Hz), 2.52–2.23 (br m), 2.23–1.97 (br m), 1.97–1.82 (br m), 1.75–1.61 (br m), 1.51–1.40 (br m), 1.20 (t, *J* = 7.0 Hz). Based by ^{1}H NMR integration: P2EEA : PVC = 0.4 : 1.0; wt% $plasticizer_{NMR}$ = 55%

FTIR: 2974 (m, alkane C─H), 2870 (m, alkane C─H), 1736 (s, alkane C─H), 1169 (m, ester C─O) 1115 (s, ether C─O)

5.3 References

(1) Niikura, K.; Nambara, K.; Okajima, T.; Matsuo, Y.; Ijiro, K. Influence of Hydrophobic Structures on the Plasma Membrane Permeability of Lipidlike Molecules. *Langmuir* **2010**, *26* (12), 9170–9175. https://doi.org/10.1021/la101039w

(2) Heyl, D.; Fessner, W.-D. Facile Direct Synthesis of Acetylenedicarboxamides. *Synthesis* **2014**, 1463–1468. https://doi.org/10.1055/s-0033-1341101

(3) Bräse, S.; Gil, C.; Knepper, K.; Zimmermann, V. Organic Azides: An Exploding Diversity of a Unique Class of Compounds. *Angew. Chem. Int. Ed.* **2005**, *44* (33), 5188–5240. https://doi.org/10.1002/anie.200400657.

(4) Hassner, A.; Stern, M. Synthesis of Alkyl Azides with a Polymeric Reagent. *Angew. Chem. Int. Ed. Engl*. **1986**, *25* (5), 478–479. https://doi.org/10.1002/anie.198604781

(5) Earla, A.; Li, L.; Costanzo, P.; Braslau, R. Phthalate Plasticizers Covalently Linked to PVC via Copper-Free or Copper Catalyzed Azide-Alkyne Cycloadditions. *Polymer* **2017**, *109* (Supplement C), 1–12. https://doi.org/10.1016/j.polymer.2016.12.014.

(6) Higa, C. M.; Tek, A. T.; Wojtecki, R. J.; Braslau, R. Nonmigratory Internal Plasticization of Poly (Vinyl Chloride) via Pendant Triazoles Bearing Alkyl or Polyether Esters. *J. Polym. Sci. Part Polym. Chem.* **2018**, *56* (21), 2397–2411. https://doi.org/10.1002/pola.29205

(7) Rusen, E.; Marculescu, B.; Butac, L.; Preda, N.; Mihut, L. The Synthesis and Characterization of Poly Vinyl Chloride Chemically Modified with C60. *Fuller. Nanotub. Carbon Nanostructures* **2008**, *16* (3), 178–185. https://doi.org/10.1080/15363830802042563.

(8) Azzam, T.; Eisenberg, A. Control of Vesicular Morphologies through Hydrophobic Block Length. *Angew. Chem. Int. Ed.* **2006**, *45* (44), 7443–7447. https://doi.org/10.1002/anie.200602897.

Addendum: Contribution to Other Published Works

Contributions to other projects from the Braslau lab in which I am a co-author, but are not included in the thesis are described as follows.

1. Earla, A.; **Li, L.**; Costanzo, P.; Braslau, R. *Polymer* **2017**, *109*, 1–12. Phthalate Plasticizers Covalently Linked to PVC via Copper-Free or Copper Catalyzed Azide-Alkyne Cycloadditions. I synthesized two alkynes bearing phthalates or phthalate mimics, and attached them to azidized PVC:

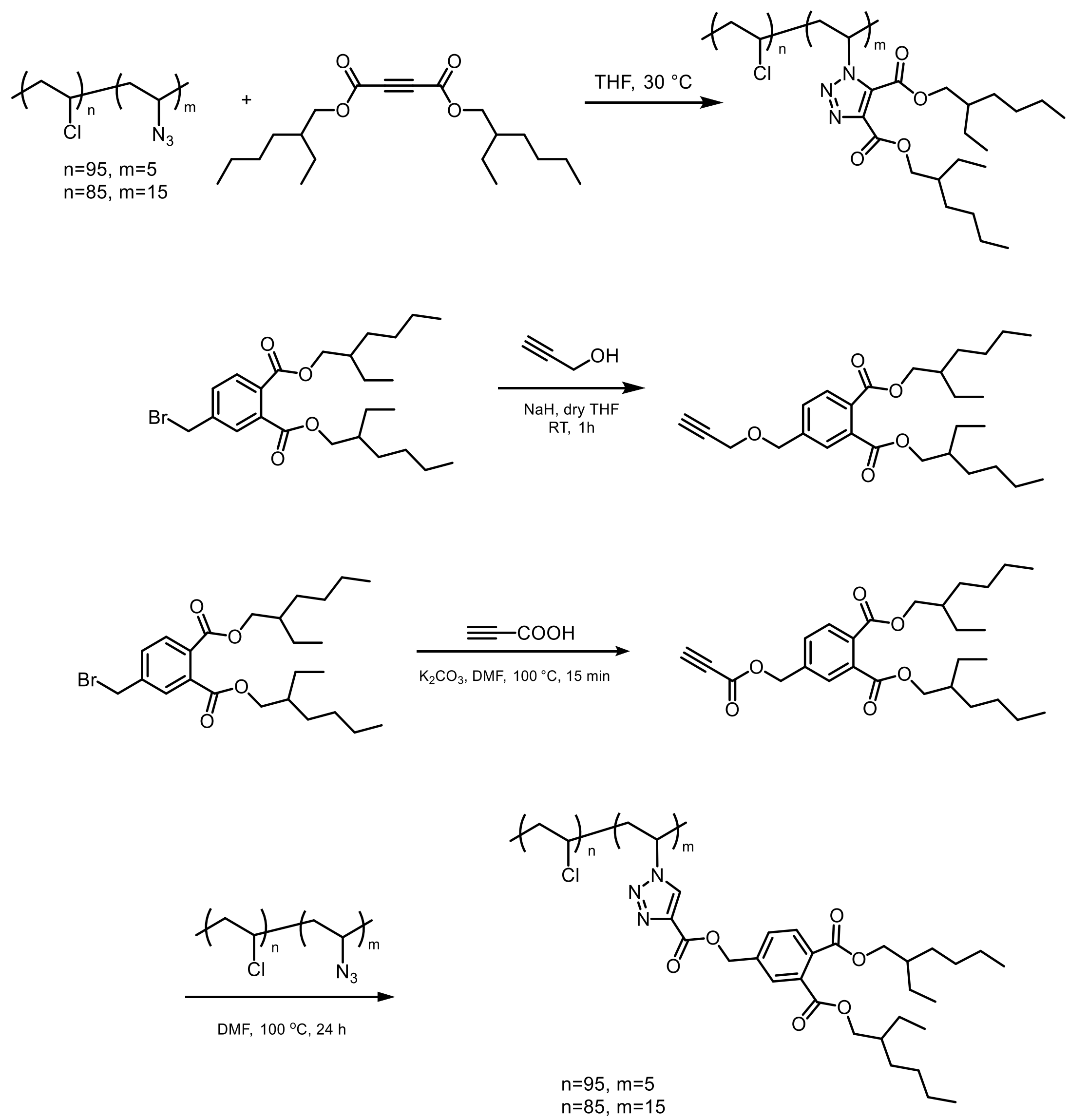

2. Skelly, P. W.; Sae-Jew, J.; Kitos Vasconcelos, A. P.; Tasnim, J.; **Li, L.**; Raskatov, J. A.; Braslau, R. *J. Org. Chem.* **2019**, *84* (21), 13615–13623. Relative Rates of Metal-Free Azide–Alkyne Cycloadditions: Tunability over 3 Orders of Magnitude. I synthesized two alkynes for Huisgen thermal cycloaddition, which were then utilized by others to determine the relative rates of various alkynes in reacting with a model azide.

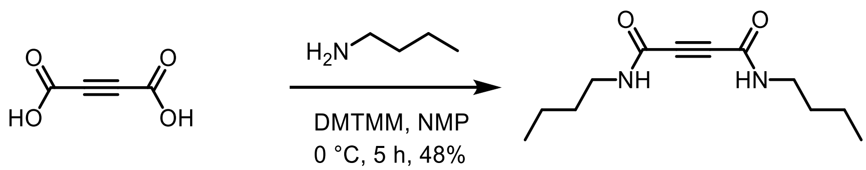

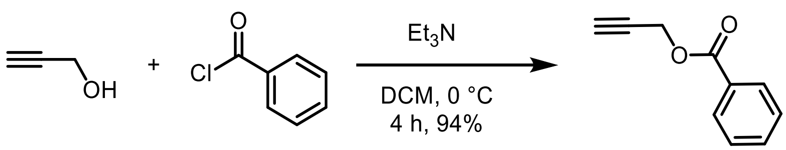

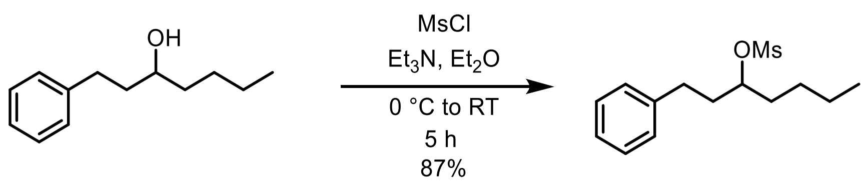

3. Rezende, T. C.; Abreu, C. M. R.; Fonseca, A. C.; Higa, C. M.; **Li, L.**; Serra, A. C.; Braslau, R.; Coelho, J. F. J. *Polymer* **2020**, *196*, 122473. Efficient Internal Plasticization of Poly(Vinyl Chloride) via Free Radical Copolymerization of Vinyl Chloride with an Acrylate Bearing a Triazole Phthalate Mimic. I synthesized an azide which I then converted to a triazole phthalate mimic, bearing a primary alcohol. This alcohol was sent to our collaborators in Portugal, where it was appended to an acrylate monomer, and then co-polymerized with vinyl chloride.

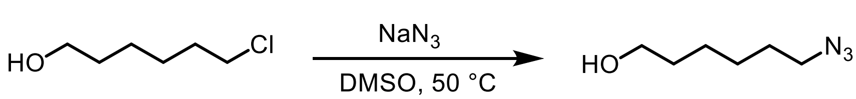

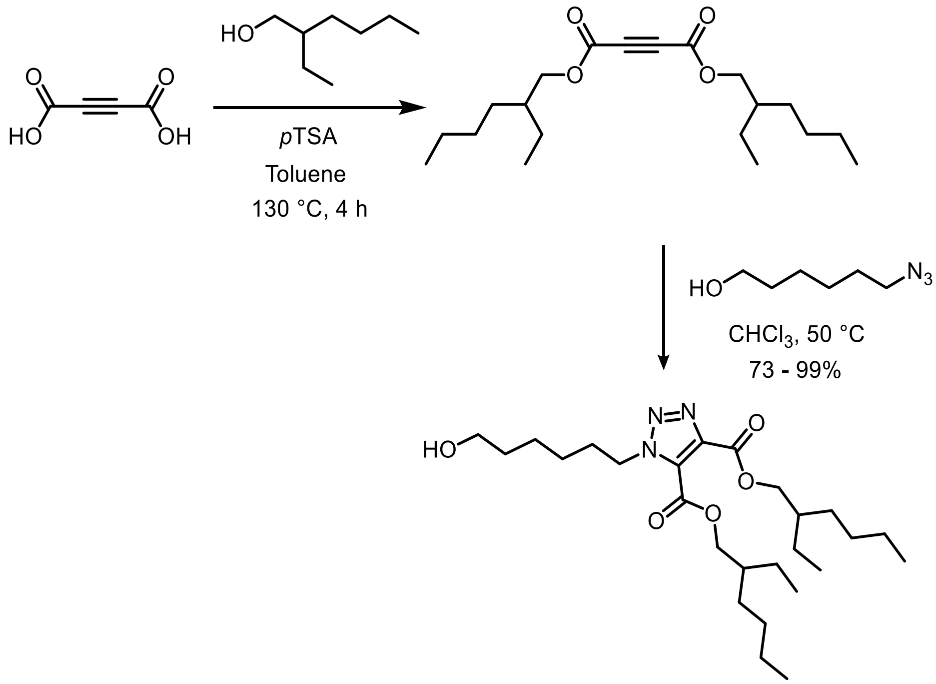
HO
pTSA
Toluene
130 °C, 4 h
HO
N3
CHCl3, 50 °C
73 - 99%

Appendix

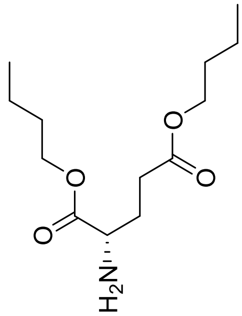

2.1a

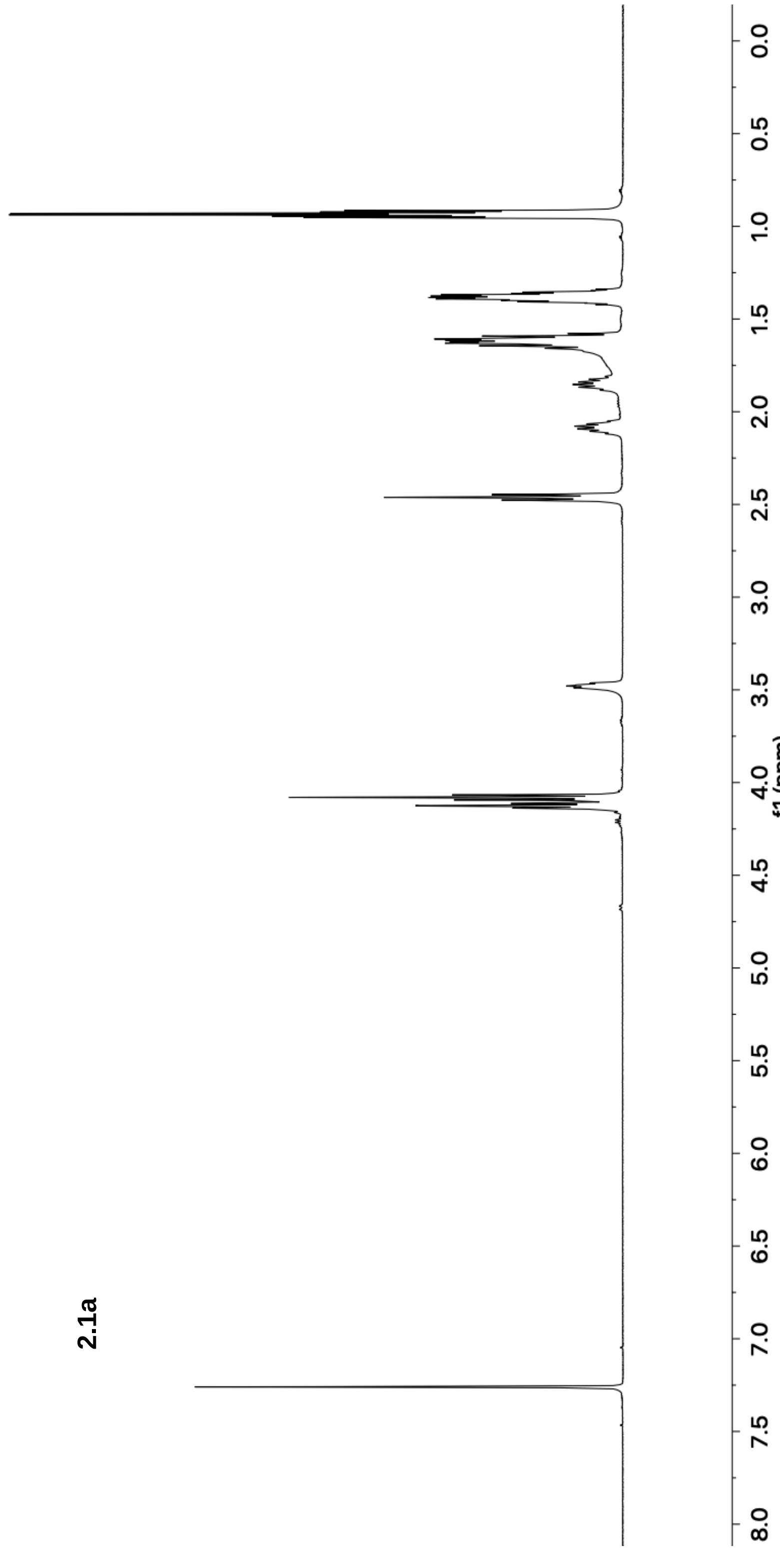

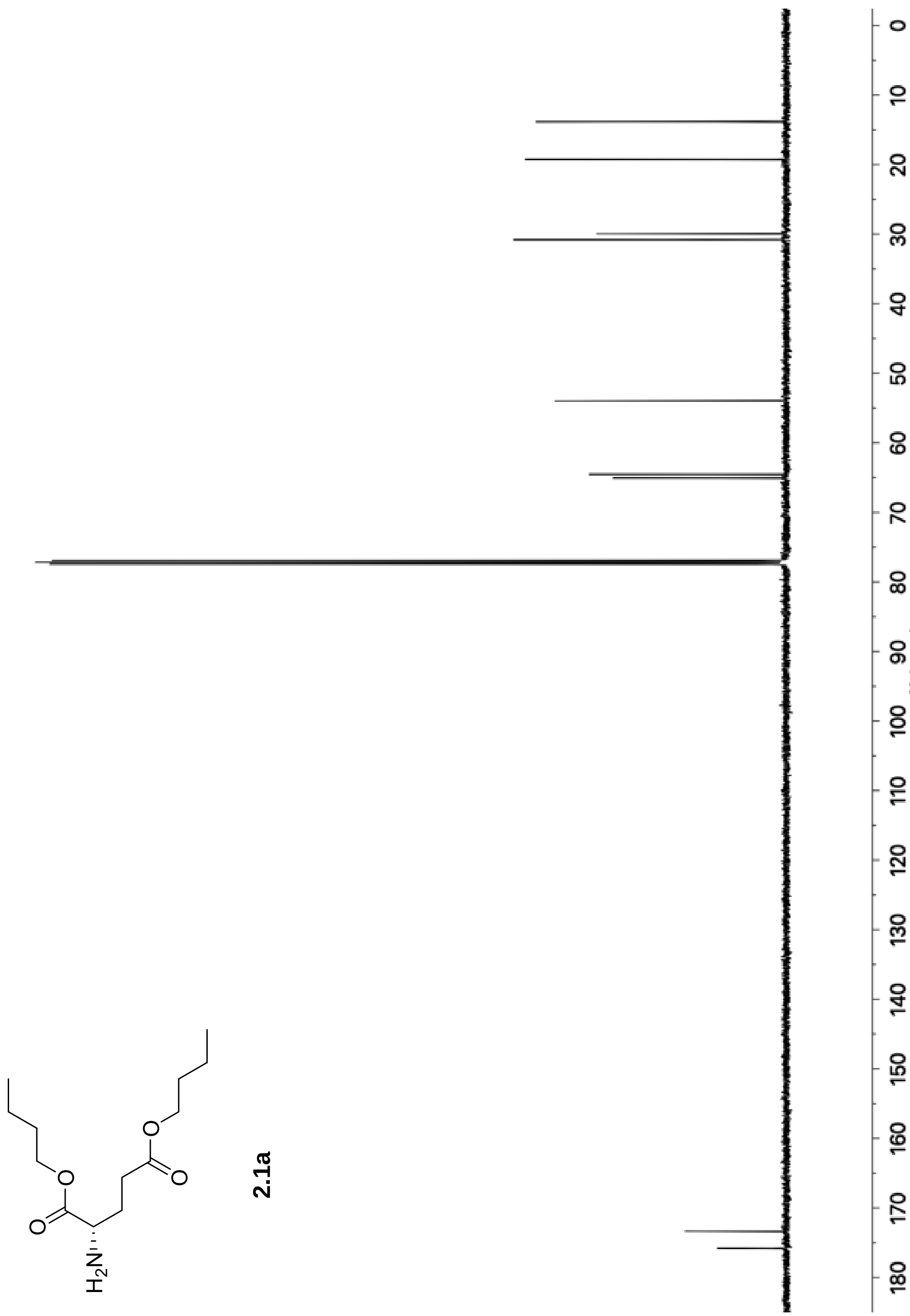
H2N
O
O
O
O
f1 (ppm)
0
10
20
30
40
50
60
70
80
90
100
110
120
130
140
150
160
170
180

2.1a

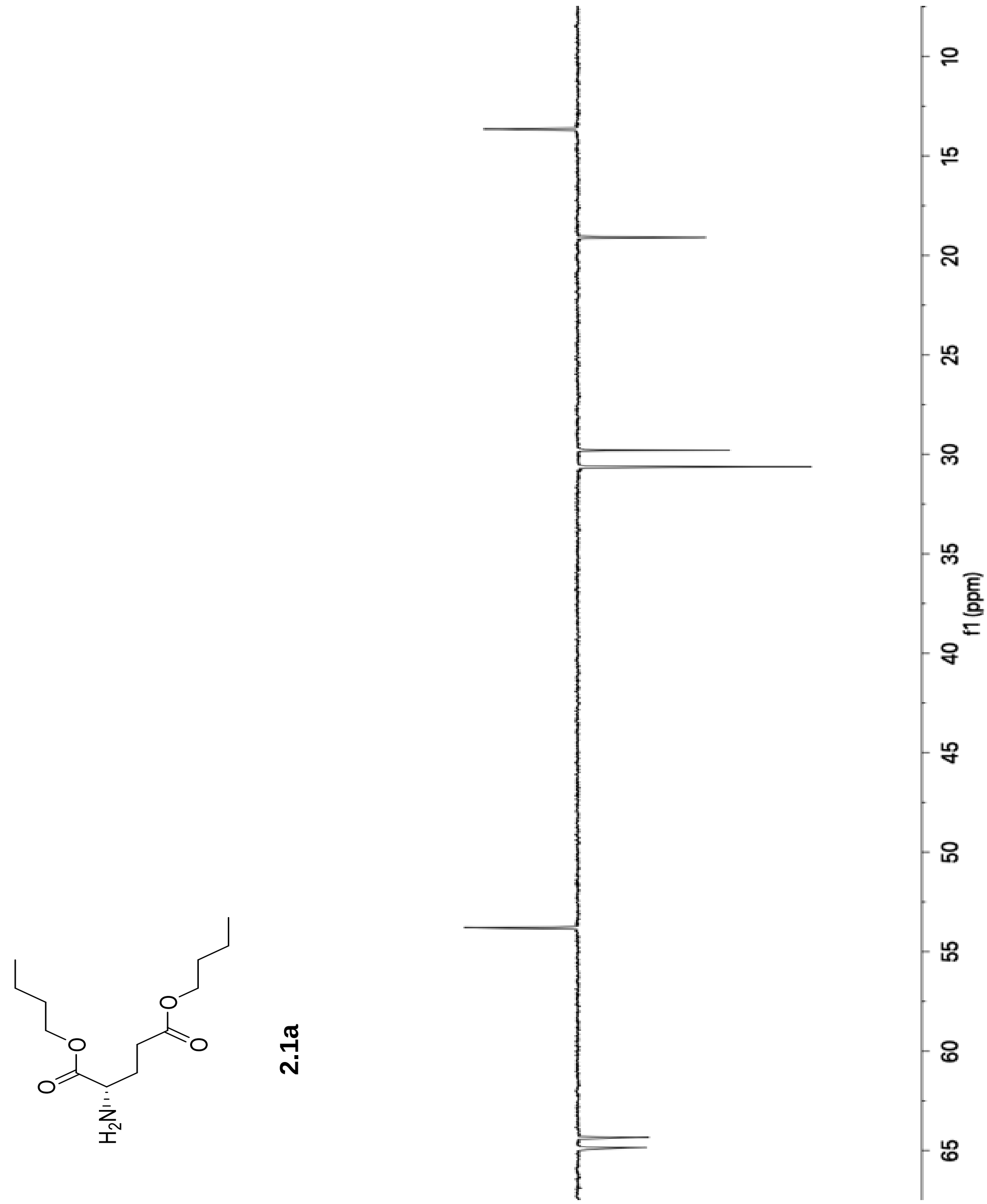
2.1a
H_2N
O
10
15
20
25
30
35
40
45
50
55
60
65
f1 (ppm)

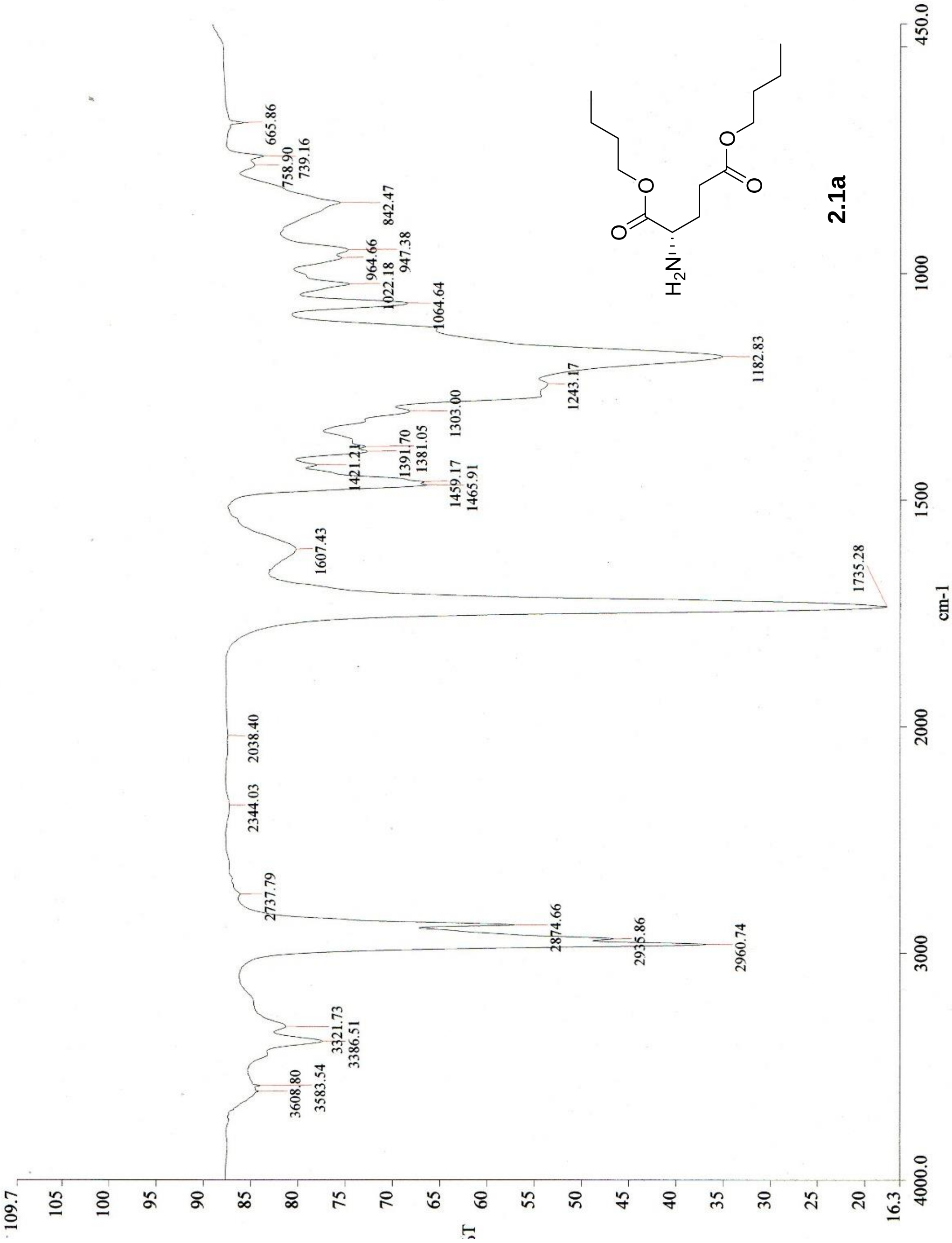

2.1a
H2N
cm-1
%T
4000.0
3000
2000
1500
1000
450.0
109.7
16.3
3608.80
3583.54
3321.73
3386.51
2960.74
2935.86
2874.66
2737.79
2344.03
2038.40
1735.28
1607.43
1465.91
1459.17
1421.21
1391.70
1381.05
1303.00
1243.17
1182.83
1064.64
1022.18
964.66
947.38
842.47
758.90
739.16
665.86

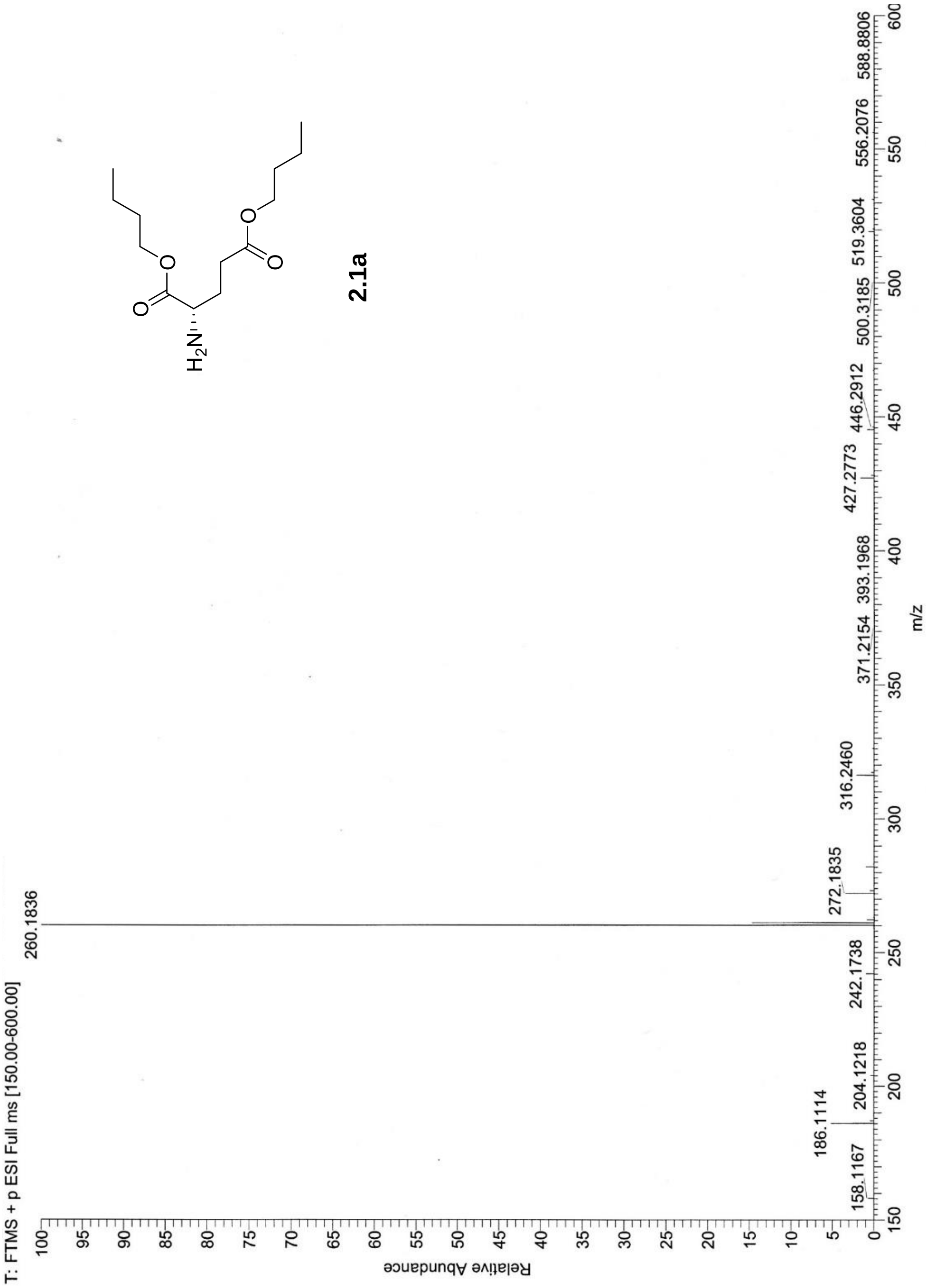
T: FTMS + p ESI Full ms [150.00-600.00]
Relative Abundance
m/z
260.1836
272.1835
316.2460
371.2154
393.1968
427.2773
446.2912
500.3185
519.3604
556.2076
588.8806
242.1738
204.1218
186.1114
158.1167
H2N
O
2.1a

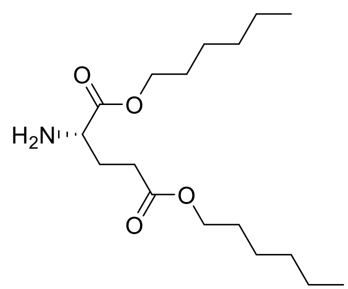

2.1b

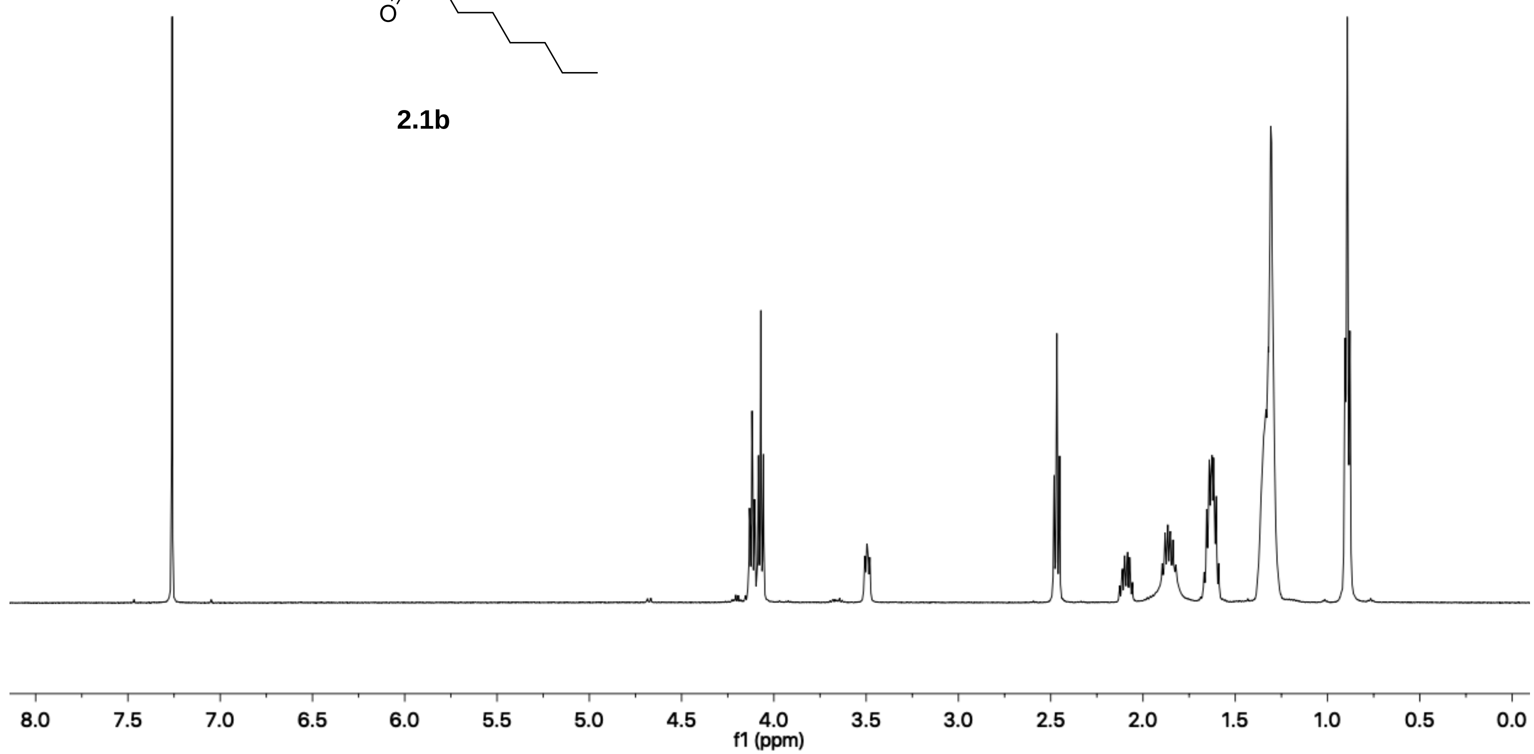

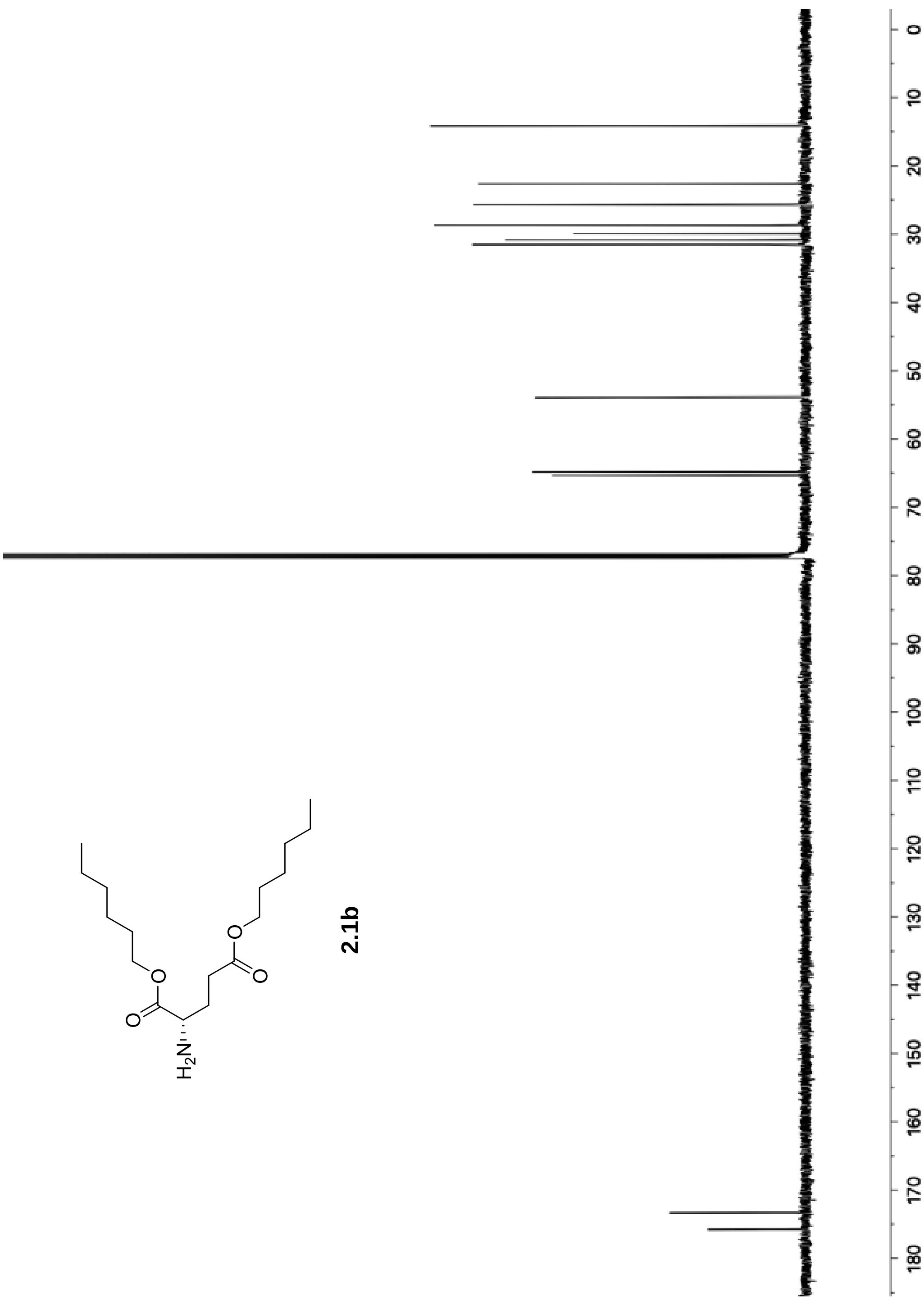
H2N
O
O
O
O
2.1b
f1 (ppm)
0
10
20
30
40
50
60
70
80
90
100
110
120
130
140
150
160
170
180

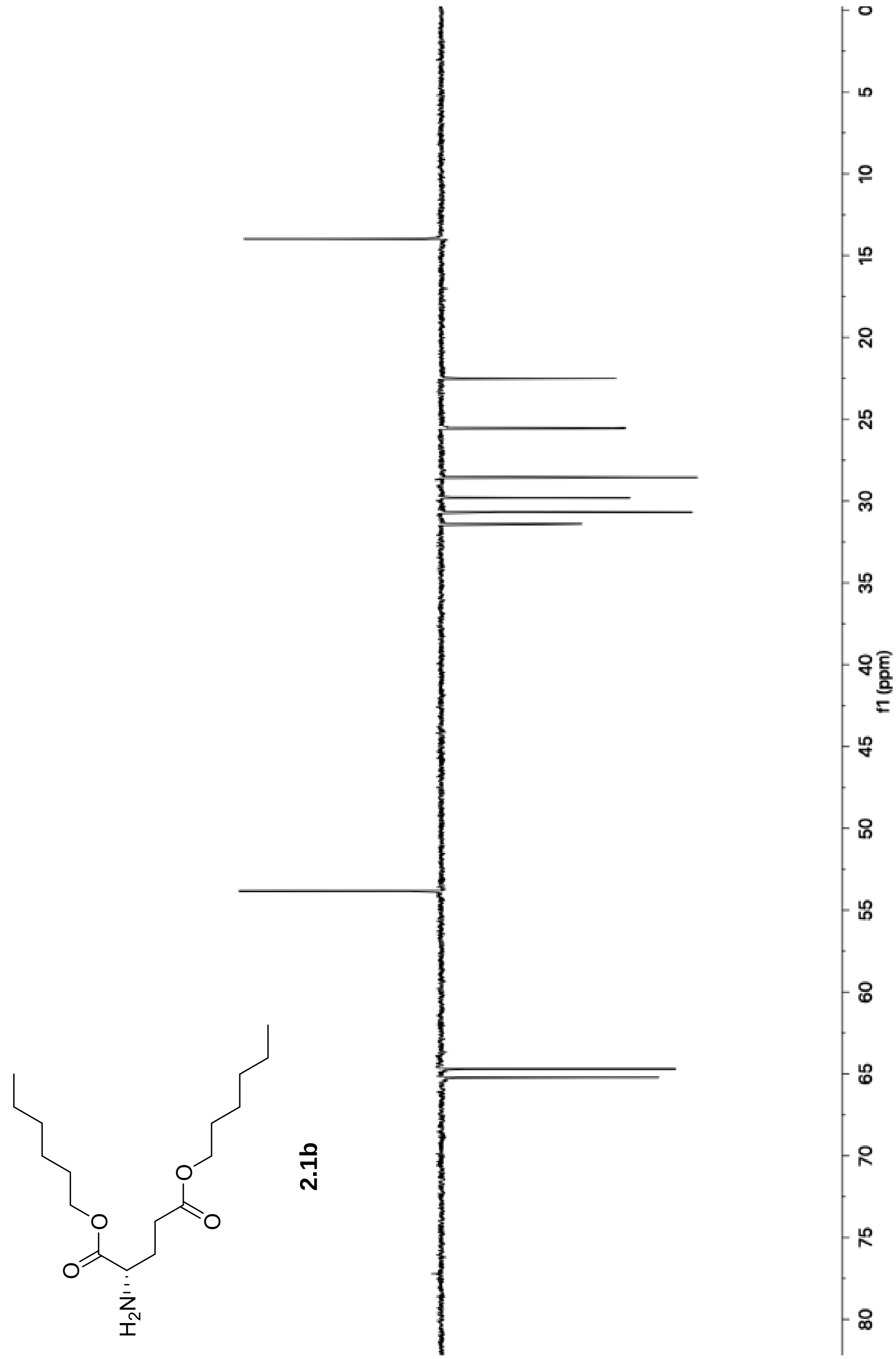

2.1b
f1 (ppm)

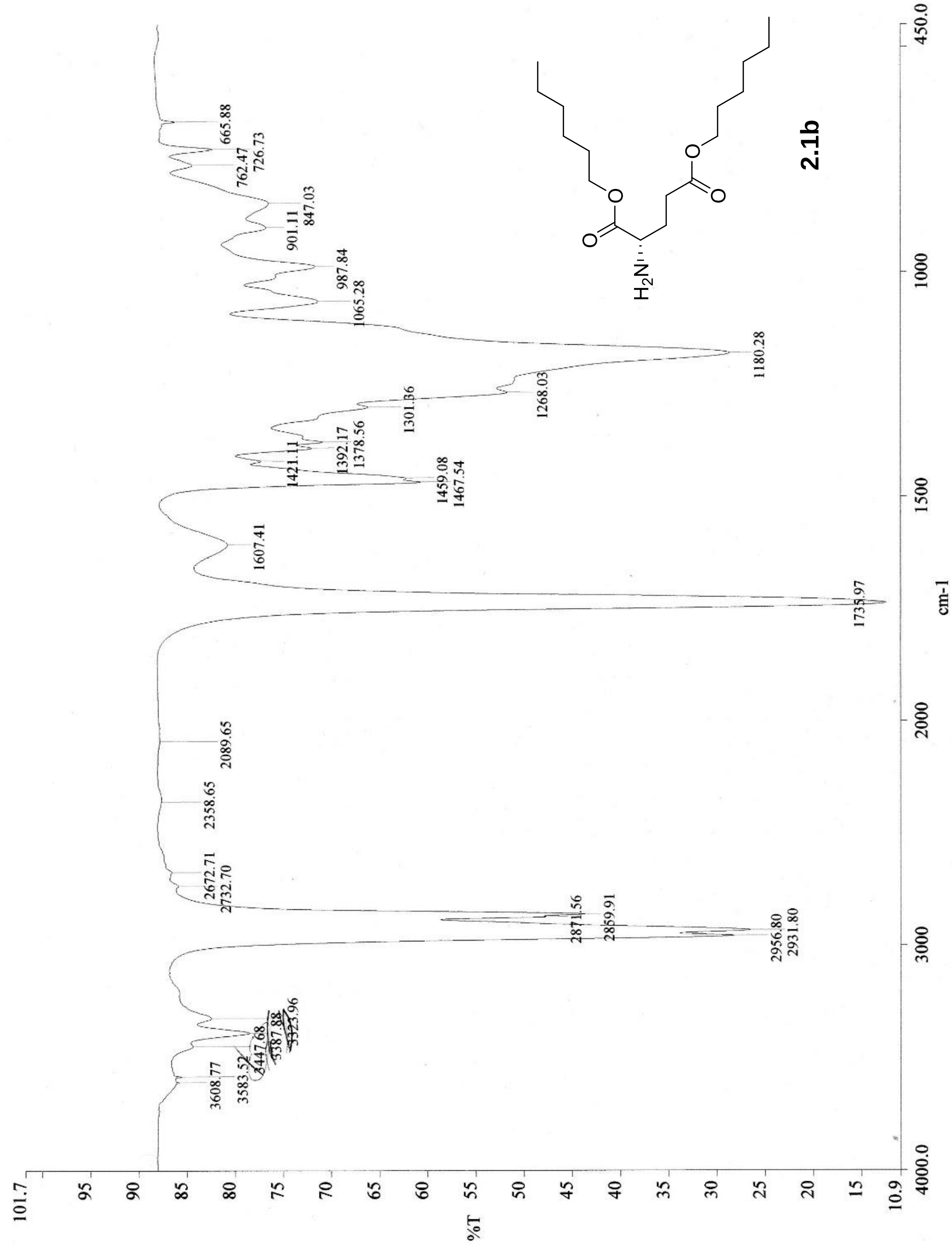

%T
cm-1
2.1b
H2N
3608.77
3583.52
3447.68
3387.88
3323.96
2956.80
2931.80
2871.56
2859.91
2732.70
2672.71
2358.65
2089.65
1735.97
1607.41
1467.54
1459.08
1421.11
1392.17
1378.56
1301.36
1268.03
1180.28
1065.28
987.84
901.11
847.03
762.47
726.73
665.88

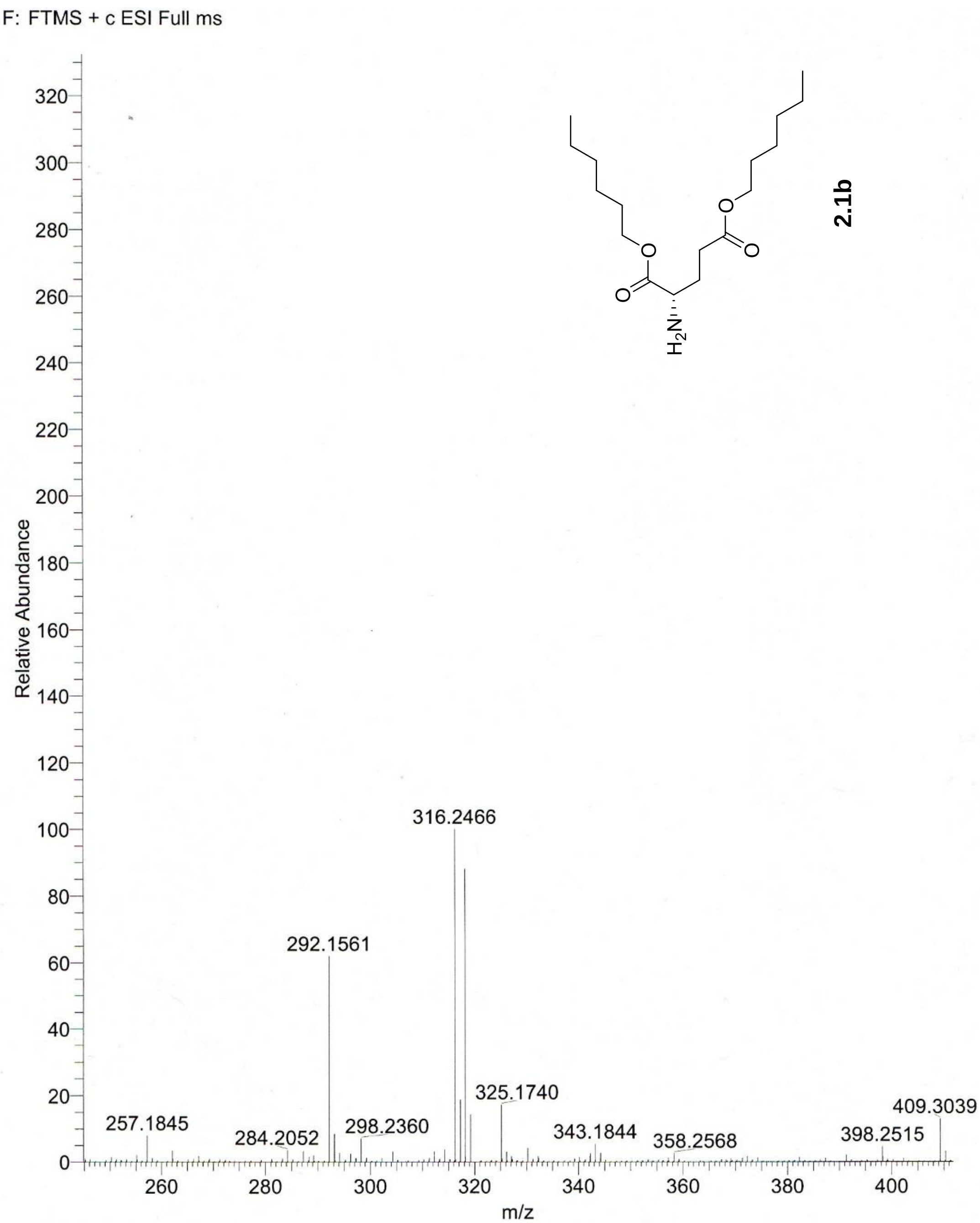
F: FTMS + c ESI Full ms
Relative Abundance
m/z
316.2466
292.1561
325.1740
409.3039
257.1845
284.2052
298.2360
343.1844
358.2568
398.2515
H2N

2.1b

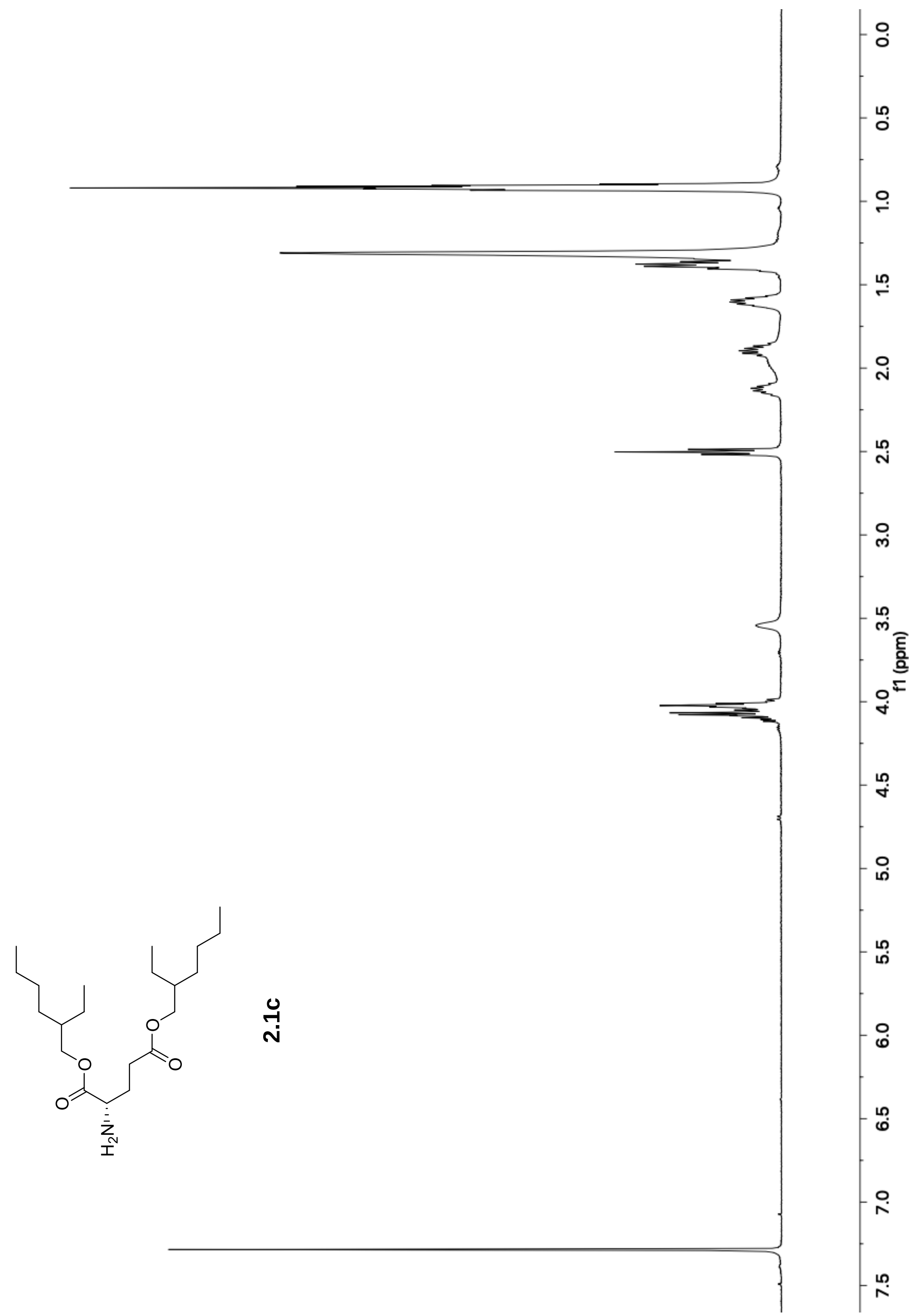
2.1c
H2N
O
0.0
0.5
1.0
1.5
2.0
2.5
3.0
3.5
4.0
4.5
5.0
5.5
6.0
6.5
7.0
7.5
f1 (ppm)

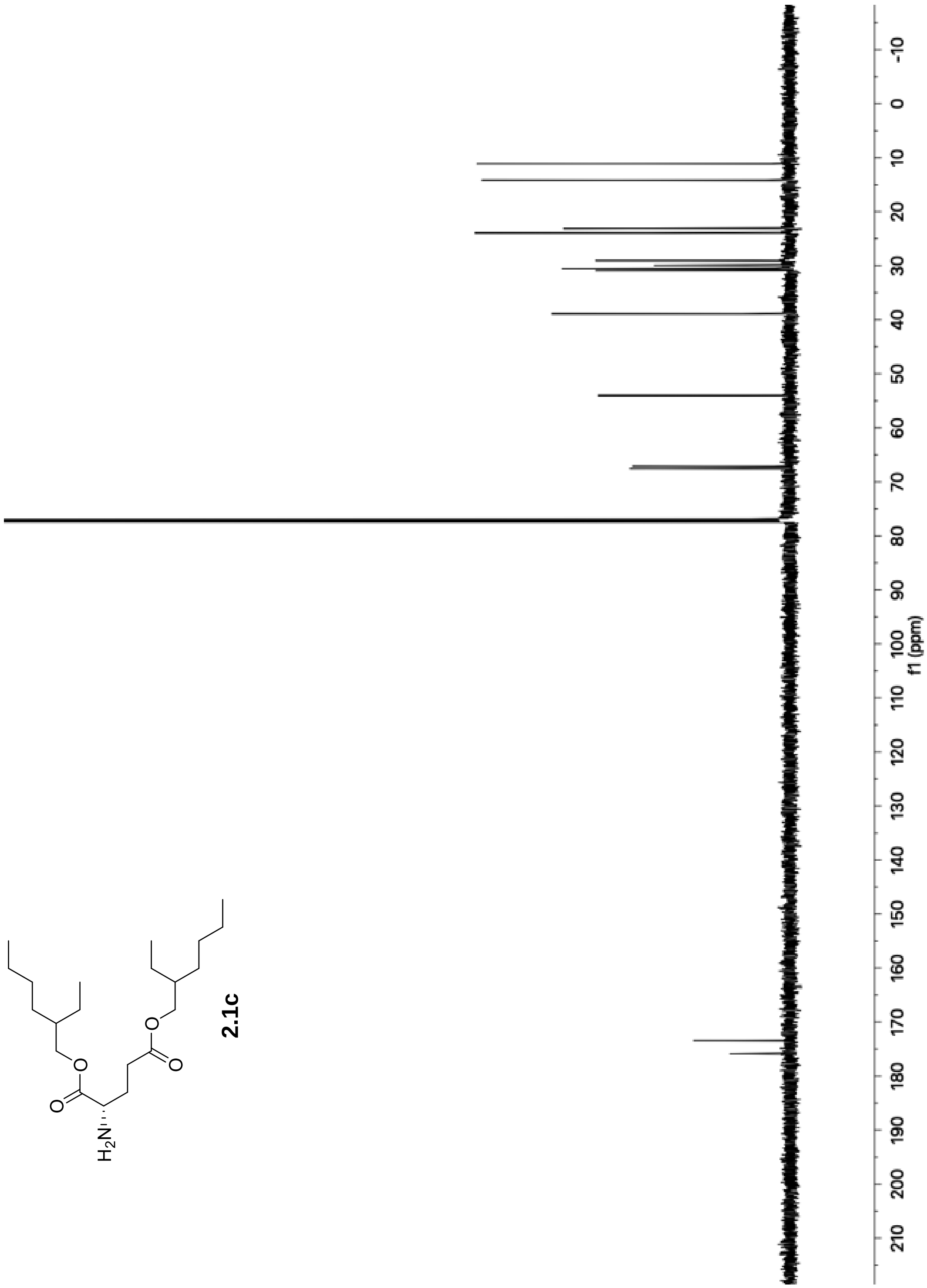

2.1c

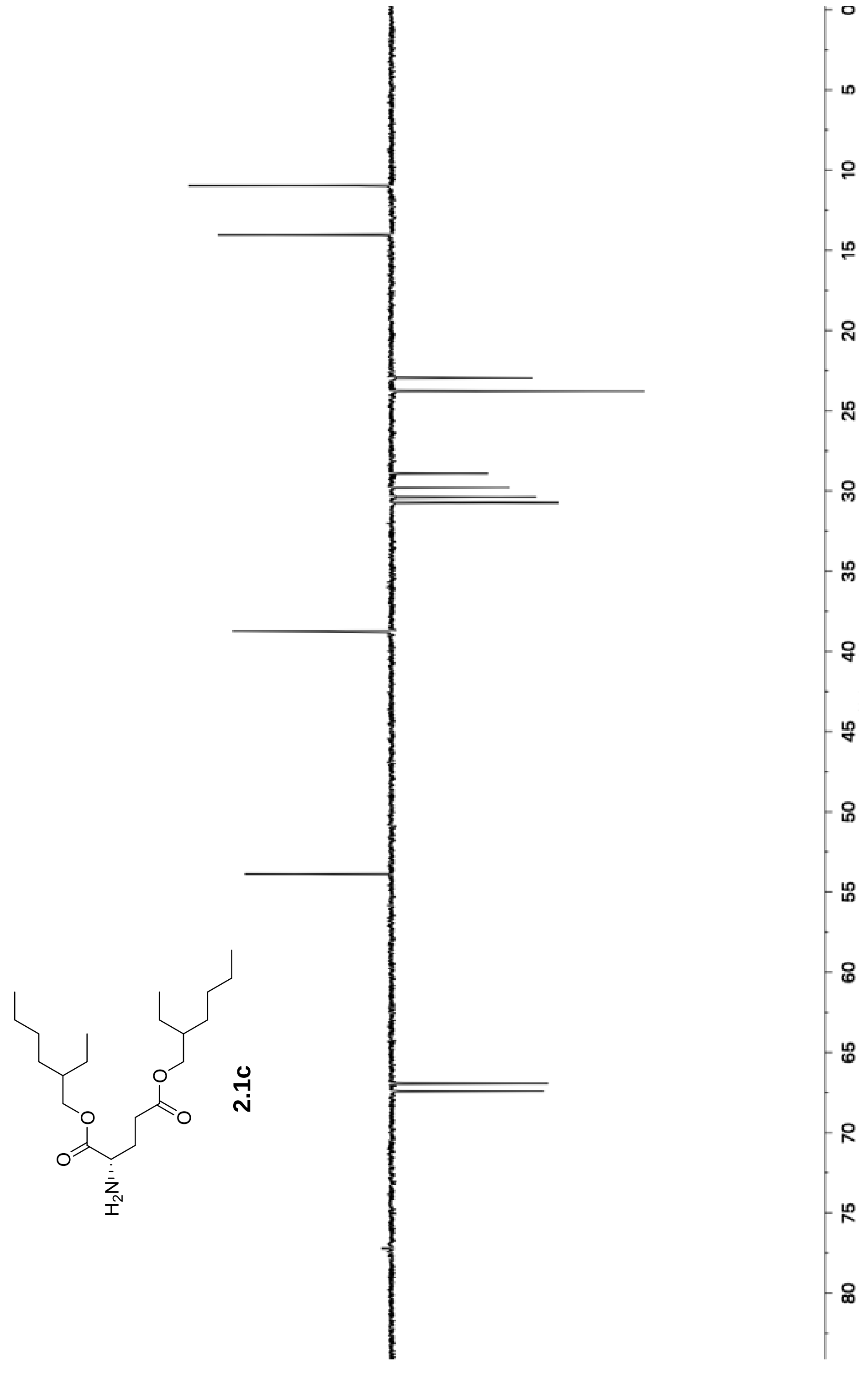
2.1c
f1 (ppm)
0
5
10
15
20
25
30
35
40
45
50
55
60
65
70
75
80

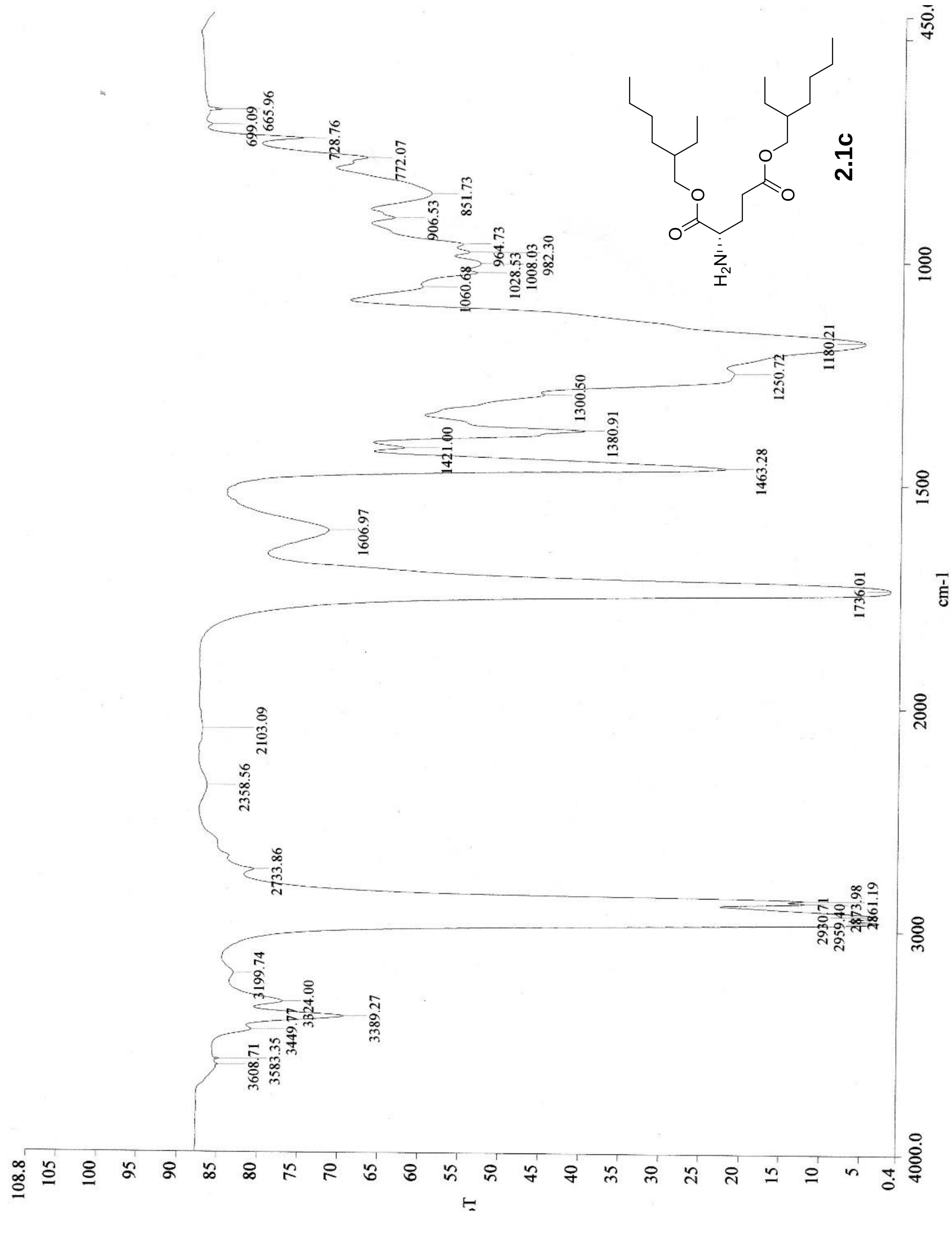
2.1c
cm-1
%T

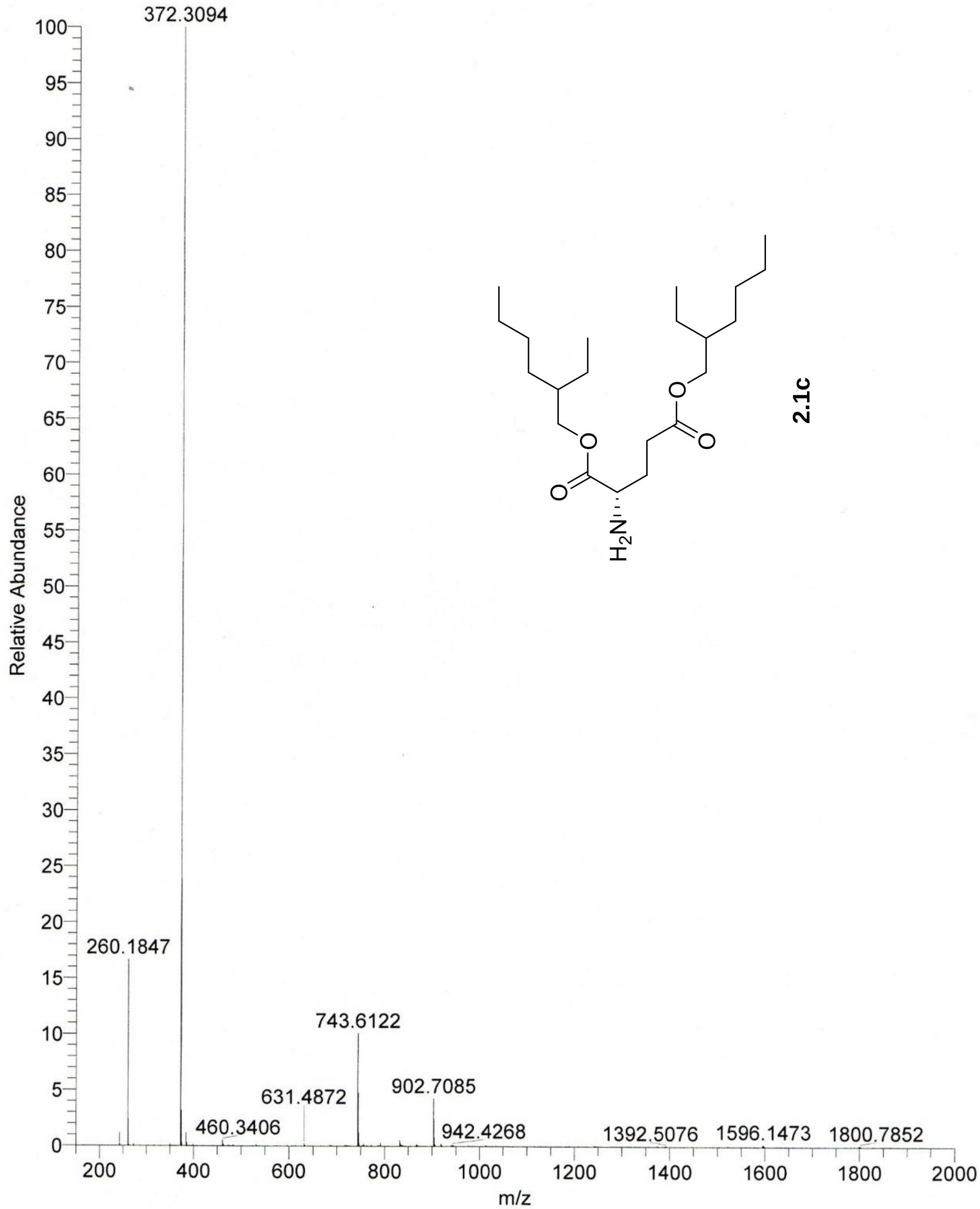
372.3094
260.1847
743.6122
631.4872
902.7085
460.3406
942.4268
1392.5076
1596.1473
1800.7852
Relative Abundance
m/z
H_2N
O

2.1c

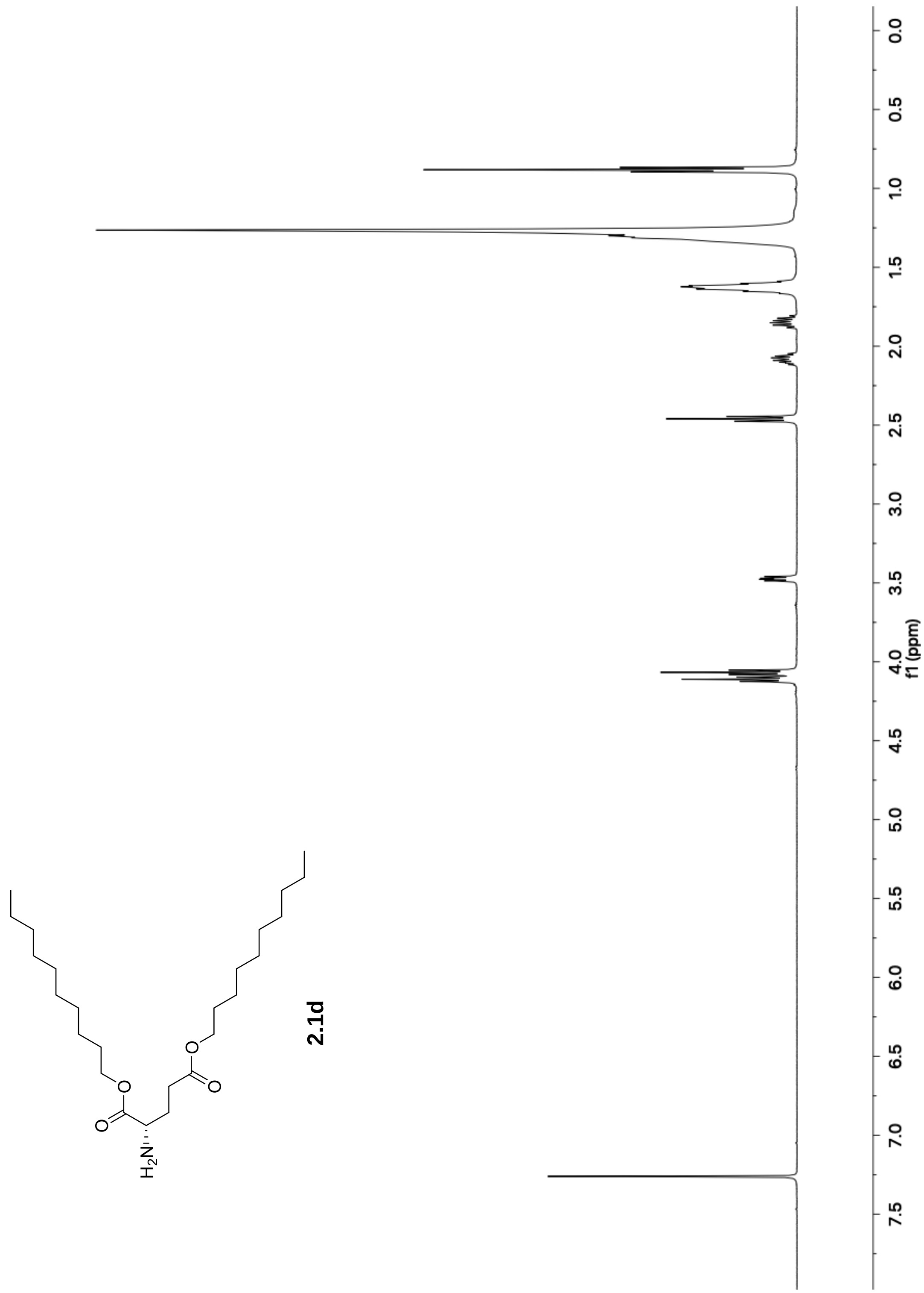

2.1d

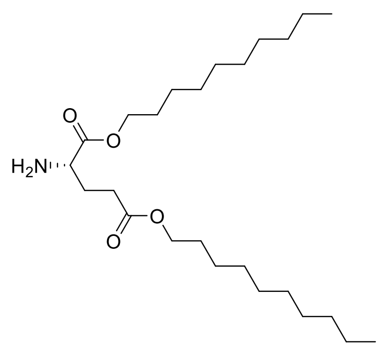

O
O
H$_2$N
O
O

2.1d

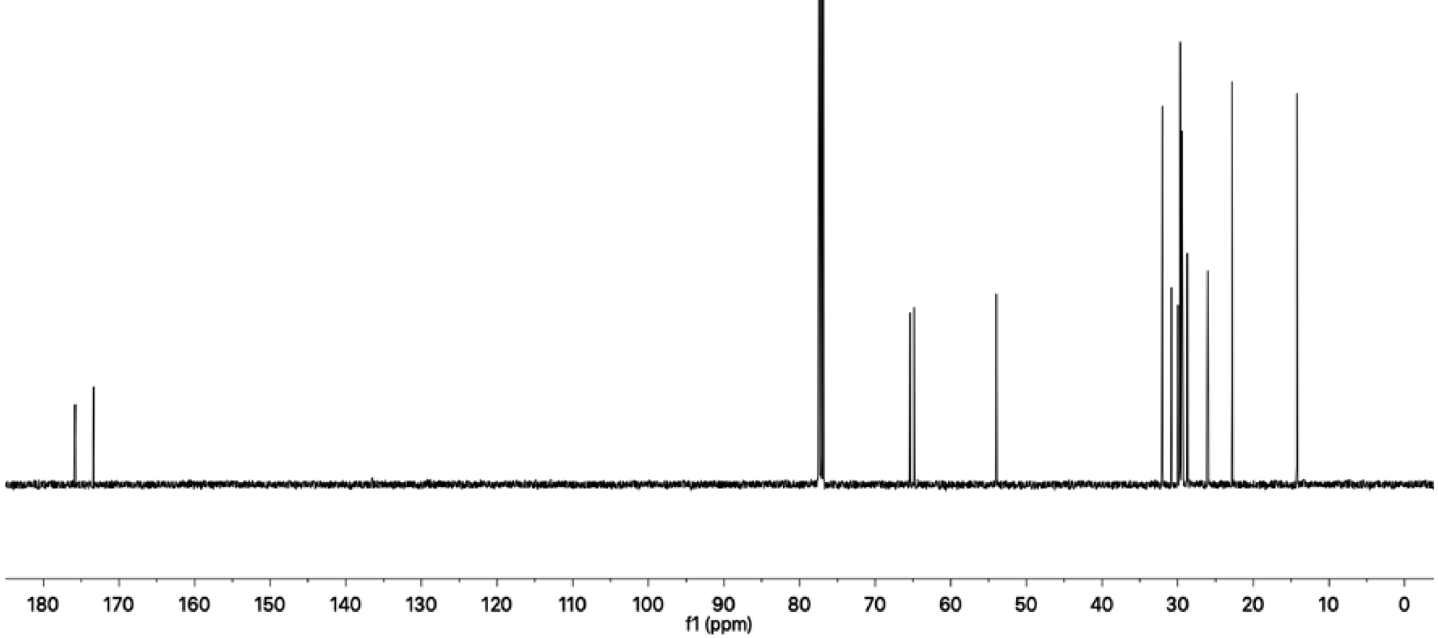

180 170 160 150 140 130 120 110 100 90 80 70 60 50 40 30 20 10 0
f1 (ppm)

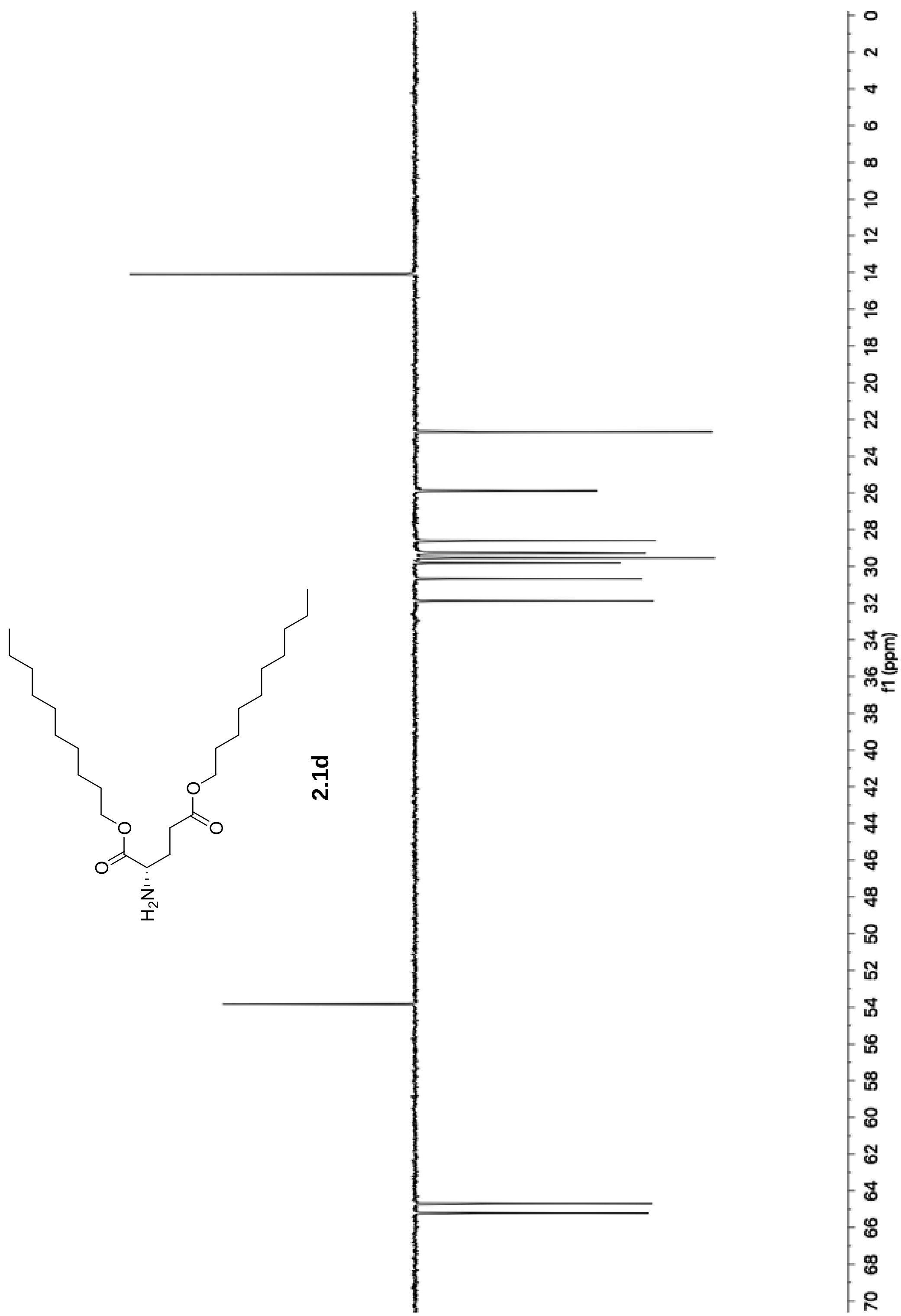

H2N
O
f1 (ppm)
0 2 4 6 8 10 12 14 16 18 20 22 24 26 28 30 32 34 36 38 40 42 44 46 48 50 52 54 56 58 60 62 64 66 68 70

2.1d

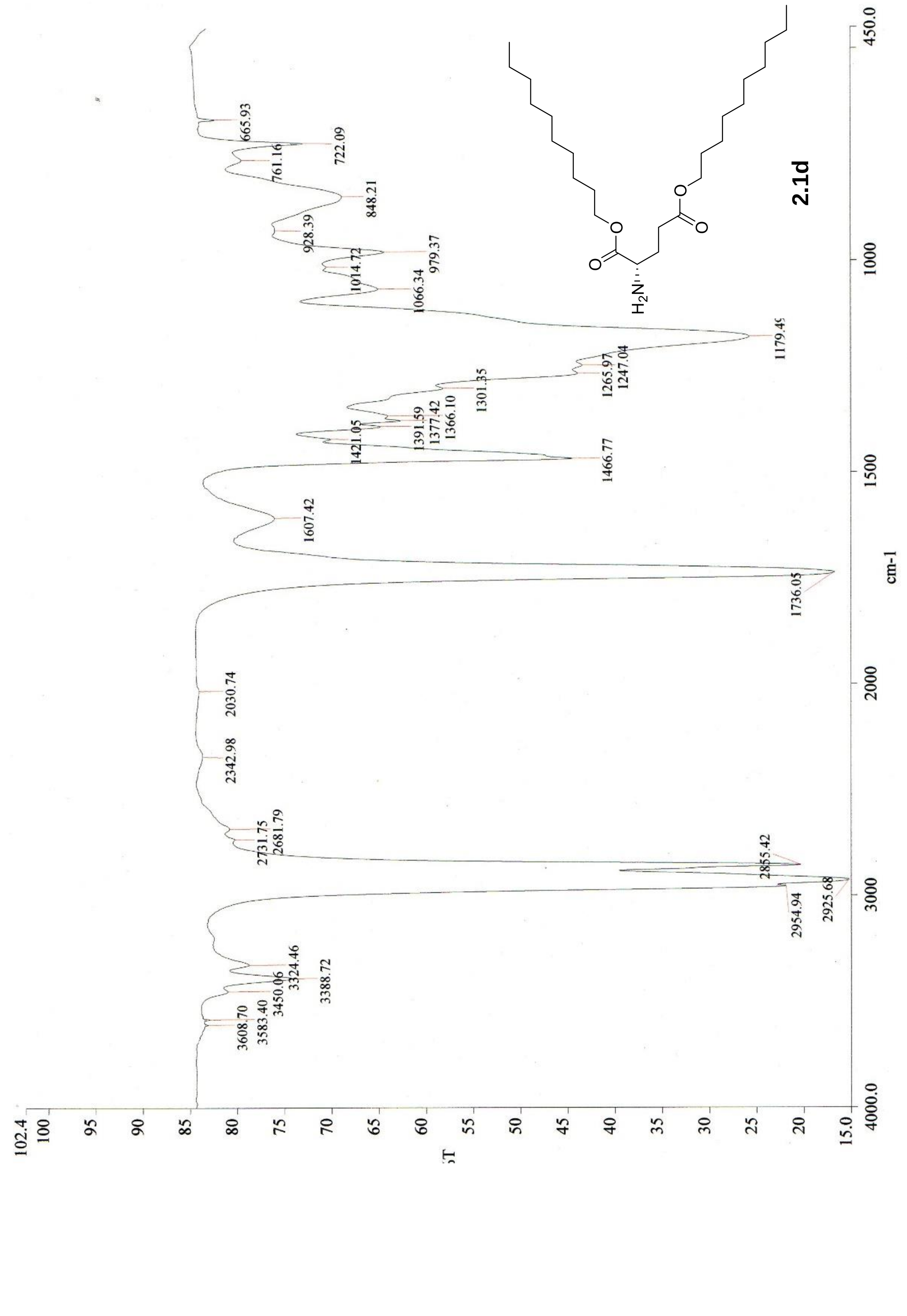

2.1d
H2N
O
cm-1
665.93
722.09
761.16
848.21
928.39
979.37
1014.72
1066.34
1247.04
1265.97
1301.35
1366.10
1377.42
1391.59
1421.05
1466.77
1607.42
1736.05
2030.74
2342.98
2681.79
2731.75
2855.42
2925.68
2954.94
3324.46
3388.72
3450.06
3583.40
3608.70

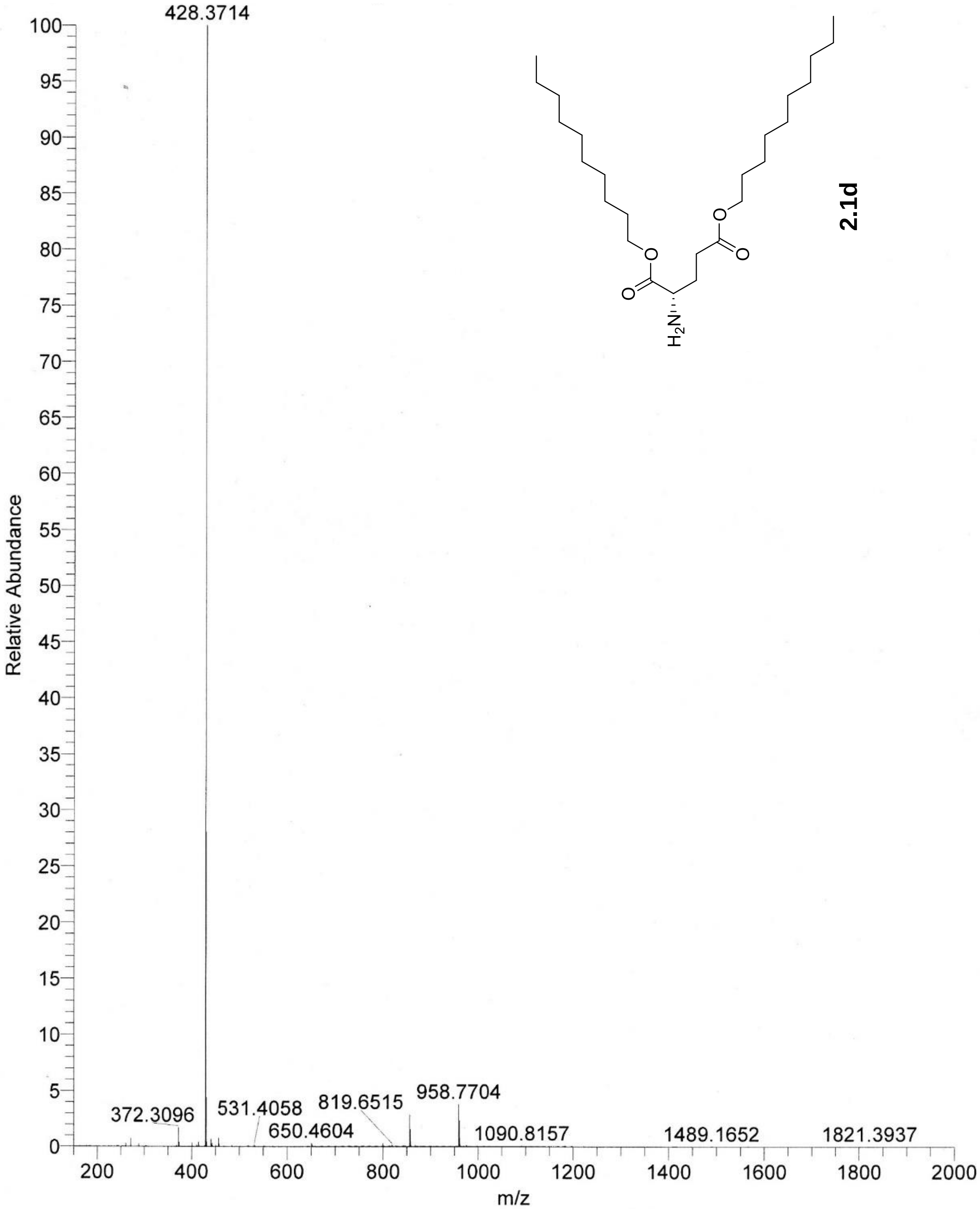
428.3714
372.3096
531.4058
650.4604
819.6515
958.7704
1090.8157
1489.1652
1821.3937
Relative Abundance
m/z
H2N
O
2.1d

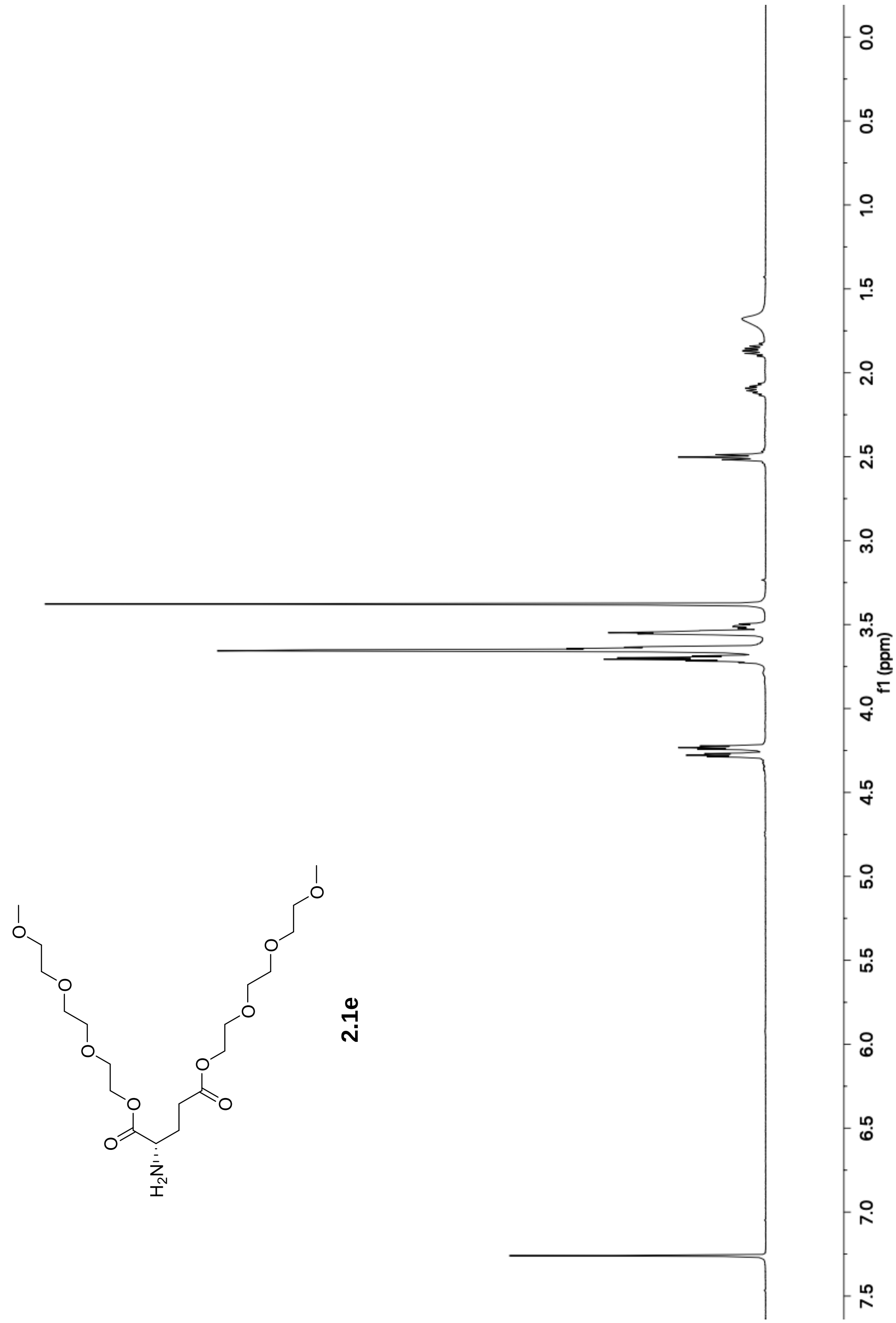

2.1e
H_2N
f1 (ppm)

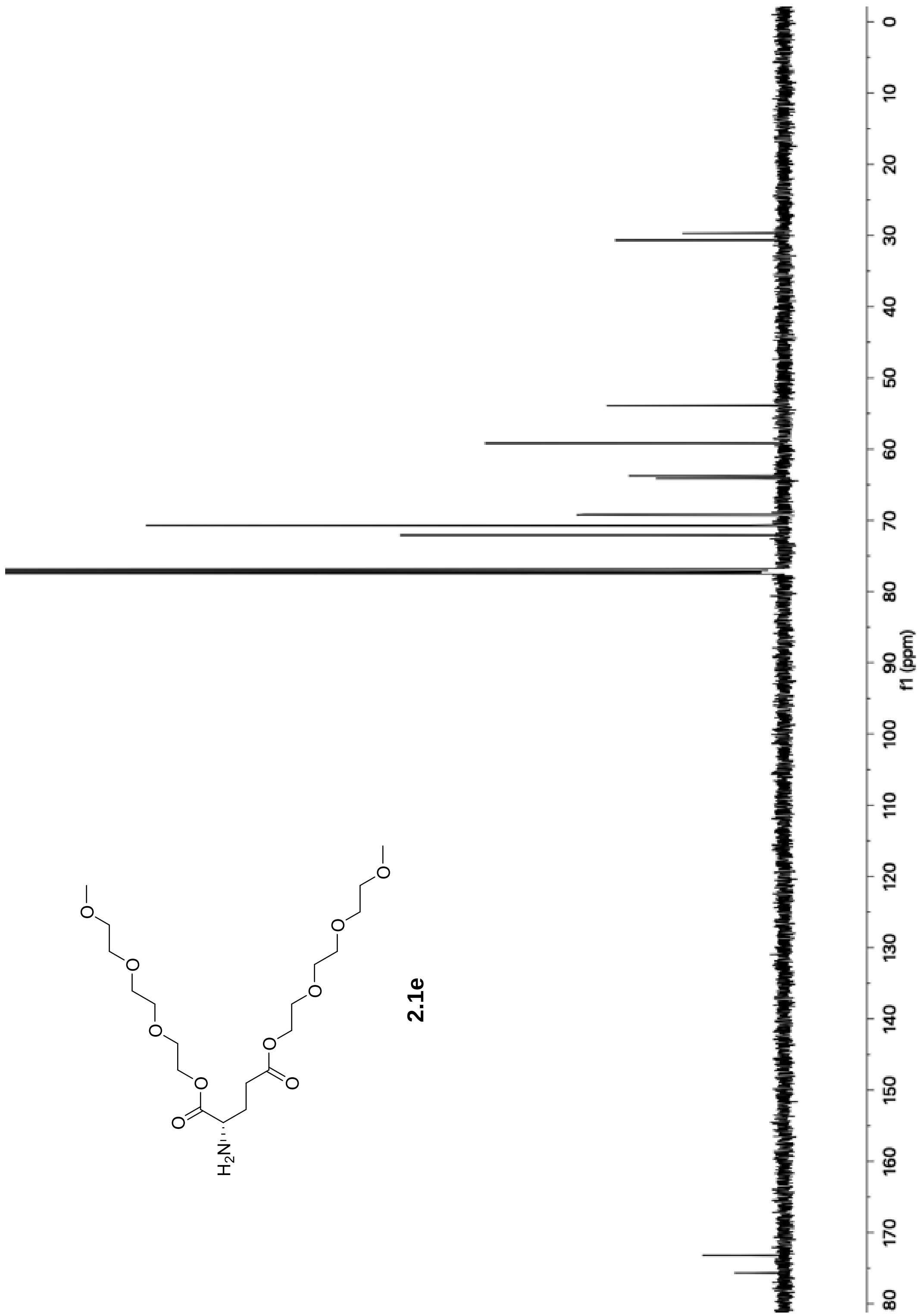

2.1e
f1 (ppm)

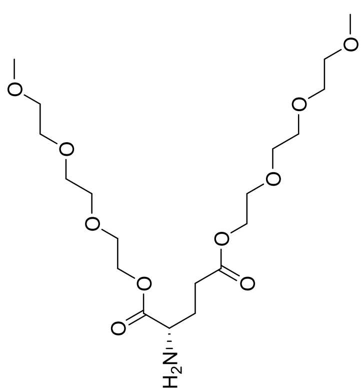

2.1e

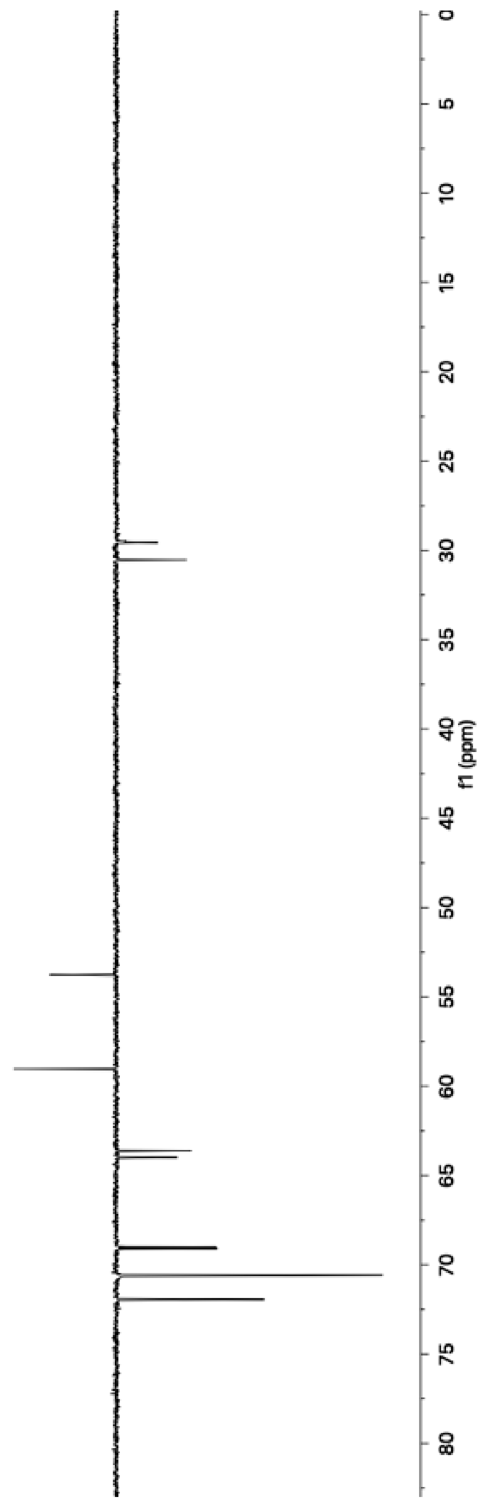

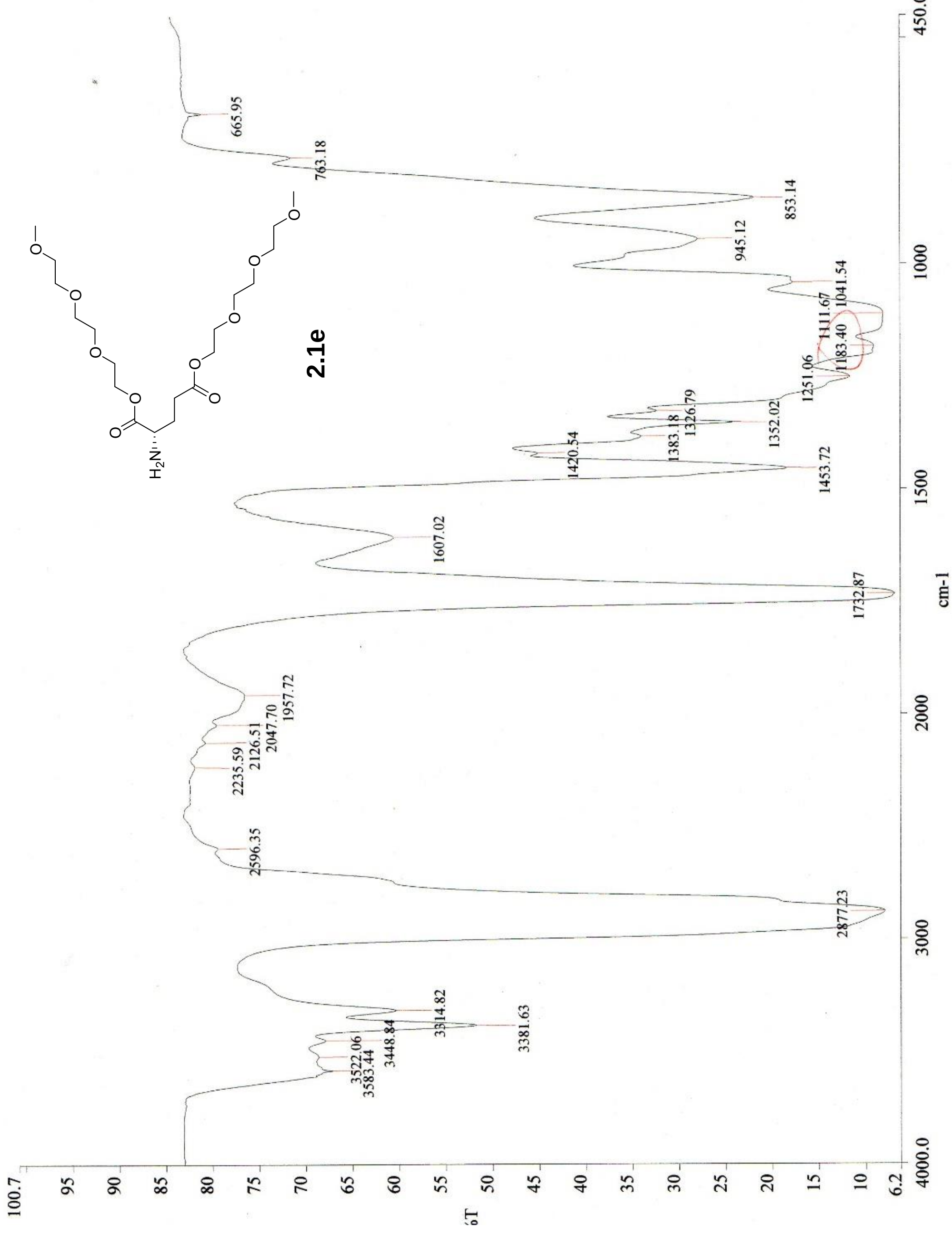

%T
cm-1
4000.0
3000
2000
1500
1000
450.0
3583.44
3522.06
3448.84
3381.63
3314.82
2877.23
2596.35
2235.59
2126.51
2047.70
1957.72
1732.87
1607.02
1453.72
1420.54
1383.18
1352.02
1326.79
1251.06
1183.40
1111.67
1041.54
945.12
853.14
763.18
665.95

2.1e

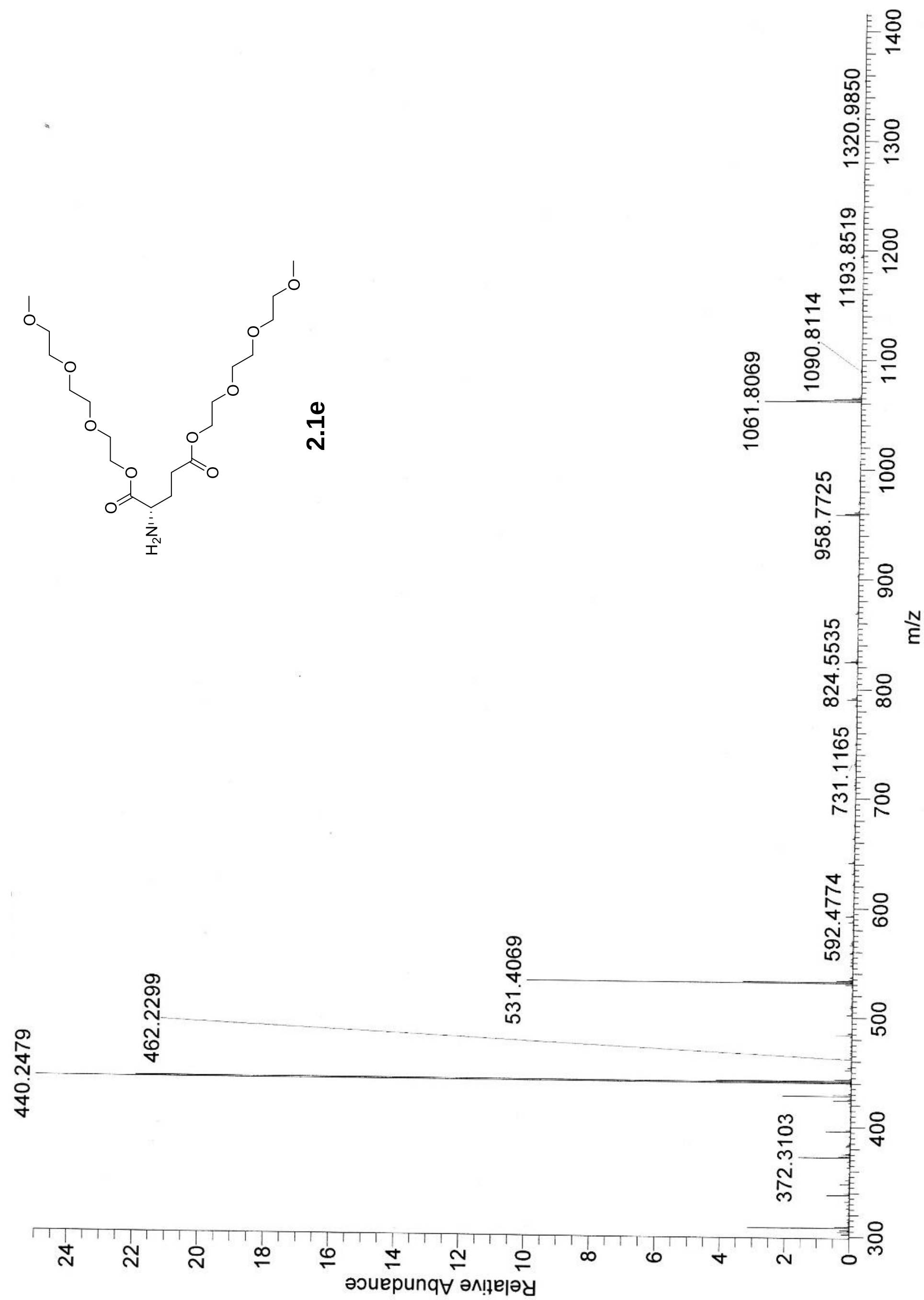
Relative Abundance
m/z
440.2479
462.2299
531.4069
372.3103
592.4774
731.1165
824.5535
958.7725
1061.8069
1090.8114
1193.8519
1320.9850
2.1e
H_2N

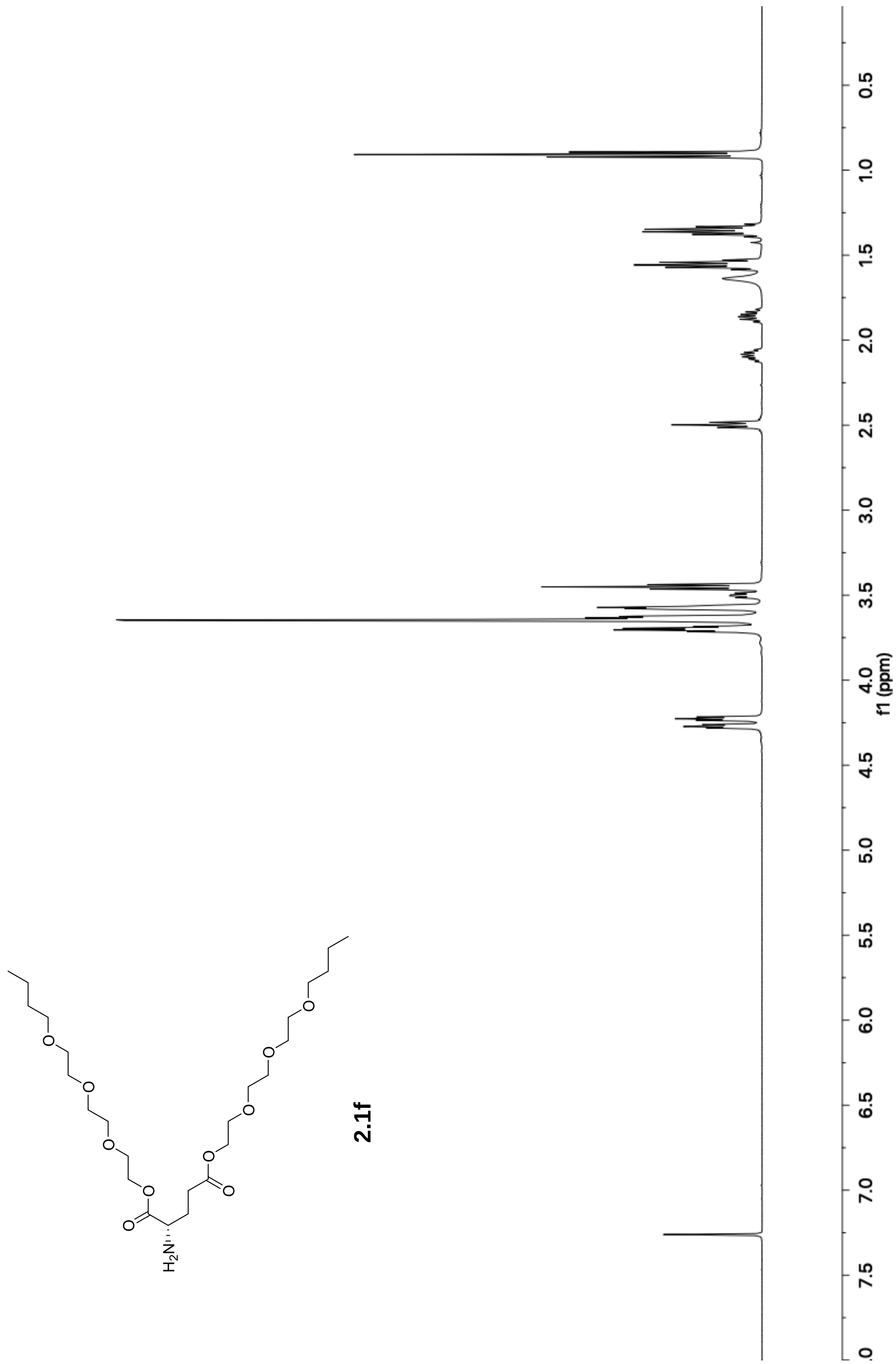

2.1f

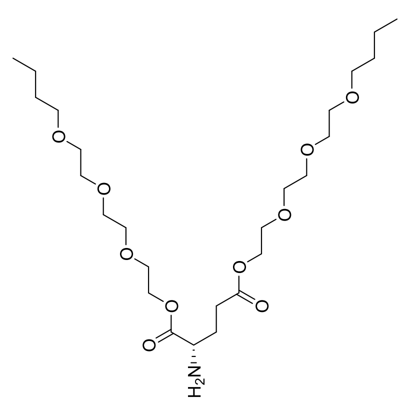

H2N
O

2.1f

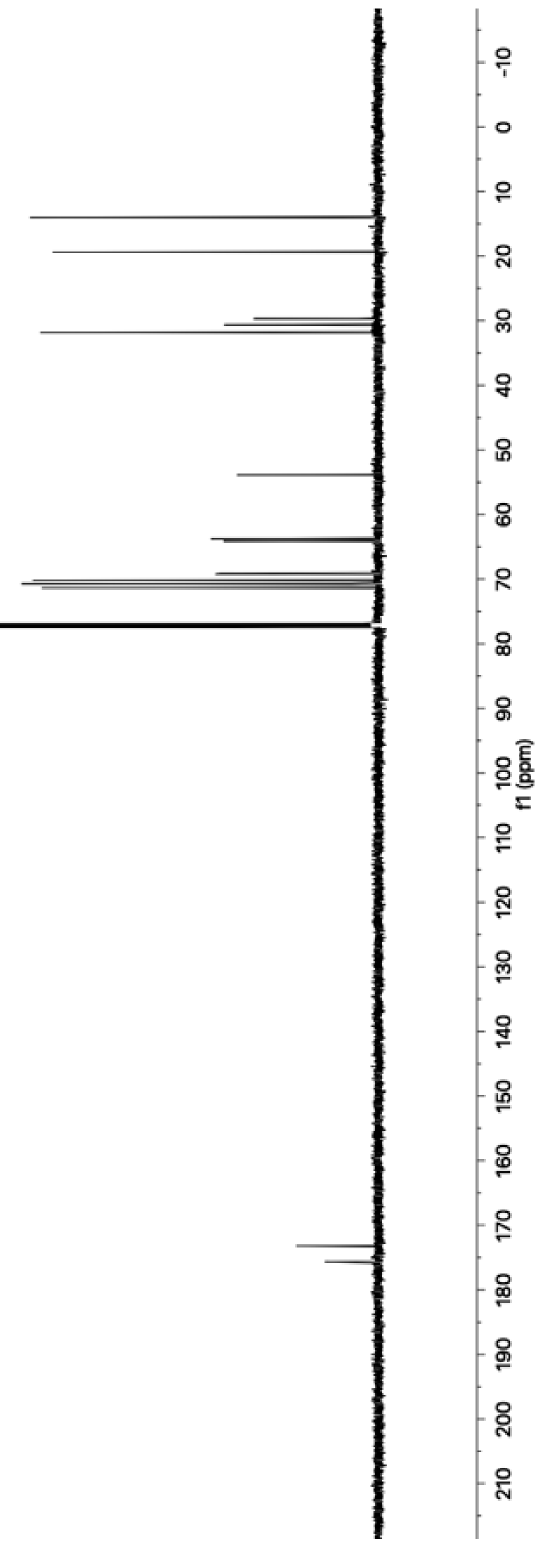

f1 (ppm)
210 200 190 180 170 160 150 140 130 120 110 100 90 80 70 60 50 40 30 20 10 0 -10

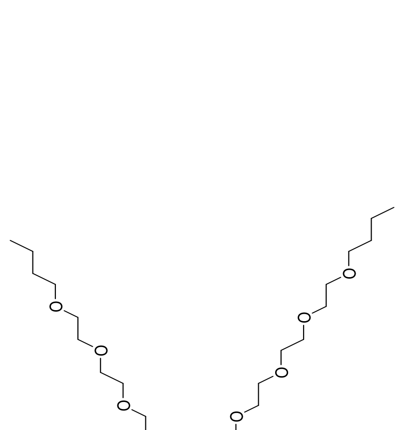

2.1f

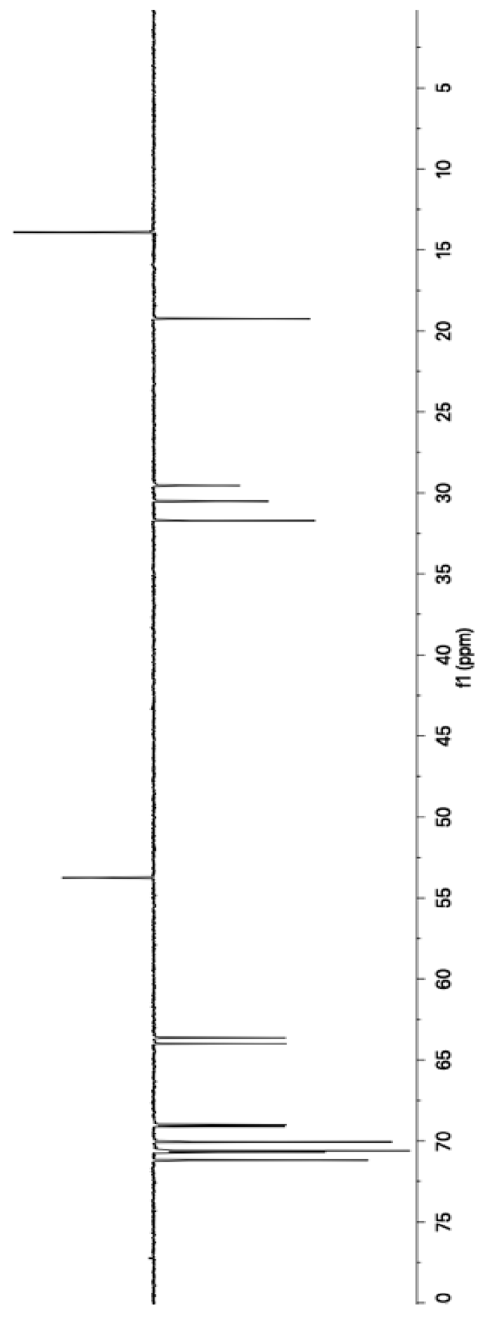

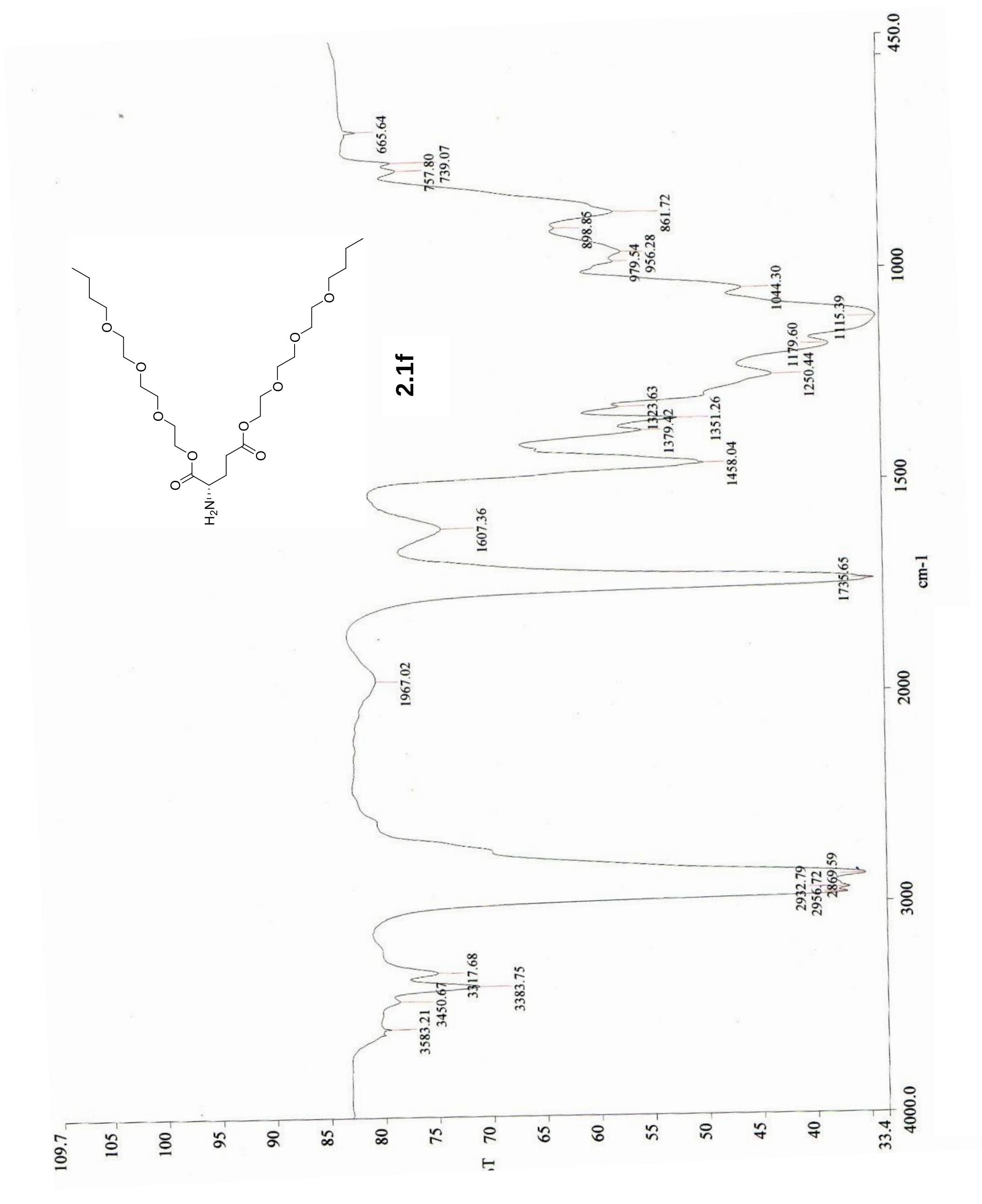

2.1f
cm-1
4000.0
3000
2000
1500
1000
450.0
109.7
105
100
95
90
85
80
75
70
65
60
55
50
45
40
33.4
3583.21
3450.67
3317.68
3383.75
2932.79
2956.72
2869.59
1967.02
1735.65
1607.36
1458.04
1379.42
1323.63
1351.26
1250.44
1179.60
1115.39
1044.30
979.54
956.28
898.85
861.72
757.80
739.07
665.64

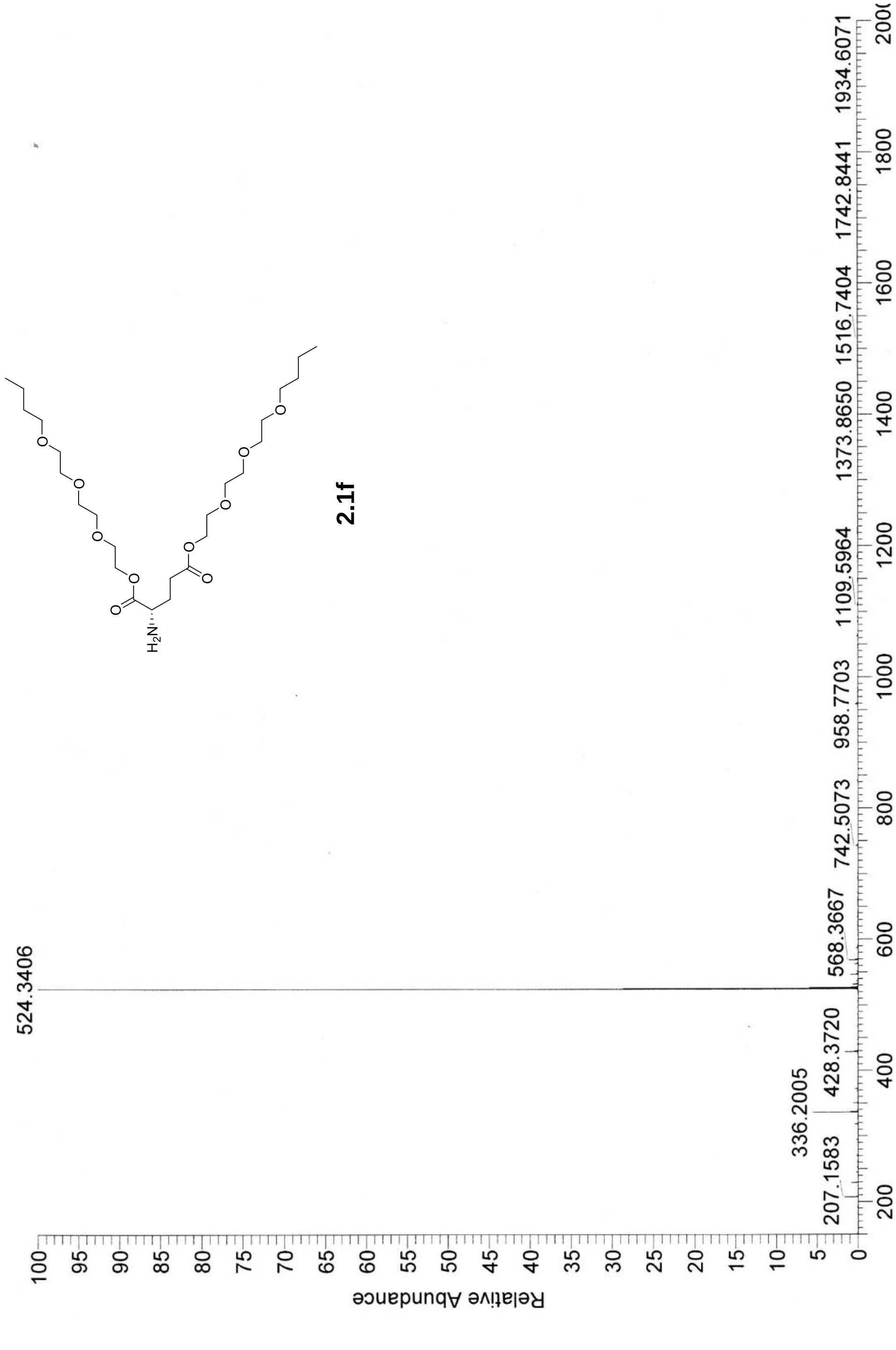
Relative Abundance
m/z
524.3406
207.1583
336.2005
428.3720
568.3667
742.5073
958.7703
1109.5964
1373.8650
1516.7404
1742.8441
1934.6071
H2N

2.1f

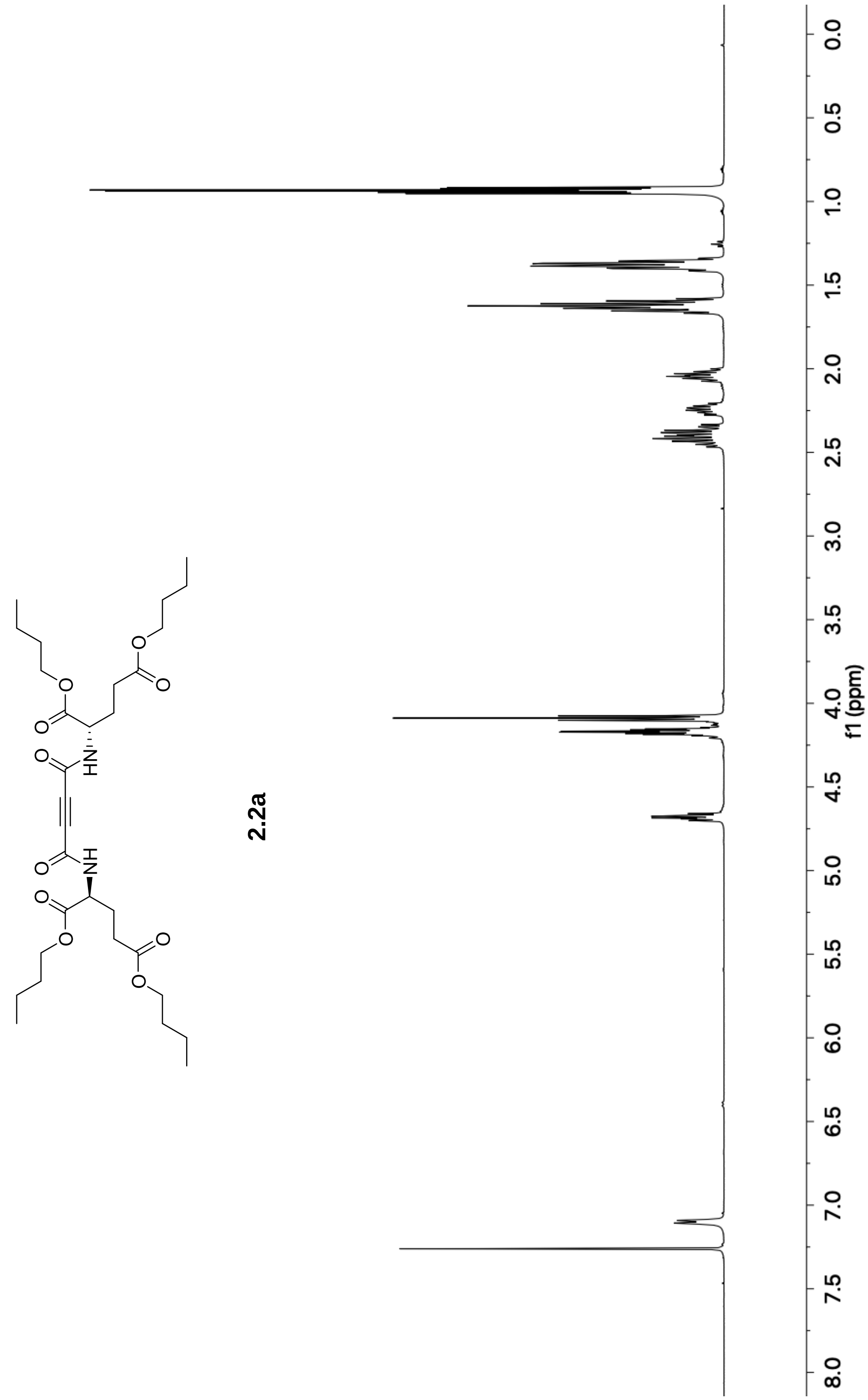
2.2a
f1 (ppm)
0.0
0.5
1.0
1.5
2.0
2.5
3.0
3.5
4.0
4.5
5.0
5.5
6.0
6.5
7.0
7.5
8.0

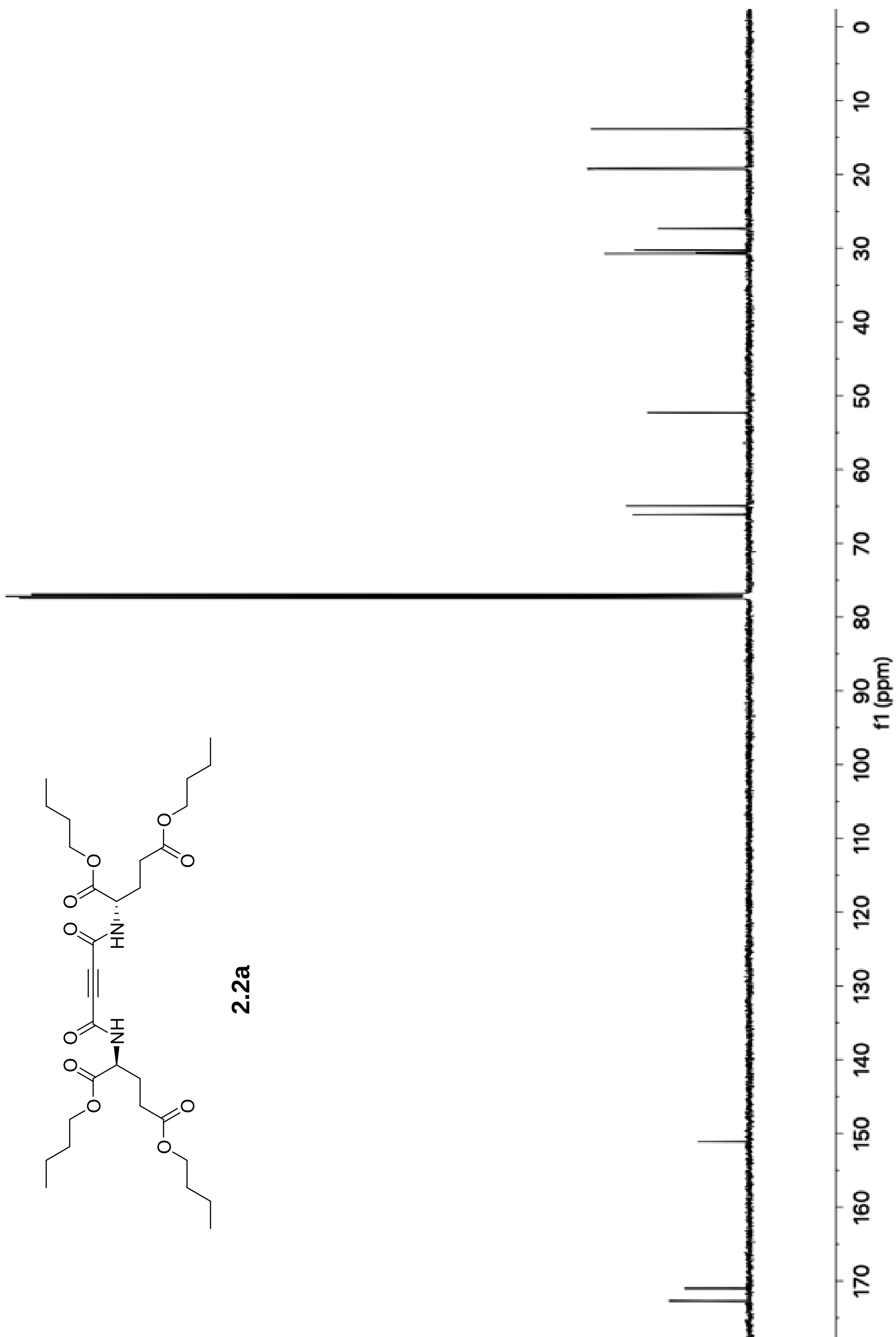
2.2a
f1 (ppm)
0
10
20
30
40
50
60
70
80
90
100
110
120
130
140
150
160
170
180

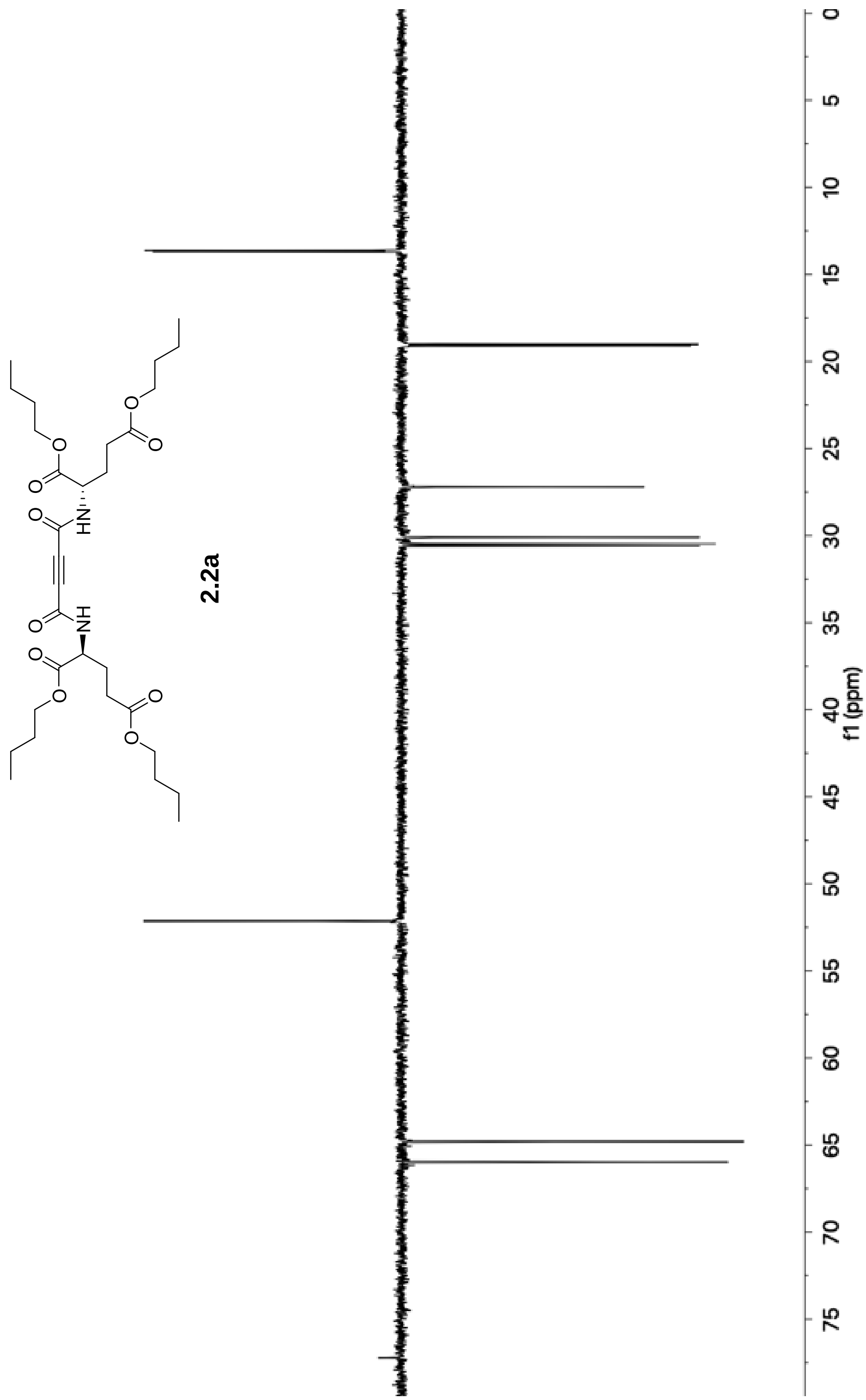

2.2a
f1 (ppm)
0 5 10 15 20 25 30 35 40 45 50 55 60 65 70 75

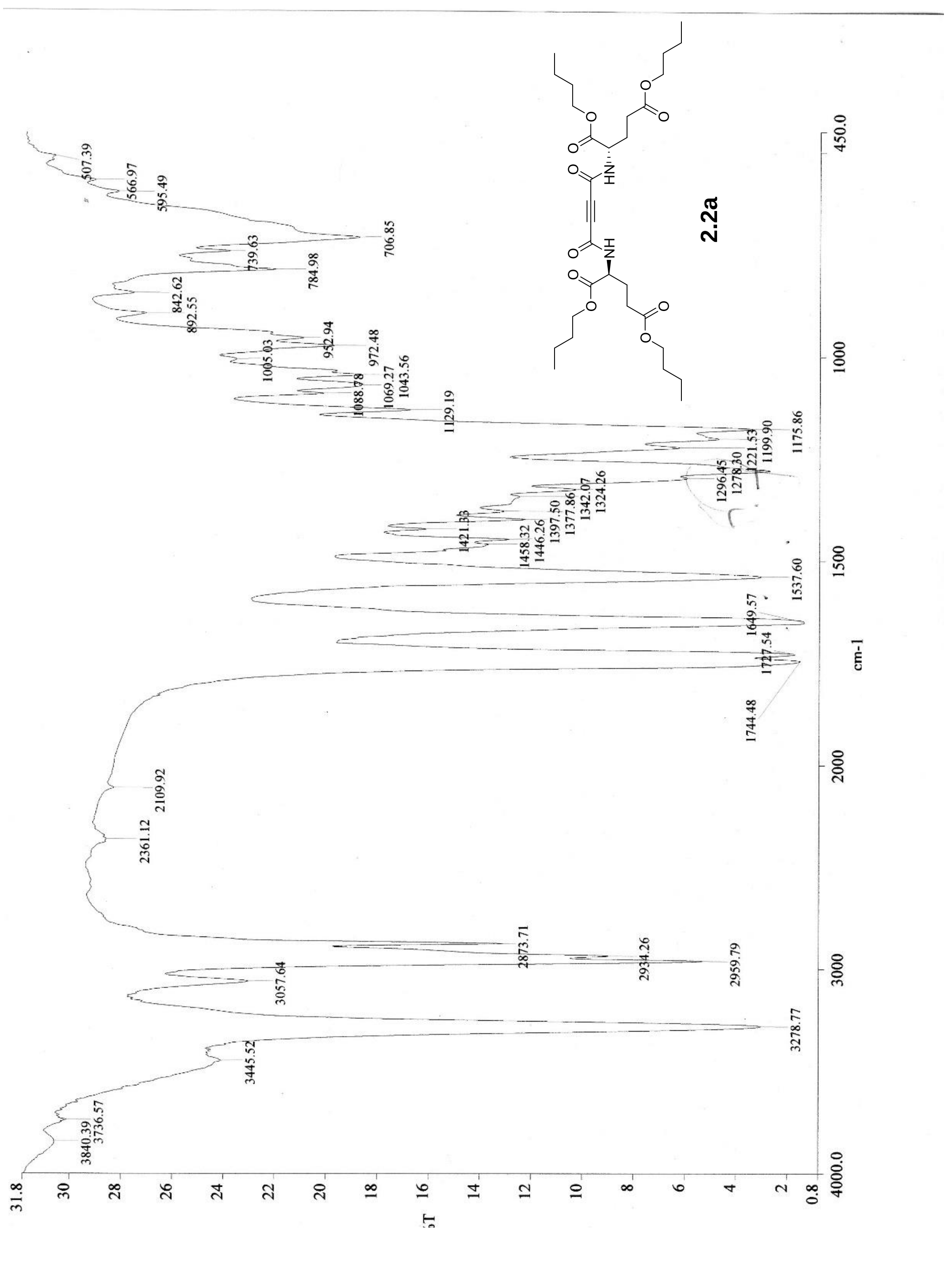
2.2a
cm-1
%T
3840.39
3736.57
3445.52
3278.77
3057.64
2959.79
2934.26
2873.71
2361.12
2109.92
1744.48
1727.54
1649.57
1537.60
1458.32
1446.26
1421.33
1397.50
1377.86
1342.07
1324.26
1296.45
1278.30
1221.53
1199.90
1175.86
1129.19
1088.78
1069.27
1043.56
1005.03
972.48
952.94
892.55
842.62
784.98
739.63
706.85
595.49
566.97
507.39
4000.0
3000
2000
1500
1000
450.0

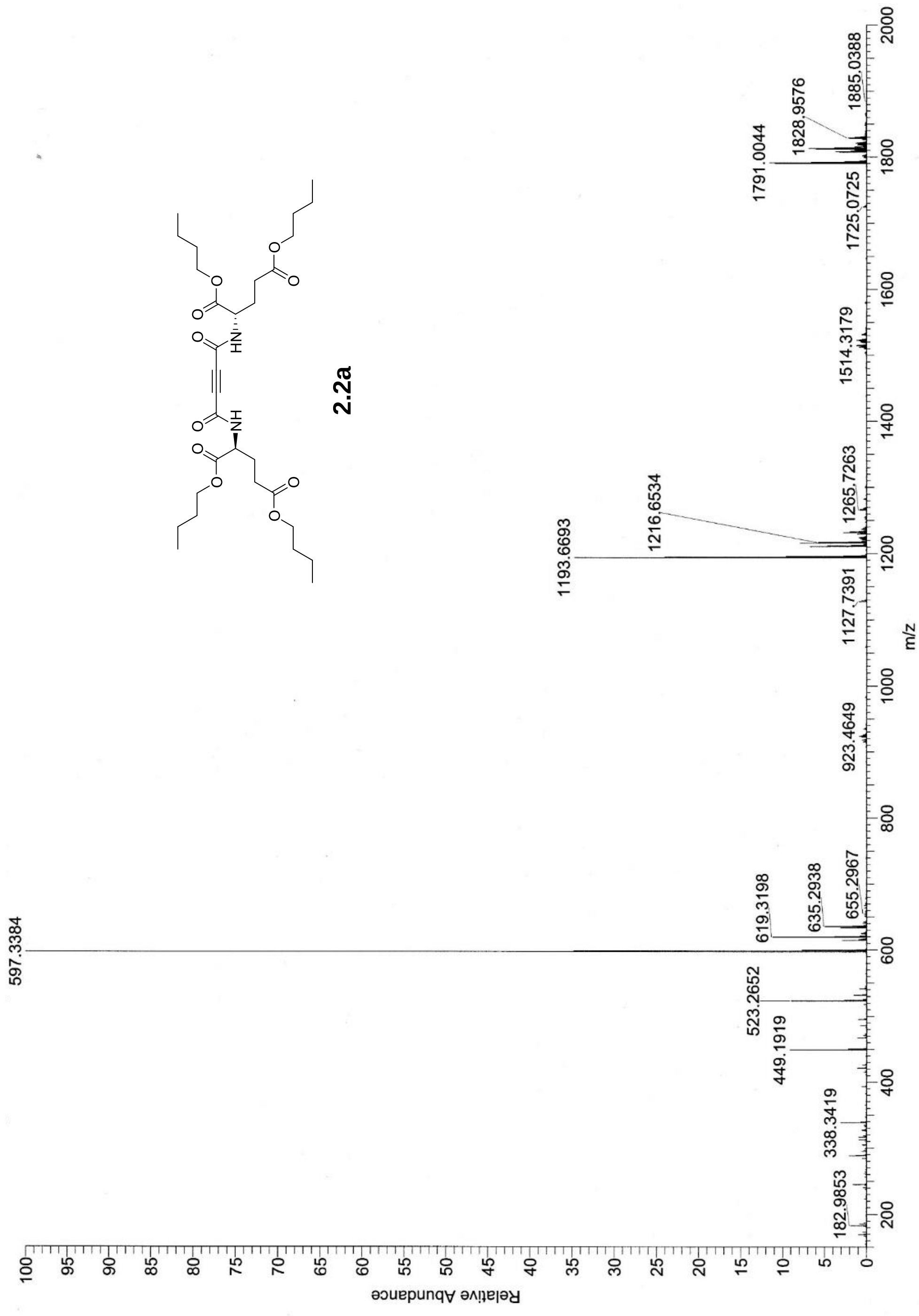
2.2a
597.3384
619.3198
635.2938
655.2967
523.2652
449.1919
338.3419
182.9853
923.4649
1127.7391
1193.6693
1216.6534
1265.7263
1514.3179
1725.0725
1791.0044
1828.9576
1885.0388
m/z
Relative Abundance

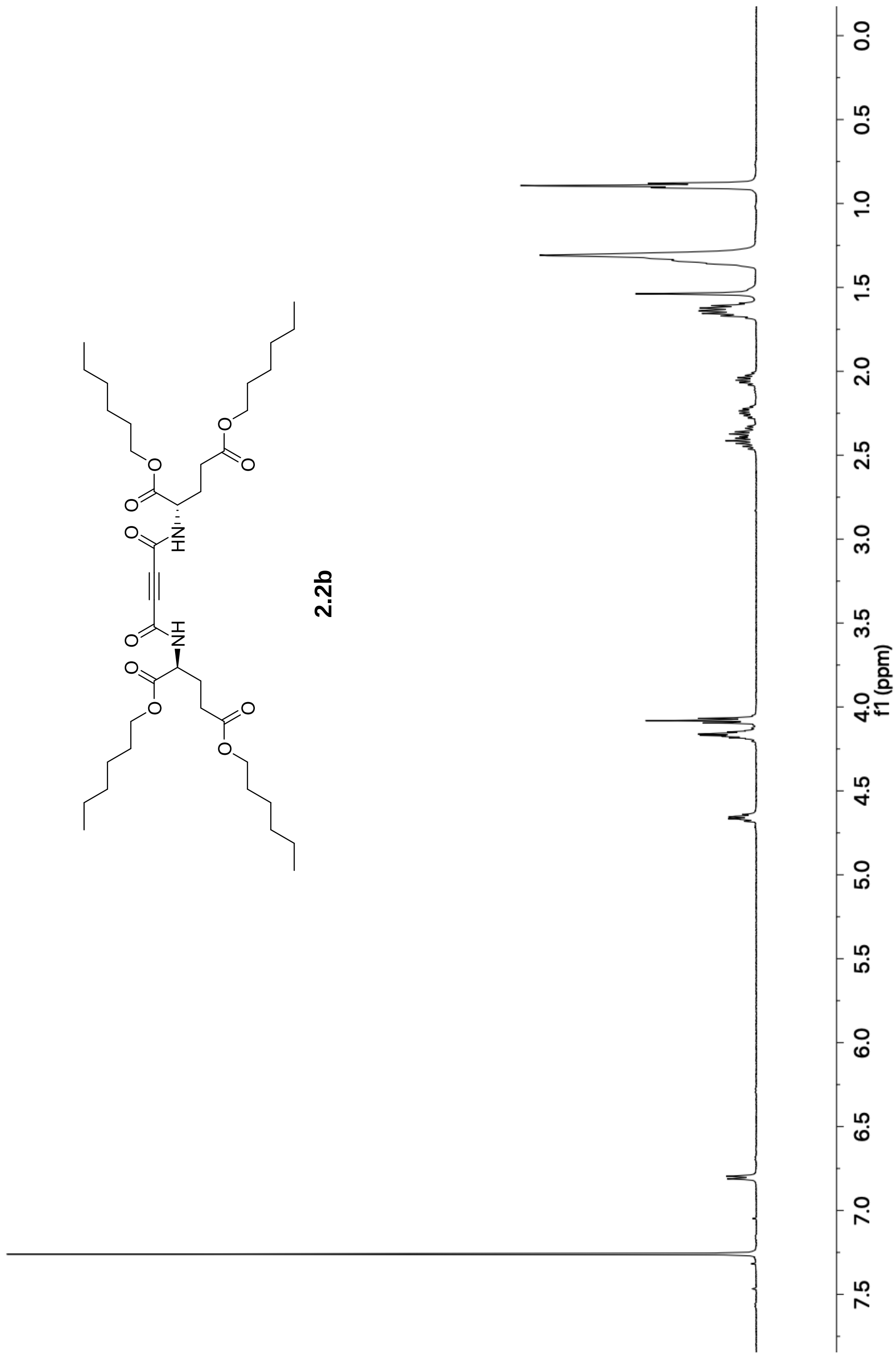

2.2b

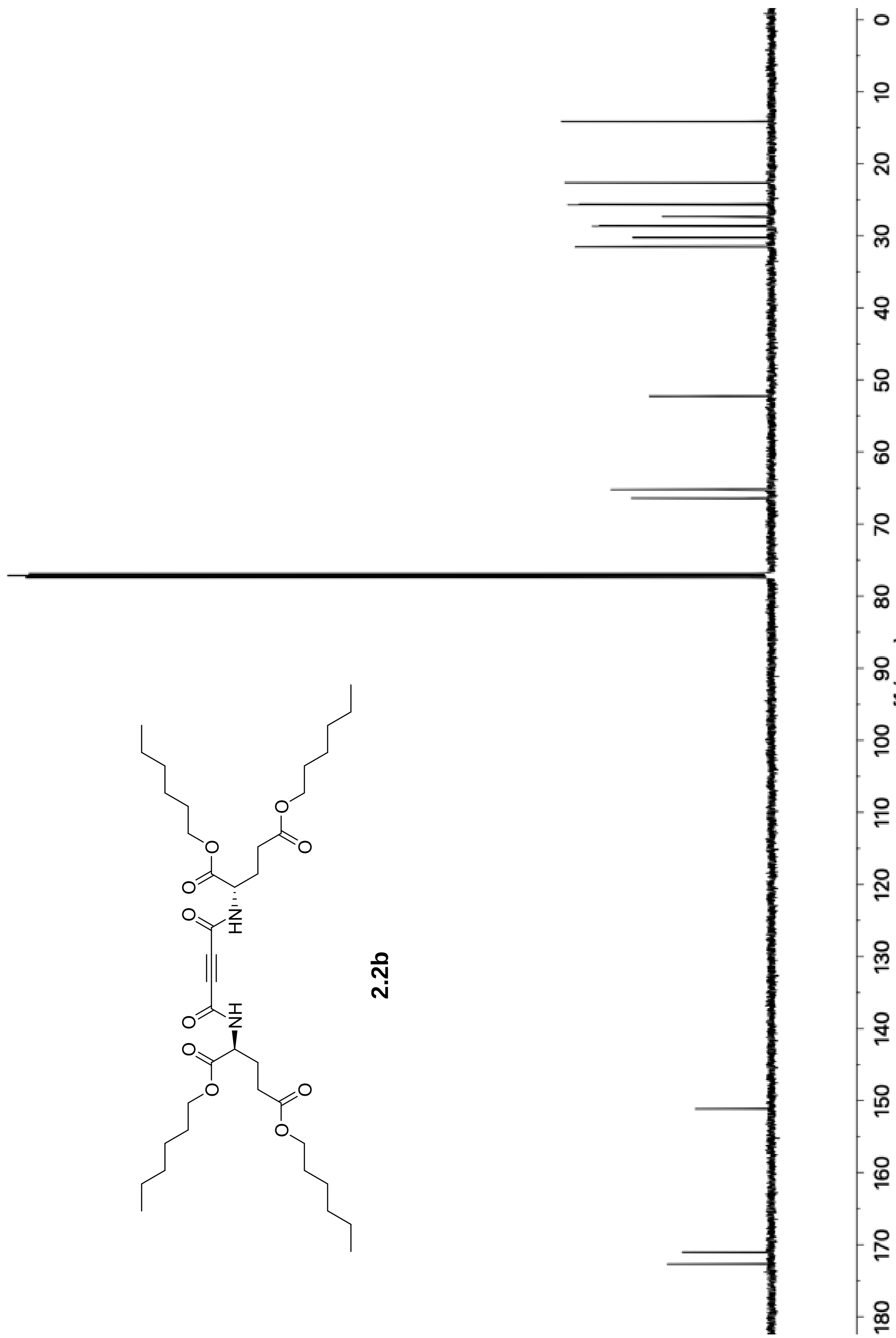
2.2b
f1 (ppm)
0 10 20 30 40 50 60 70 80 90 100 110 120 130 140 150 160 170 180

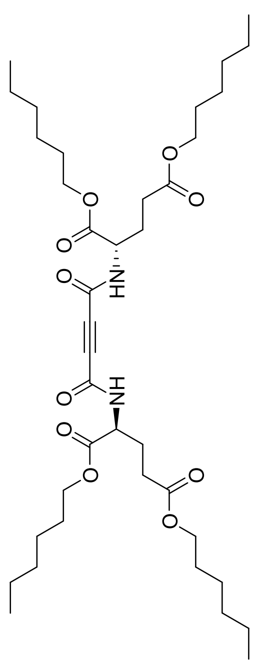

2.2b

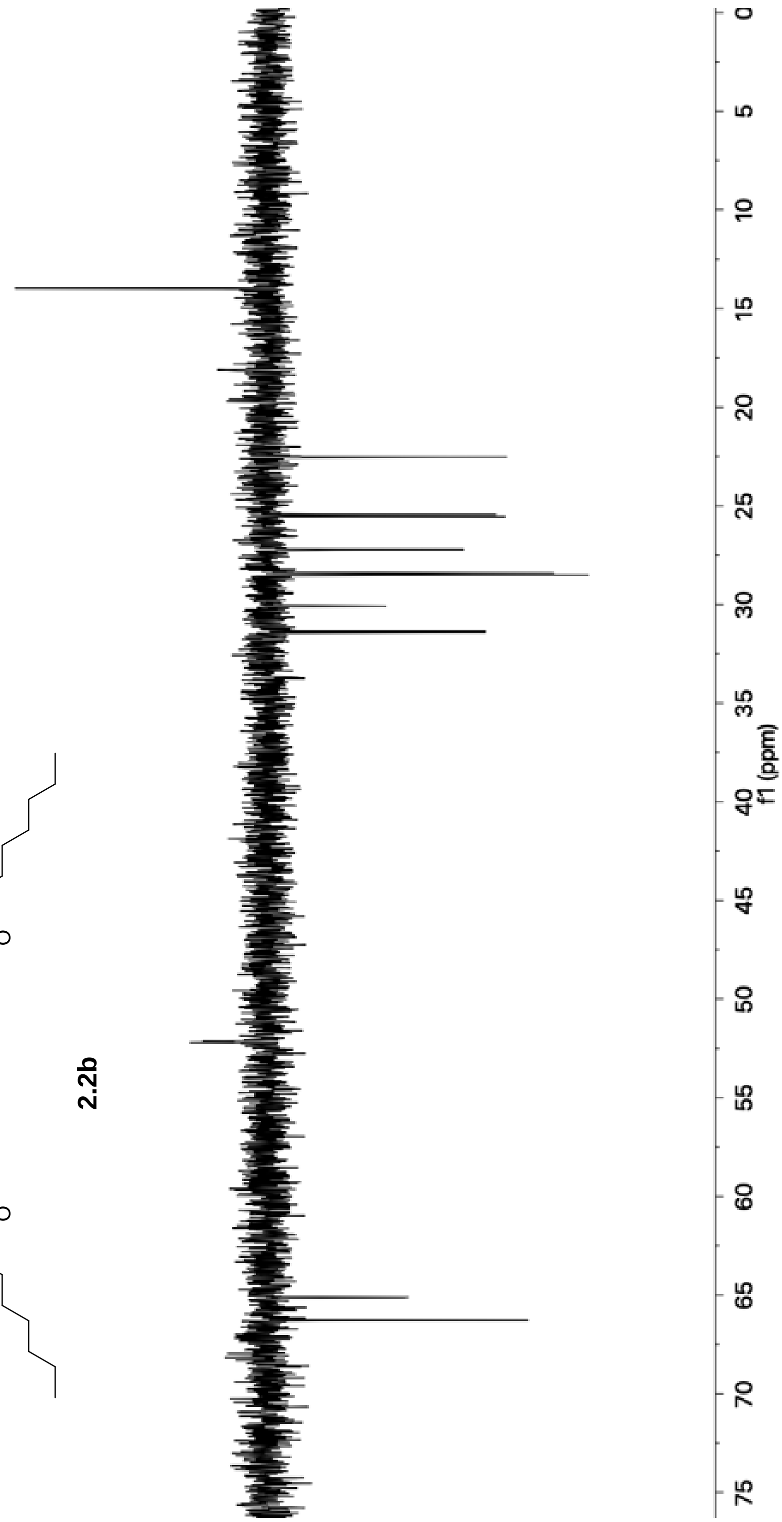

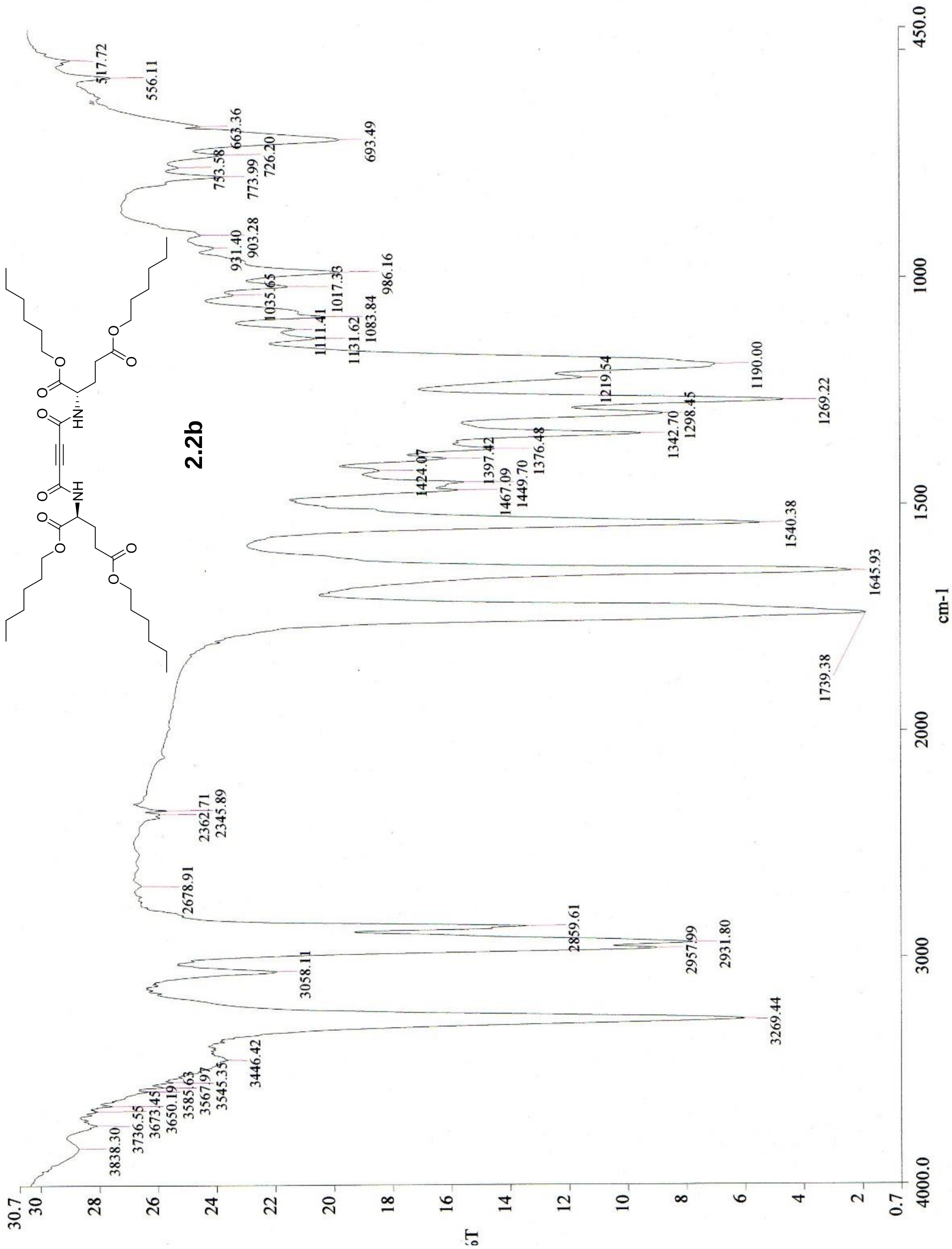

4000.0
3000
2000
1500
1000
450.0
cm-1
%T
3838.30
3736.55
3673.45
3650.19
3585.63
3567.97
3545.35
3446.42
3269.44
3058.11
2957.99
2931.80
2859.61
2678.91
2362.71
2345.89
1739.38
1645.93
1540.38
1467.09
1449.70
1424.07
1397.42
1376.48
1342.70
1298.45
1269.22
1219.54
1190.00
1131.62
1111.41
1083.84
1035.65
1017.33
986.16
931.40
903.28
773.99
753.58
726.20
693.49
663.36
556.11
517.72
HN
NH
O

2.2b

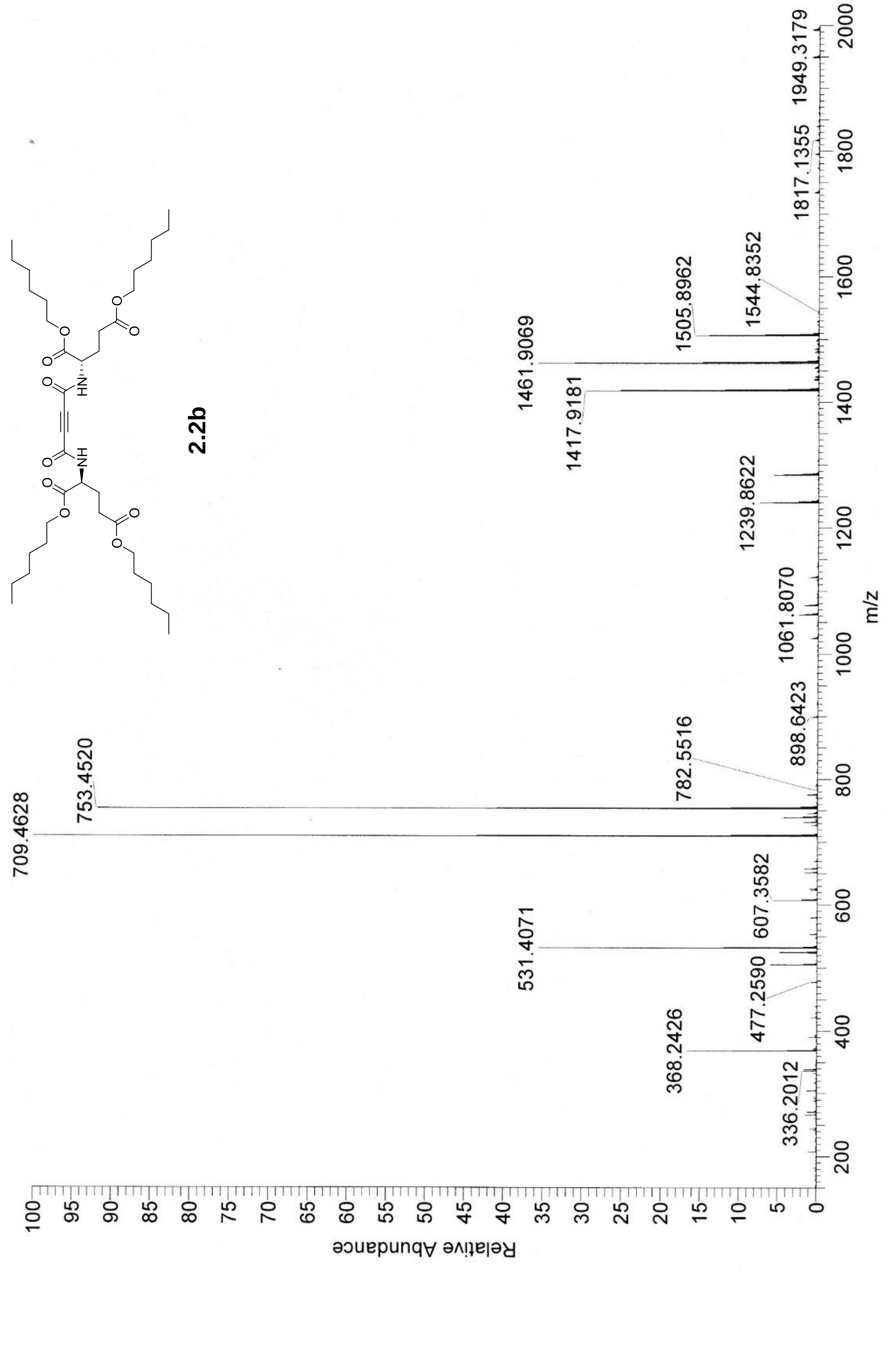
2.2b
Relative Abundance
m/z
709.4628
753.4520
531.4071
368.2426
336.2012
477.2590
607.3582
782.5516
898.6423
1061.8070
1239.8622
1417.9181
1461.9069
1505.8962
1544.8352
1817.1355
1949.3179

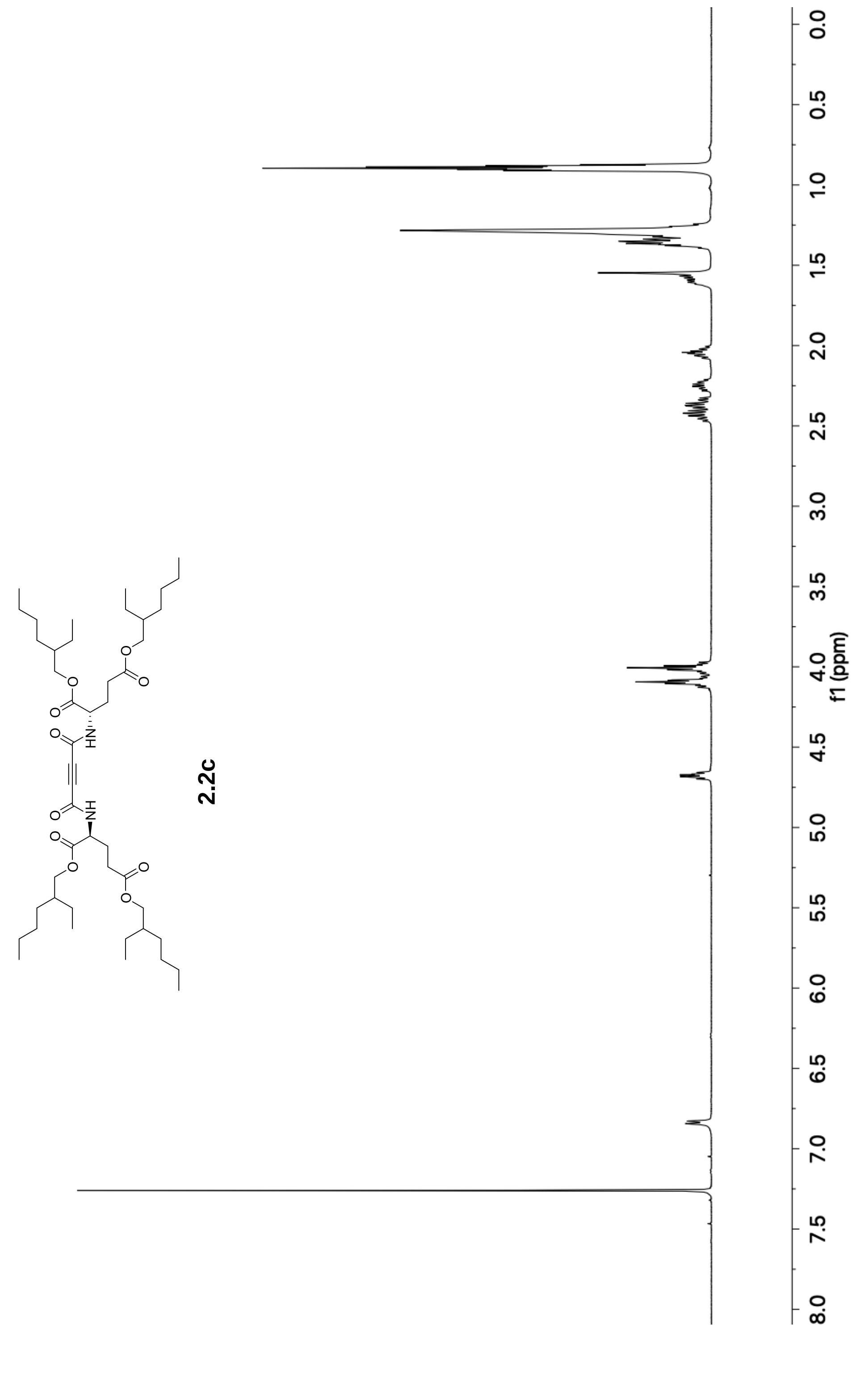
2.2c
f1 (ppm)
0.0
0.5
1.0
1.5
2.0
2.5
3.0
3.5
4.0
4.5
5.0
5.5
6.0
6.5
7.0
7.5
8.0

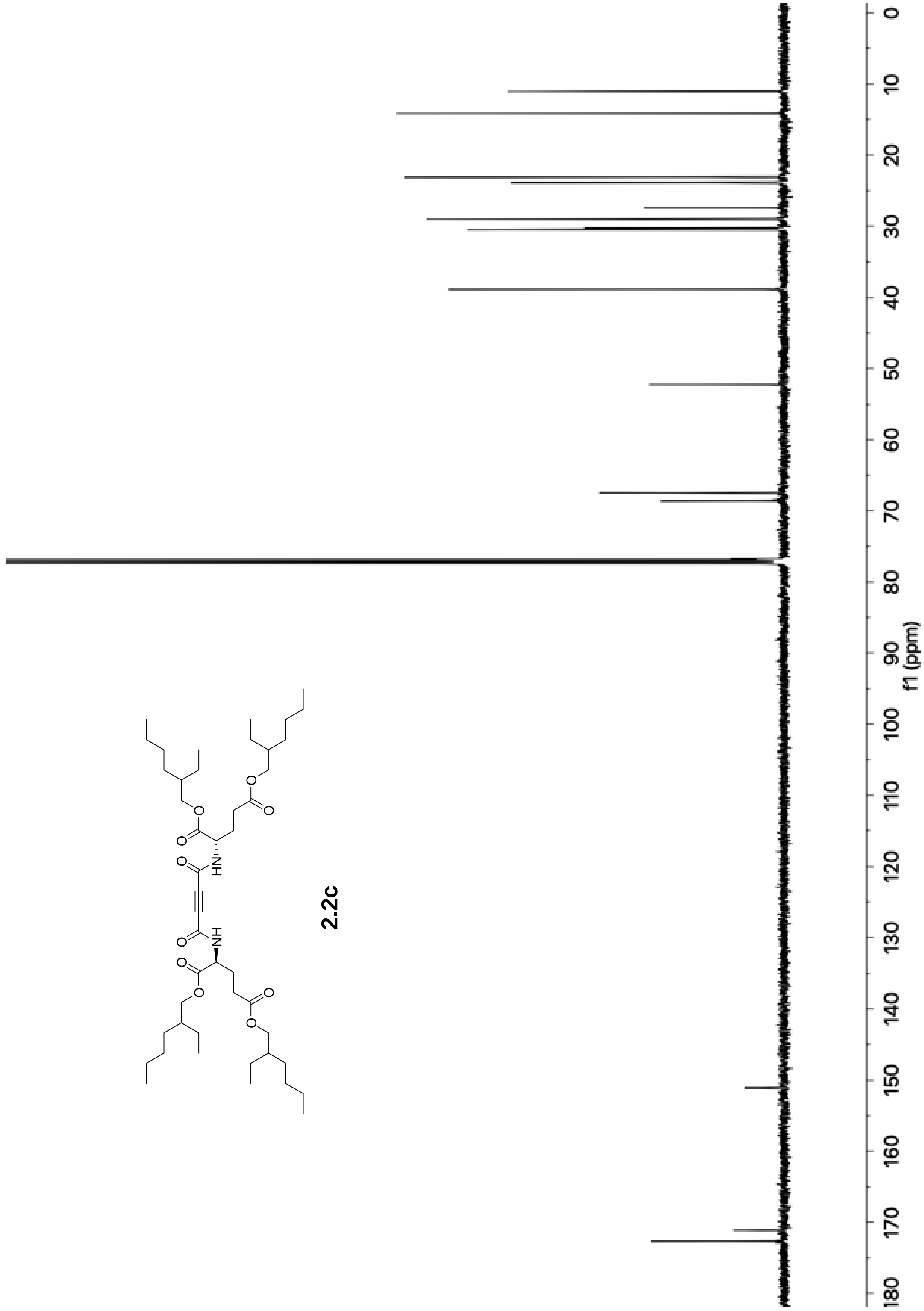

2.2c
O
HN
NH
0
10
20
30
40
50
60
70
80
90
100
110
120
130
140
150
160
170
180
f1 (ppm)

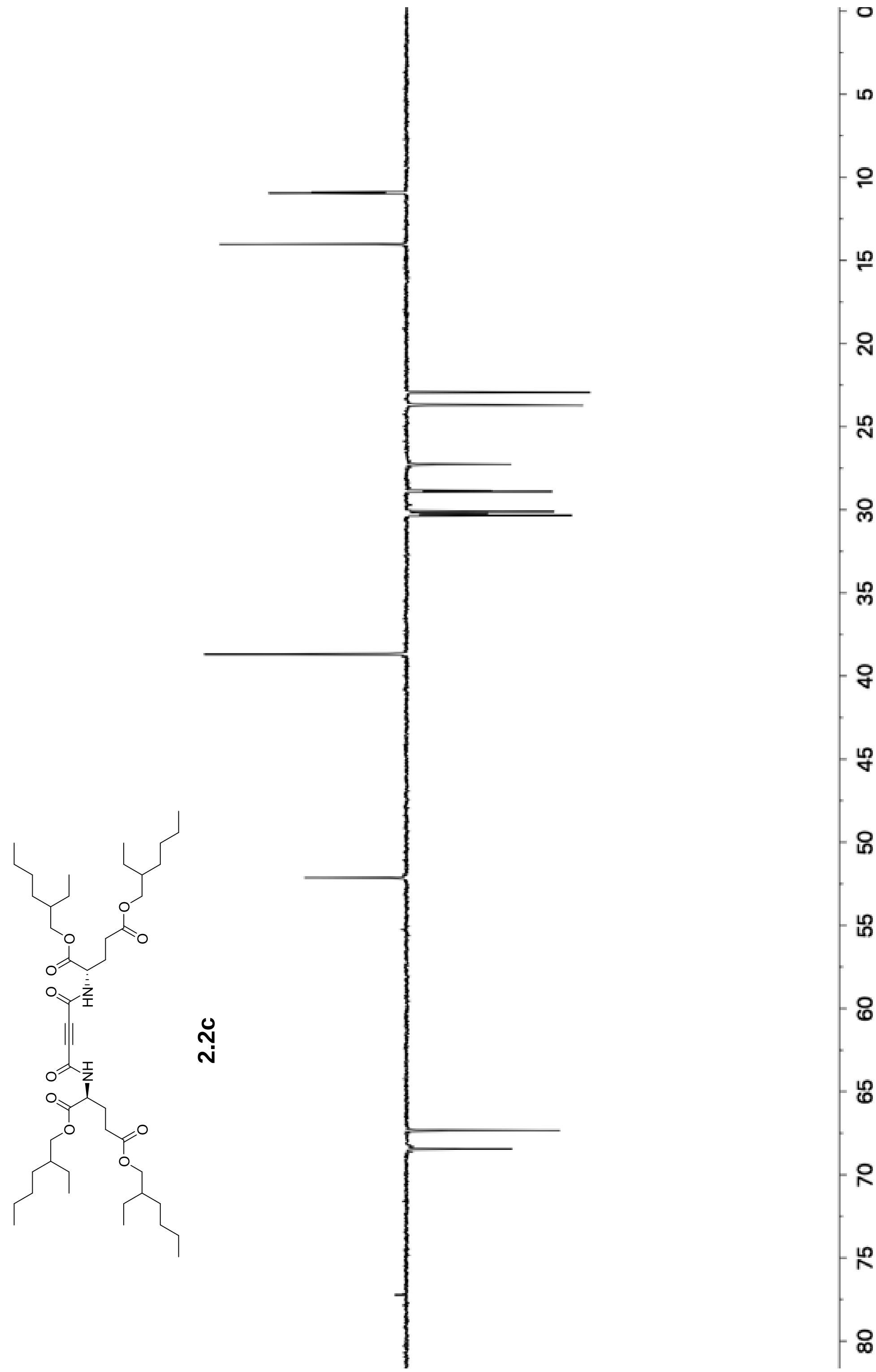

2.2c
HN
NH
O
f1 (ppm)
0
5
10
15
20
25
30
35
40
45
50
55
60
65
70
75
80

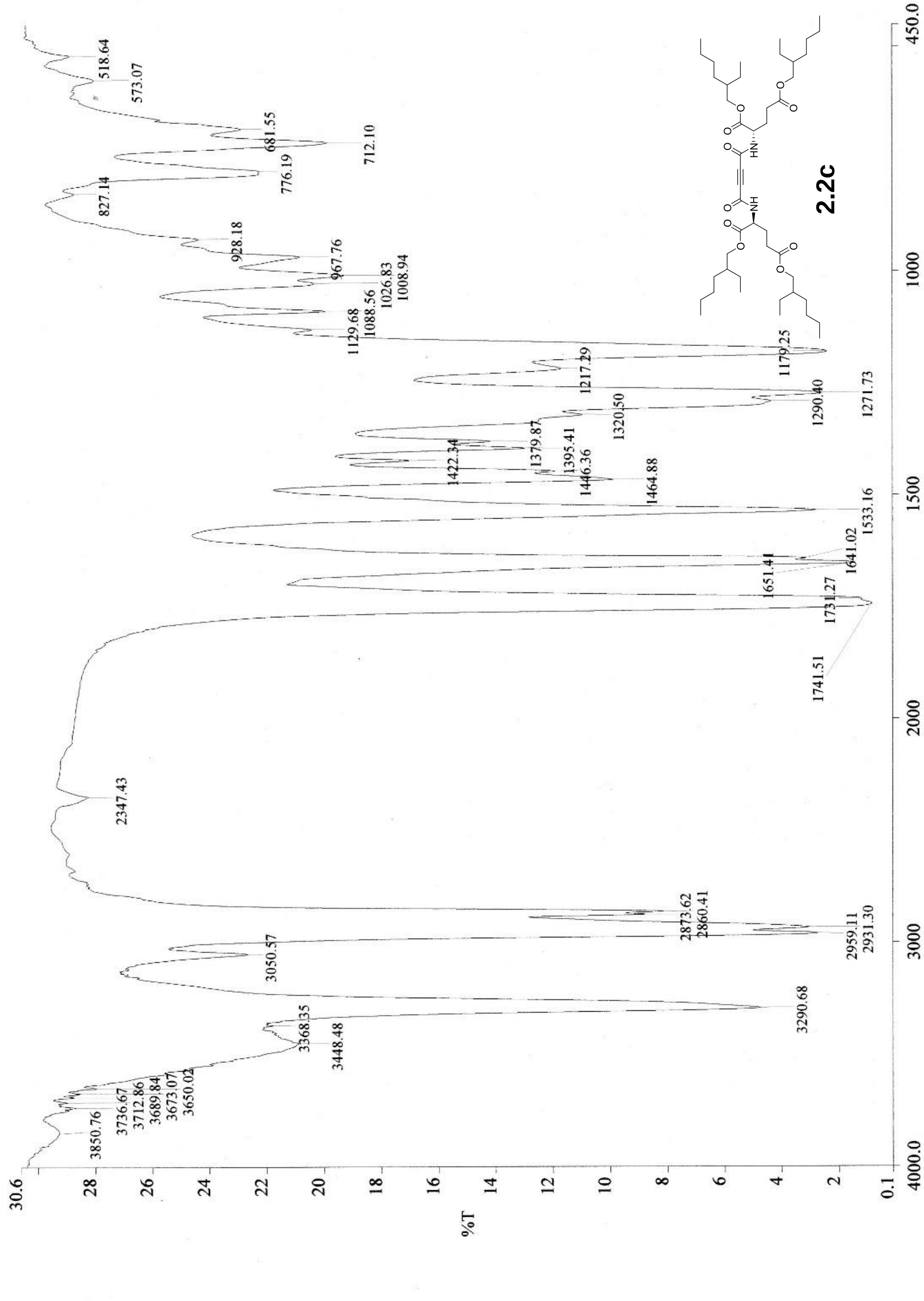
%T
cm-1
30.6
28
26
24
22
20
18
16
14
12
10
8
6
4
2
0.1
4000.0
3000
2000
1500
1000
450.0
3850.76
3736.67
3712.86
3689.84
3673.07
3650.02
3448.48
3368.35
3290.68
3050.57
2959.11
2931.30
2873.62
2860.41
2347.43
1741.51
1731.27
1651.41
1641.02
1533.16
1464.88
1446.36
1422.34
1395.41
1379.87
1320.50
1290.40
1271.73
1217.29
1179.25
1129.68
1088.56
1026.83
1008.94
967.76
928.18
827.14
776.19
712.10
681.55
573.07
518.64
HN
NH
O

2.2c

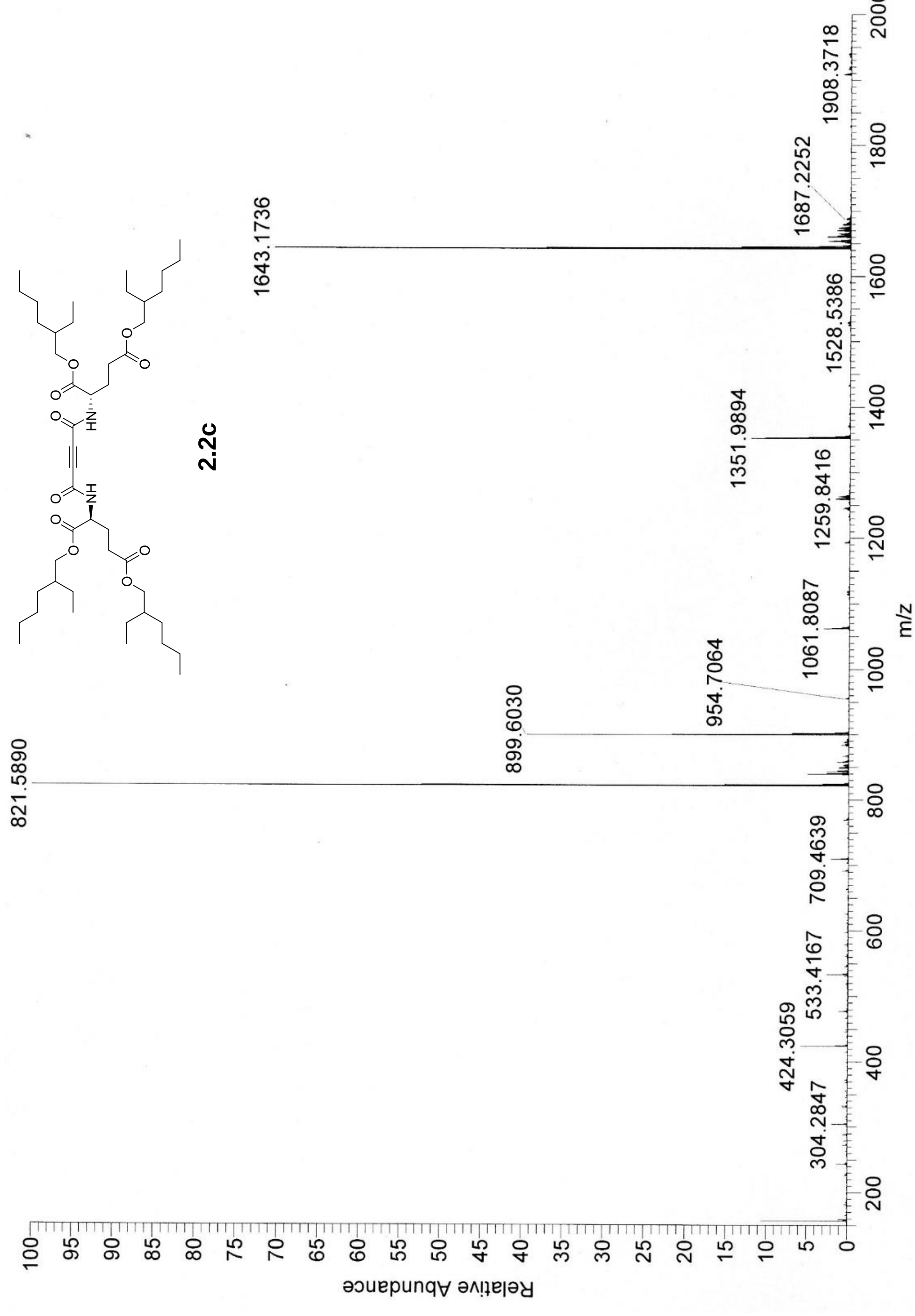
2.2c
821.5890
899.6030
954.7064
1061.8087
1259.8416
1351.9894
1528.5386
1643.1736
1687.2252
1908.3718
304.2847
424.3059
533.4167
709.4639
m/z
Relative Abundance

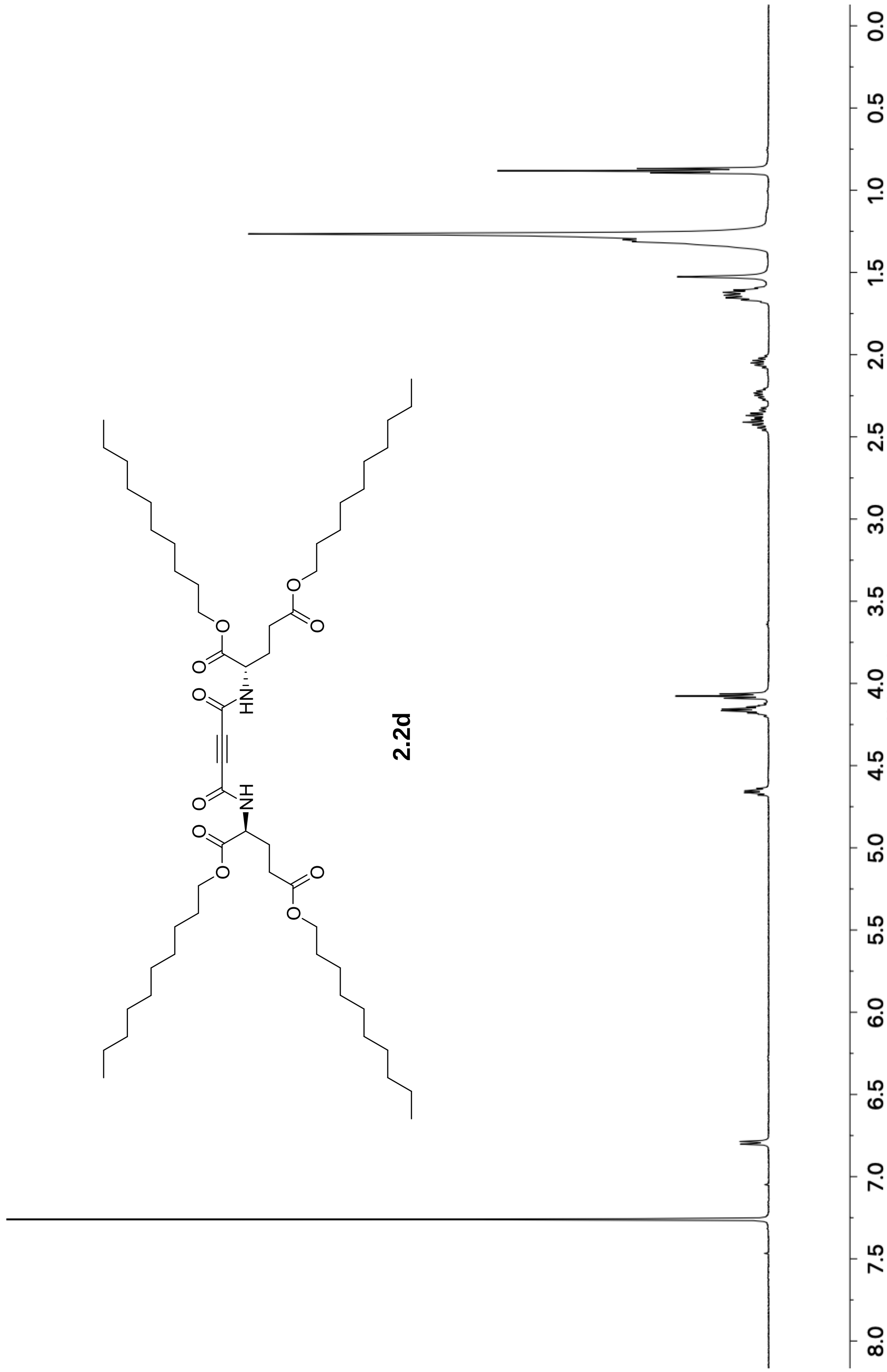

2.2d

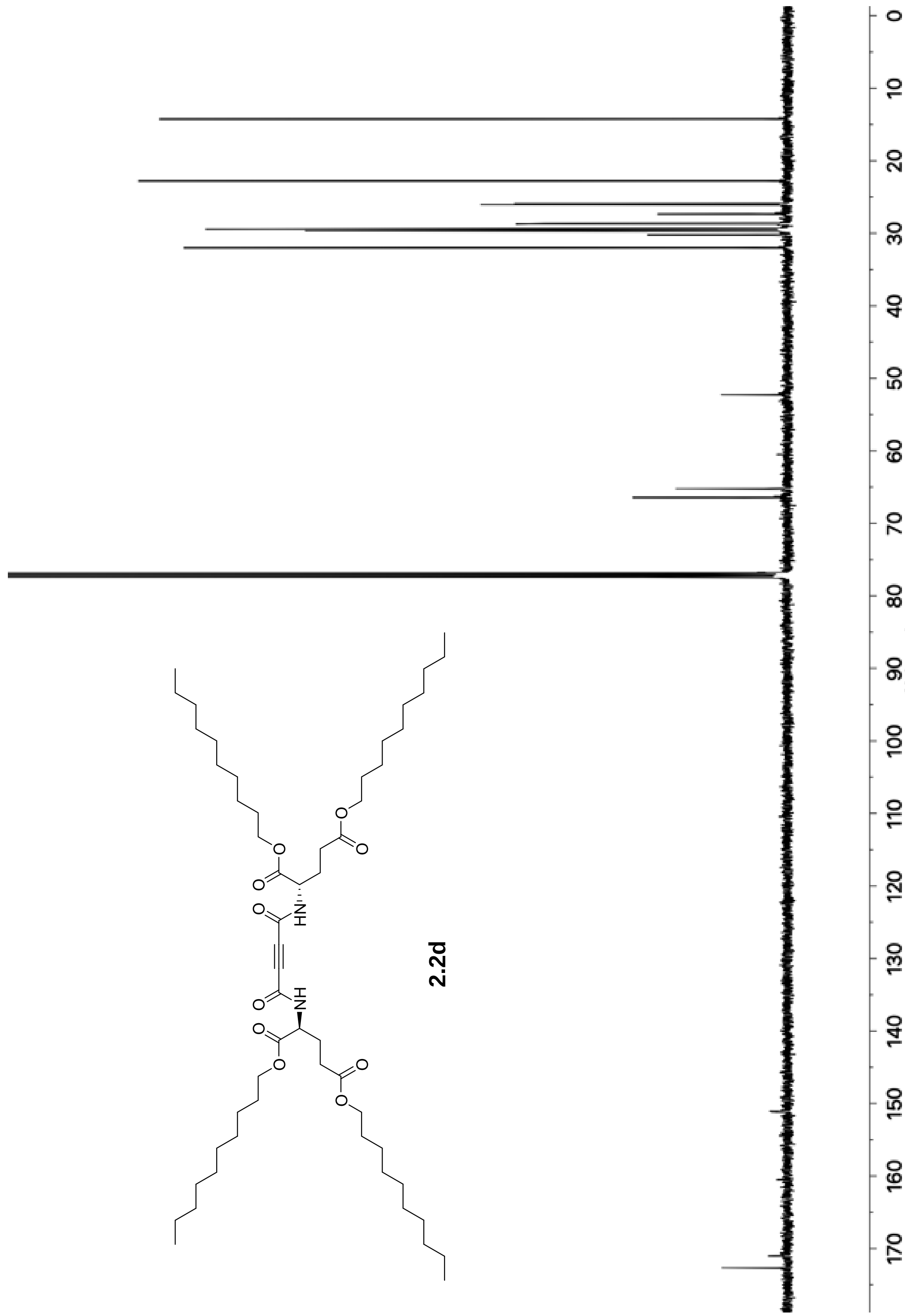

2.2d
f1 (ppm)
0
10
20
30
40
50
60
70
80
90
100
110
120
130
140
150
160
170

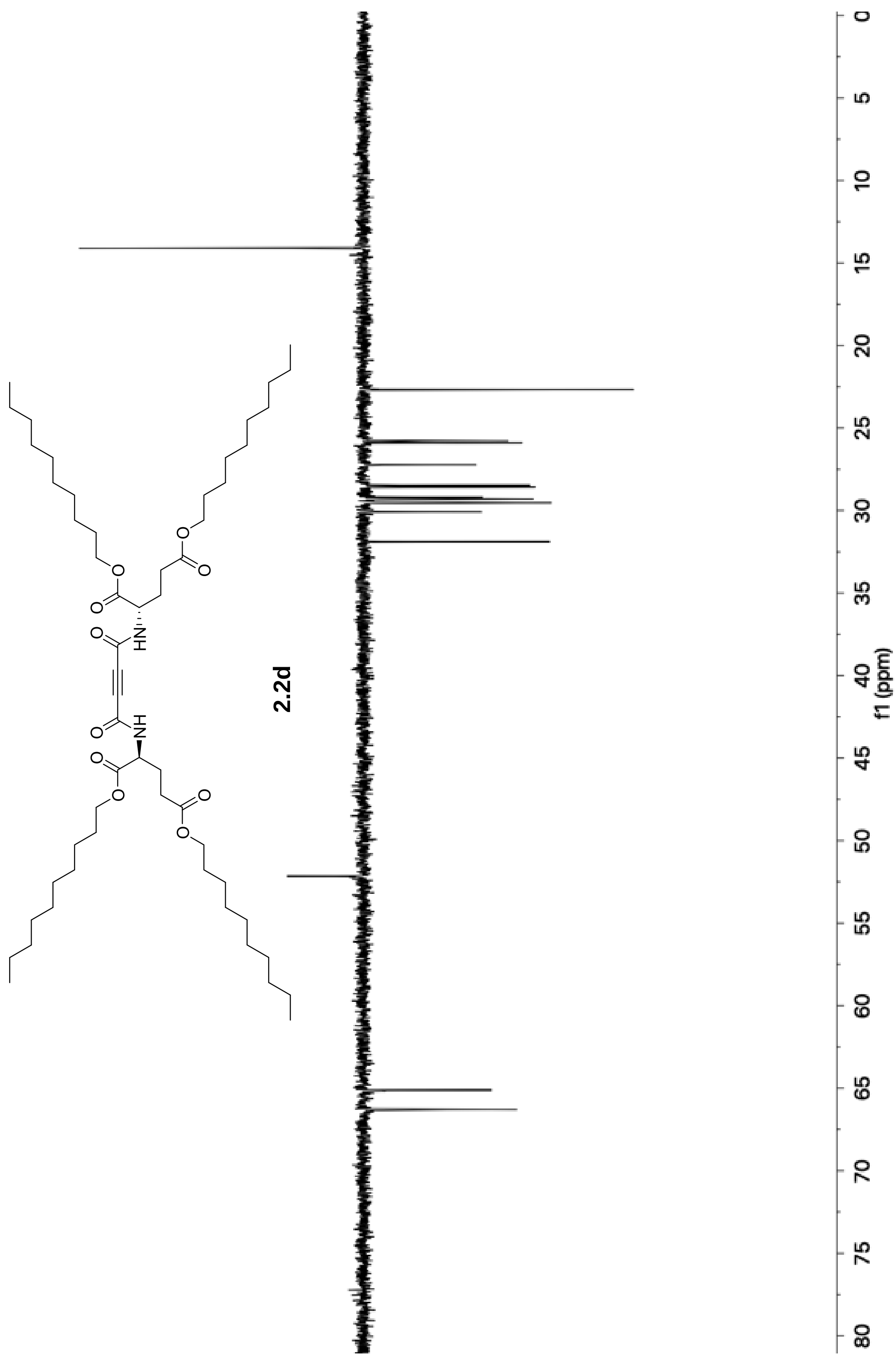

2.2d
HN
NH
O
f1 (ppm)
0
5
10
15
20
25
30
35
40
45
50
55
60
65
70
75
80

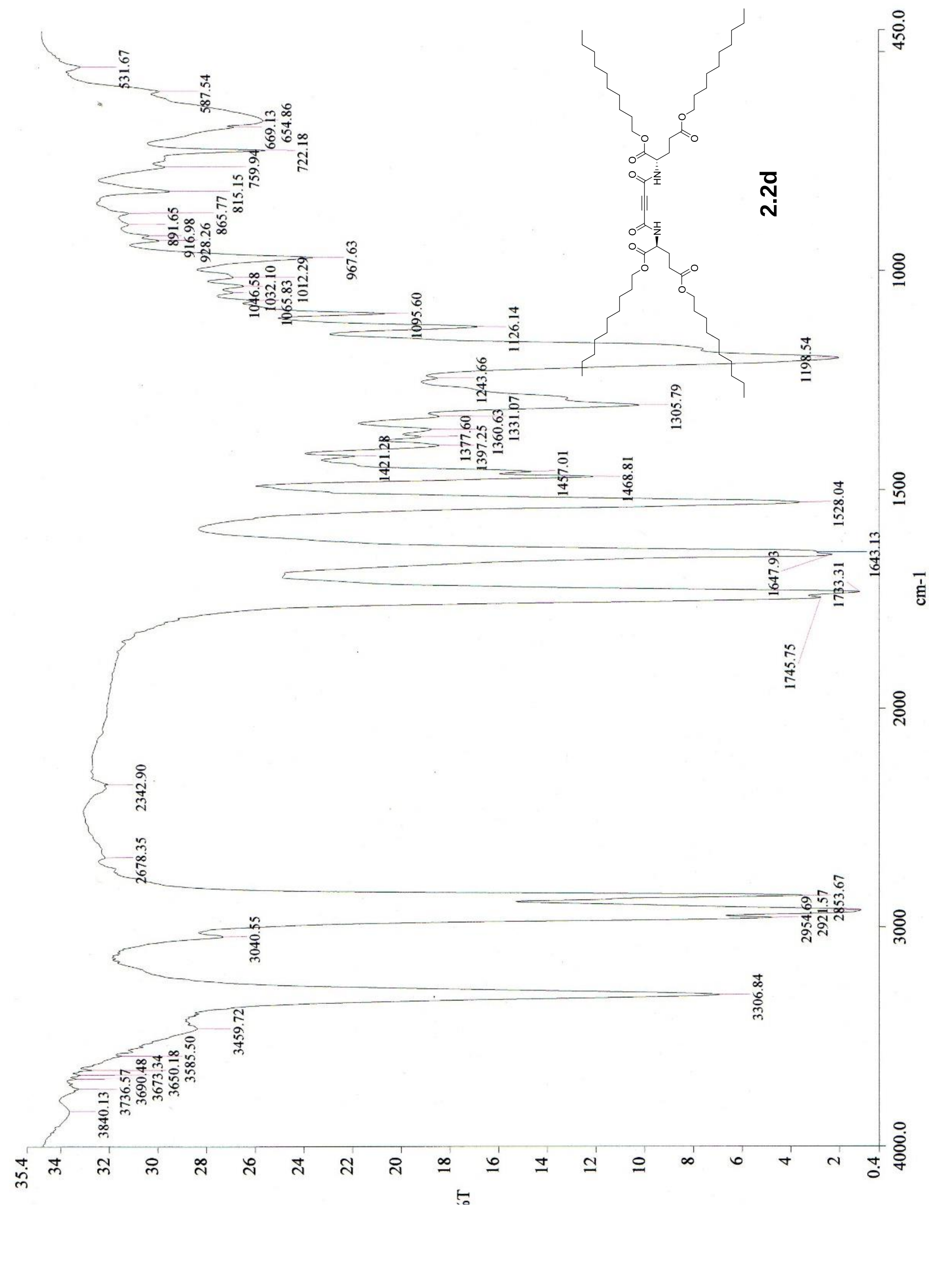
2.2d
cm-1
%T
3840.13
3736.57
3690.48
3673.34
3650.18
3585.50
3459.72
3306.84
3040.55
2954.69
2921.57
2853.67
2678.35
2342.90
1745.75
1733.31
1647.93
1643.13
1528.04
1468.81
1457.01
1421.28
1397.25
1377.60
1360.63
1331.07
1305.79
1243.66
1198.54
1126.14
1095.60
1065.83
1046.58
1032.10
1012.29
967.63
928.26
916.98
891.65
865.77
815.15
759.94
722.18
669.13
654.86
587.54
531.67

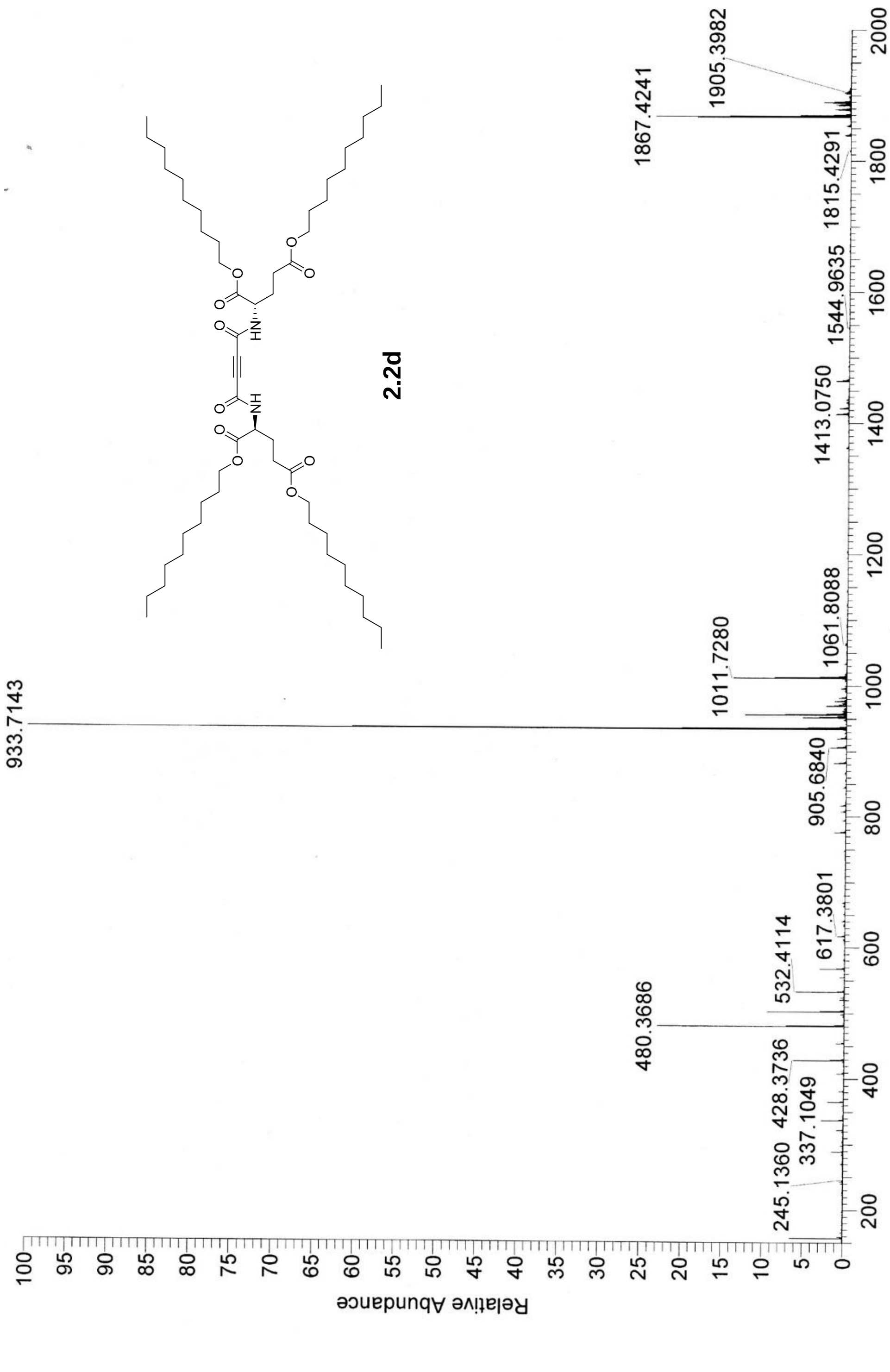

2.2d
933.7143
480.3686
1011.7280
1061.8088
1867.4241
1905.3982
1815.4291
1544.9635
1413.0750
905.6840
617.3801
532.4114
428.3736
337.1049
245.1360
Relative Abundance
m/z

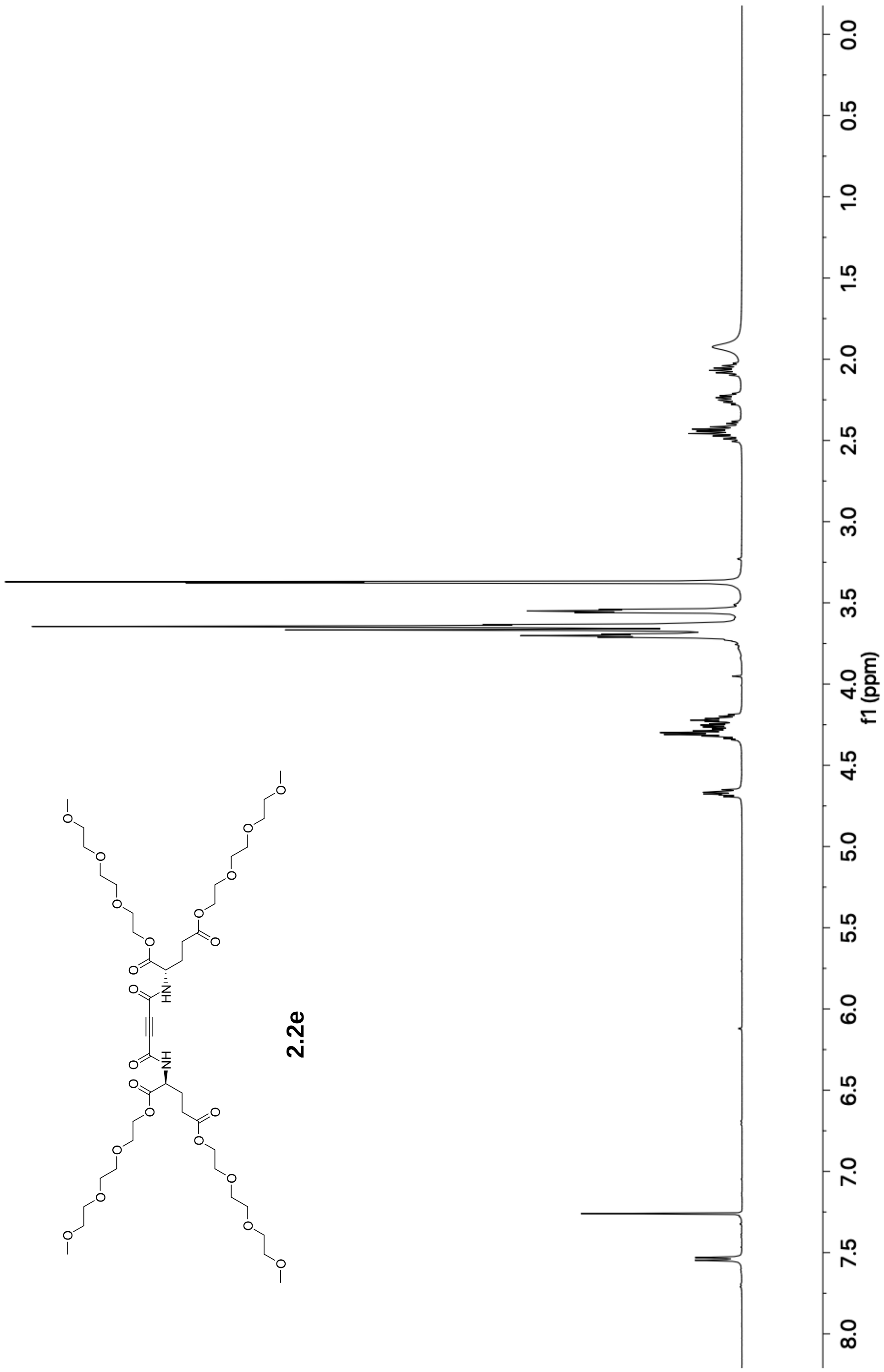
2.2e
0.0
0.5
1.0
1.5
2.0
2.5
3.0
3.5
4.0
4.5
5.0
5.5
6.0
6.5
7.0
7.5
8.0
f1 (ppm)

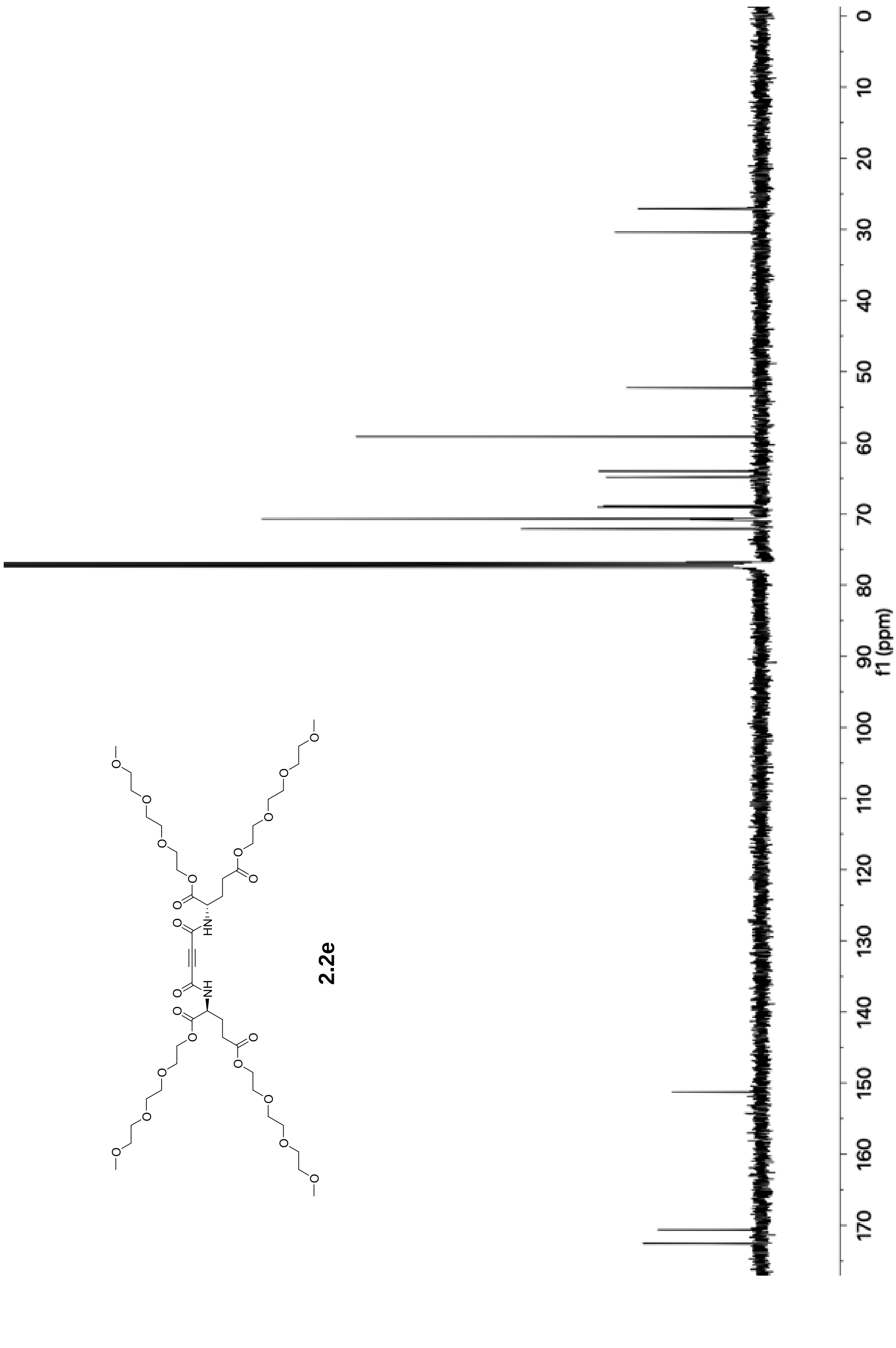

2.2e

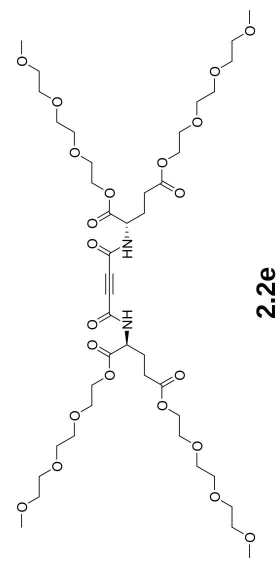

2.2e

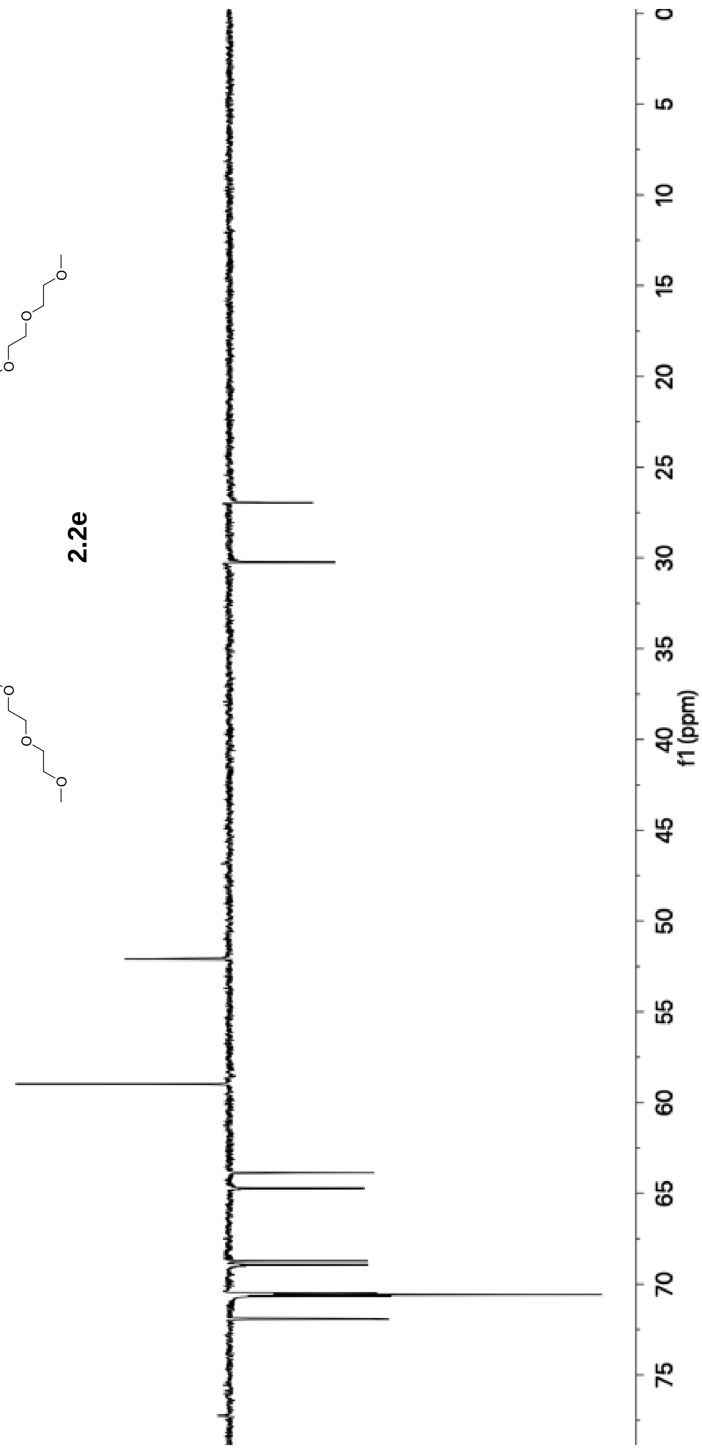

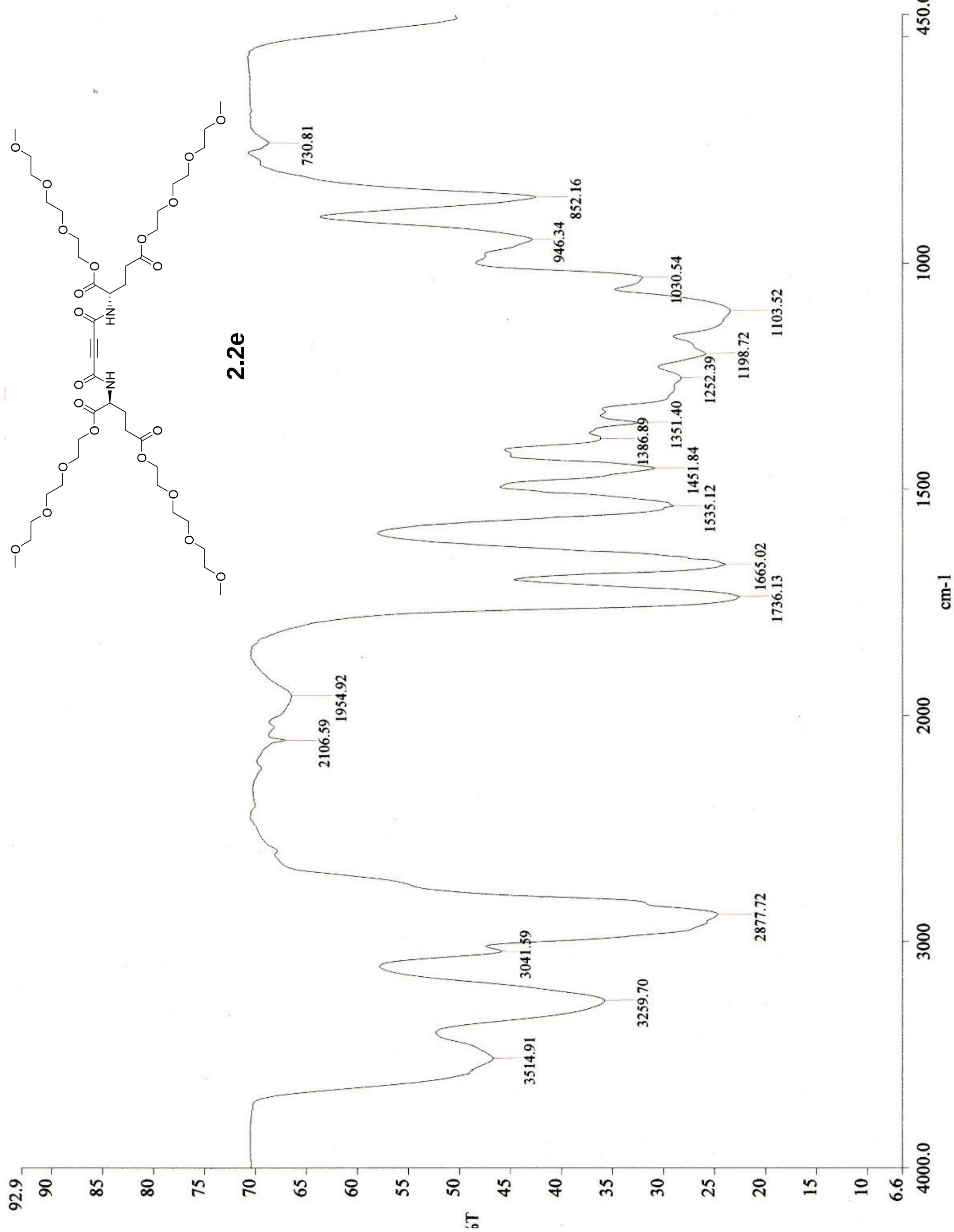

2.2e
%T
cm-1
4000.0
3000
2000
1500
1000
450.0
3514.91
3259.70
3041.59
2877.72
2106.59
1954.92
1736.13
1665.02
1535.12
1451.84
1386.89
1351.40
1252.39
1198.72
1103.52
1030.54
946.34
852.16
730.81

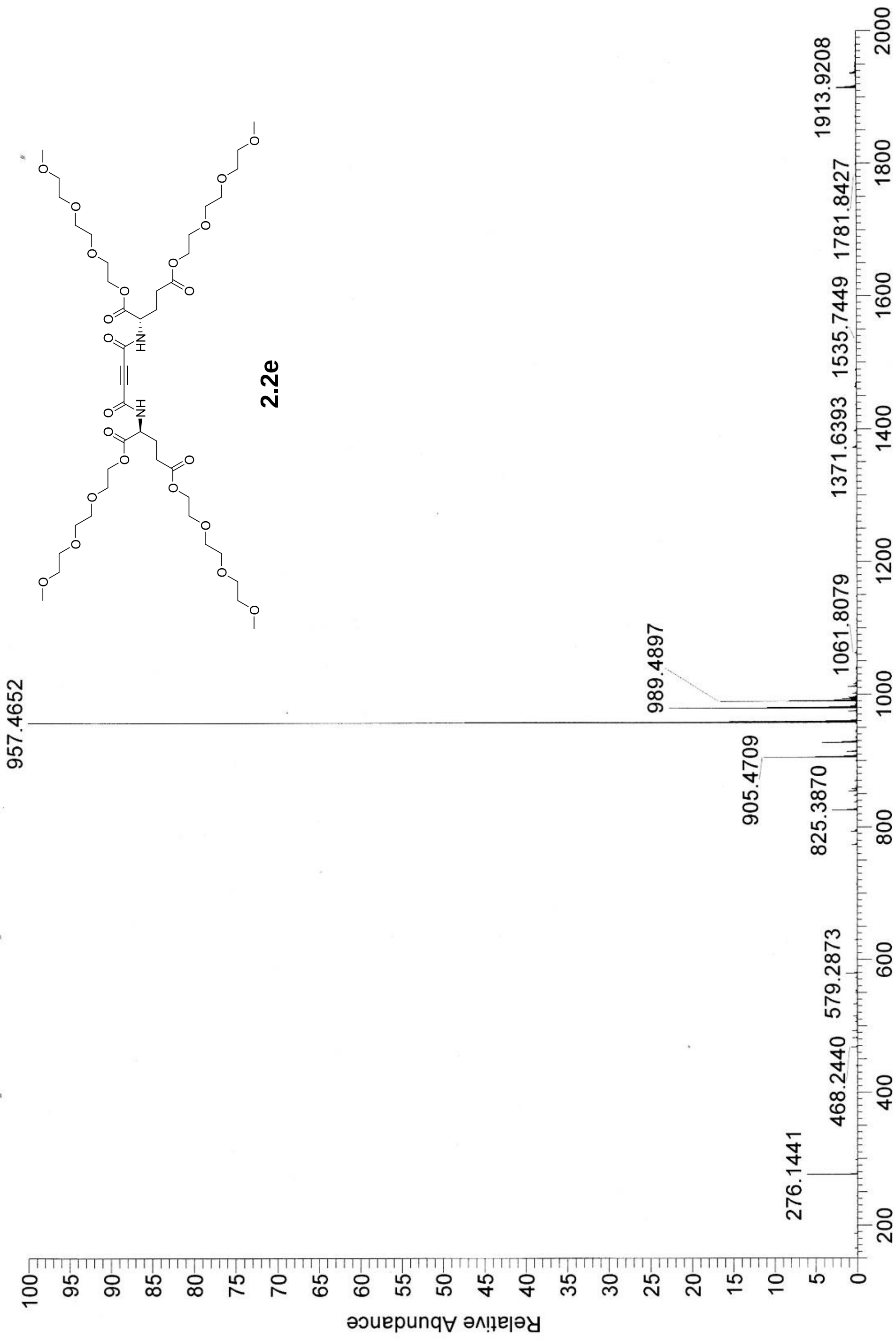
2.2e
957.4652
989.4897
905.4709
825.3870
1061.8079
1371.6393
1535.7449
1781.8427
1913.9208
579.2873
468.2440
276.1441
m/z
Relative Abundance

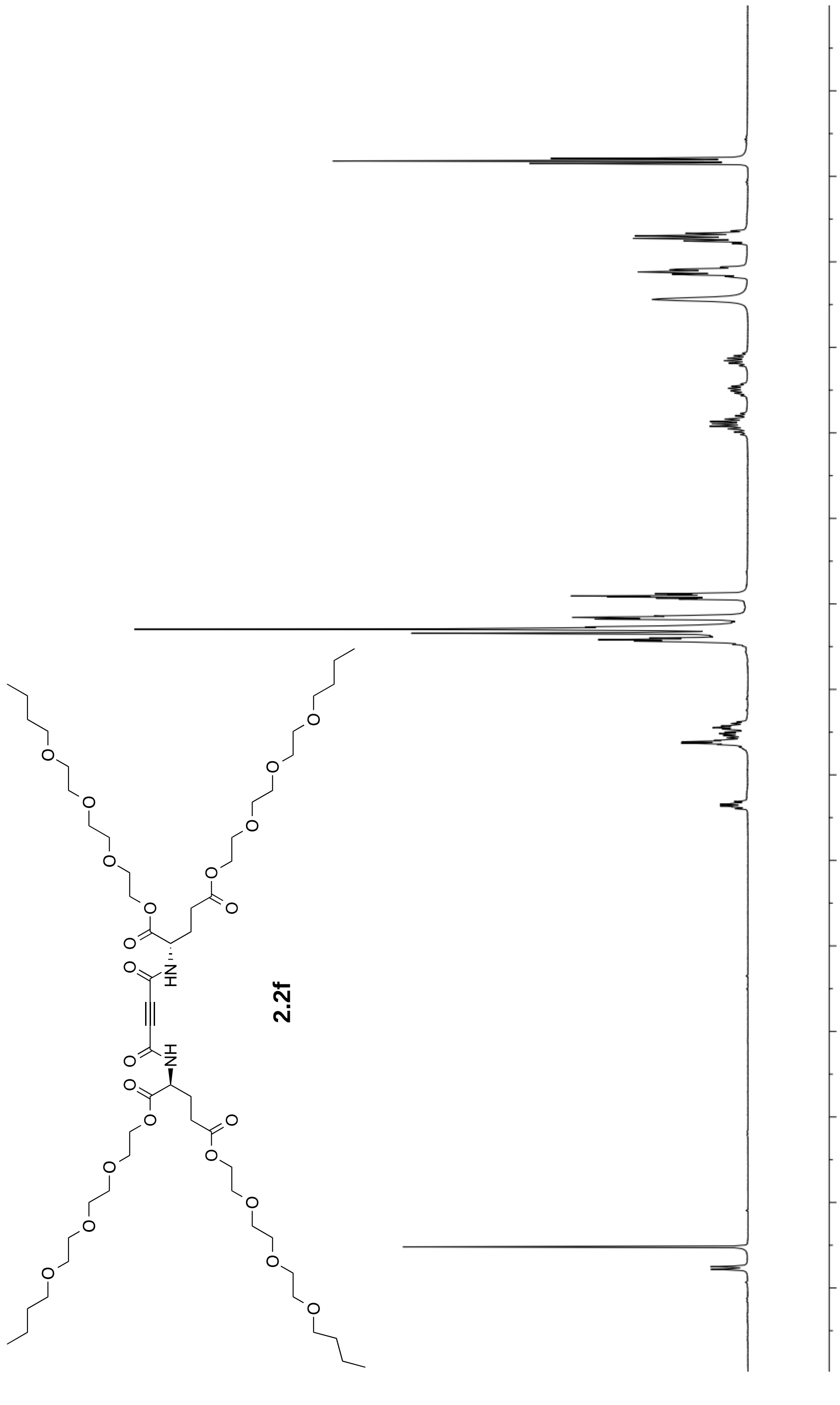

2.2f

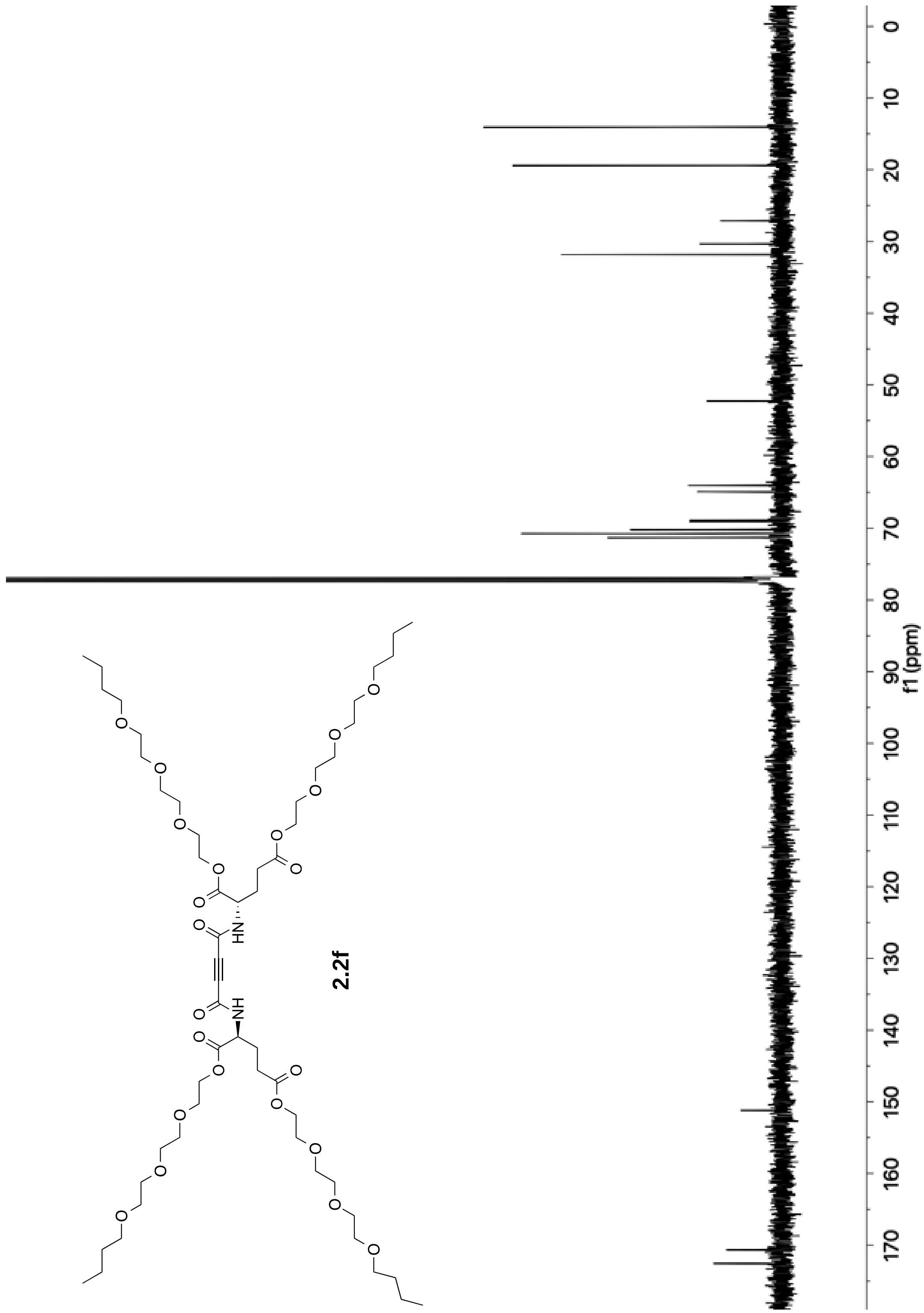
2.2f
f1 (ppm)

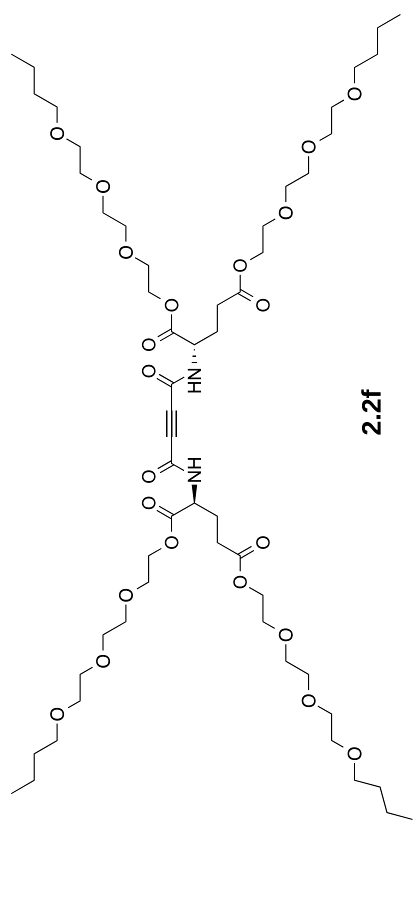

2.2f

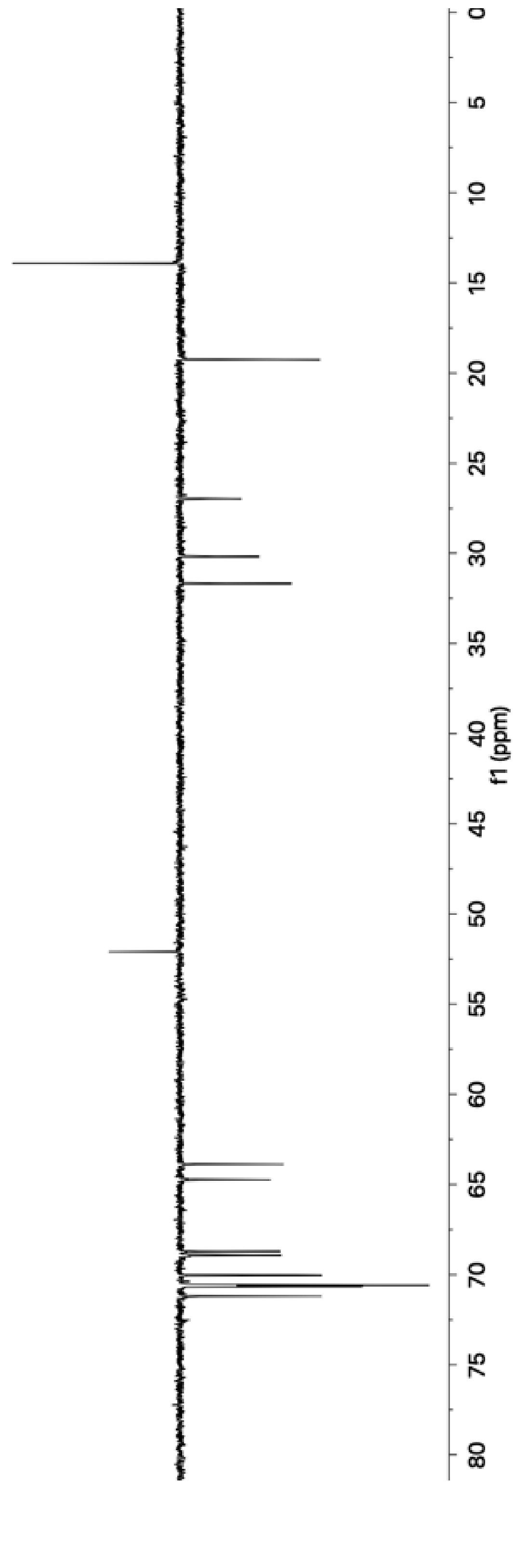

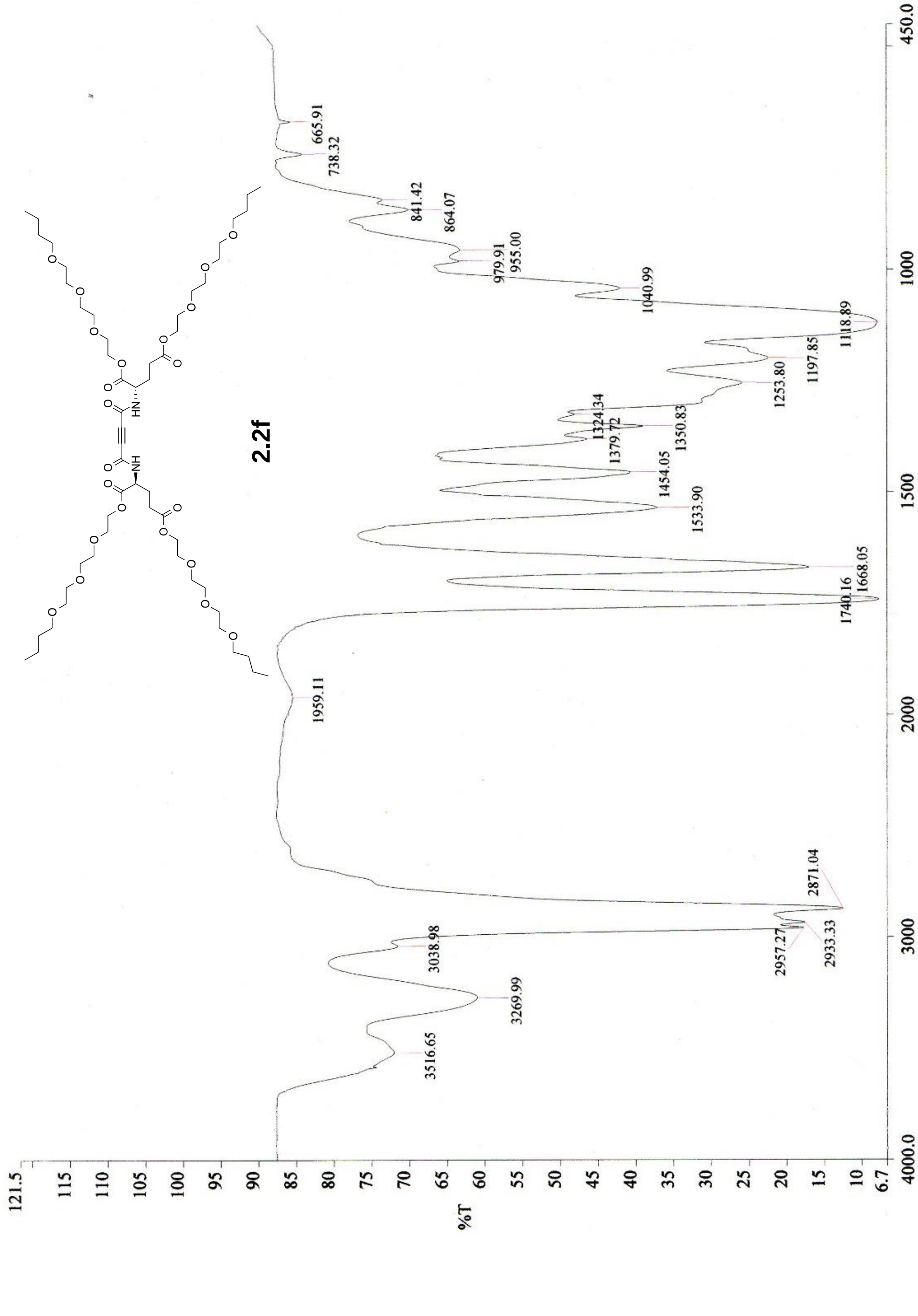
2.2f
%T
cm-1
121.5
115
110
105
100
95
90
85
80
75
70
65
60
55
50
45
40
35
30
25
20
15
10
6.7
4000.0
3000
2000
1500
1000
450.0
3516.65
3269.99
3038.98
2957.27
2933.33
2871.04
1959.11
1740.16
1668.05
1533.90
1454.05
1379.72
1350.83
1324.34
1253.80
1197.85
1118.89
1040.99
979.91
955.00
864.07
841.42
738.32
665.91

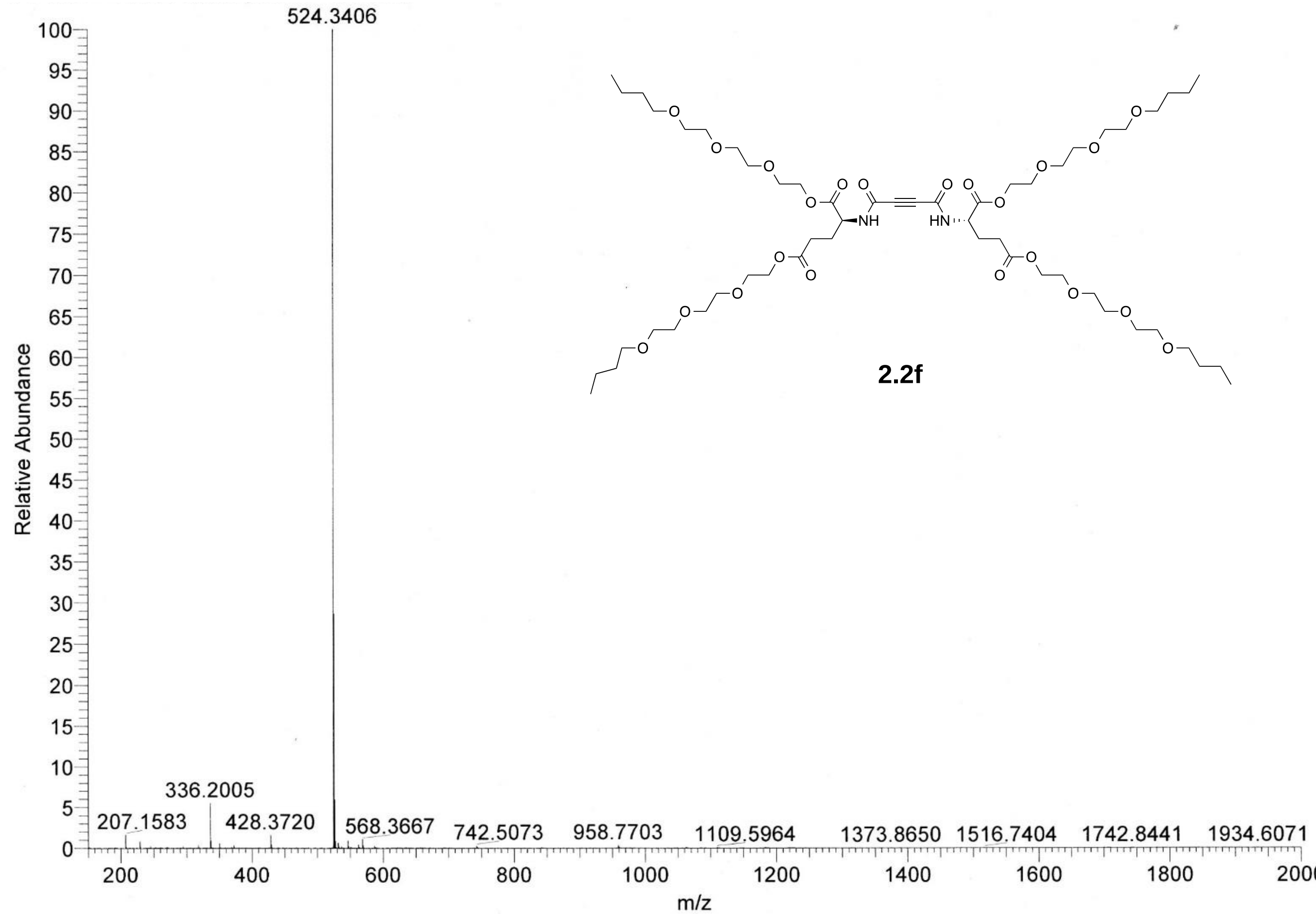
524.3406
Relative Abundance
100
95
90
85
80
75
70
65
60
55
50
45
40
35
30
25
20
15
10
5
0
336.2005
207.1583
428.3720
568.3667
742.5073
958.7703
1109.5964
1373.8650
1516.7404
1742.8441
1934.6071
200
400
600
800
1000
1200
1400
1600
1800
2000
m/z
O
NH
HN
2.2f

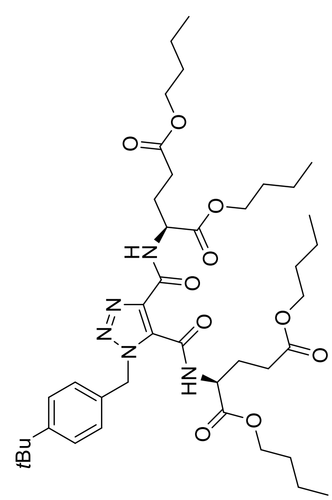
tBu
N
N=N
O
HN
O
O
O
O
HN
O
O
O
O

2.4

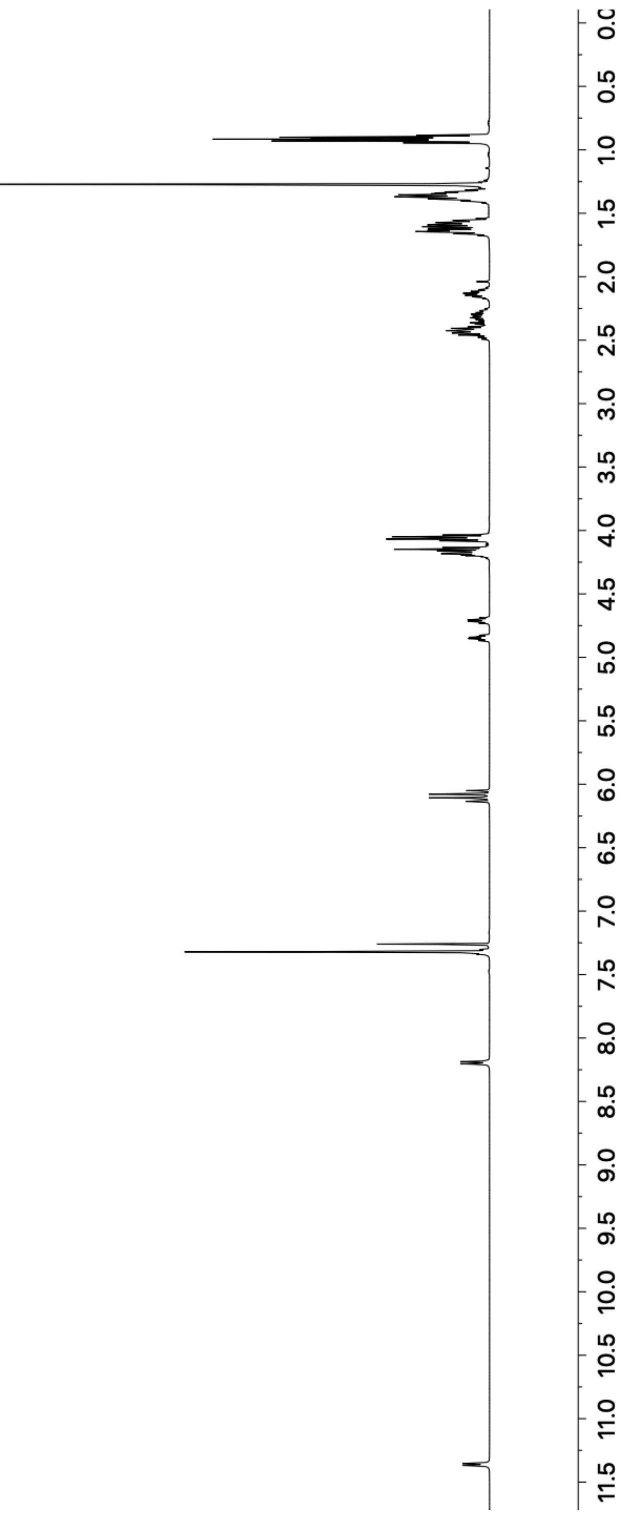
0.0
0.5
1.0
1.5
2.0
2.5
3.0
3.5
4.0
4.5
5.0
5.5
6.0
6.5
7.0
7.5
8.0
8.5
9.0
9.5
10.0
10.5
11.0
11.5
f1 (ppm)

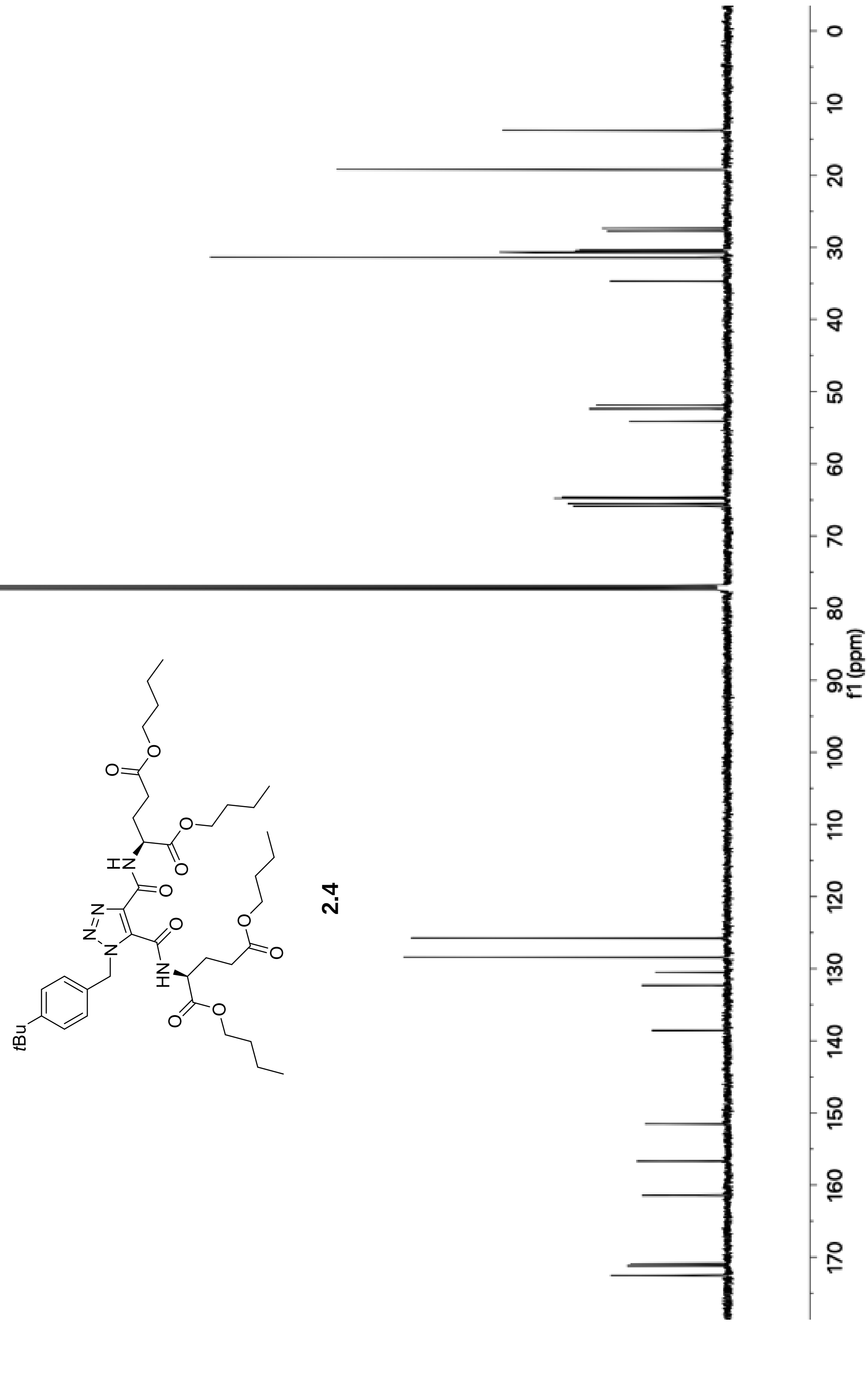

tBu
N
N
N
O
HN
O
O
O
O
H
N
O
O
O
O
O
2.4
f1 (ppm)
0
10
20
30
40
50
60
70
80
90
100
110
120
130
140
150
160
170

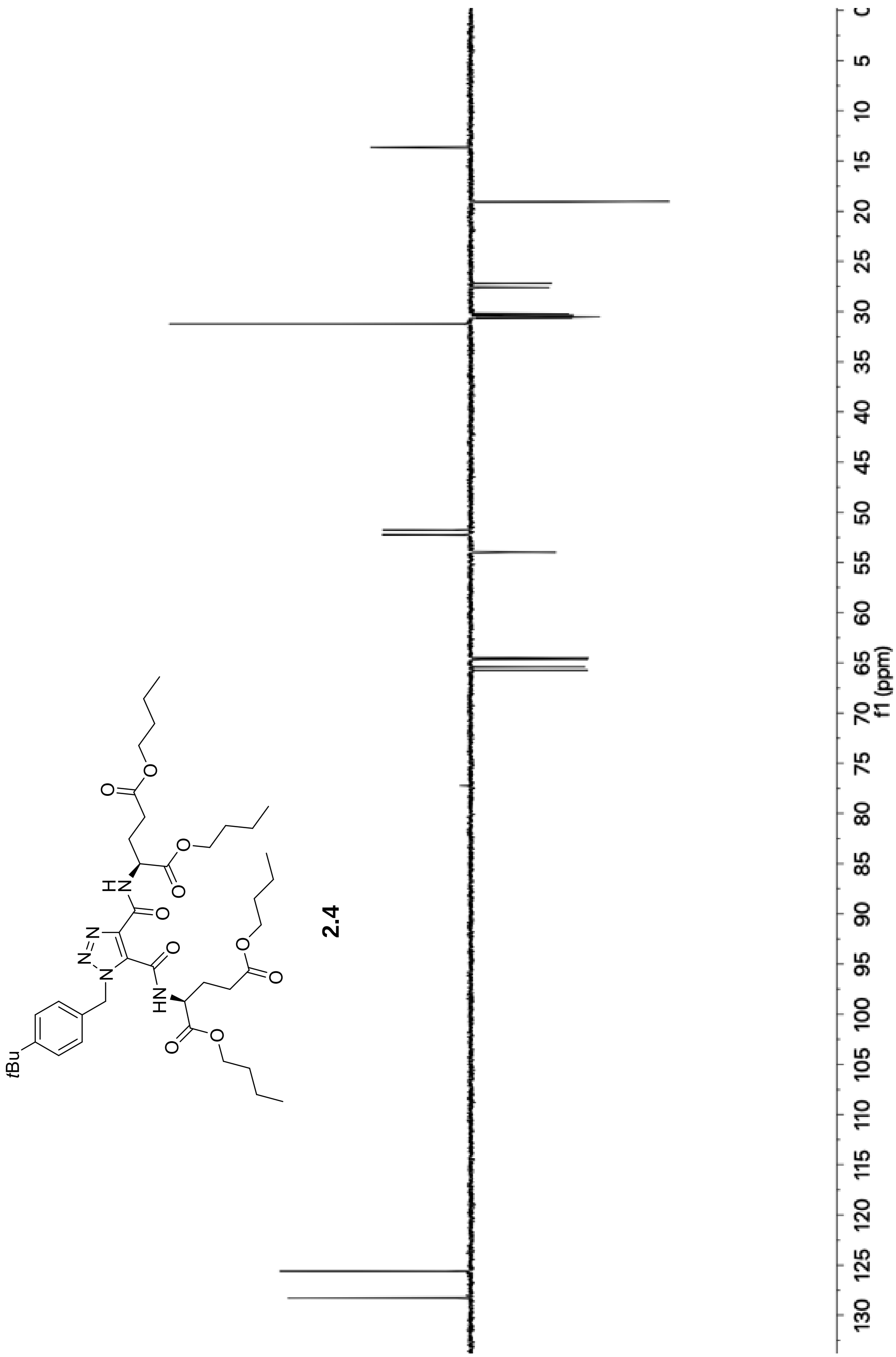
2.4
f1 (ppm)

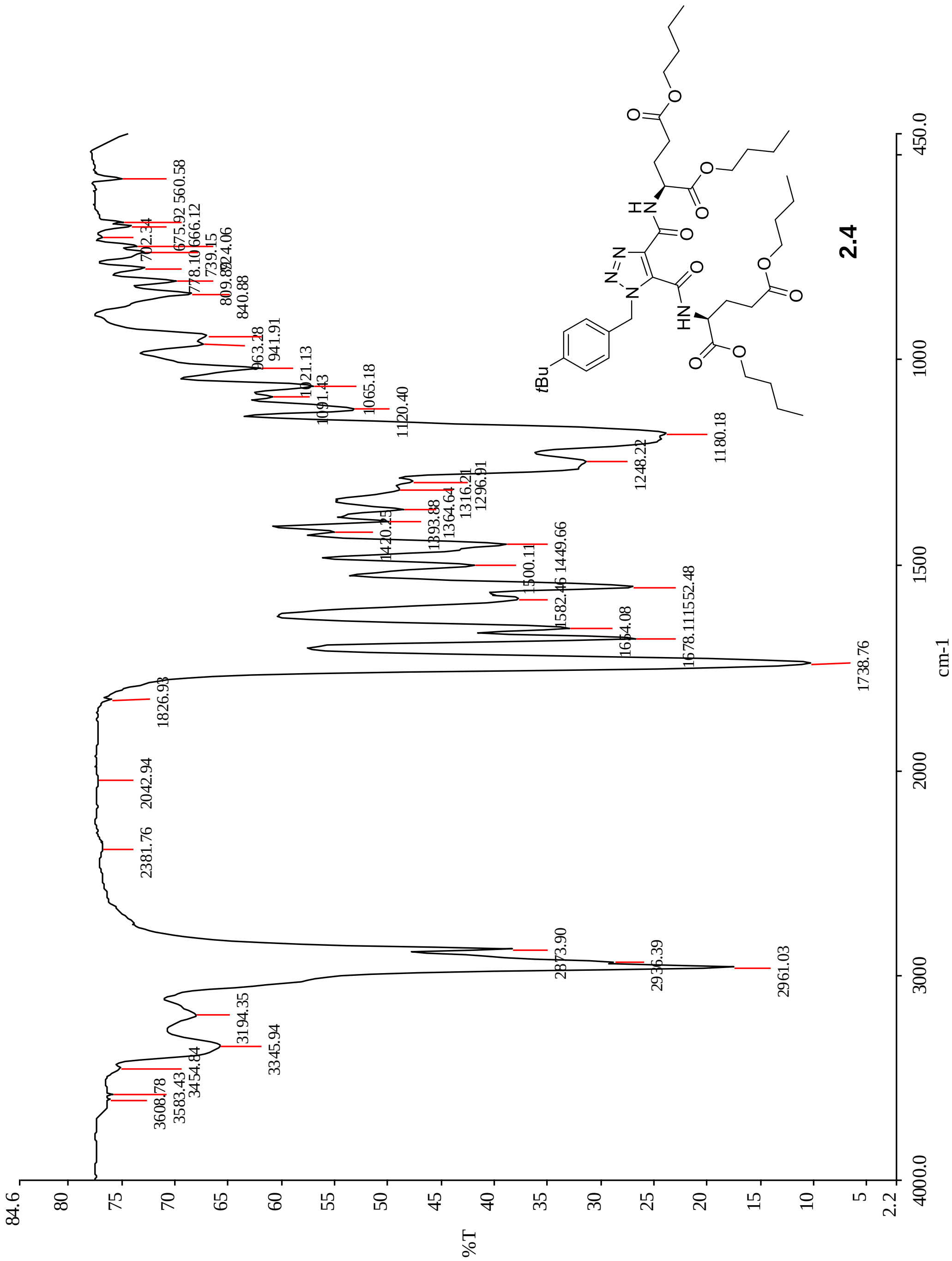
%T
cm-1
tBu
2.4

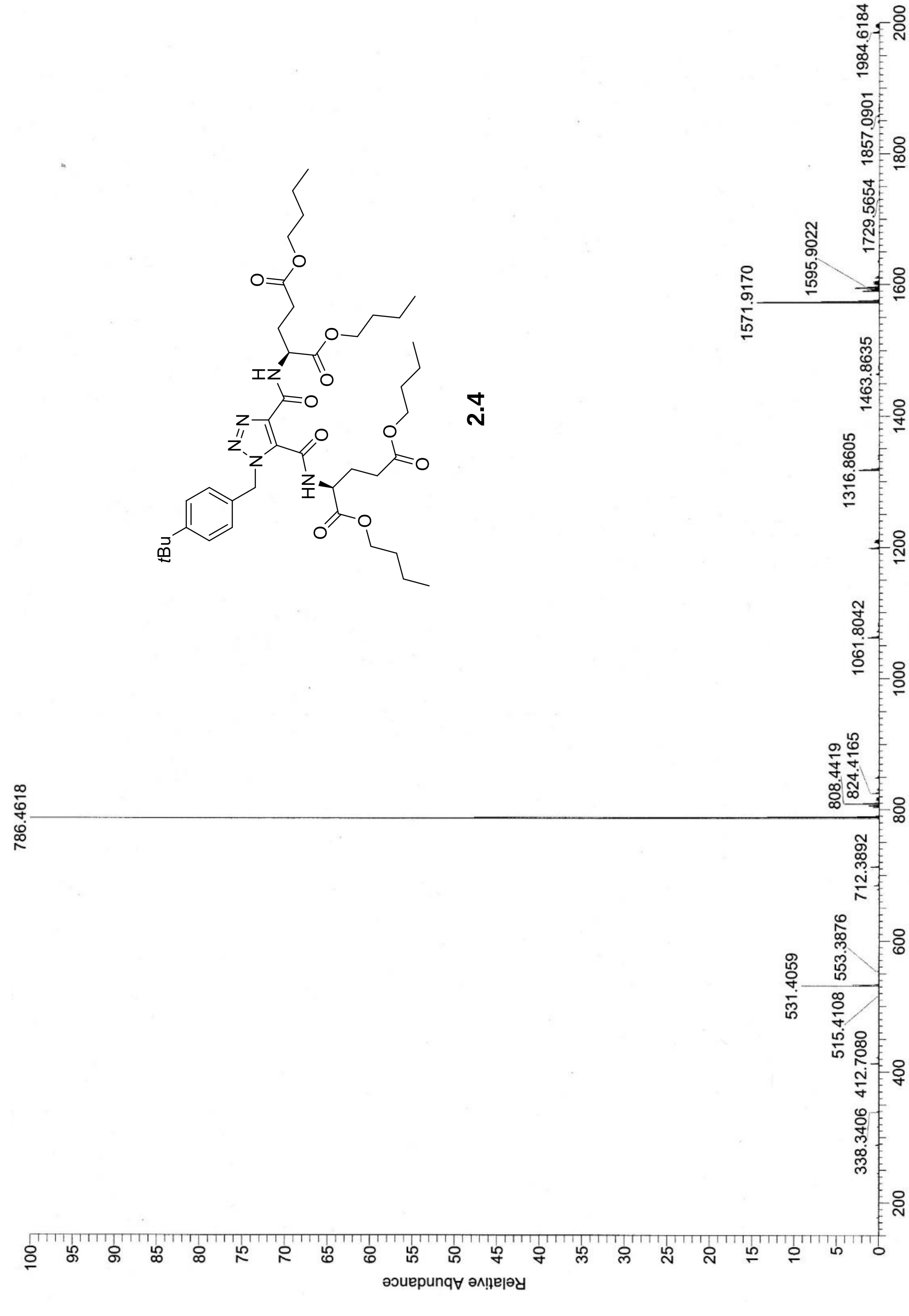

786.4618
531.4059
515.4108
553.3876
412.7080
338.3406
712.3892
808.4419
824.4165
1061.8042
1316.8605
1463.8635
1571.9170
1595.9022
1729.5654
1857.0901
1984.6184
m/z
Relative Abundance
tBu
2.4

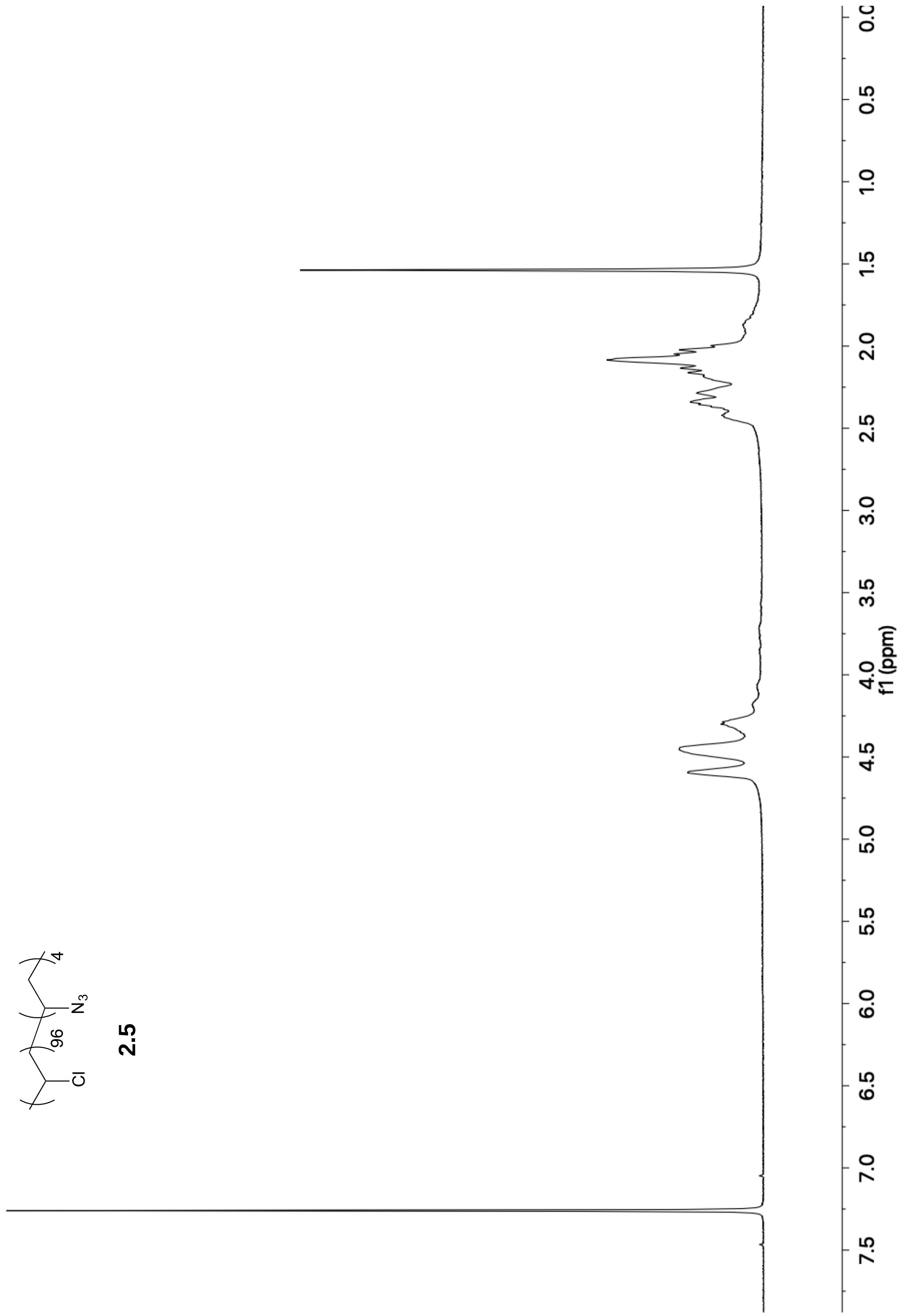
Cl
96
N3
4
2.5
7.5
7.0
6.5
6.0
5.5
5.0
4.5
4.0
3.5
3.0
2.5
2.0
1.5
1.0
0.5
0.0
f1 (ppm)

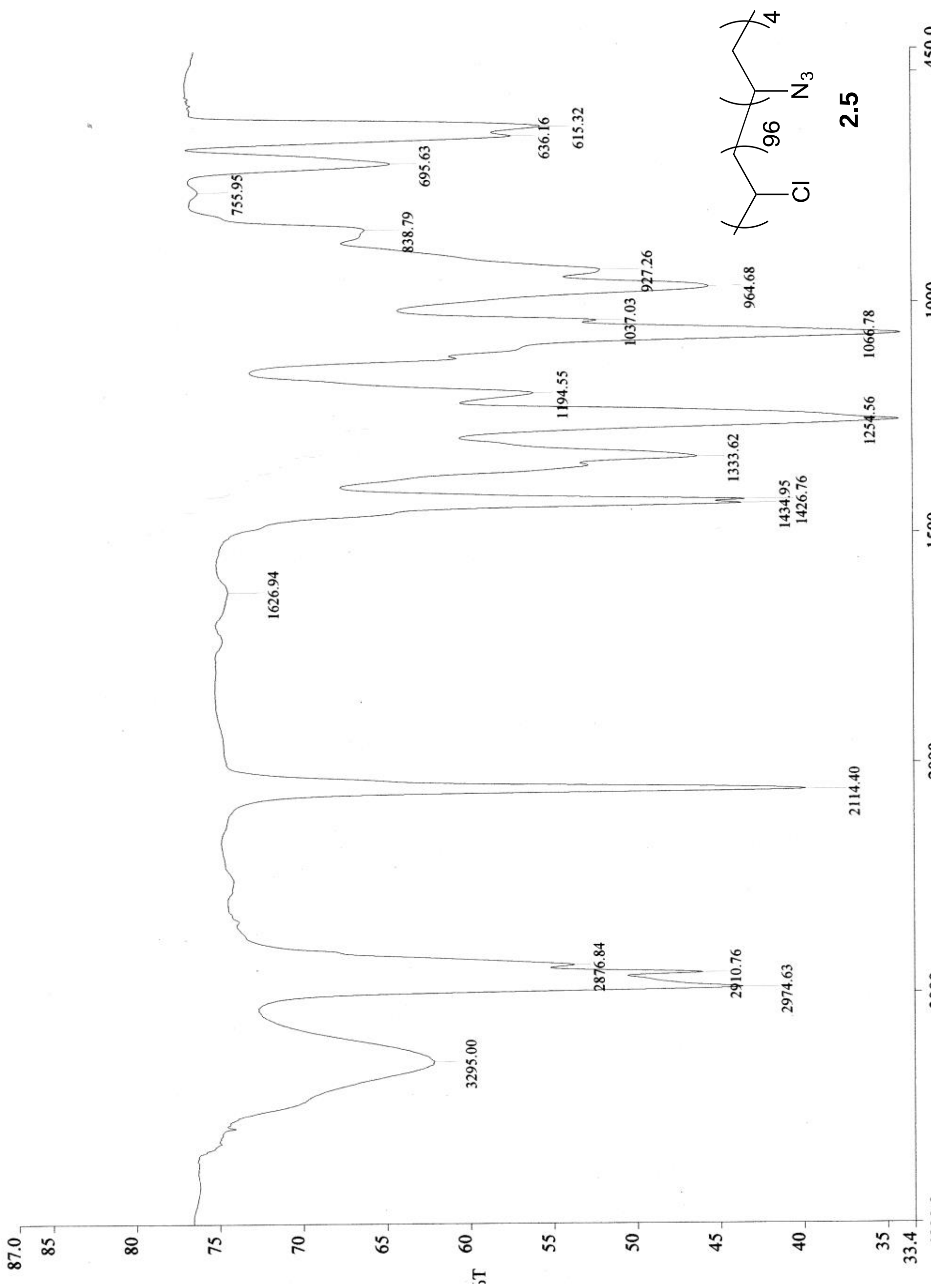

%T
cm-1
4000.0
3000
2000
1500
1000
450.0
87.0
85
80
75
70
65
60
55
50
45
40
35
33.4
3295.00
2974.63
2910.76
2876.84
2114.40
1626.94
1434.95
1426.76
1333.62
1254.56
1194.55
1066.78
1037.03
964.68
927.26
838.79
755.95
695.63
636.16
615.32
Cl
N3
96
4
2.5

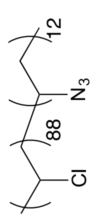

2.5'

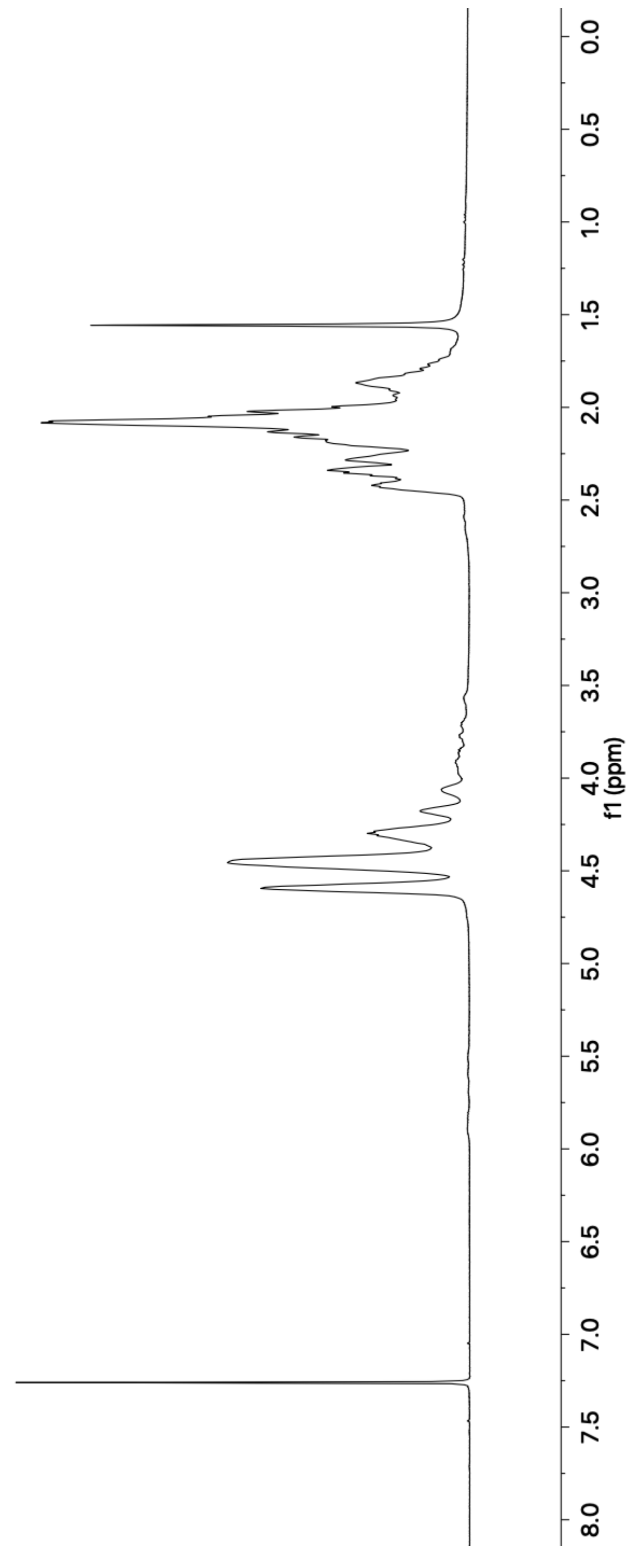

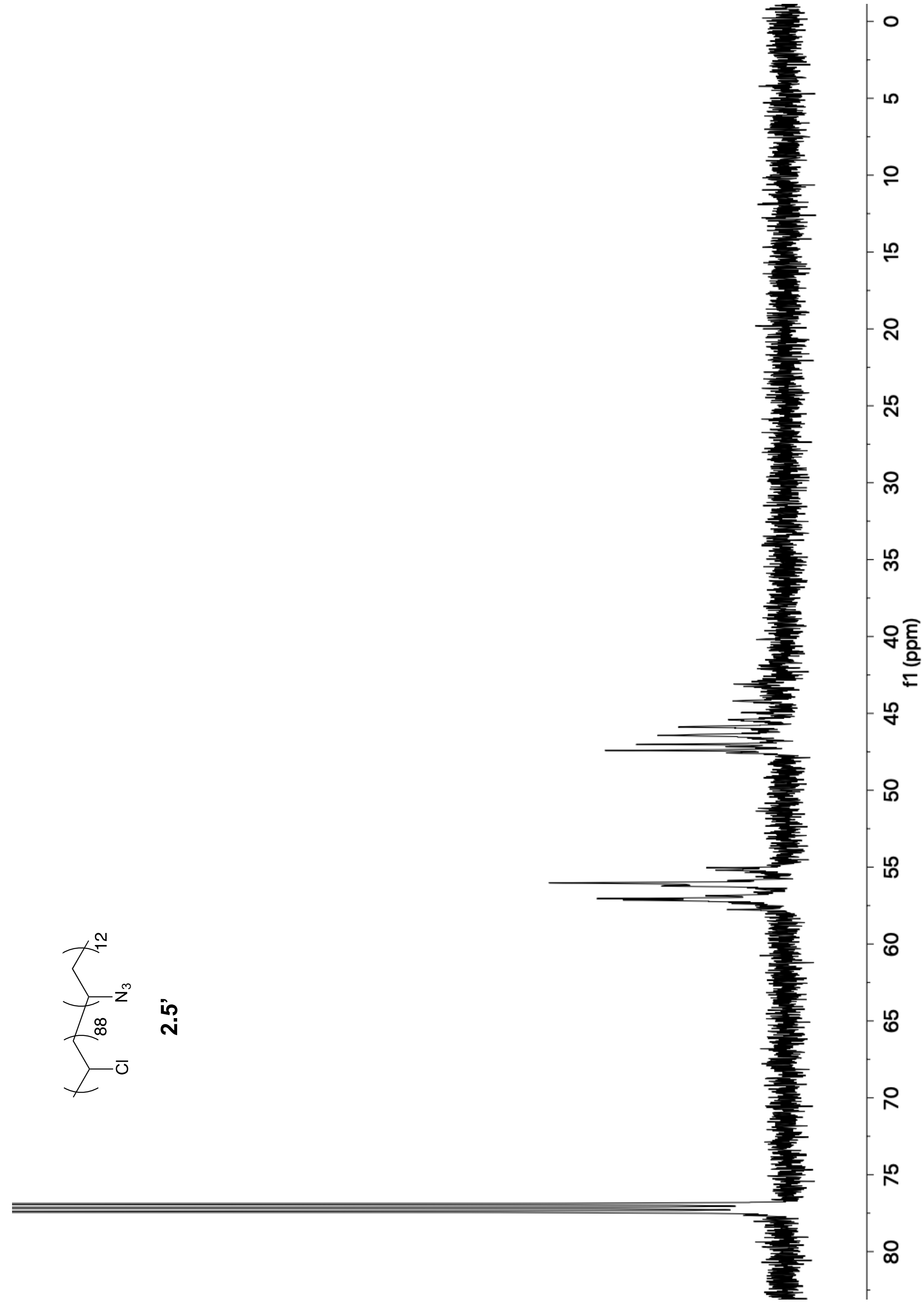

2.5'

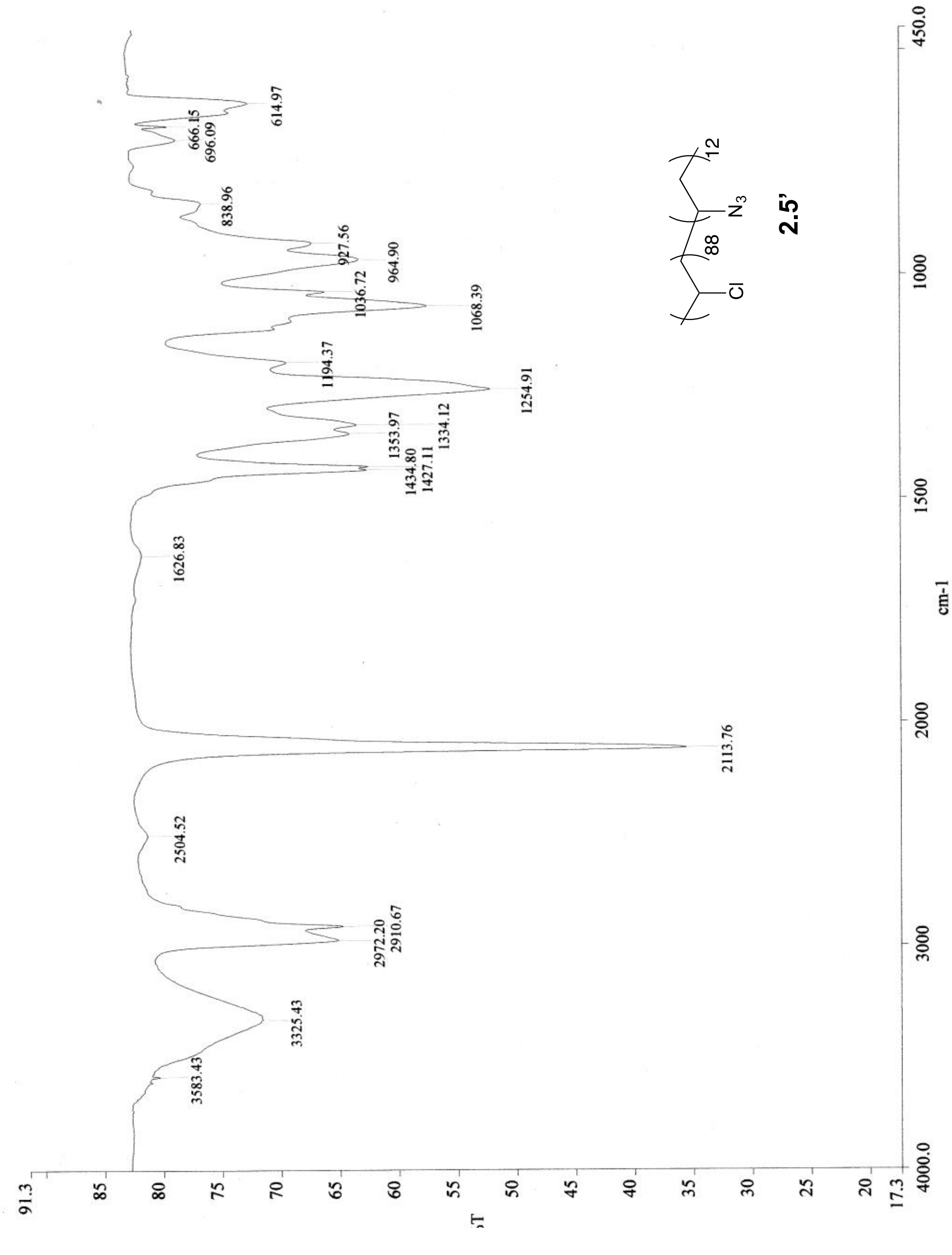

%T
cm-1
4000.0
3000
2000
1500
1000
450.0
91.3
85
80
75
70
65
60
55
50
45
40
35
30
25
20
17.3
3583.43
3325.43
2972.20
2910.67
2504.52
2113.76
1626.83
1434.80
1427.11
1353.97
1334.12
1254.91
1194.37
1068.39
1036.72
964.90
927.56
838.96
696.09
666.15
614.97
Cl
88
N3
12
2.5'

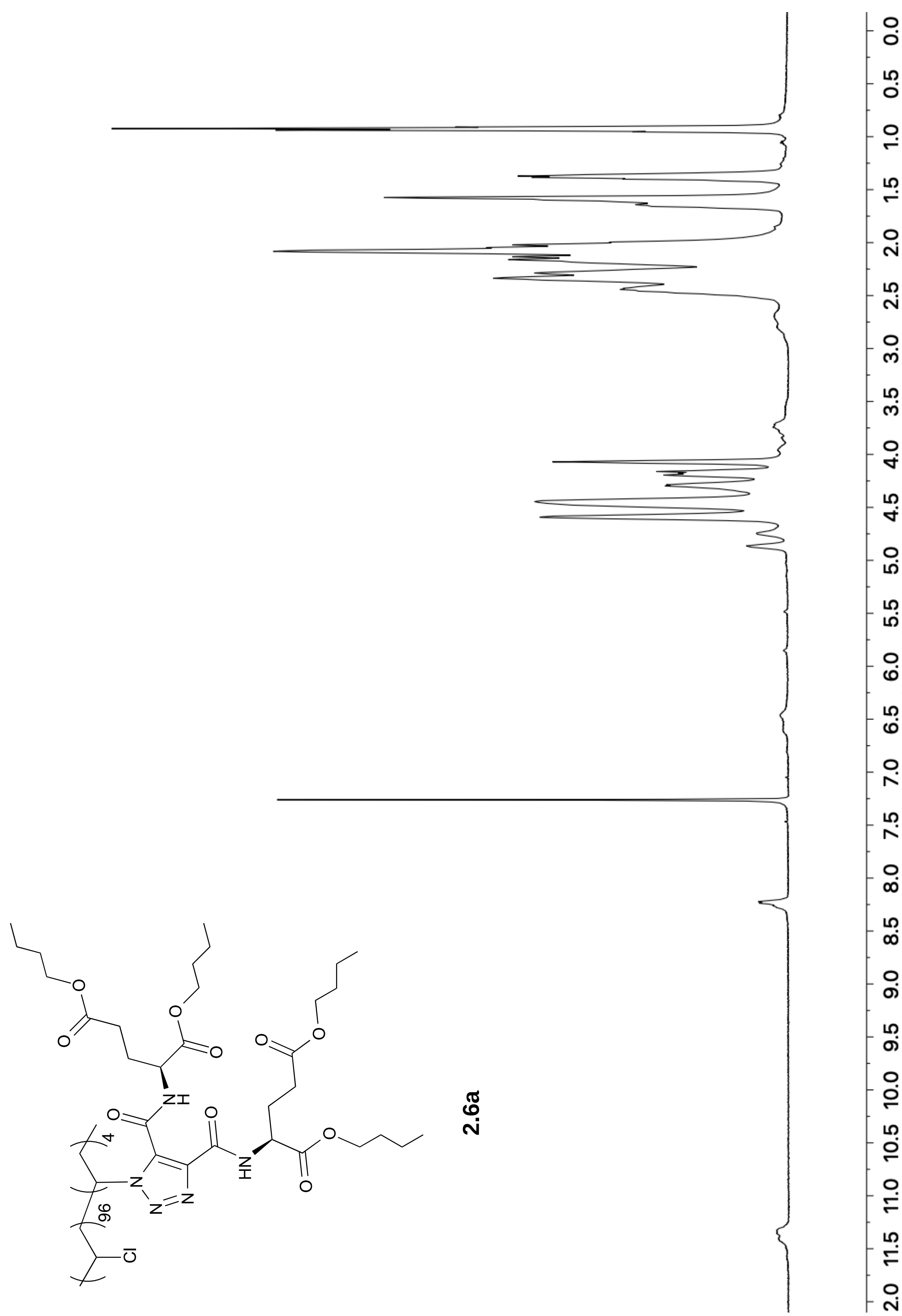
2.6a
f1 (ppm)

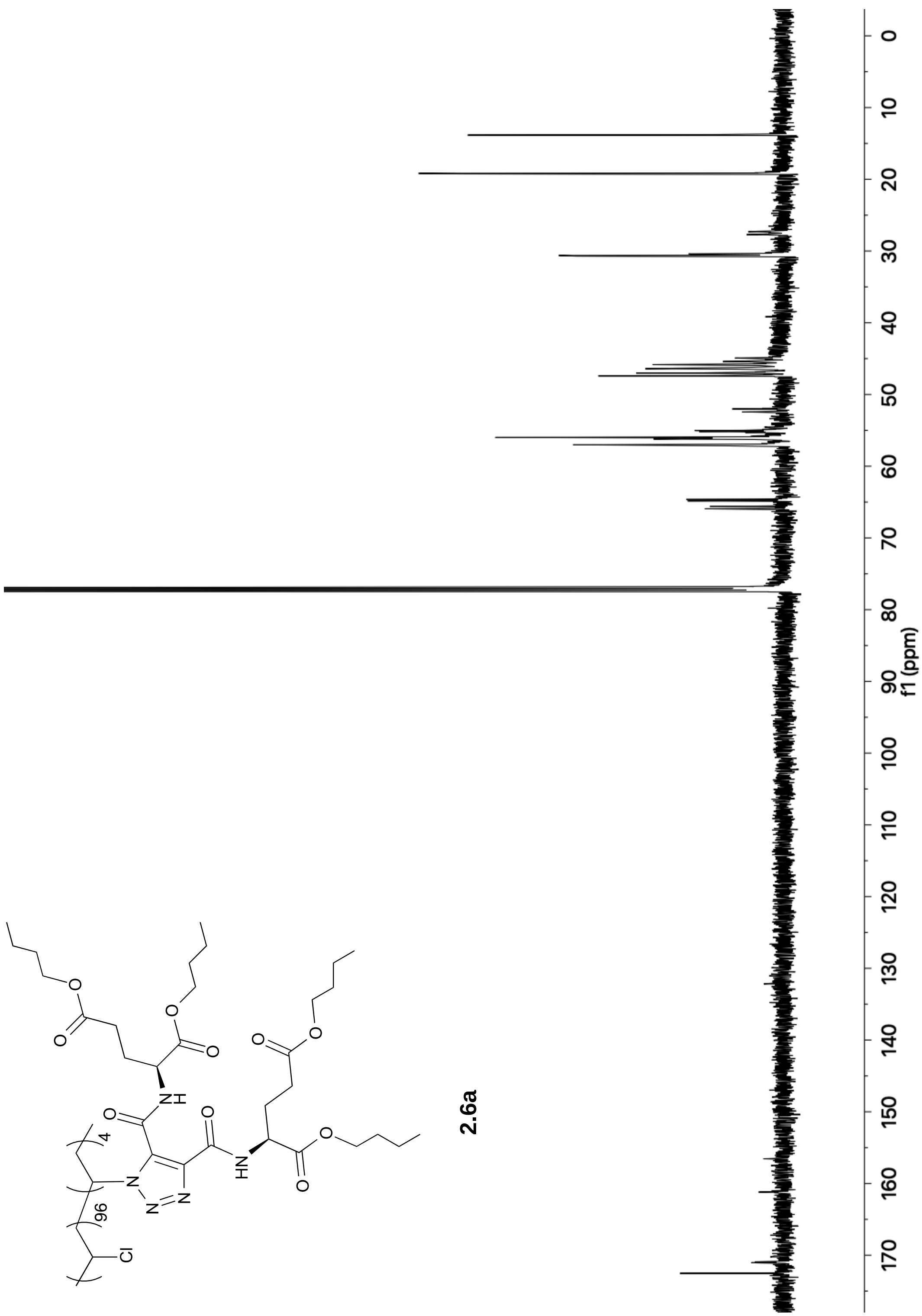

2.6a

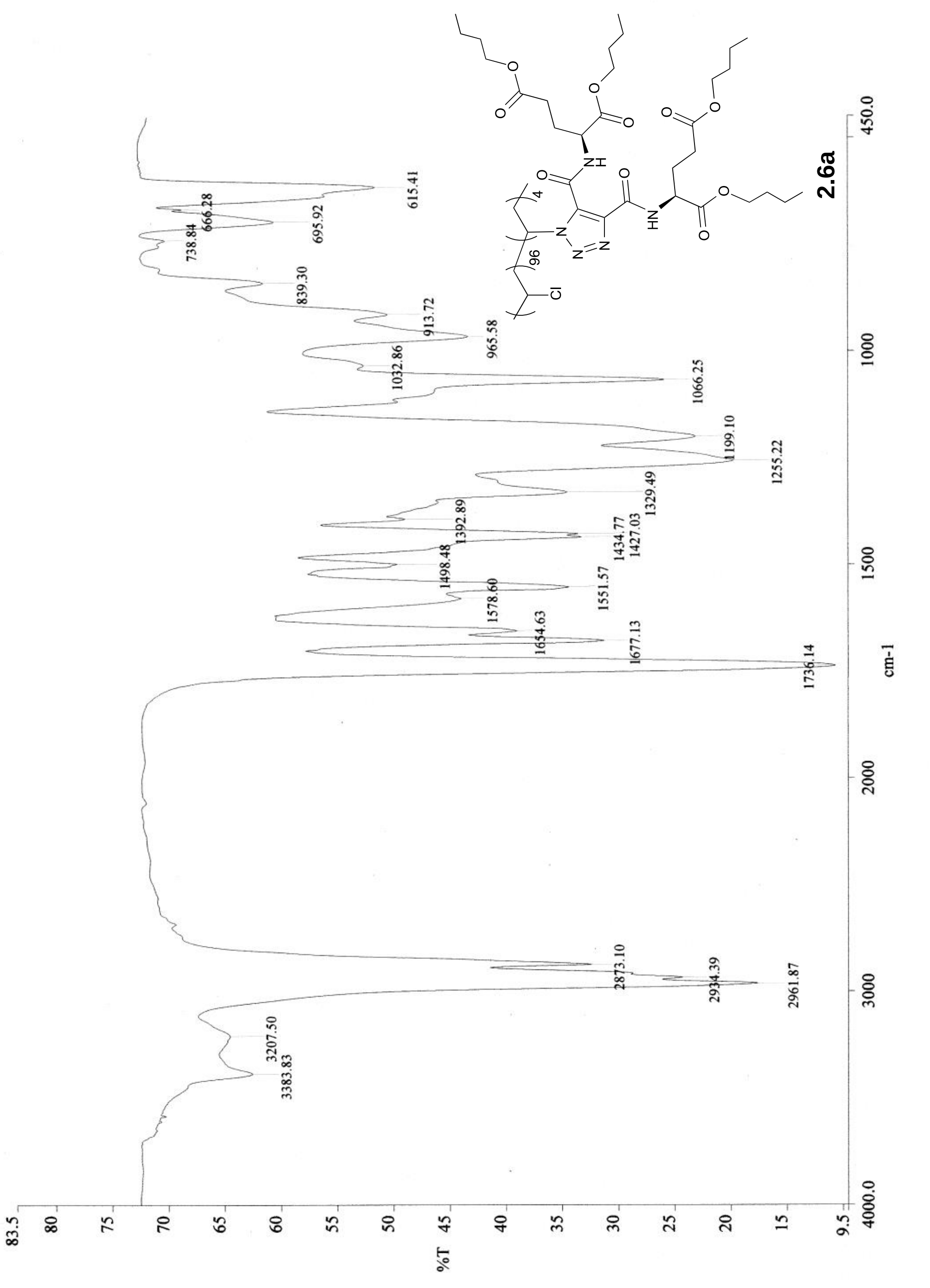
2.6a
%T
cm-1
1736.14
1677.13
1654.63
1578.60
1551.57
1498.48
1434.77
1427.03
1392.89
1329.49
1255.22
1199.10
1066.25
1032.86
965.58
913.72
839.30
738.84
695.92
666.28
615.41
2961.87
2934.39
2873.10
3207.50
3383.83

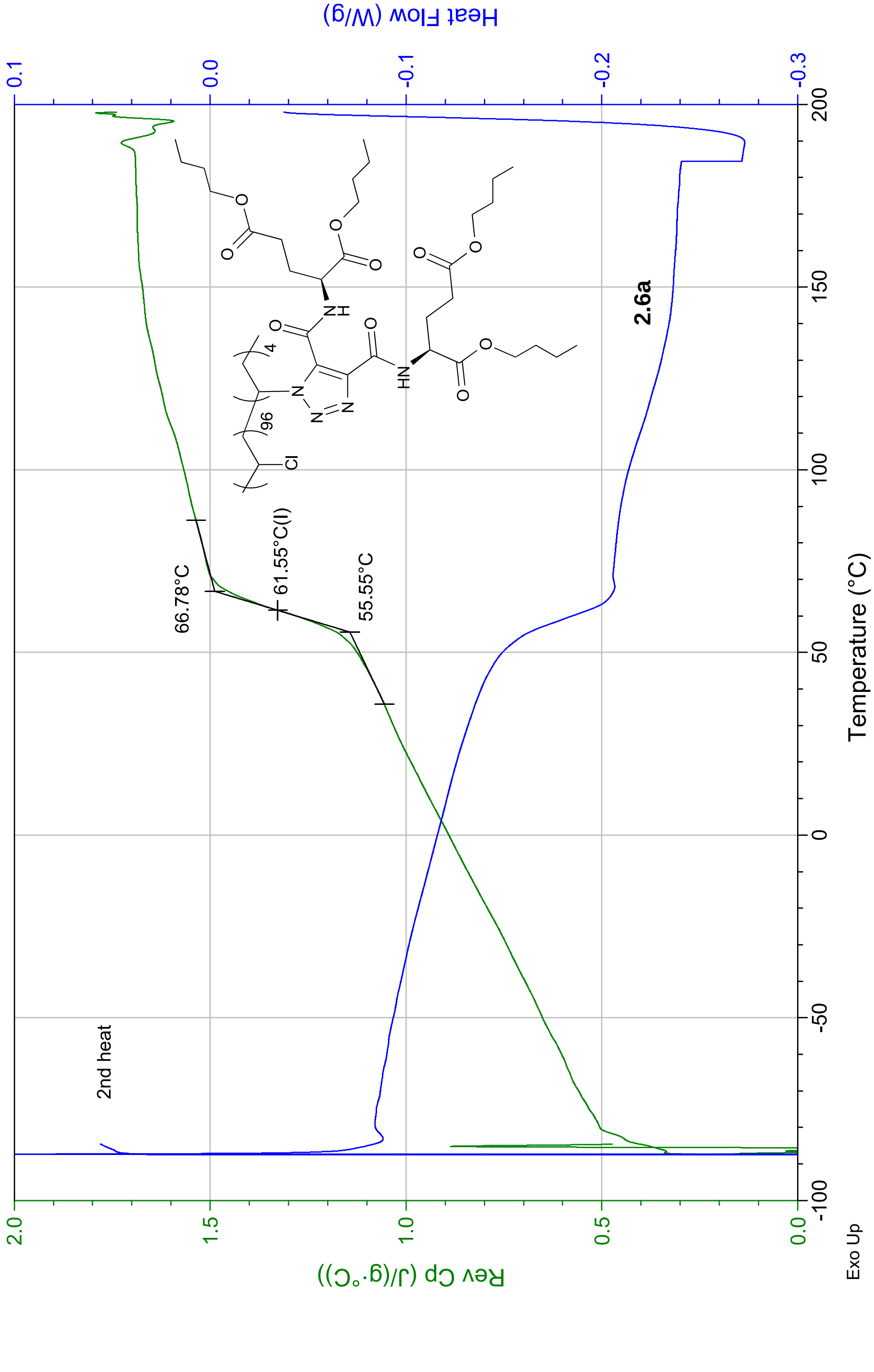
2nd heat
66.78°C
61.55°C(I)
55.55°C
2.6a
Temperature (°C)
Heat Flow (W/g)
Rev Cp (J/(g·°C))
Exo Up

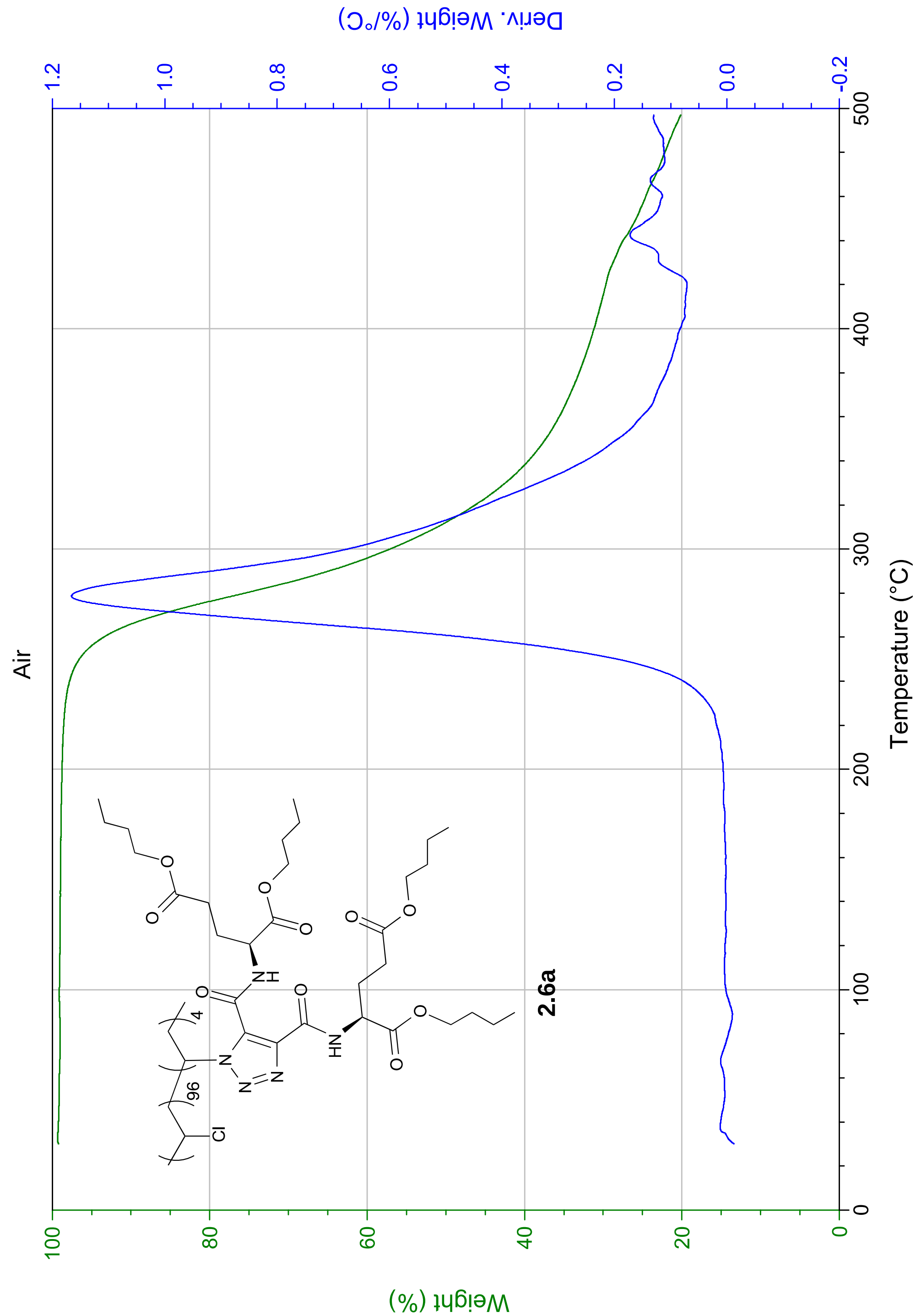
Air
Temperature (°C)
Weight (%)
Deriv. Weight (%/°C)
2.6a
0
100
200
300
400
500
20
40
60
80
-0.2
0.0
0.2
0.4
0.6
0.8
1.0
1.2
Cl
96
4
N
HN
NH
O

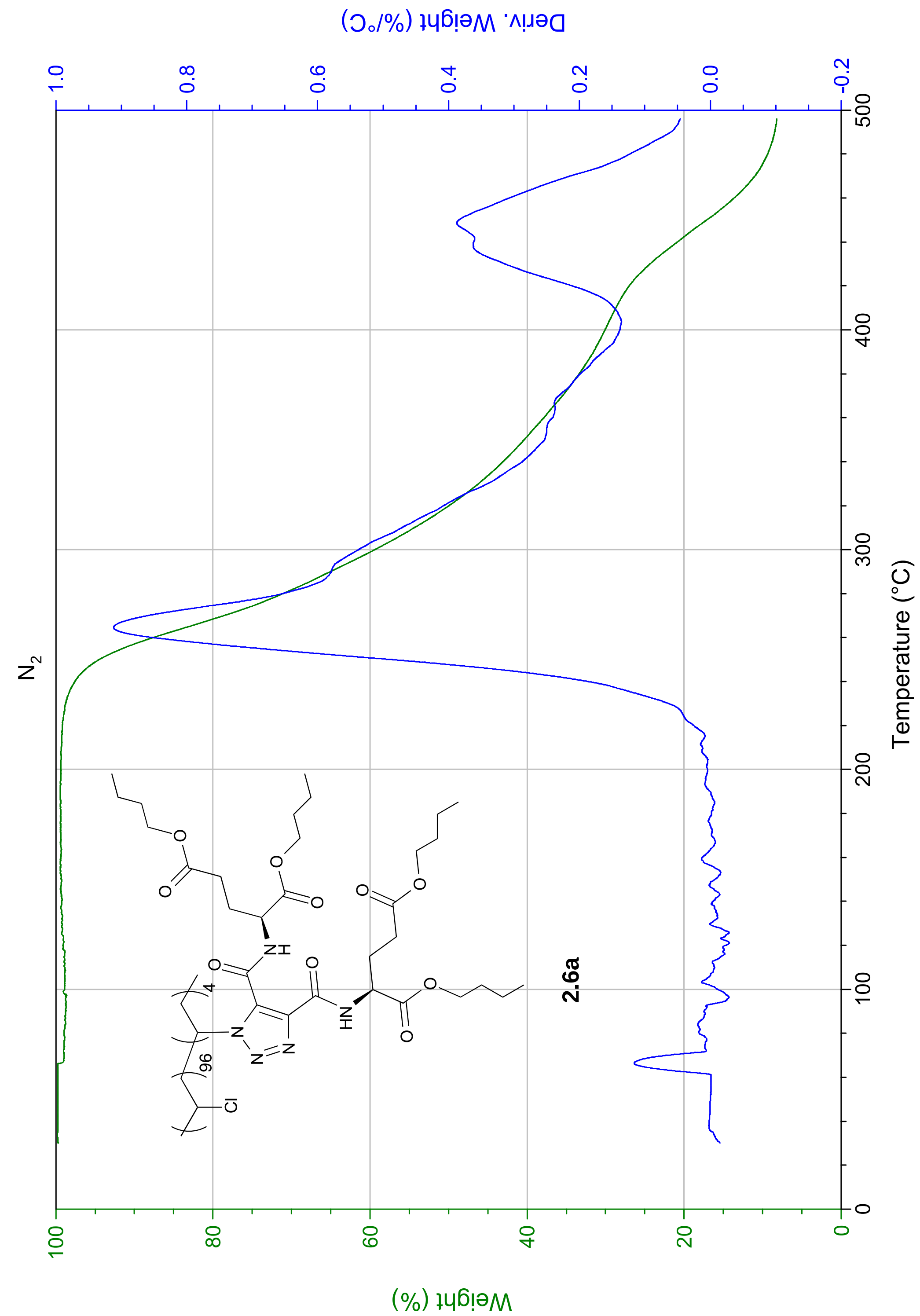
N$_2$
Weight (%)
Deriv. Weight (%/°C)
Temperature (°C)
2.6a

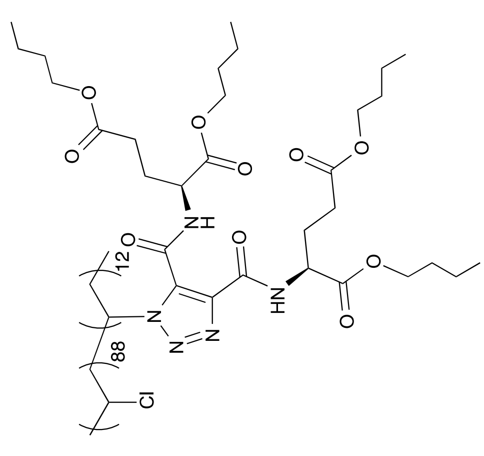

2.6'a

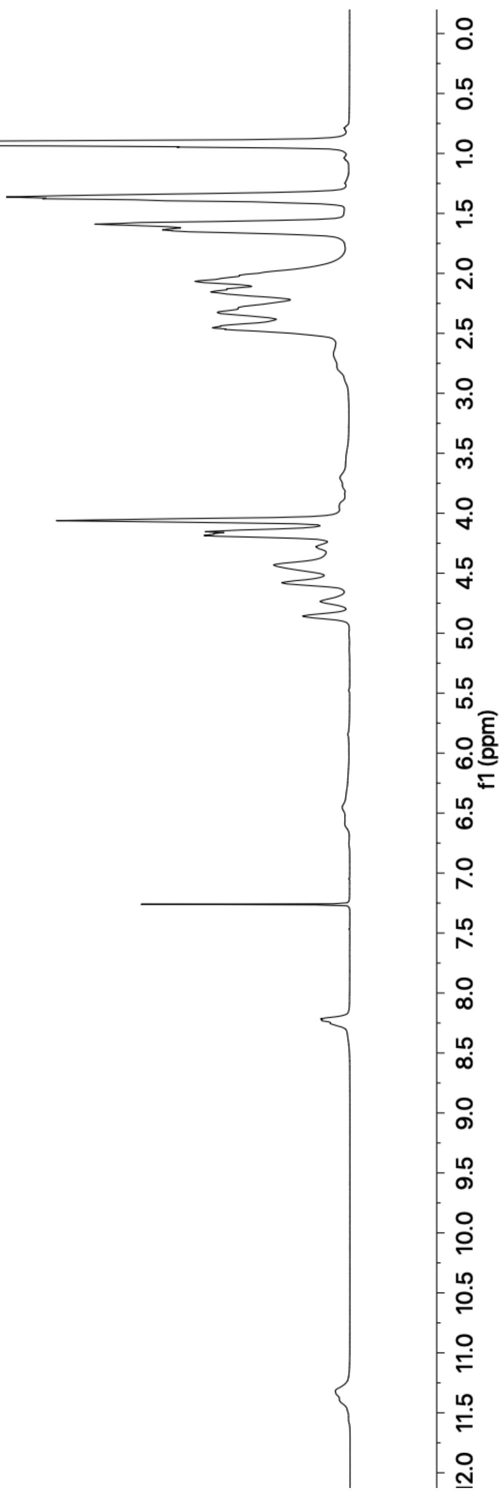

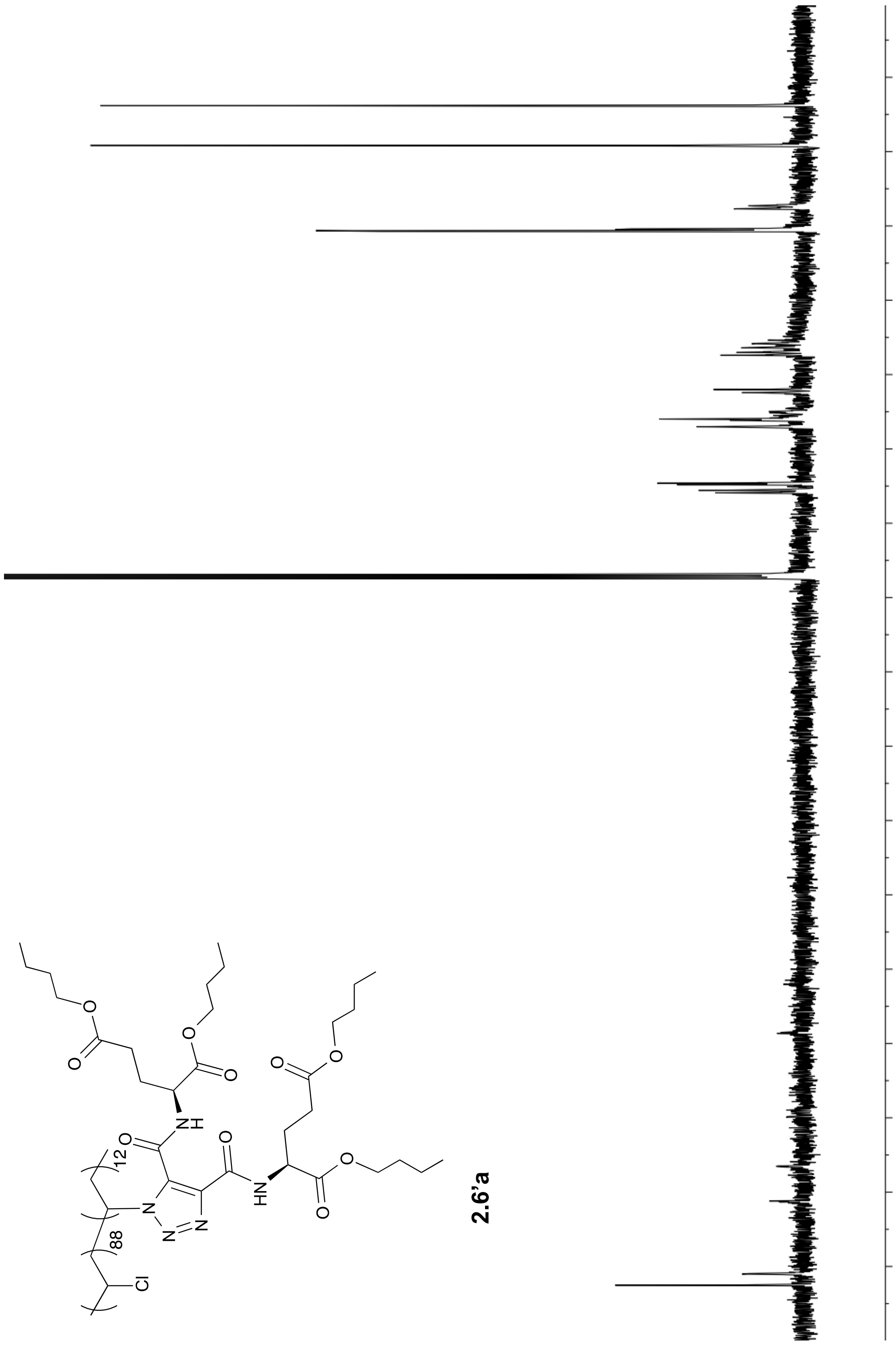
2.6'a
f1 (ppm)

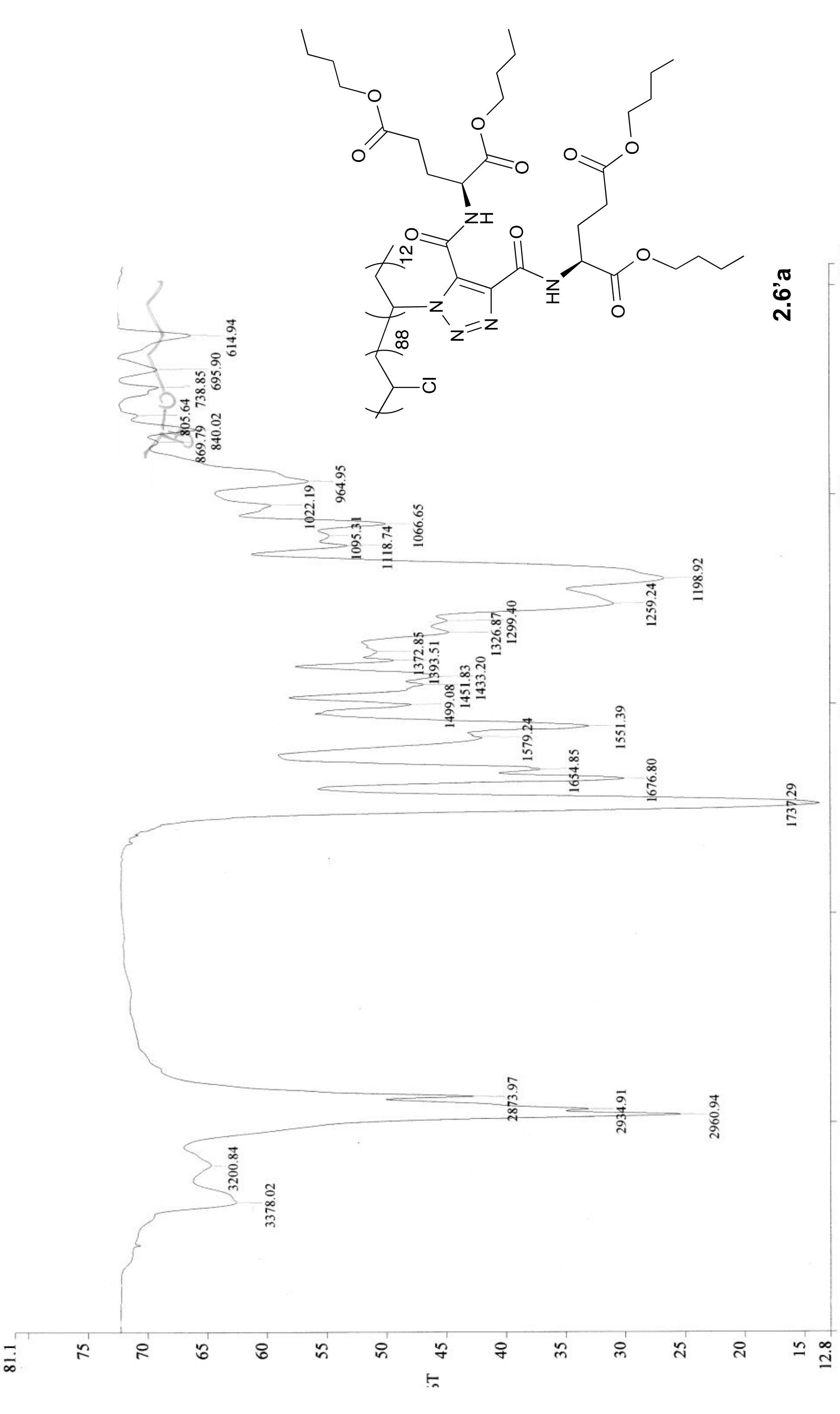
3378.02
3200.84
2960.94
2934.91
2873.97
1737.29
1676.80
1654.85
1579.24
1551.39
1499.08
1451.83
1433.20
1393.51
1372.85
1326.87
1299.40
1259.24
1198.92
1118.74
1095.31
1066.65
1022.19
964.95
869.79
840.02
805.64
738.85
695.90
614.94
4000.0
3000
2000
1500
1000
450.0
cm-1
81.1
75
70
65
60
55
50
45
40
35
30
25
20
15
12.8
%T
88
12
Cl
N
HN
NH
O

2.6'a

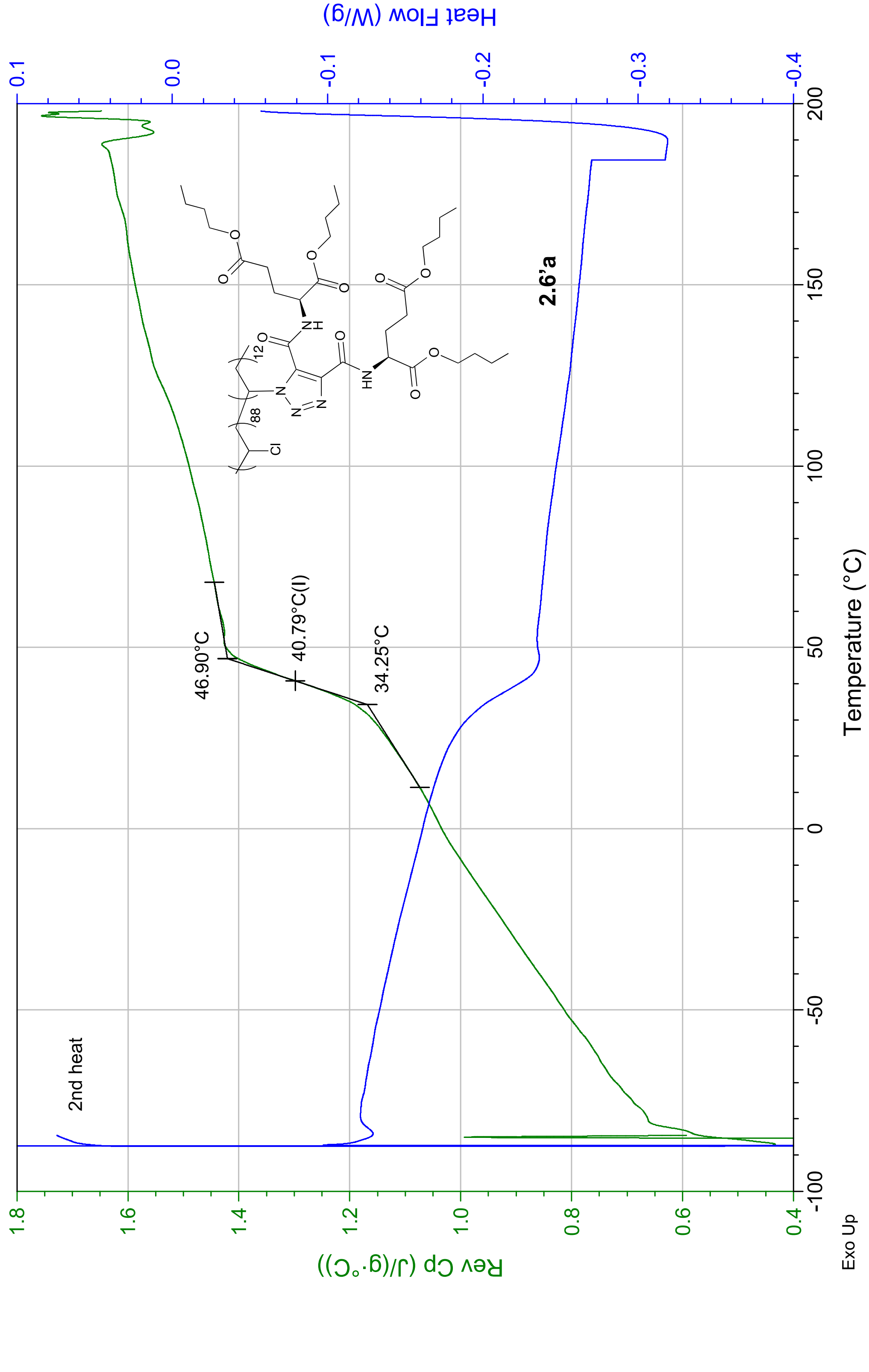

Heat Flow (W/g)
Rev Cp (J/(g·°C))
Temperature (°C)
Exo Up
2nd heat
46.90°C
40.79°C(I)
34.25°C
2.6’a

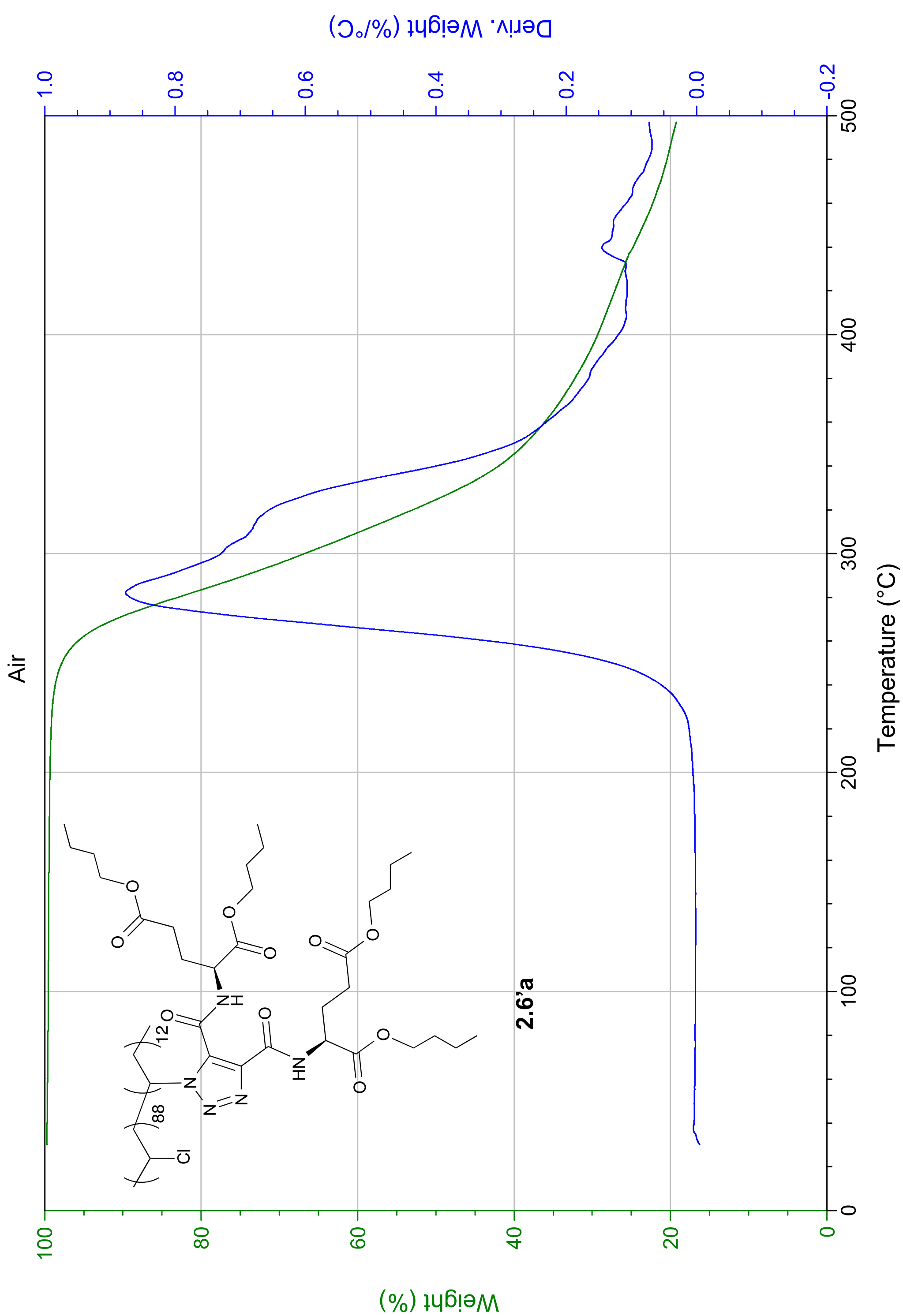
Air
Temperature (°C)
Weight (%)
Deriv. Weight (%/°C)
2.6'a

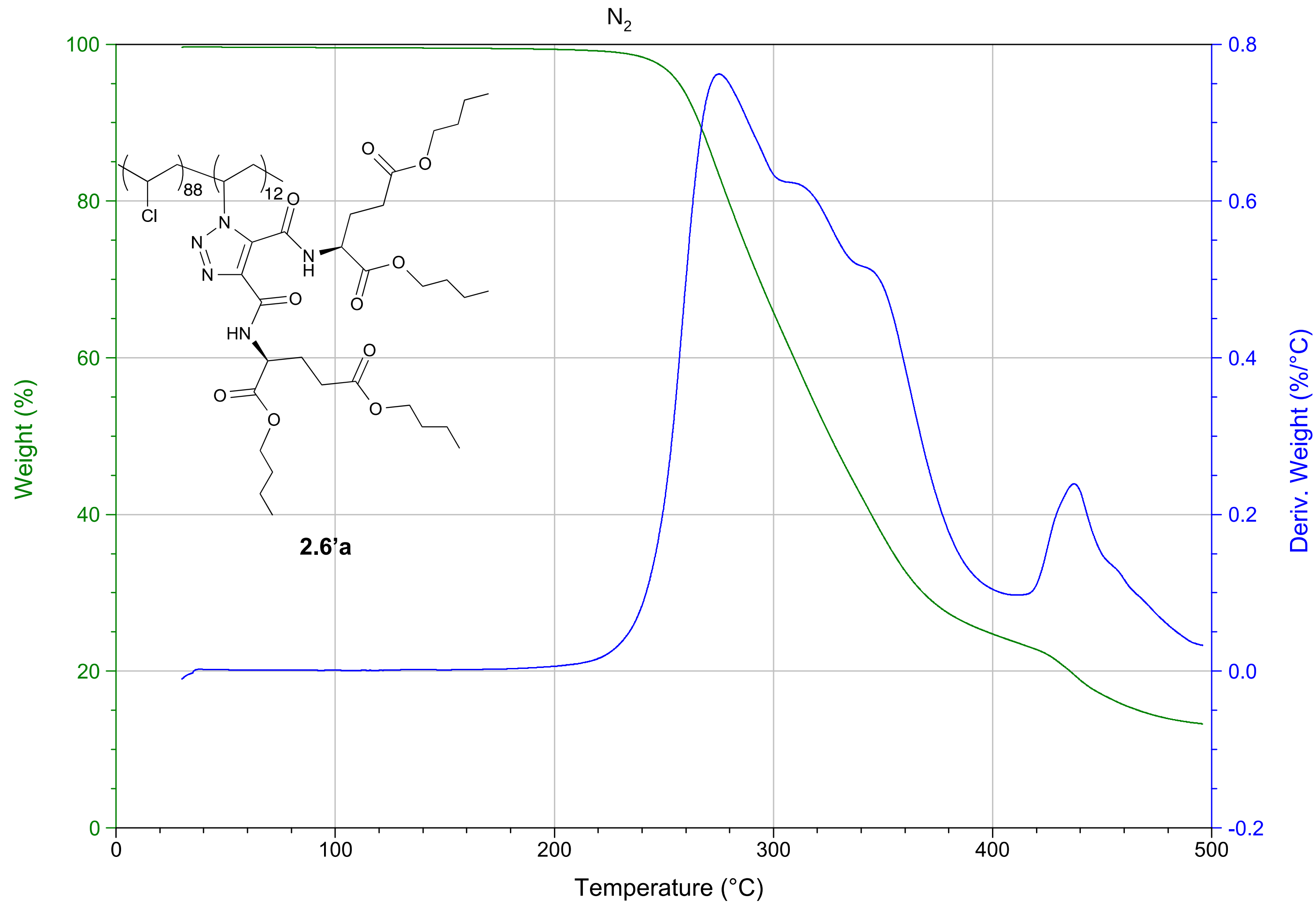
N2
2.6’a
Cl
88
12
Weight (%)
Deriv. Weight (%/°C)
Temperature (°C)
0
20
40
60
80
100
-0.2
0.0
0.2
0.4
0.6
0.8
0
100
200
300
400
500

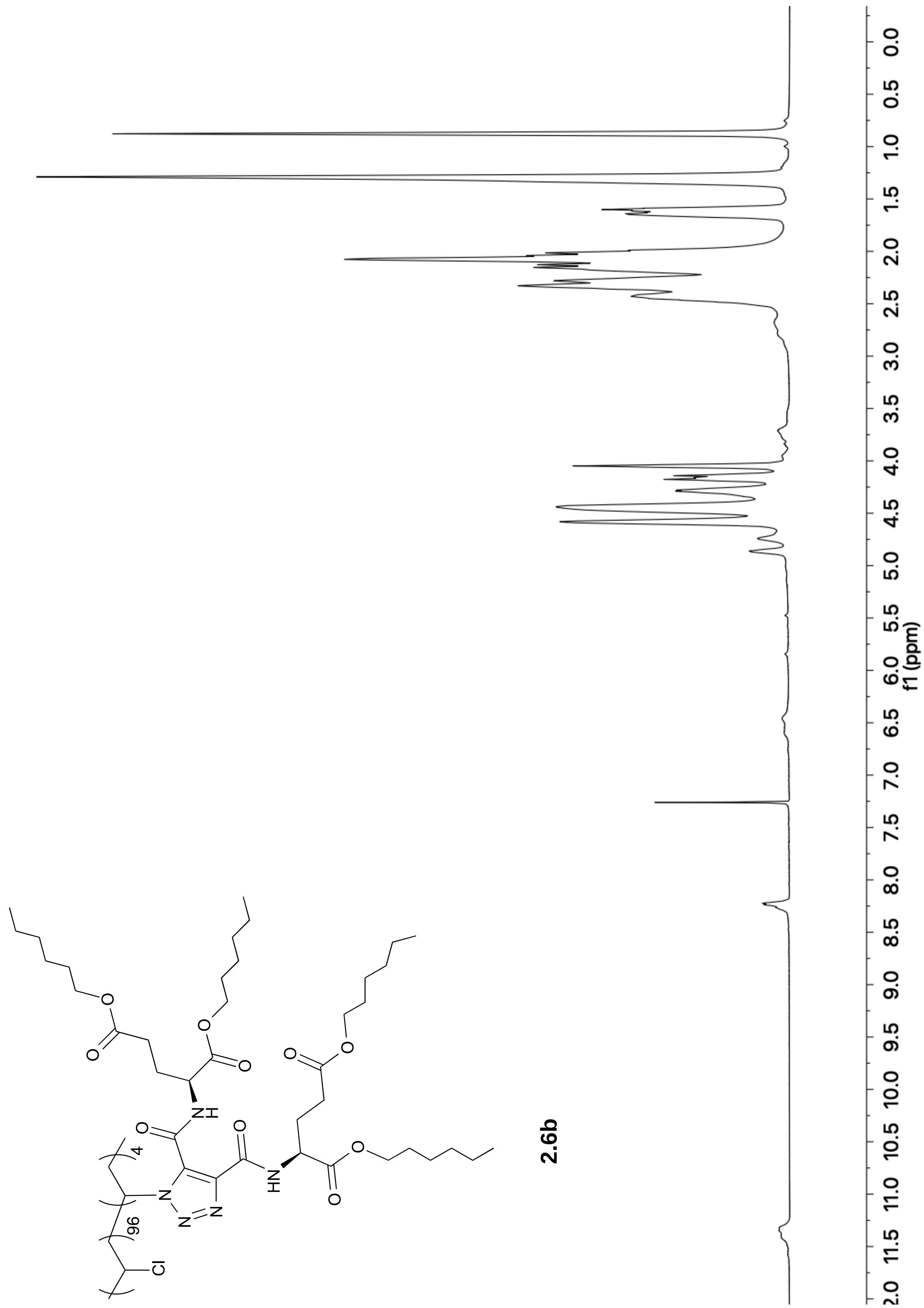

2.6b

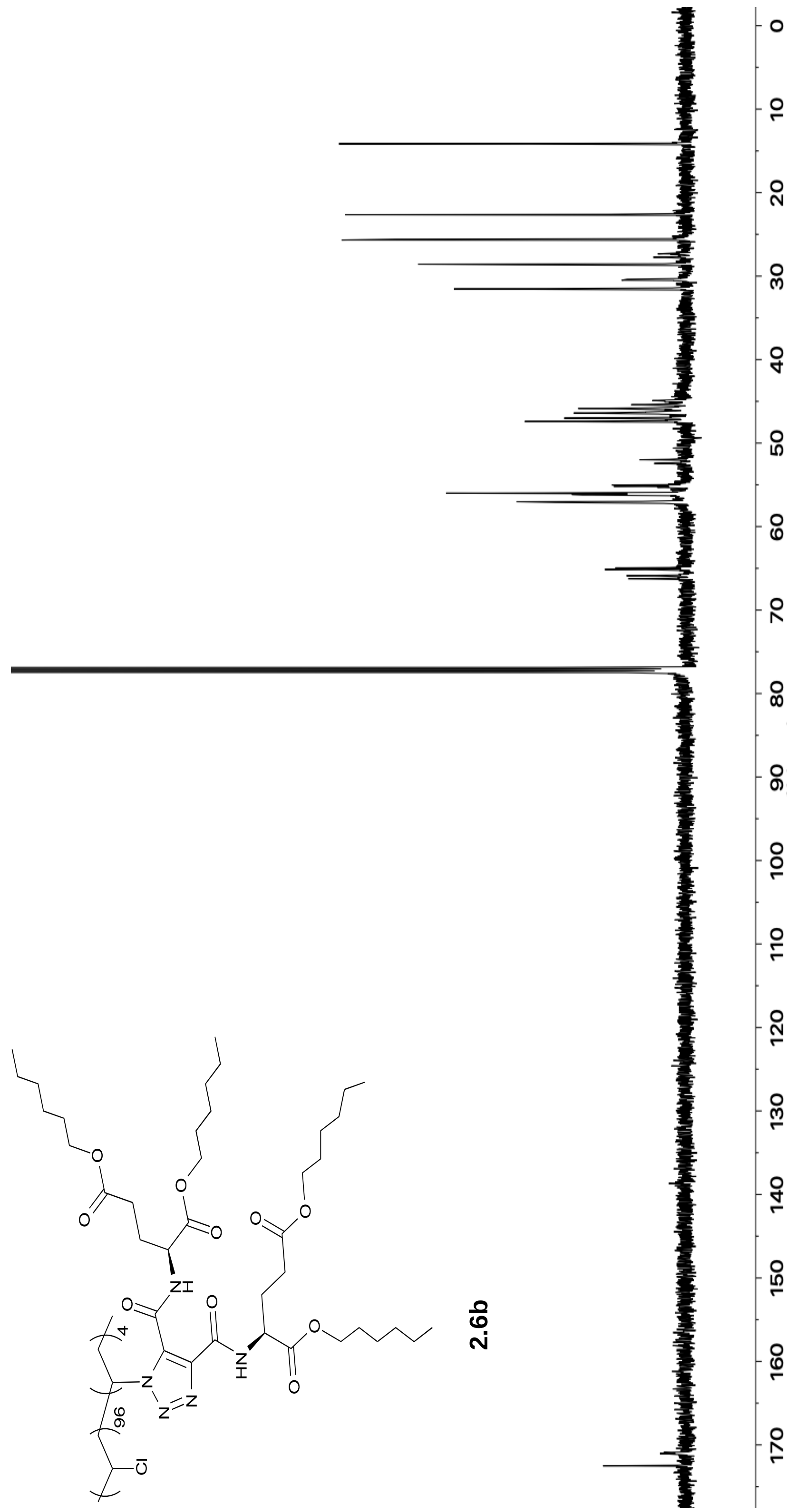
f1 (ppm)
0
10
20
30
40
50
60
70
80
90
100
110
120
130
140
150
160
170
Cl
96
4
HN
O

2.6b

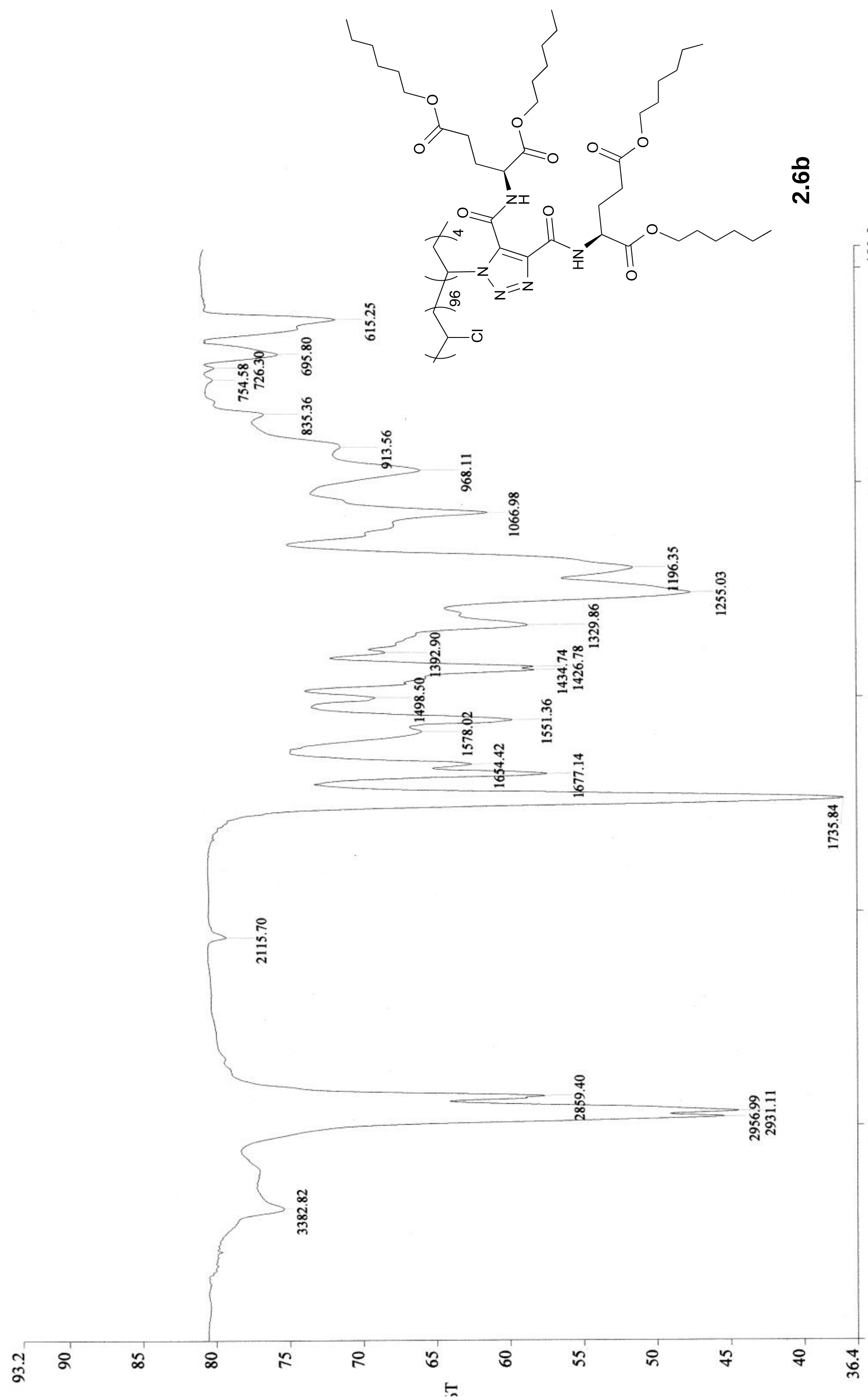
2.6b
615.25
695.80
726.30
754.58
835.36
913.56
968.11
1066.98
1196.35
1255.03
1329.86
1392.90
1434.74
1426.78
1498.50
1551.36
1578.02
1654.42
1677.14
1735.84
2115.70
2859.40
2956.99
2931.11
3382.82
cm-1
4000.0
3000
2000
1500
1000
450.0
93.2
36.4

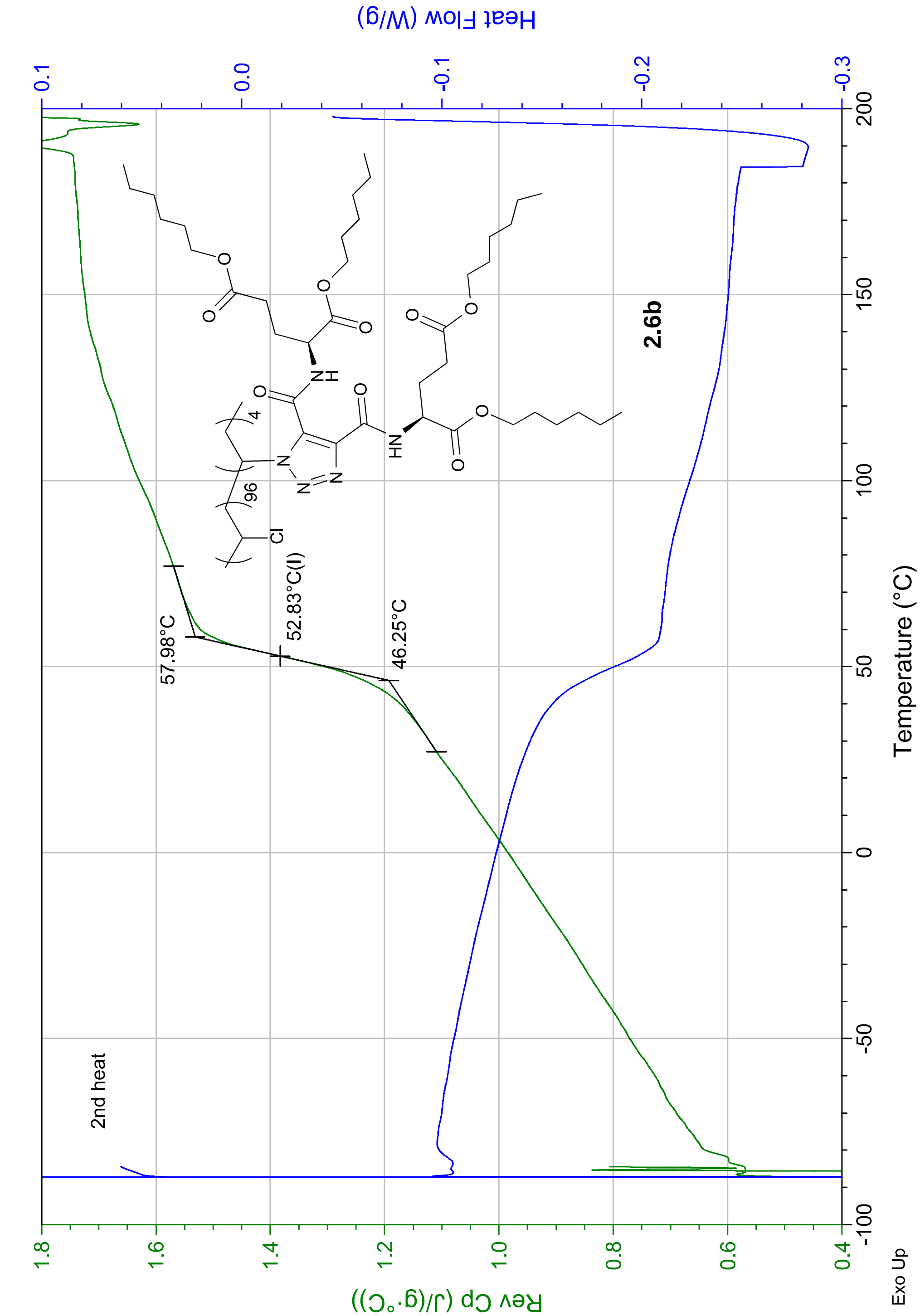

Heat Flow (W/g)
Rev Cp (J/(g·°C))
Temperature (°C)
Exo Up
2nd heat
57.98°C
52.83°C(I)
46.25°C
2.6b

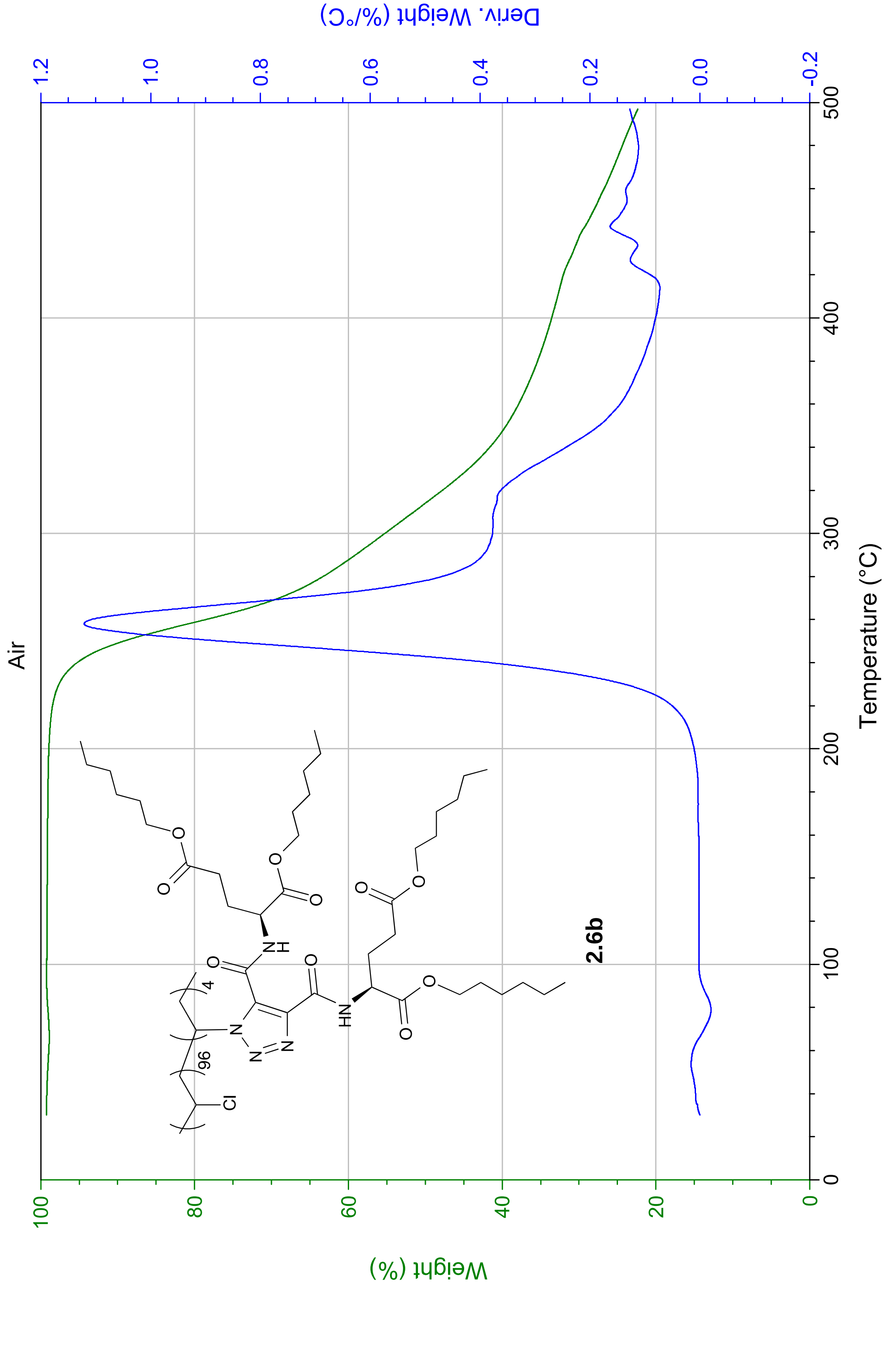
Air
Temperature (°C)
Weight (%)
Deriv. Weight (%/°C)
2.6b

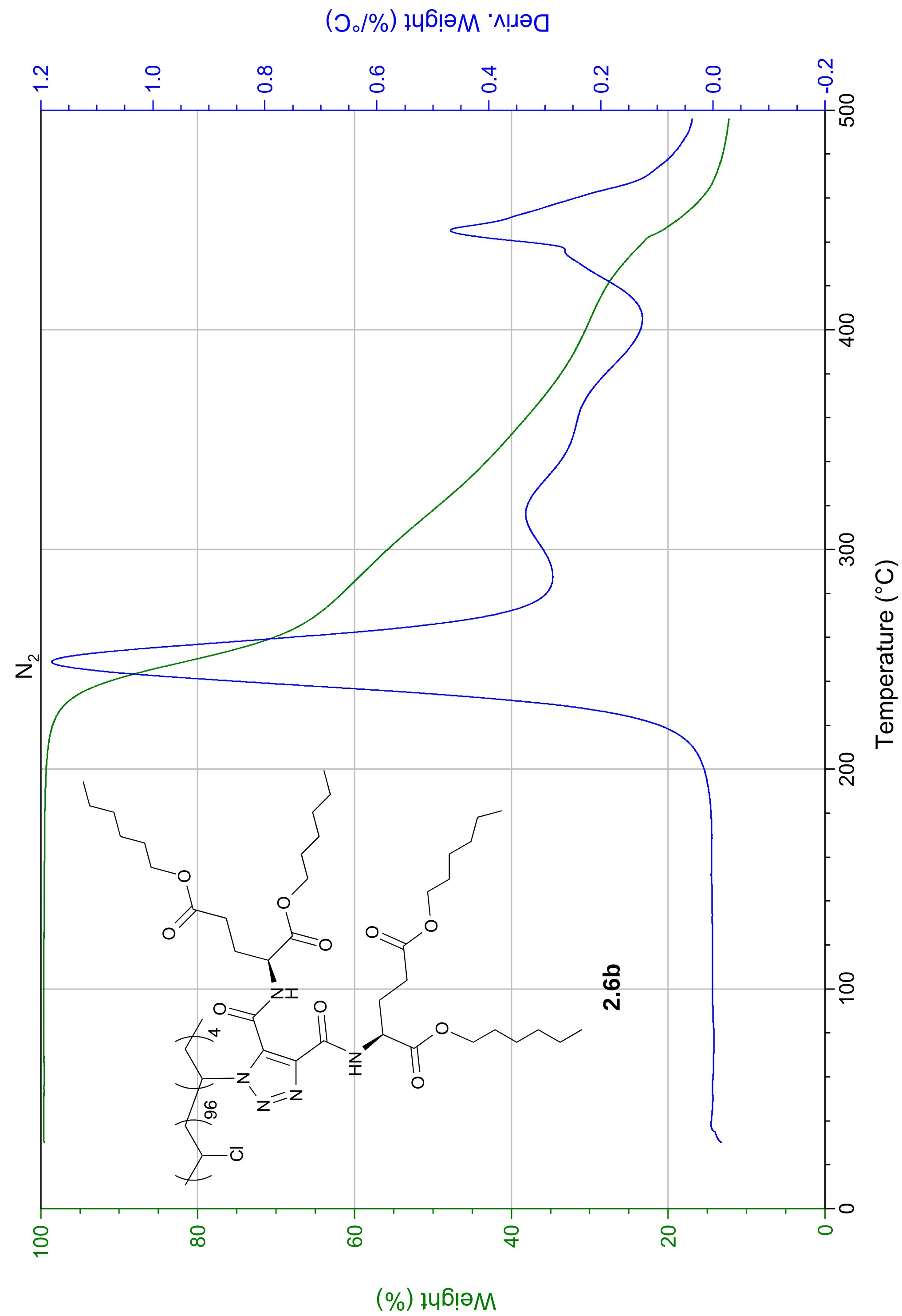
N$_2$
2.6b
Cl
96
4
Temperature (°C)
Weight (%)
Deriv. Weight (%/°C)
0
100
200
300
400
500
20
40
60
80
-0.2
0.0
0.2
0.4
0.6
0.8
1.0
1.2

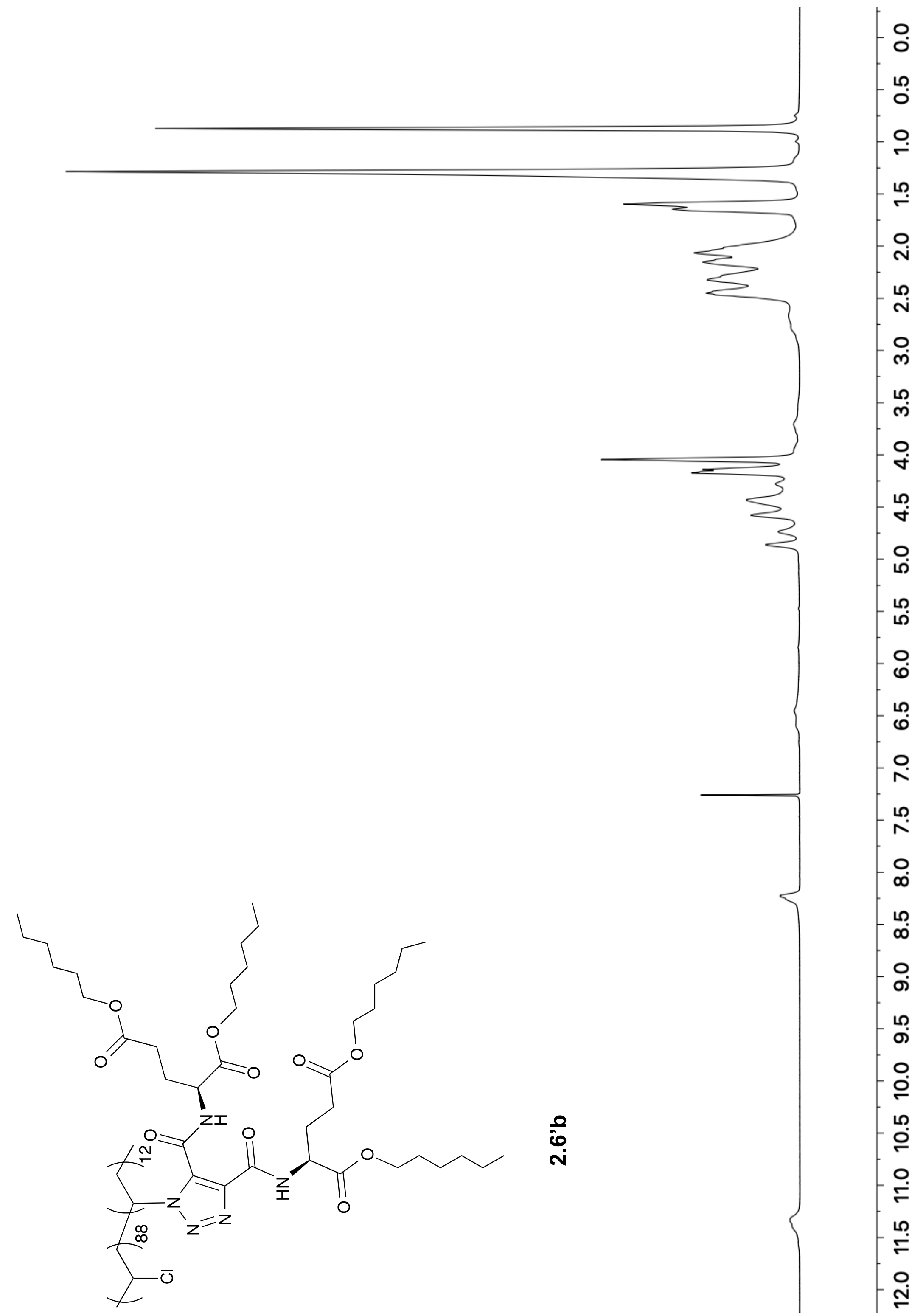
0.0 0.5 1.0 1.5 2.0 2.5 3.0 3.5 4.0 4.5 5.0 5.5 6.0 6.5 7.0 7.5 8.0 8.5 9.0 9.5 10.0 10.5 11.0 11.5 12.0
f1 (ppm)

2.6'b

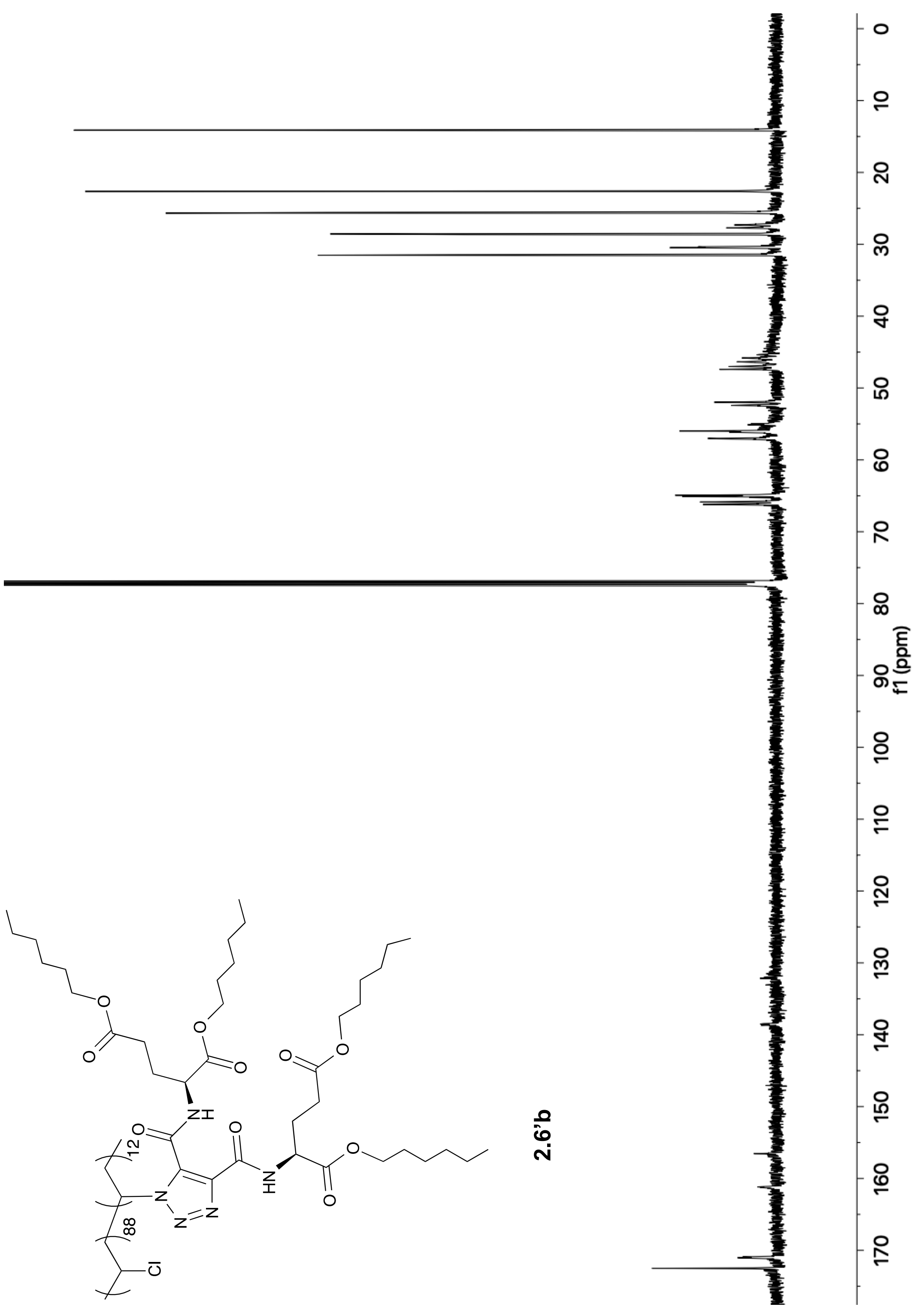

2.6'b

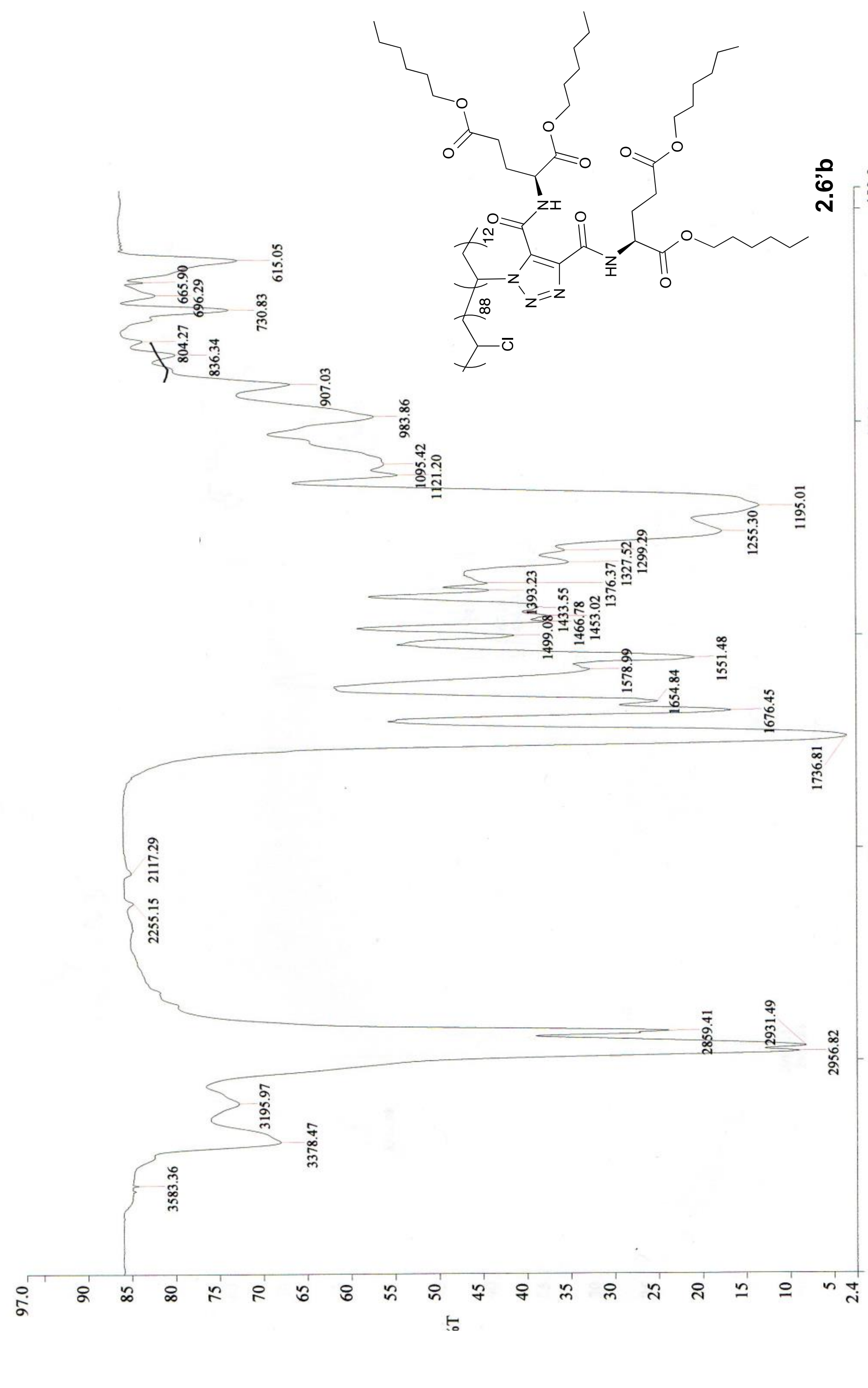
2.6'b
%T
cm-1
3583.36
3378.47
3195.97
2956.82
2931.49
2859.41
2255.15
2117.29
1736.81
1676.45
1654.84
1578.99
1551.48
1499.08
1466.78
1453.02
1433.55
1393.23
1376.37
1327.52
1299.29
1255.30
1195.01
1121.20
1095.42
983.86
907.03
836.34
804.27
730.83
696.29
665.90
615.05

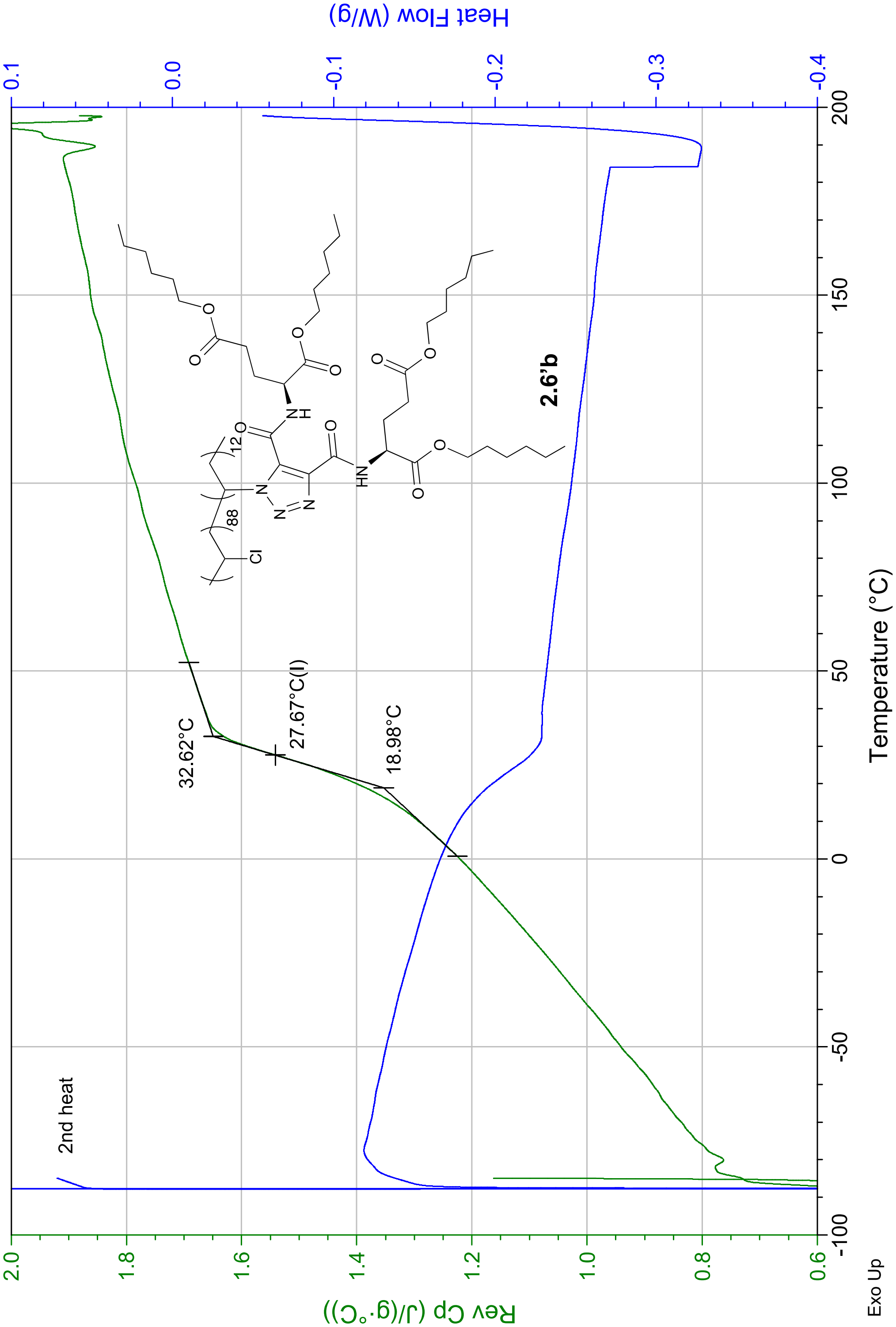
Heat Flow (W/g)
0.1
0.0
-0.1
-0.2
-0.3
-0.4
Rev Cp (J/(g·°C))
2.0
1.8
1.6
1.4
1.2
1.0
0.8
0.6
Exo Up
-100
-50
0
50
100
150
200
Temperature (°C)
2nd heat
32.62°C
27.67°C(I)
18.98°C
2.6'b
Cl
88
12
N
HN
NH
O

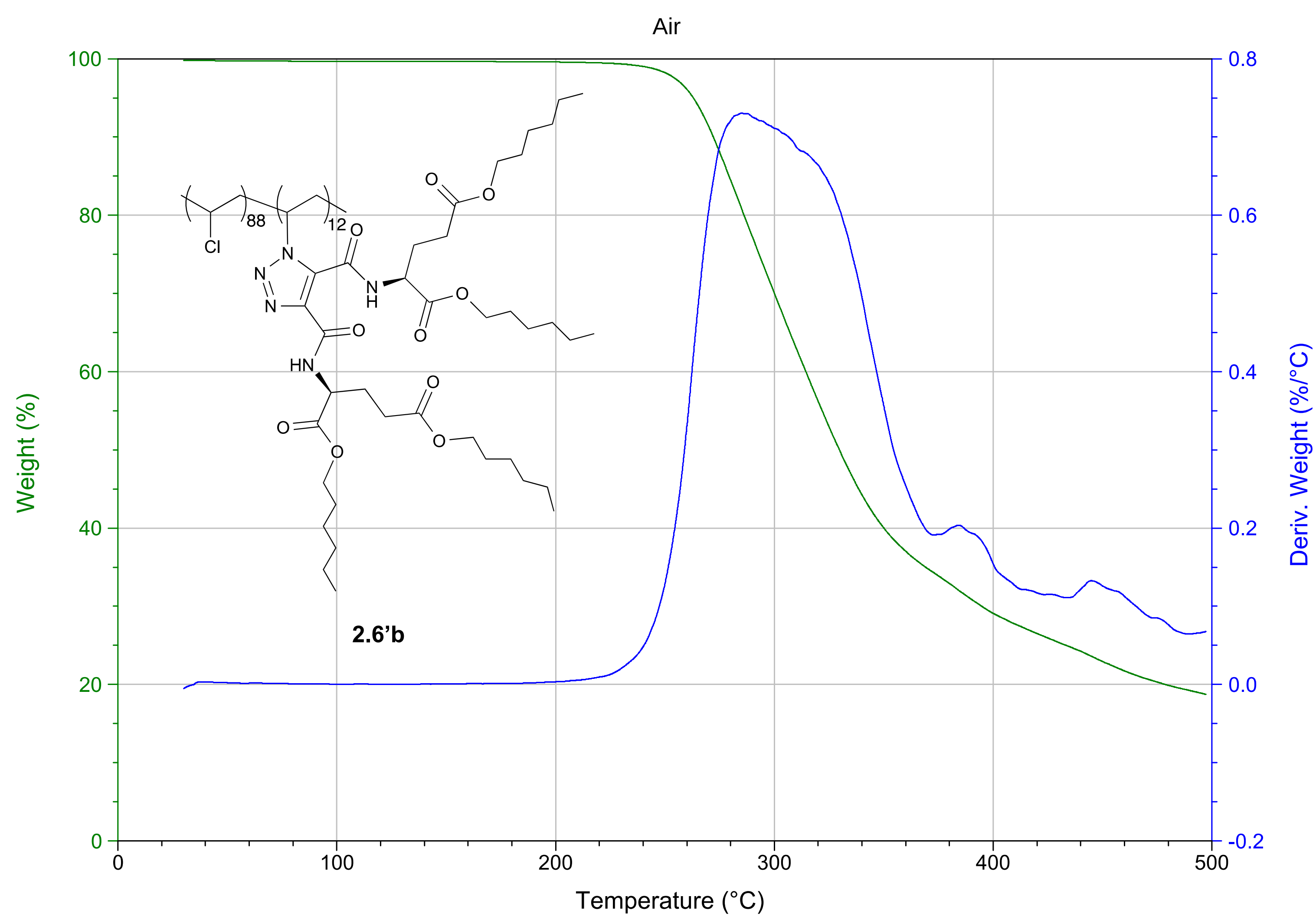
Air
Weight (%)
Deriv. Weight (%/°C)
Temperature (°C)
0
100
200
300
400
500
20
40
60
80
-0.2
0.0
0.2
0.4
0.6
0.8
88
12
Cl
2.6'b

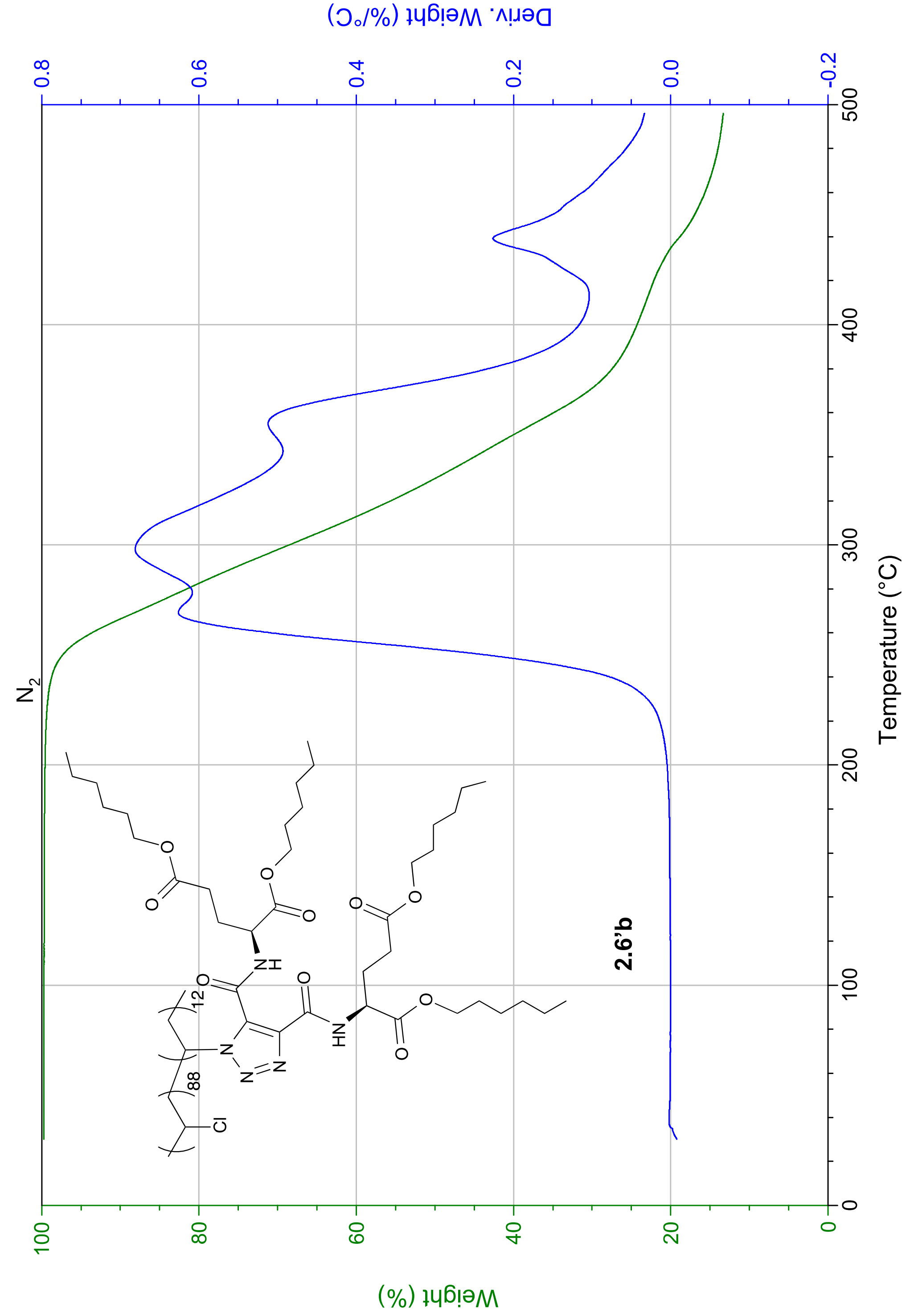

N$_2$
2.6'b
Weight (%)
Deriv. Weight (%/°C)
Temperature (°C)
0
20
40
60
80
100
-0.2
0.0
0.2
0.4
0.6
0.8
0
100
200
300
400
500
Cl
88
12
N
N
N
HN
NH
O

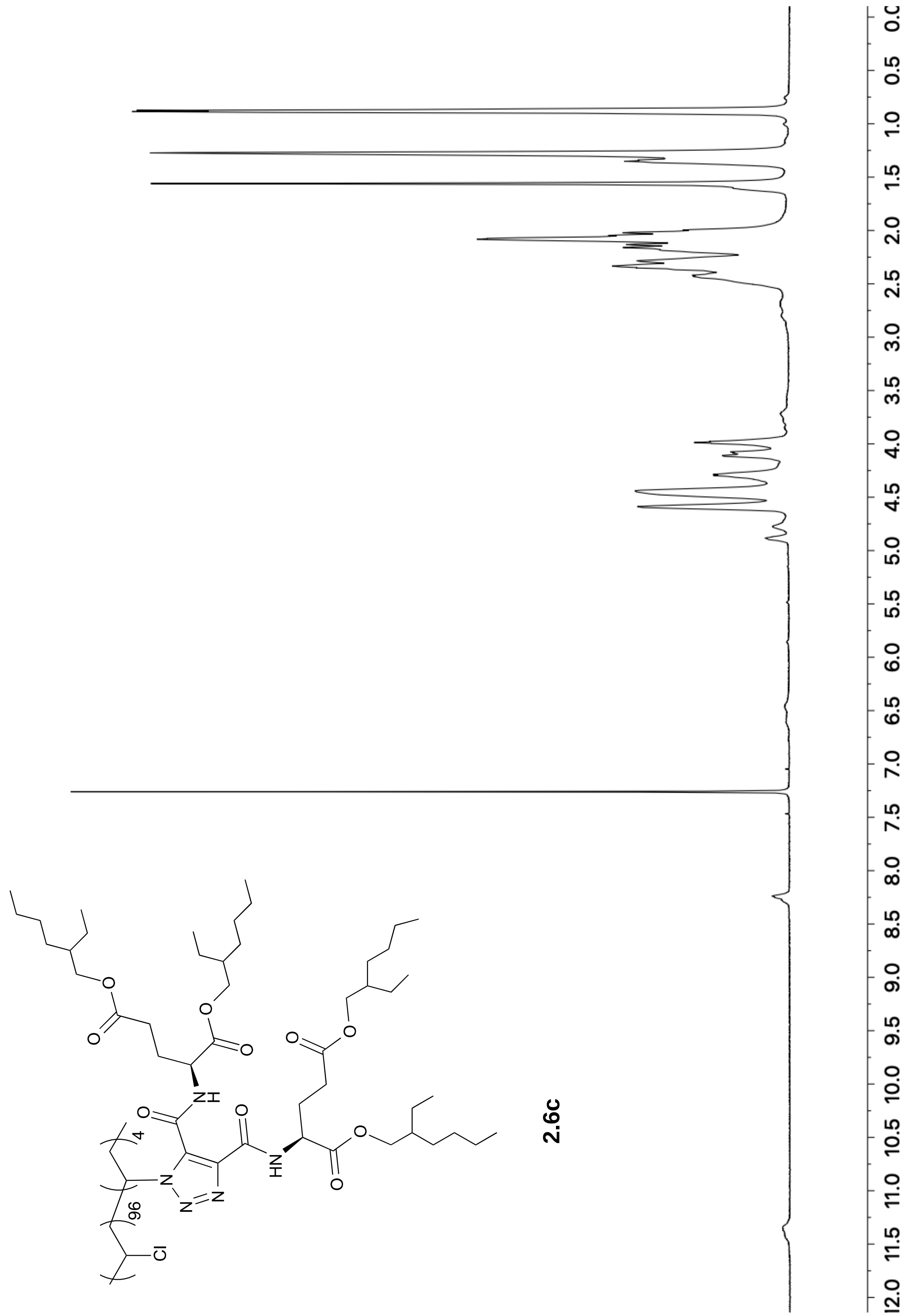

2.6c

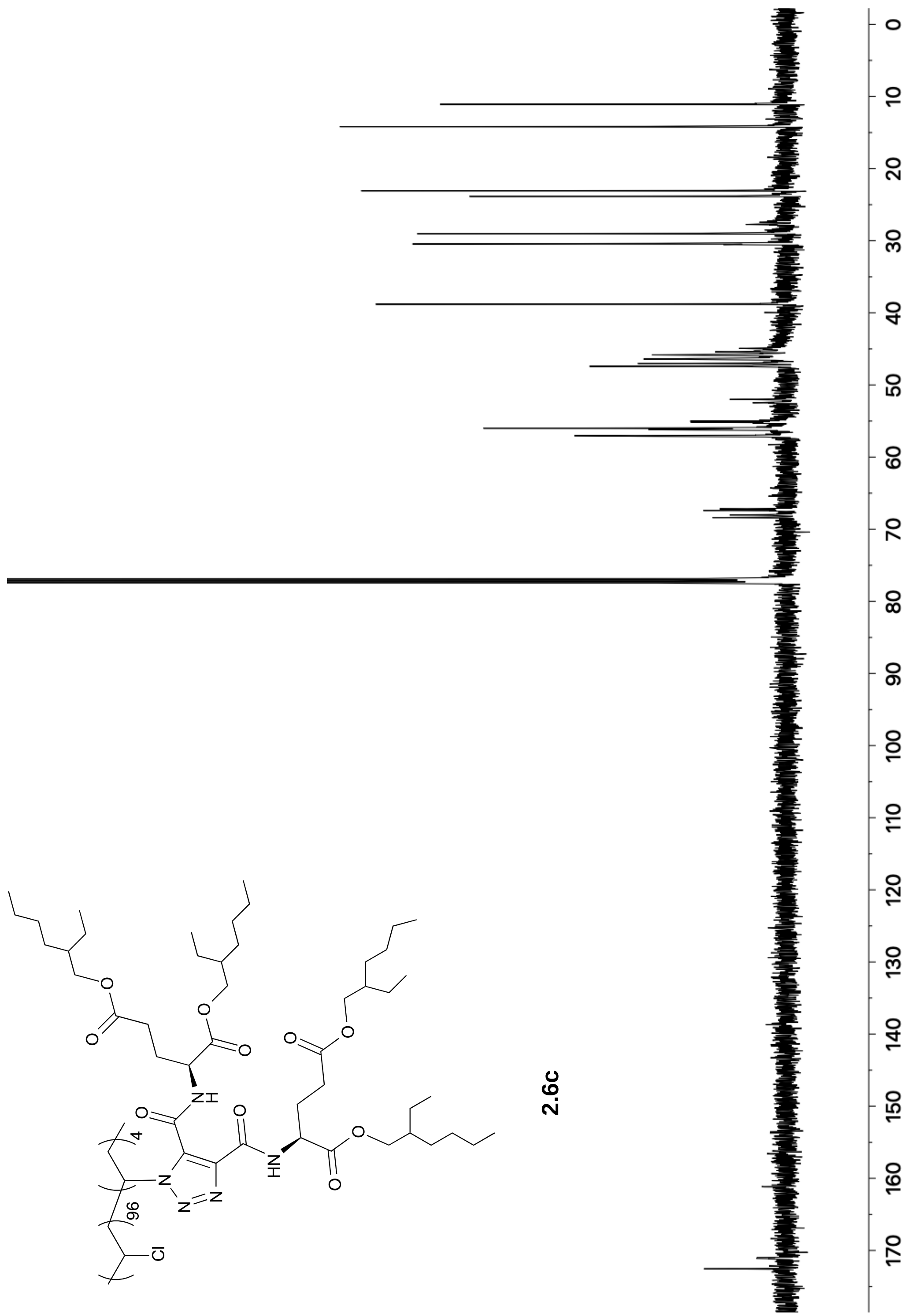

2.6c

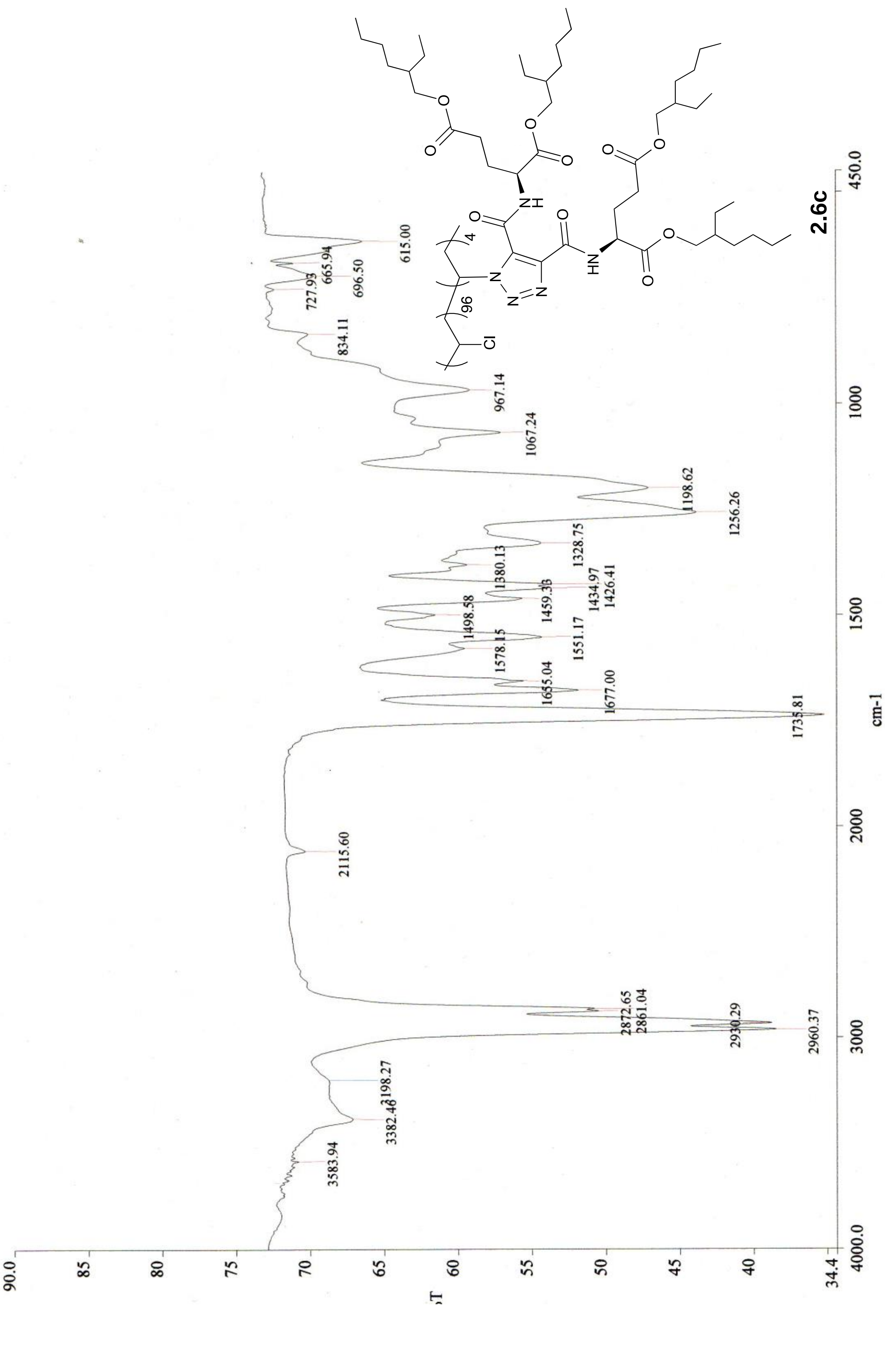
2.6c
%T
cm-1
4000.0
3000
2000
1500
1000
450.0
90.0
34.4
3583.94
3382.46
3198.27
2960.37
2930.29
2872.65
2861.04
2115.60
1735.81
1677.00
1655.04
1578.15
1551.17
1498.58
1459.33
1434.97
1426.41
1380.13
1328.75
1256.26
1198.62
1067.24
967.14
834.11
727.93
696.50
665.94
615.00
Cl
96
4

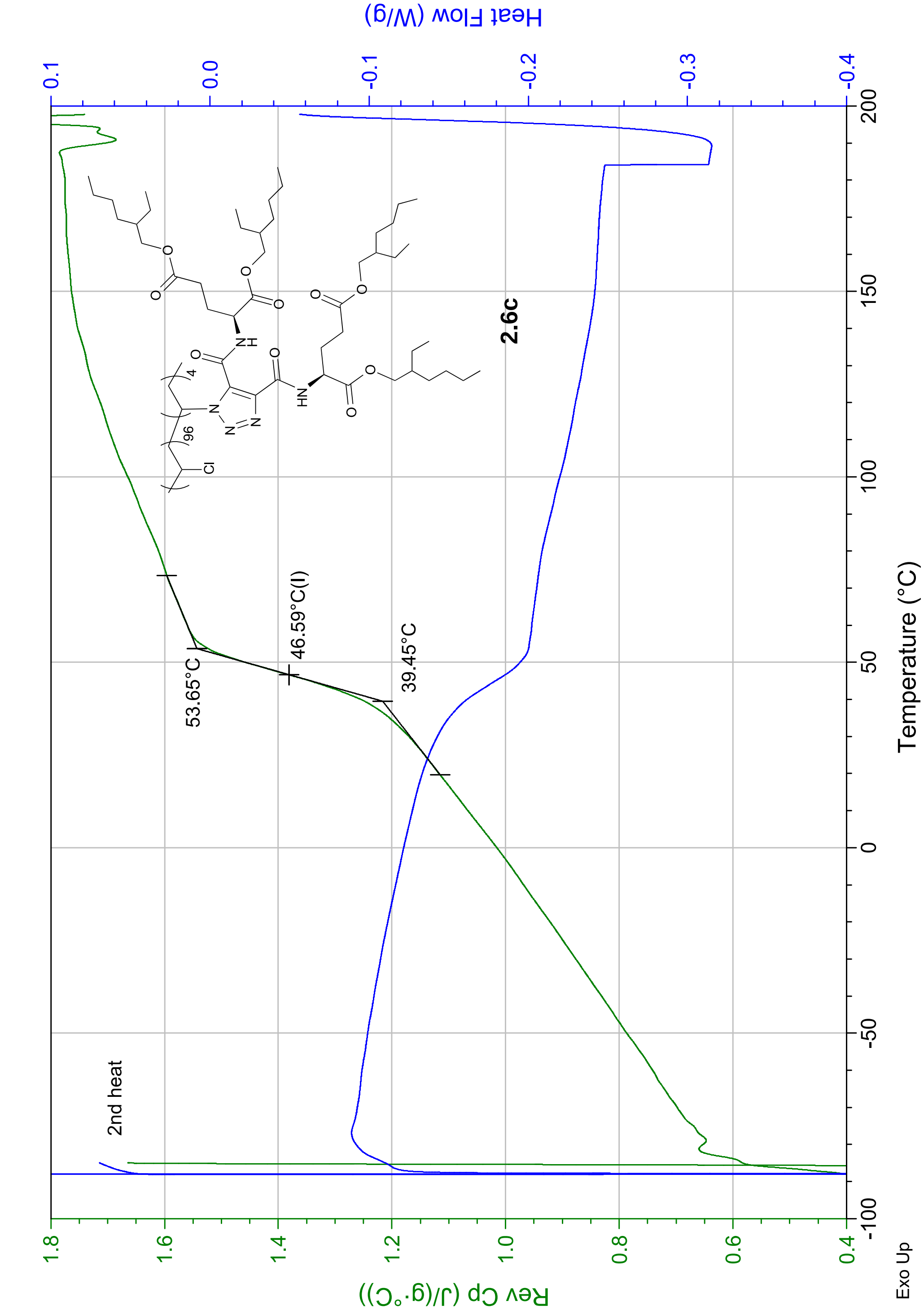

Heat Flow (W/g)
0.1
0.0
-0.1
-0.2
-0.3
-0.4
Rev Cp (J/(g·°C))
1.8
1.6
1.4
1.2
1.0
0.8
0.6
0.4
Exo Up
Temperature (°C)
-100
-50
0
50
100
150
200
2nd heat
53.65°C
46.59°C(I)
39.45°C
2.6c

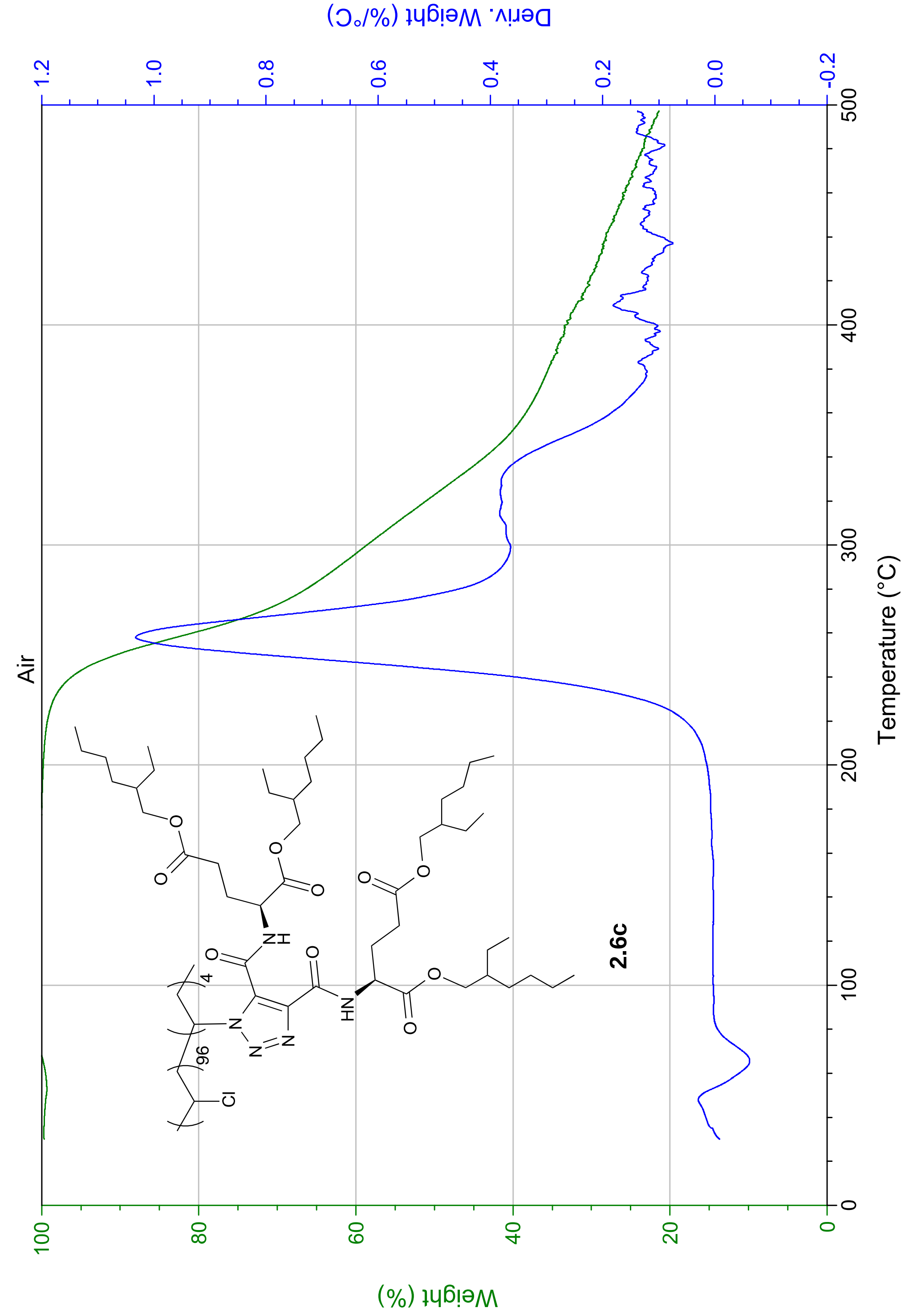
Air
Temperature (°C)
Weight (%)
Deriv. Weight (%/°C)
0
100
200
300
400
500
0
20
40
60
80
100
-0.2
0.0
0.2
0.4
0.6
0.8
1.0
1.2
2.6c

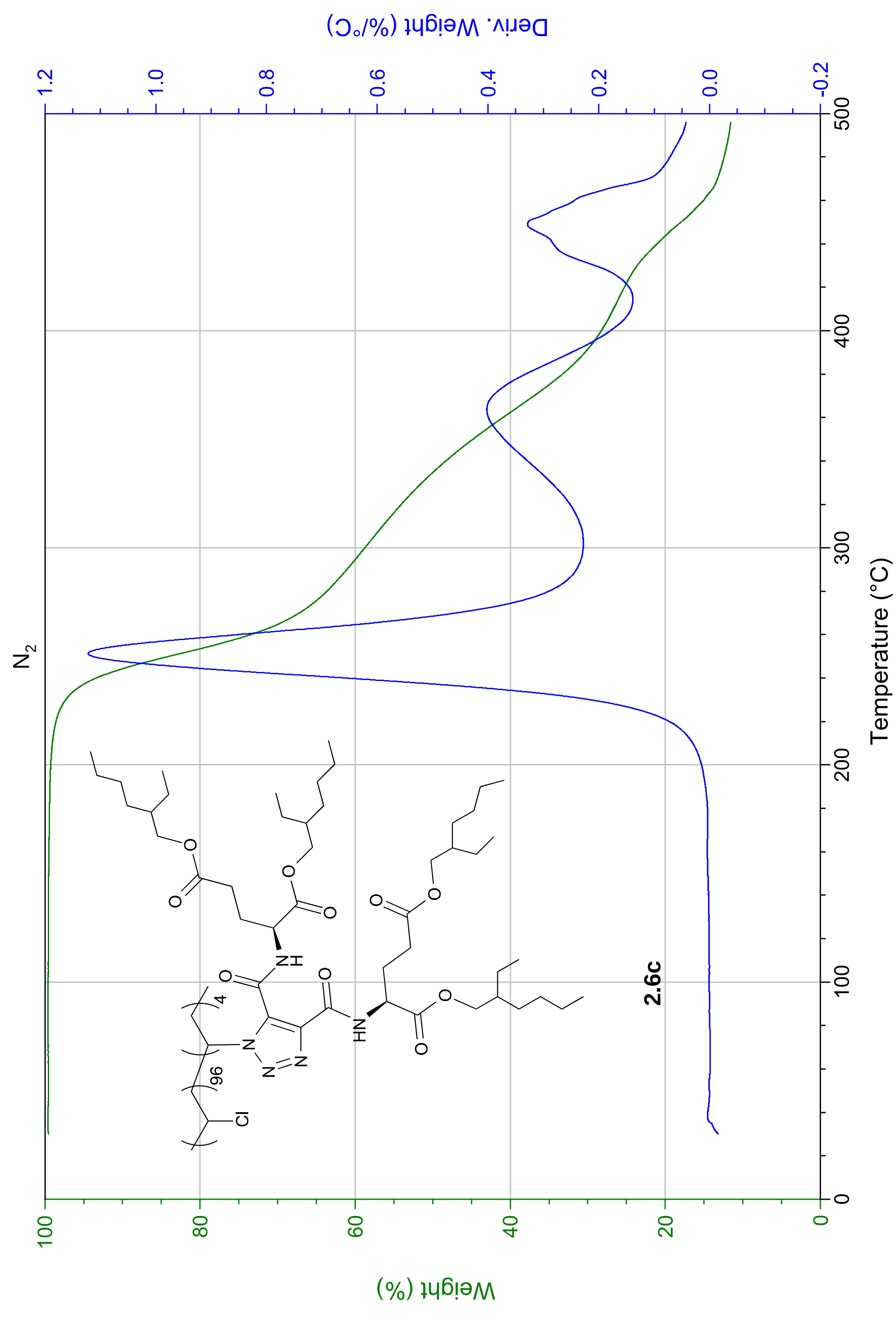

N2
Weight (%)
Deriv. Weight (%/°C)
Temperature (°C)
2.6c

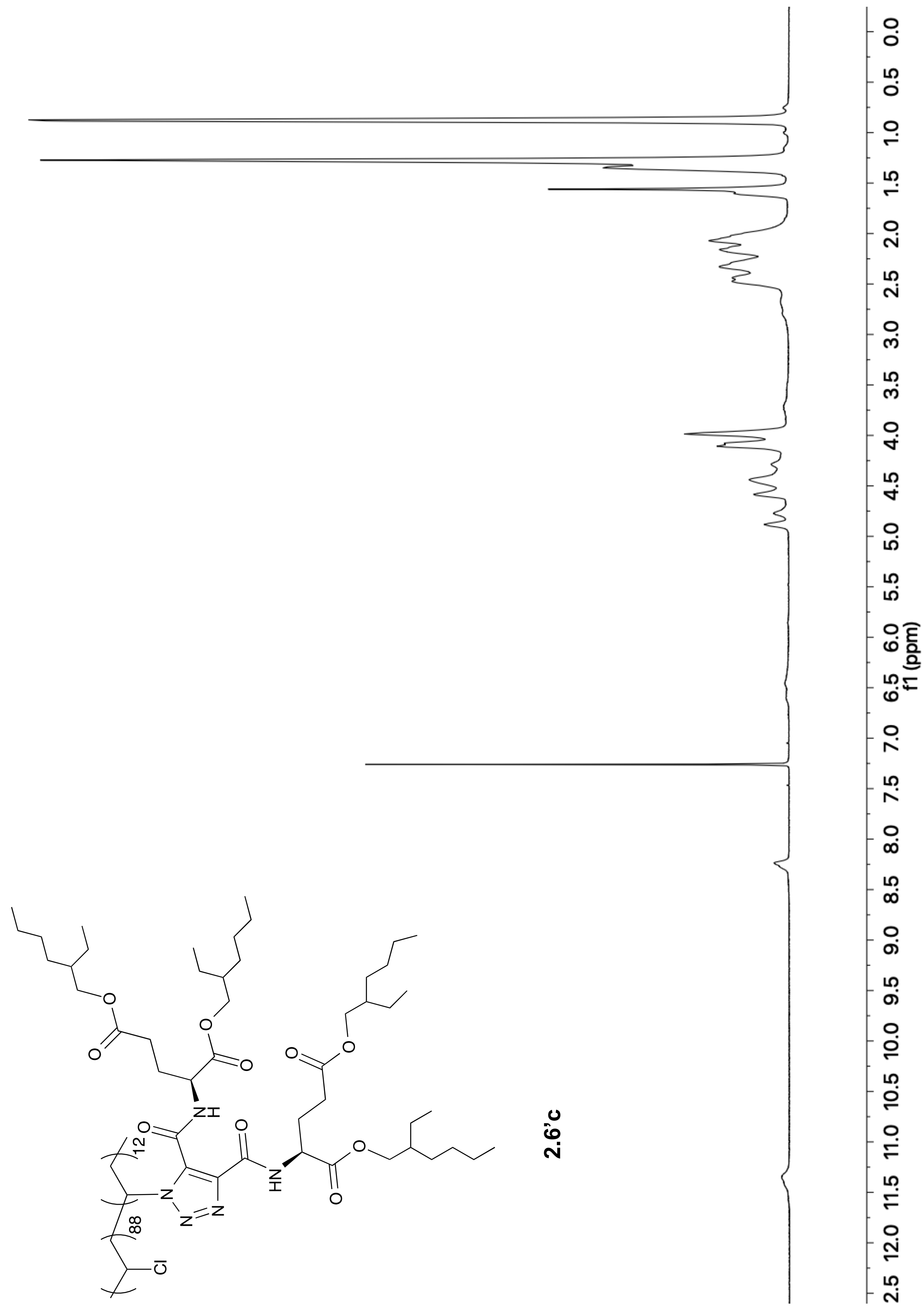

2.6'c

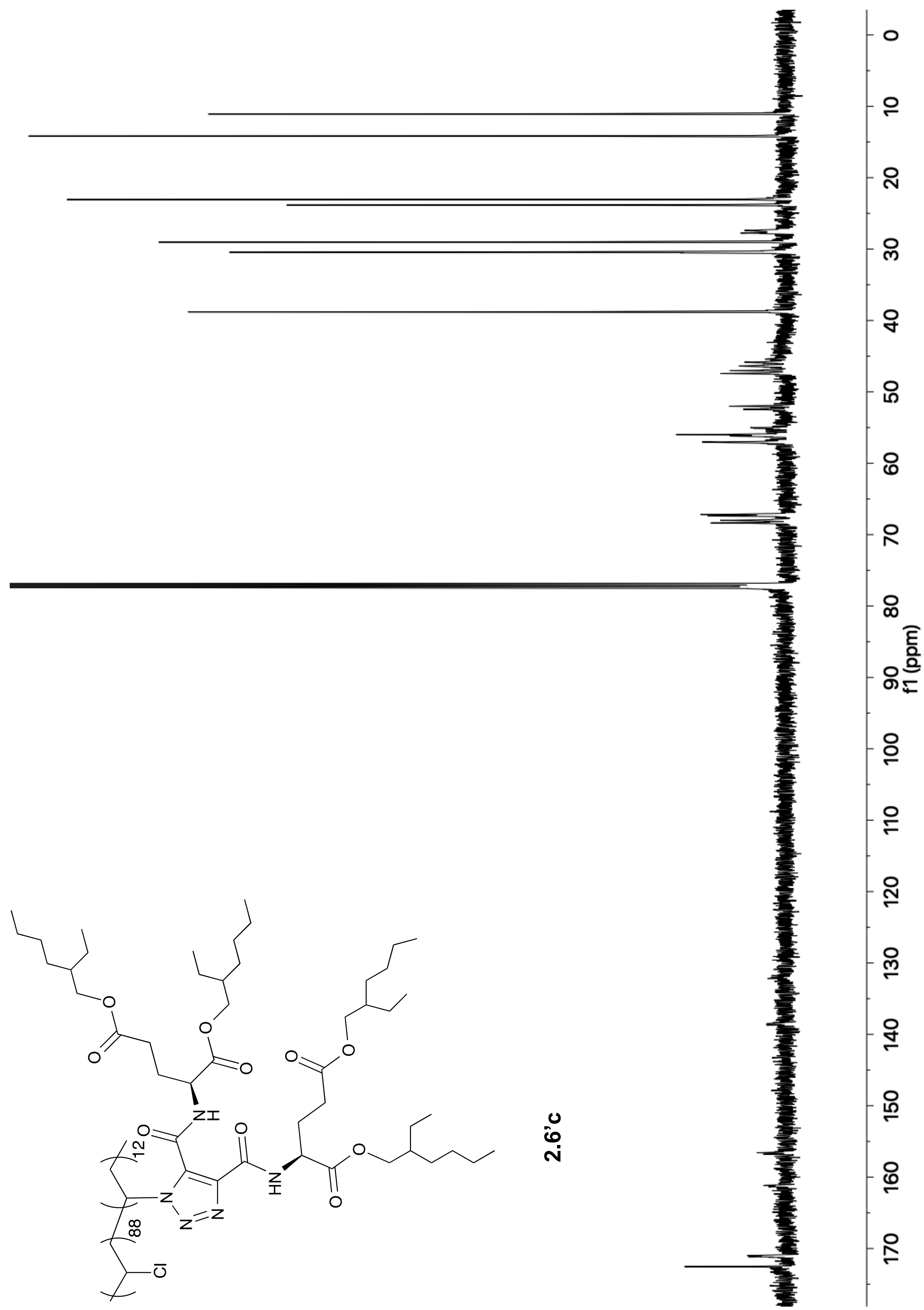

f1 (ppm)
0
10
20
30
40
50
60
70
80
90
100
110
120
130
140
150
160
170
Cl
88
12
N
HN
O

2.6'c

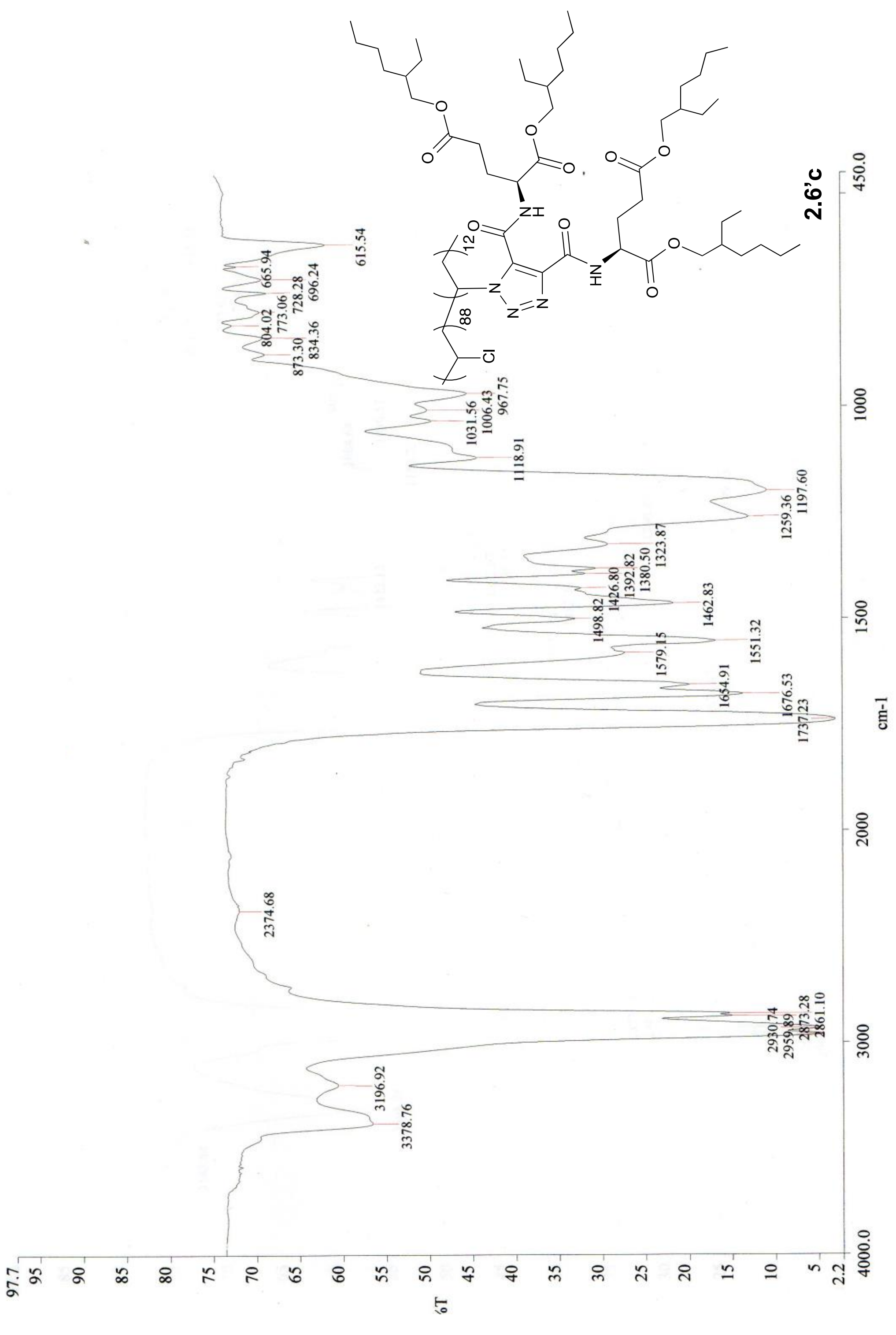
%T
cm-1
4000.0
3000
2000
1500
1000
450.0
3378.76
3196.92
2930.74
2959.89
2873.28
2861.10
2374.68
1737.23
1676.53
1654.91
1579.15
1551.32
1498.82
1462.83
1426.80
1392.82
1380.50
1323.87
1259.36
1197.60
1118.91
1031.56
1006.43
967.75
873.30
834.36
804.02
773.06
728.28
696.24
665.94
615.54
Cl
88
12
HN
NH

2.6'c

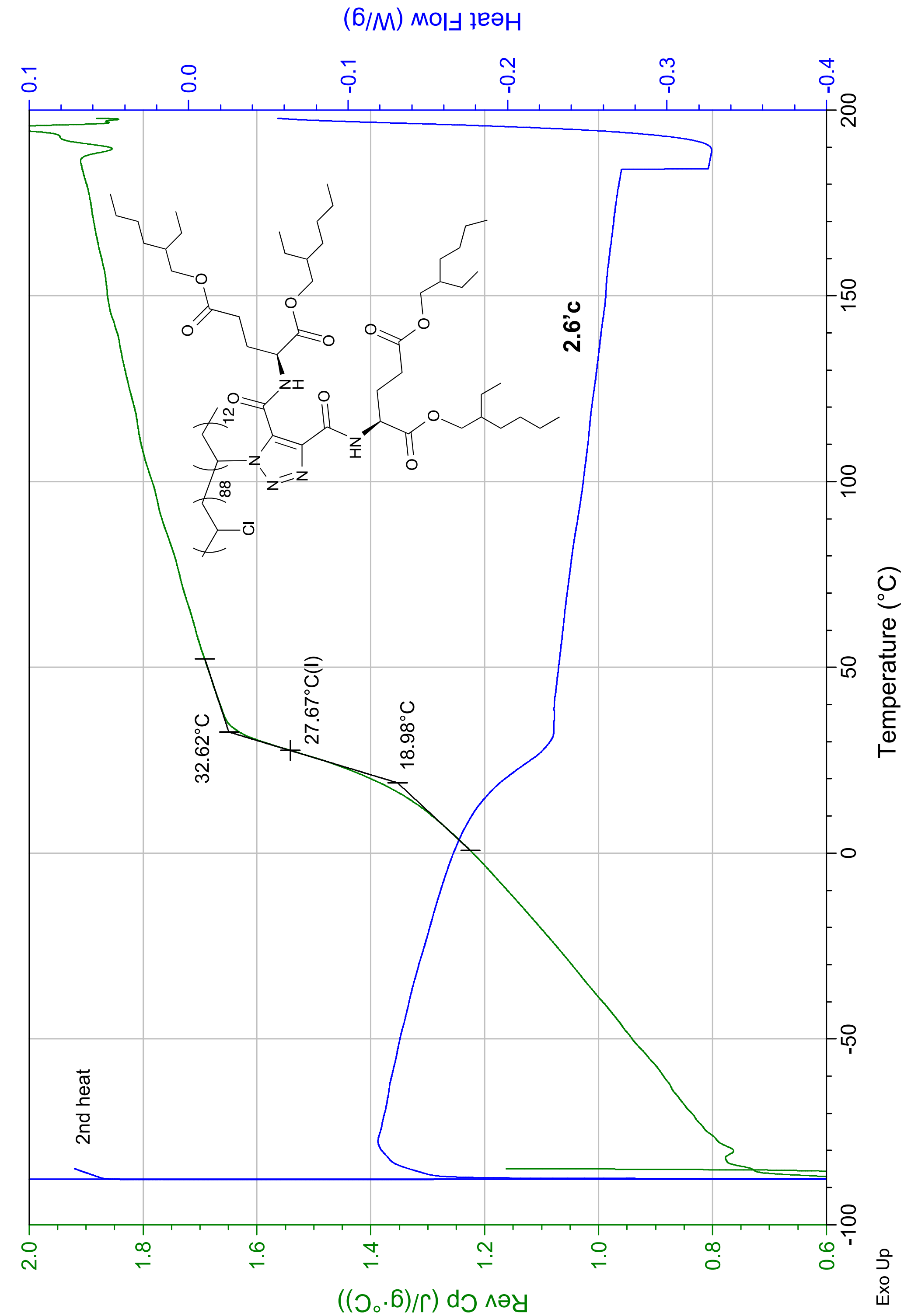
2nd heat
32.62°C
27.67°C(I)
18.98°C
2.6'c
Temperature (°C)
Rev Cp (J/(g·°C))
Heat Flow (W/g)
Exo Up

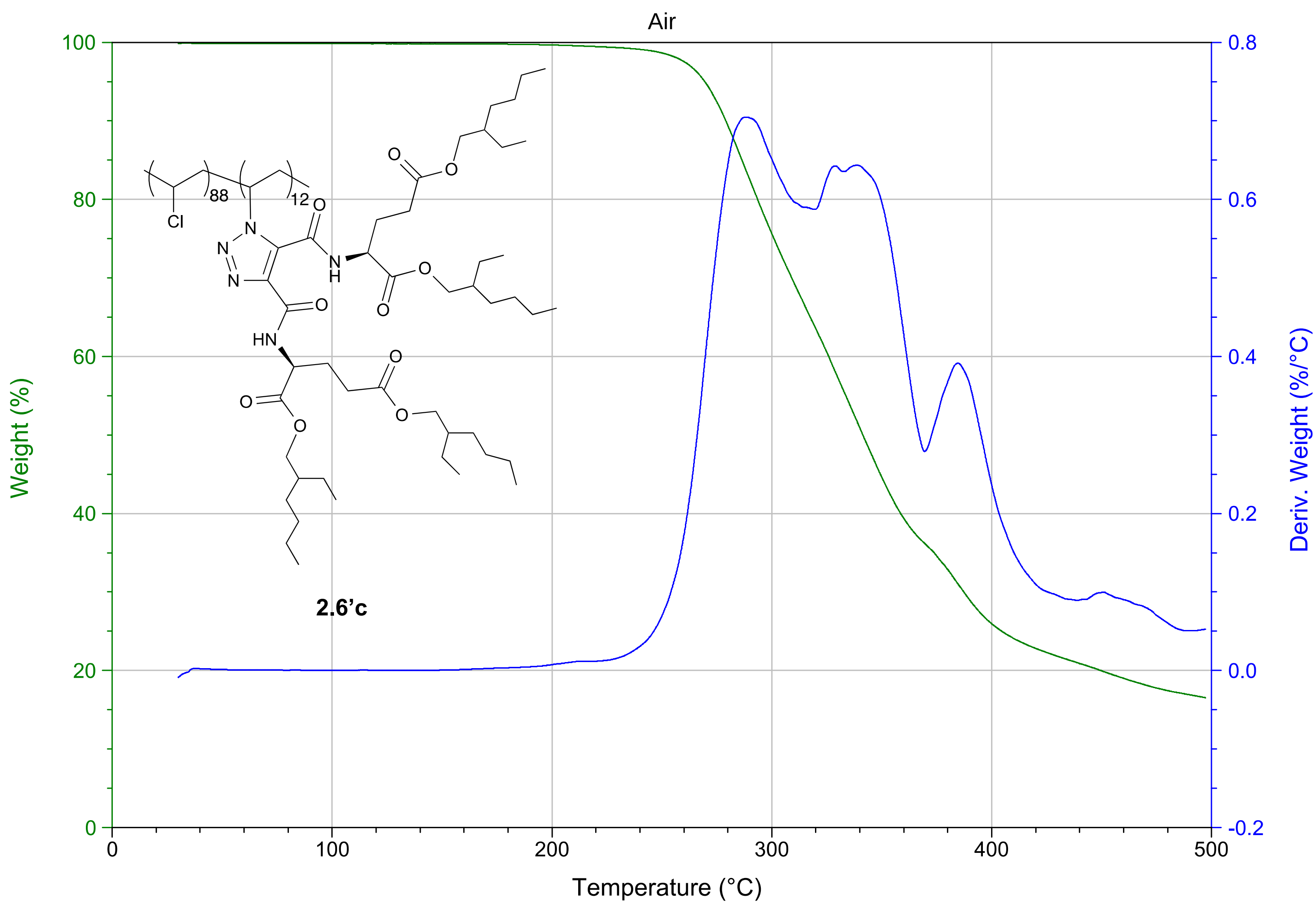
Air
2.6'c
Weight (%)
Deriv. Weight (%/°C)
Temperature (°C)

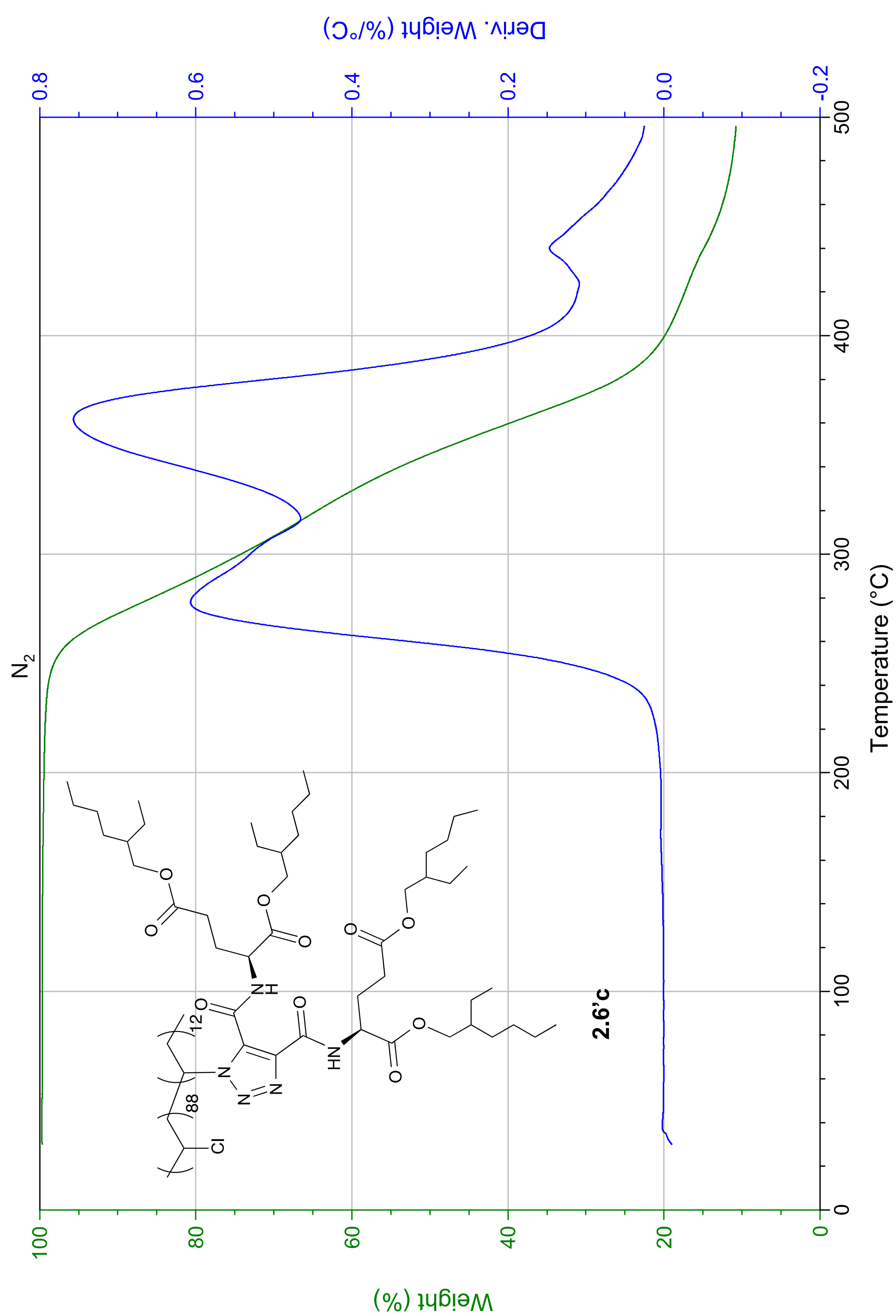
N2
2.6'c
Temperature (°C)
Weight (%)
Deriv. Weight (%/°C)
0
100
200
300
400
500
20
40
60
80
-0.2
0.0
0.2
0.4
0.6
0.8

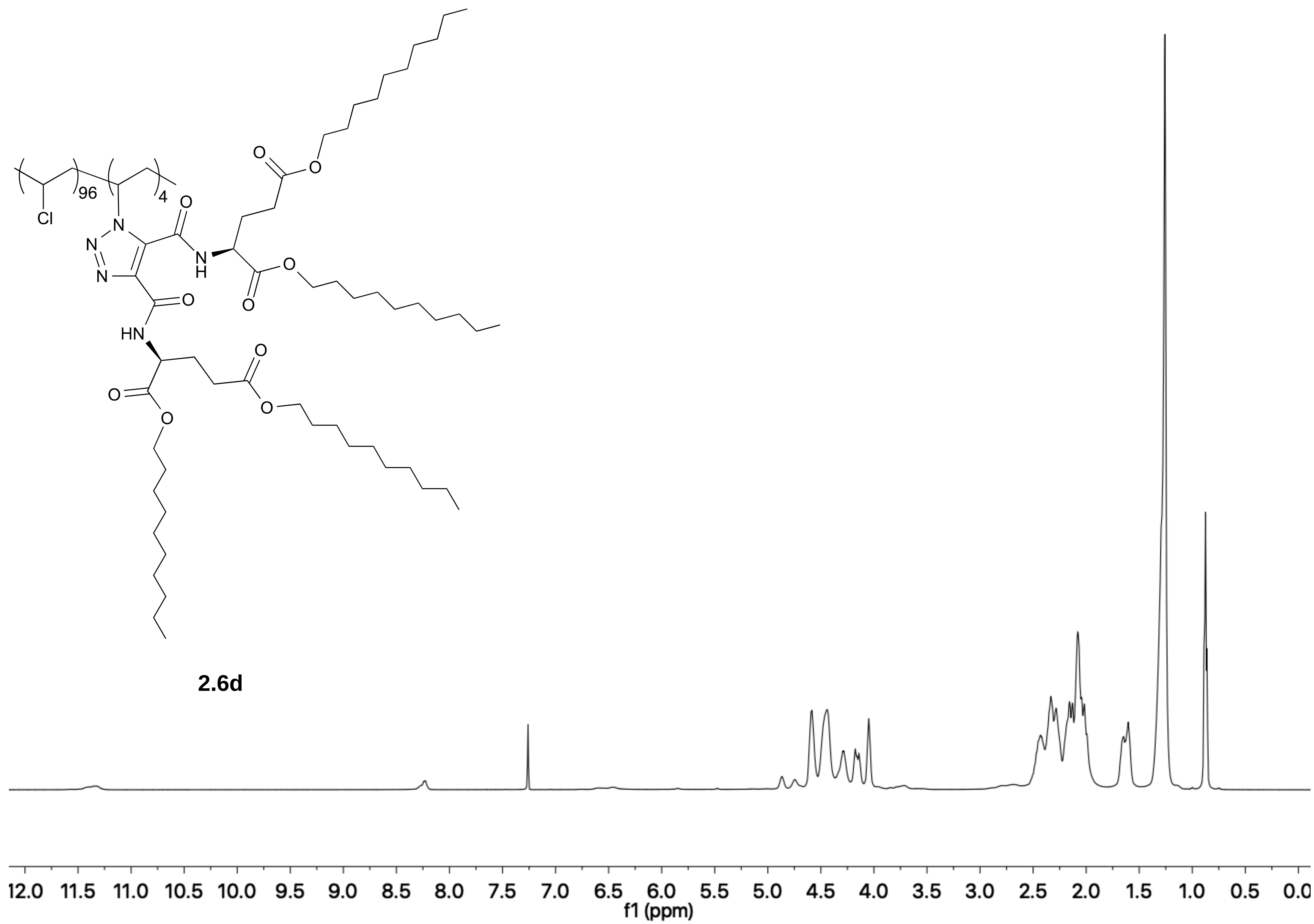
96
4
Cl
N
N
N
O
H
N
O
HN
O
O
O
O
O
O
12.0 11.5 11.0 10.5 10.0 9.5 9.0 8.5 8.0 7.5 7.0 6.5 6.0 5.5 5.0 4.5 4.0 3.5 3.0 2.5 2.0 1.5 1.0 0.5 0.0
f1 (ppm)

2.6d

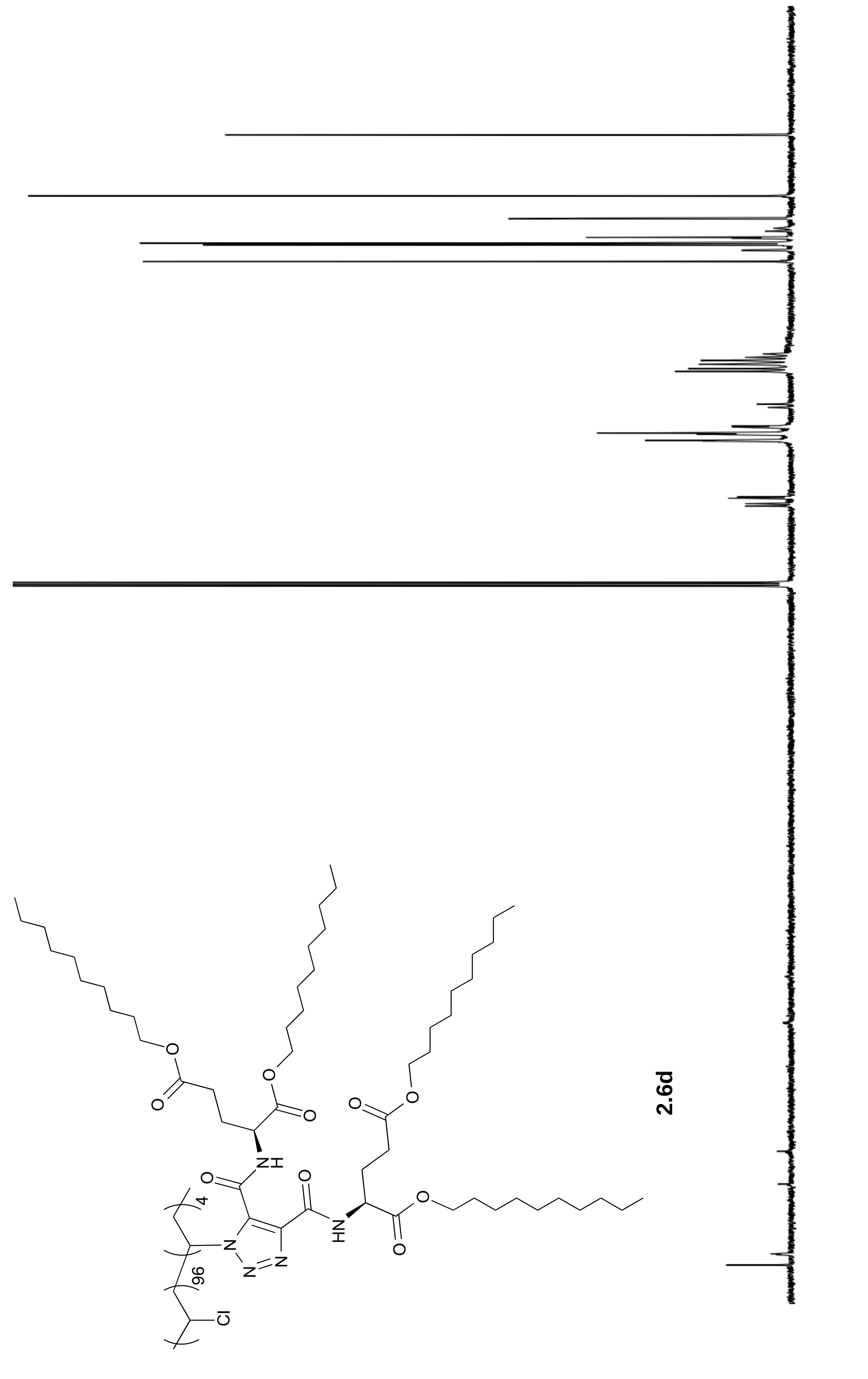

2.6d

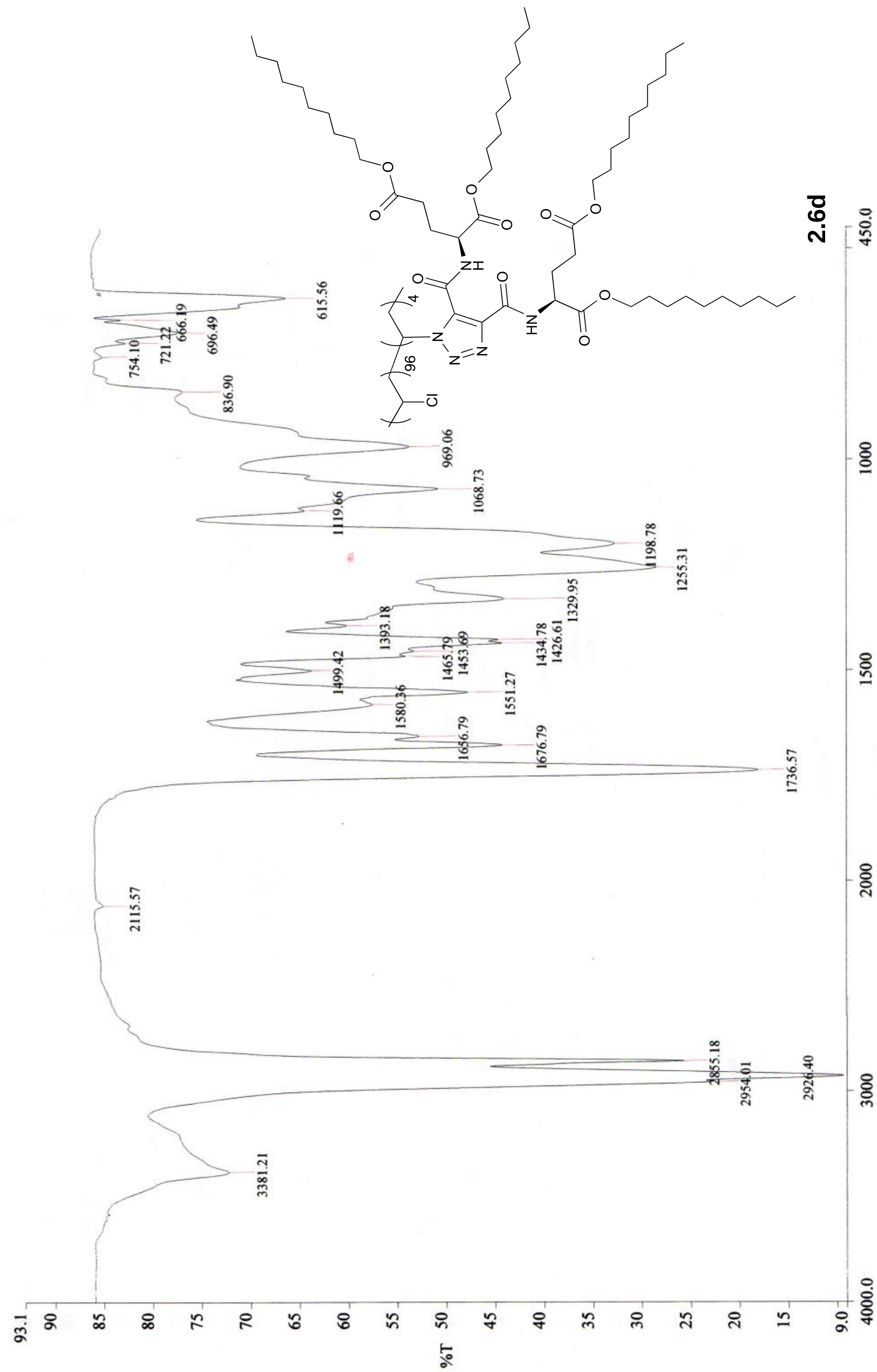

2.6d

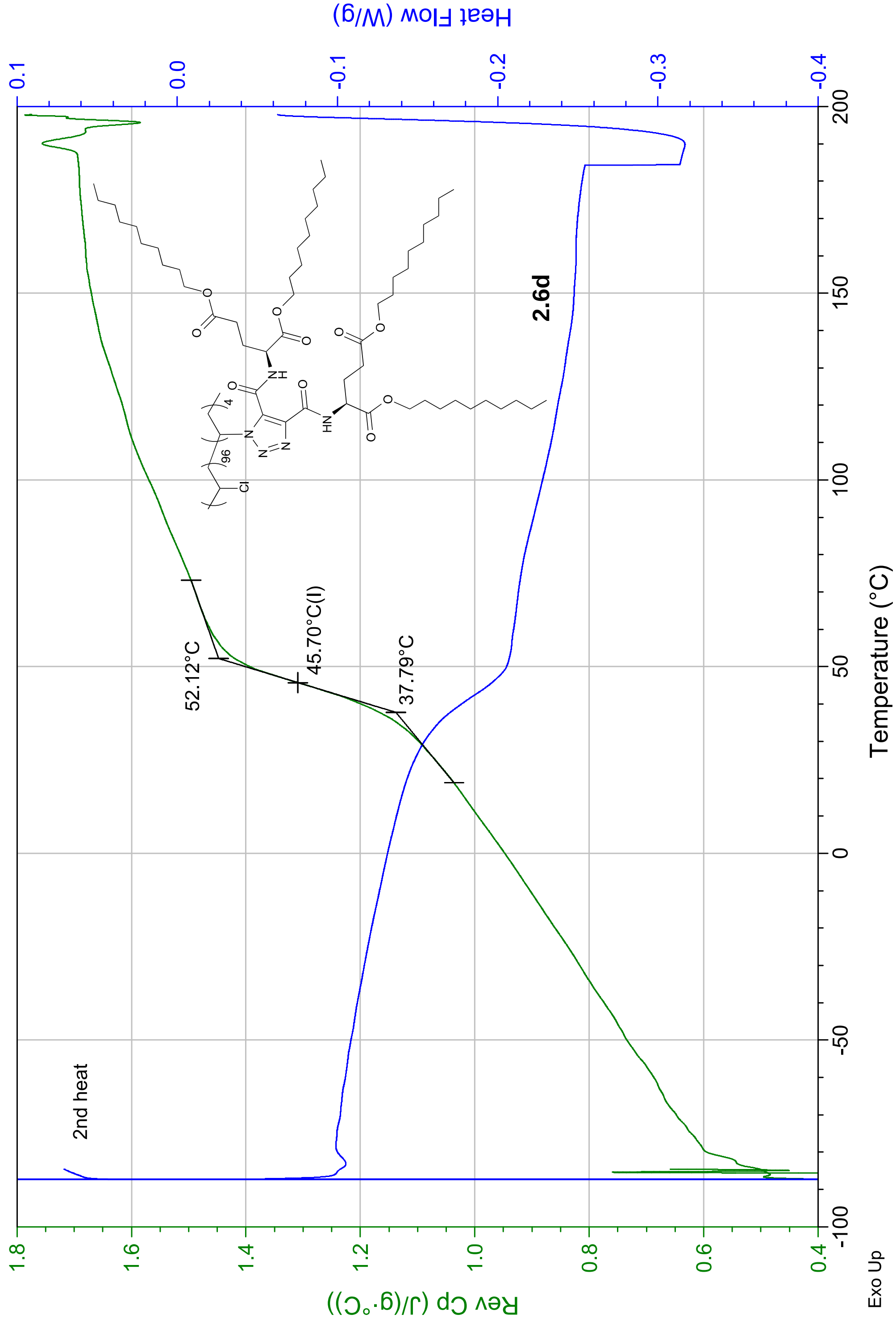

Heat Flow (W/g)
Rev Cp (J/(g·°C))
Temperature (°C)
Exo Up
2nd heat
52.12°C
45.70°C(I)
37.79°C
2.6d

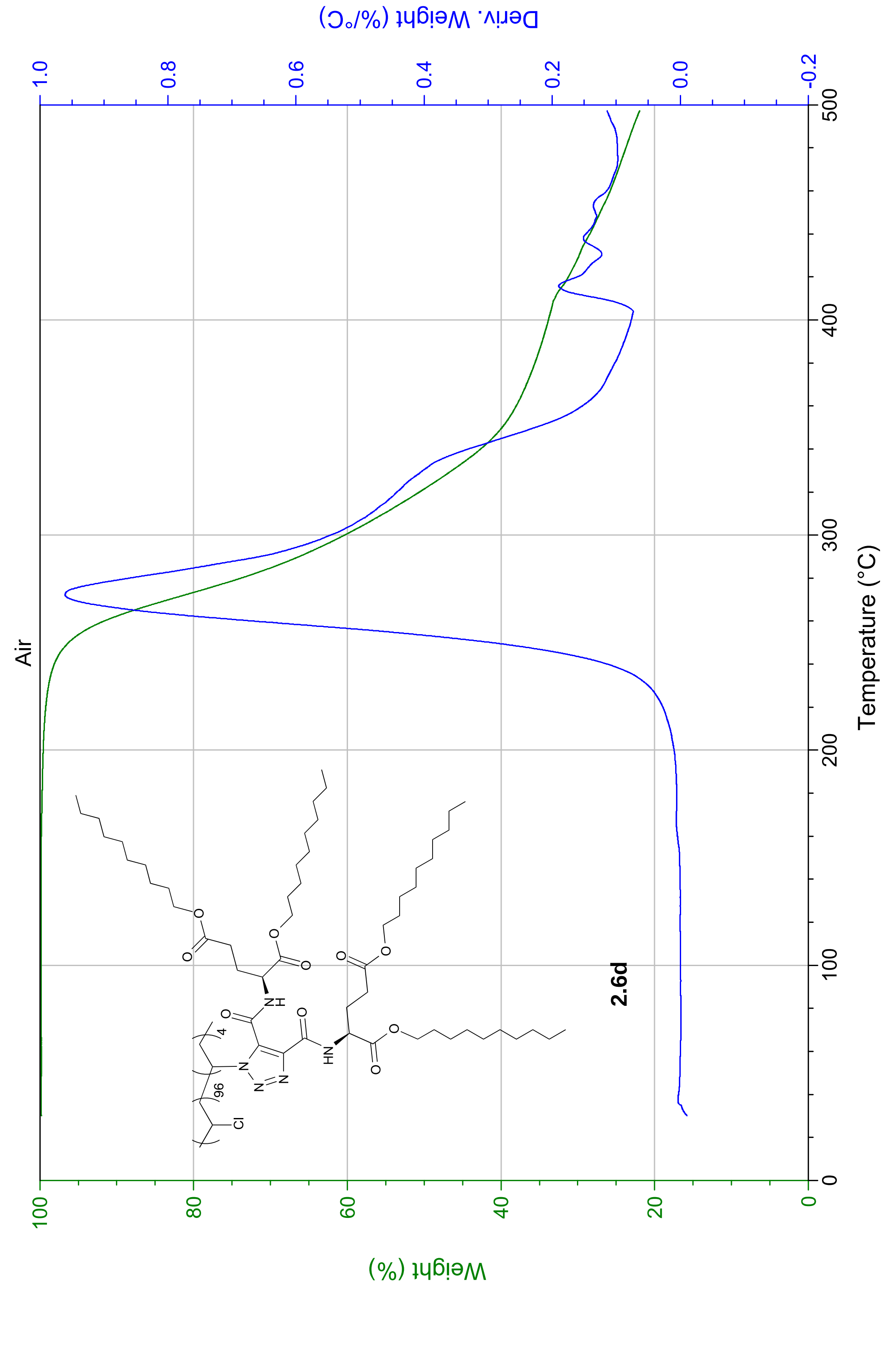
Air
Temperature (°C)
Weight (%)
Deriv. Weight (%/°C)
2.6d
0
100
200
300
400
500
0
20
40
60
80
100
-0.2
0.0
0.2
0.4
0.6
0.8
1.0

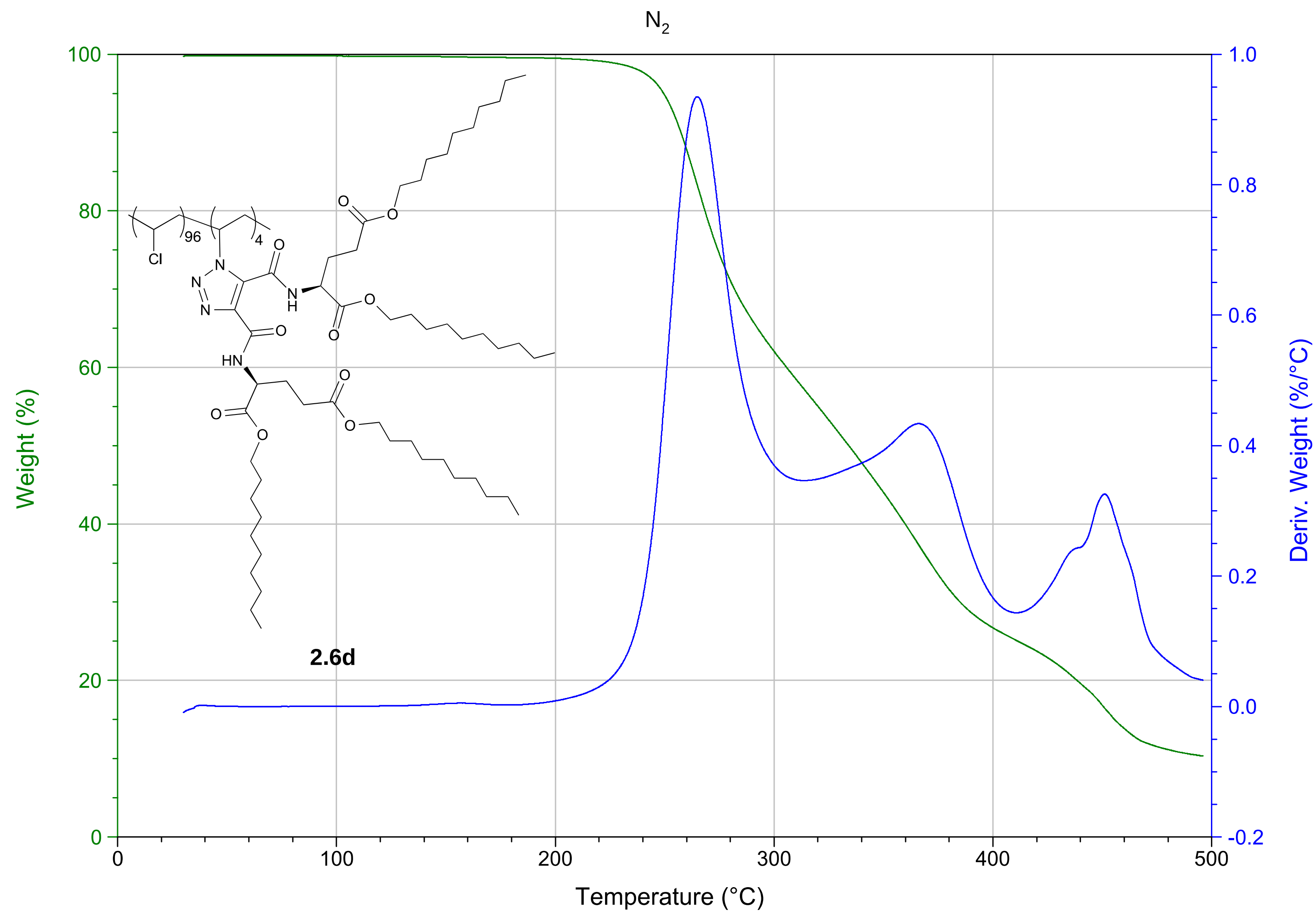

N2
Weight (%)
Deriv. Weight (%/°C)
Temperature (°C)
2.6d

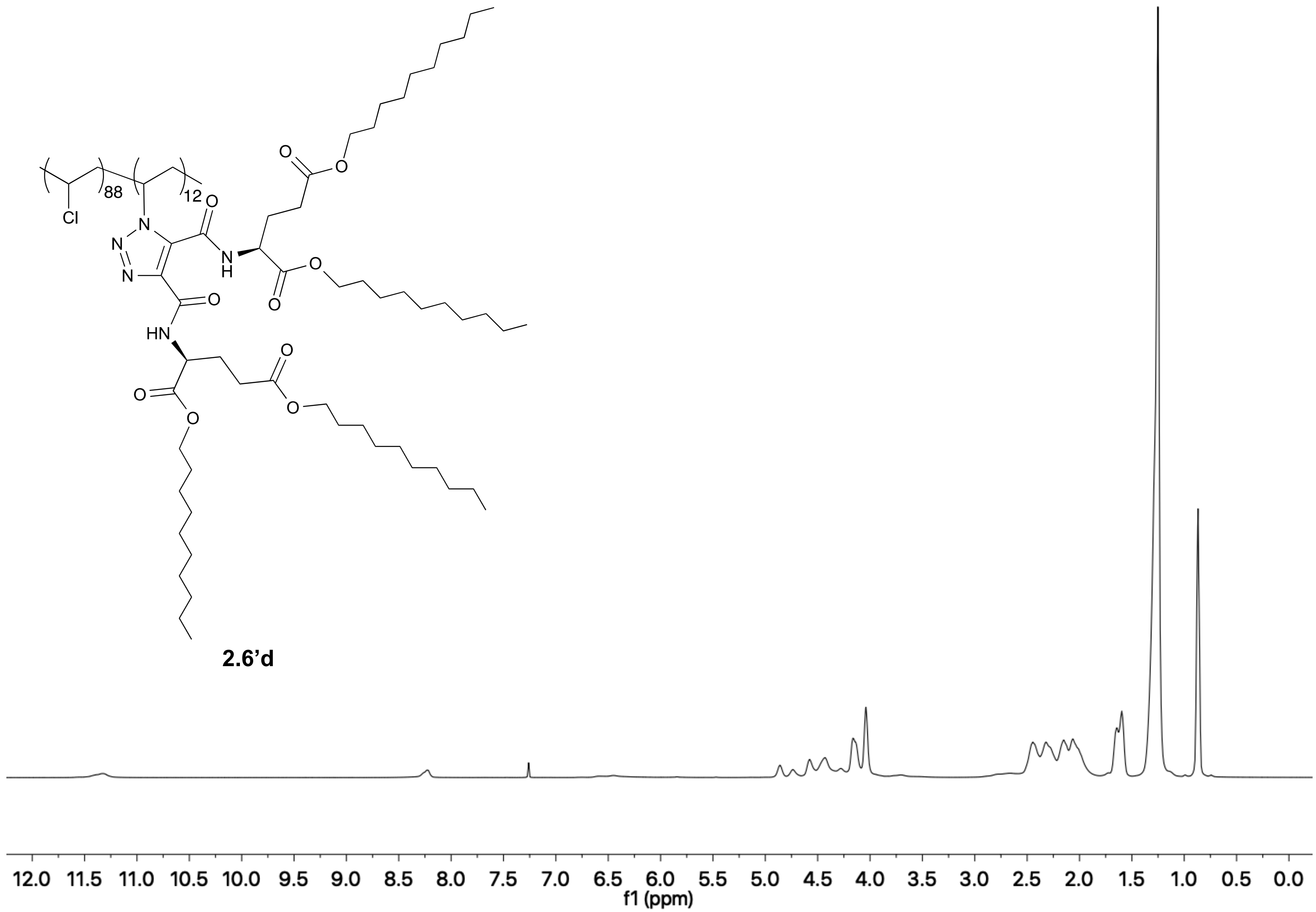
Cl
88
12
O
N
N
N
NH
O
O
O
HN
O
O
O
O
12.0 11.5 11.0 10.5 10.0 9.5 9.0 8.5 8.0 7.5 7.0 6.5 6.0 5.5 5.0 4.5 4.0 3.5 3.0 2.5 2.0 1.5 1.0 0.5 0.0
f1 (ppm)

2.6’d

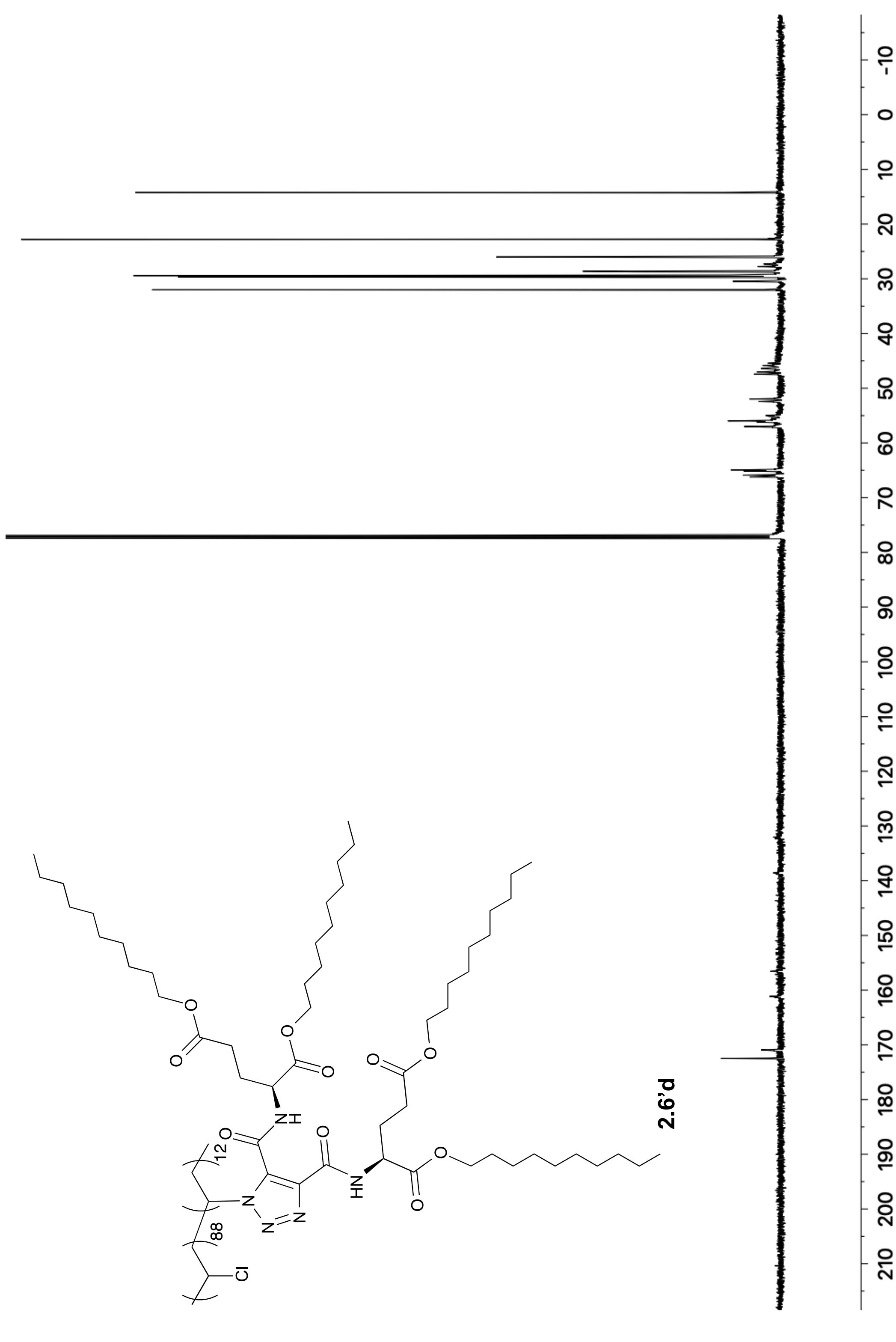
2.6'd
f1 (ppm)
210 200 190 180 170 160 150 140 130 120 110 100 90 80 70 60 50 40 30 20 10 0 -10

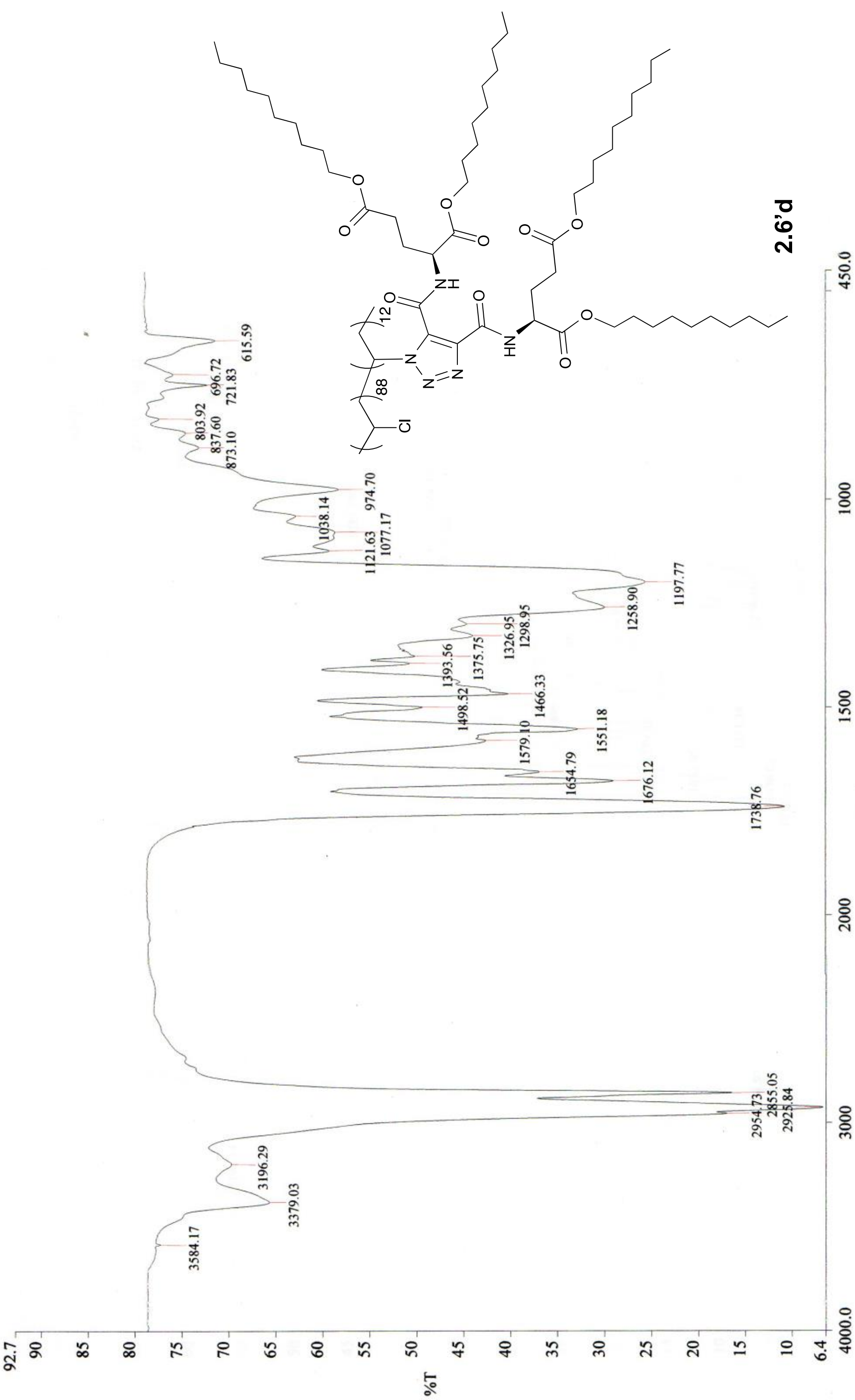
%T
cm-1
4000.0
3000
2000
1500
1000
450.0
3584.17
3379.03
3196.29
2954.73
2925.84
2855.05
1738.76
1676.12
1654.79
1579.10
1551.18
1498.52
1466.33
1393.56
1375.75
1326.95
1298.95
1258.90
1197.77
1121.63
1077.17
1038.14
974.70
873.10
837.60
803.92
721.83
696.72
615.59
Cl
88
12
N
NH
HN
O

2.6'd

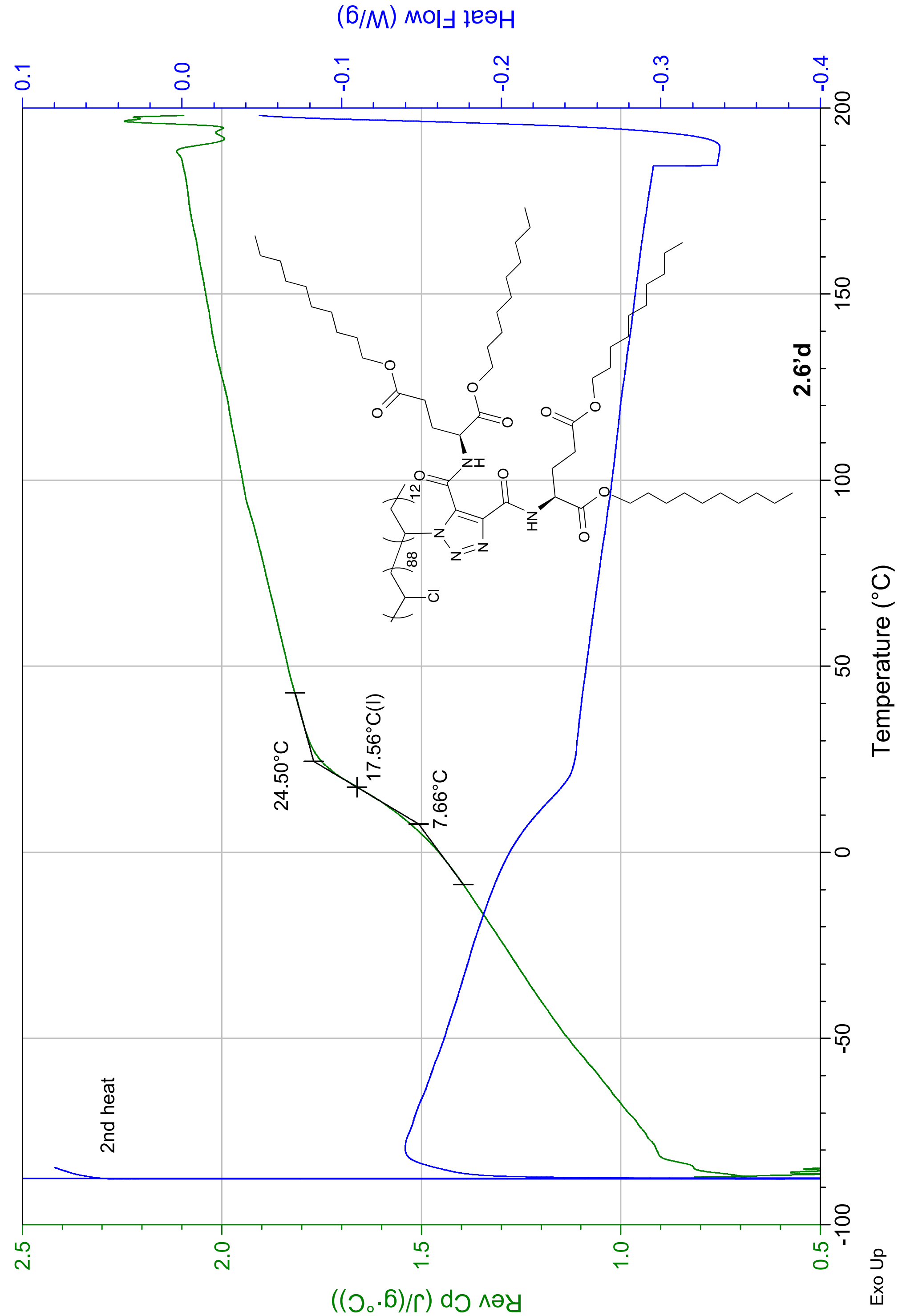

Heat Flow (W/g)
Rev Cp (J/(g·°C))
Temperature (°C)
Exo Up
2nd heat
24.50°C
17.56°C(I)
7.66°C
2.6'd

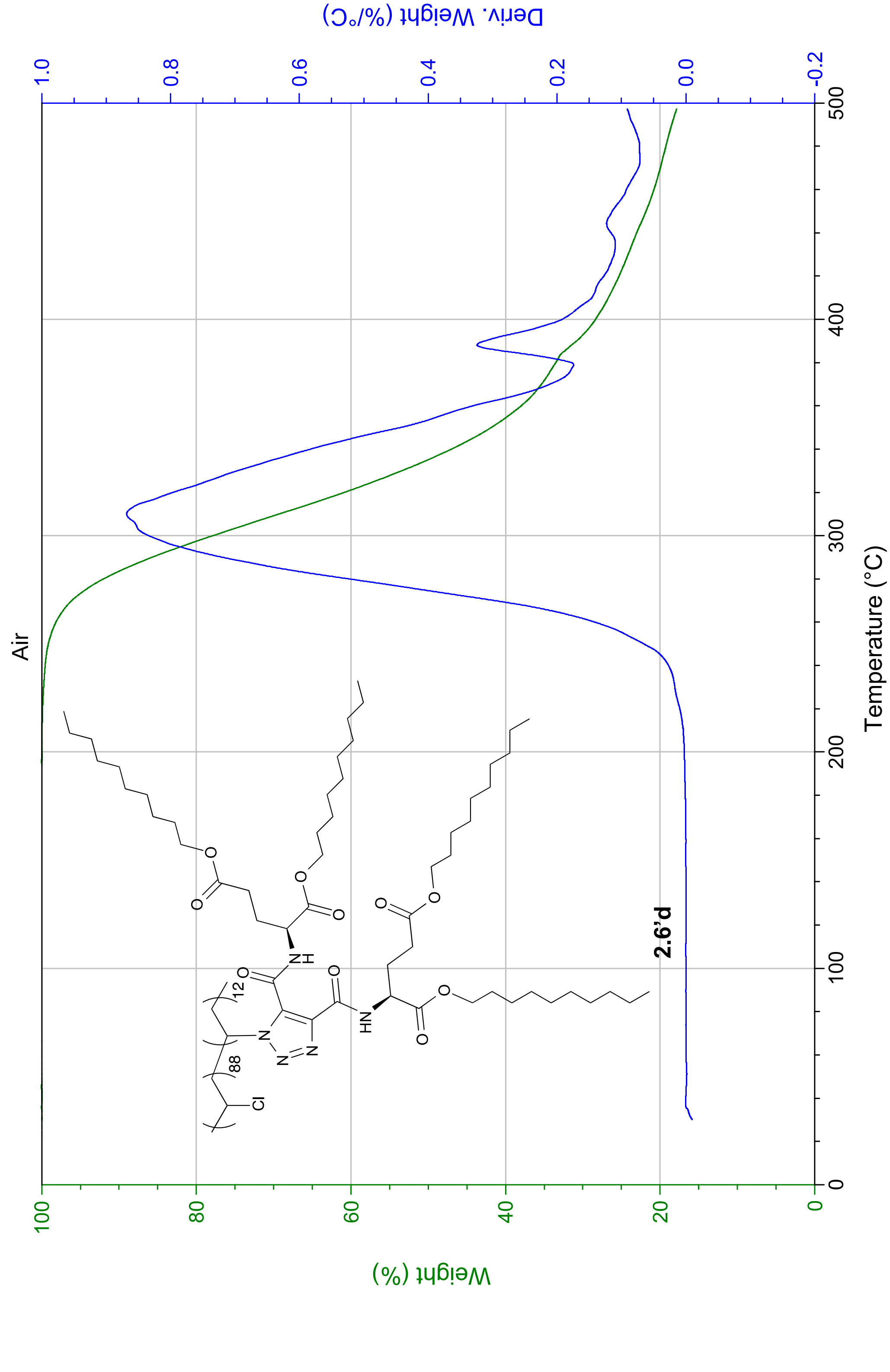
Air
2.6'd
Temperature (°C)
Weight (%)
Deriv. Weight (%/°C)
0
100
200
300
400
500
20
40
60
80
-0.2
0.0
0.2
0.4
0.6
0.8
1.0
Cl
88
12

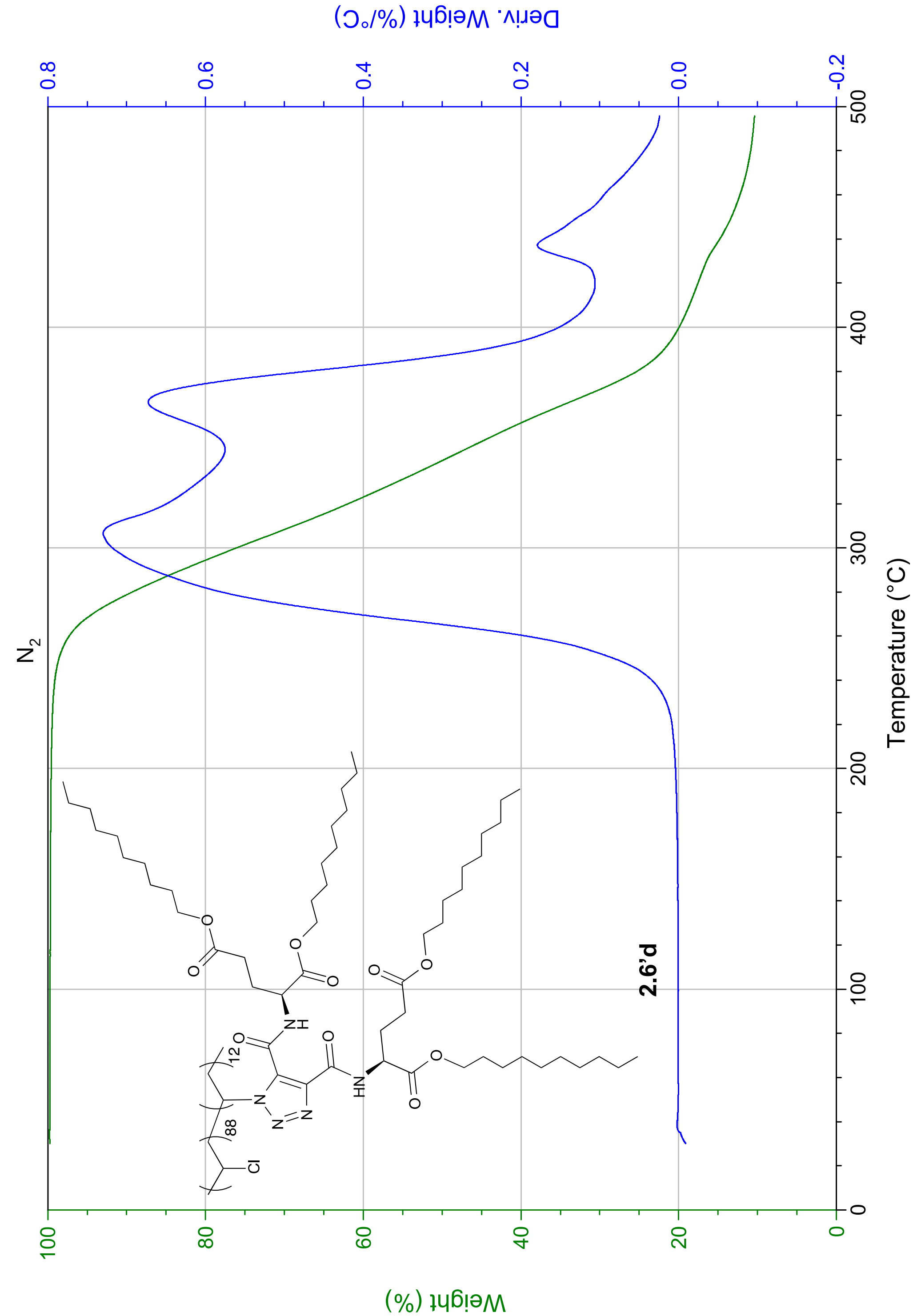
N$_2$
2.6'd
Temperature (°C)
Weight (%)
Deriv. Weight (%/°C)
0
100
200
300
400
500
20
40
60
80
-0.2
0.0
0.2
0.4
0.6
0.8

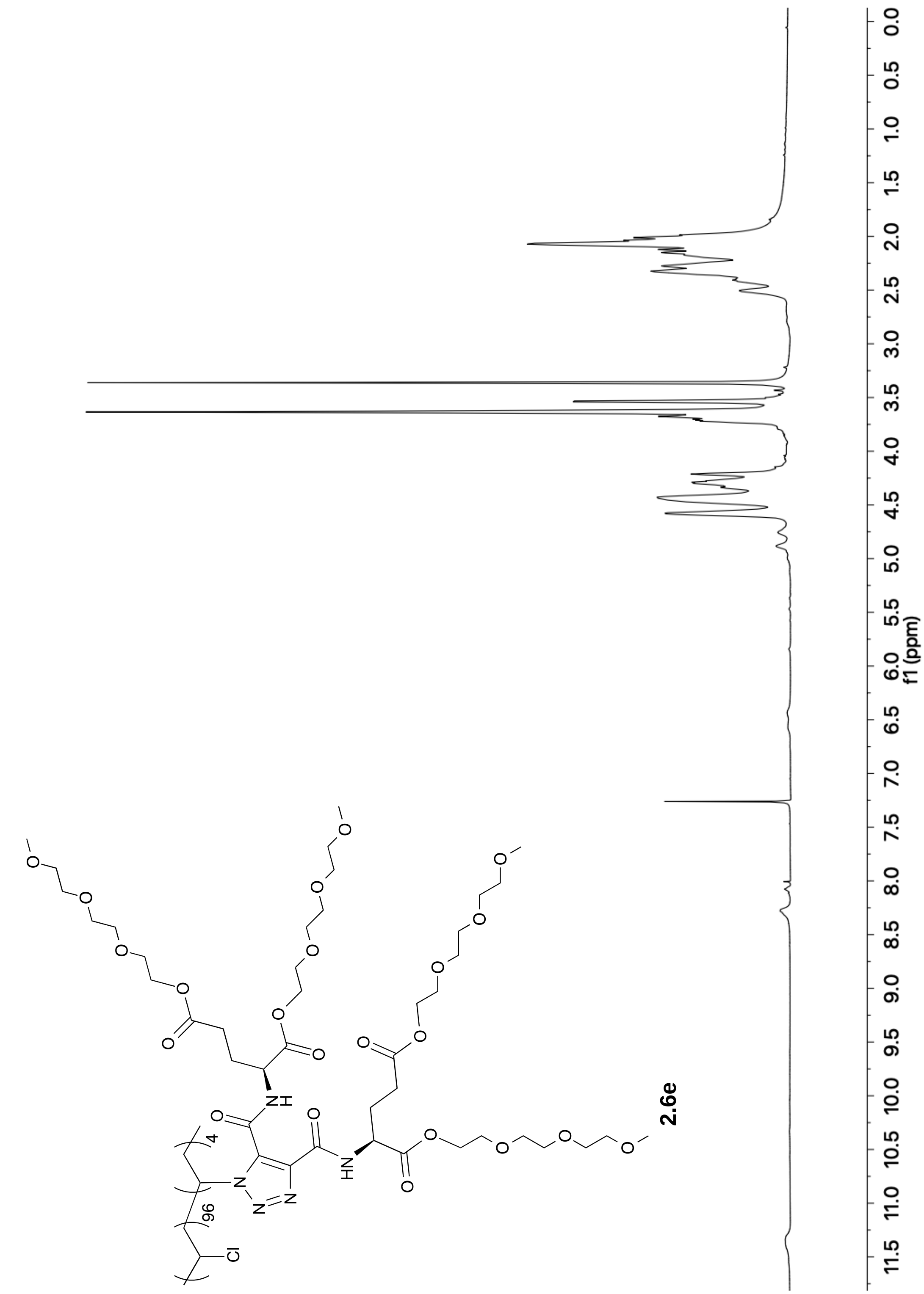
2.6e
f1 (ppm)
0.0 0.5 1.0 1.5 2.0 2.5 3.0 3.5 4.0 4.5 5.0 5.5 6.0 6.5 7.0 7.5 8.0 8.5 9.0 9.5 10.0 10.5 11.0 11.5

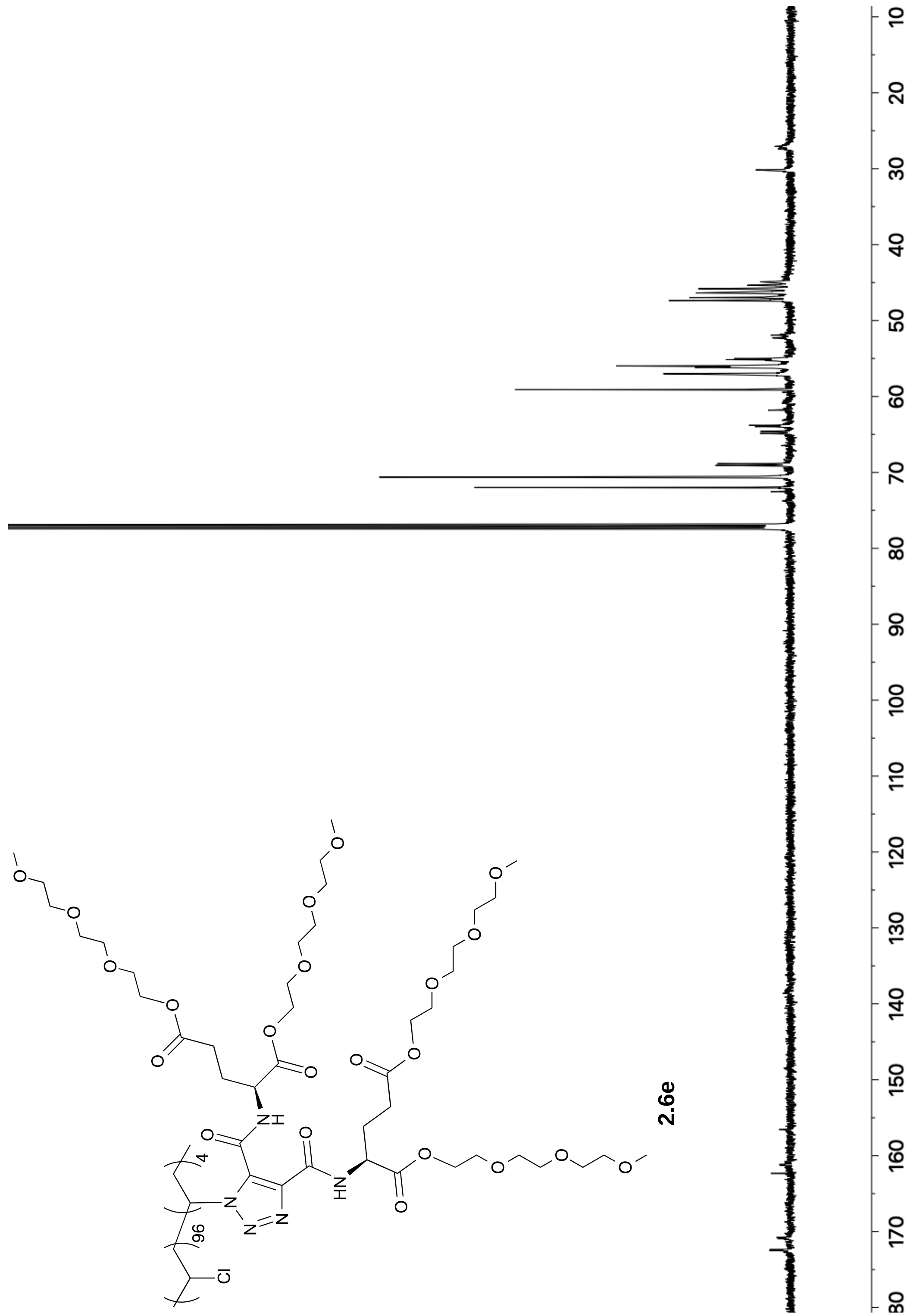
2.6e
f1 (ppm)
180
170
160
150
140
130
120
110
100
90
80
70
60
50
40
30
20
10

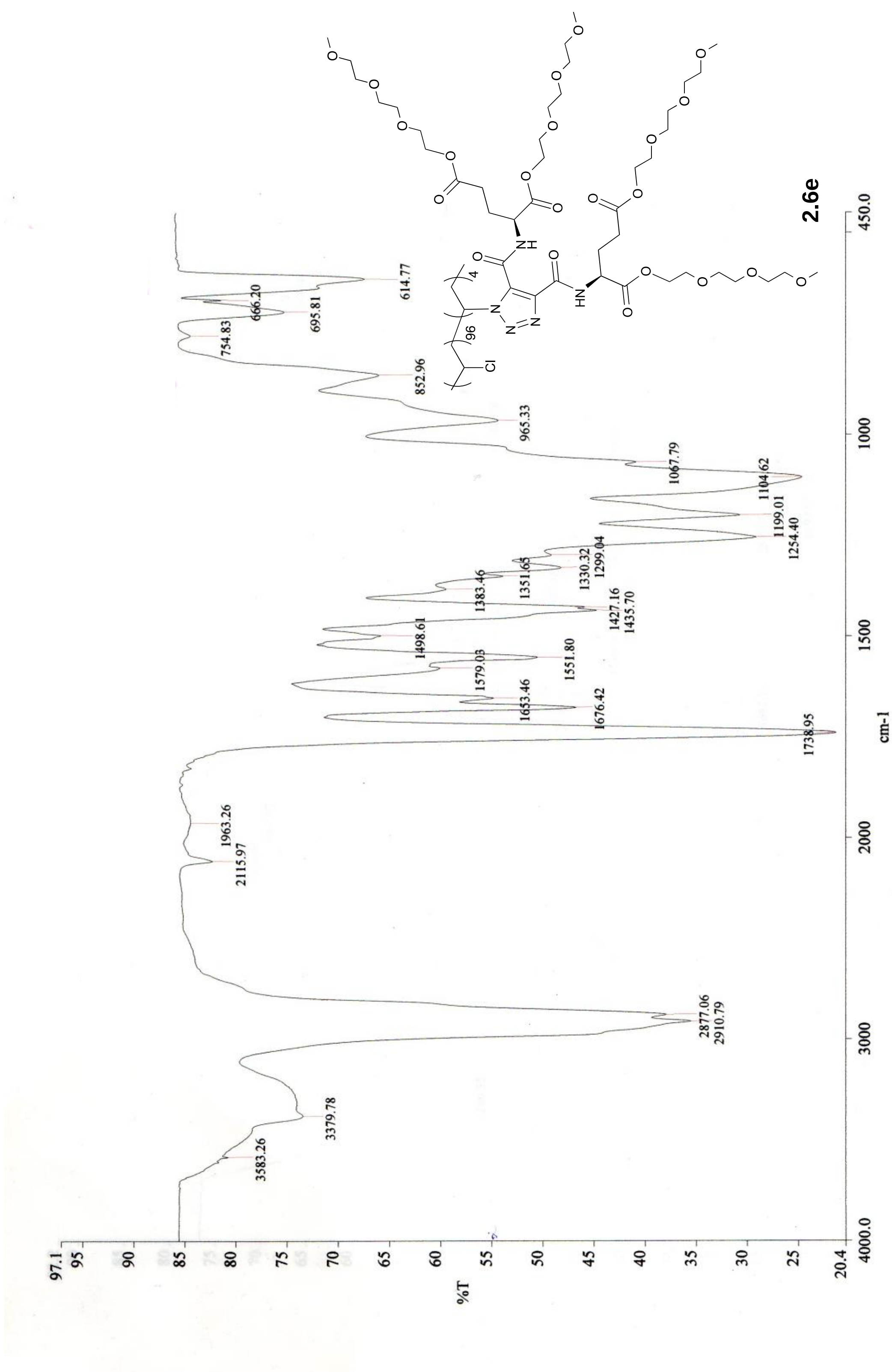

2.6e
%T
cm-1
97.1
95
90
85
80
75
70
65
60
55
50
45
40
35
30
25
20.4
4000.0
3000
2000
1500
1000
450.0
3583.26
3379.78
2877.06
2910.79
2115.97
1963.26
1738.95
1676.42
1653.46
1579.03
1551.80
1498.61
1435.70
1427.16
1383.46
1351.65
1330.32
1299.04
1254.40
1199.01
1104.62
1067.79
965.33
852.96
754.83
695.81
666.20
614.77

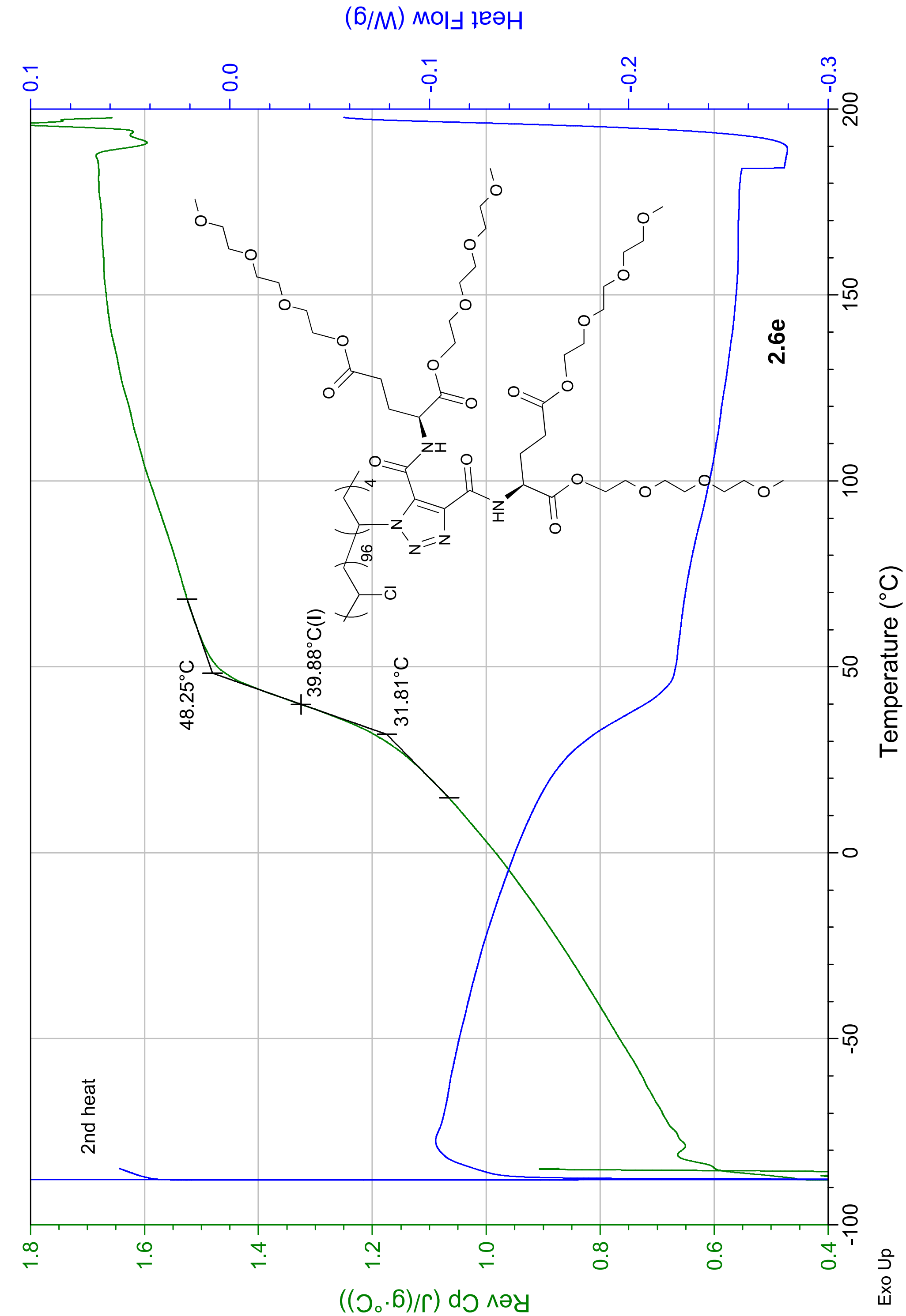
Heat Flow (W/g)
Rev Cp (J/(g·°C))
Temperature (°C)
Exo Up
2nd heat
48.25°C
39.88°C(I)
31.81°C
2.6e

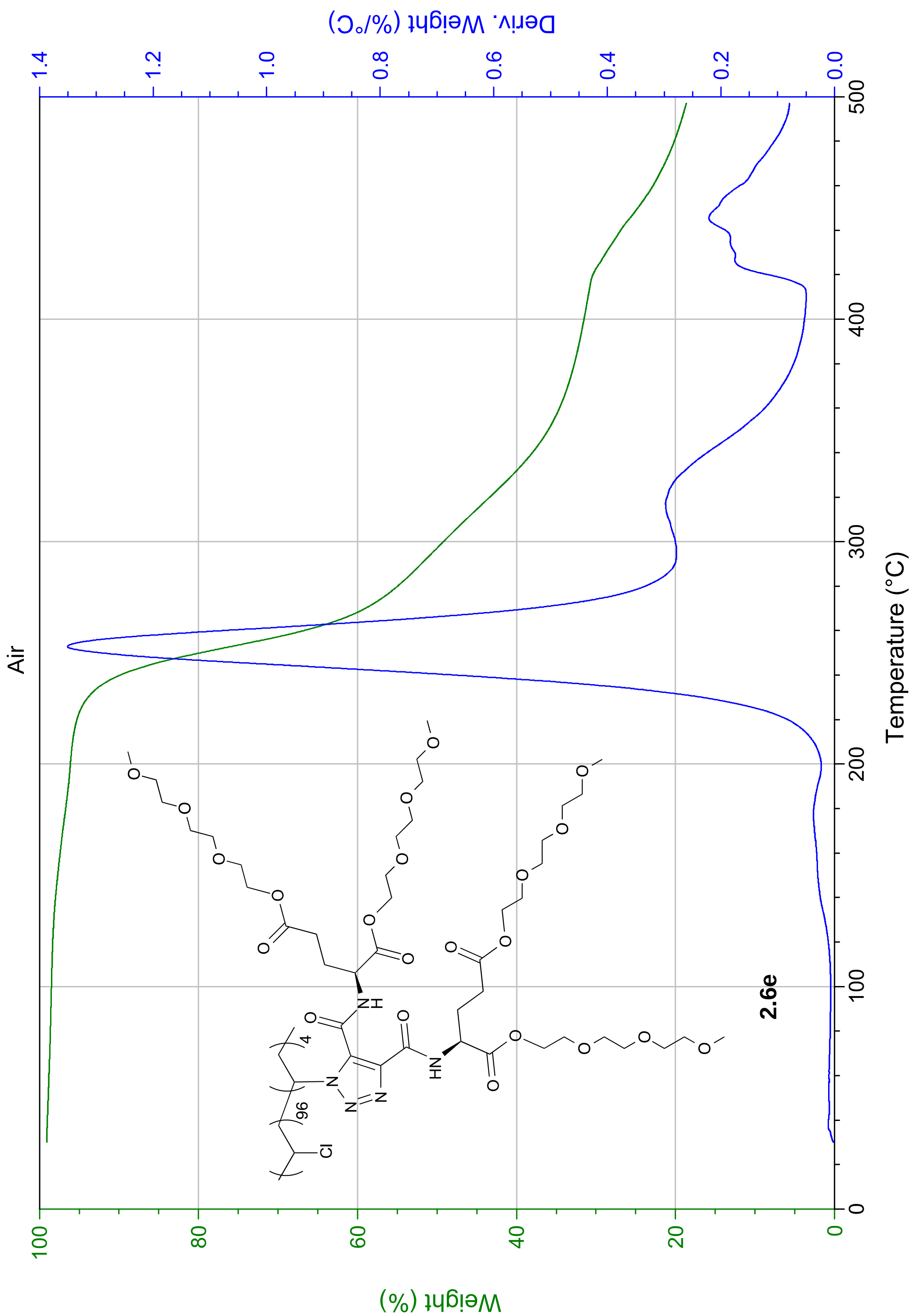

Air
Temperature (°C)
Weight (%)
Deriv. Weight (%/°C)
2.6e

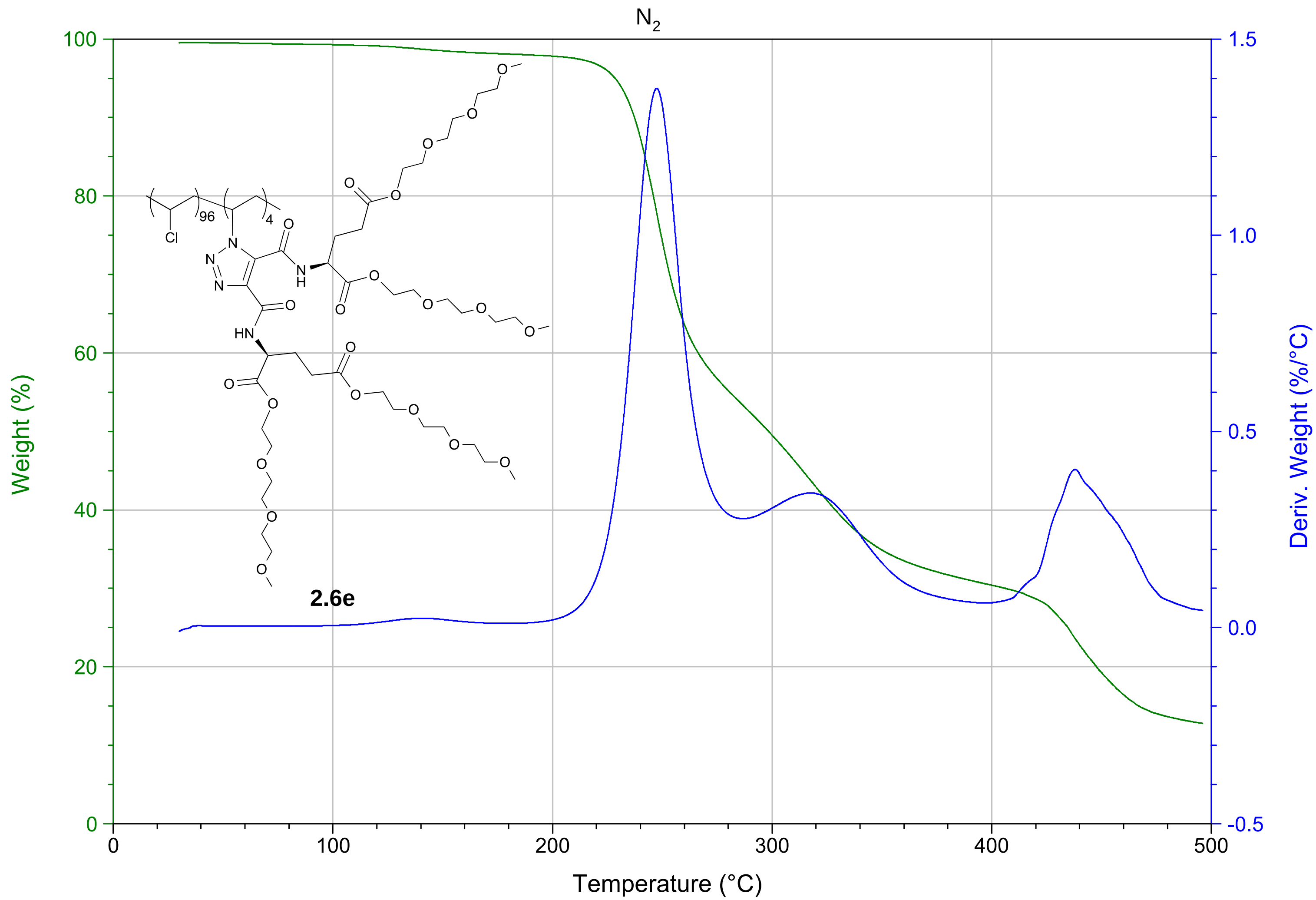
N2
Weight (%)
Deriv. Weight (%/°C)
Temperature (°C)
2.6e
100
80
60
40
20
0
1.5
1.0
0.5
0.0
-0.5
0
100
200
300
400
500

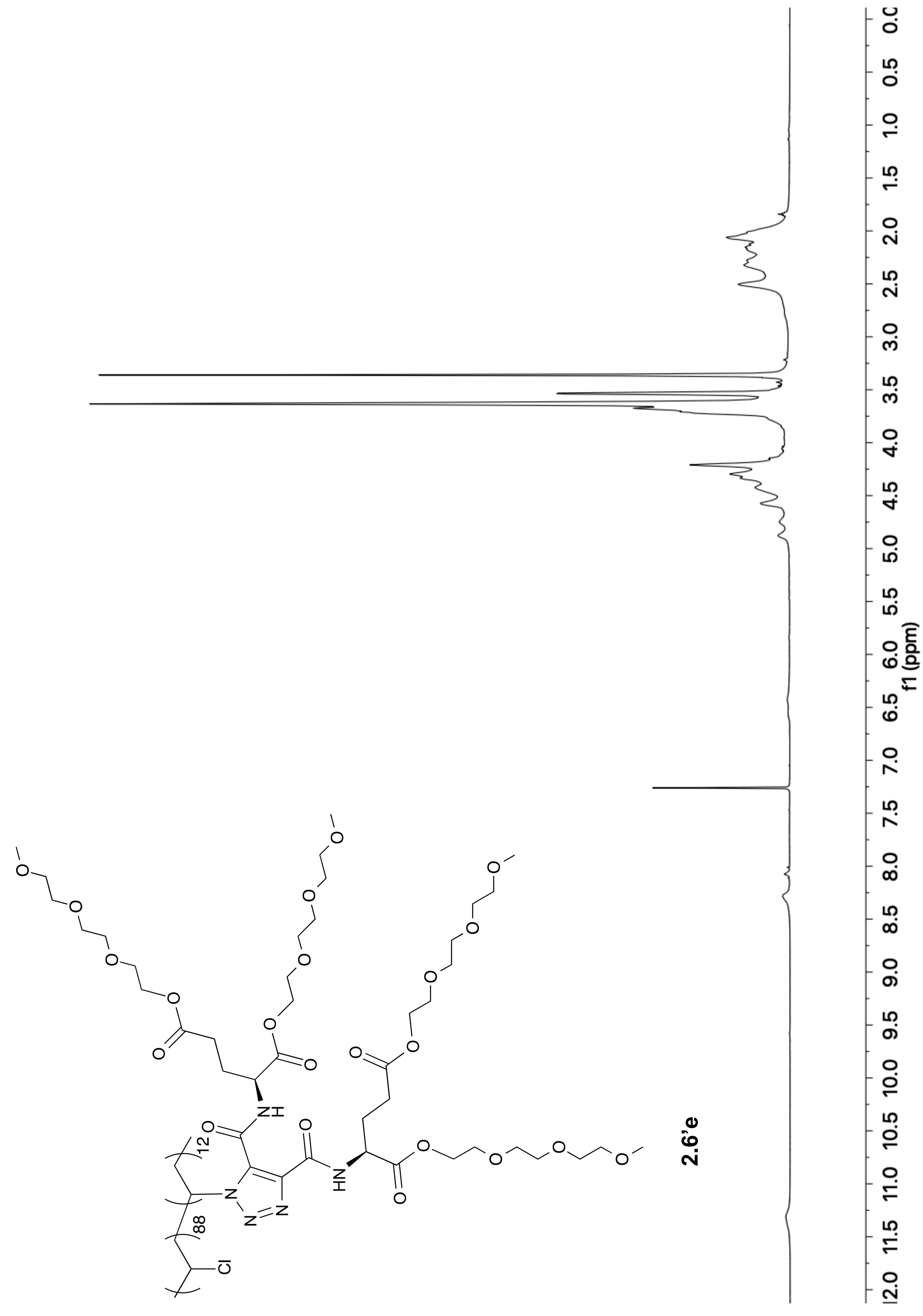
2.6'e
f1 (ppm)
0.0 0.5 1.0 1.5 2.0 2.5 3.0 3.5 4.0 4.5 5.0 5.5 6.0 6.5 7.0 7.5 8.0 8.5 9.0 9.5 10.0 10.5 11.0 11.5 12.0

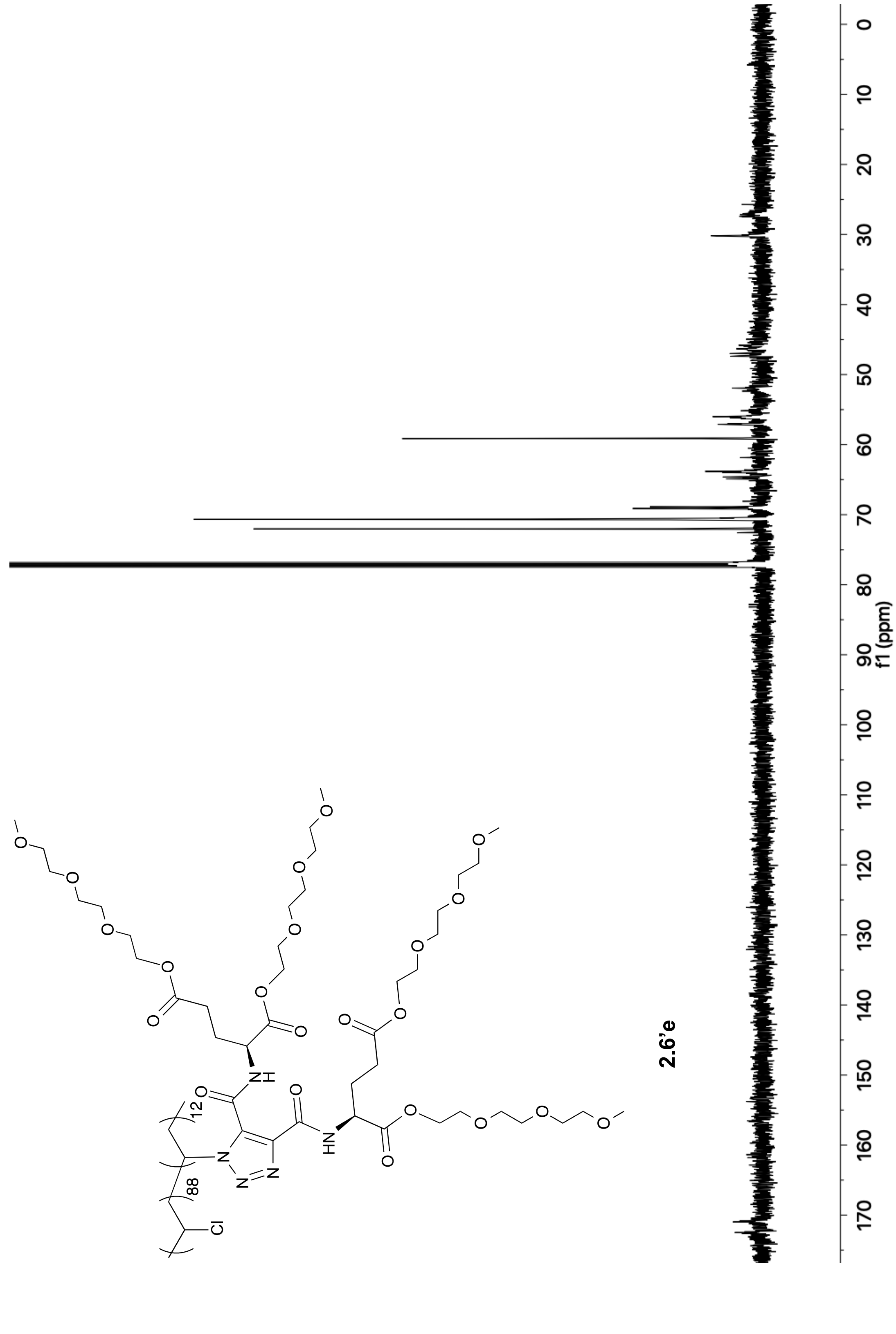
2.6'e
f1 (ppm)
0
10
20
30
40
50
60
70
80
90
100
110
120
130
140
150
160
170

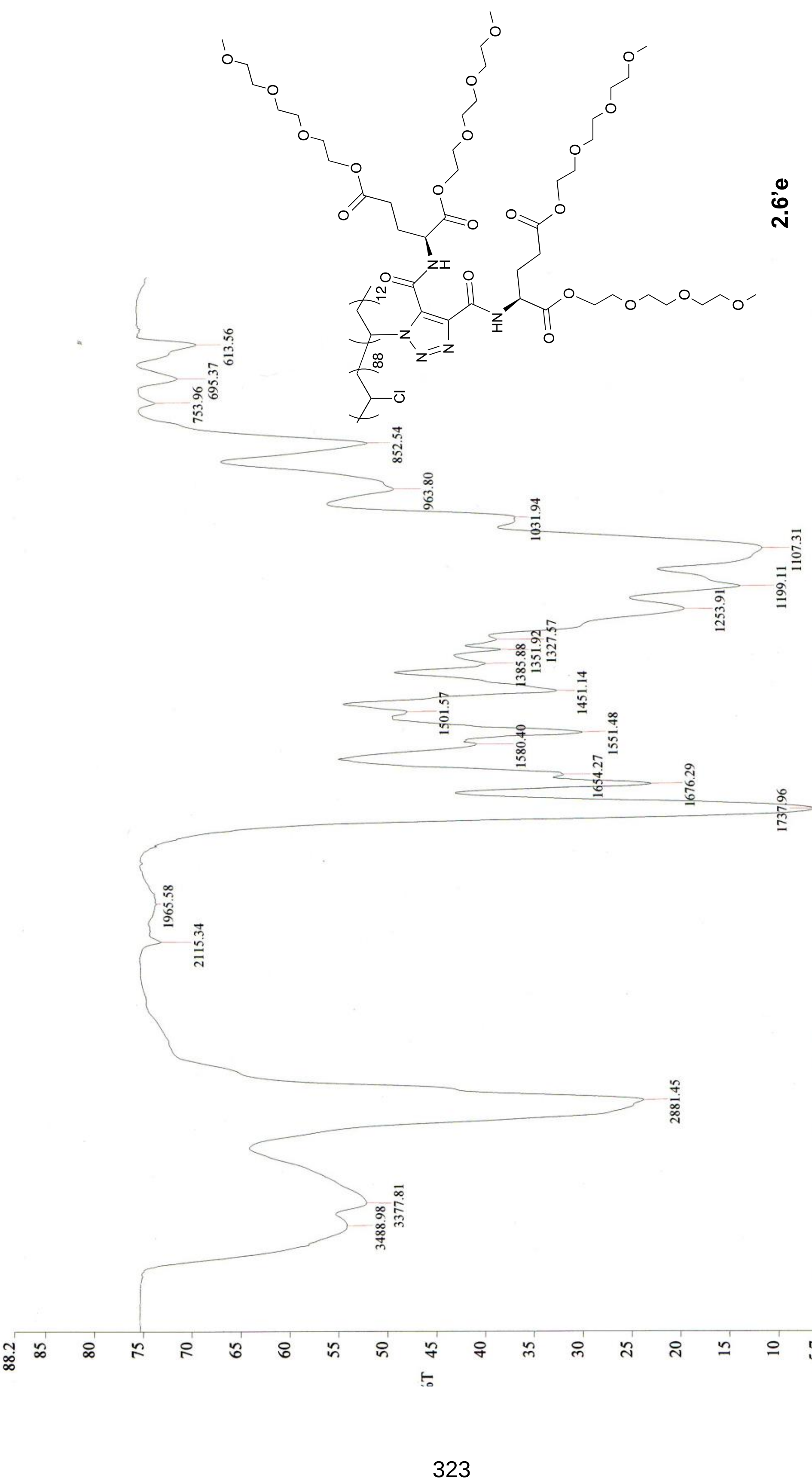
%T
cm-1
4000.0
3000
2000
1500
1000
450.0
88.2
85
80
75
70
65
60
55
50
45
40
35
30
25
20
15
10
5.7
3488.98
3377.81
2881.45
2115.34
1965.58
1737.96
1676.29
1654.27
1580.40
1551.48
1501.57
1451.14
1385.88
1351.92
1327.57
1253.91
1199.11
1107.31
1031.94
963.80
852.54
753.96
695.37
613.56
Cl
88
12

2.6'e

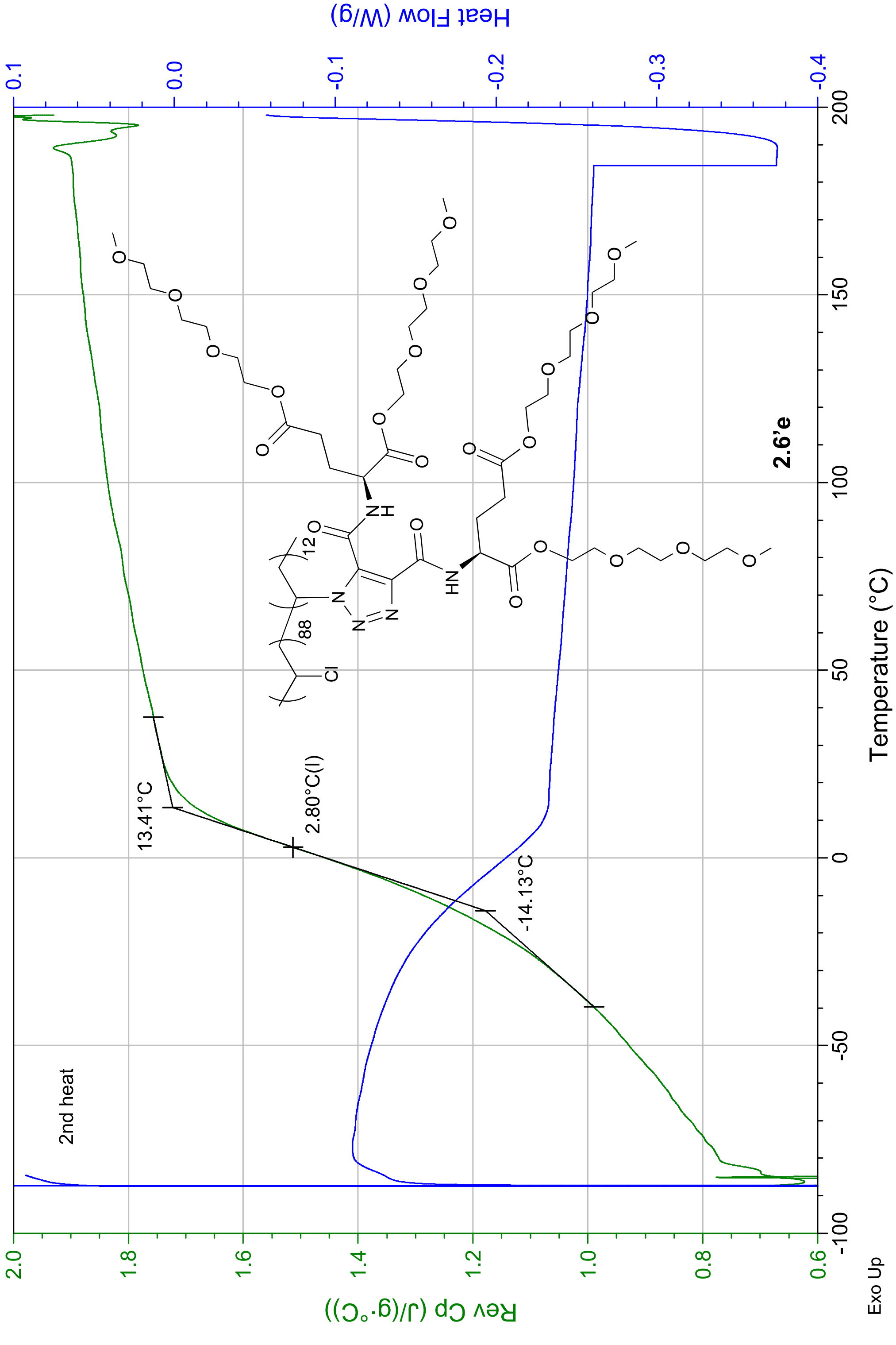
Heat Flow (W/g)
Rev Cp (J/(g·°C))
Temperature (°C)
Exo Up
2nd heat
13.41°C
2.80°C(I)
-14.13°C
2.6'e

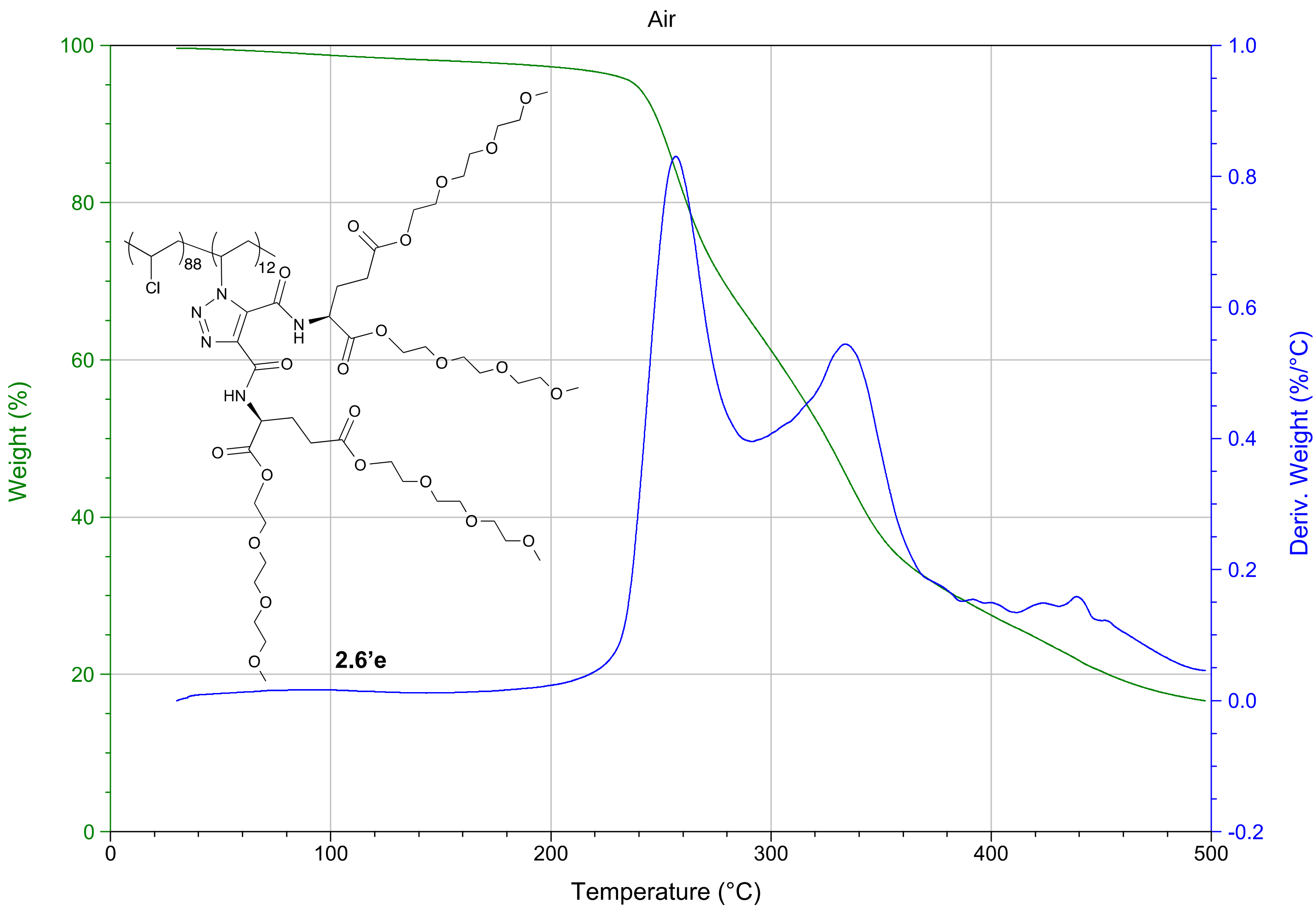
Air
Weight (%)
Deriv. Weight (%/°C)
Temperature (°C)
2.6'e
0
20
40
60
80
100
0
100
200
300
400
500
-0.2
0.0
0.2
0.4
0.6
0.8
1.0

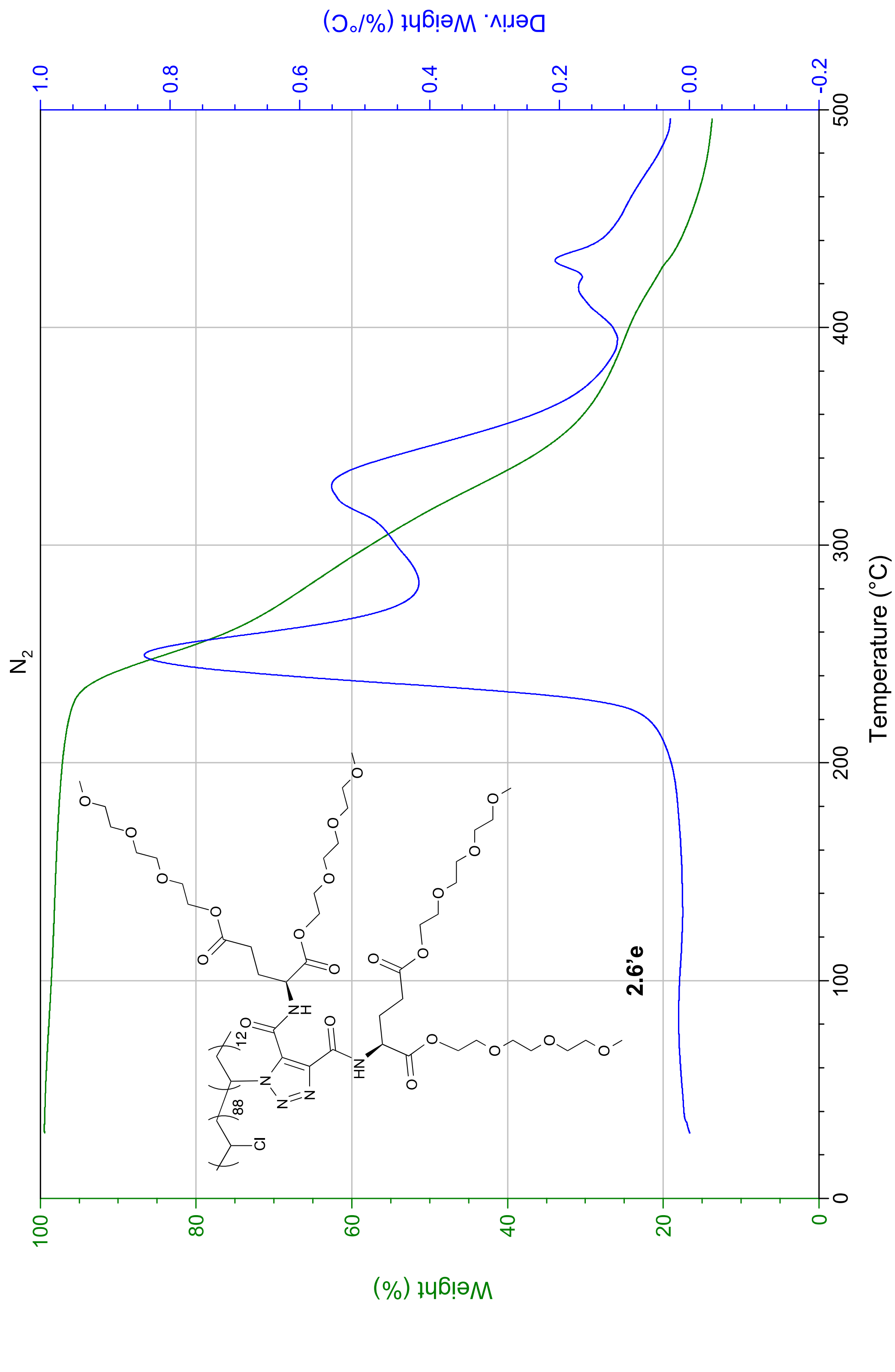
N$_2$
Temperature (°C)
Weight (%)
Deriv. Weight (%/°C)
2.6’e

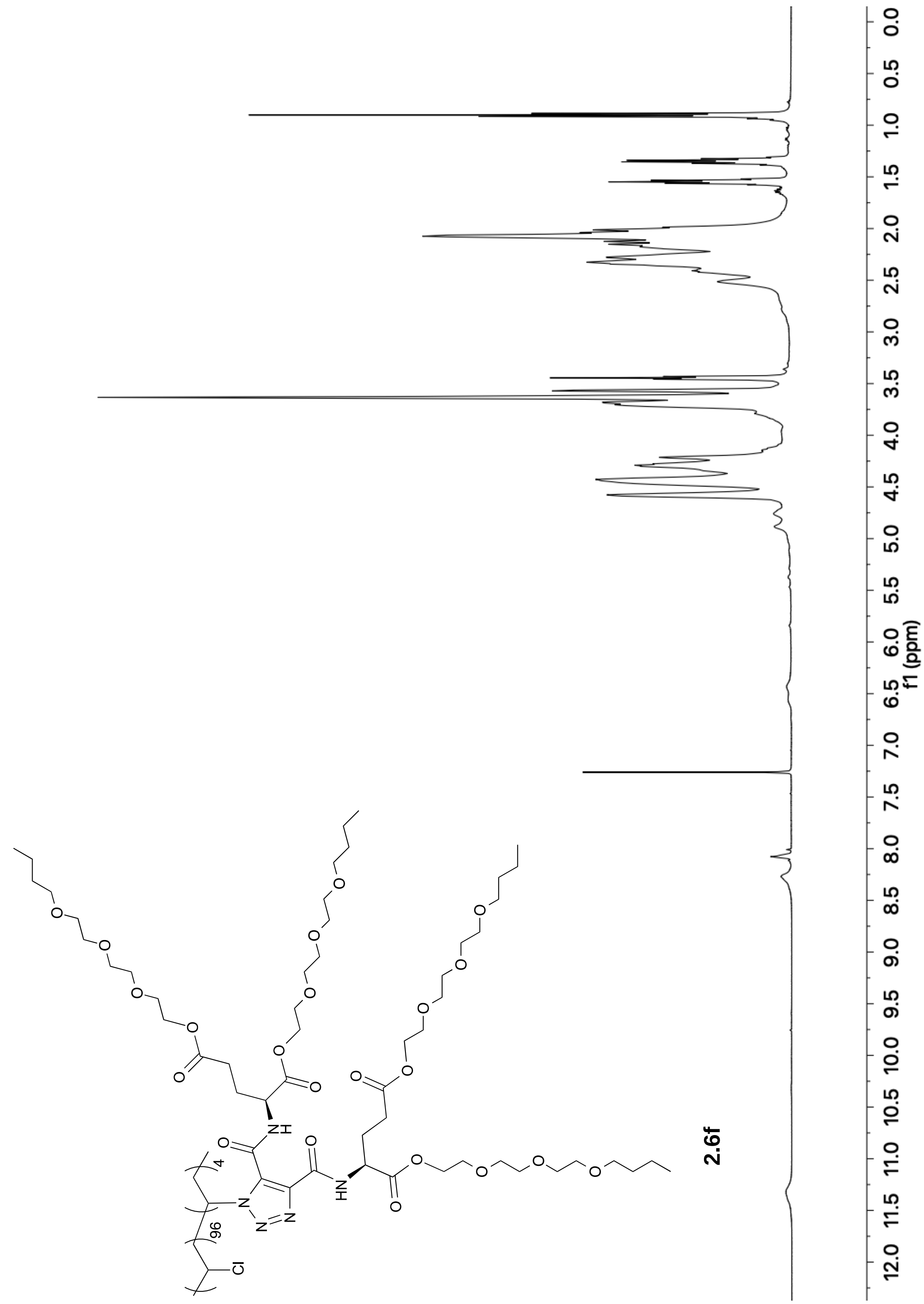
2.6f
f1 (ppm)
0.0 0.5 1.0 1.5 2.0 2.5 3.0 3.5 4.0 4.5 5.0 5.5 6.0 6.5 7.0 7.5 8.0 8.5 9.0 9.5 10.0 10.5 11.0 11.5 12.0

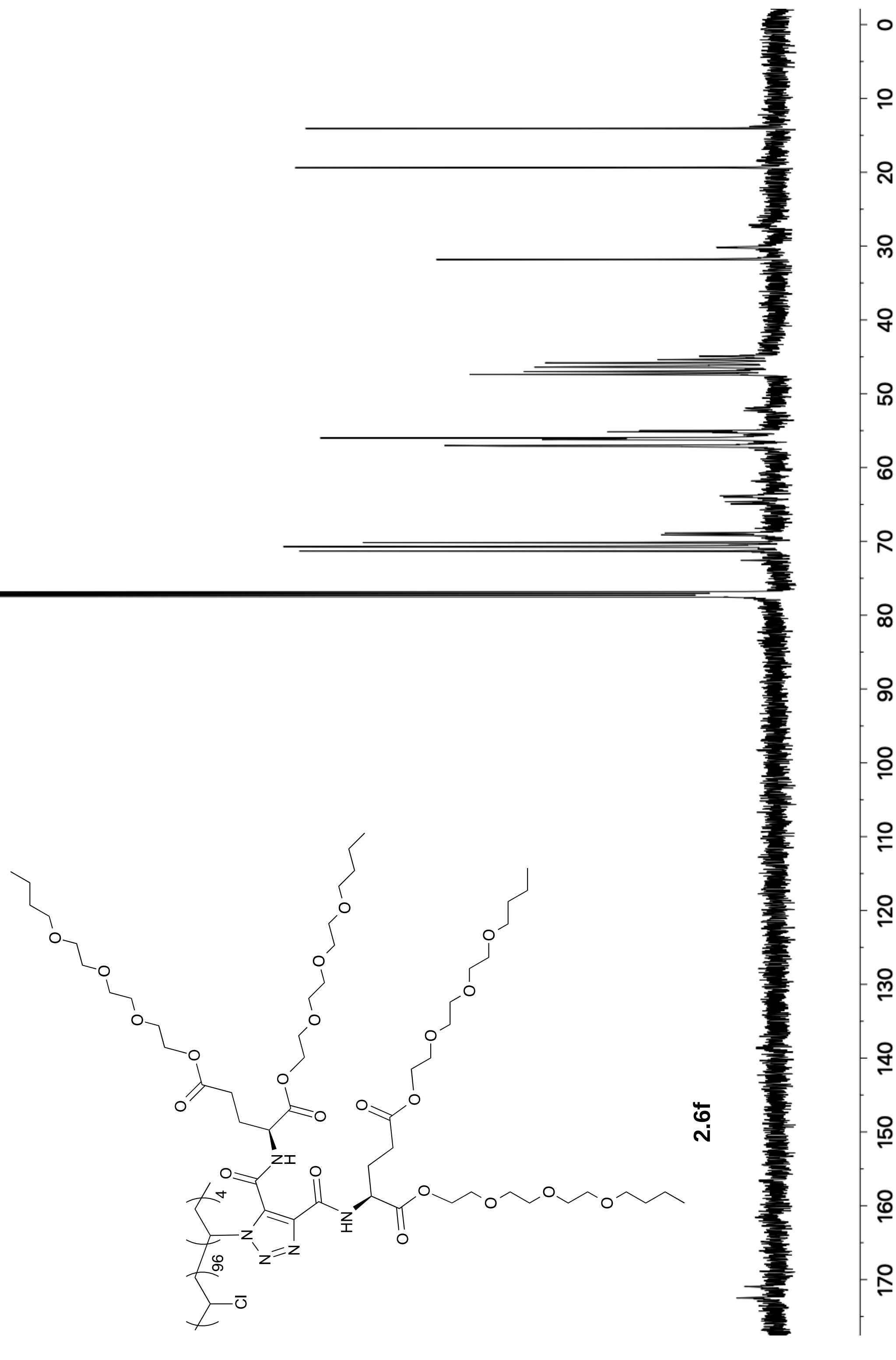
f1 (ppm)
0
10
20
30
40
50
60
70
80
90
100
110
120
130
140
150
160
170
NH
HN
Cl
96
4

2.6f

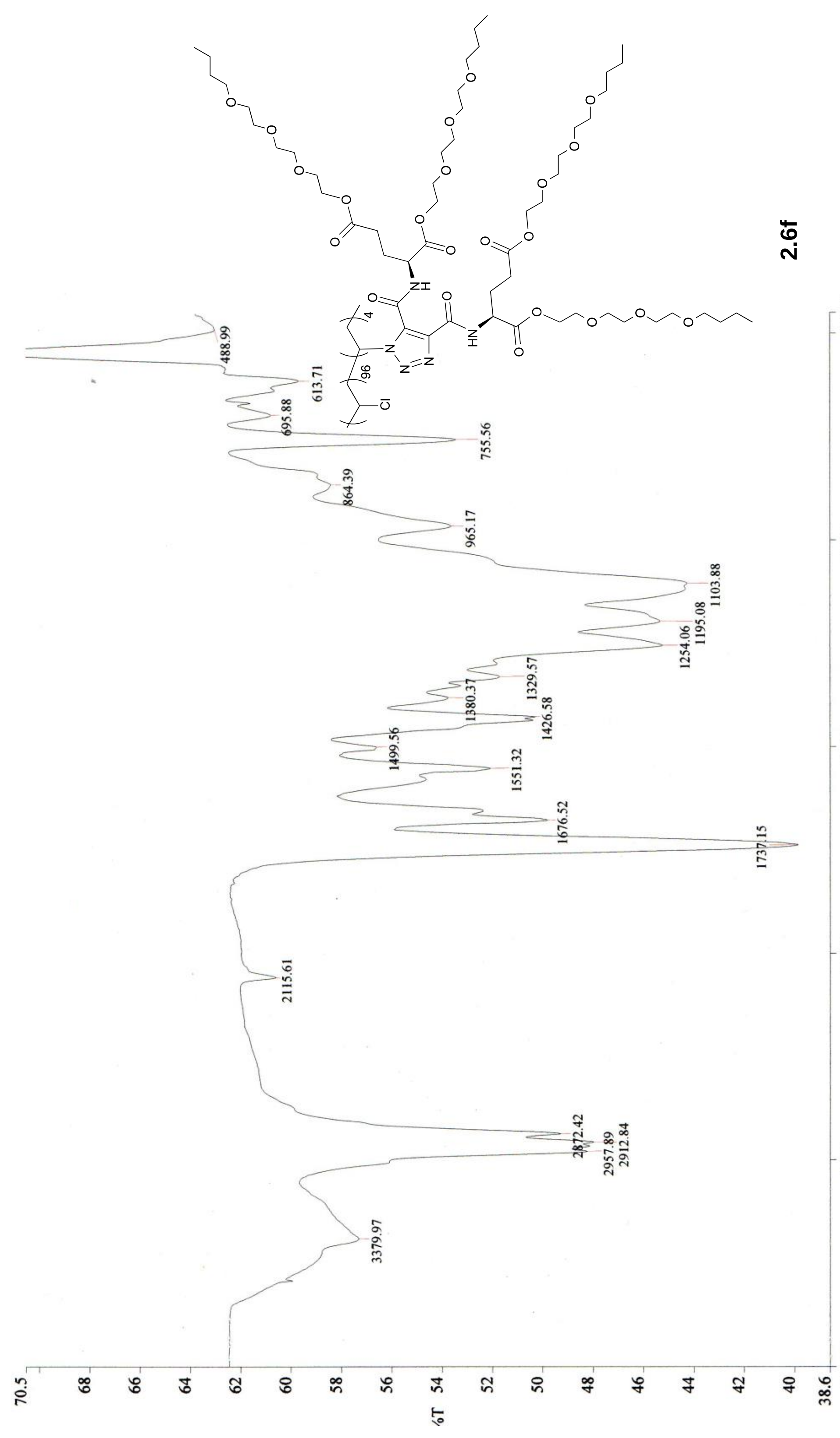
%T
cm-1
3379.97
2957.89
2912.84
2872.42
2115.61
1737.15
1676.52
1551.32
1499.56
1426.58
1380.37
1329.57
1254.06
1195.08
1103.88
965.17
864.39
755.56
695.88
613.71
488.99

2.6f

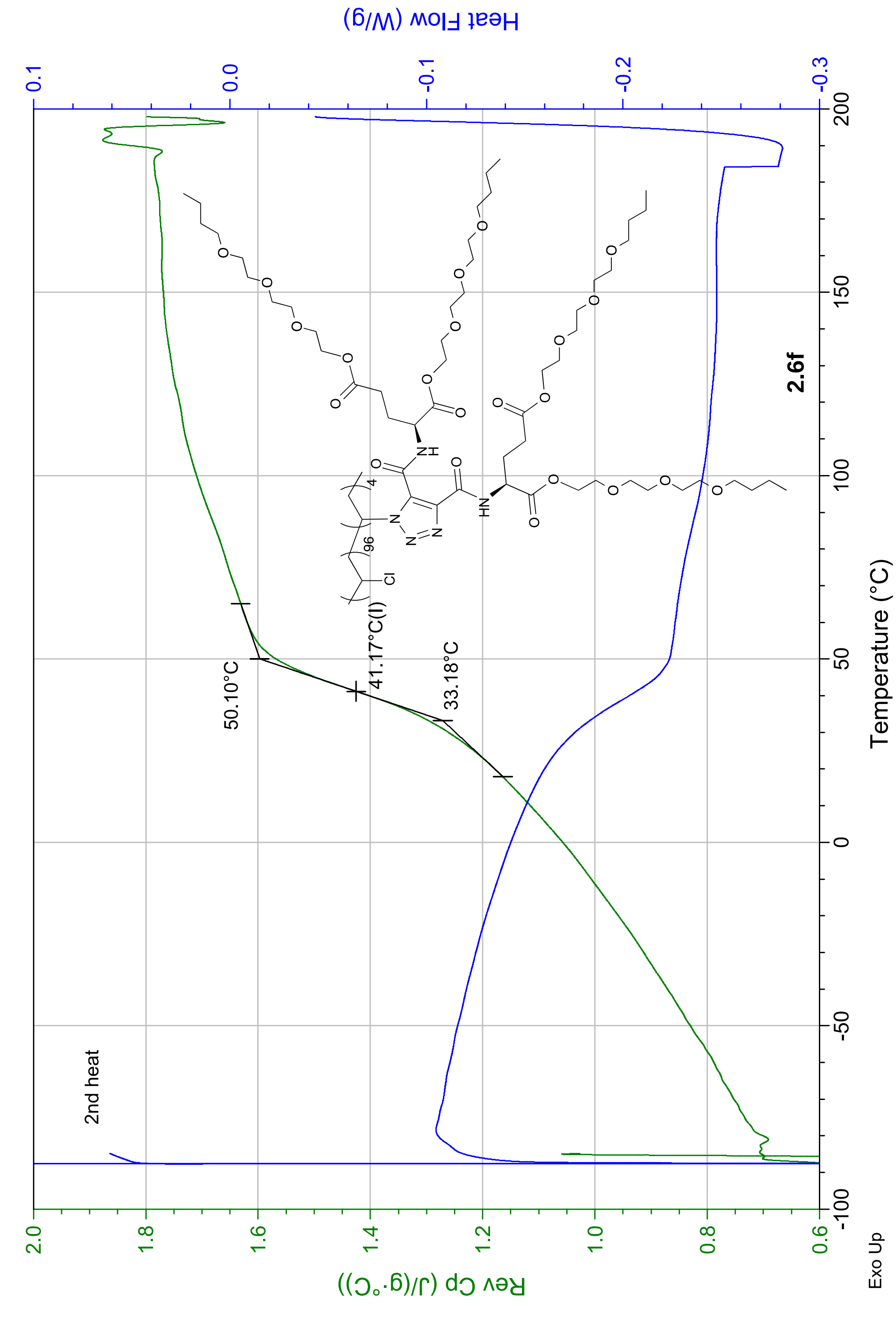

Heat Flow (W/g)
Rev Cp (J/(g·°C))
Temperature (°C)
Exo Up
2nd heat
50.10°C
41.17°C(I)
33.18°C
2.6f

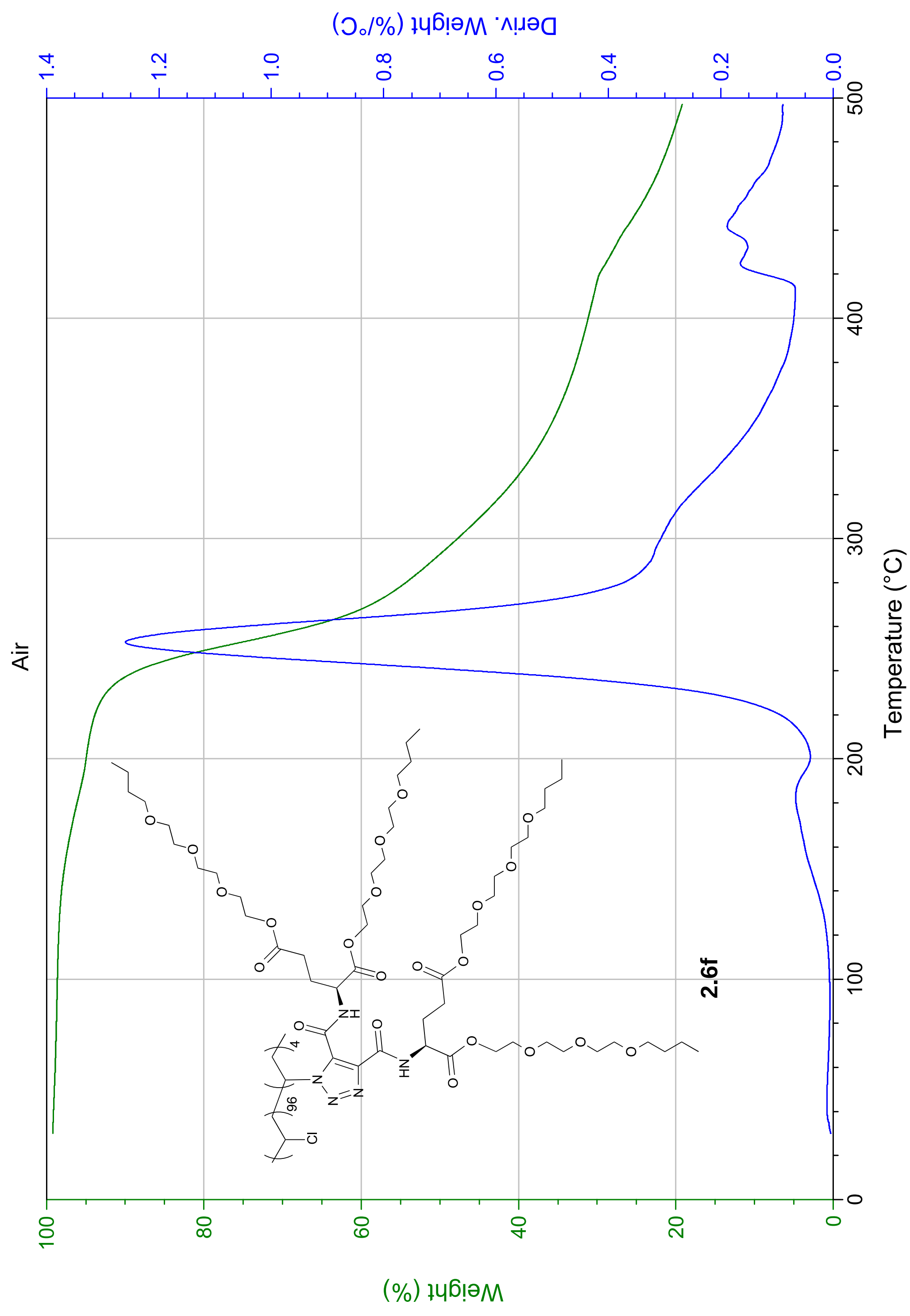
Air
2.6f
Temperature (°C)
Weight (%)
Deriv. Weight (%/°C)

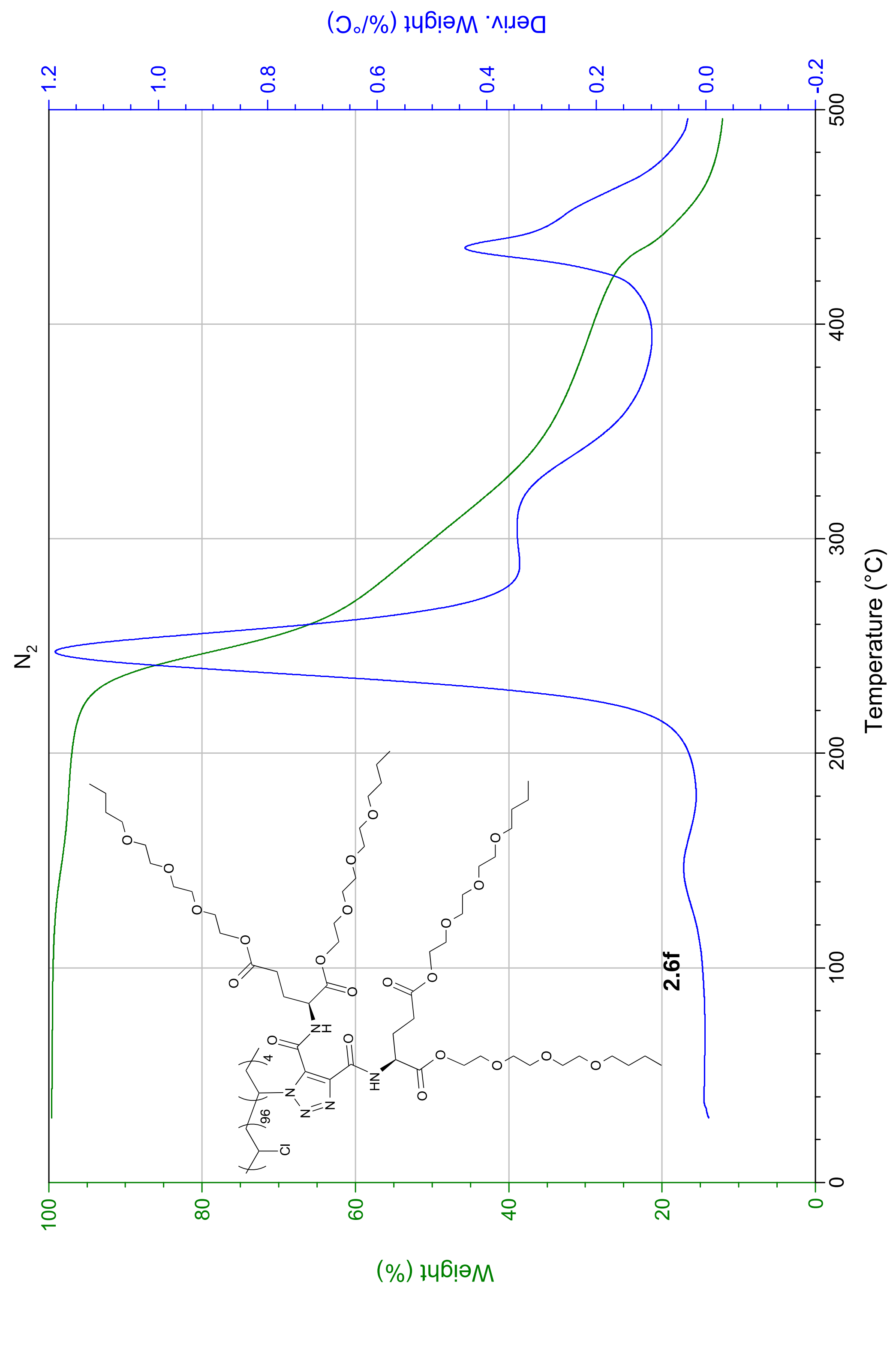

N2
2.6f
Temperature (°C)
Weight (%)
Deriv. Weight (%/°C)
0
100
200
300
400
500
0
20
40
60
80
100
-0.2
0.0
0.2
0.4
0.6
0.8
1.0
1.2

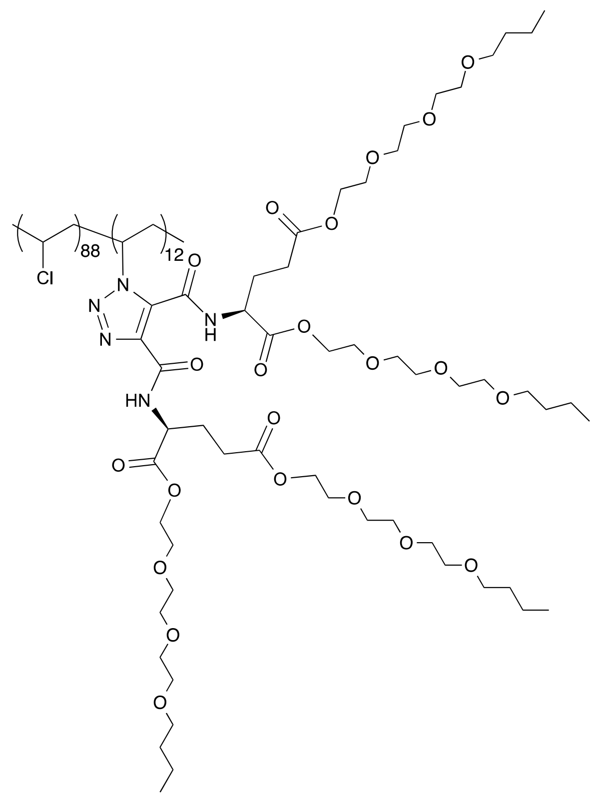
Cl
88
12
O
N
N
N
N
O
NH
HN
O
O
O
O
O
O
O
O
O
O
O
O
O
O
O
O
O

2.6'f

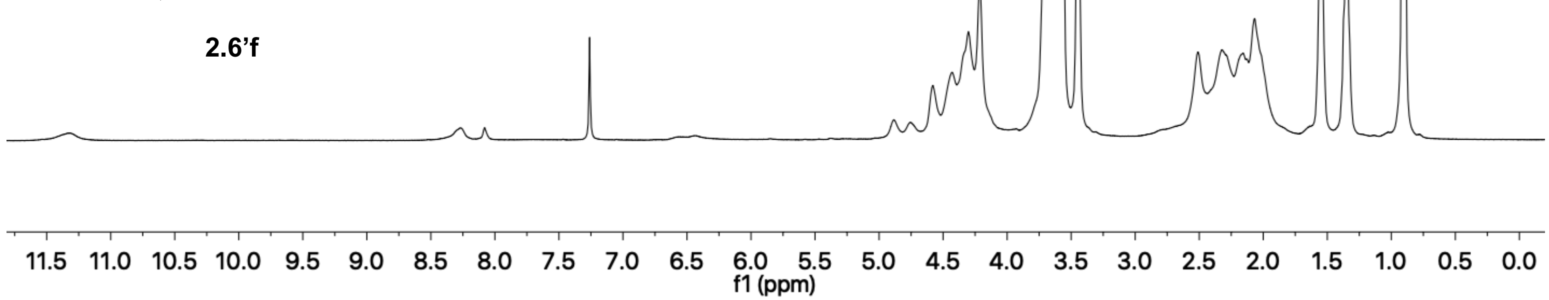
11.5 11.0 10.5 10.0 9.5 9.0 8.5 8.0 7.5 7.0 6.5 6.0 5.5 5.0 4.5 4.0 3.5 3.0 2.5 2.0 1.5 1.0 0.5 0.0
f1 (ppm)

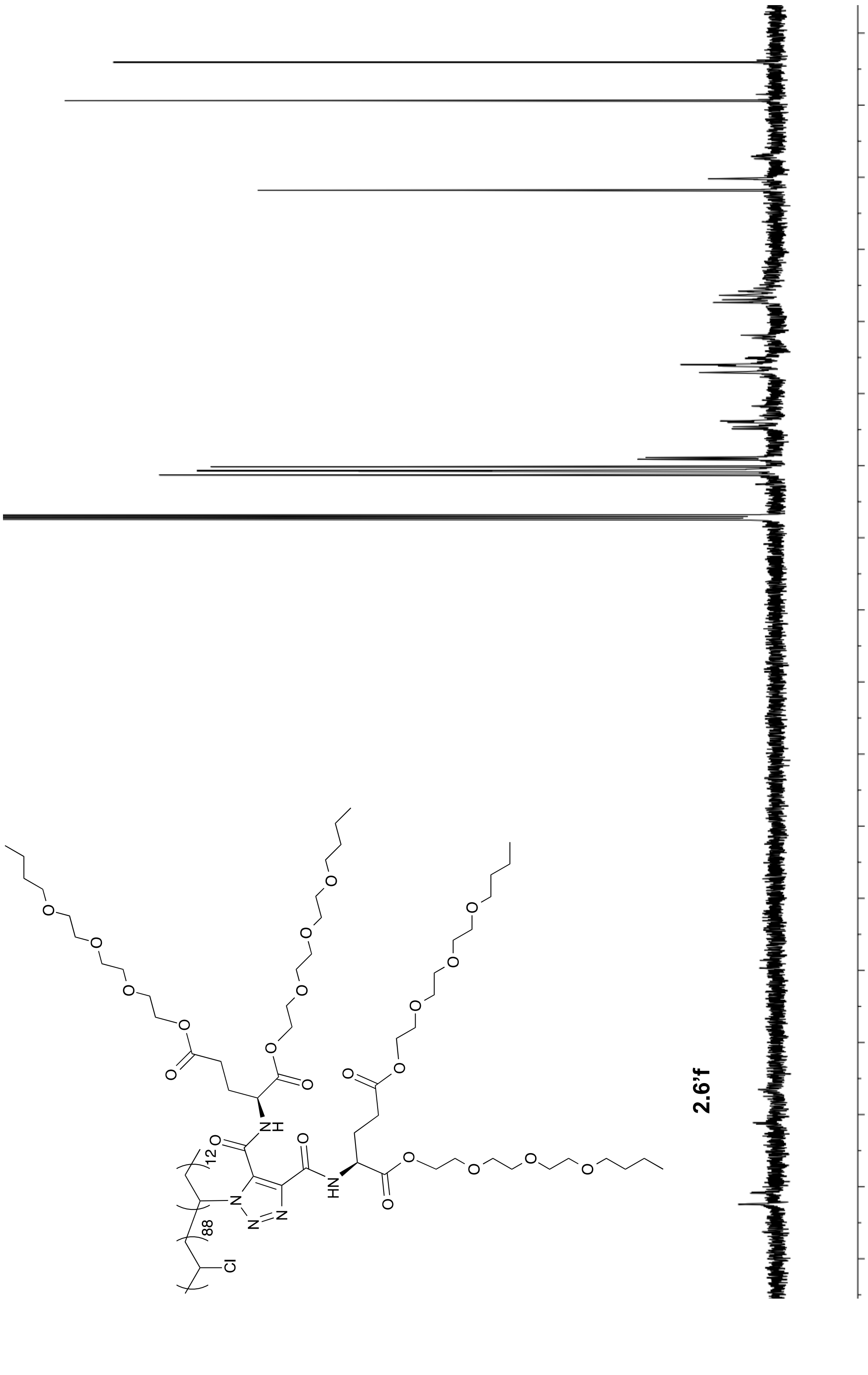
2.6'f
f1 (ppm)
10
20
30
40
50
60
70
80
90
100
110
120
130
140
150
160
170
180
Cl
88
12
NH
HN

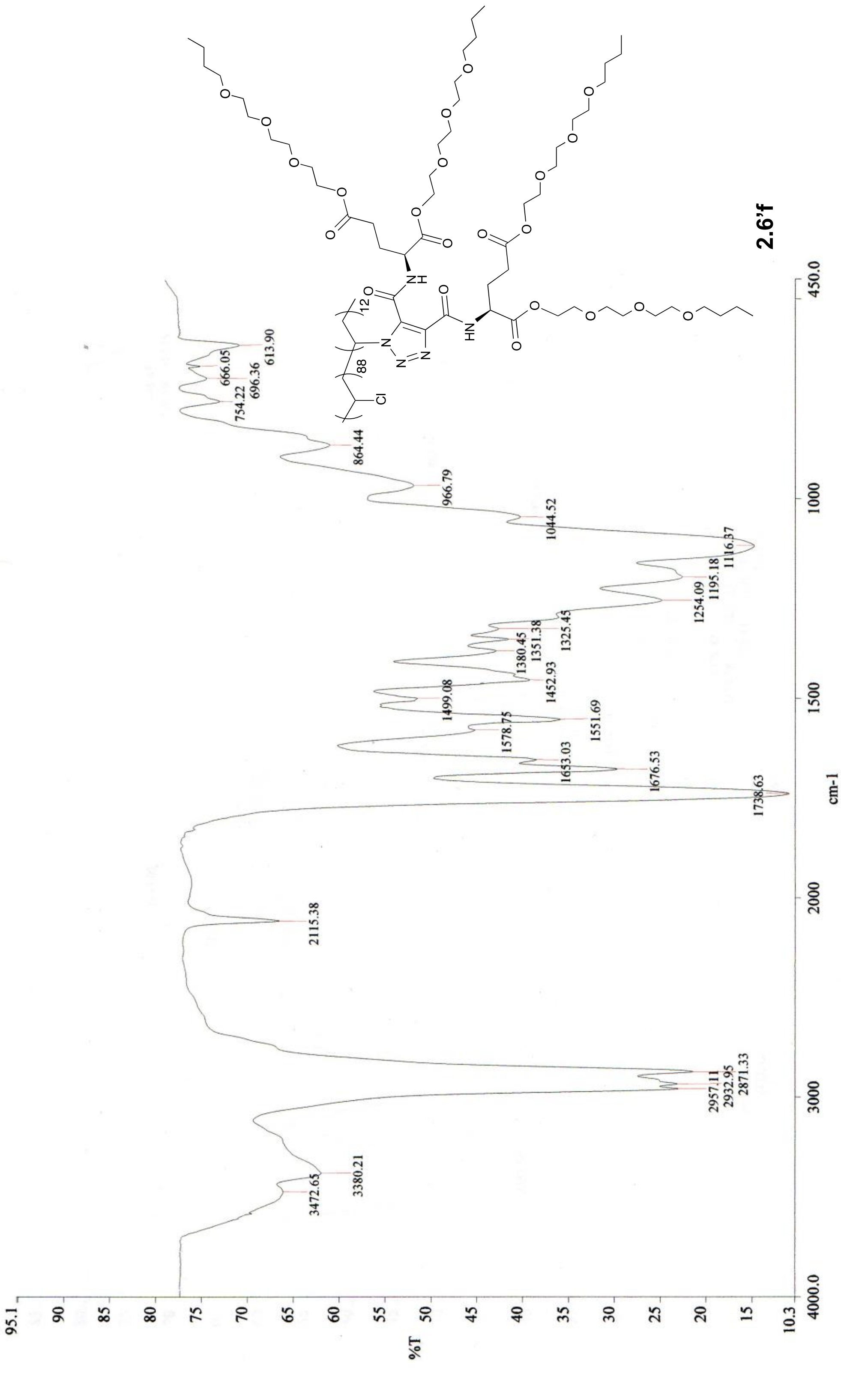

%T
cm-1
95.1
90
85
80
75
70
65
60
55
50
45
40
35
30
25
20
15
10.3
4000.0
3000
2000
1500
1000
450.0
3472.65
3380.21
2957.11
2932.95
2871.33
2115.38
1738.63
1676.53
1653.03
1578.75
1551.69
1499.08
1452.93
1380.45
1351.38
1325.45
1254.09
1195.18
1116.37
1044.52
966.79
864.44
754.22
696.36
666.05
613.90

2.6'f

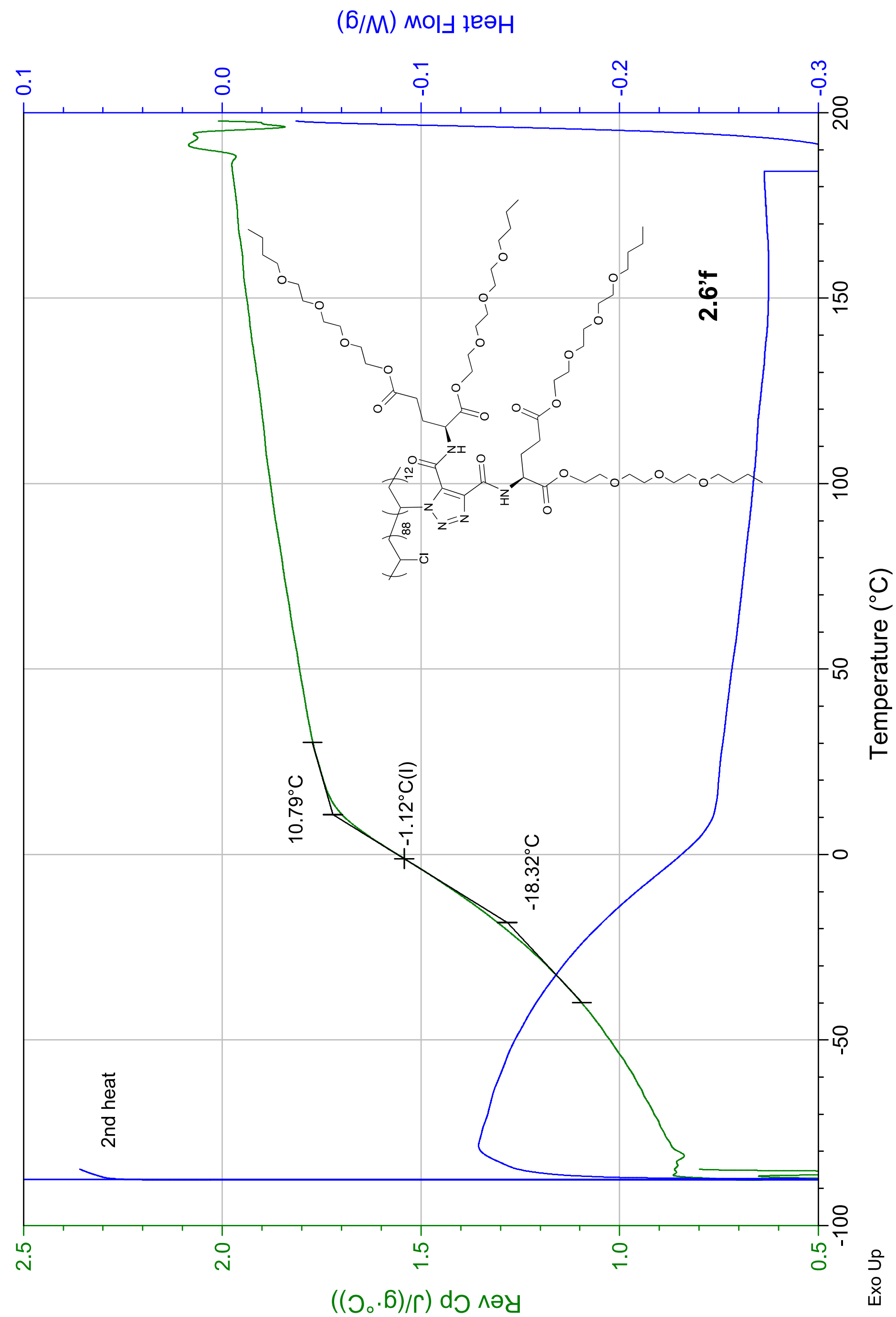

Heat Flow (W/g)
Rev Cp (J/(g·°C))
Temperature (°C)
Exo Up
2nd heat
10.79°C
-1.12°C(I)
-18.32°C
2.6'f

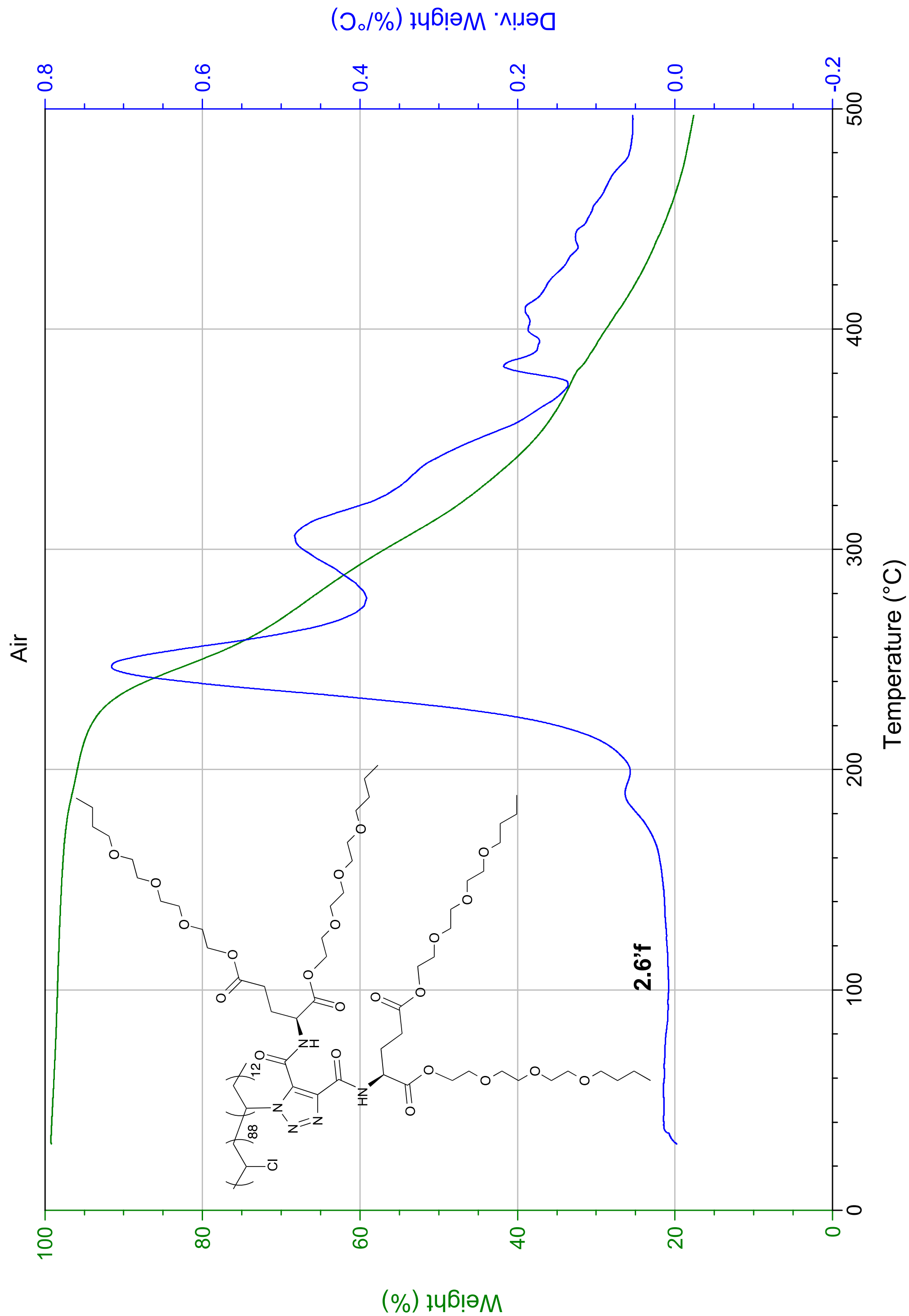

Air
2.6'f
Weight (%)
Deriv. Weight (%/°C)
Temperature (°C)
0
100
200
300
400
500
20
40
60
80
-0.2
0.0
0.2
0.4
0.6
0.8

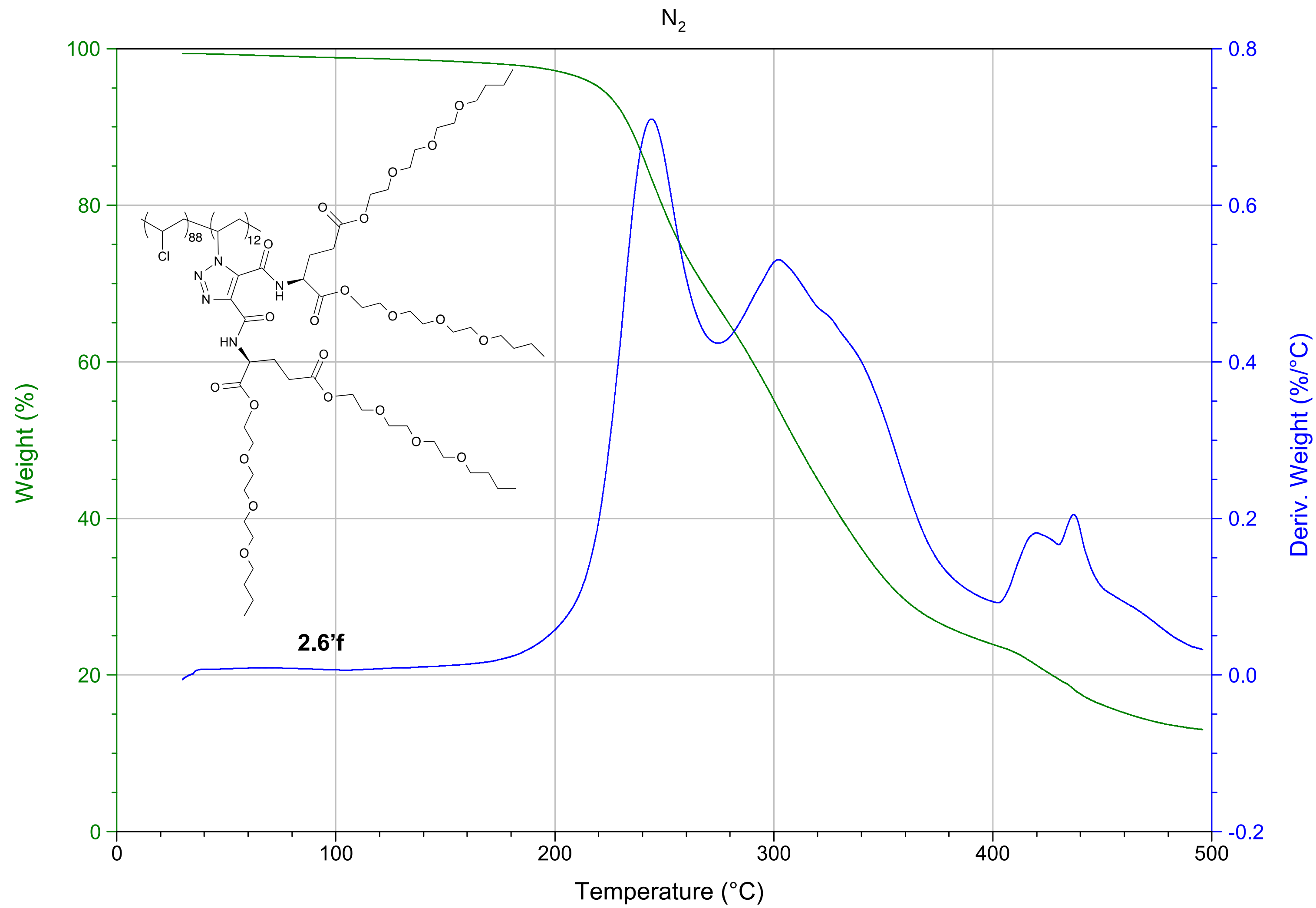
N2
2.6'f
Weight (%)
Deriv. Weight (%/°C)
Temperature (°C)
0
20
40
60
80
100
0.8
0.6
0.4
0.2
0.0
-0.2
0
100
200
300
400
500
Cl
88
12
N
N
N
O
H
HN
O
O
O
O
O
O
O
O

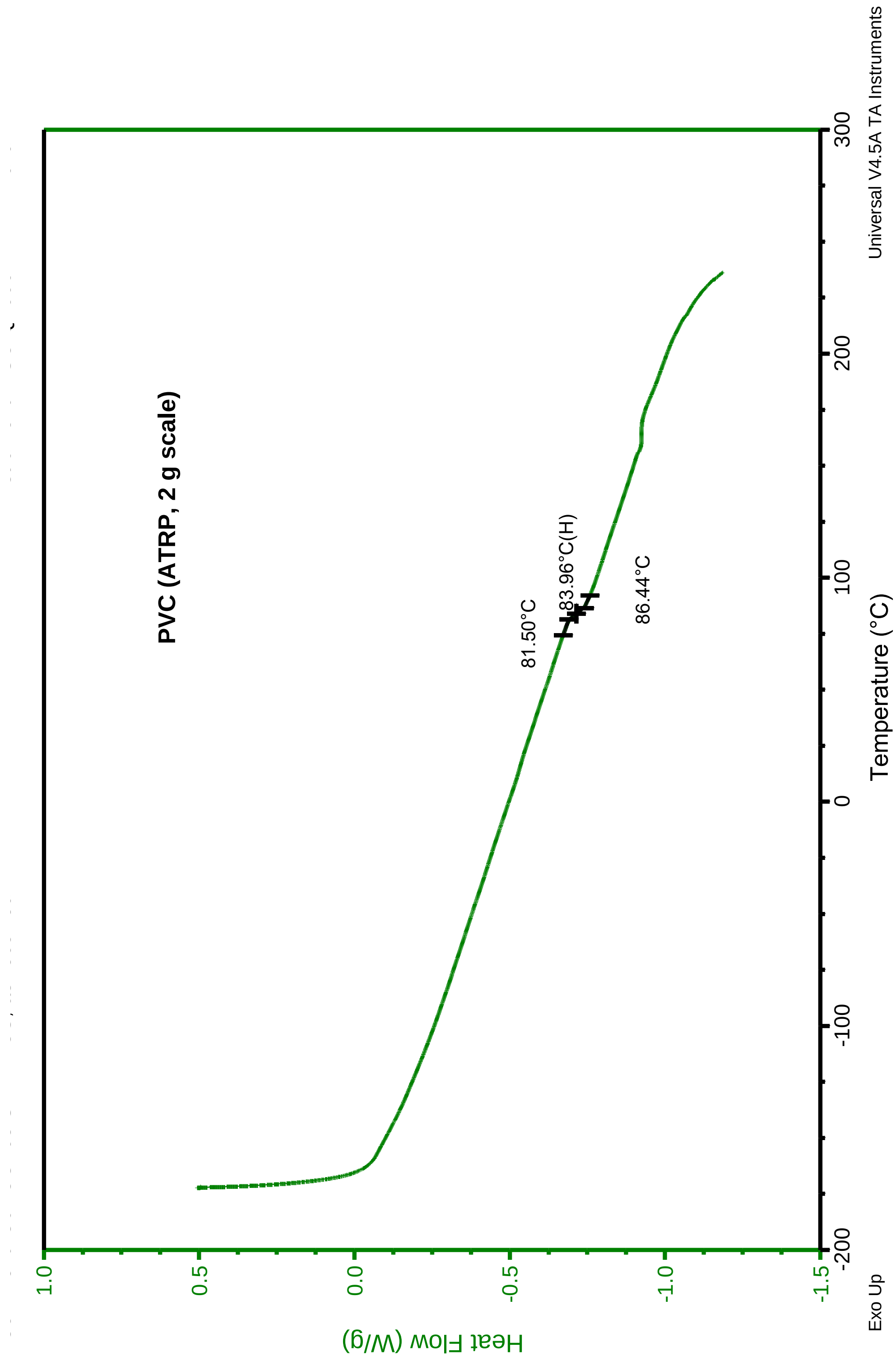
PVC (ATRP, 2 g scale)
81.50°C
83.96°C(H)
86.44°C
Heat Flow (W/g)
1.0
0.5
0.0
-0.5
-1.0
-1.5
Exo Up
-200
-100
0
100
200
300
Temperature (°C)
Universal V4.5A TA Instruments

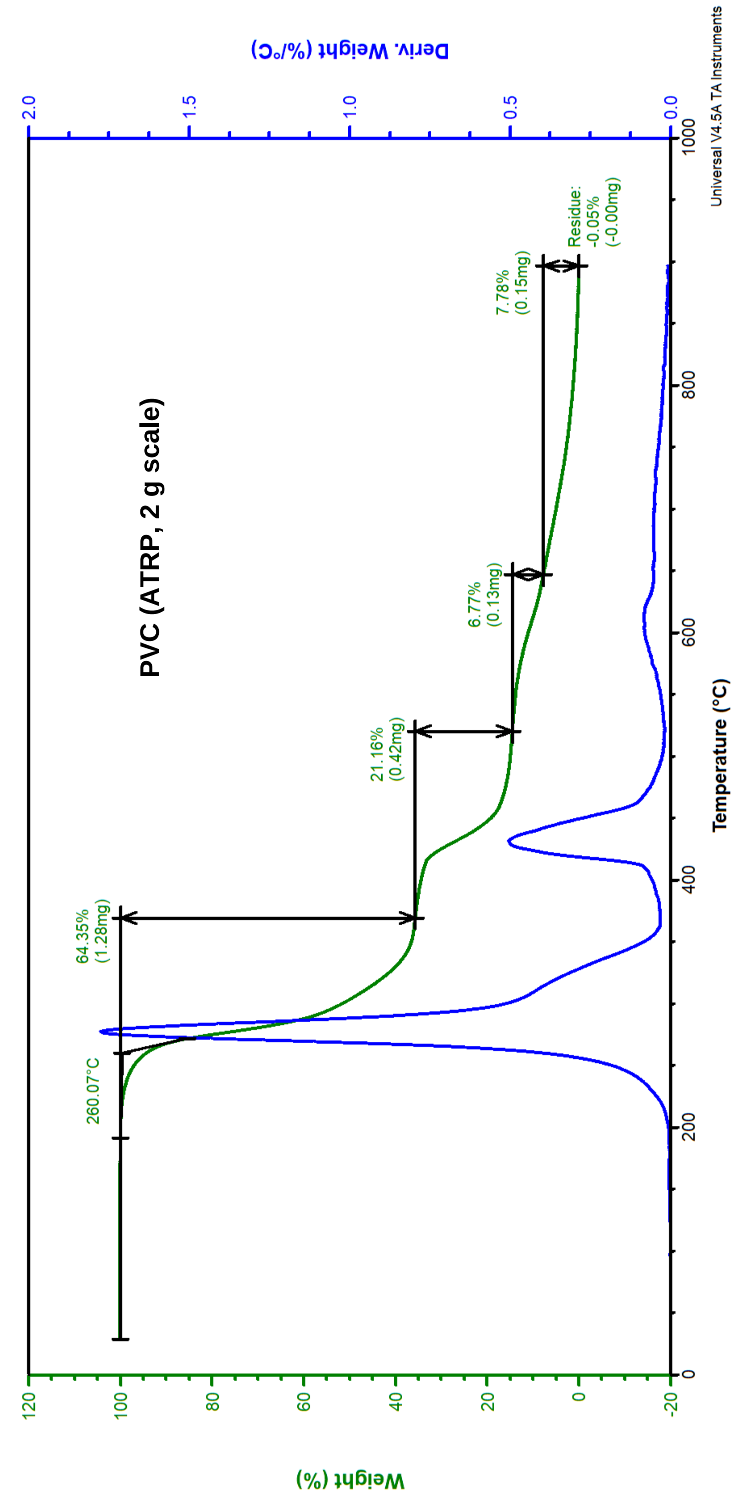
PVC (ATRP, 2 g scale)
260.07°C
64.35%
(1.28mg)
21.16%
(0.42mg)
6.77%
(0.13mg)
7.78%
(0.15mg)
Residue:
-0.05%
(-0.00mg)
Weight (%)
Deriv. Weight (%/°C)
Temperature (°C)
Universal V4.5A TA Instruments

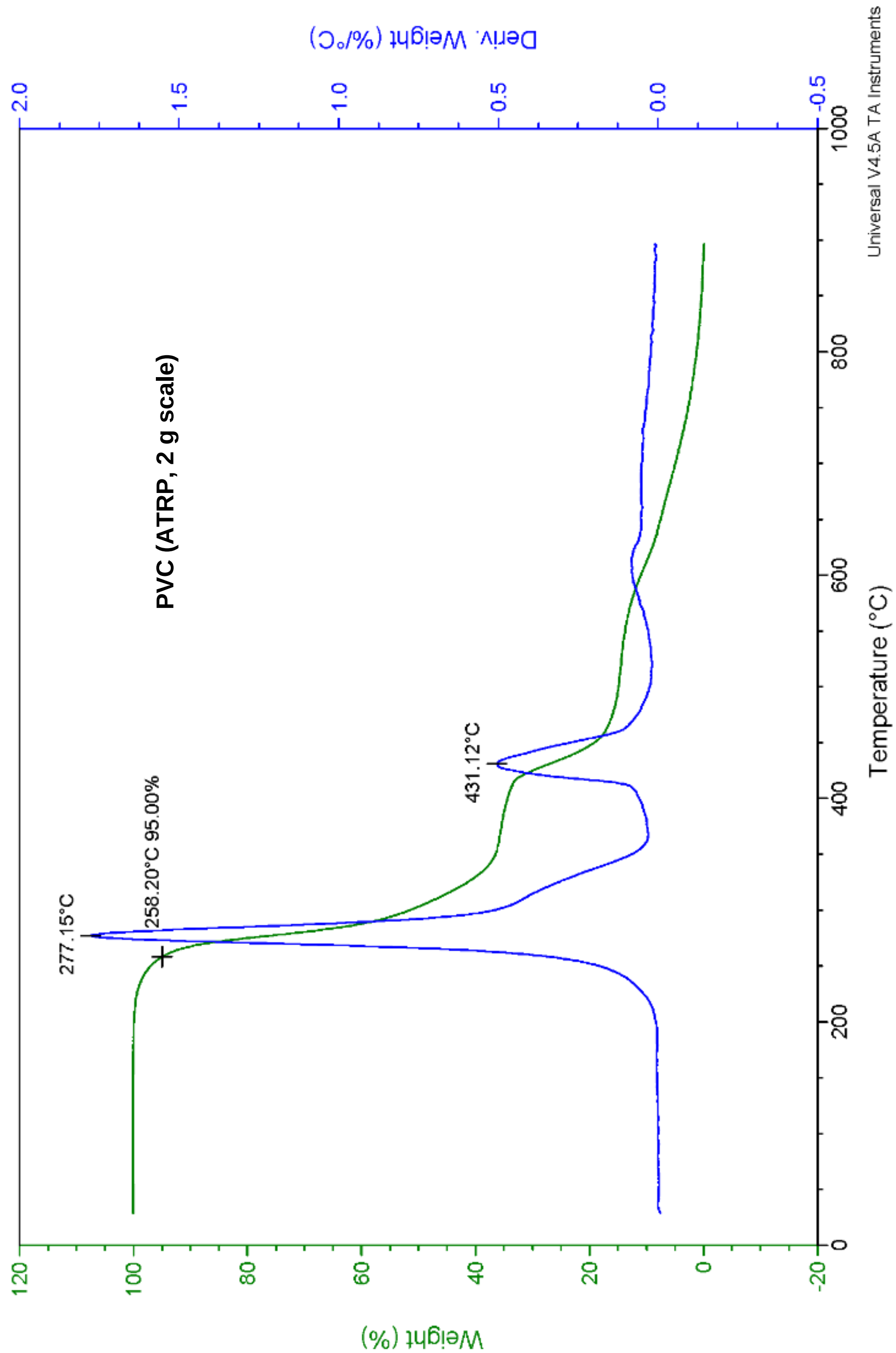
PVC (ATRP, 2 g scale)
277.15°C
258.20°C 95.00%
431.12°C
Weight (%)
Deriv. Weight (%/°C)
Temperature (°C)
Universal V4.5A TA Instruments
120
100
80
60
40
20
0
-20
2.0
1.5
1.0
0.5
0.0
-0.5
0
200
400
600
800
1000

PVC (ATRP, 2 g scale)

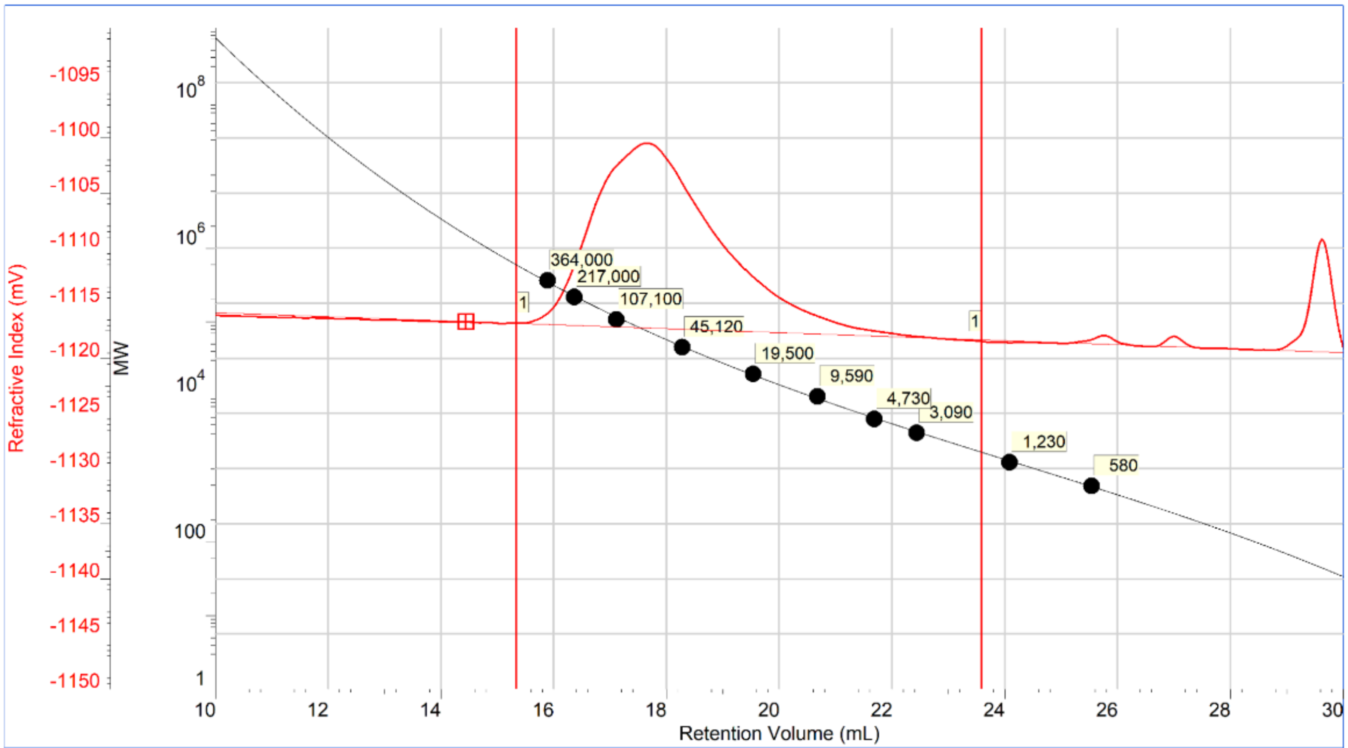

Peak	Ret Time	Mp	Mn	Mw	Mz	Mw/Mn	RI Area
1	17.647	74,652	39,315	80,177	130,744	2.039	43.32

PVC (ATRP, 2 g scale)

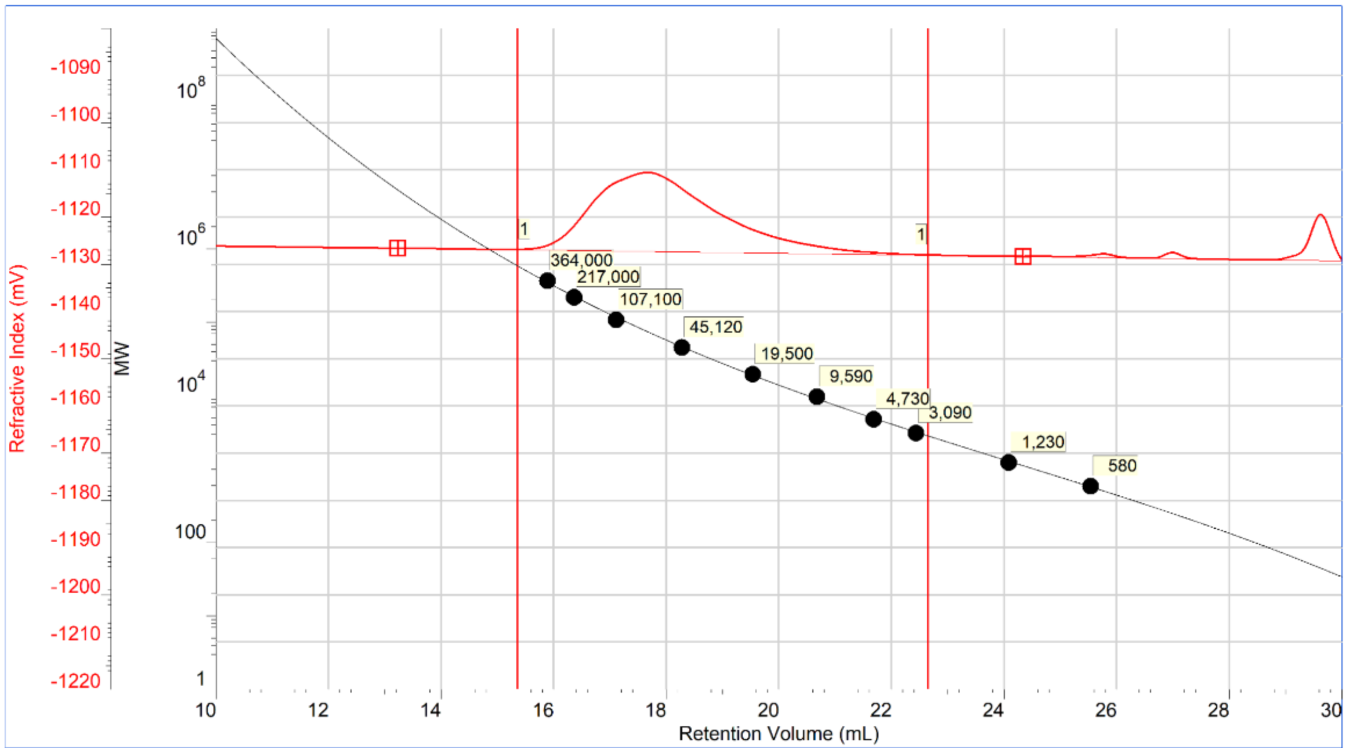

Peak	Ret Time	Mp	Mn	Mw	Mz	Mw/Mn	RI Area
1	17.660	73,931	38,321	79,654	130,426	2.079	43.48

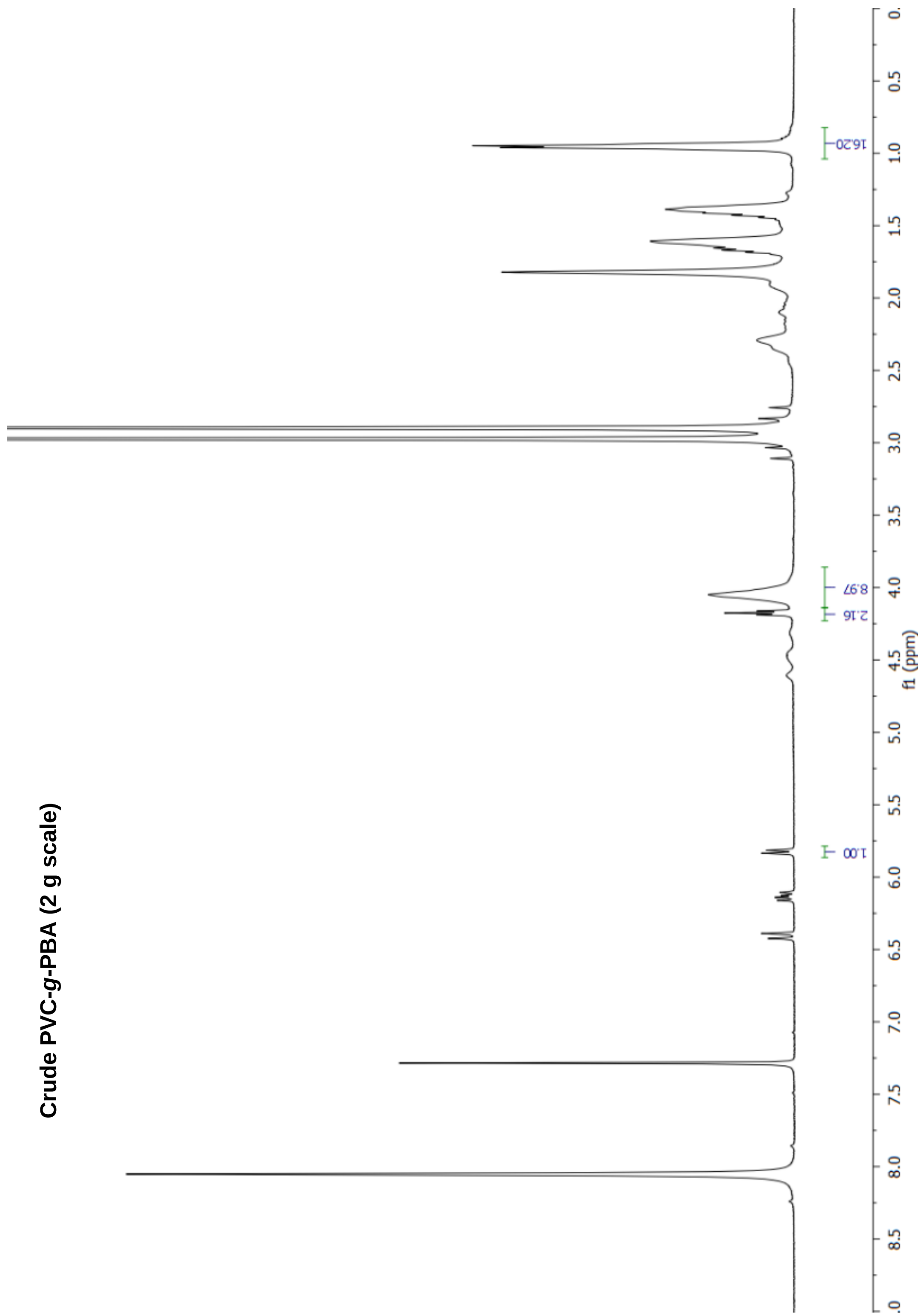
Crude PVC-*g*-PBA (2 g scale)
f1 (ppm)
16.20
8.97
2.16
1.00

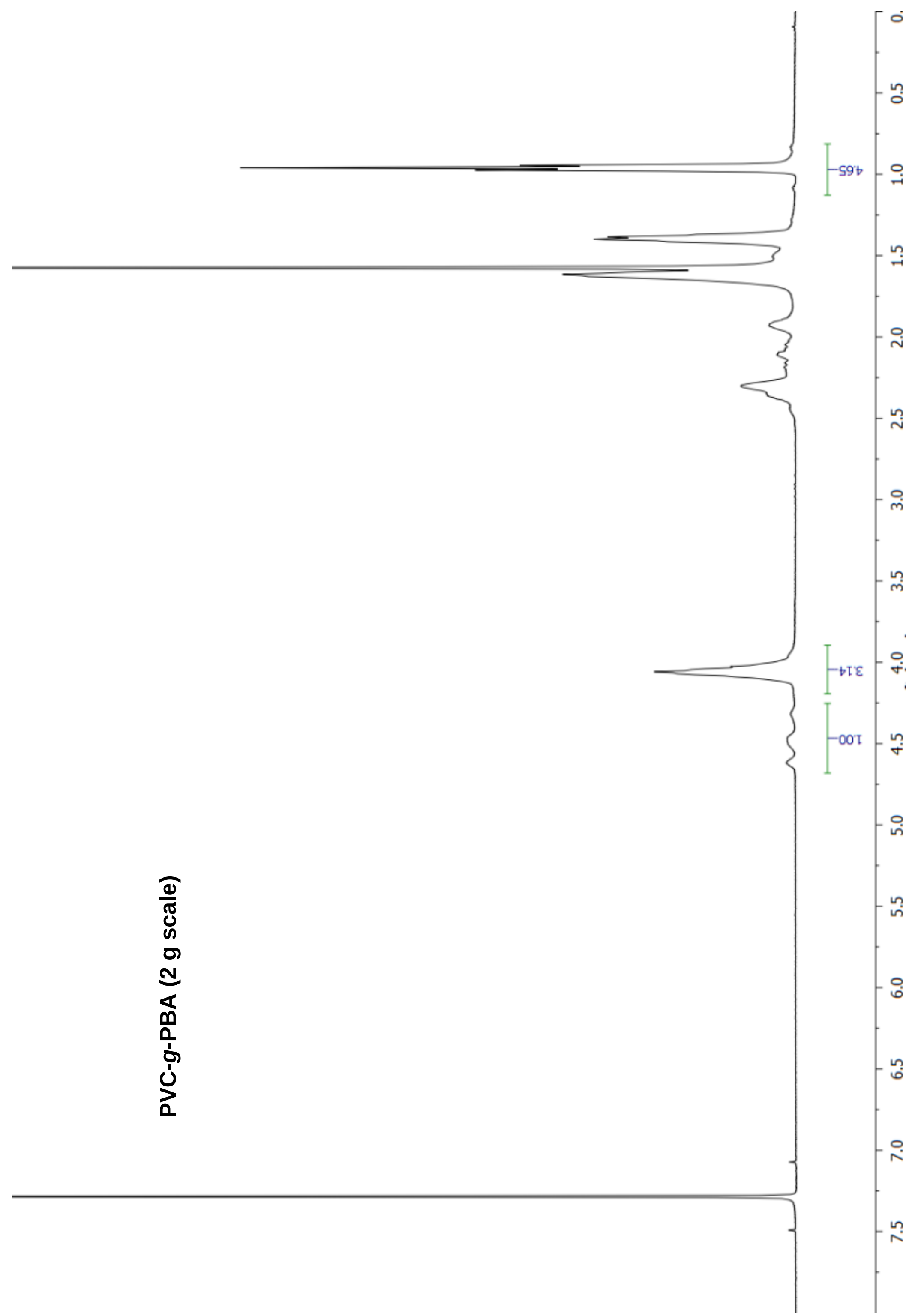

PVC-g-PBA (2 g scale)
4.65
3.14
1.00
f1 (ppm)

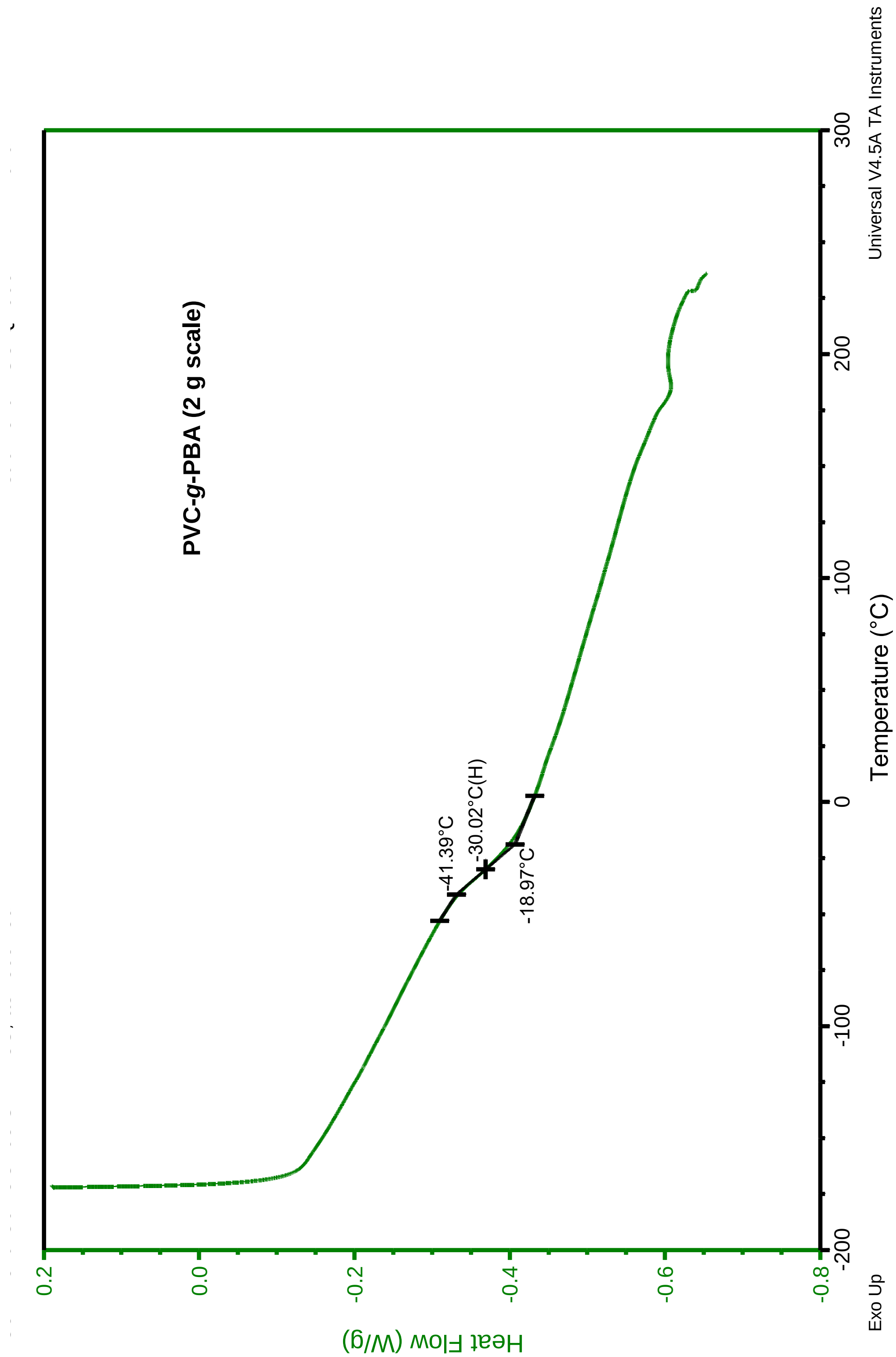

PVC-*g*-PBA (2 g scale)
-41.39°C
-30.02°C(H)
-18.97°C
Heat Flow (W/g)
0.2
0.0
-0.2
-0.4
-0.6
-0.8
Temperature (°C)
-200
-100
0
100
200
300
Exo Up
Universal V4.5A TA Instruments

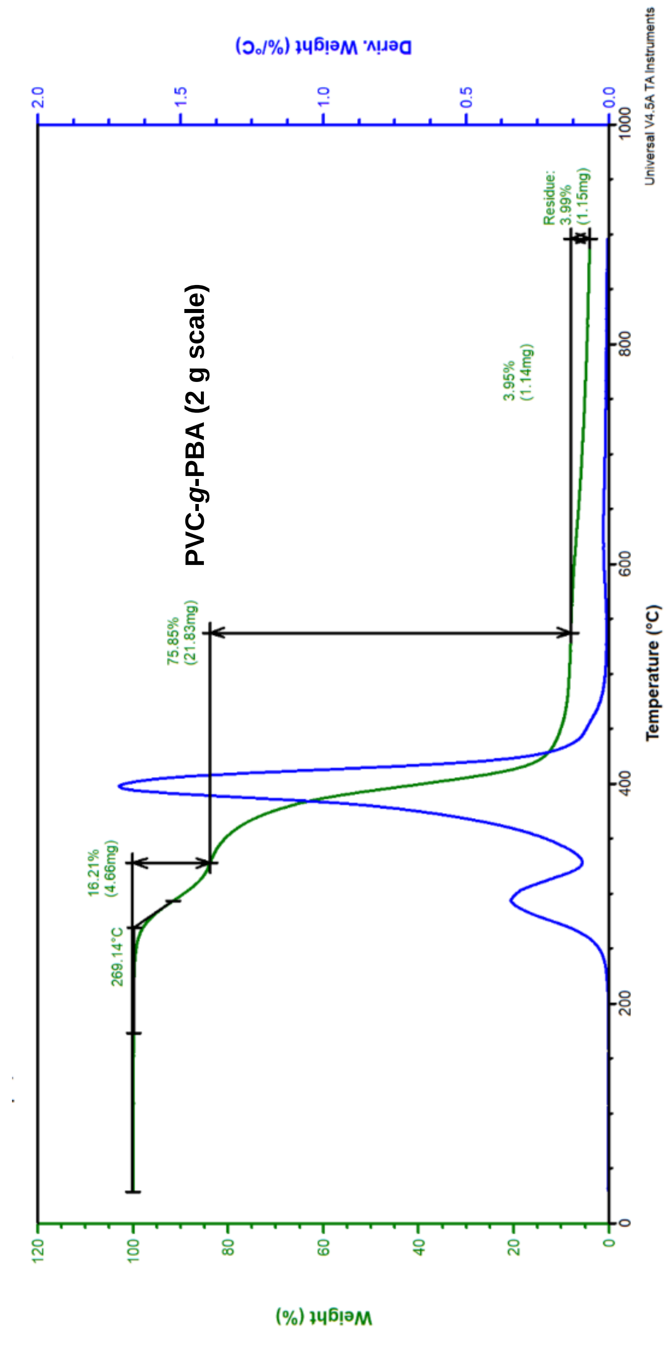

PVC-*g*-PBA (2 g scale)
Weight (%)
Deriv. Weight (%/°C)
Temperature (°C)
269.14°C
16.21%
(4.66mg)
75.85%
(21.83mg)
3.95%
(1.14mg)
Residue:
3.99%
(1.15mg)
Universal V4.5A TA Instruments

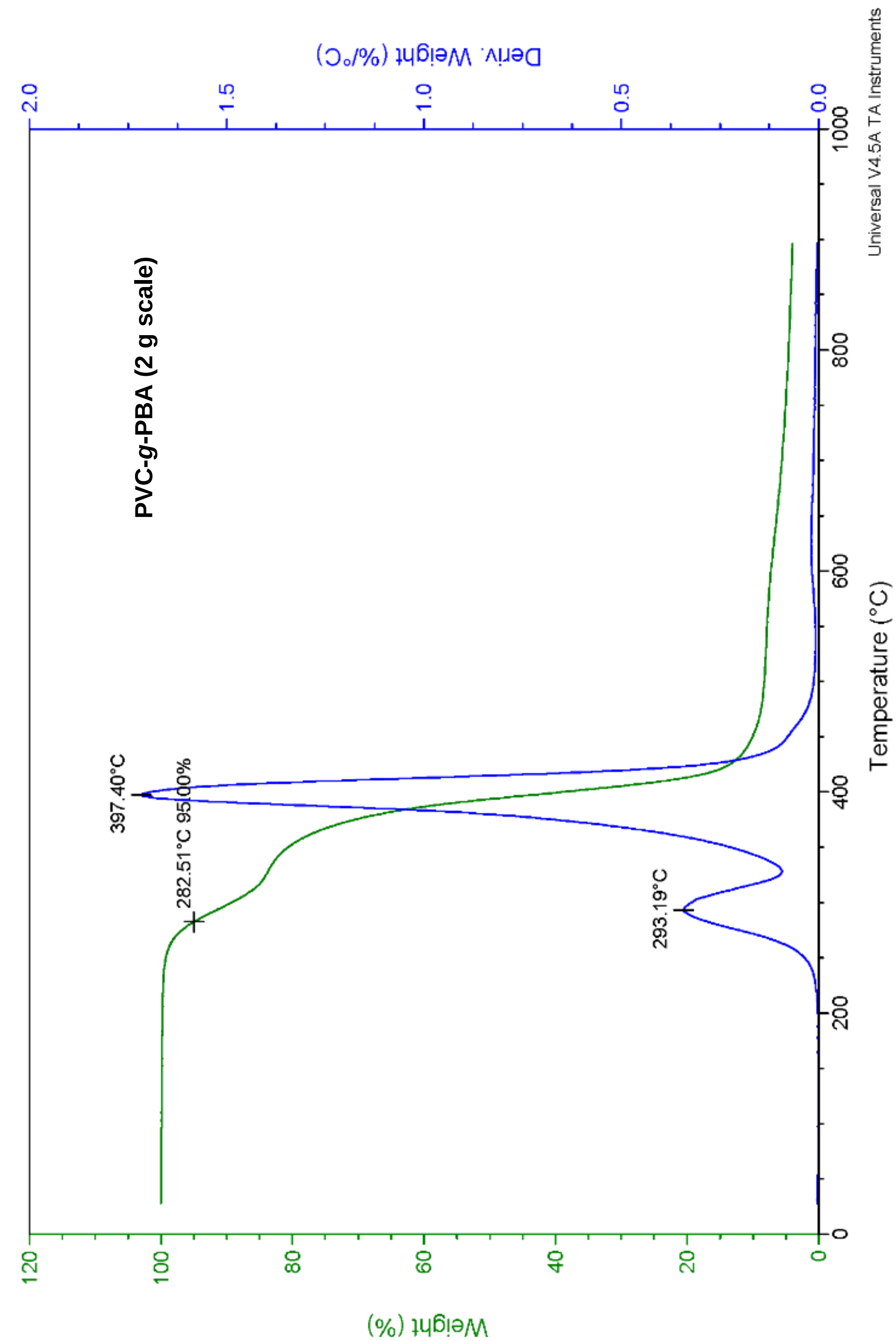
PVC-g-PBA (2 g scale)
397.40°C
282.51°C 95.00%
293.19°C
Weight (%)
0
20
40
60
80
100
120
Deriv. Weight (%/°C)
0.0
0.5
1.0
1.5
2.0
Temperature (°C)
0
200
400
600
800
1000
Universal V4.5A TA Instruments

PVC-*g*-PBA (2 g scale)

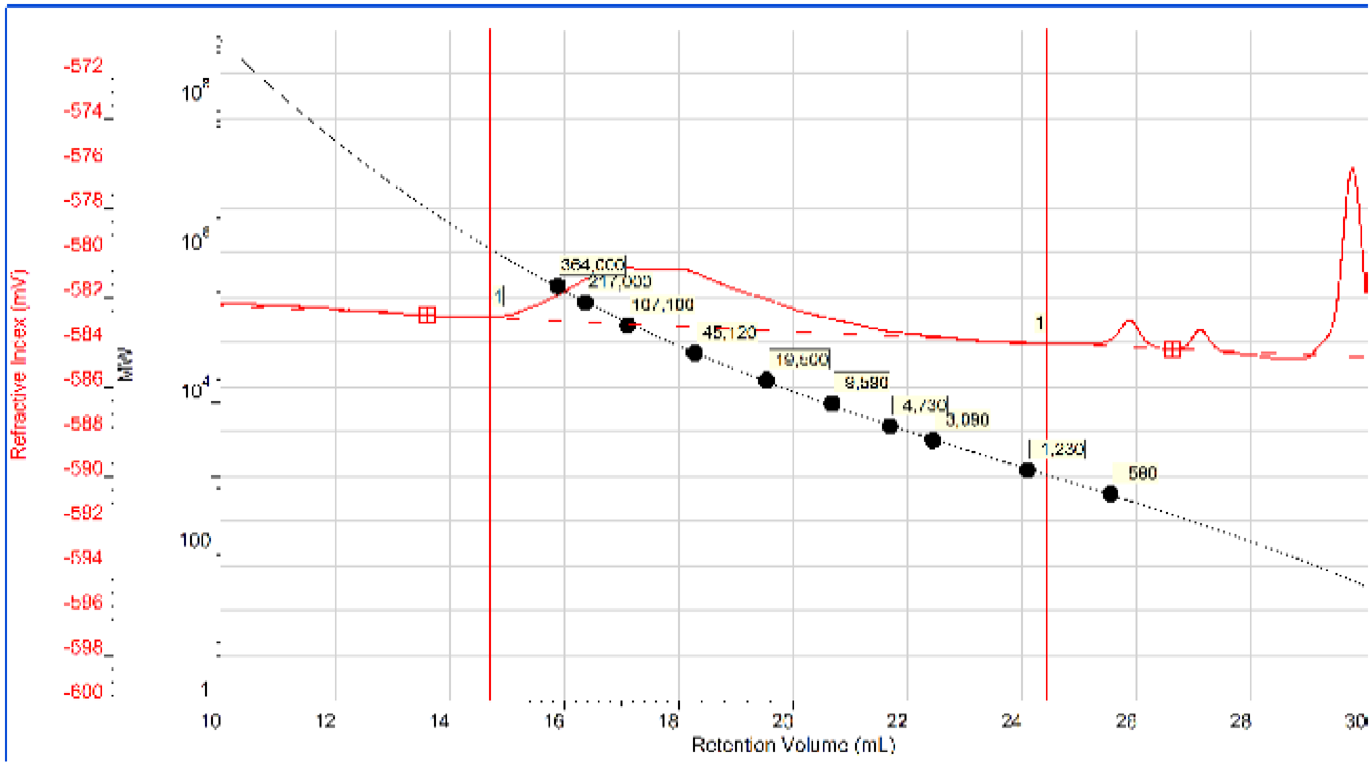

Peak	Ret Time	Mp	Mn	Mw	Mz	Mw/Mn	RI Area
1	17.993	56,972	36,580	112,274	280,121	3.069	9.94

PVC-*g*-PBA (2 g scale)

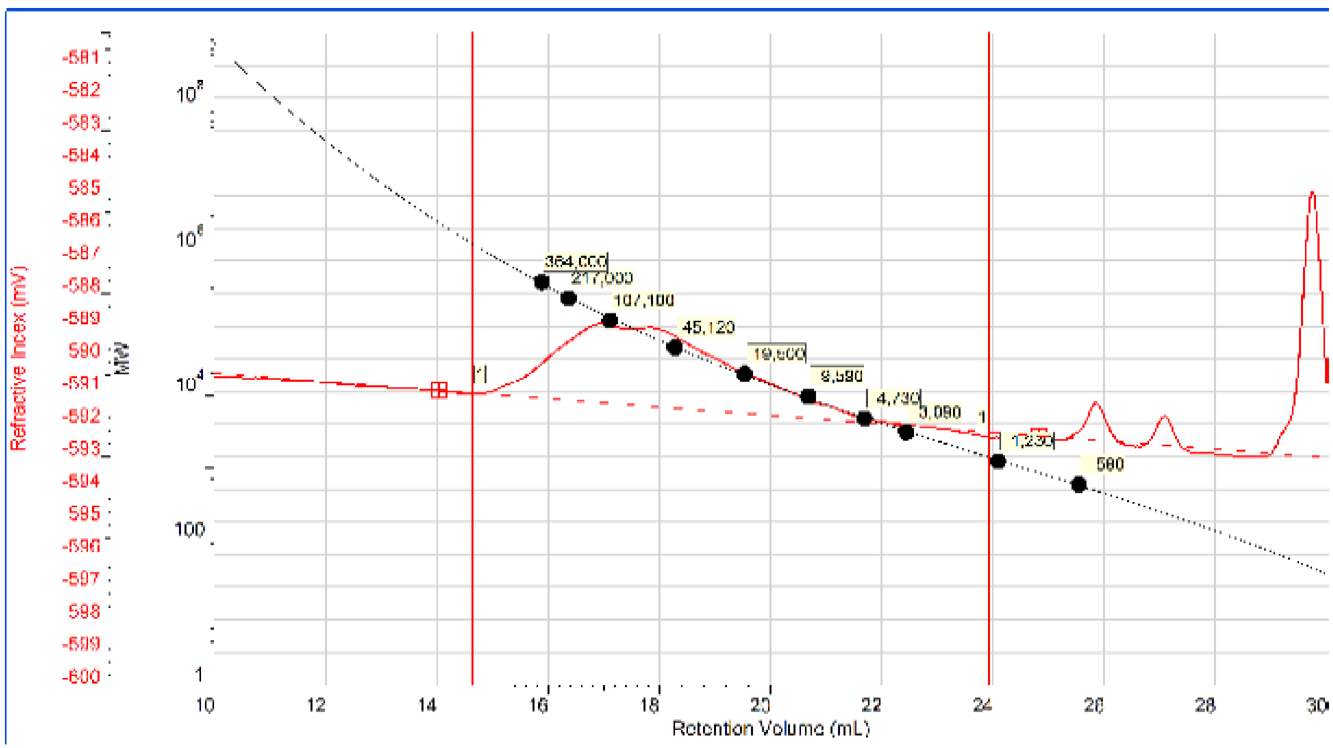

Peak	Ret Time	Mp	Mn	Mw	Mz	Mw/Mn	RI Area
1	16.997	127,483	39,700	113,565	284,191	2.861	9.09

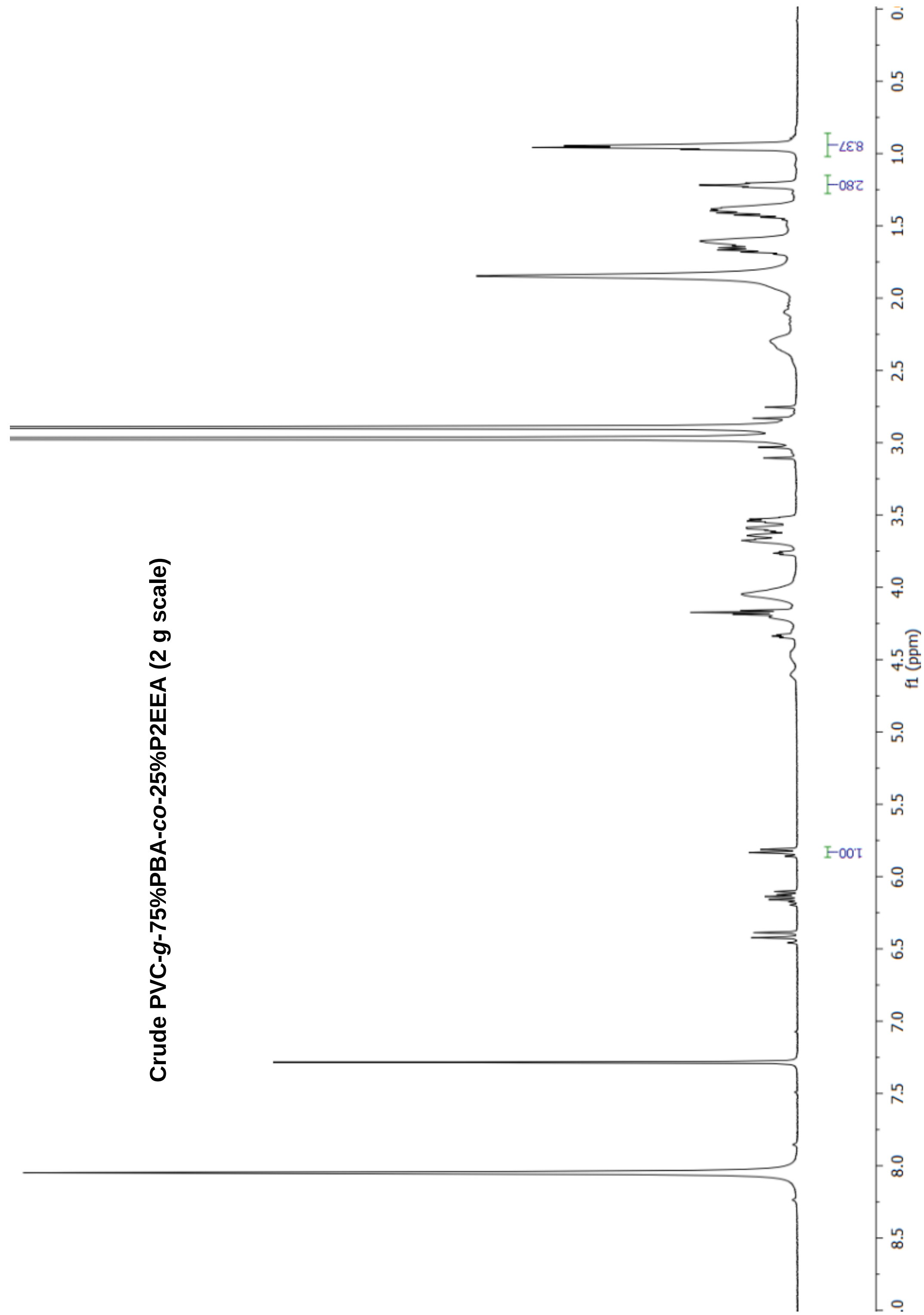
Crude PVC-*g*-75%PBA-*co*-25%P2EEA (2 g scale)
f1 (ppm)
0.5
1.0
1.5
2.0
2.5
3.0
3.5
4.0
4.5
5.0
5.5
6.0
6.5
7.0
7.5
8.0
8.5
8.37
2.80
1.00

PVC-*g*-75%PBA-*co*-25%P2EEA (2 g scale)

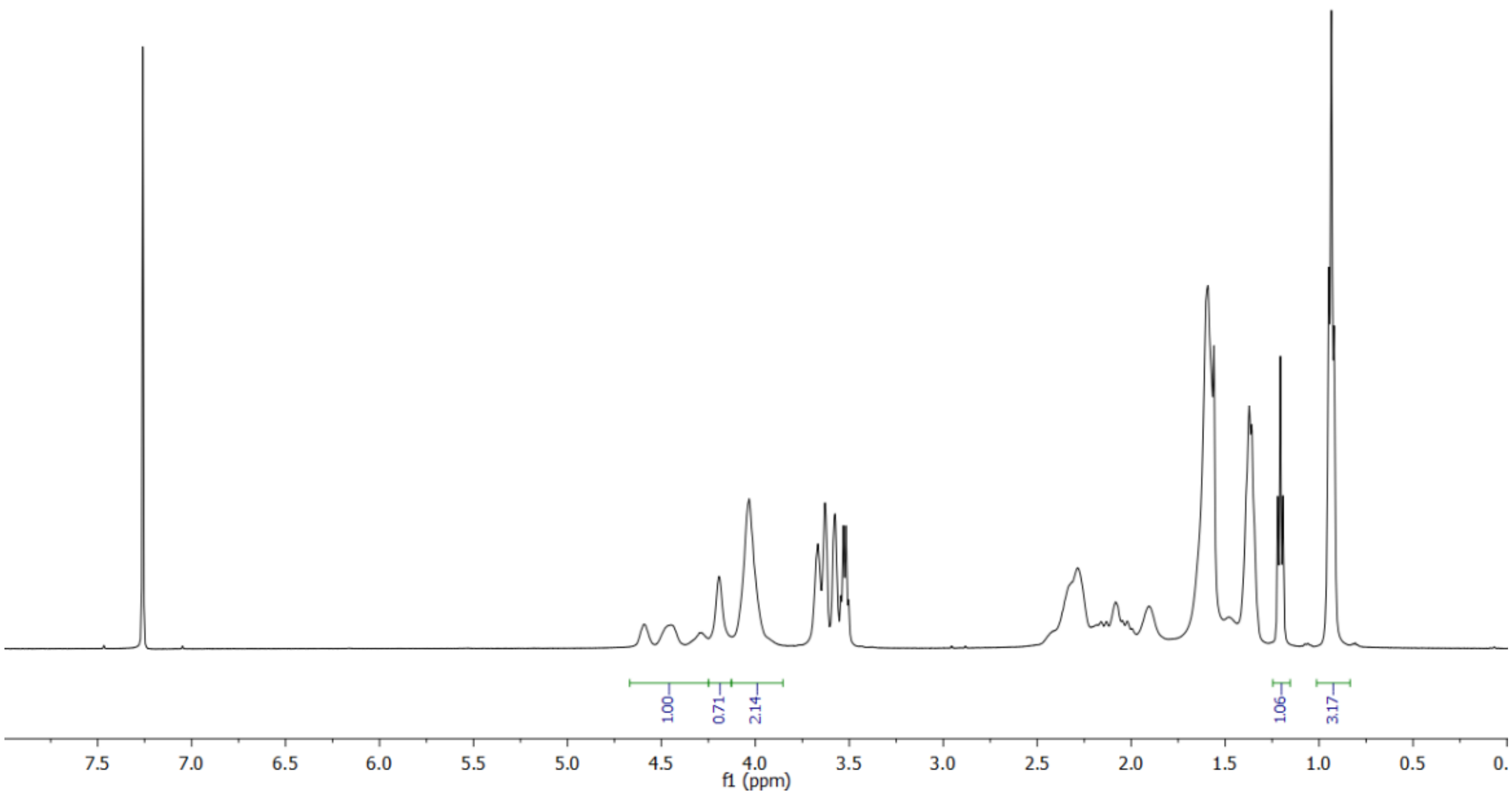

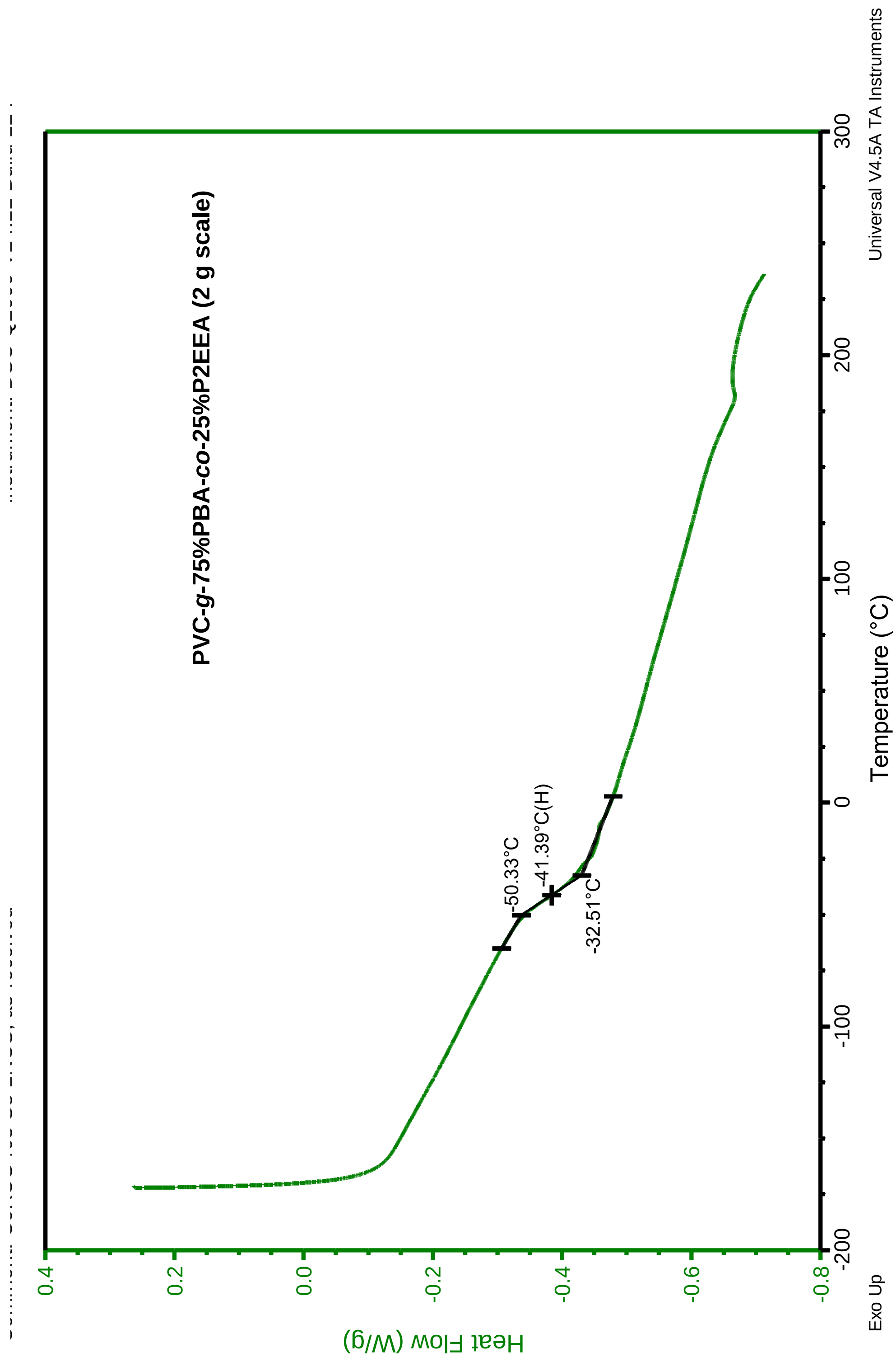
PVC-g-75%PBA-co-25%P2EEA (2 g scale)
-50.33°C
-41.39°C(H)
-32.51°C
Heat Flow (W/g)
0.4
0.2
0.0
-0.2
-0.4
-0.6
-0.8
-200
-100
0
100
200
300
Temperature (°C)
Exo Up
Universal V4.5A TA Instruments

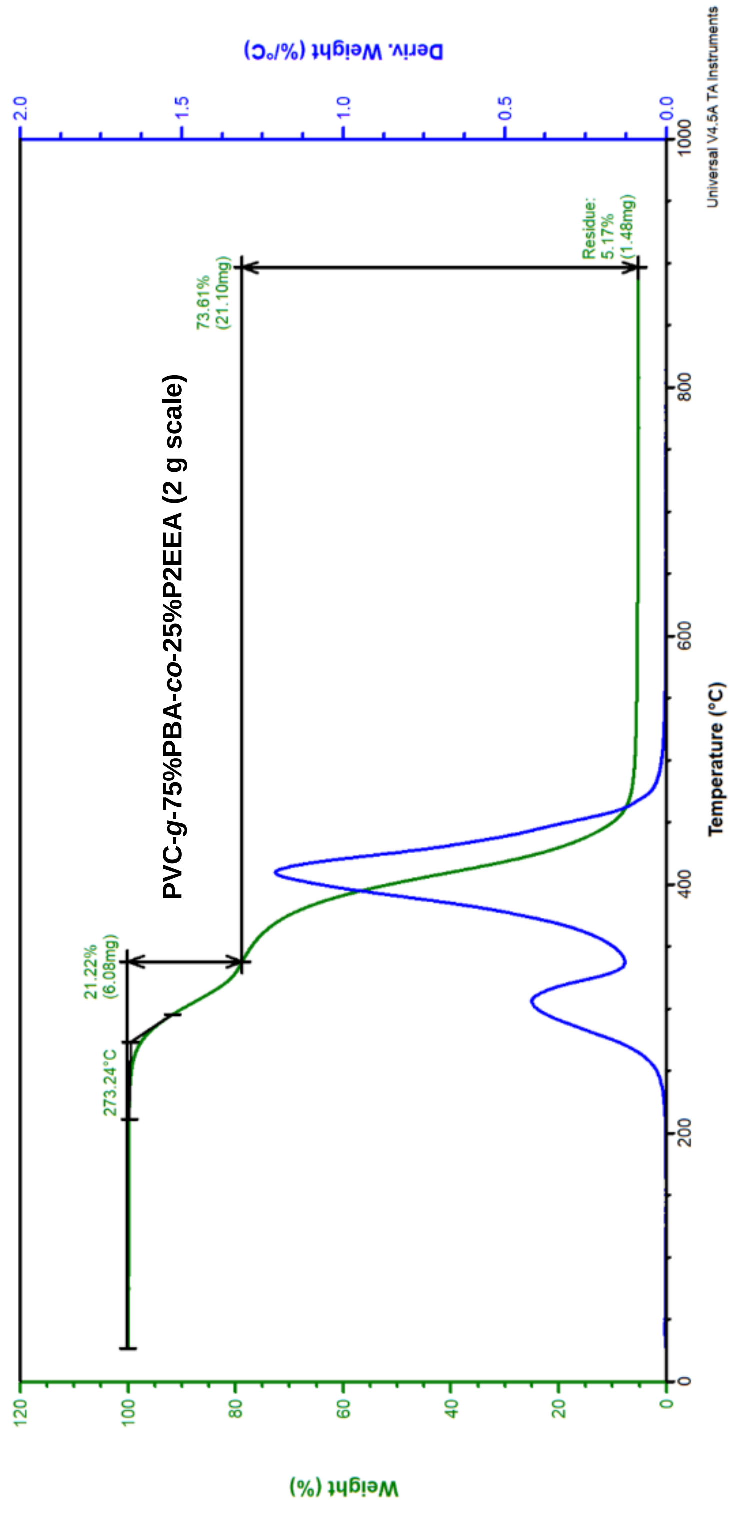

PVC-g-75%PBA-co-25%P2EEA (2 g scale)
273.24°C
21.22%
(6.08mg)
73.61%
(21.10mg)
Residue:
5.17%
(1.48mg)
Weight (%)
Deriv. Weight (%/°C)
Temperature (°C)
Universal V4.5A TA Instruments

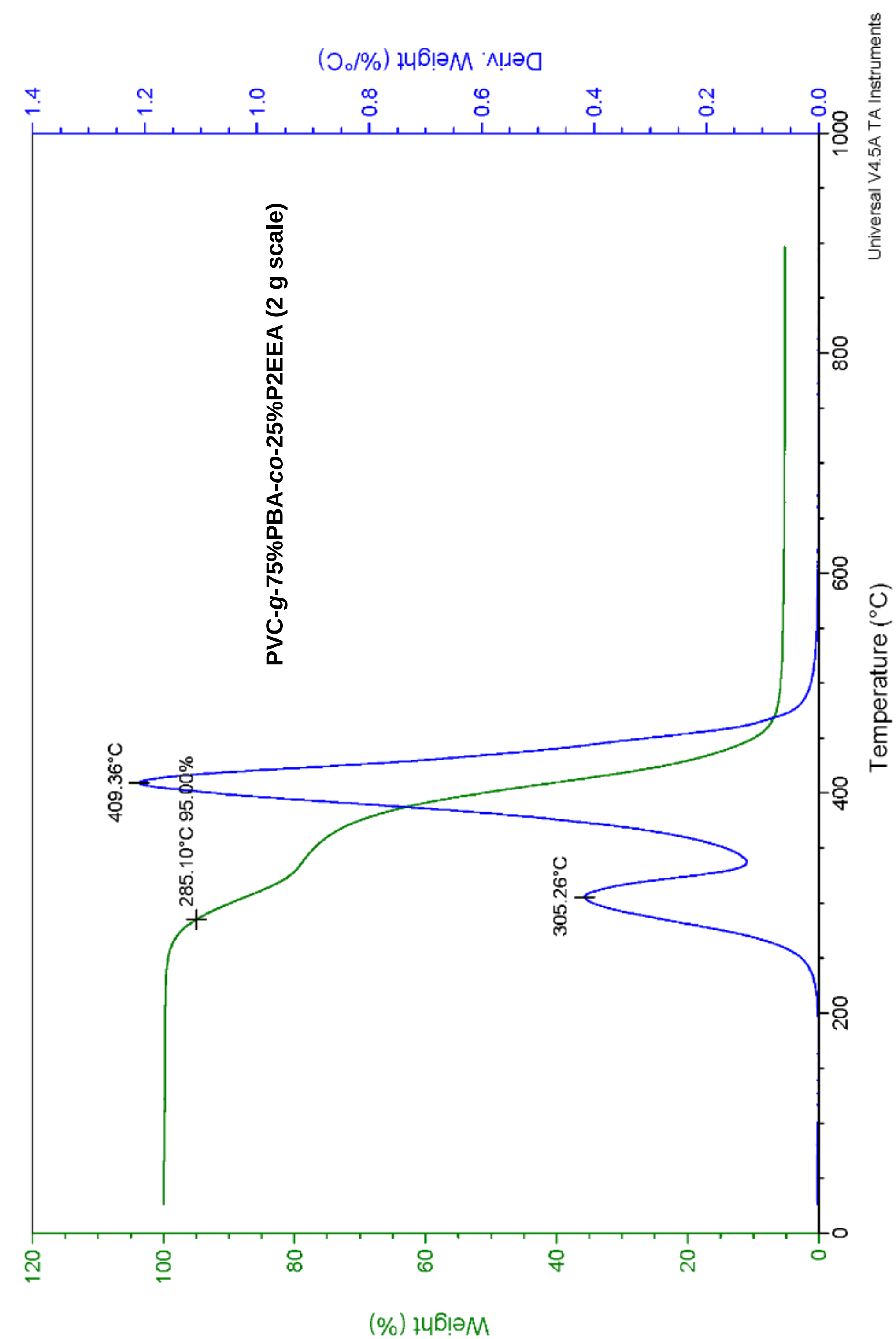

PVC-g-75%PBA-co-25%P2EEA (2 g scale)
409.36°C
285.10°C 95.00%
305.26°C
Weight (%)
Deriv. Weight (%/°C)
Temperature (°C)
Universal V4.5A TA Instruments

PVC-*g*-75%PBA-*co*-25%P2EEA (2 g scale)

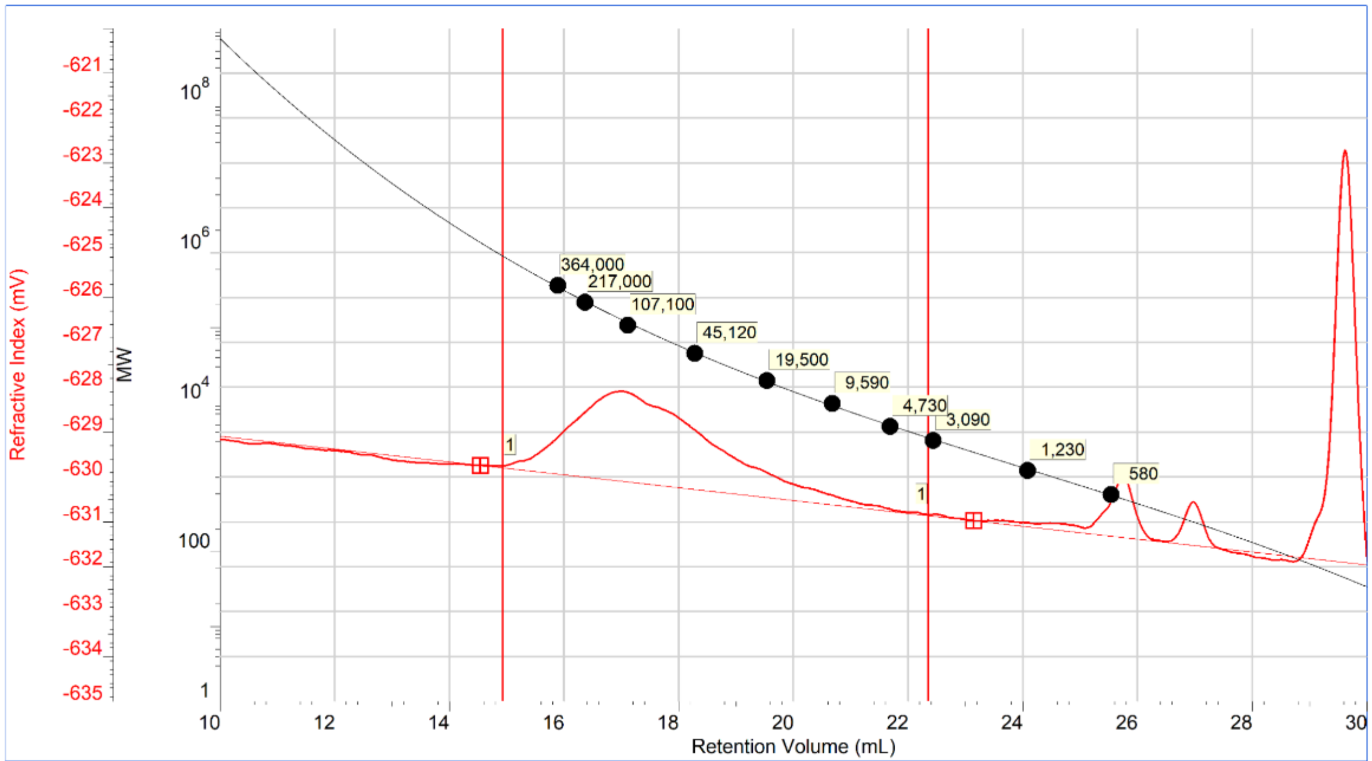

Peak	Ret Time	Mp	Mn	Mw	Mz	Mw/Mn	RI Area
1	17.003	126,773	45,936	125,179	248,350	2.725	5.87

PVC-*g*-75%PBA-*co*-25%P2EEA (2 g scale)

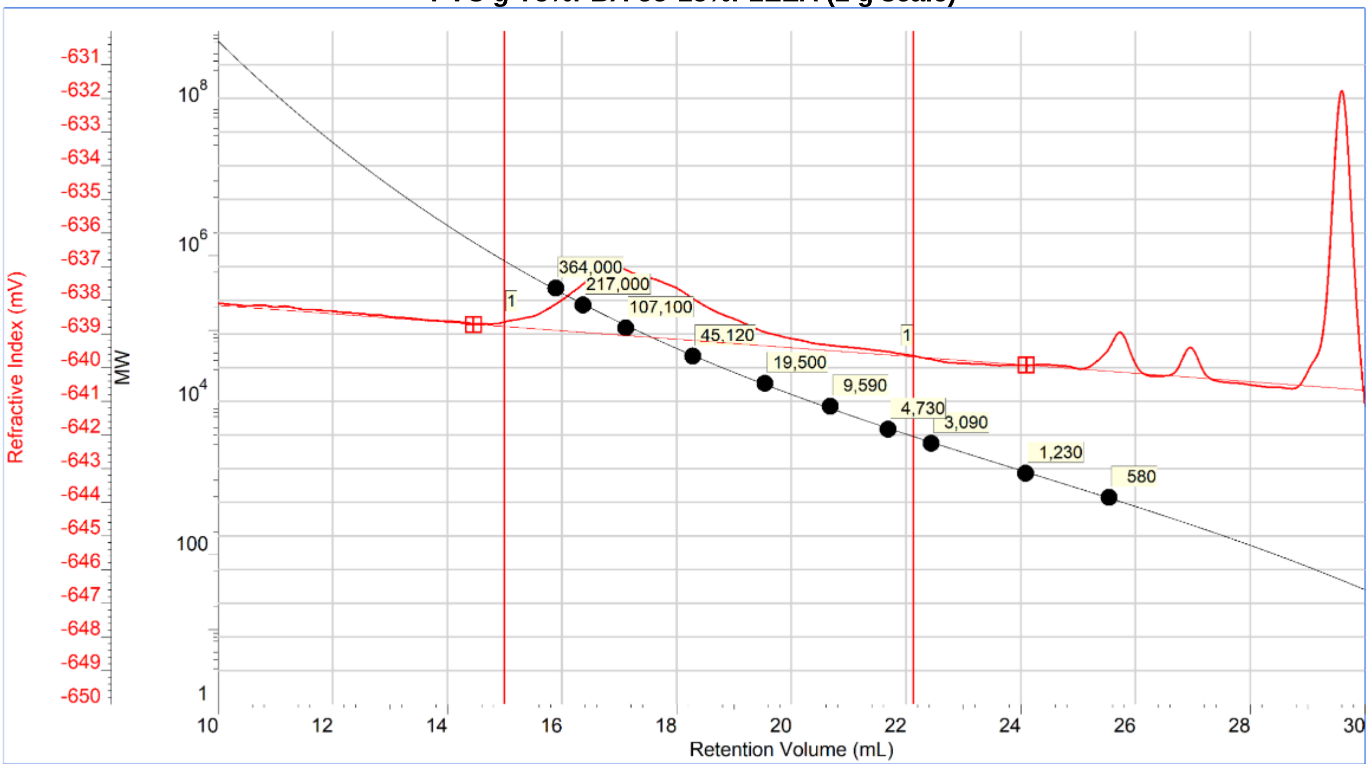

Peak	Ret Time	Mp	Mn	Mw	Mz	Mw/Mn	RI Area
1	16.977	129,680	46,978	127,608	247,117	2.716	5.63

Crude PVC-*g*-50%PBA-*co*-50%P2EEA (2 g scale)

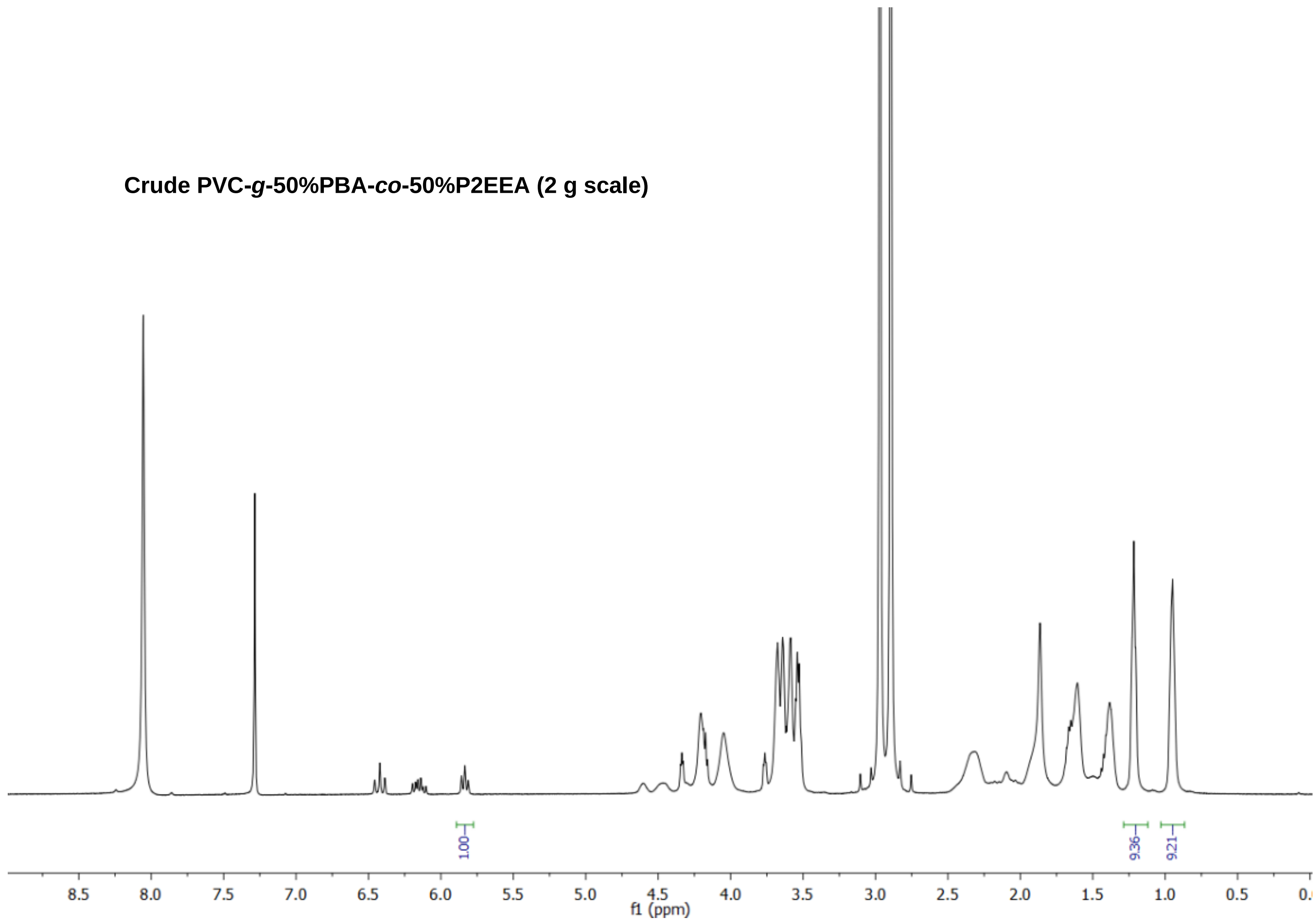

PVC-*g*-50%PBA-*co*-50%P2EEA (2 g scale)

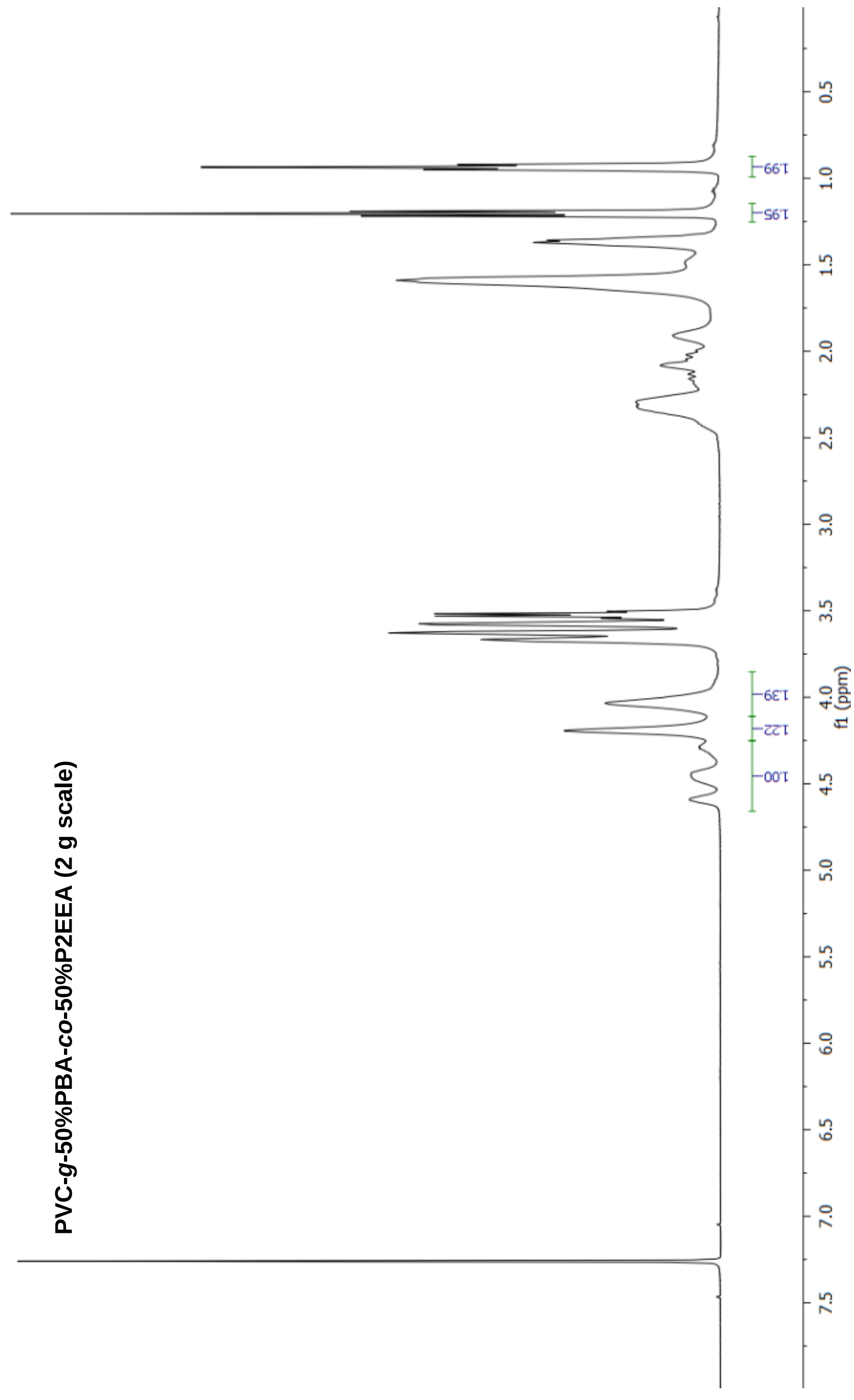

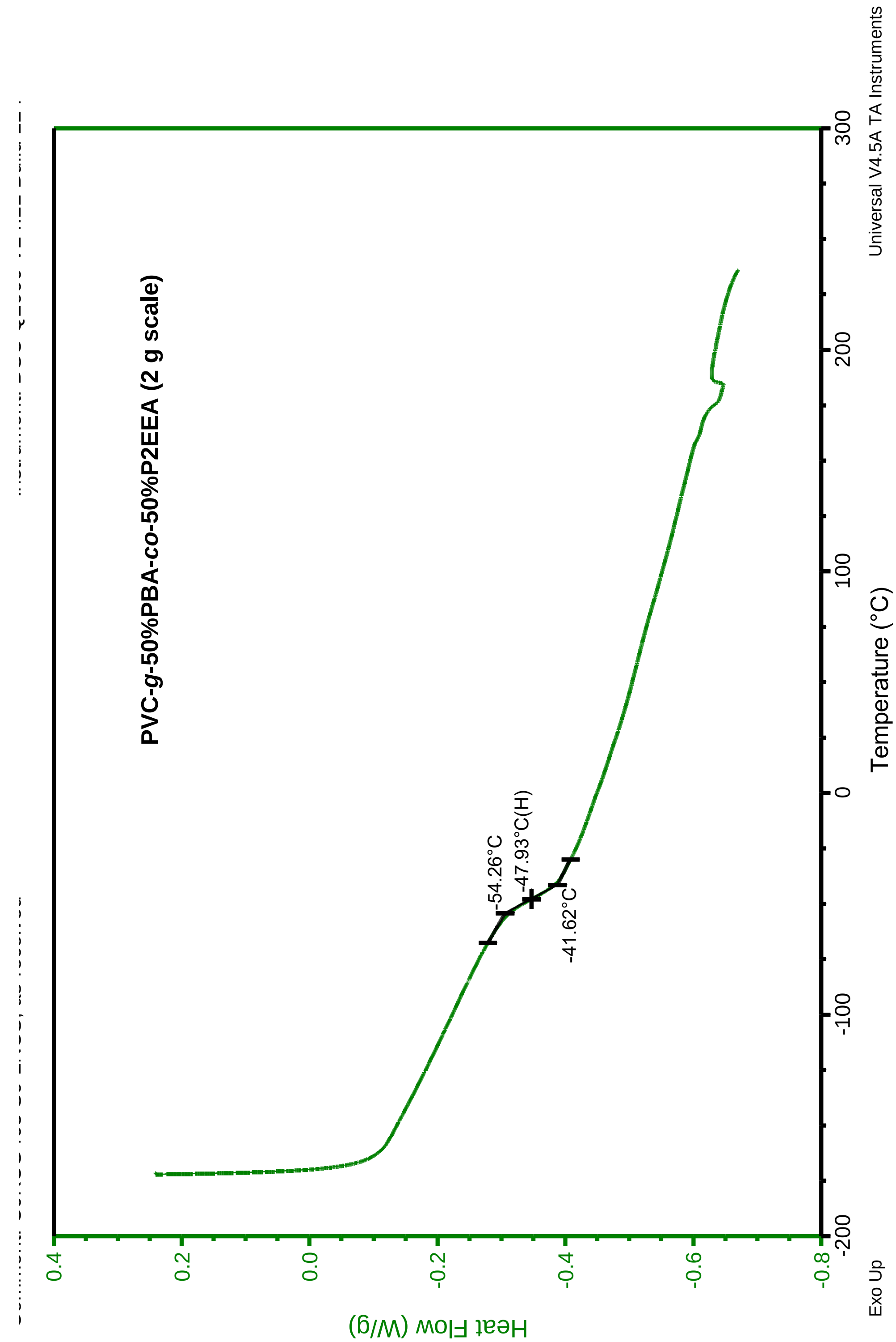

PVC-g-50%PBA-co-50%P2EEA (2 g scale)
Heat Flow (W/g)
Temperature (°C)
-54.26°C
-47.93°C(H)
-41.62°C
0.4
0.2
0.0
-0.2
-0.4
-0.6
-0.8
-200
-100
0
100
200
300
Exo Up
Universal V4.5A TA Instruments

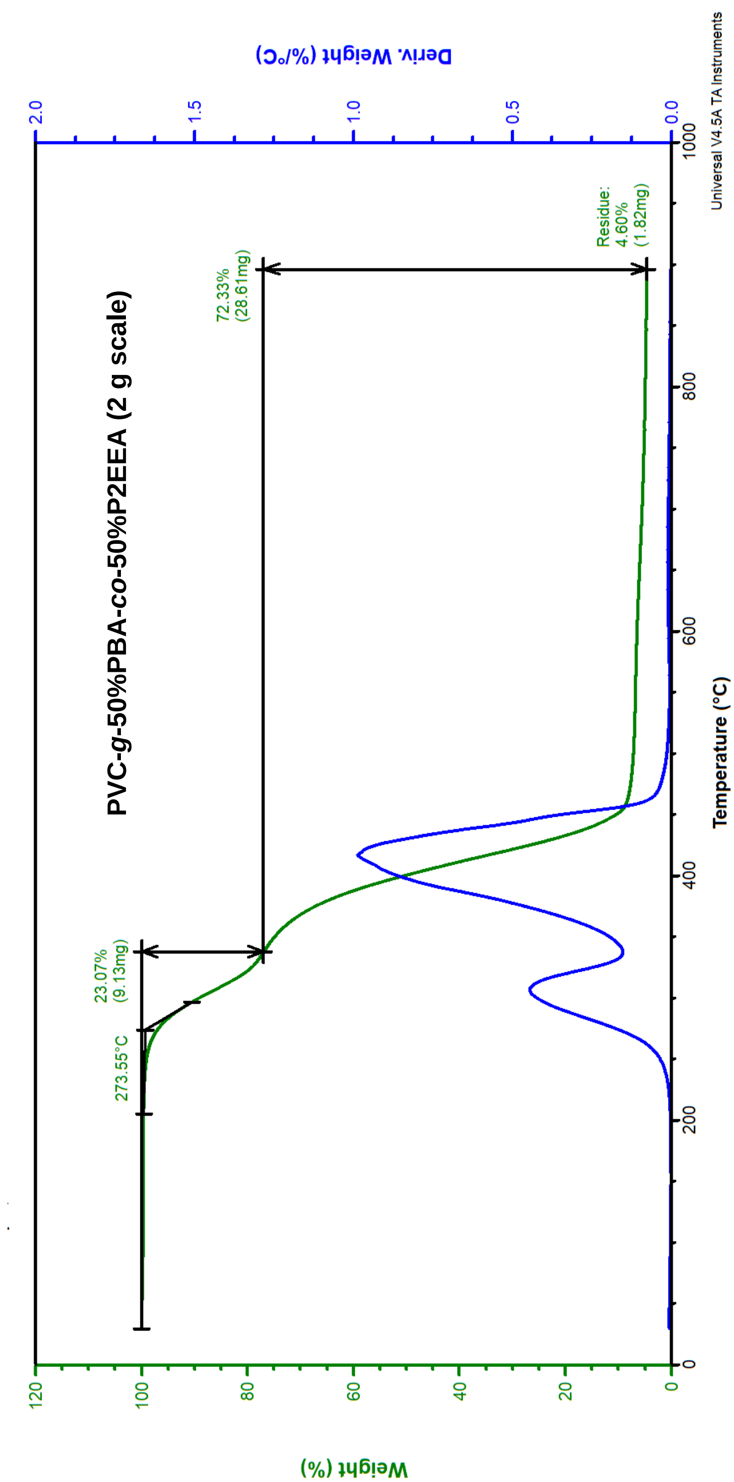

PVC-*g*-50%PBA-*co*-50%P2EEA (2 g scale)
273.55°C
23.07%
(9.13mg)
72.33%
(28.61mg)
Residue:
4.60%
(1.82mg)
Weight (%)
Deriv. Weight (%/°C)
Temperature (°C)
Universal V4.5A TA Instruments

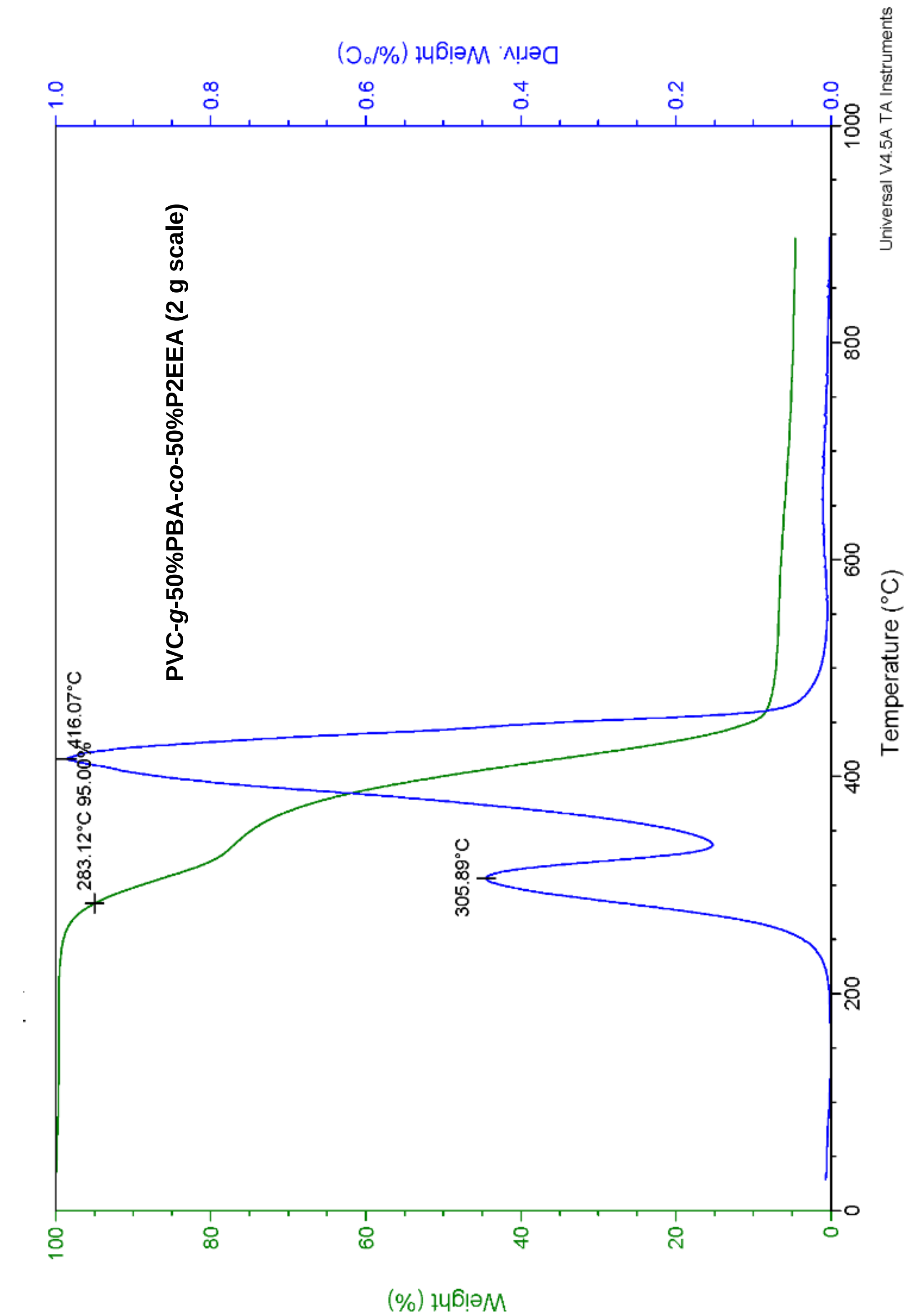

PVC-g-50%PBA-co-50%P2EEA (2 g scale)
283.12°C 95.00%
416.07°C
305.89°C
Weight (%)
100
80
60
40
20
0
Deriv. Weight (%/°C)
1.0
0.8
0.6
0.4
0.2
0.0
Temperature (°C)
0
200
400
600
800
1000
Universal V4.5A TA Instruments

PVC-*g*-50%PBA-*co*-50%P2EEA (2 g scale)

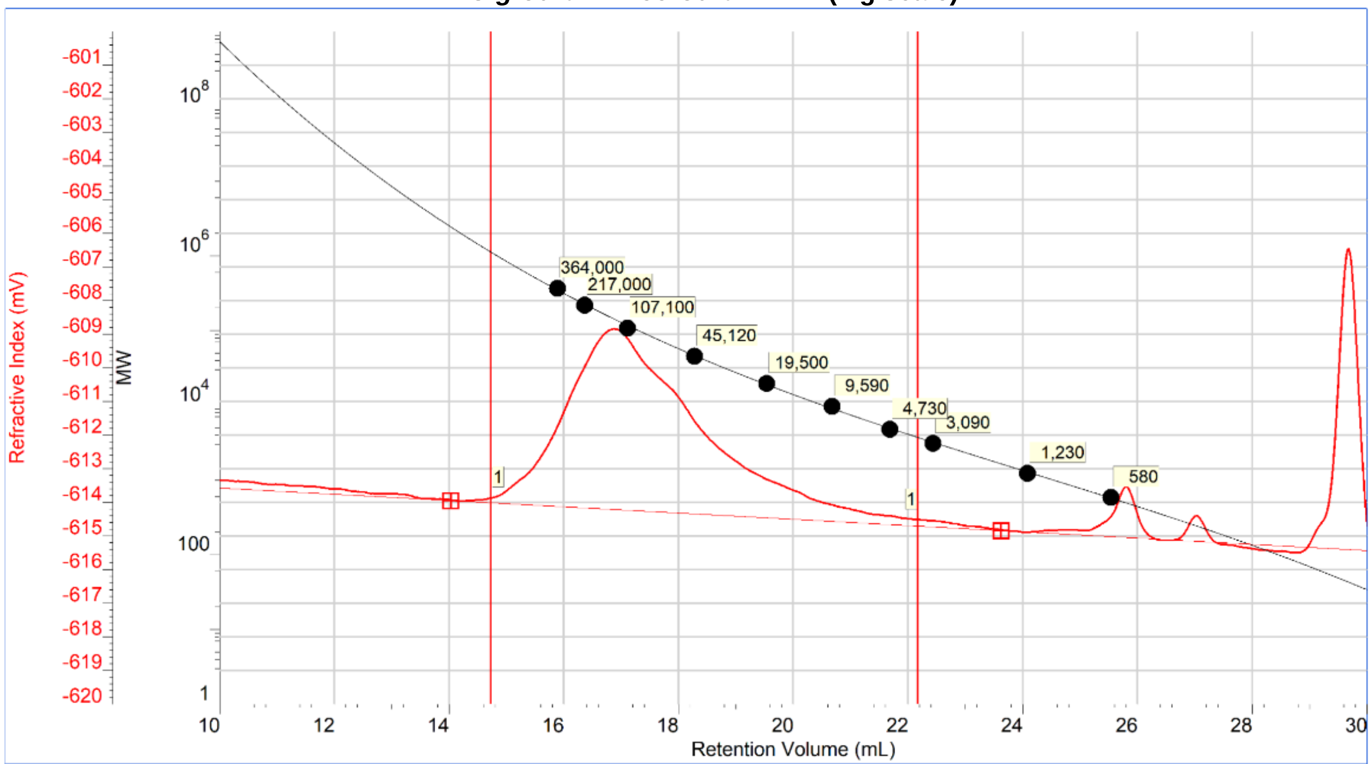

Peak	Ret Time	Mp	Mn	Mw	Mz	Mw/Mn	RI Area
1	16.880	140,864	46,537	141,136	283,867	3.033	14.73

PVC-*g*-50%PBA-*co*-50%P2EEA (2 g scale)

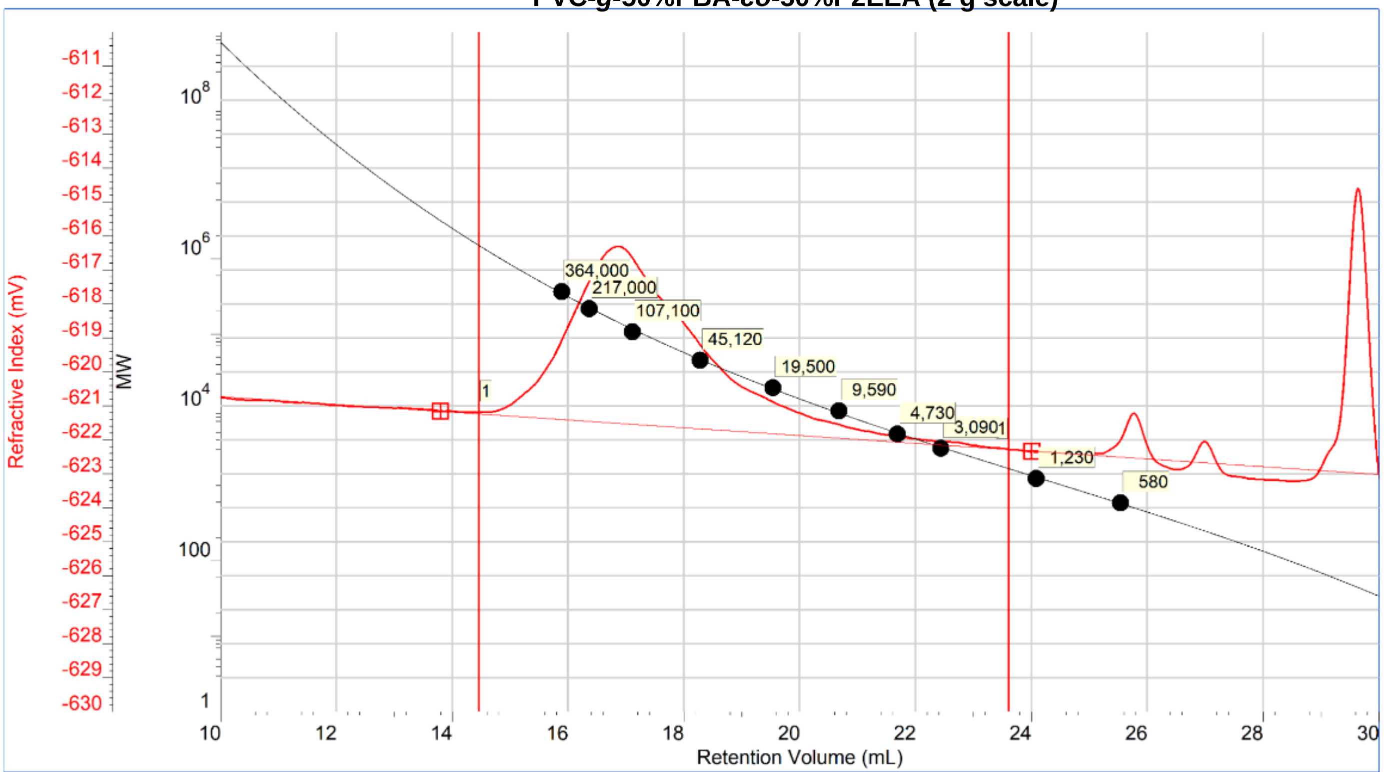

Peak	Ret Time	Mp	Mn	Mw	Mz	Mw/Mn	RI Area
1	16.857	143,711	45,482	149,291	309,480	3.282	13.65

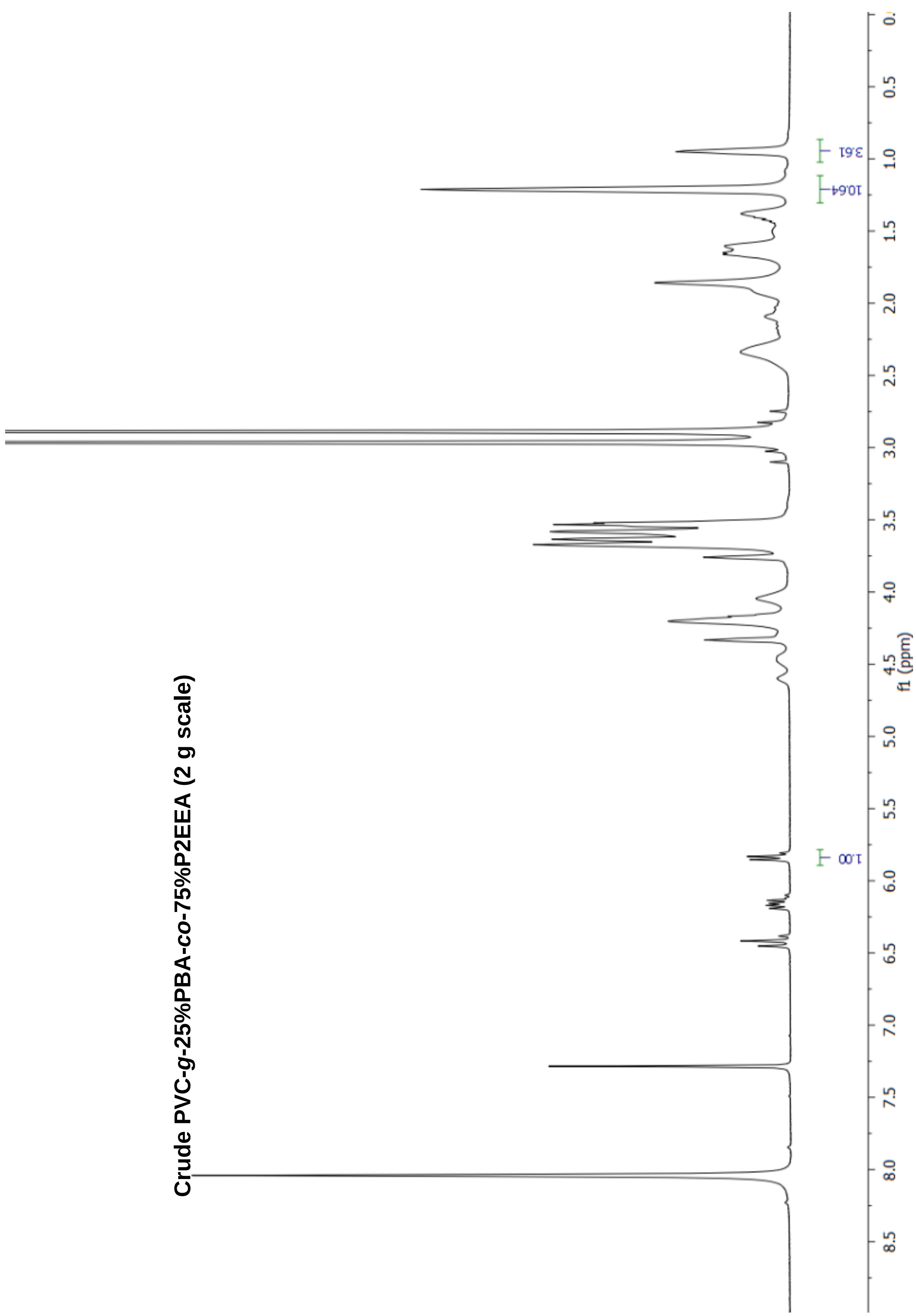
Crude PVC-g-25%PBA-co-75%P2EEA (2 g scale)
f1 (ppm)
3.61
10.64
1.00
0.5
1.0
1.5
2.0
2.5
3.0
3.5
4.0
4.5
5.0
5.5
6.0
6.5
7.0
7.5
8.0
8.5

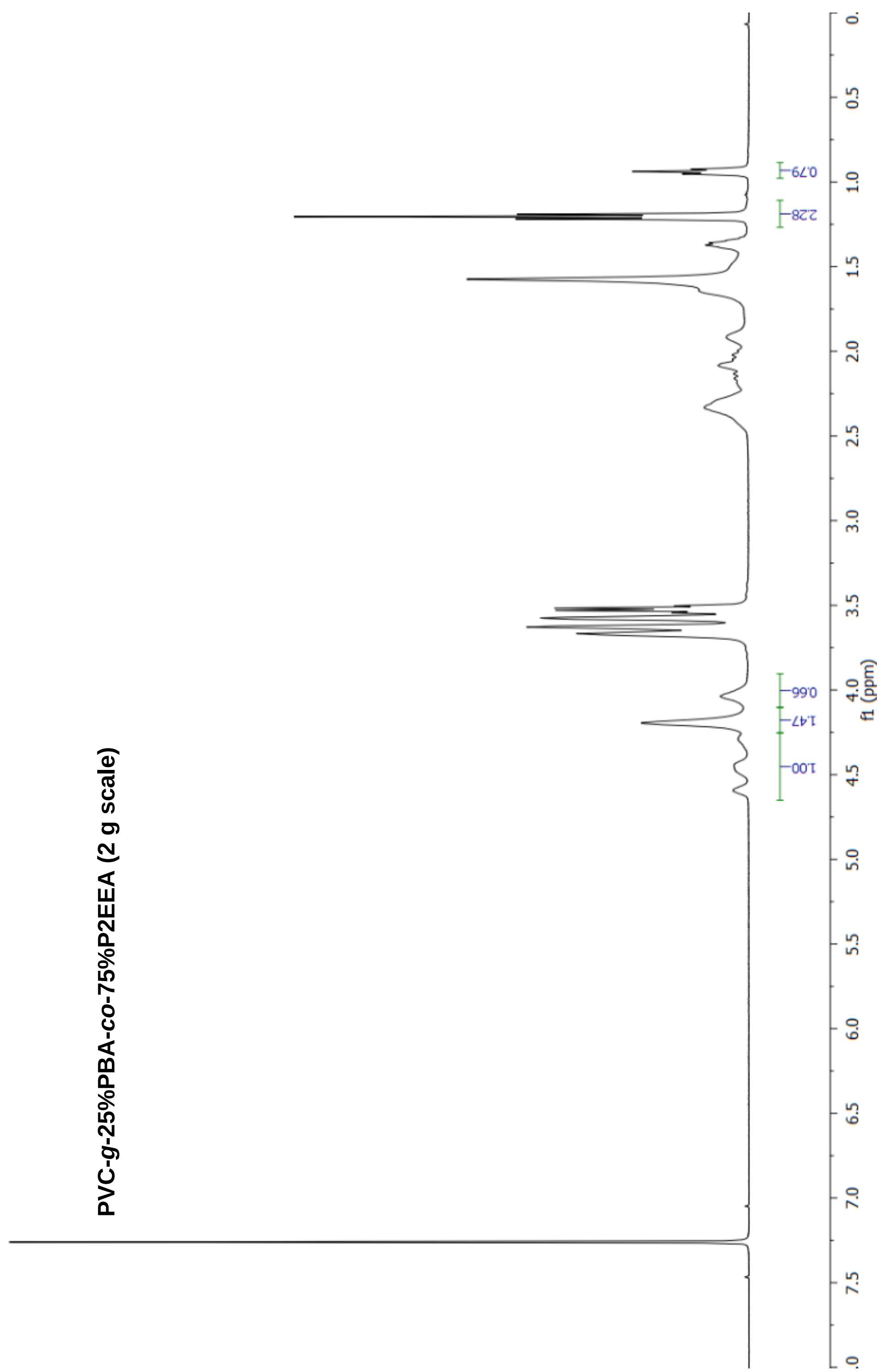

PVC-*g*-25%PBA-*co*-75%P2EEA (2 g scale)

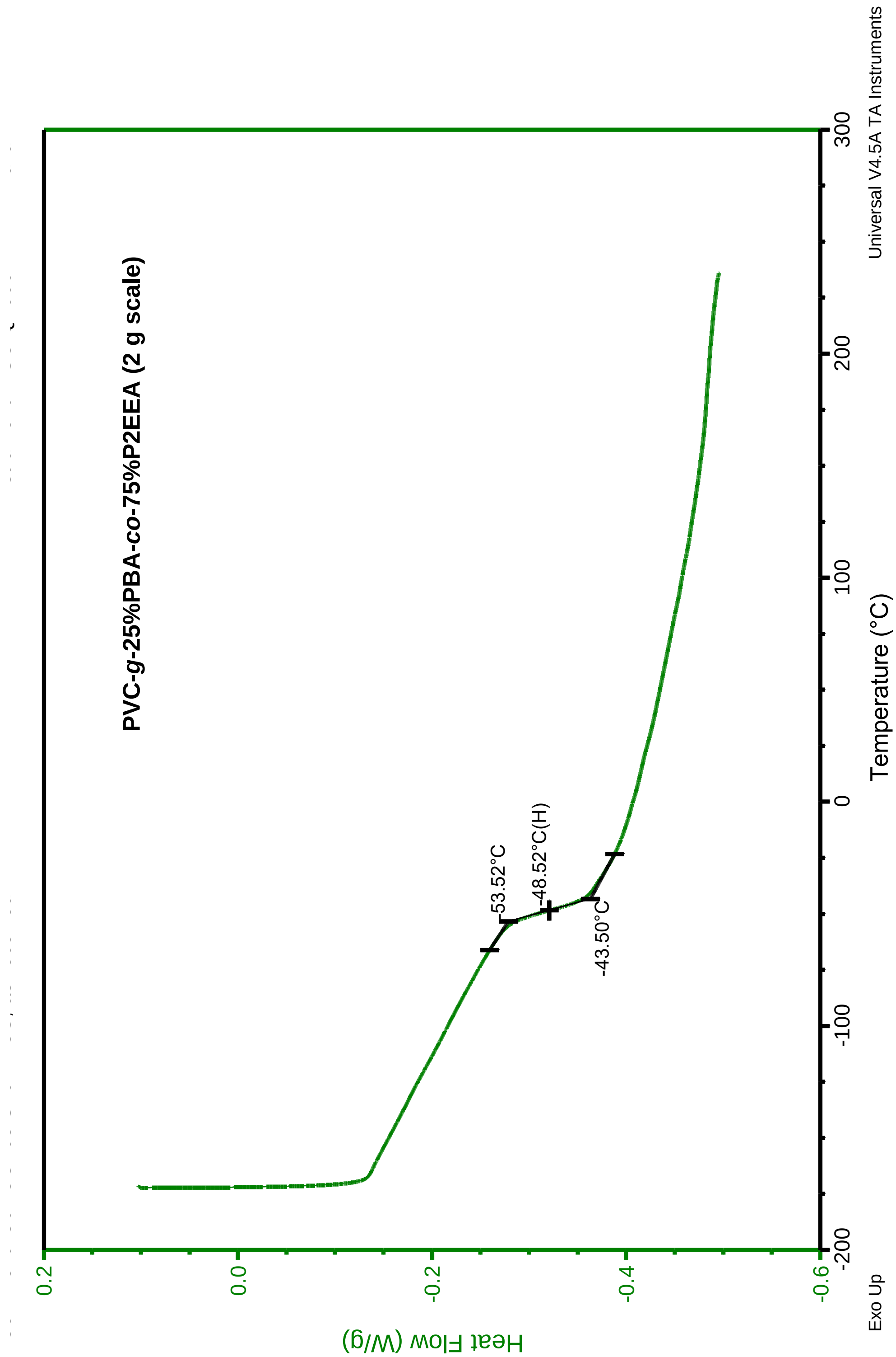

PVC-*g*-25%PBA-*co*-75%P2EEA (2 g scale)
-53.52°C
-48.52°C(H)
-43.50°C
Heat Flow (W/g)
0.2
0.0
-0.2
-0.4
-0.6
Exo Up
-200
-100
0
100
200
300
Temperature (°C)
Universal V4.5A TA Instruments

PVC-*g*-25%PBA-*co*-75%P2EEA (2 g scale)

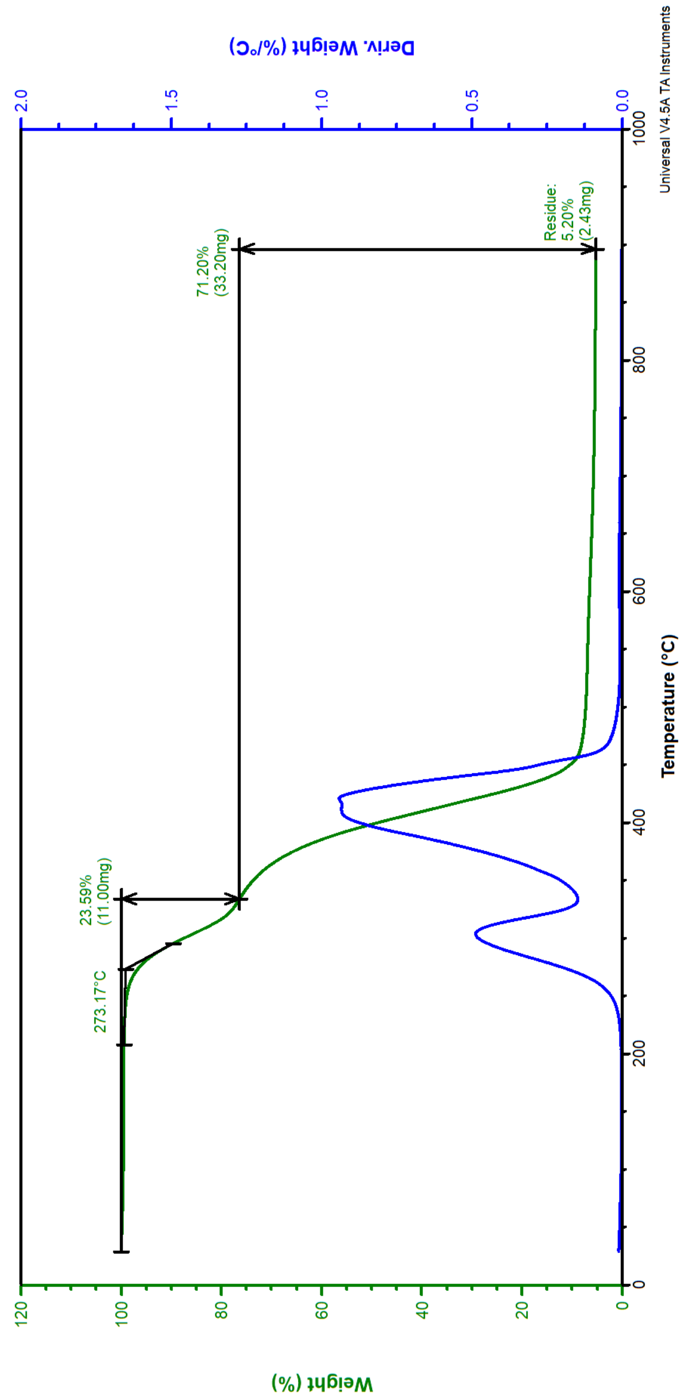

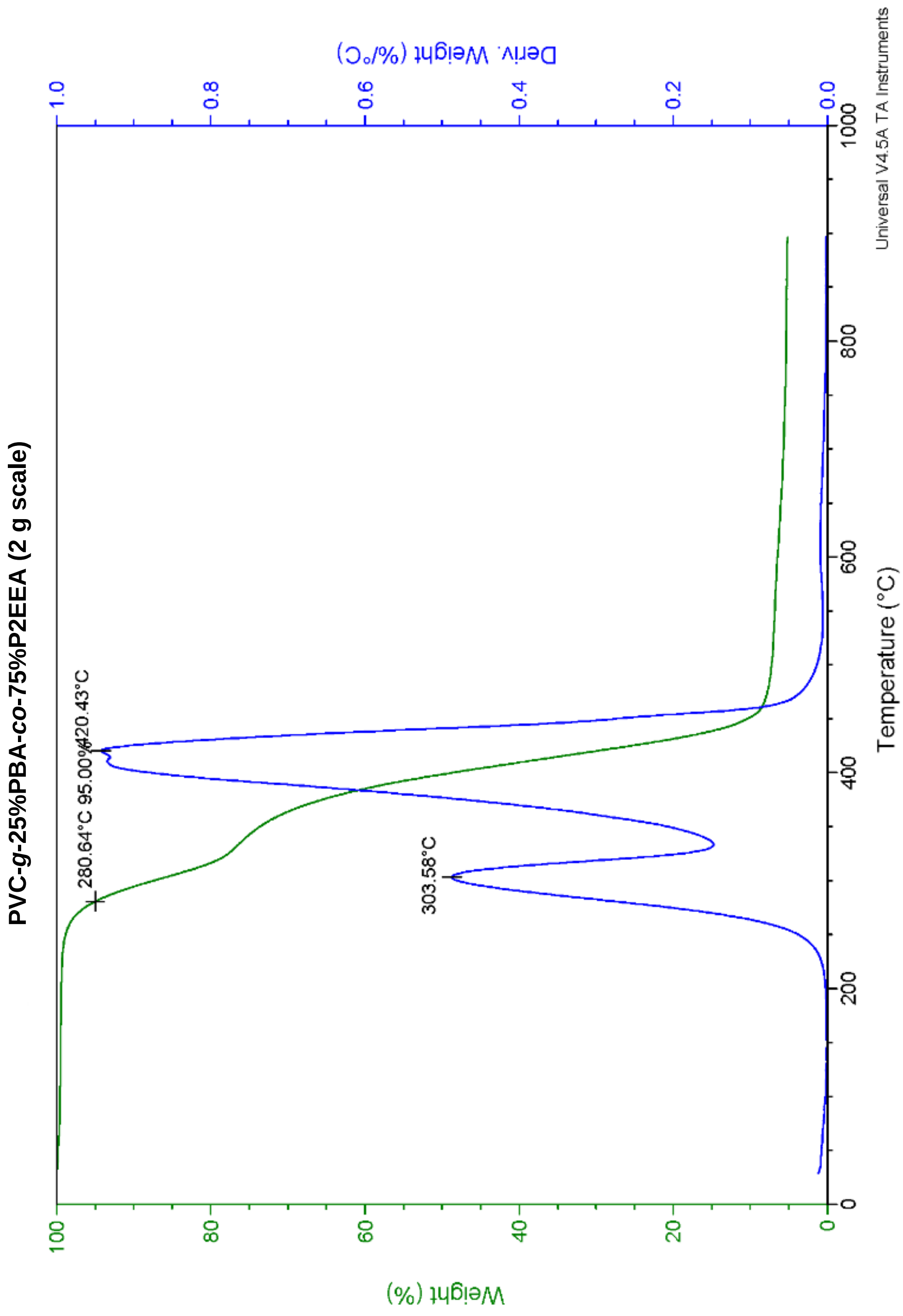
PVC-*g*-25%PBA-*co*-75%P2EEA (2 g scale)
280.64°C 95.00%
420.43°C
303.58°C
Weight (%)
Deriv. Weight (%/°C)
Temperature (°C)
Universal V4.5A TA Instruments

PVC-*g*-25%PBA-*co*-75%P2EEA (2 g scale)

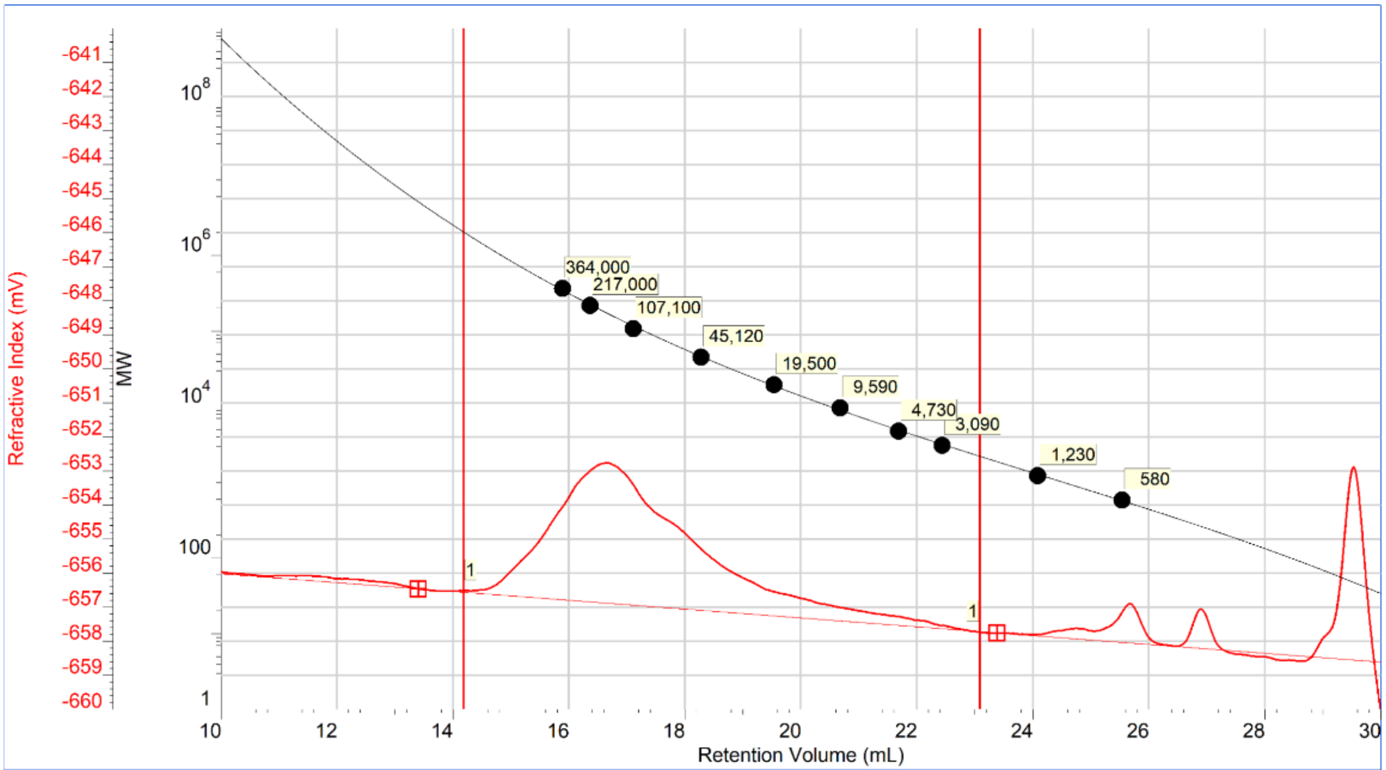

Peak	Ret Time	Mp	Mn	Mw	Mz	Mw/Mn	RI Area
1	16.647	172,407	46,521	187,320	417,640	4.027	11.80

PVC-*g*-25%PBA-*co*-75%P2EEA (2 g scale)

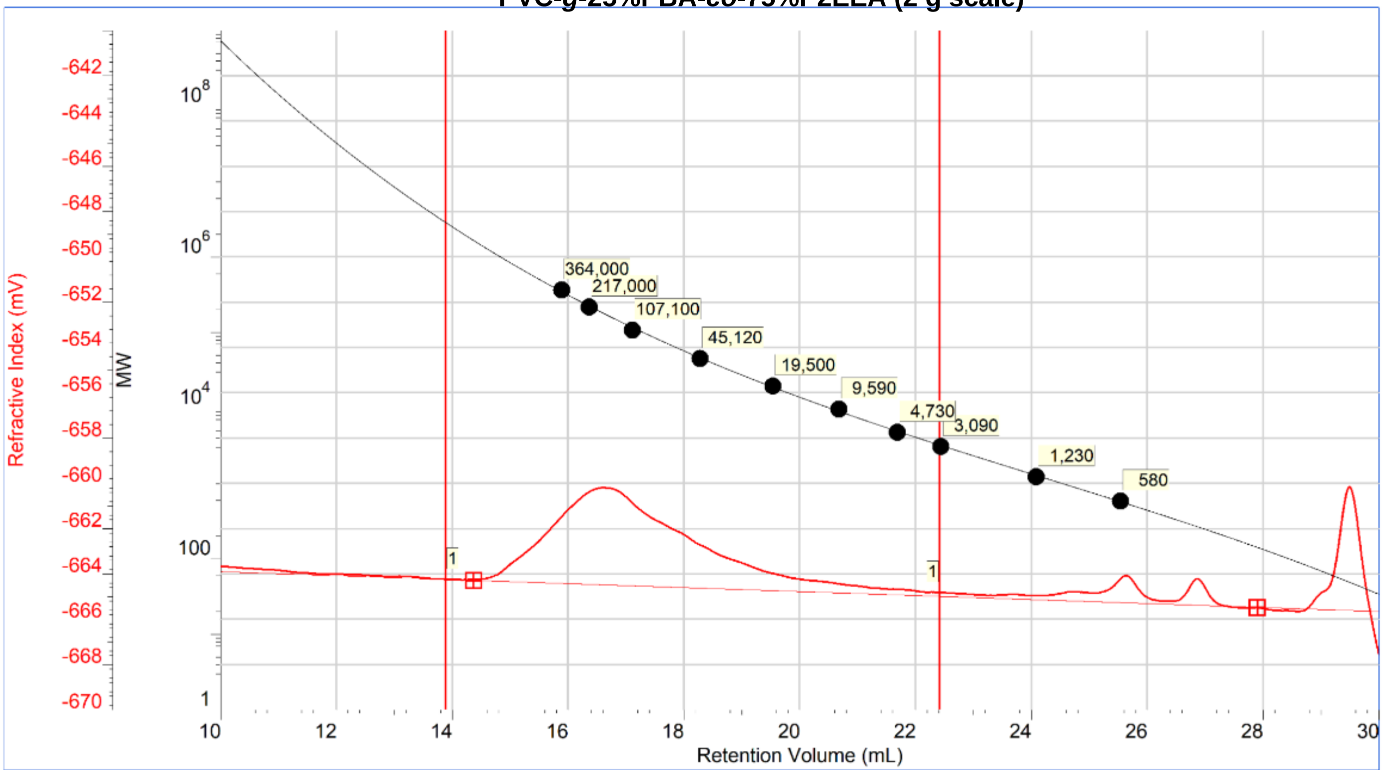

Peak	Ret Time	Mp	Mn	Mw	Mz	Mw/Mn	RI Area
1	16.633	174,772	48,451	187,568	420,907	3.871	12.42

Crude PVC-*g*-P2EEA (2 g scale)

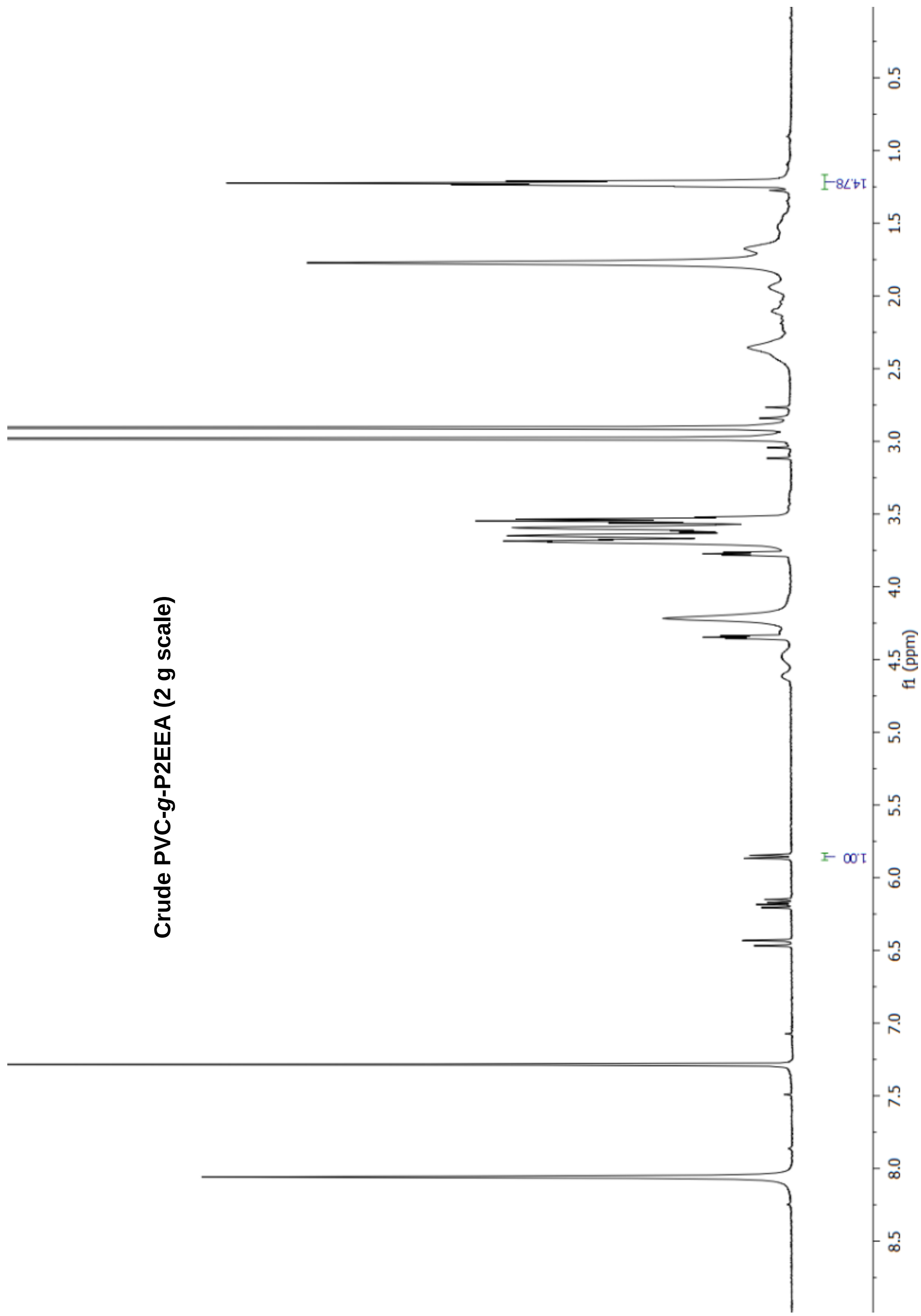

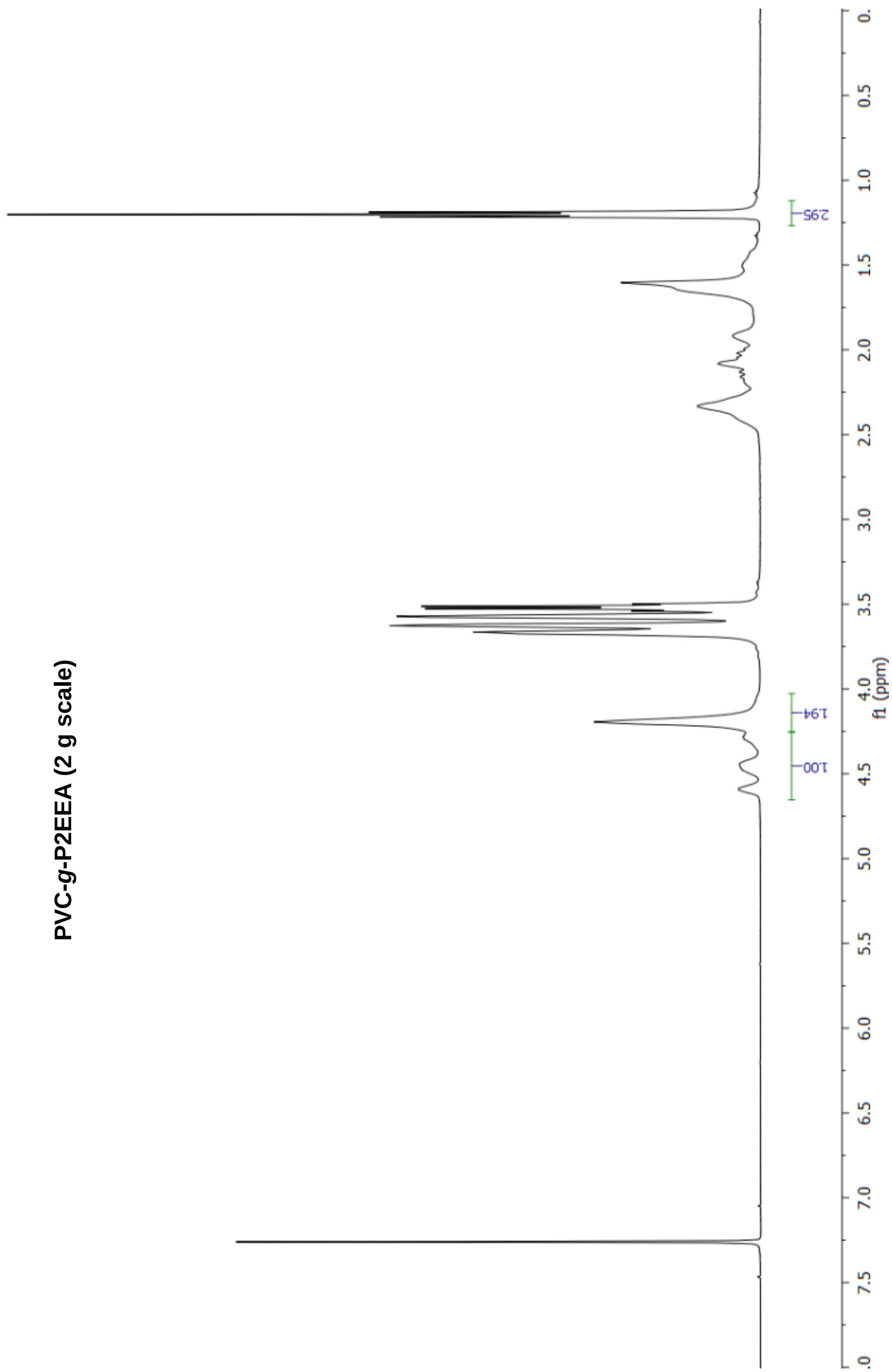
PVC-*g*-P2EEA (2 g scale)
f1 (ppm)
2.95
1.94
1.00

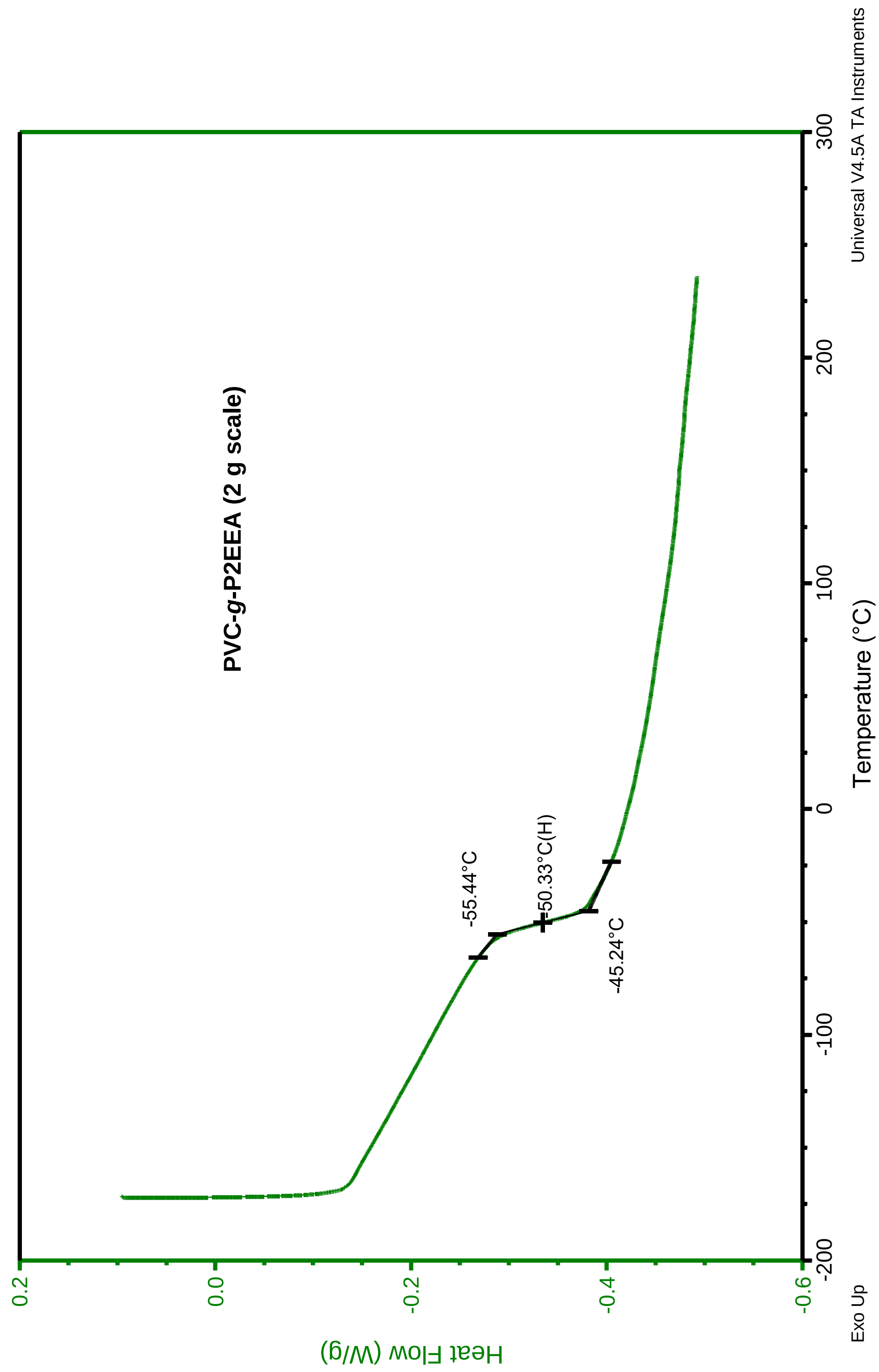
PVC-g-P2EEA (2 g scale)
-55.44°C
-50.33°C(H)
-45.24°C
Heat Flow (W/g)
Temperature (°C)
Exo Up
Universal V4.5A TA Instruments
0.2
0.0
-0.2
-0.4
-0.6
-200
-100
0
100
200
300

PVC-*g*-P2EEA (2 g scale)

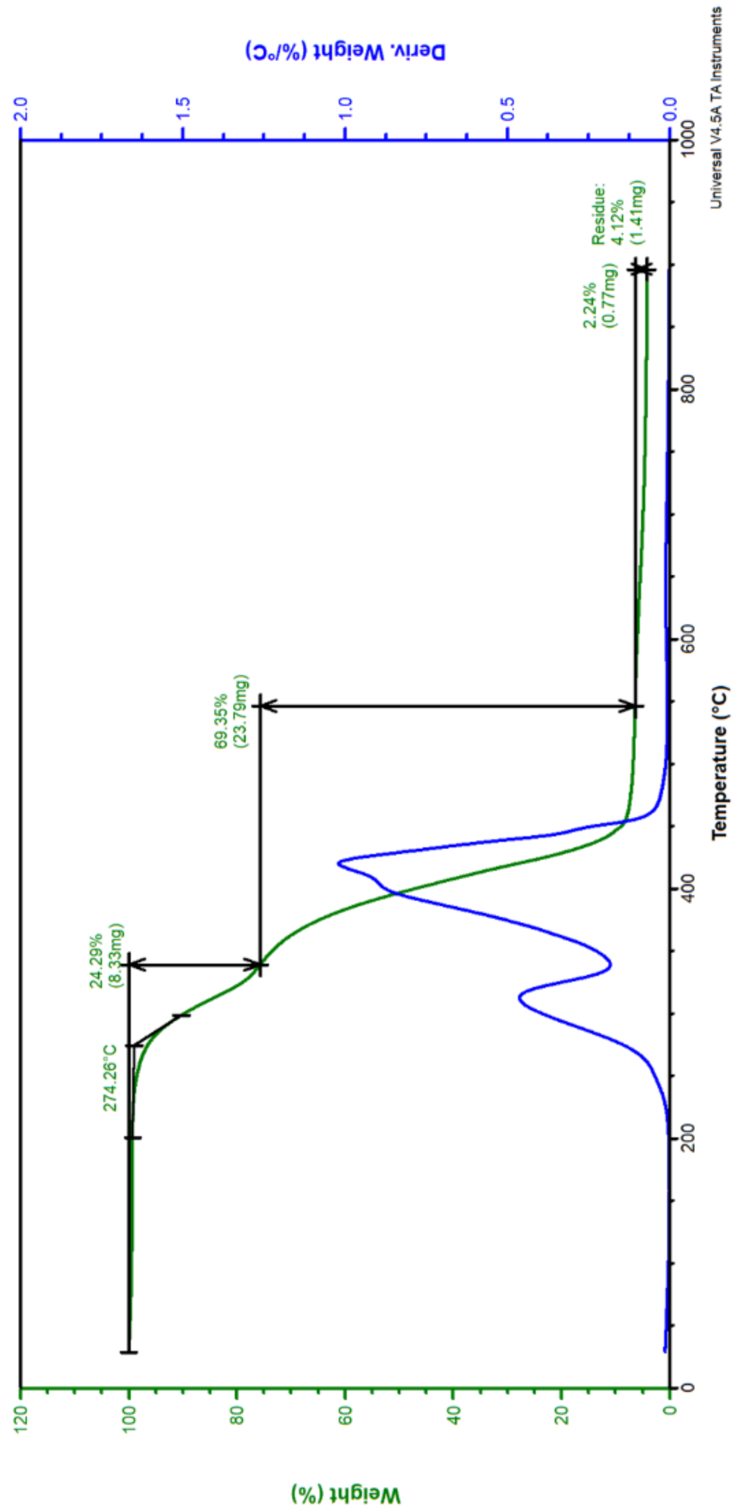

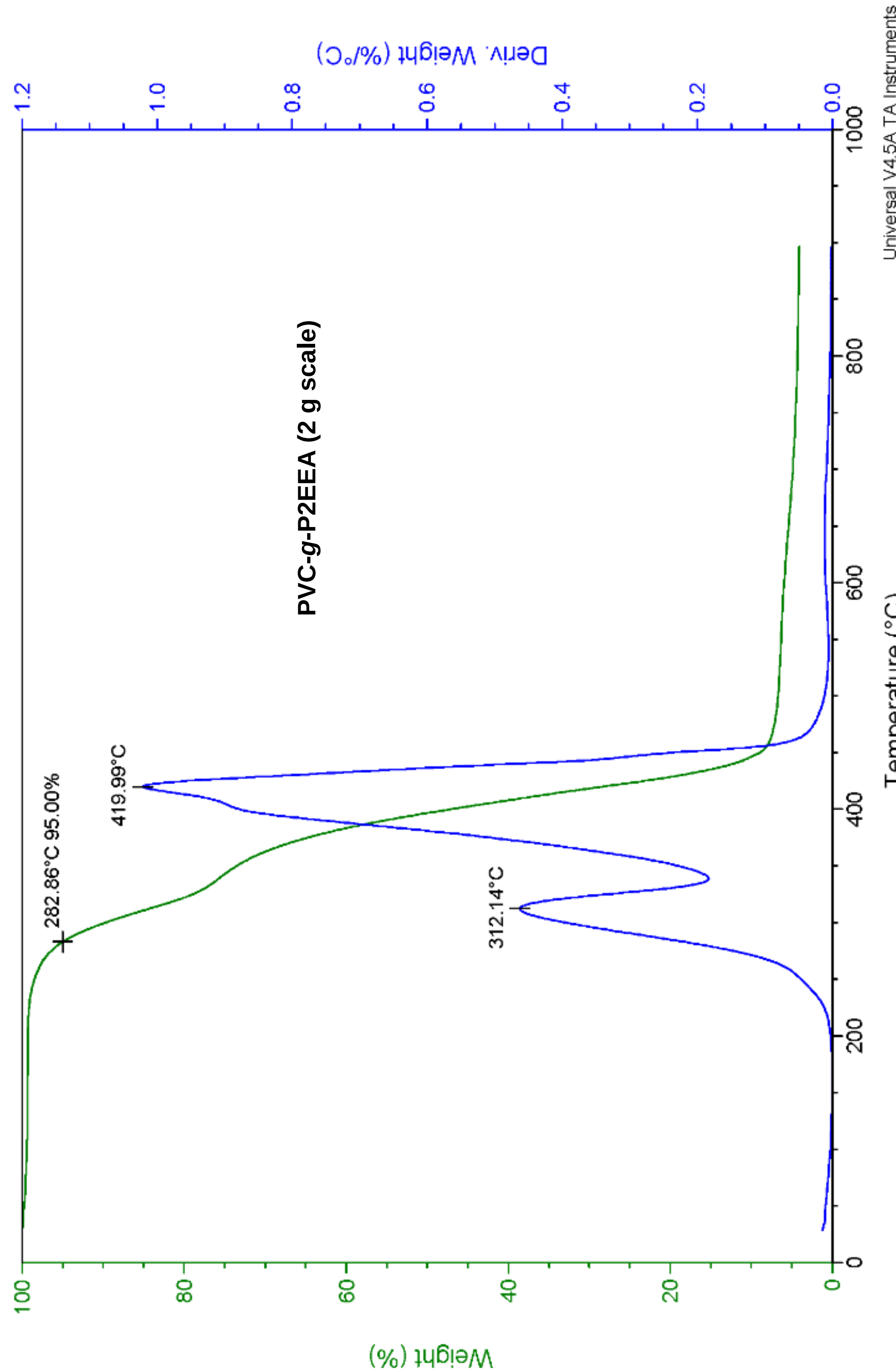
PVC-g-P2EEA (2 g scale)
282.86°C 95.00%
312.14°C
419.99°C
Weight (%)
Deriv. Weight (%/°C)
Temperature (°C)
Universal V4.5A TA Instruments
0
200
400
600
800
1000
20
40
60
80
100
0.0
0.2
0.4
0.6
0.8
1.0
1.2

PVC-*g*-P2EEA (2 g scale)

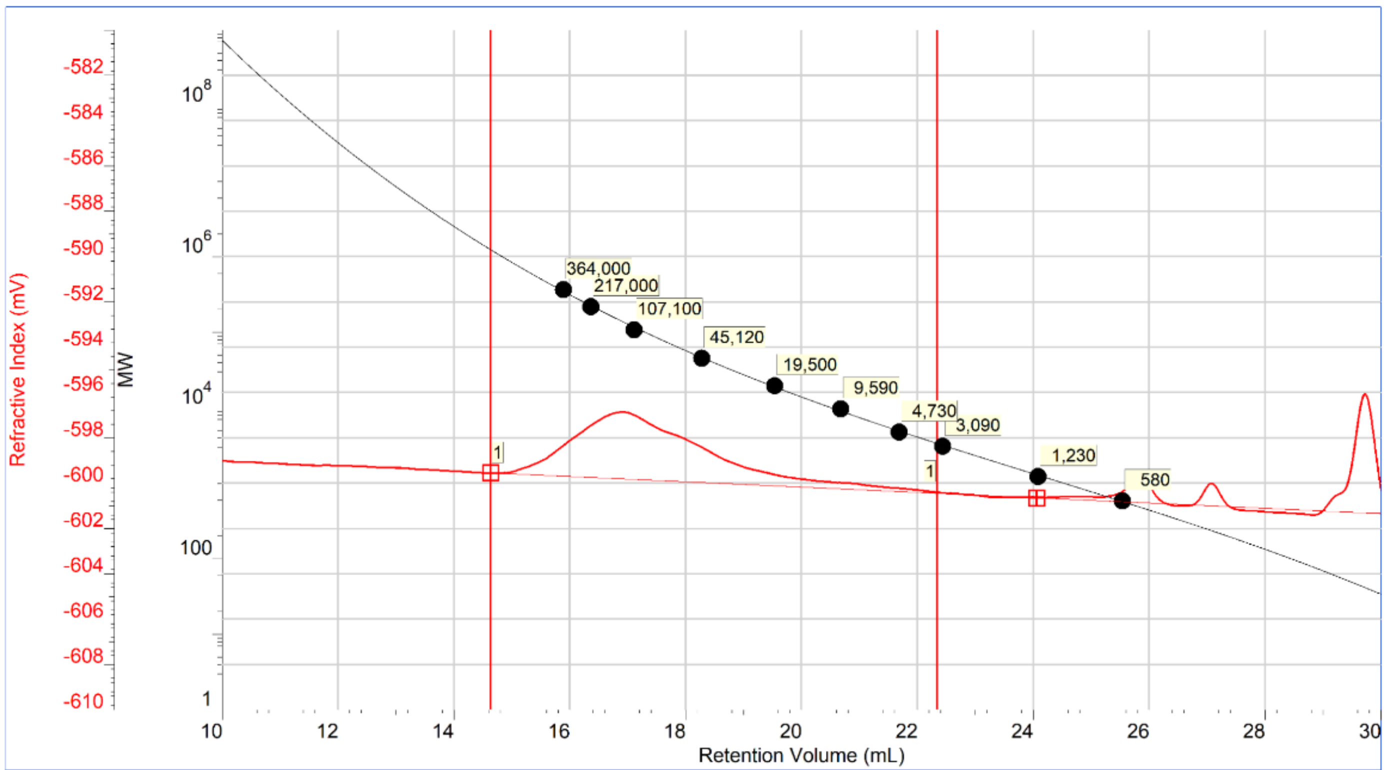

Peak	Ret Time	Mp	Mn	Mw	Mz	Mw/Mn	RI Area
1	16.907	137,679	47,072	142,932	285,085	3.036	7.86

PVC-*g*-P2EEA (2 g scale)

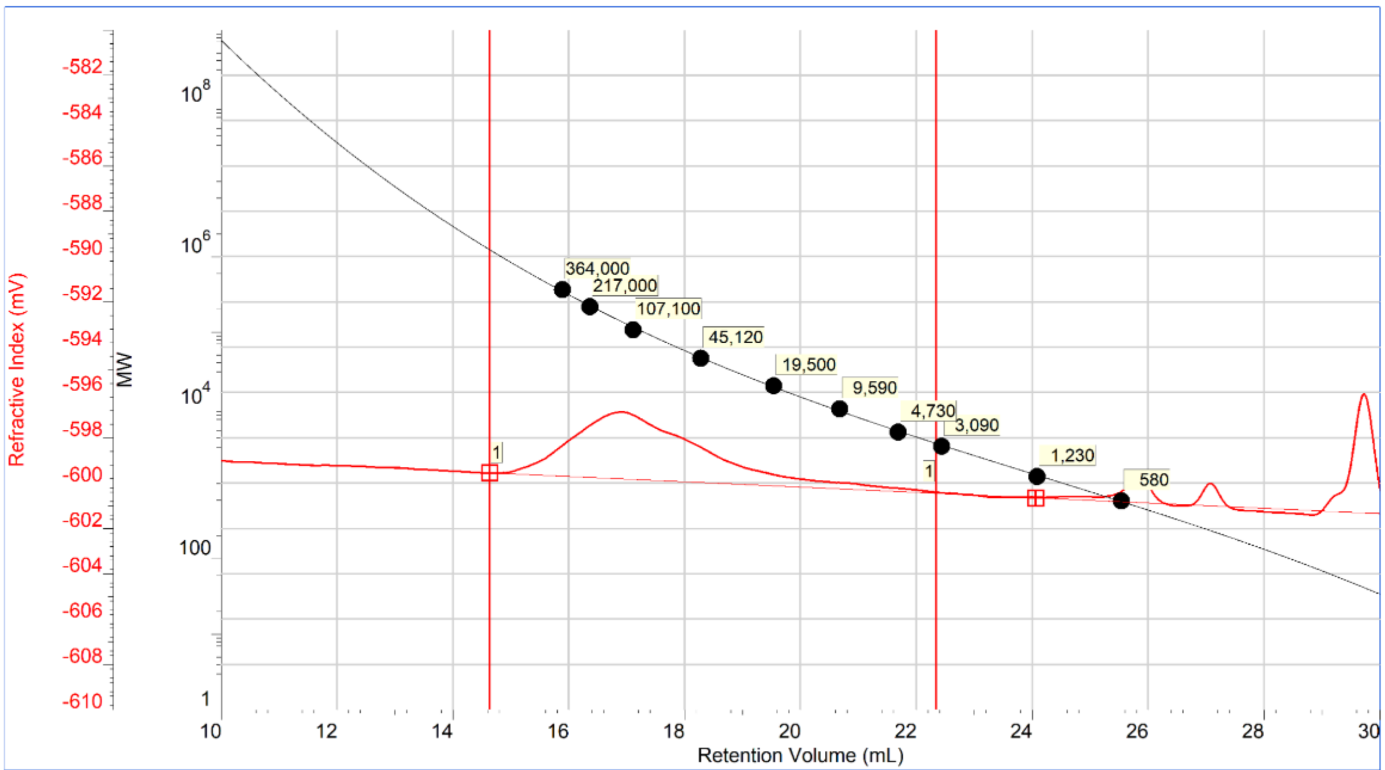

Peak	Ret Time	Mp	Mn	Mw	Mz	Mw/Mn	RI Area
1	16.907	137,679	47,072	142,932	285,085	3.036	7.86

Control reaction (Crude, 2 g scale)

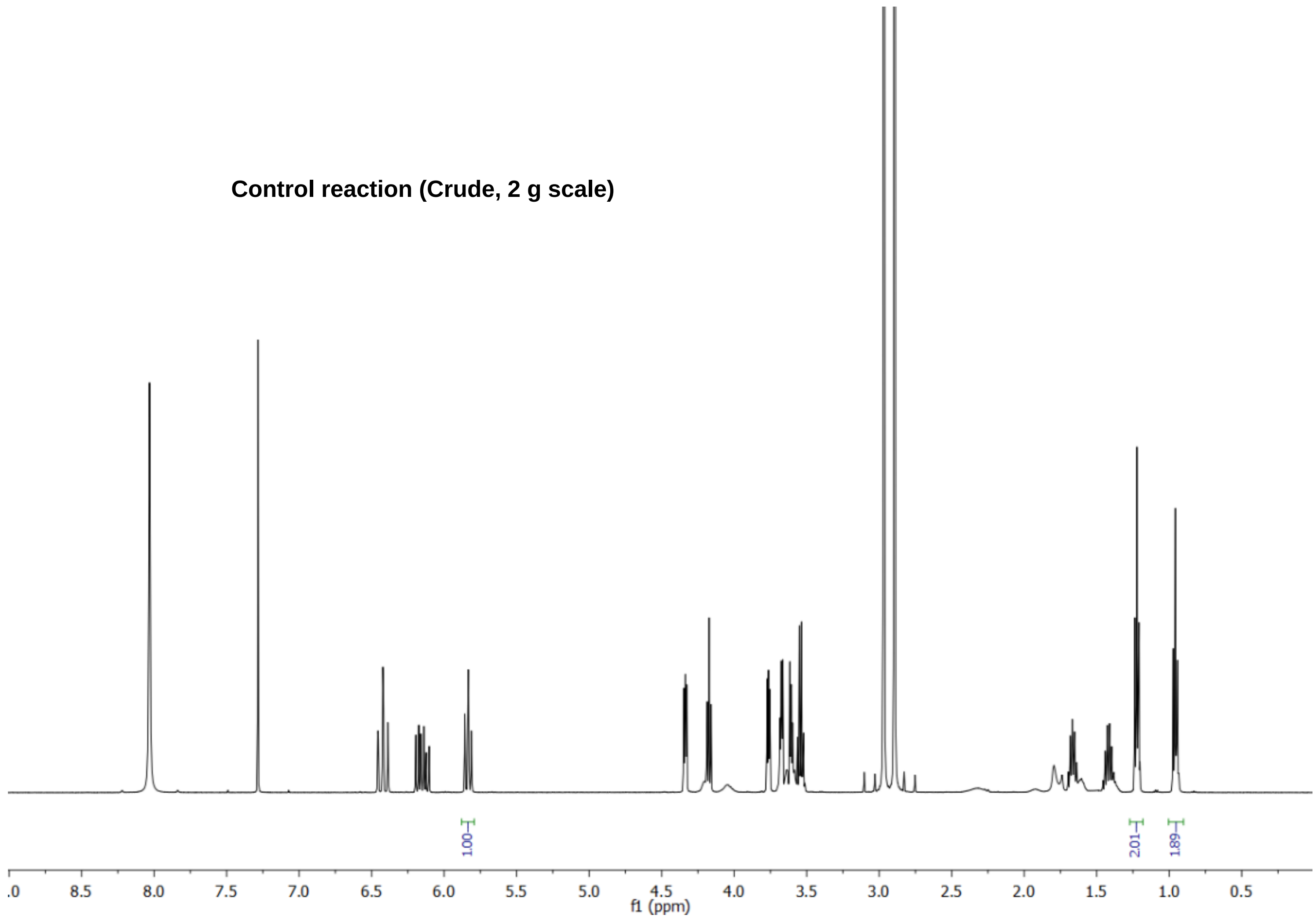

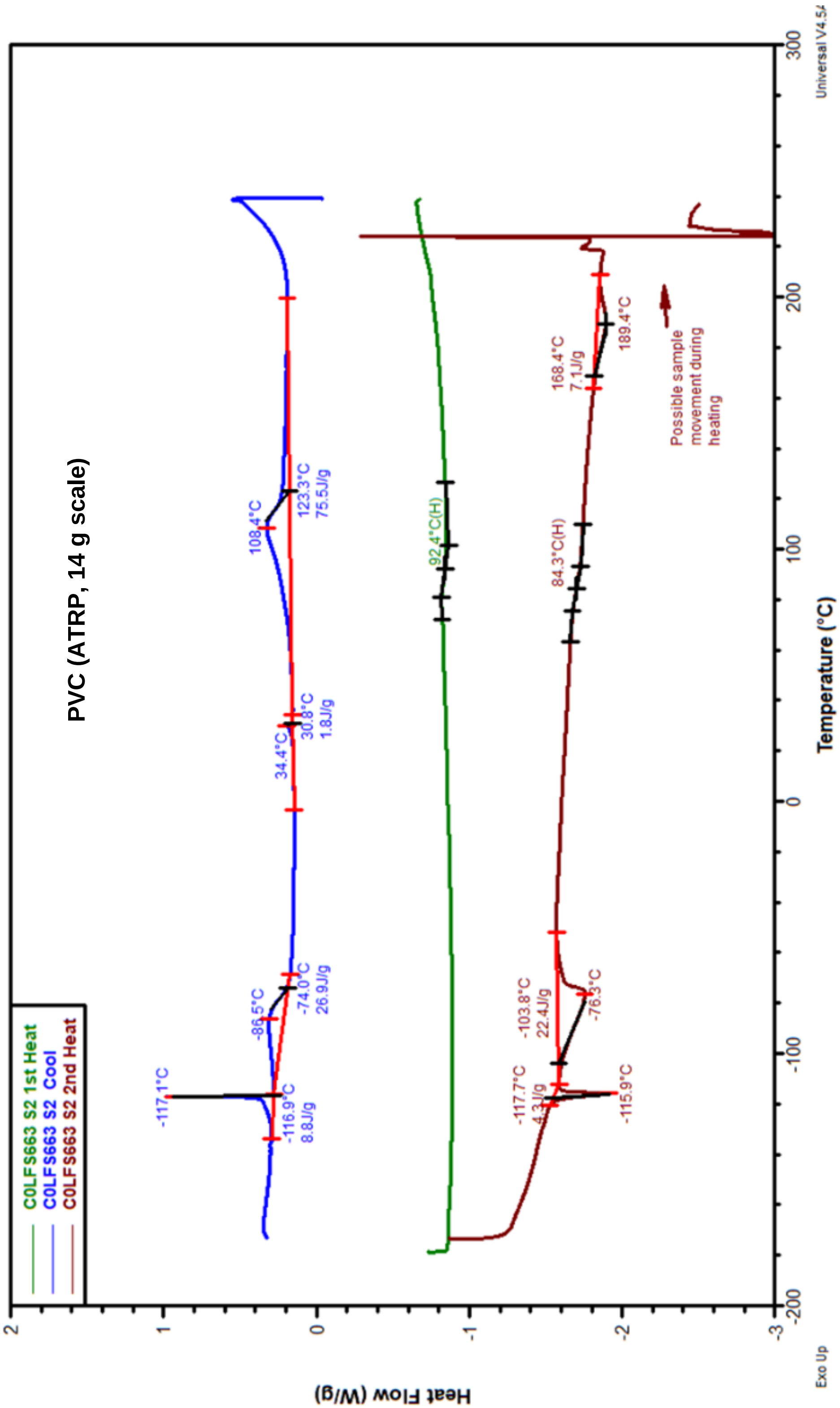
PVC (ATRP, 14 g scale)
C0LFS663 S2 1st Heat
C0LFS663 S2 Cool
C0LFS663 S2 2nd Heat
-117.1°C
-116.9°C
8.8J/g
-86.5°C
-74.0°C
26.9J/g
34.4°C
30.8°C
1.8J/g
108.4°C
123.3°C
75.5J/g
92.4°C(H)
84.3°C(H)
-117.7°C
4.3J/g
-115.9°C
-103.8°C
22.4J/g
-76.3°C
168.4°C
7.1J/g
189.4°C
Possible sample movement during heating
Heat Flow (W/g)
Temperature (°C)
Exo Up
Universal V4.5A

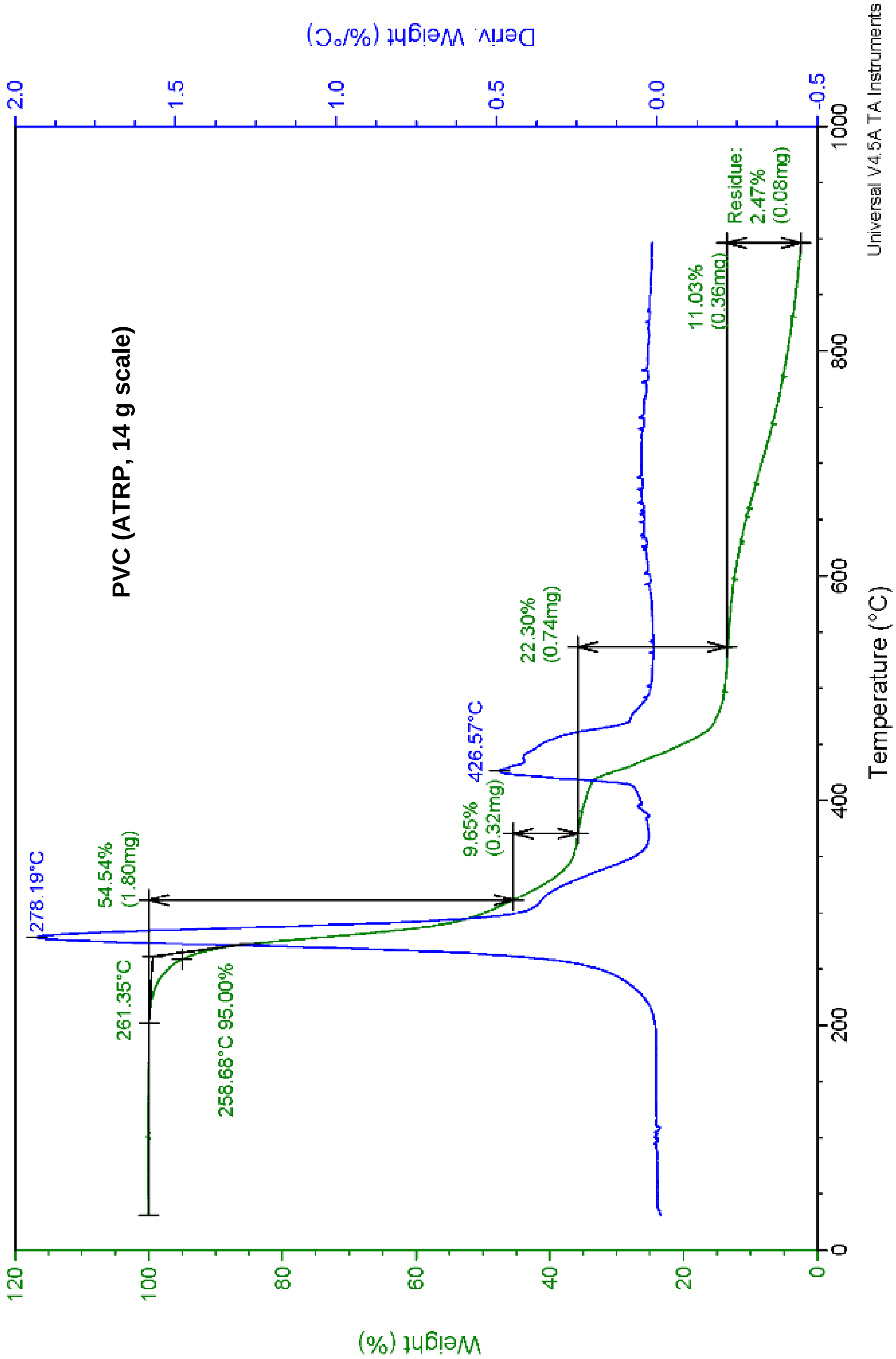
PVC (ATRP, 14 g scale)
Weight (%)
Deriv. Weight (%/°C)
Temperature (°C)
278.19°C
261.35°C
258.68°C 95.00%
54.54%
(1.80mg)
9.65%
(0.32mg)
426.57°C
22.30%
(0.74mg)
11.03%
(0.36mg)
Residue:
2.47%
(0.08mg)
Universal V4.5A TA Instruments

PVC (ATRP, 14 g scale)

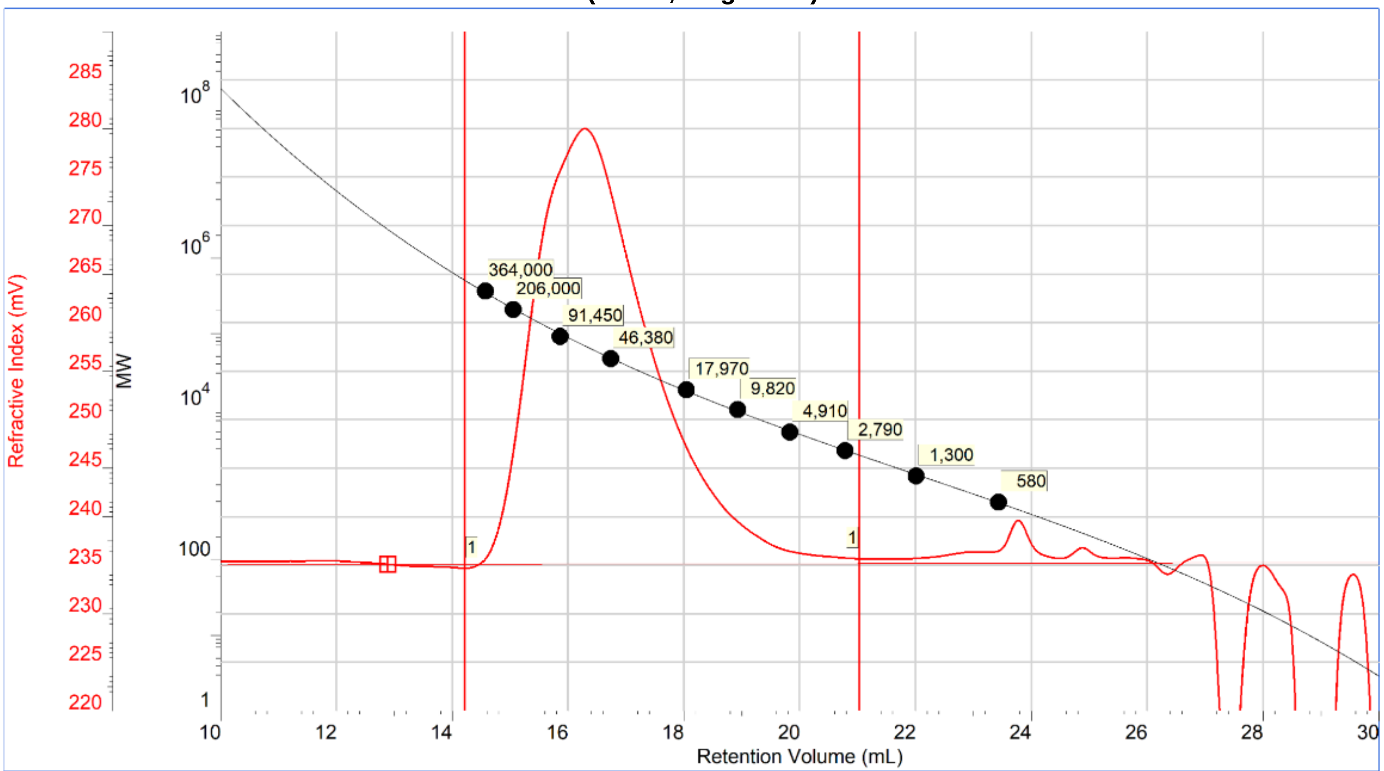

Peak	Ret Time	Mp	Mn	Mw	Mz	Mw/Mn	RI Area
1	16.280	68,699	36,029	72,192	111,606	2.004	103.85

PVC (ATRP, 14 g scale)

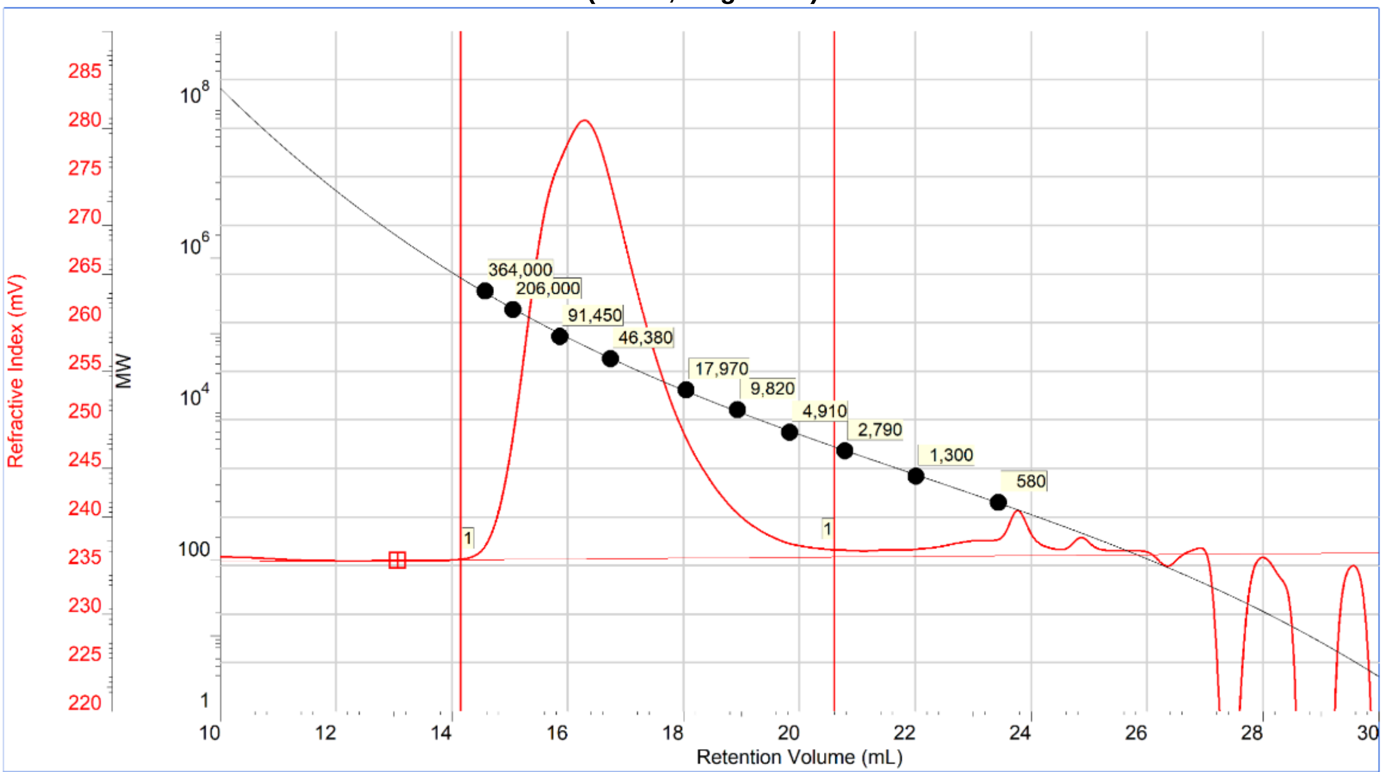

Peak	Ret Time	Mp	Mn	Mw	Mz	Mw/Mn	RI Area
1	16.273	69,039	36,793	73,914	117,273	2.009	106.17

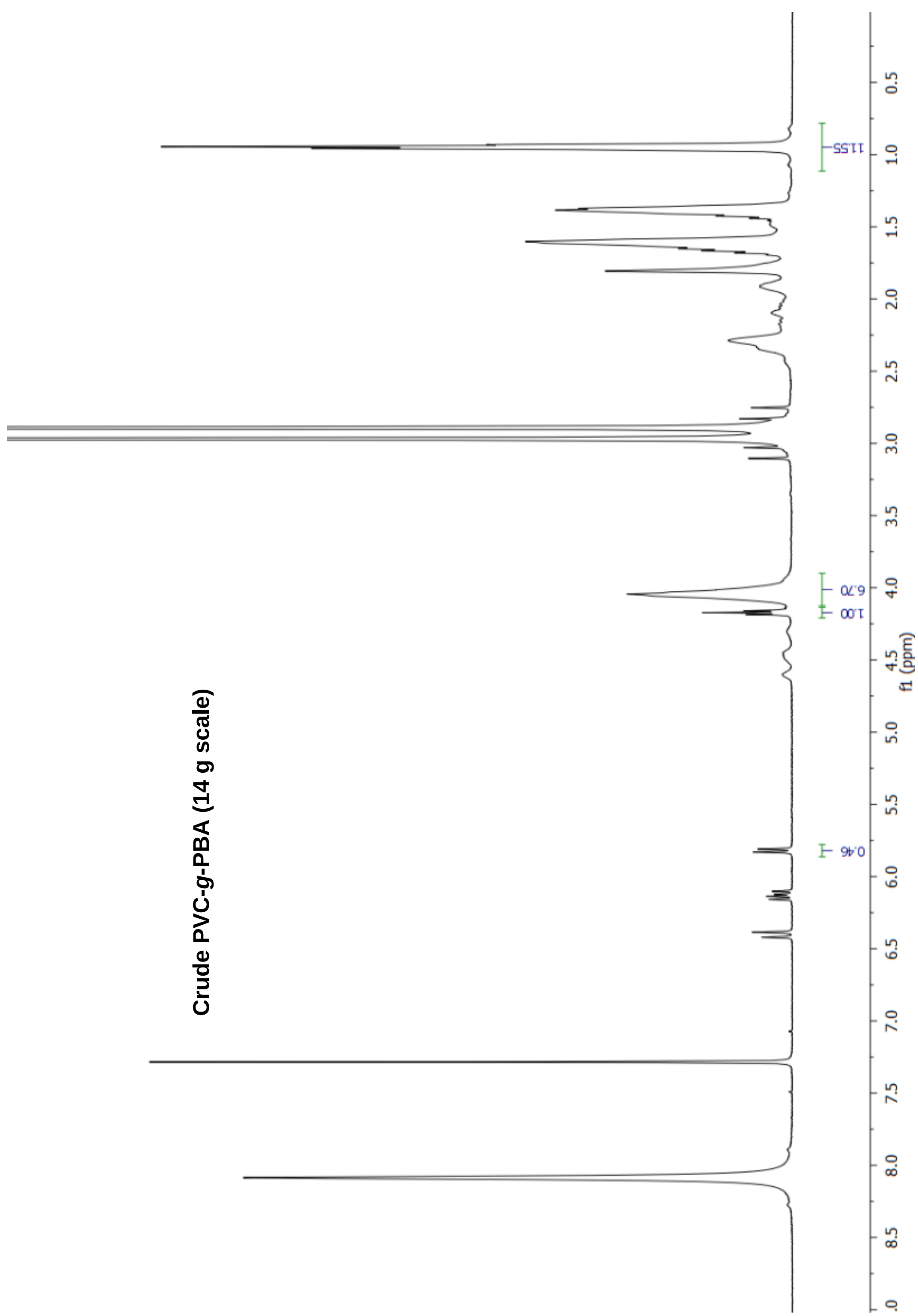
Crude PVC-*g*-PBA (14 g scale)
11.55
6.70
1.00
0.46
0.5 1.0 1.5 2.0 2.5 3.0 3.5 4.0 4.5 5.0 5.5 6.0 6.5 7.0 7.5 8.0 8.5
f1 (ppm)

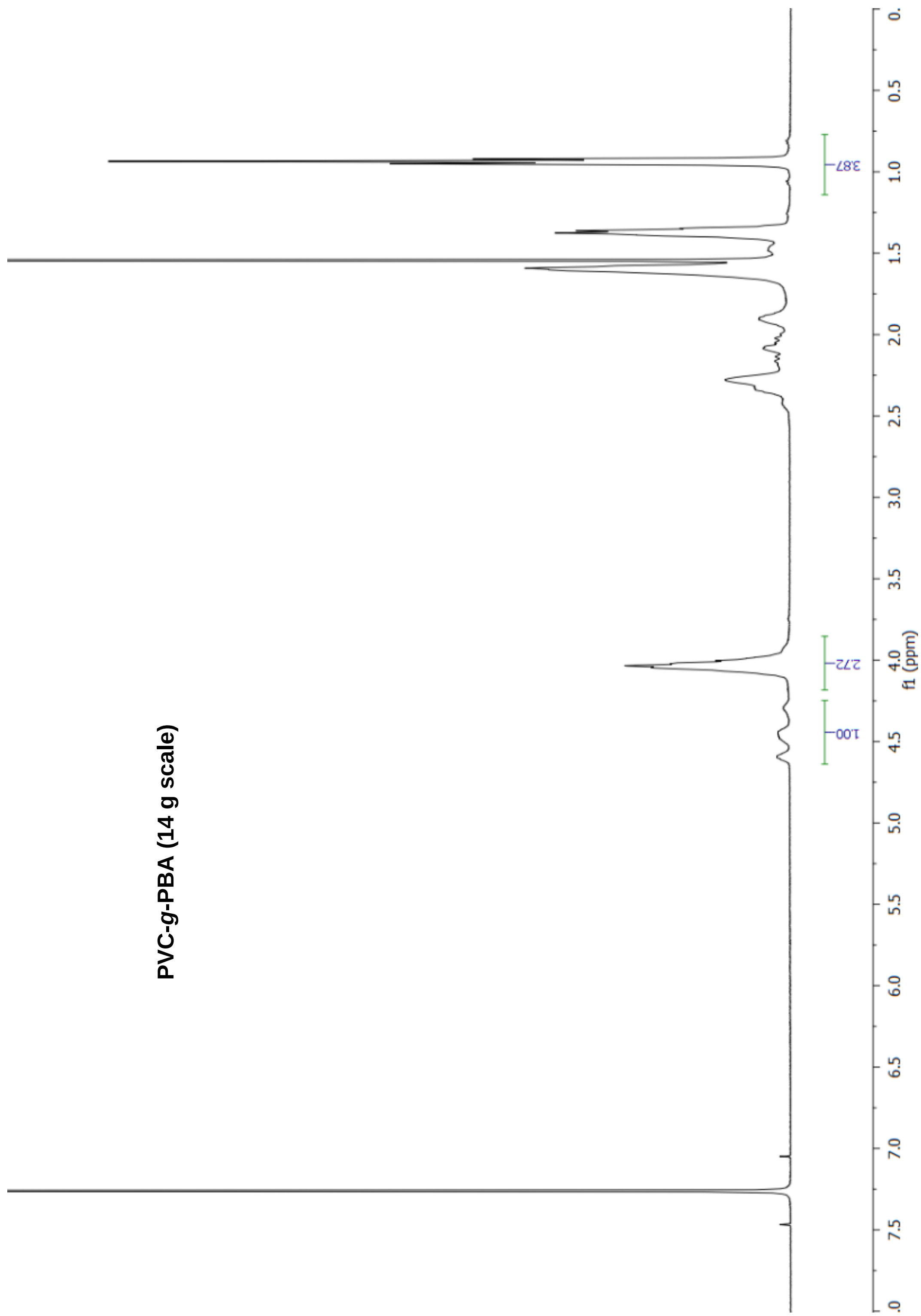
PVC-g-PBA (14 g scale)
3.87
2.72
1.00
0.5
1.0
1.5
2.0
2.5
3.0
3.5
4.0
4.5
5.0
5.5
6.0
6.5
7.0
7.5
f1 (ppm)

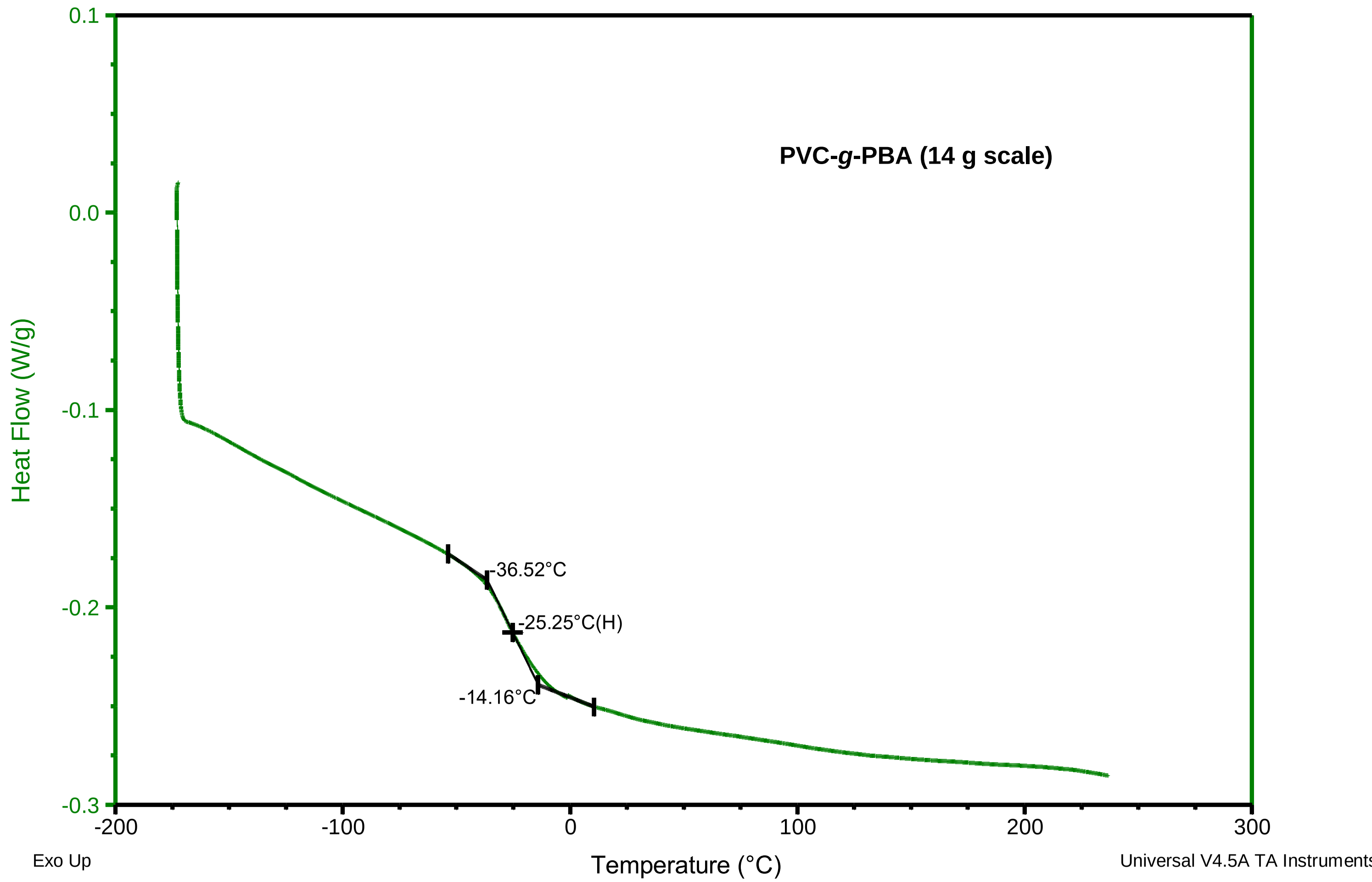
PVC-g-PBA (14 g scale)
-36.52°C
-25.25°C(H)
-14.16°C
Heat Flow (W/g)
0.1
0.0
-0.1
-0.2
-0.3
-200
-100
0
100
200
300
Exo Up
Temperature (°C)
Universal V4.5A TA Instruments

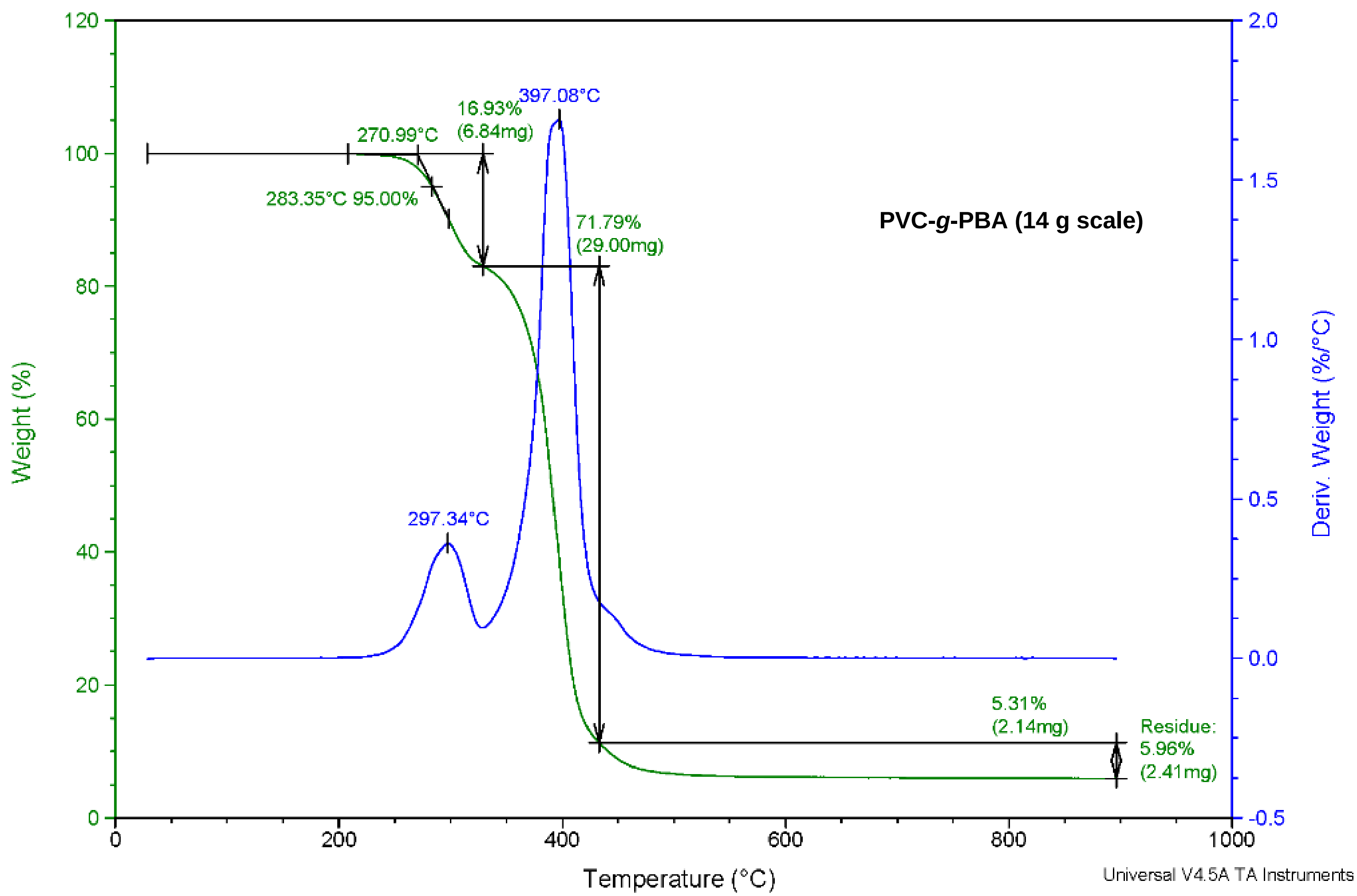
PVC-g-PBA (14 g scale)
270.99°C
283.35°C 95.00%
16.93%
(6.84mg)
397.08°C
71.79%
(29.00mg)
297.34°C
5.31%
(2.14mg)
Residue:
5.96%
(2.41mg)
Weight (%)
Deriv. Weight (%/°C)
Temperature (°C)
Universal V4.5A TA Instruments
0
20
40
60
80
100
120
200
400
600
800
1000
-0.5
0.0
0.5
1.0
1.5
2.0

PVC-*g*-PBA (14 g scale)

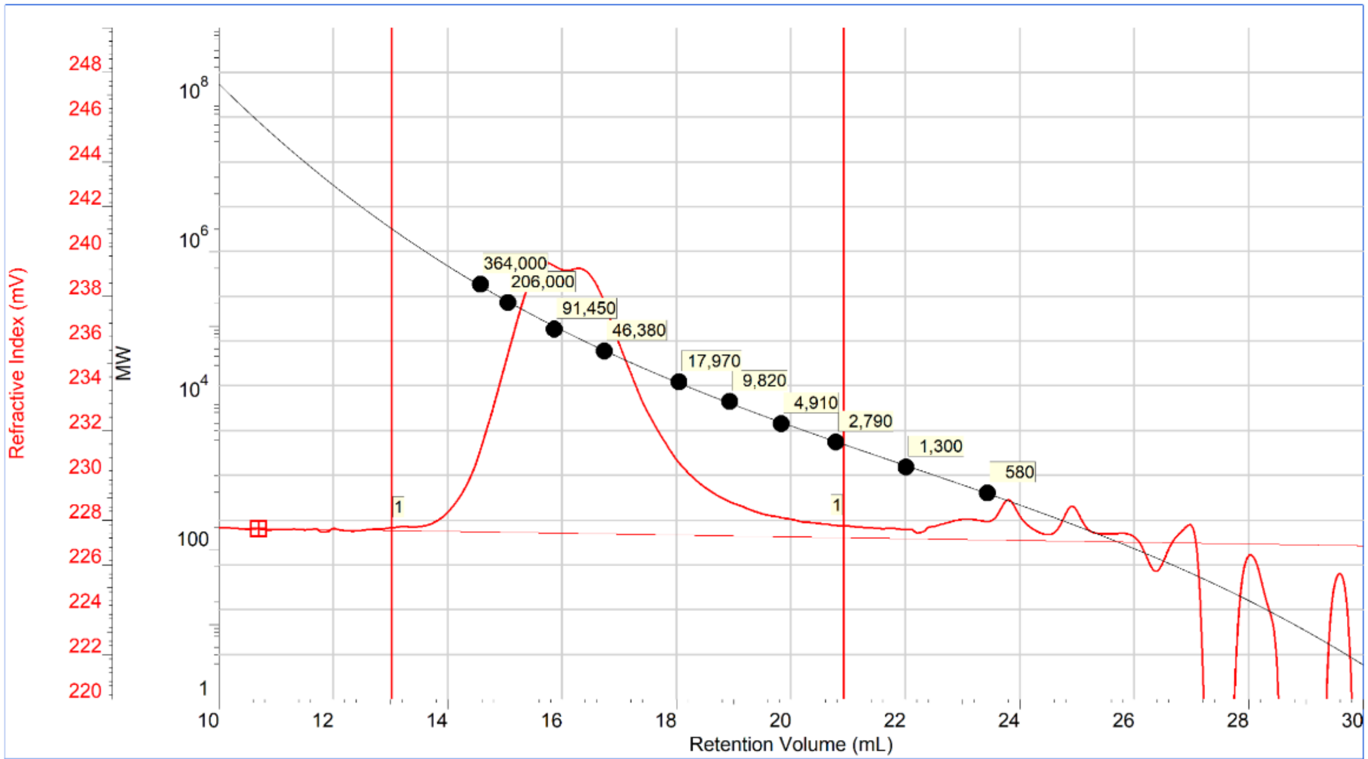

Peak	Ret Time	Mp	Mn	Mw	Mz	Mw/Mn	RI Area
1	15.723	112,551	35,015	107,422	242,947	3.068	35.11

PVC-*g*-PBA (14 g scale)

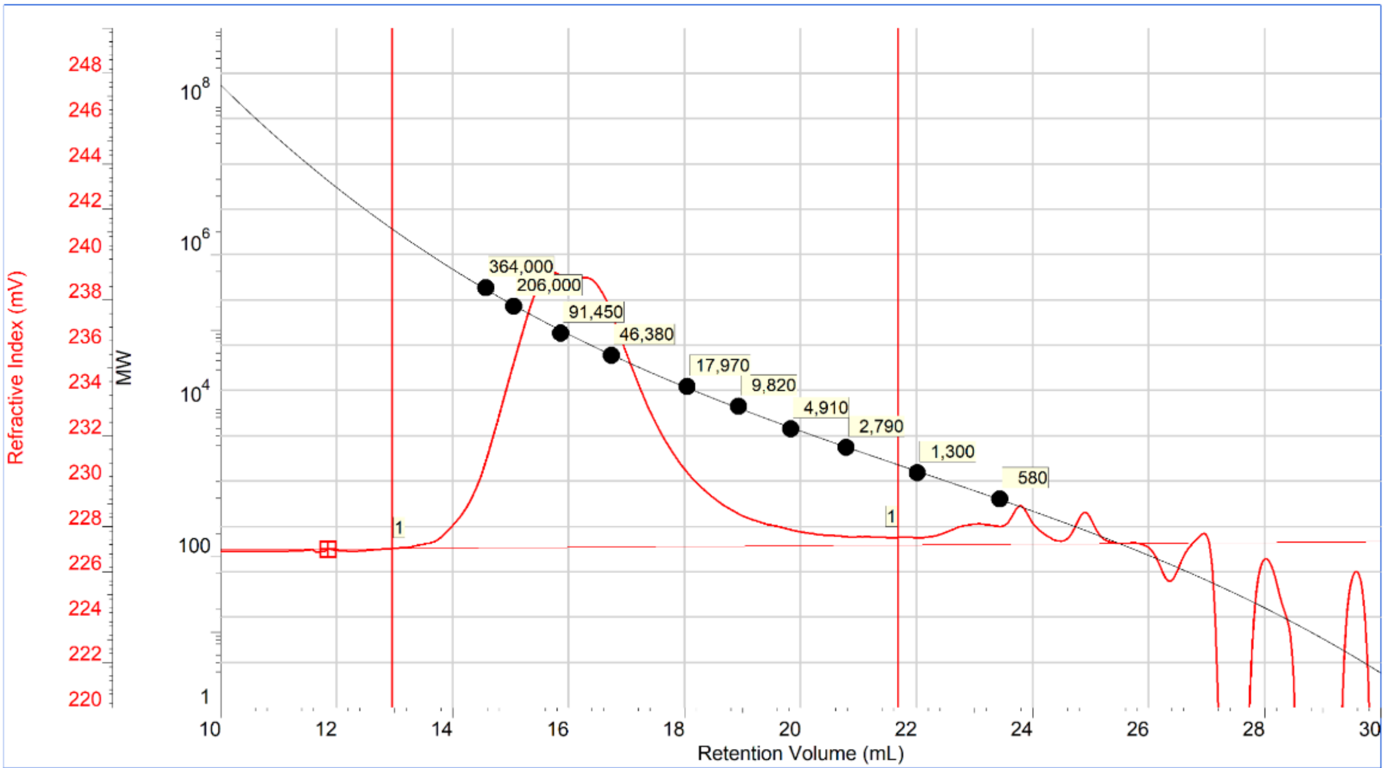

Peak	Ret Time	Mp	Mn	Mw	Mz	Mw/Mn	RI Area
1	15.723	112,534	33,052	108,961	245,638	3.297	35.41

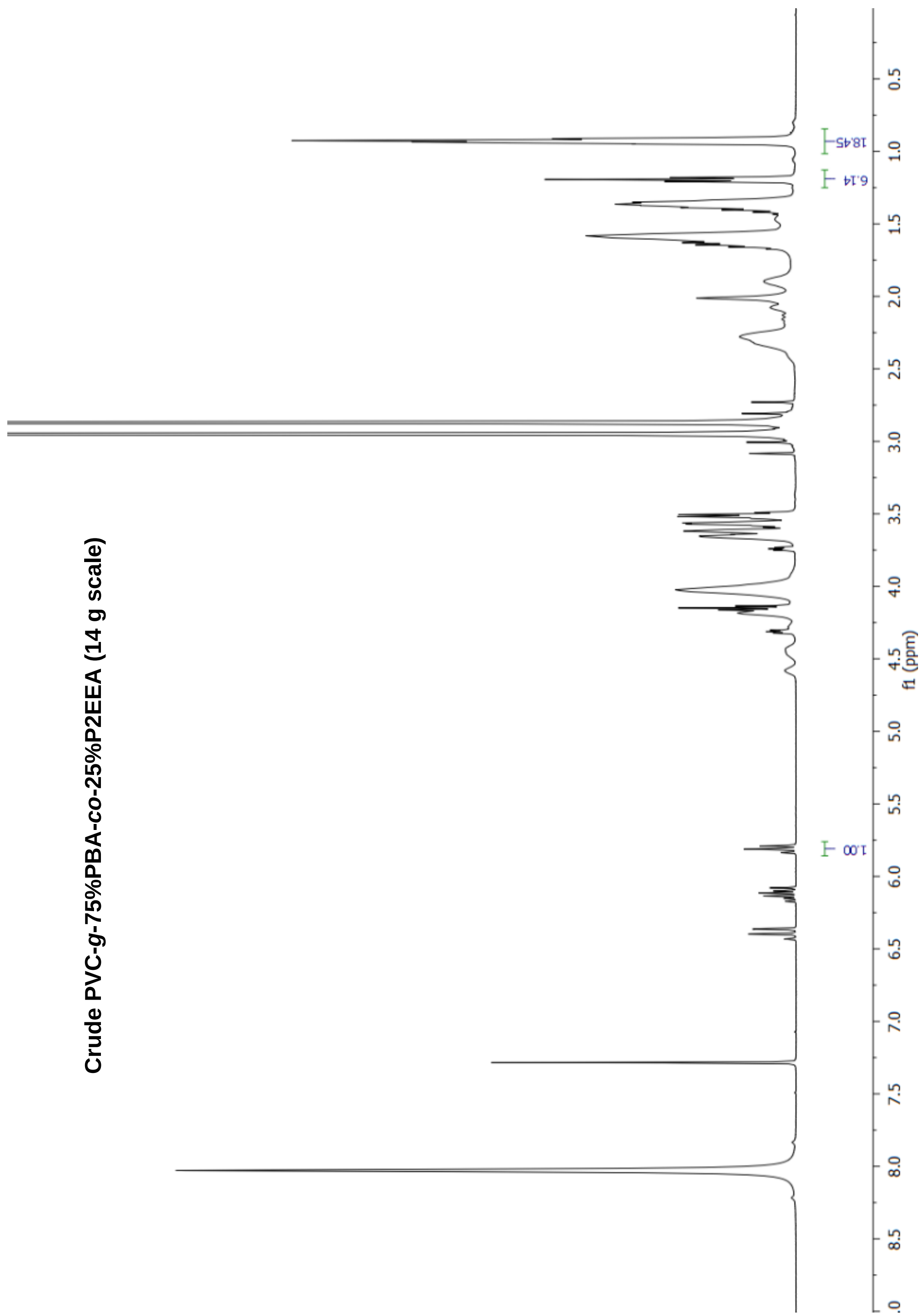
Crude PVC-*g*-75%PBA-*co*-25%P2EEA (14 g scale)
18.45
6.14
1.00
0.5
1.0
1.5
2.0
2.5
3.0
3.5
4.0
4.5
5.0
5.5
6.0
6.5
7.0
7.5
8.0
8.5
f1 (ppm)

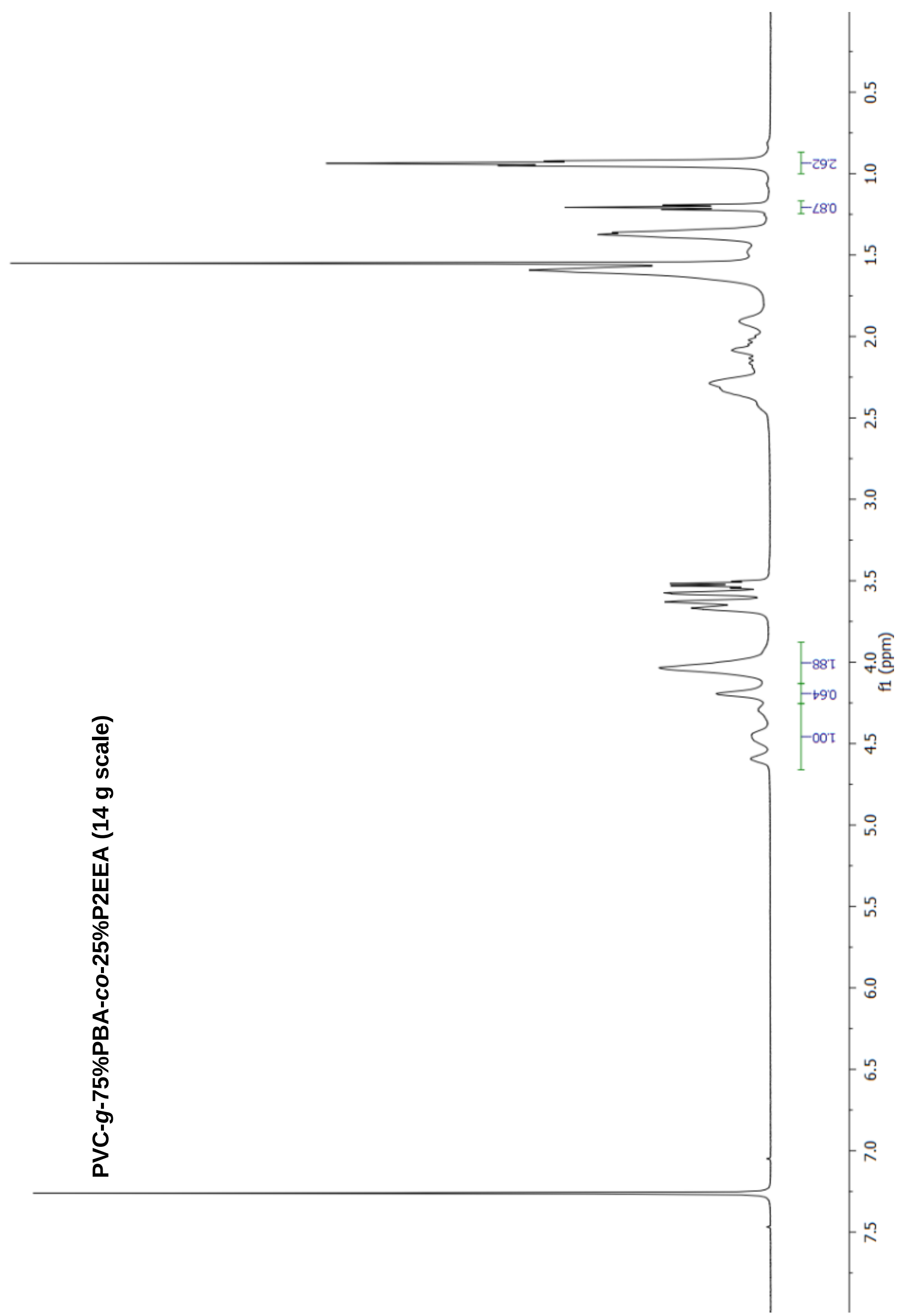
PVC-*g*-75%PBA-*co*-25%P2EEA (14 g scale)
2.62
0.87
1.88
0.64
1.00
0.5
1.0
1.5
2.0
2.5
3.0
3.5
4.0
4.5
5.0
5.5
6.0
6.5
7.0
7.5
f1 (ppm)

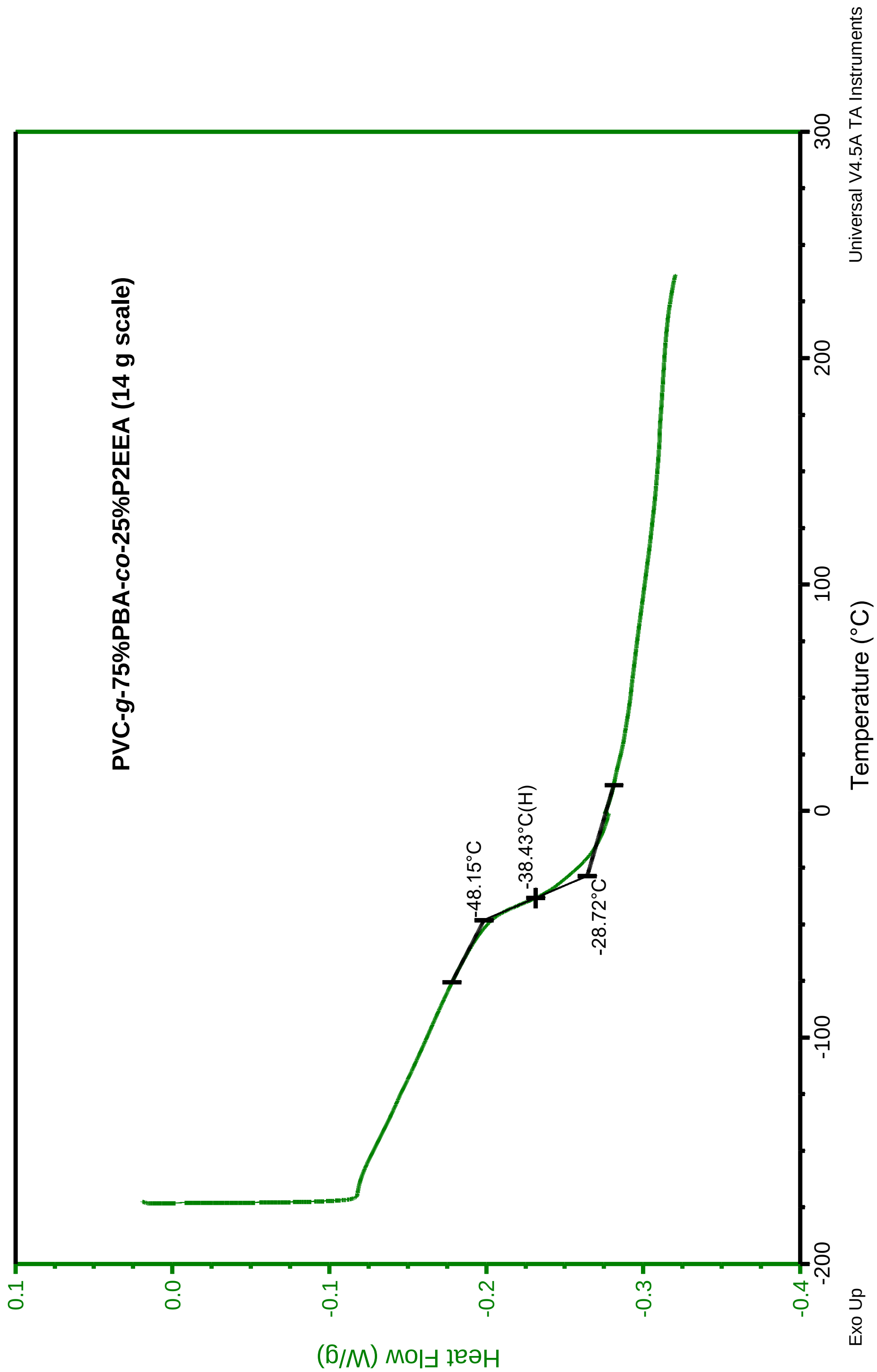
PVC-g-75%PBA-co-25%P2EEA (14 g scale)
-48.15°C
-38.43°C(H)
-28.72°C
Heat Flow (W/g)
Temperature (°C)
Exo Up
Universal V4.5A TA Instruments
0.1
0.0
-0.1
-0.2
-0.3
-0.4
-200
-100
0
100
200
300

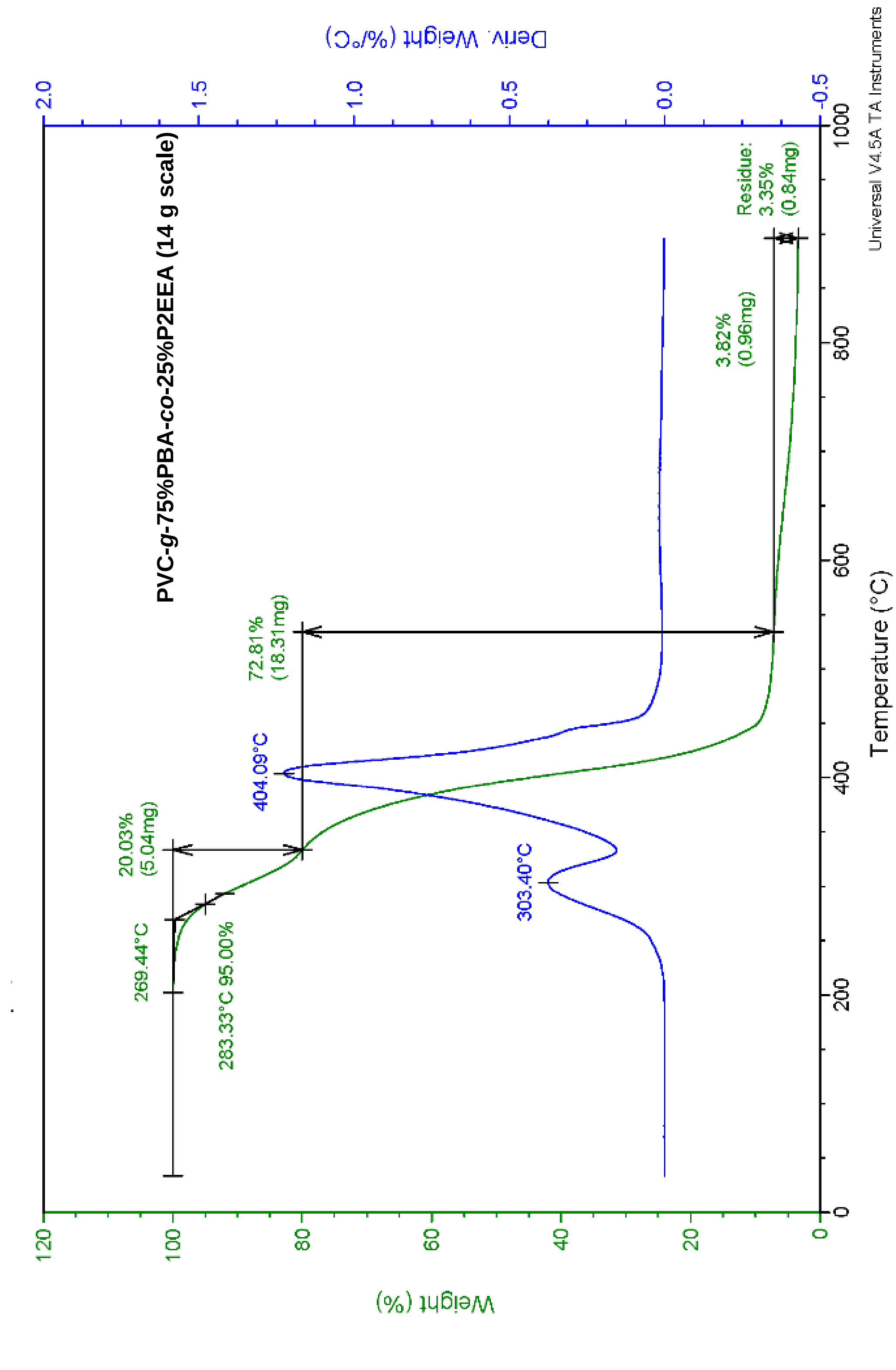
PVC-g-75%PBA-co-25%P2EEA (14 g scale)
Weight (%)
Deriv. Weight (%/°C)
Temperature (°C)
269.44°C
283.33°C 95.00%
20.03%
(5.04mg)
72.81%
(18.31mg)
404.09°C
303.40°C
3.82%
(0.96mg)
Residue:
3.35%
(0.84mg)
Universal V4.5A TA Instruments

PVC-*g*-75%PBA-*co*-25%P2EEA (14 g scale)

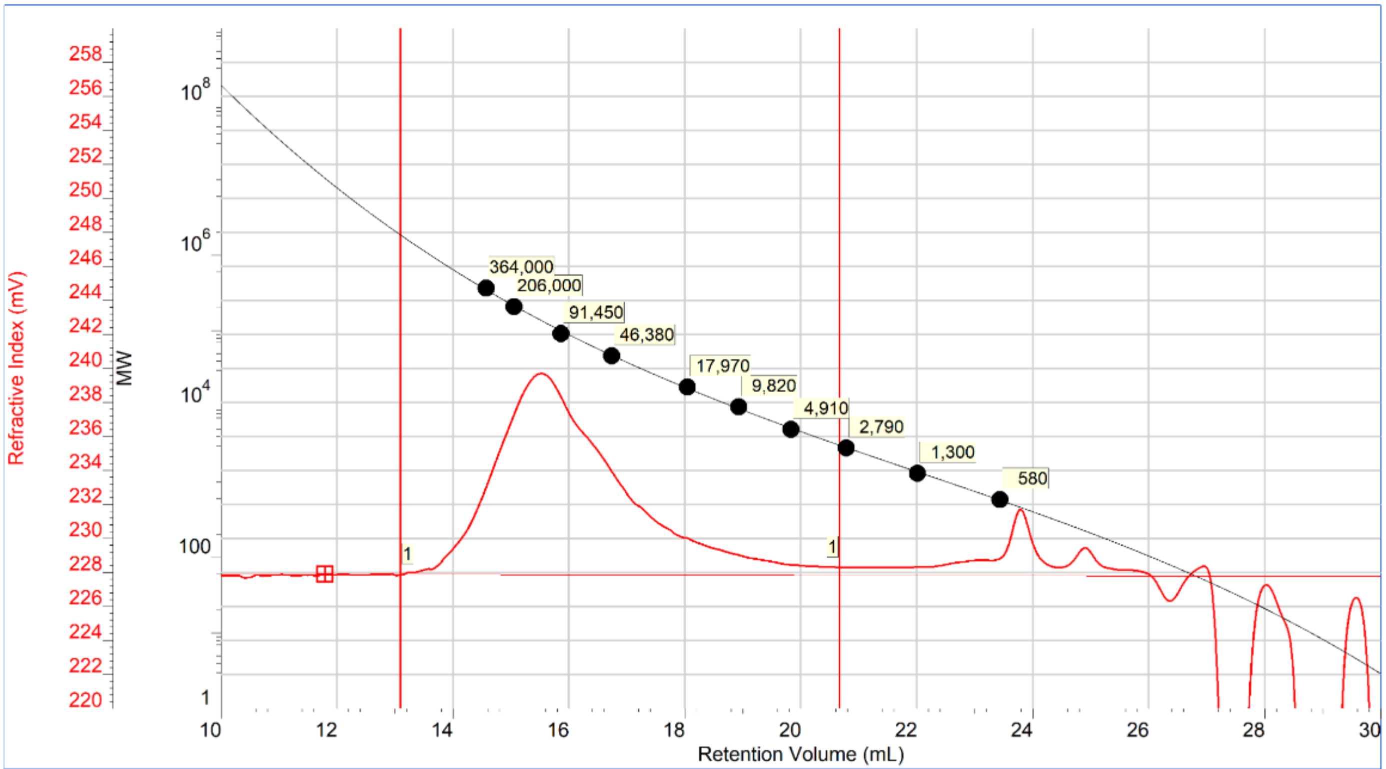

Peak	Ret Time	Mp	Mn	Mw	Mz	Mw/Mn	RI Area
1	15.510	136,923	42,773	140,460	293,907	3.284	29.28

PVC-*g*-75%PBA-*co*-25%P2EEA (14 g scale)

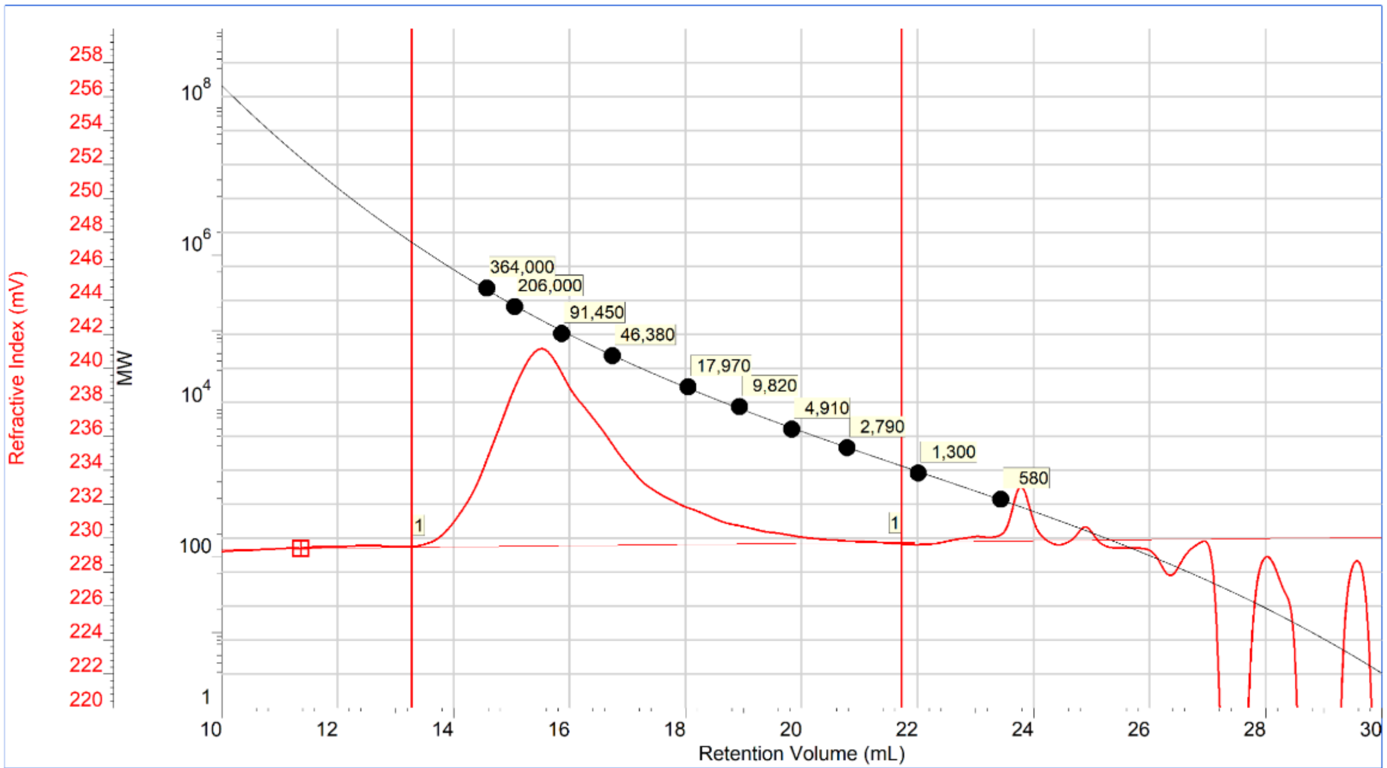

Peak	Ret Time	Mp	Mn	Mw	Mz	Mw/Mn	RI Area
1	15.503	137,756	46,511	140,448	279,156	3.020	28.46

Crude PVC-*g*-50%PBA-*co*-50%P2EEA (14 g scale)

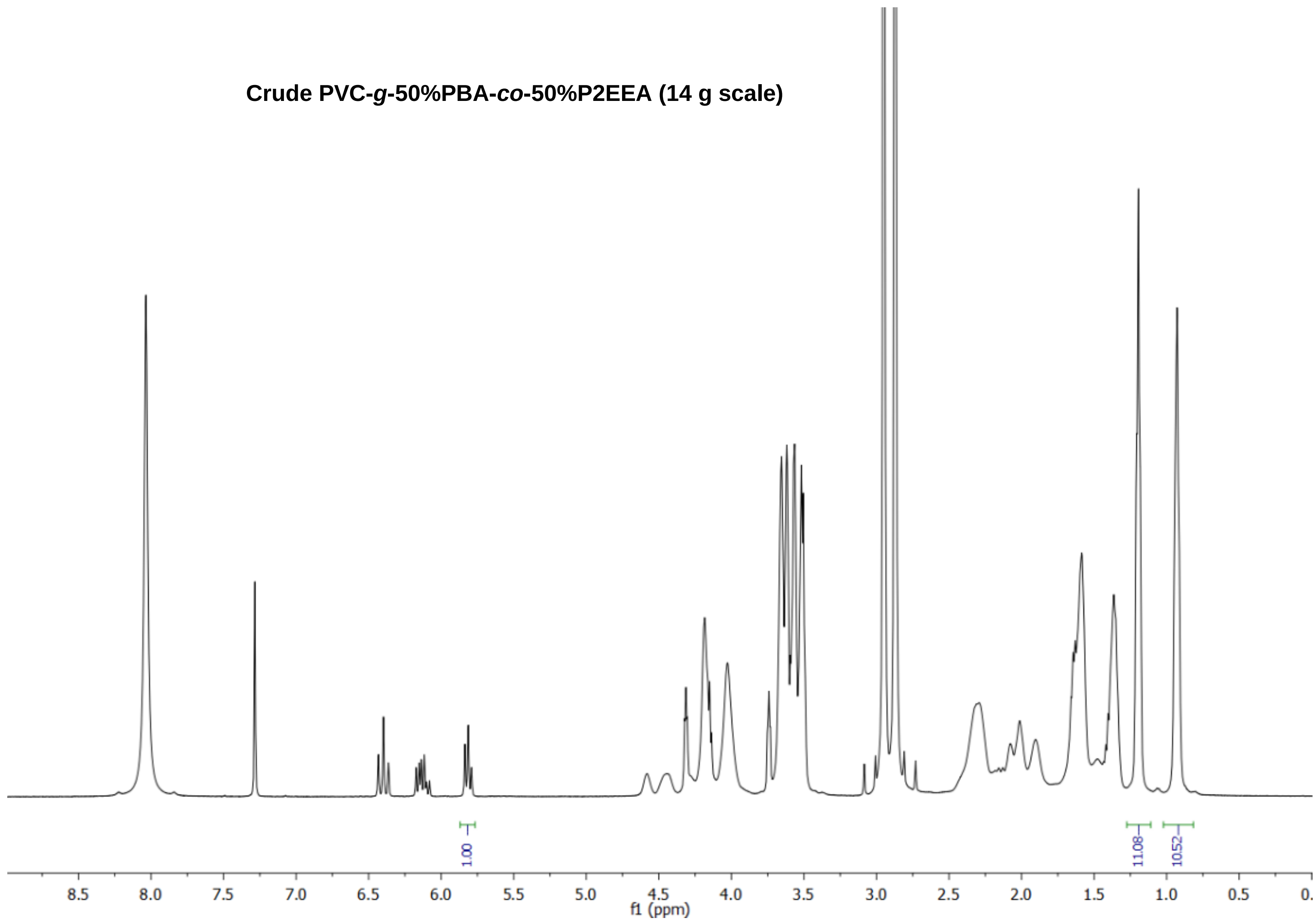

PVC-*g*-50%PBA-*co*-50%P2EEA (14 g scale)

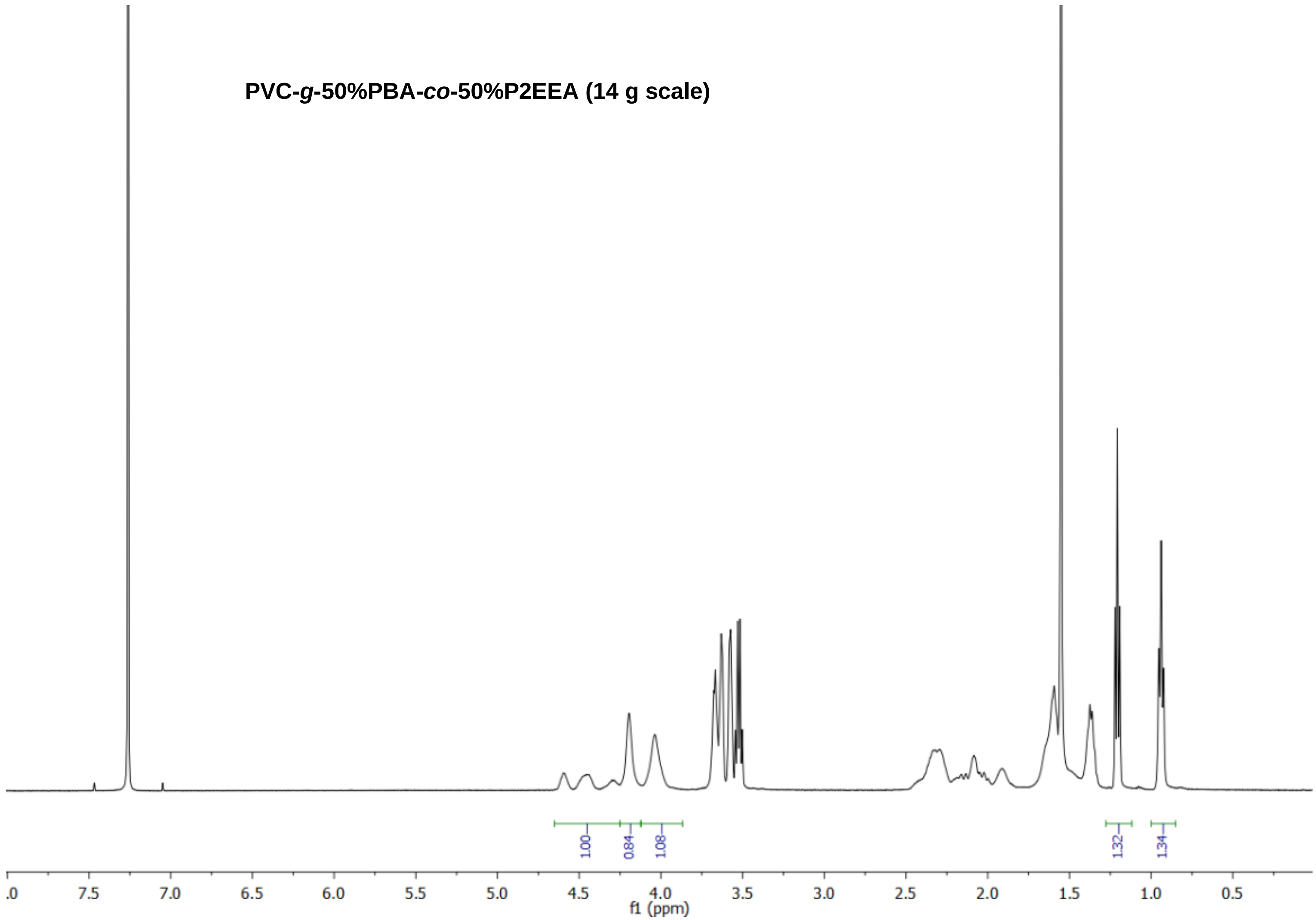

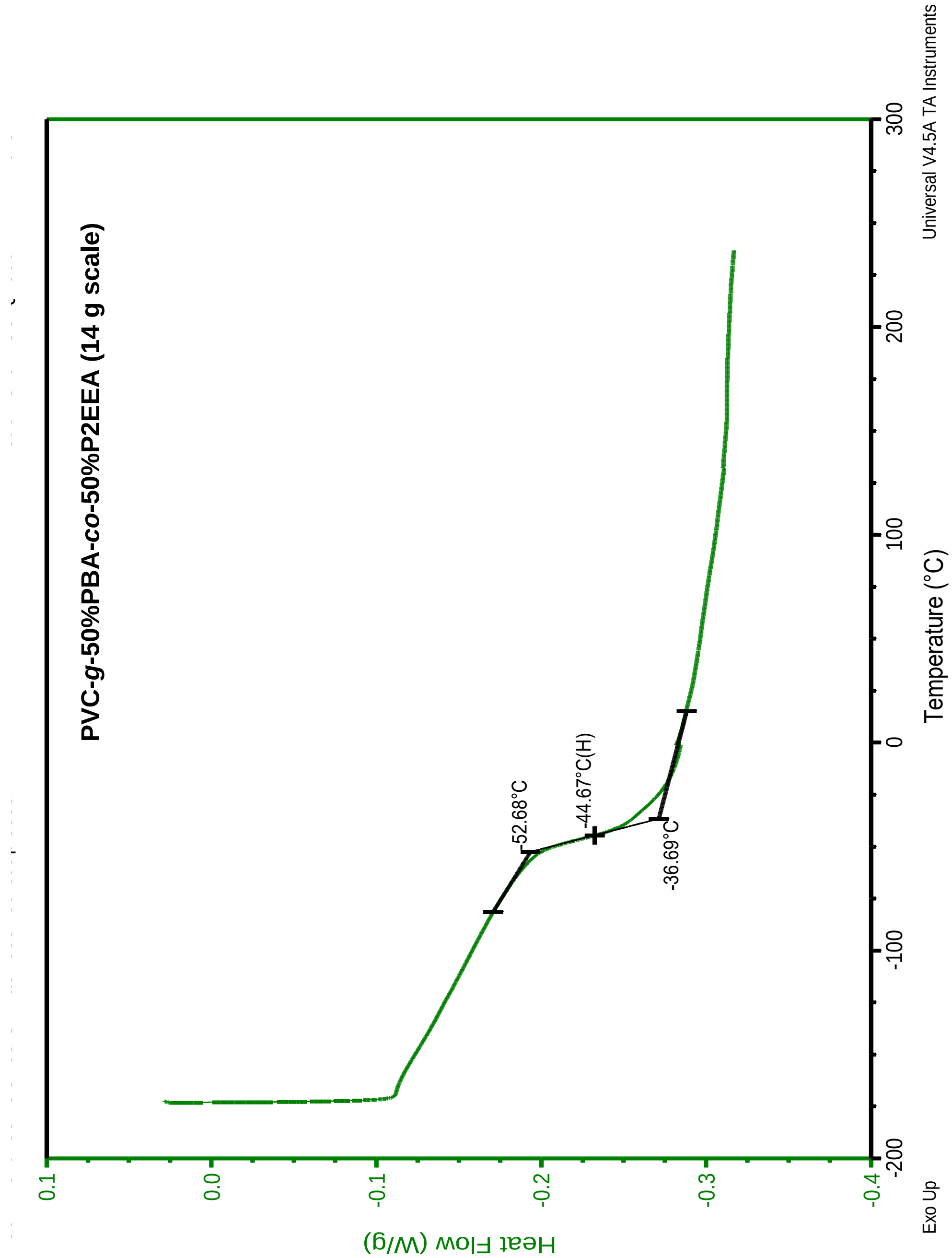

PVC-*g*-50%PBA-*co*-50%P2EEA (14 g scale)
Heat Flow (W/g)
0.1
0.0
-0.1
-0.2
-0.3
-0.4
Exo Up
Temperature (°C)
-200
-100
0
100
200
300
52.68°C
-44.67°C(H)
-36.69°C
Universal V4.5A TA Instruments

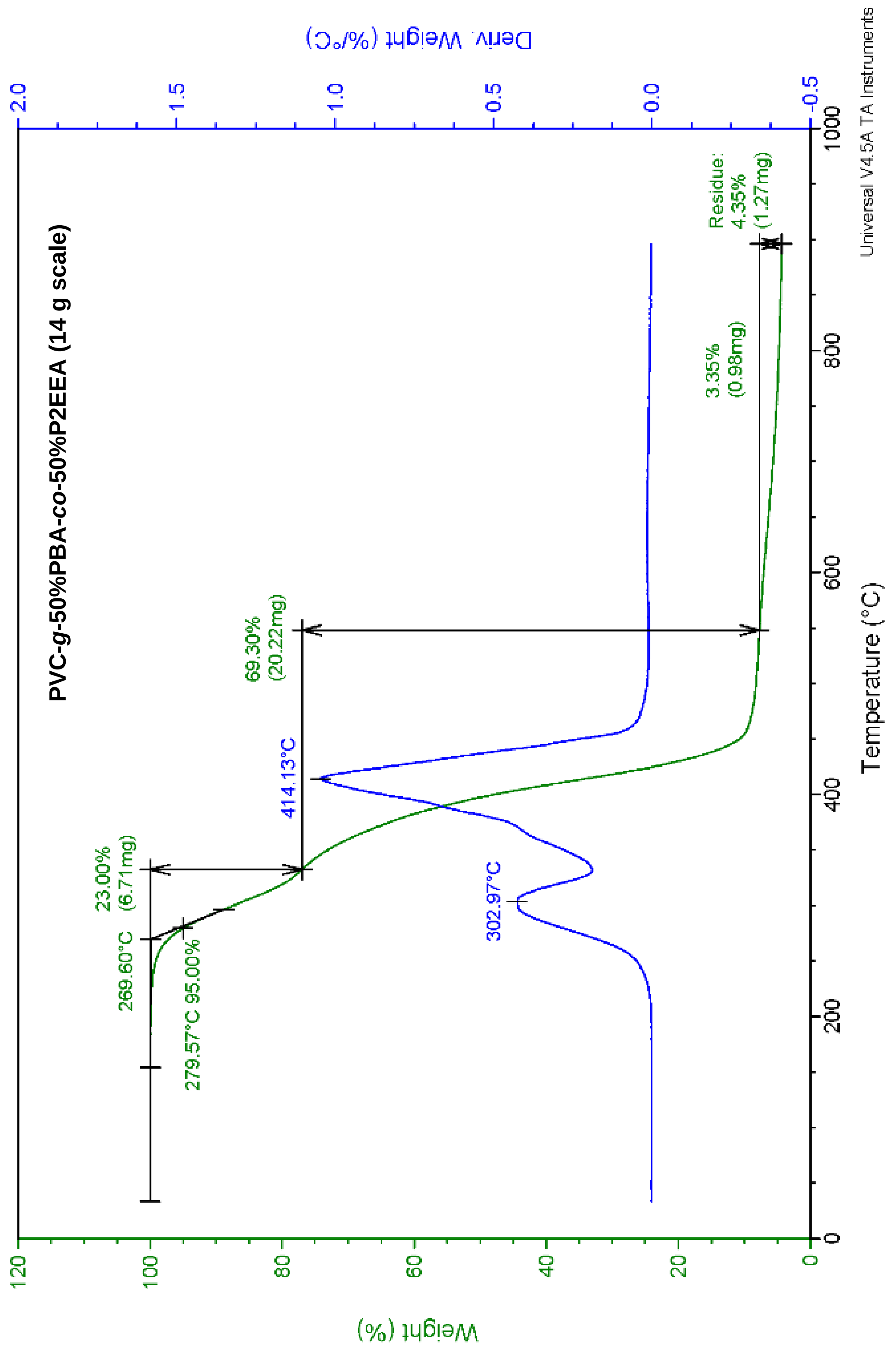
PVC-g-50%PBA-co-50%P2EEA (14 g scale)
Weight (%)
Deriv. Weight (%/°C)
Temperature (°C)
269.60°C
279.57°C 95.00%
23.00%
(6.71mg)
302.97°C
414.13°C
69.30%
(20.22mg)
3.35%
(0.98mg)
Residue:
4.35%
(1.27mg)
Universal V4.5A TA Instruments

PVC-*g*-50%PBA-*co*-50%P2EEA (14 g scale)

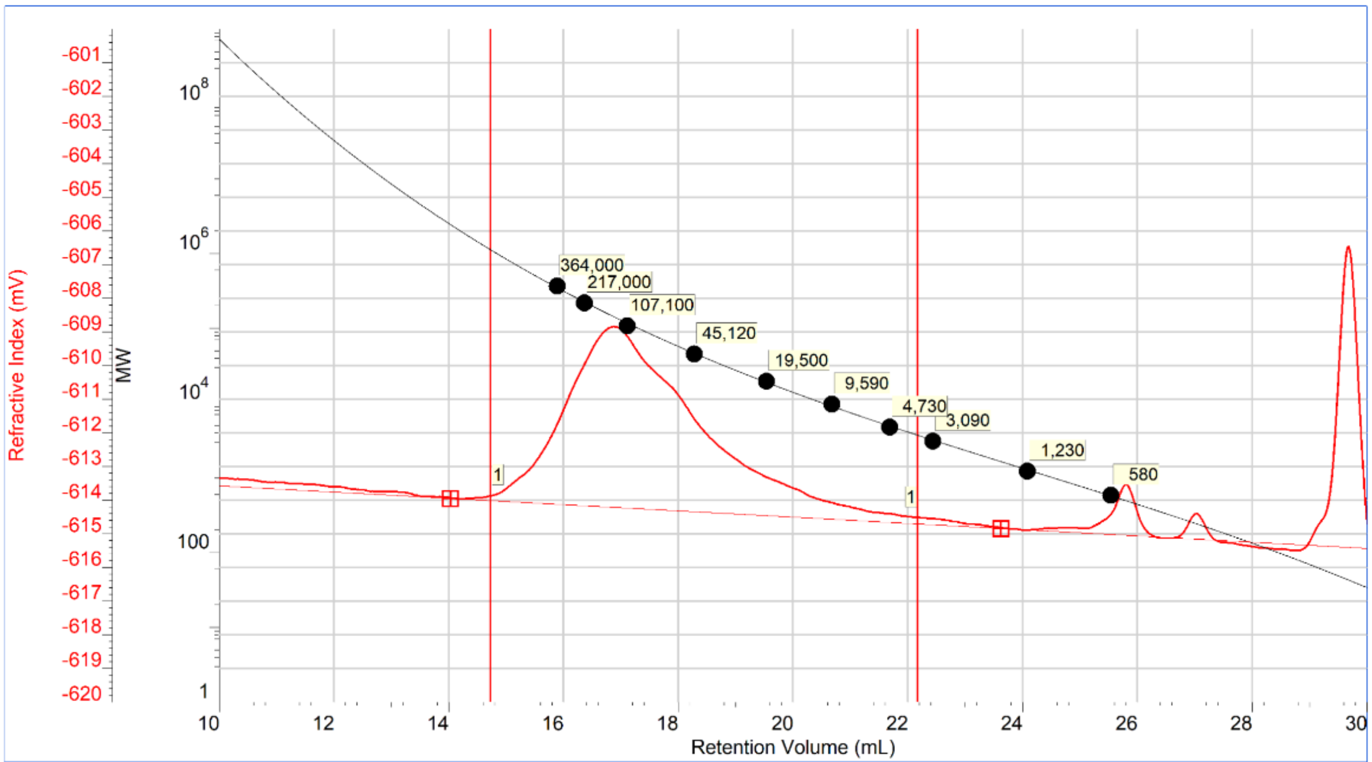

Peak	Ret Time	Mp	Mn	Mw	Mz	Mw/Mn	RI Area
1	16.880	140,864	46,537	141,136	283,867	3.033	14.73

PVC-*g*-50%PBA-*co*-50%P2EEA (14 g scale)

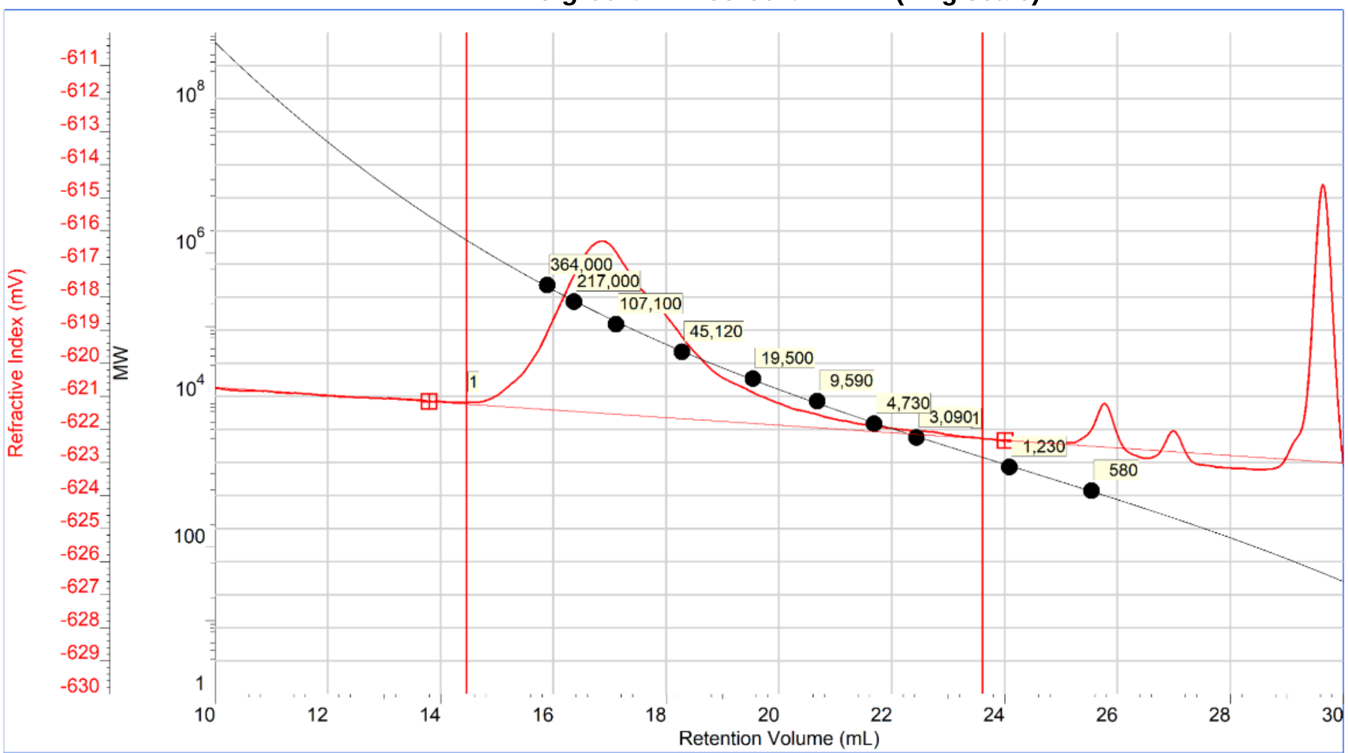

Peak	Ret Time	Mp	Mn	Mw	Mz	Mw/Mn	RI Area
1	16.857	143,711	45,482	149,291	309,480	3.282	13.65

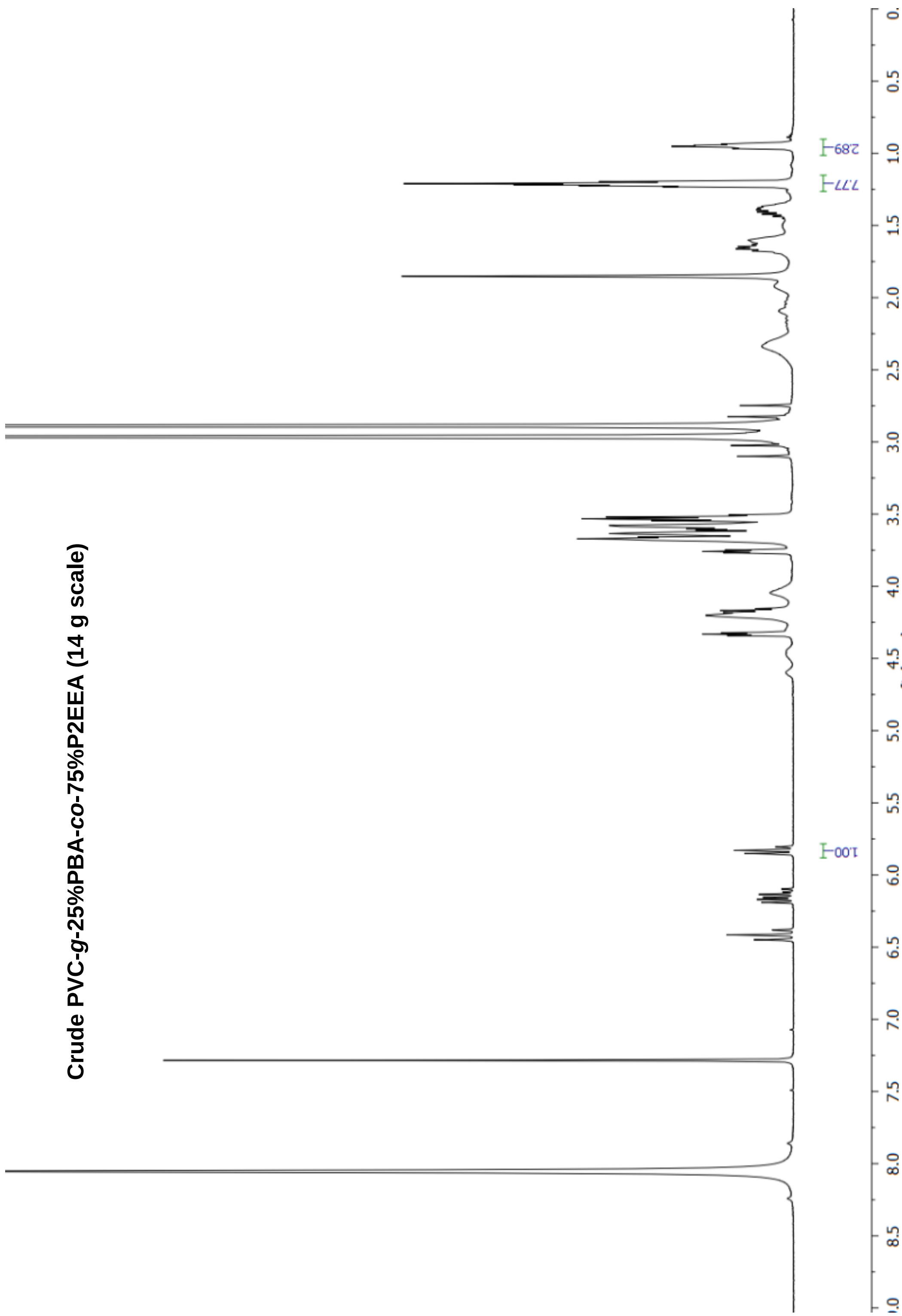
Crude PVC-*g*-25%PBA-*co*-75%P2EEA (14 g scale)
f1 (ppm)
2.89
7.77
1.00

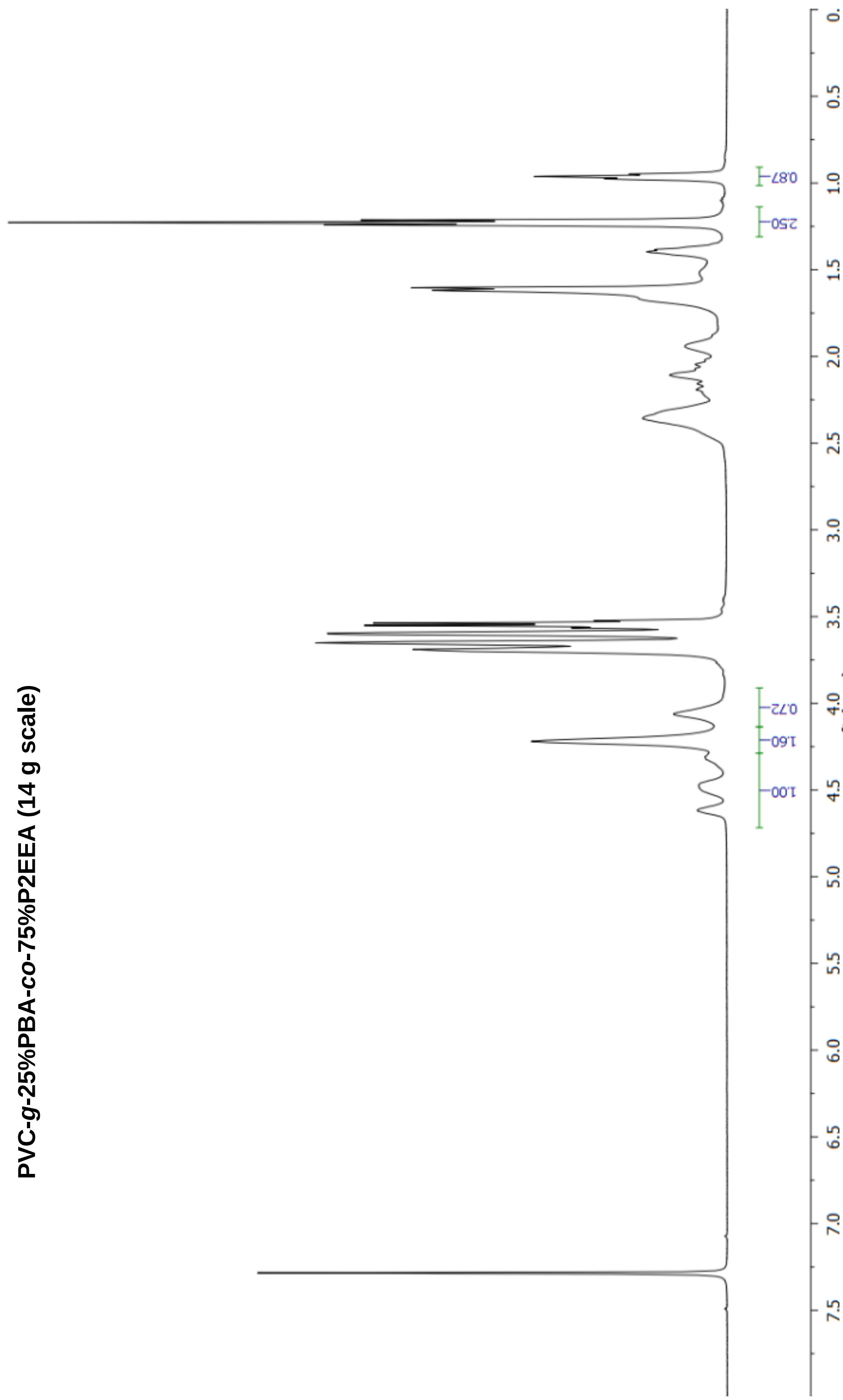

PVC-*g*-25%PBA-*co*-75%P2EEA (14 g scale)

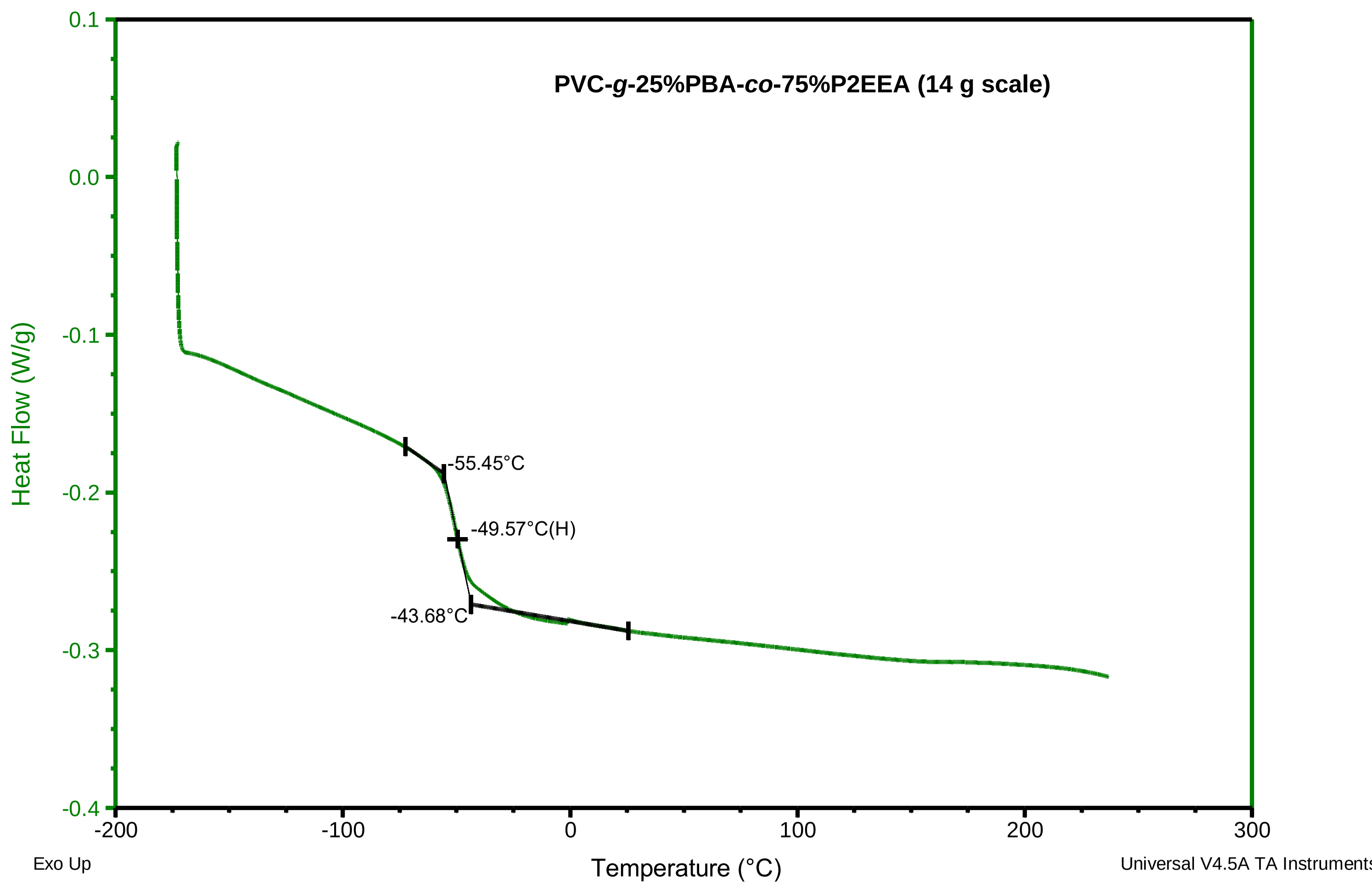
PVC-*g*-25%PBA-*co*-75%P2EEA (14 g scale)
-55.45°C
-49.57°C(H)
-43.68°C
Heat Flow (W/g)
0.1
0.0
-0.1
-0.2
-0.3
-0.4
-200
-100
0
100
200
300
Temperature (°C)
Exo Up
Universal V4.5A TA Instruments

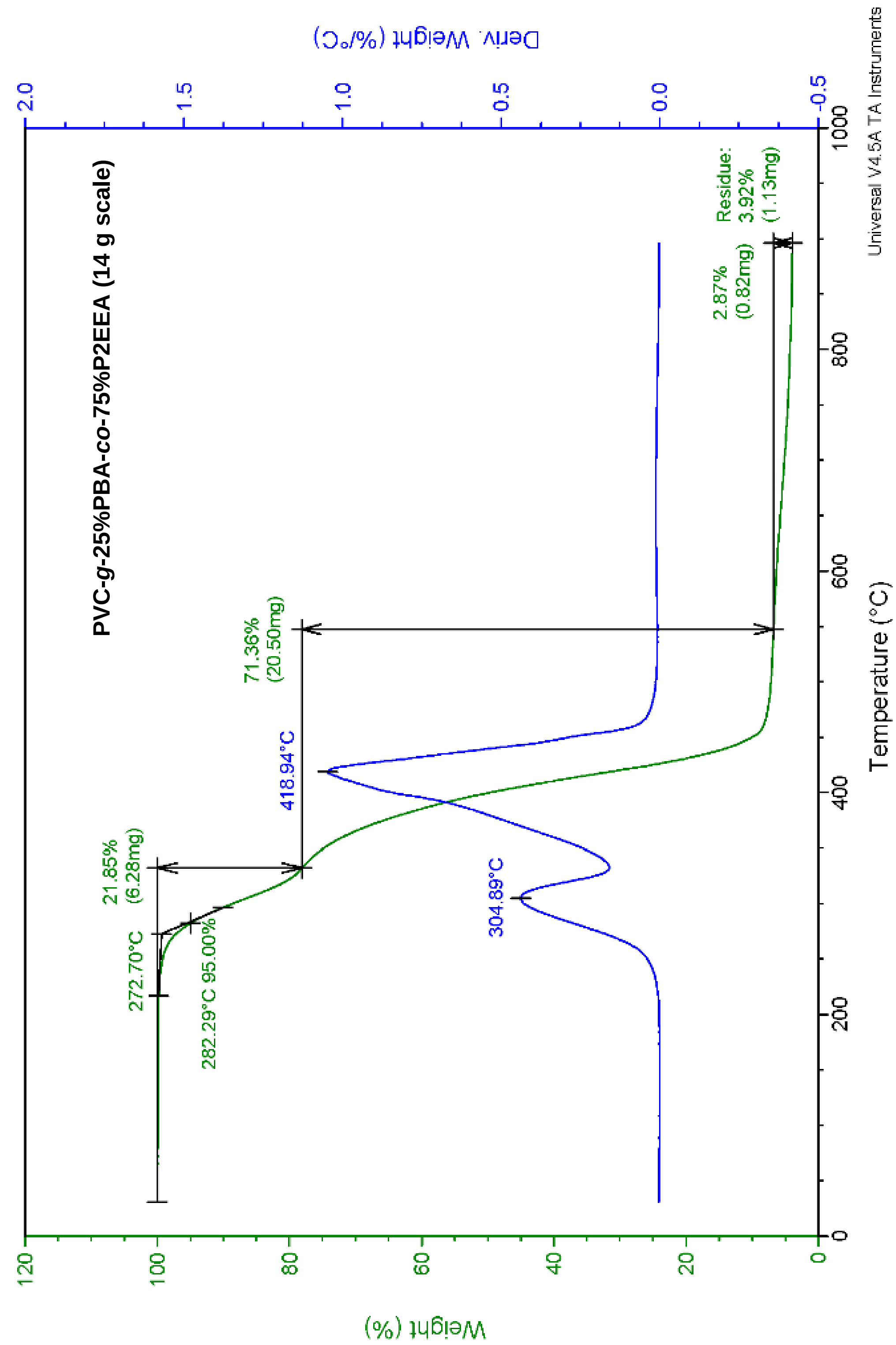
PVC-g-25%PBA-co-75%P2EEA (14 g scale)
Weight (%)
Deriv. Weight (%/°C)
Temperature (°C)
272.70°C
282.29°C 95.00%
21.85%
(6.28mg)
304.89°C
418.94°C
71.36%
(20.50mg)
2.87%
(0.82mg)
Residue:
3.92%
(1.13mg)
Universal V4.5A TA Instruments

PVC-*g*-25%PBA-*co*-75%P2EEA (14 g scale)

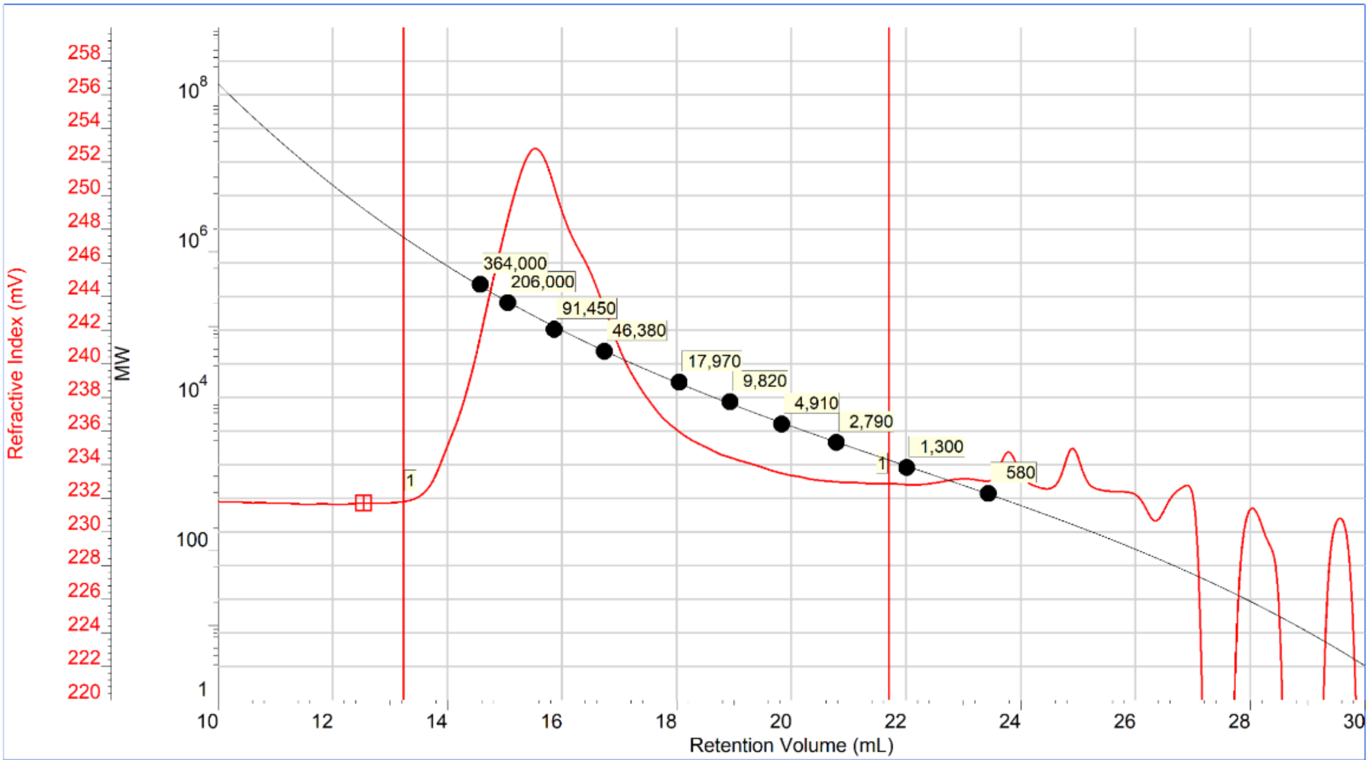

Peak	Ret Time	Mp	Mn	Mw	Mz	Mw/Mn	RI Area
1	15.523	135,516	29,149	137,002	292,854	4.700	56.13

PVC-*g*-25%PBA-*co*-75%P2EEA (14 g scale)

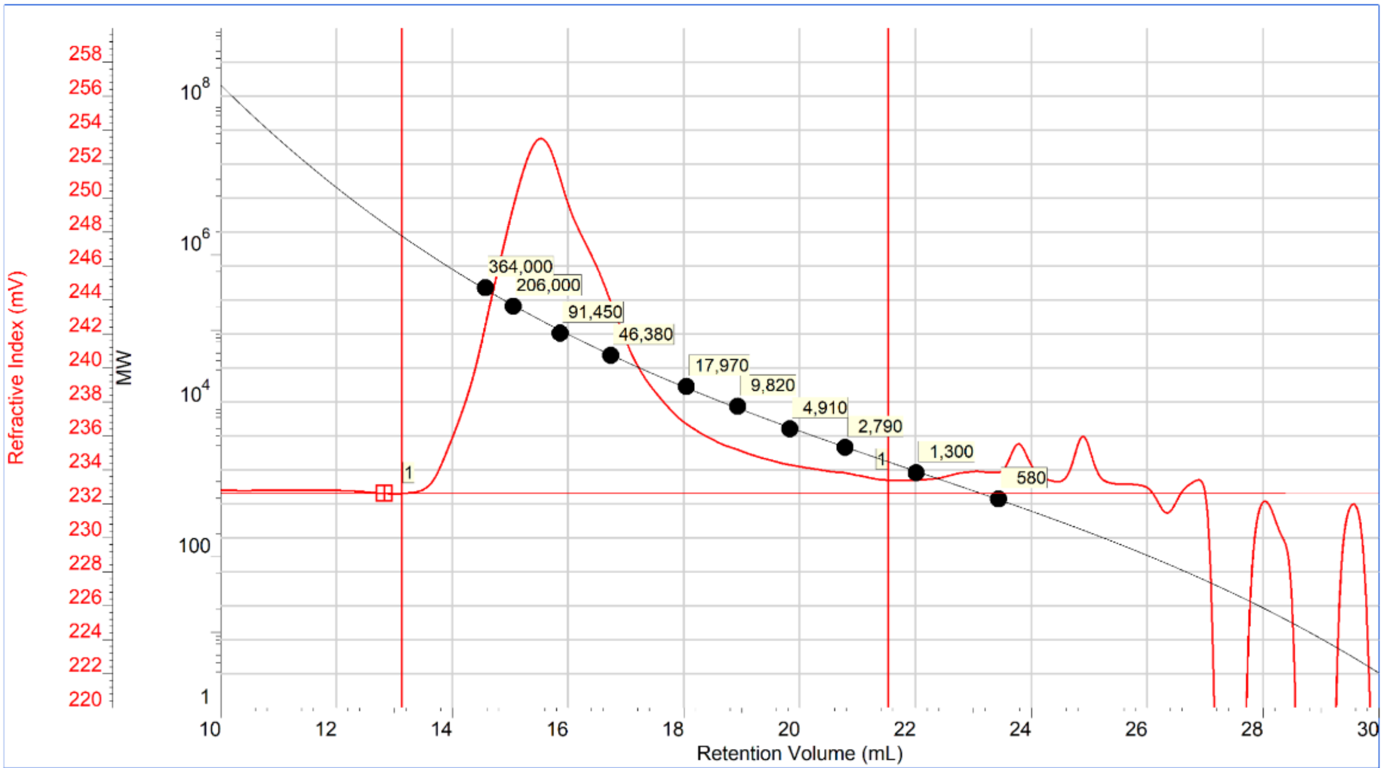

Peak	Ret Time	Mp	Mn	Mw	Mz	Mw/Mn	RI Area
1	15.520	135,756	30,766	136,801	286,717	4.446	55.36

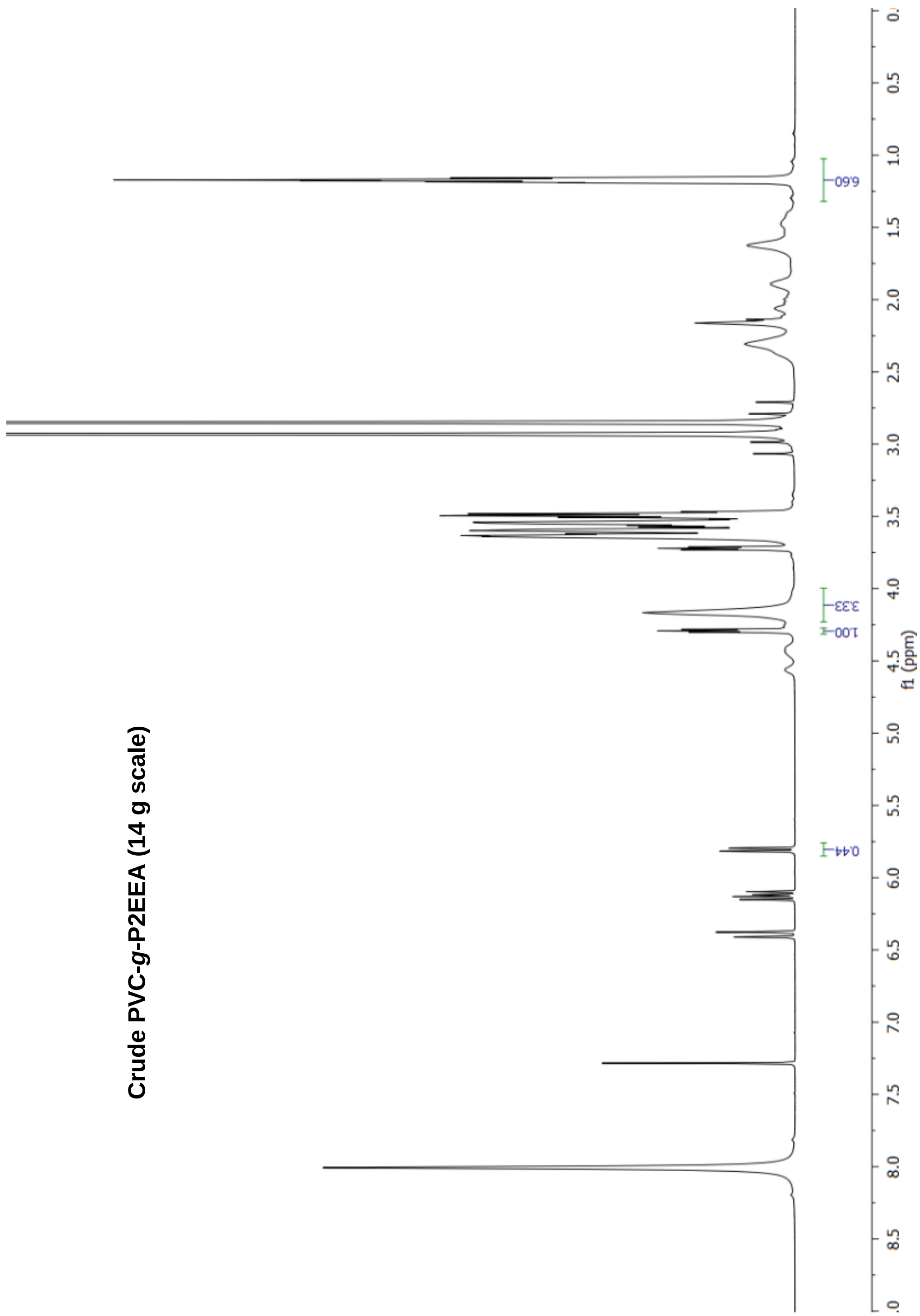

Crude PVC-g-P2EEA (14 g scale)
6.60
3.33
1.00
0.44
f1 (ppm)

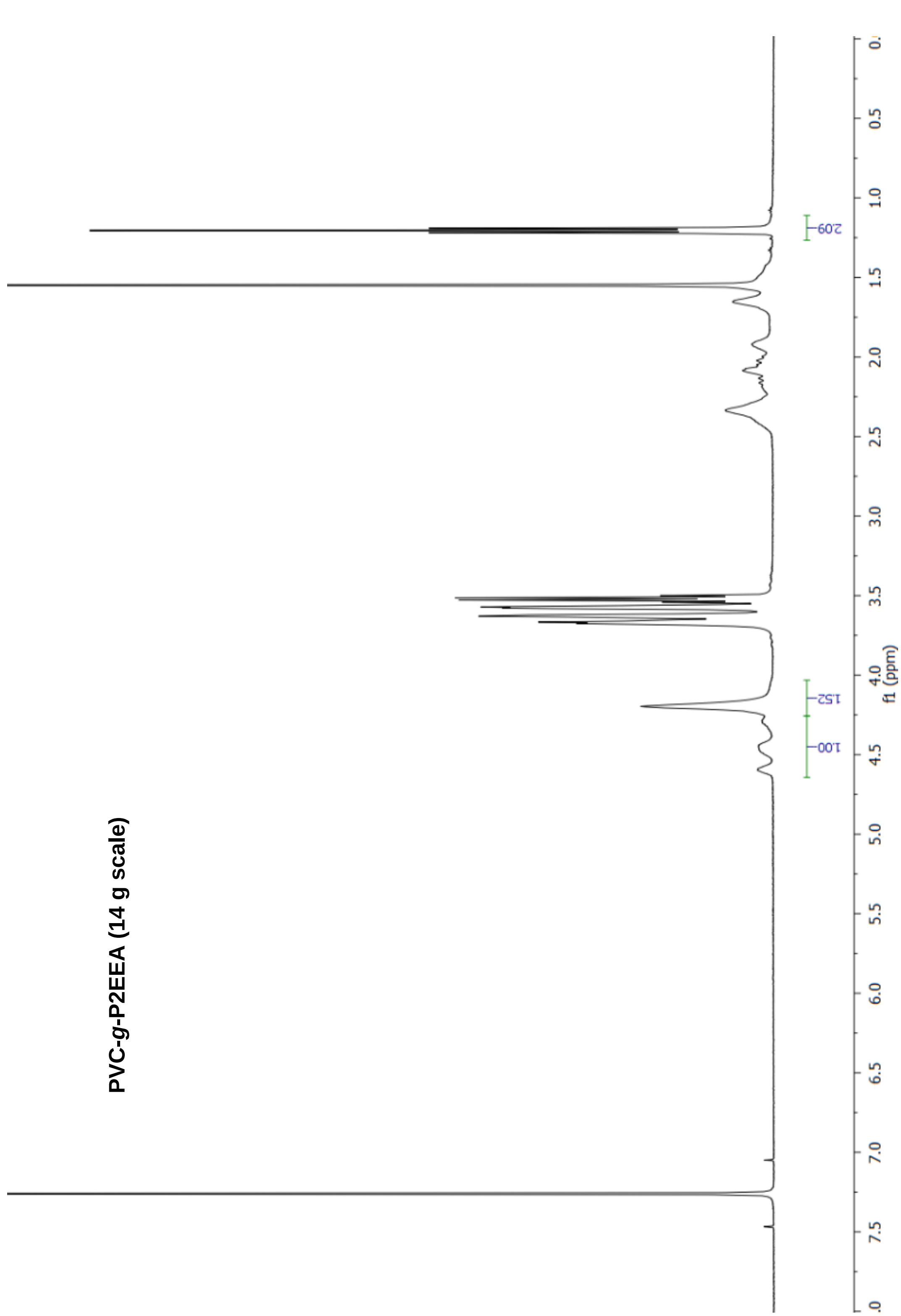
PVC-g-P2EEA (14 g scale)
2.09
1.52
1.00
f1 (ppm)
0.5
1.0
1.5
2.0
2.5
3.0
3.5
4.0
4.5
5.0
5.5
6.0
6.5
7.0
7.5

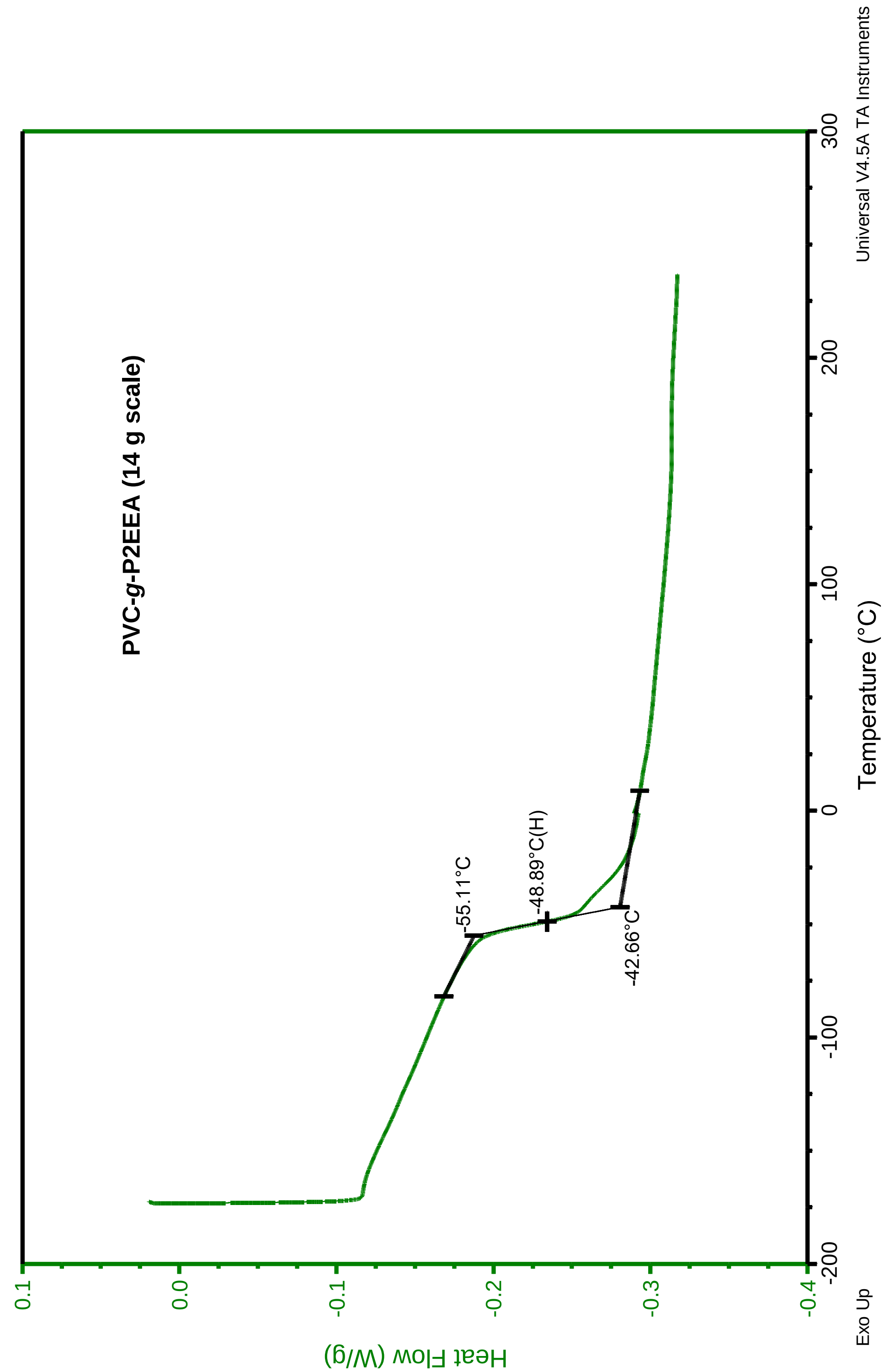
PVC-g-P2EEA (14 g scale)
-55.11°C
-48.89°C(H)
-42.66°C
Heat Flow (W/g)
Temperature (°C)
Exo Up
Universal V4.5A TA Instruments
0.1
0.0
-0.1
-0.2
-0.3
-0.4
-200
-100
0
100
200
300

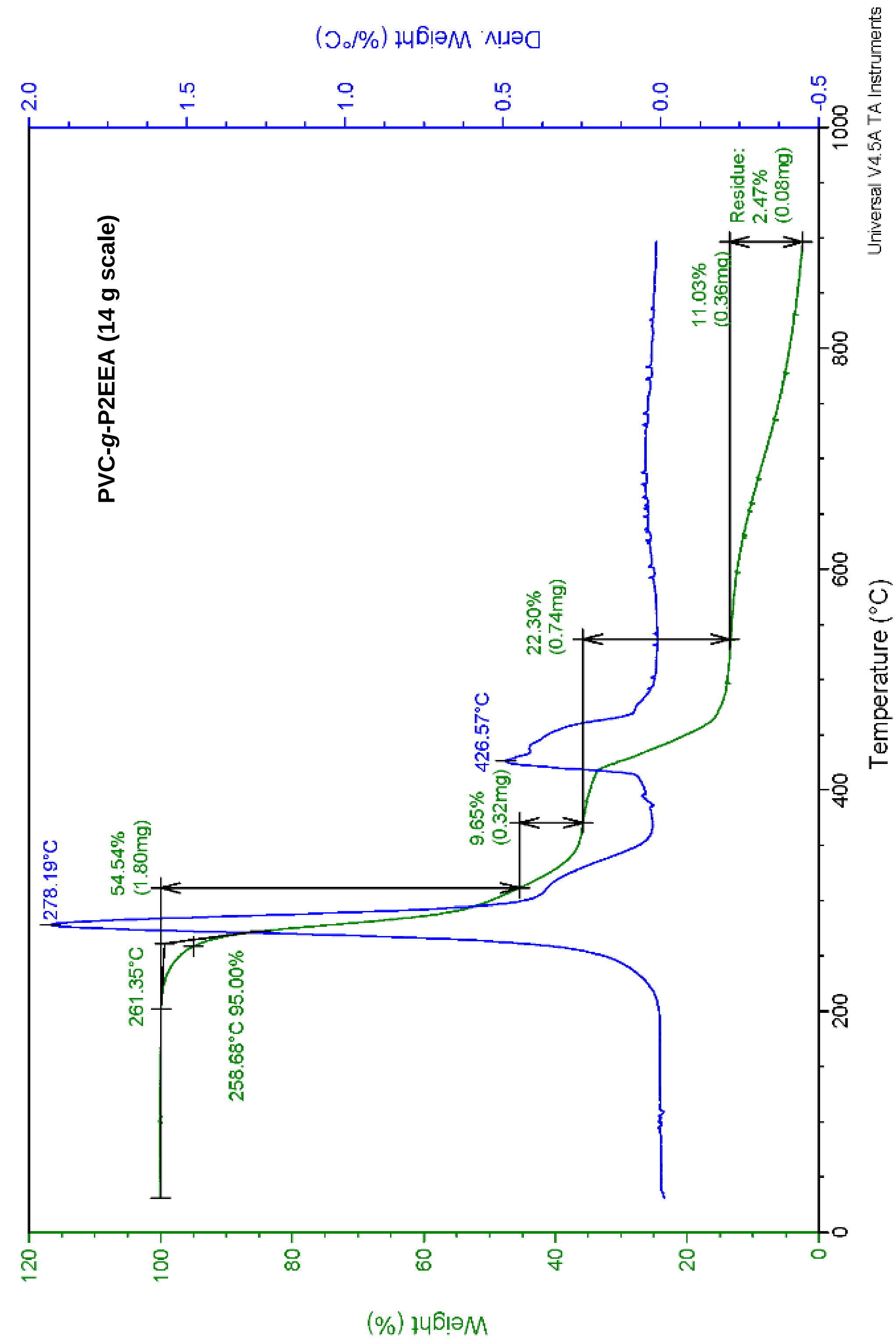
PVC-*g*-P2EEA (14 g scale)
278.19°C
426.57°C
261.35°C
258.68°C 95.00%
54.54%
(1.80mg)
9.65%
(0.32mg)
22.30%
(0.74mg)
11.03%
(0.36mg)
Residue:
2.47%
(0.08mg)
Weight (%)
Deriv. Weight (%/°C)
Temperature (°C)
Universal V4.5A TA Instruments

PVC-*g*-P2EEA (14 g scale)

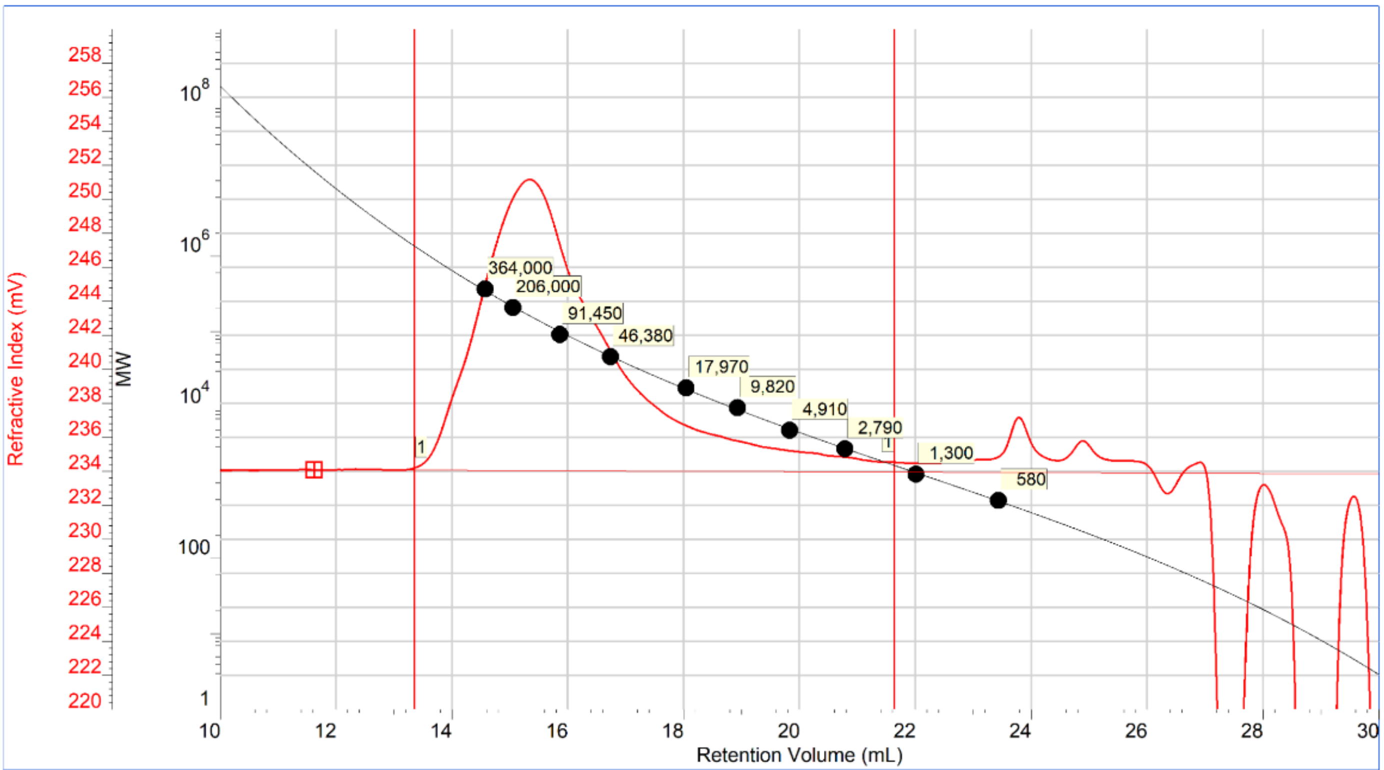

Peak	Ret Time	Mp	Mn	Mw	Mz	Mw/Mn	RI Area
1	15.333	161,735	33,257	165,677	329,111	4.982	44.00

PVC-*g*-P2EEA (14 g scale)

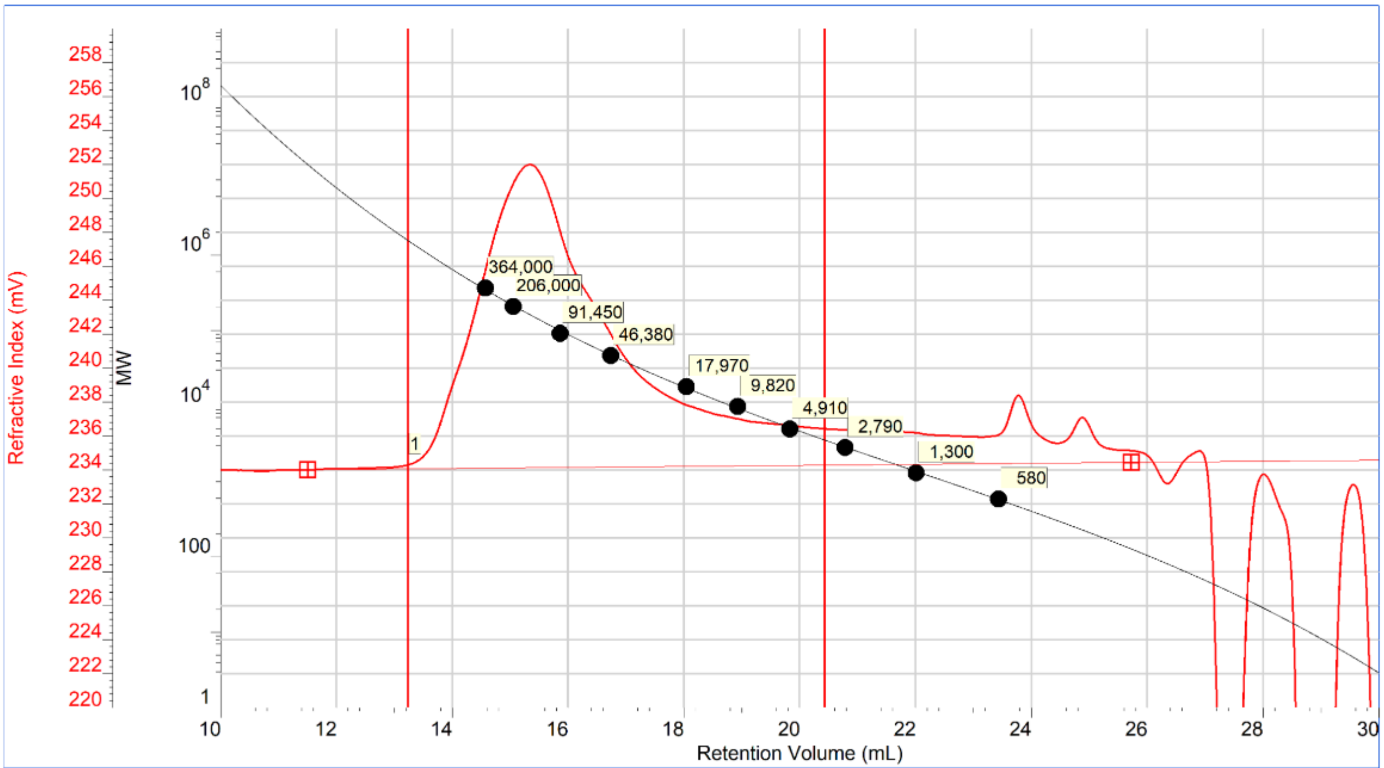

Peak	Ret Time	Mp	Mn	Mw	Mz	Mw/Mn	RI Area
1	15.327	163,161	35,416	165,548	355,290	4.674	48.96

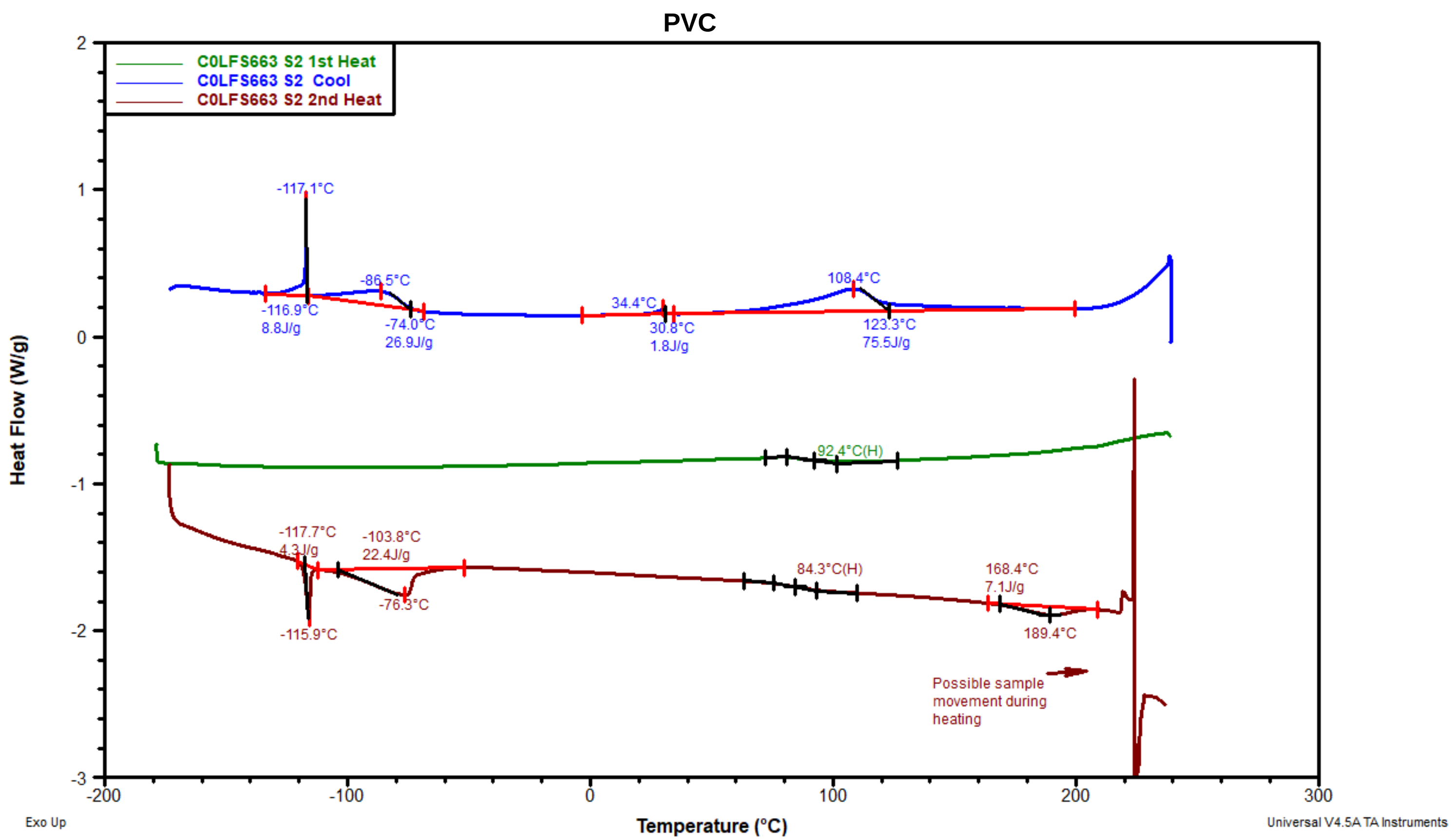
PVC
C0LFS663 S2 1st Heat
C0LFS663 S2 Cool
C0LFS663 S2 2nd Heat
-117.1°C
-86.5°C
-116.9°C
8.8J/g
-74.0°C
26.9J/g
34.4°C
30.8°C
1.8J/g
108.4°C
123.3°C
75.5J/g
92.4°C(H)
-117.7°C
4.3J/g
-103.8°C
22.4J/g
-76.3°C
-115.9°C
84.3°C(H)
168.4°C
7.1J/g
189.4°C
Possible sample movement during heating
Heat Flow (W/g)
Temperature (°C)
Exo Up
Universal V4.5A TA Instruments

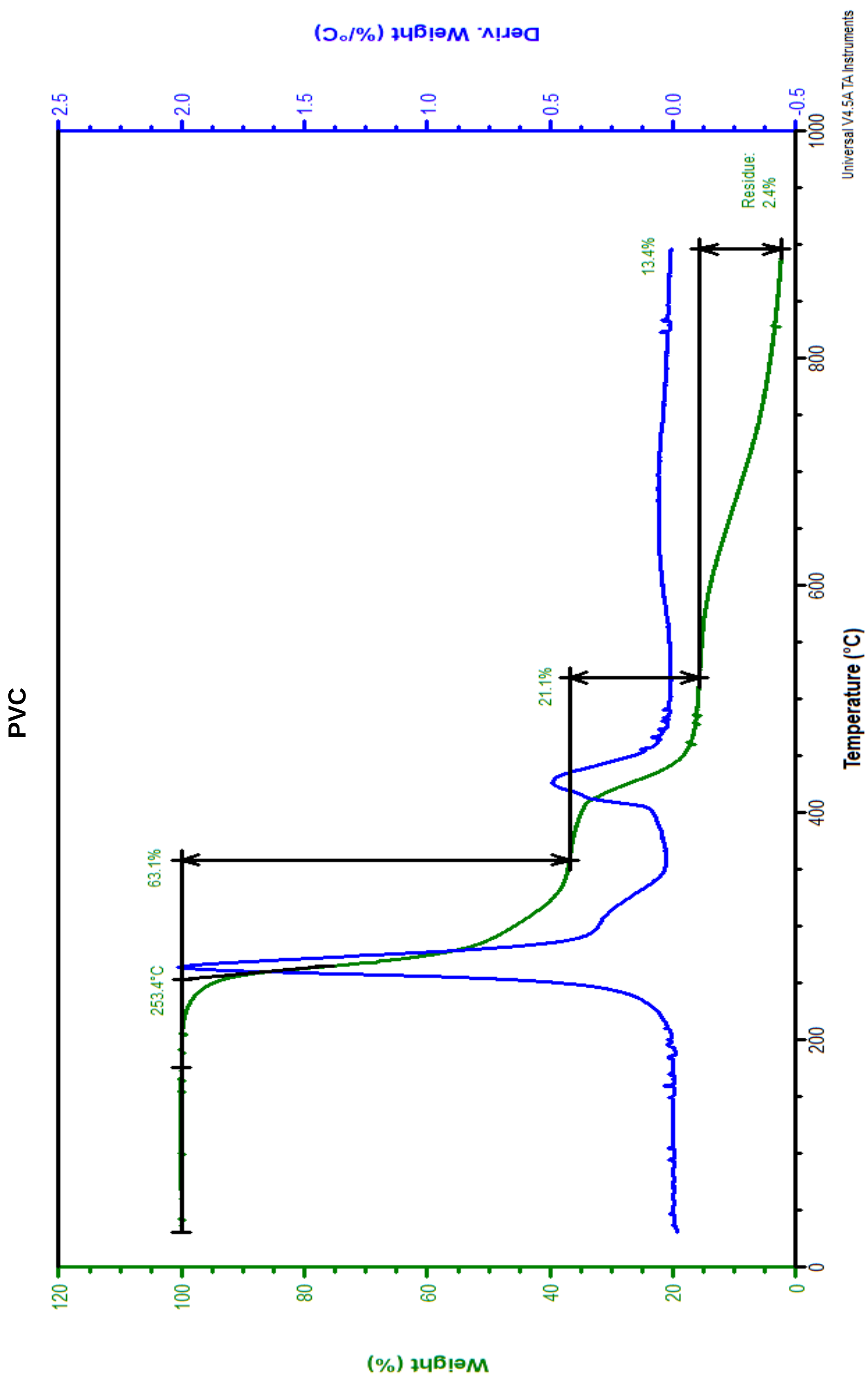

PVC
Deriv. Weight (%/°C)
Weight (%)
Temperature (°C)
253.4°C
63.1%
21.1%
13.4%
Residue:
2.4%
Universal V4.5A TA Instruments

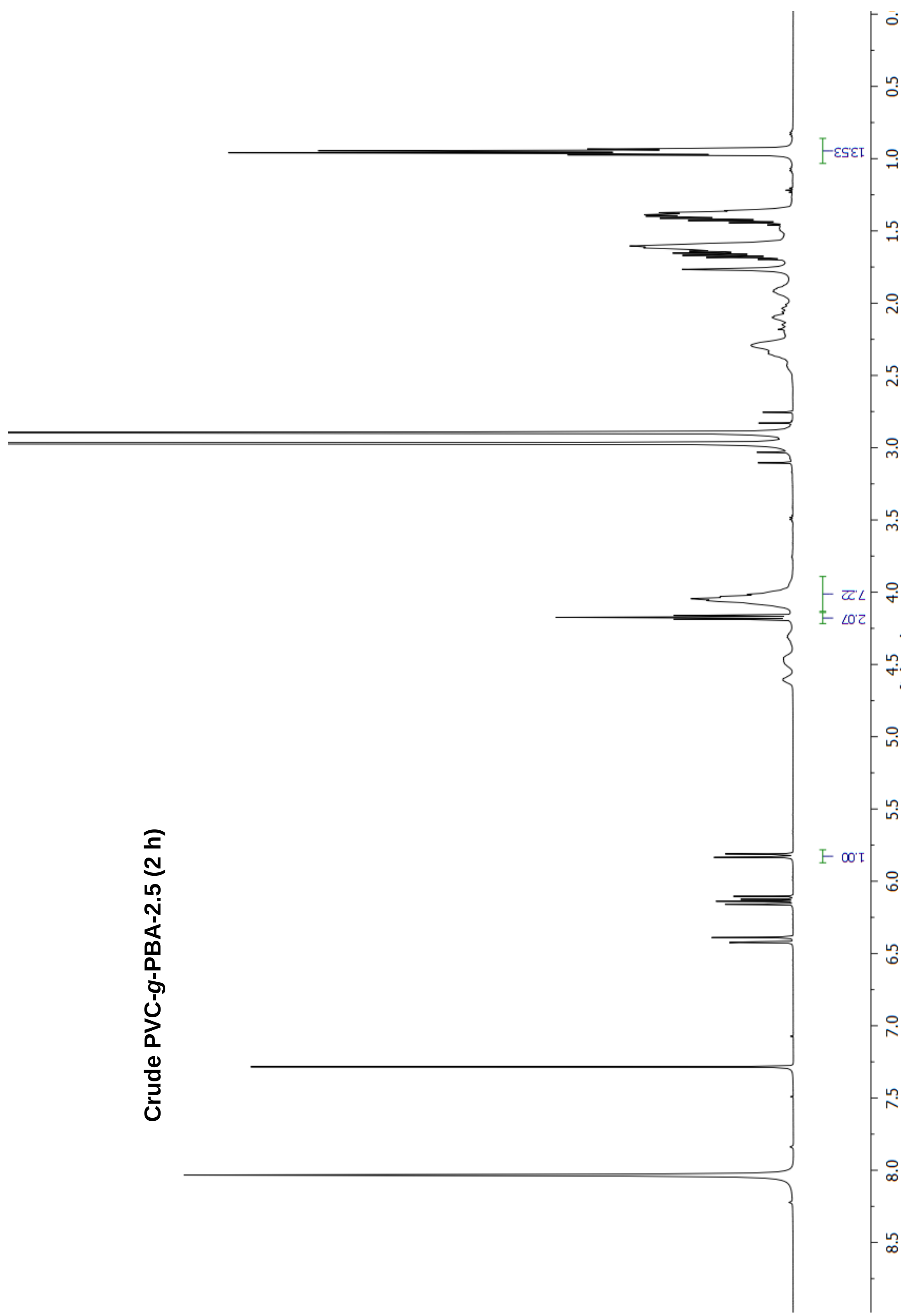
Crude PVC-*g*-PBA-2.5 (2 h)
13.53
7.22
2.07
1.00
f1 (ppm)
0.0
0.5
1.0
1.5
2.0
2.5
3.0
3.5
4.0
4.5
5.0
5.5
6.0
6.5
7.0
7.5
8.0
8.5

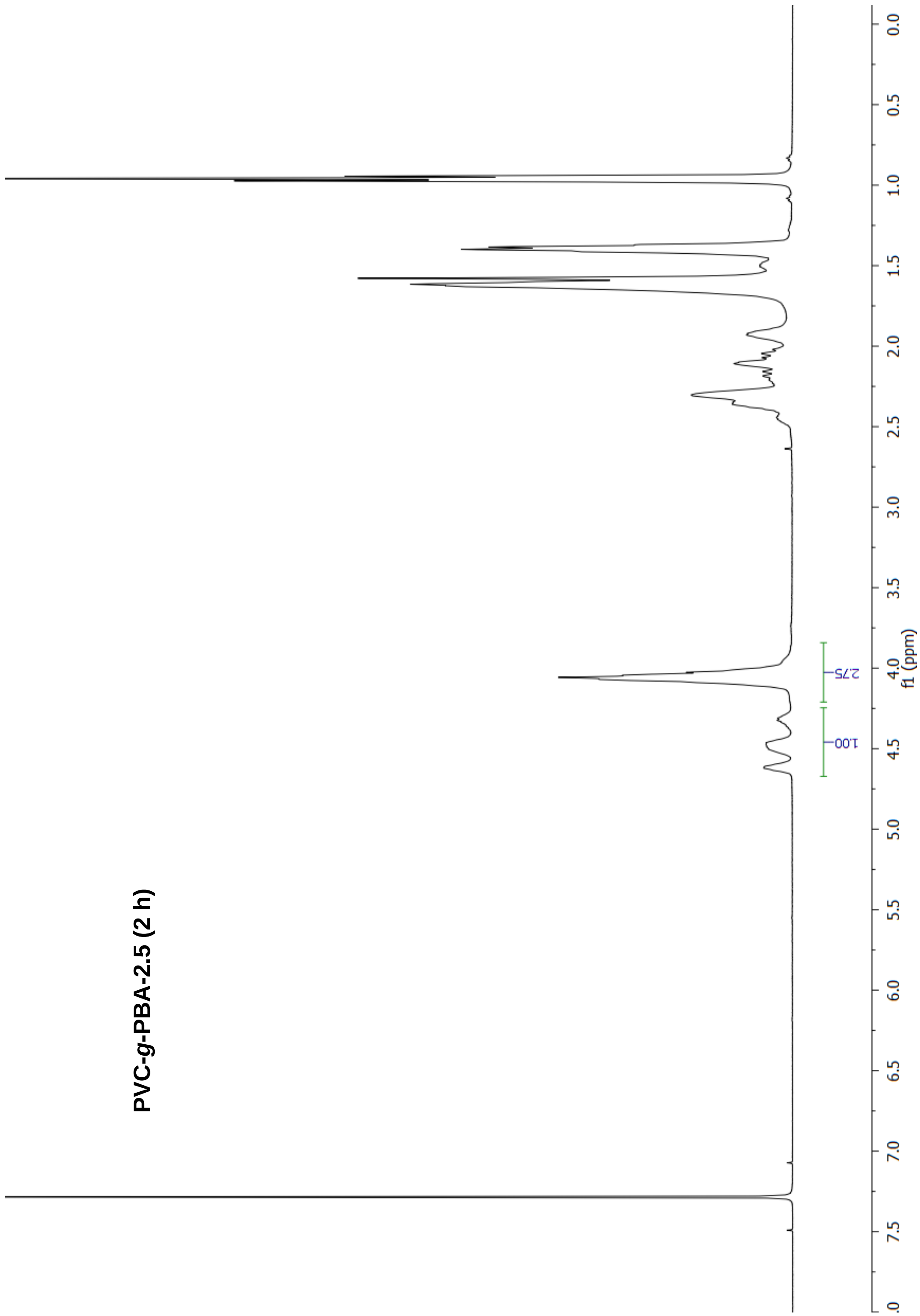
PVC-*g*-PBA-2.5 (2 h)
2.75
1.00
0.0
0.5
1.0
1.5
2.0
2.5
3.0
3.5
4.0
4.5
5.0
5.5
6.0
6.5
7.0
7.5
f1 (ppm)

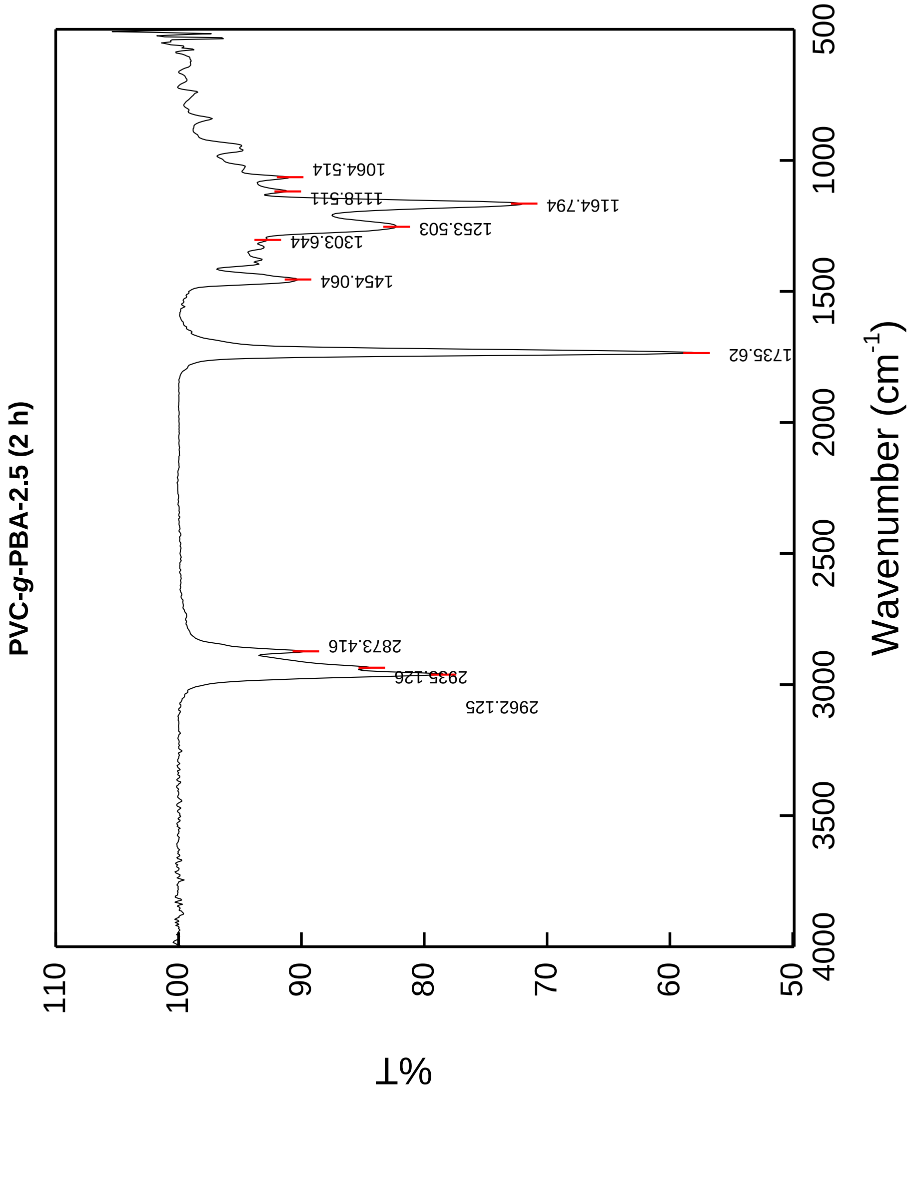
PVC-*g*-PBA-2.5 (2 h)
%T
Wavenumber (cm-1)
110
100
90
80
70
60
50
4000
3500
3000
2500
2000
1500
1000
500
2962.125
2935.126
2873.416
1735.62
1454.064
1303.644
1253.503
1164.794
1118.511
1064.514

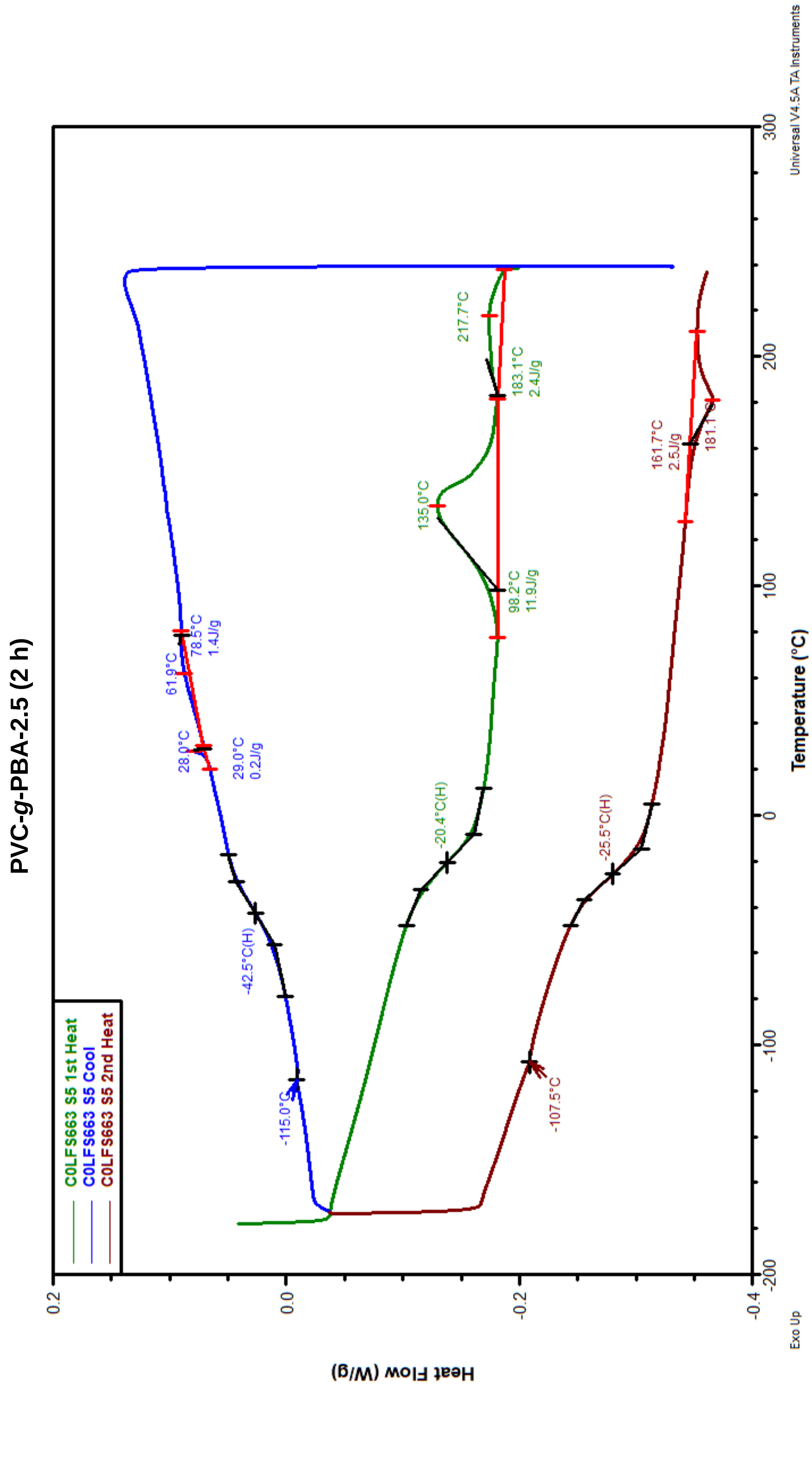

PVC-g-PBA-2.5 (2 h)
C0LFS663 S5 1st Heat
C0LFS663 S5 Cool
C0LFS663 S5 2nd Heat
Heat Flow (W/g)
Temperature (°C)
Exo Up
Universal V4.5A TA Instruments
-115.0°C
-42.5°C(H)
28.0°C
29.0°C
0.2J/g
61.9°C
78.5°C
1.4J/g
-20.4°C(H)
98.2°C
11.9J/g
135.0°C
183.1°C
2.4J/g
217.7°C
-107.5°C
-25.5°C(H)
161.7°C
2.5J/g
181.1°C

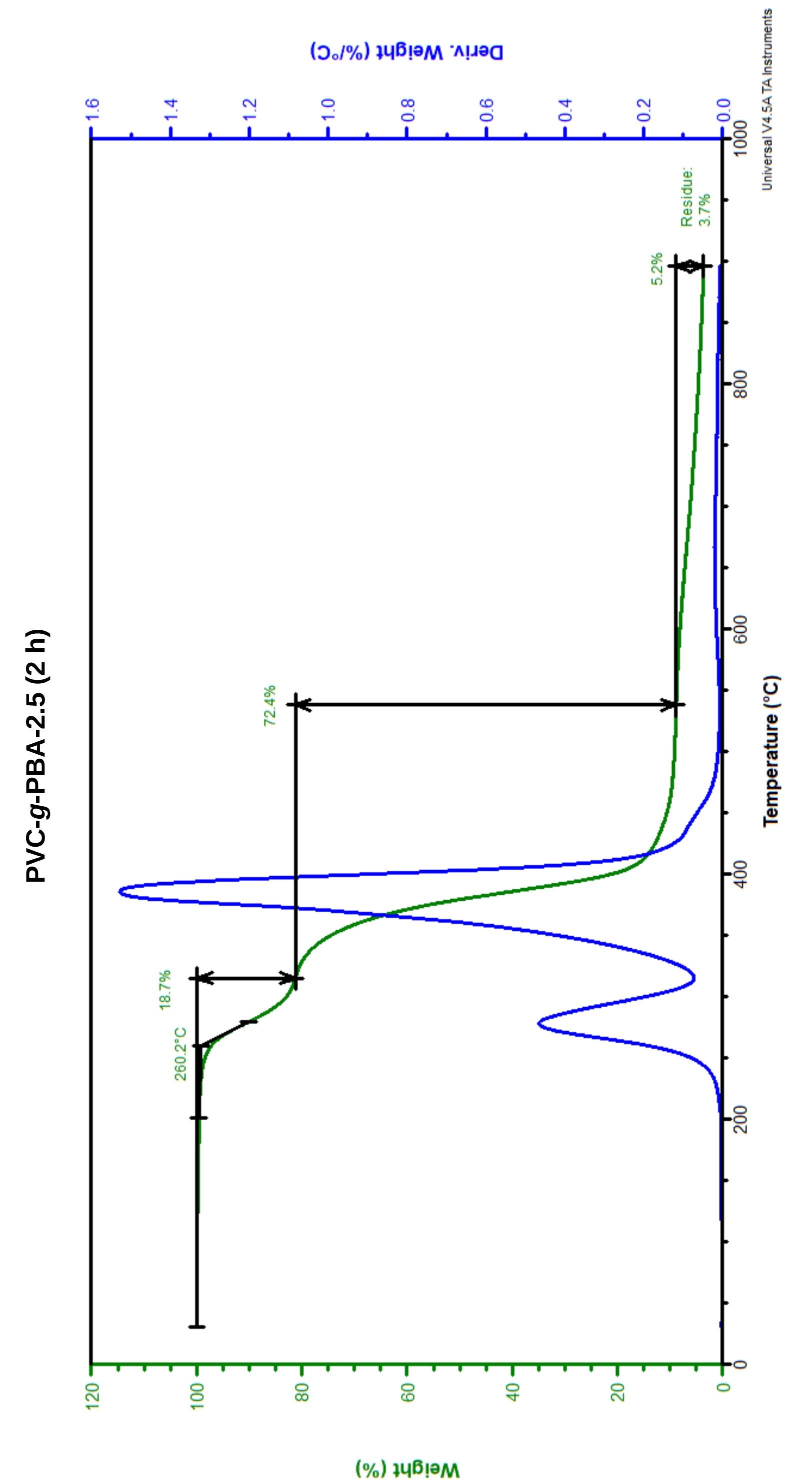

PVC-g-PBA-2.5 (2 h)
Weight (%)
Deriv. Weight (%/°C)
Temperature (°C)
260.2°C
18.7%
72.4%
5.2%
Residue:
3.7%
Universal V4.5A TA Instruments

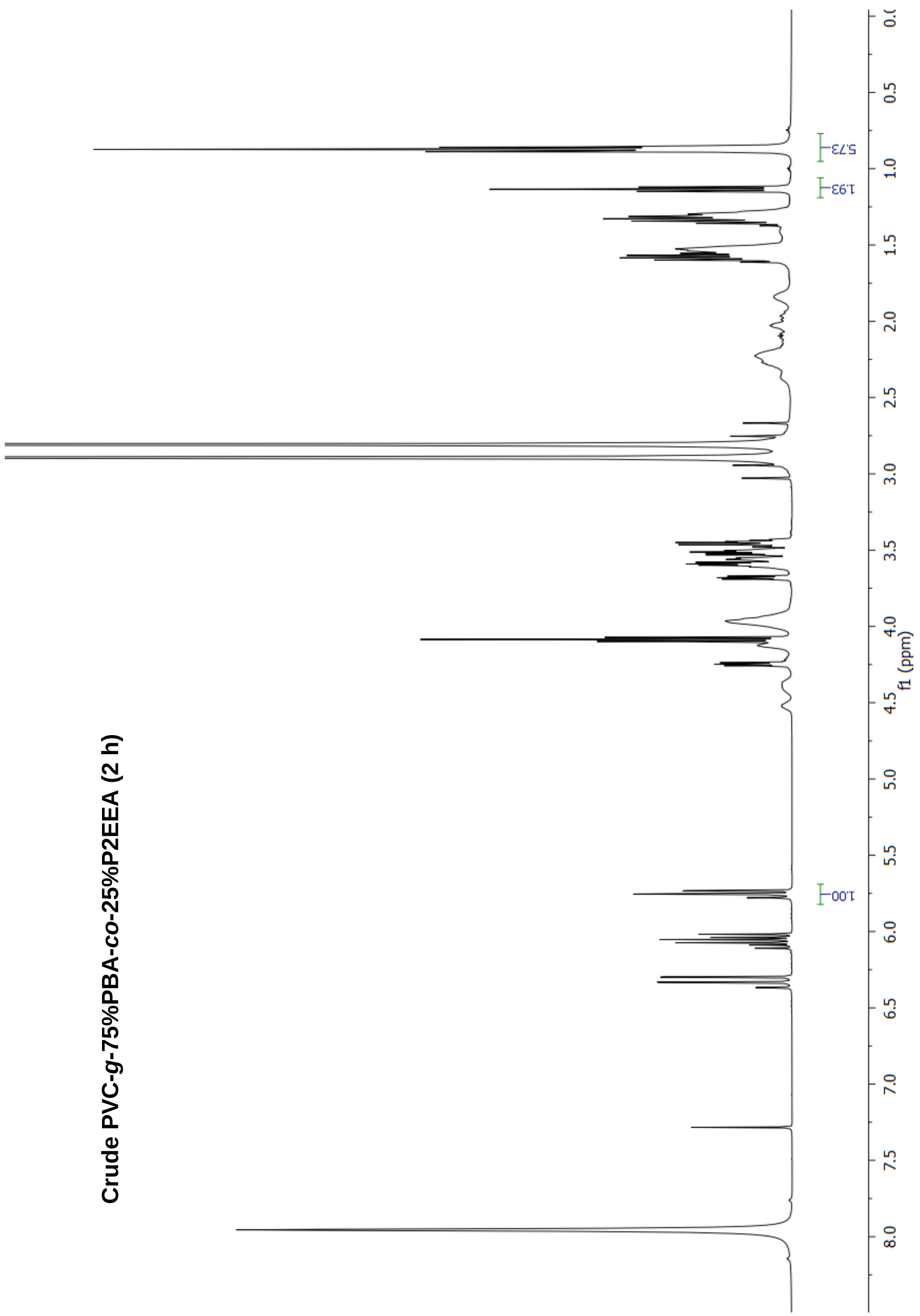
Crude PVC-g-75%PBA-co-25%P2EEA (2 h)
5.73
1.93
1.00
f1 (ppm)
0.0
0.5
1.0
1.5
2.0
2.5
3.0
3.5
4.0
4.5
5.0
5.5
6.0
6.5
7.0
7.5
8.0

PVC-*g*-75%PBA-*co*-25%P2EEA (2 h)

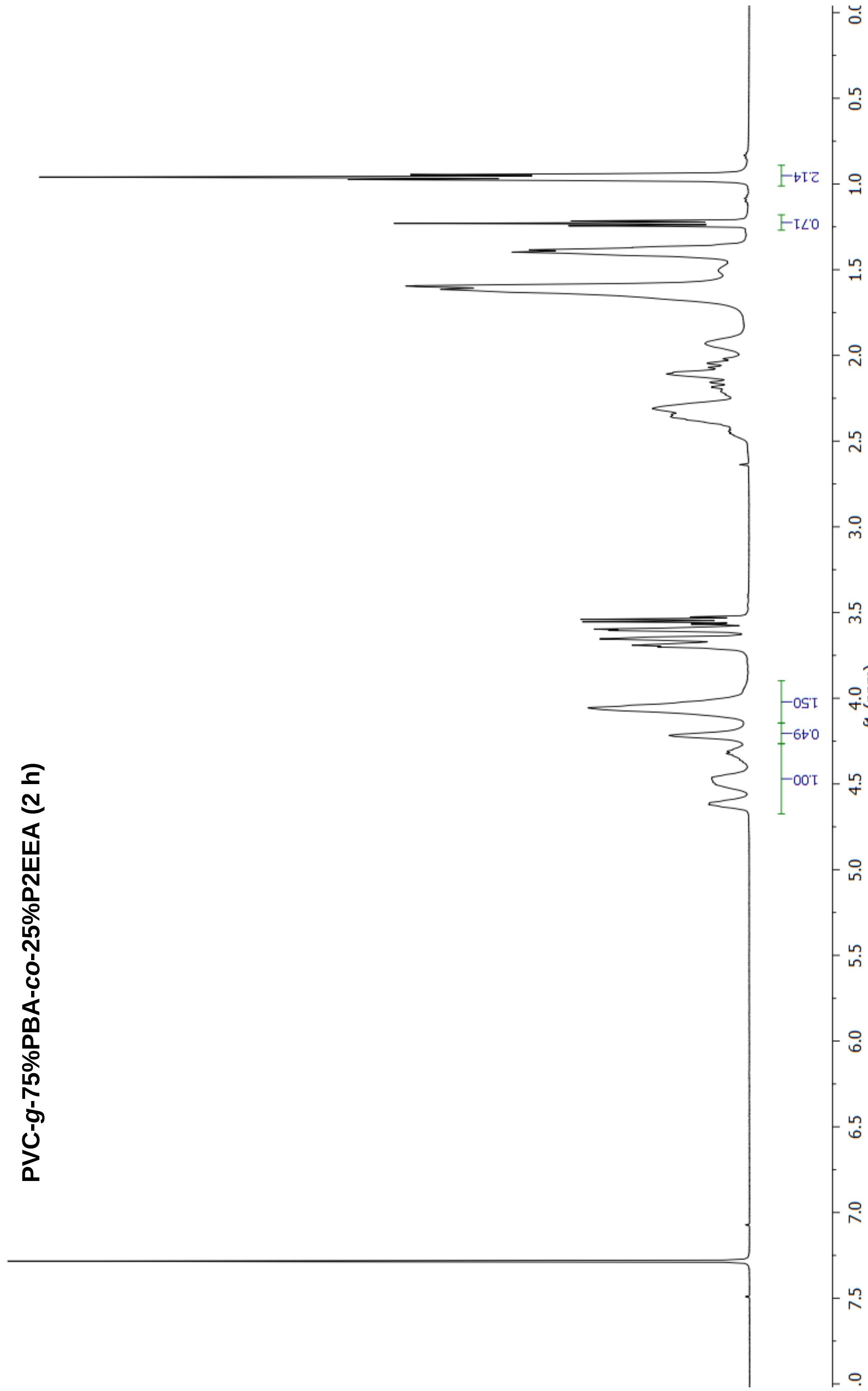

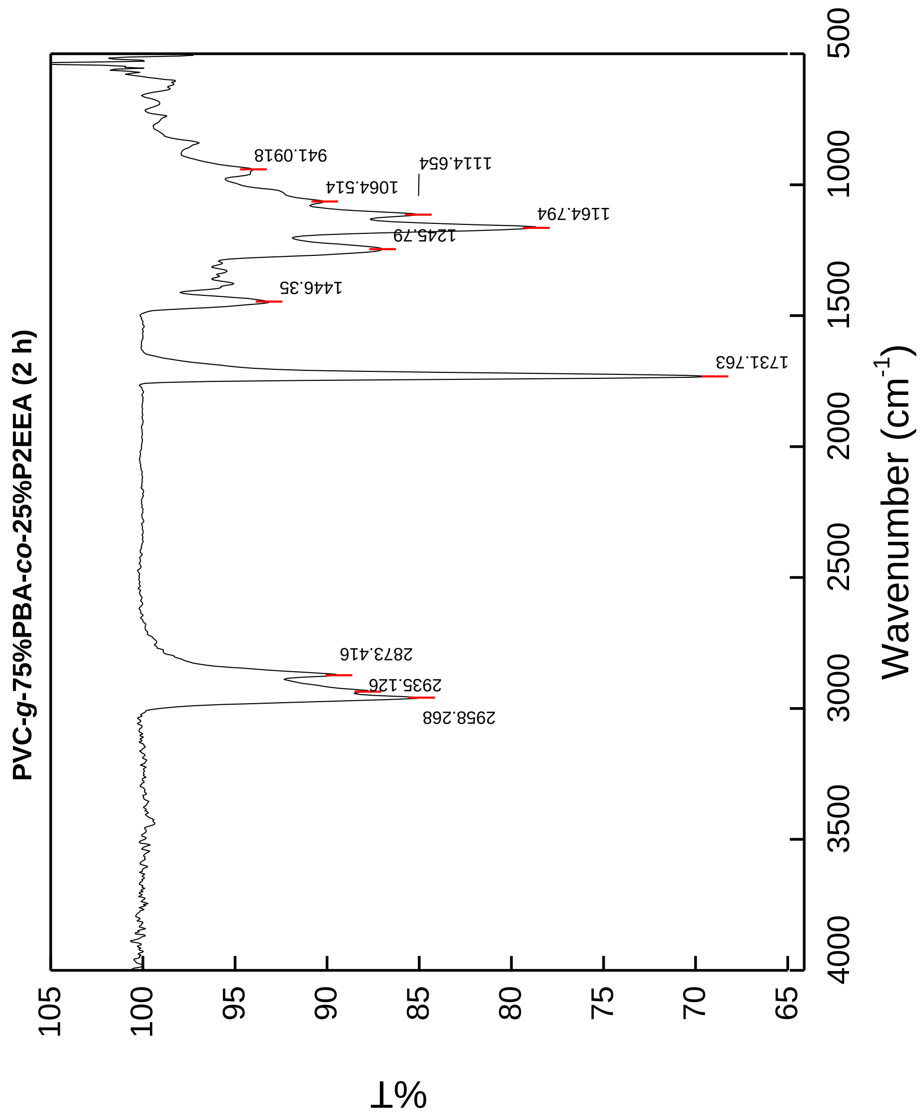
PVC-*g*-75%PBA-*co*-25%P2EEA (2 h)
%T
Wavenumber (cm^{-1})
941.0918
1064.514
1114.654
1164.794
1245.79
1446.35
1731.763
2873.416
2935.126
2958.268

PVC-*g*-75%PBA-*co*-25%P2EEA (2 h)

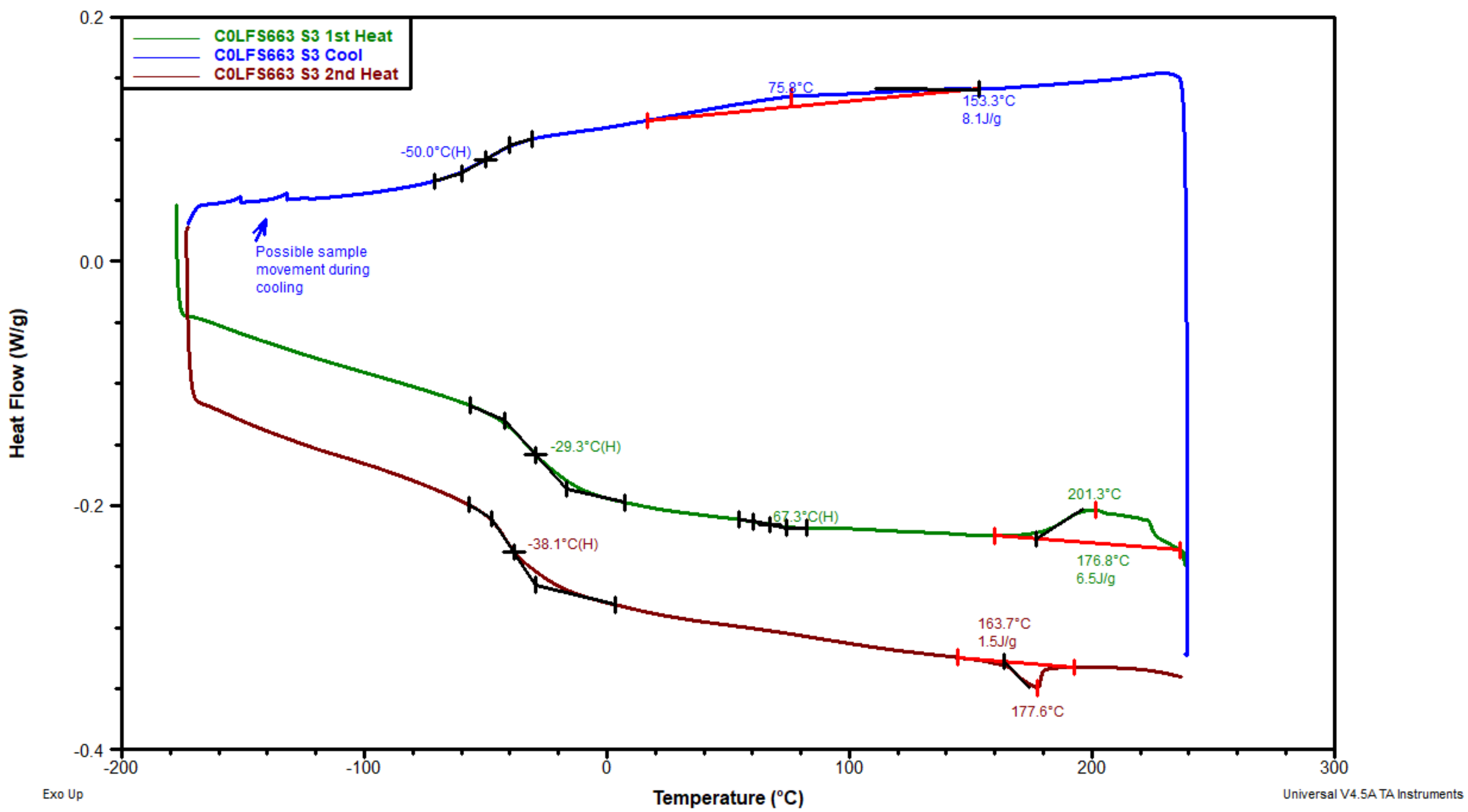

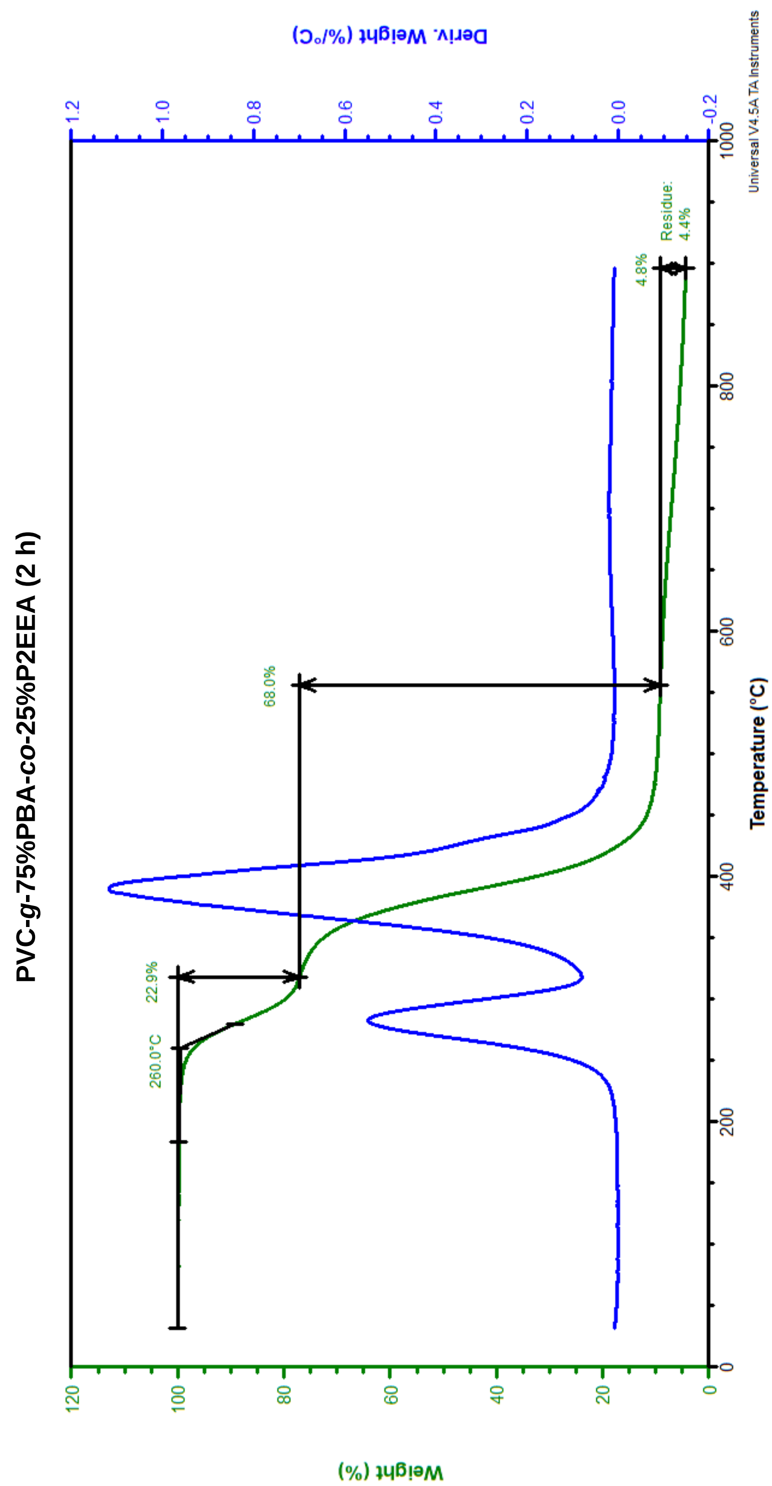
PVC-g-75%PBA-co-25%P2EEA (2 h)
Weight (%)
Deriv. Weight (%/°C)
Temperature (°C)
260.0°C
22.9%
68.0%
4.8%
Residue:
4.4%
Universal V4.5A TA Instruments
0
20
40
60
80
100
120
-0.2
0.0
0.2
0.4
0.6
0.8
1.0
1.2
0
200
400
600
800
1000

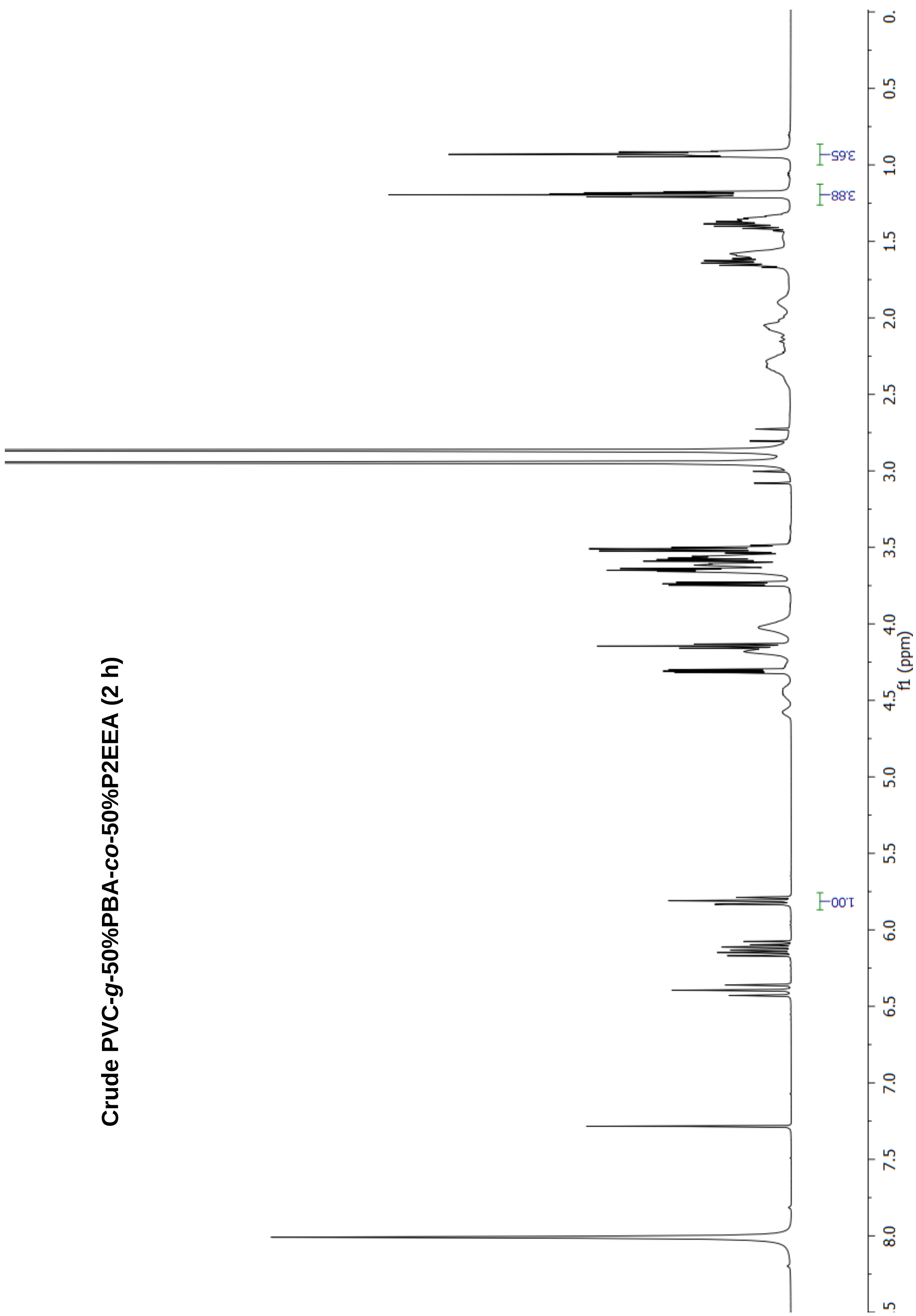
Crude PVC-*g*-50%PBA-*co*-50%P2EEA (2 h)
3.65
3.88
1.00
0.
0.5
1.0
1.5
2.0
2.5
3.0
3.5
4.0
4.5
5.0
5.5
6.0
6.5
7.0
7.5
8.0
.5
f1 (ppm)

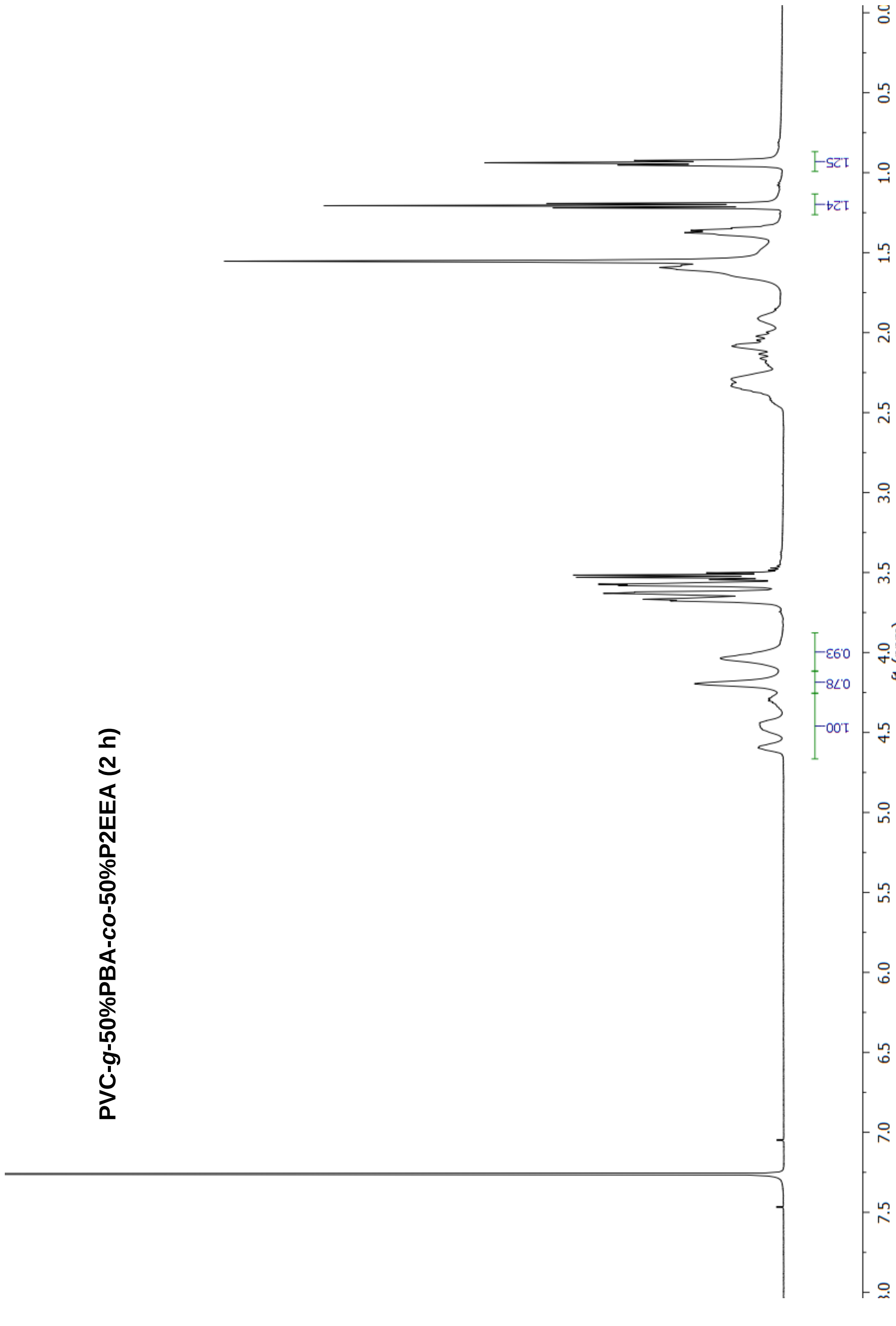
PVC-*g*-50%PBA-*co*-50%P2EEA (2 h)
1.25
1.24
0.93
0.78
1.00
0.0
0.5
1.0
1.5
2.0
2.5
3.0
3.5
4.0
4.5
5.0
5.5
6.0
6.5
7.0
7.5
8.0
f1 (ppm)

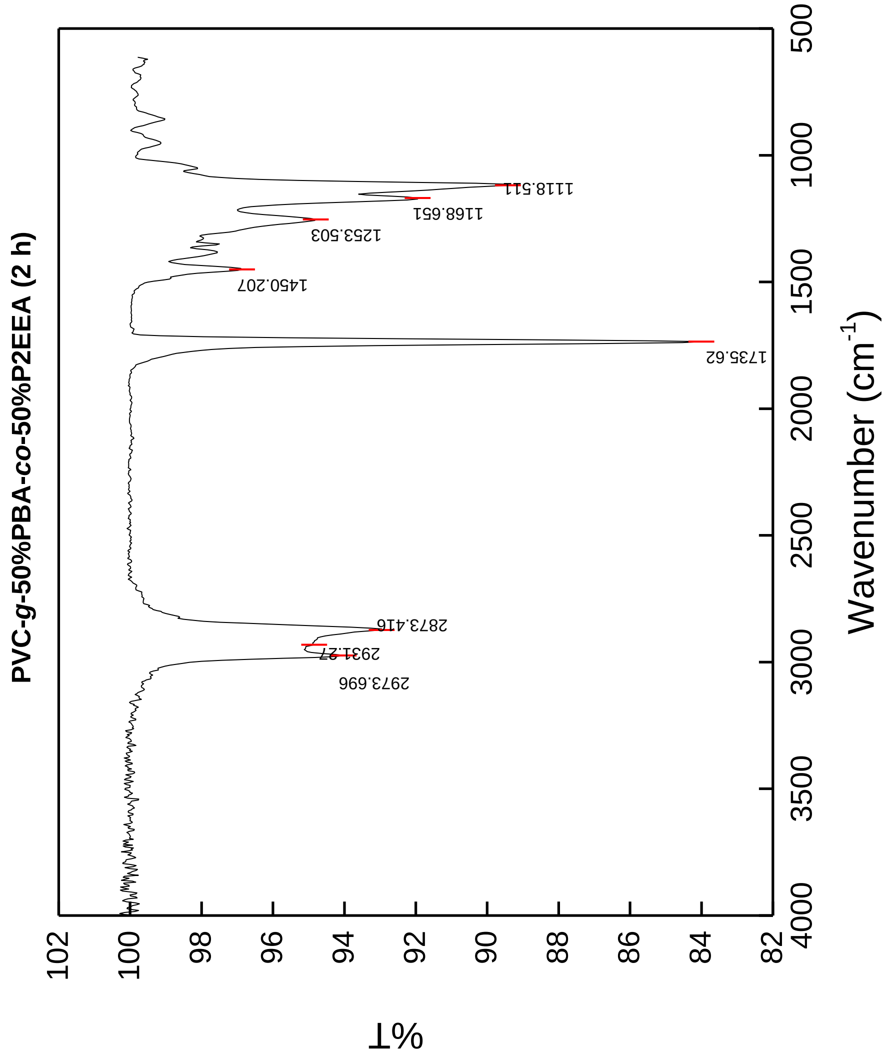
PVC-g-50%PBA-co-50%P2EEA (2 h)
%T
Wavenumber (cm-1)
1118.511
1168.651
1253.503
1450.207
1735.62
2873.416
2931.27
2973.696
102
100
98
96
94
92
90
88
86
84
82
4000
3500
3000
2500
2000
1500
1000
500

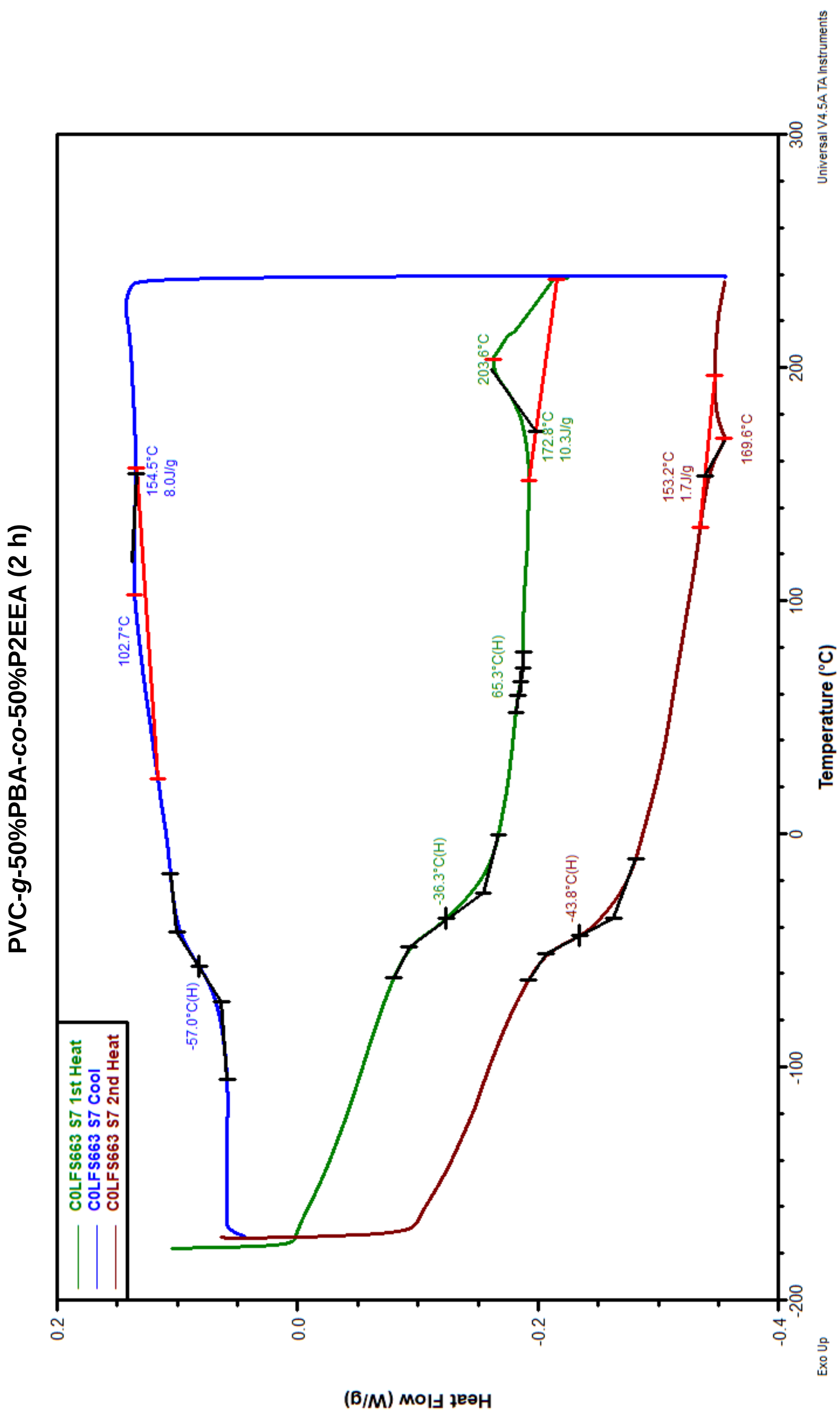

PVC-g-50%PBA-co-50%P2EEA (2 h)
C0LFS663 S7 1st Heat
C0LFS663 S7 Cool
C0LFS663 S7 2nd Heat
-57.0°C(H)
102.7°C
154.5°C
8.0J/g
-36.3°C(H)
65.3°C(H)
203.6°C
172.8°C
10.3J/g
-43.8°C(H)
153.2°C
1.7J/g
169.6°C
Heat Flow (W/g)
Temperature (°C)
Exo Up
Universal V4.5A TA Instruments
0.2
0.0
-0.2
-0.4
-200
-100
0
100
200
300

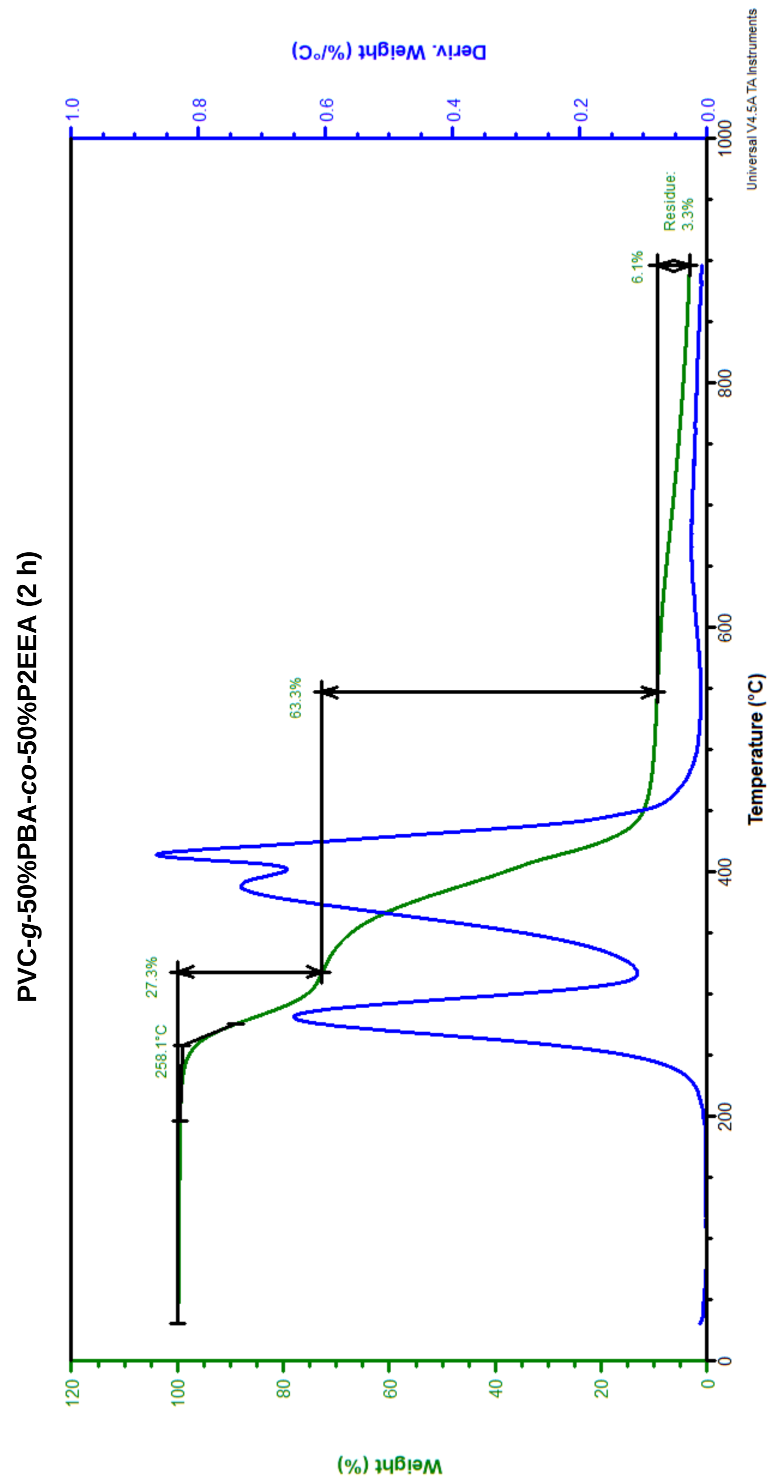
PVC-g-50%PBA-co-50%P2EEA (2 h)
Weight (%)
Deriv. Weight (%/°C)
Temperature (°C)
258.1°C
27.3%
63.3%
6.1%
Residue:
3.3%
0
20
40
60
80
100
120
0.0
0.2
0.4
0.6
0.8
1.0
0
200
400
600
800
1000
Universal V4.5A TA Instruments

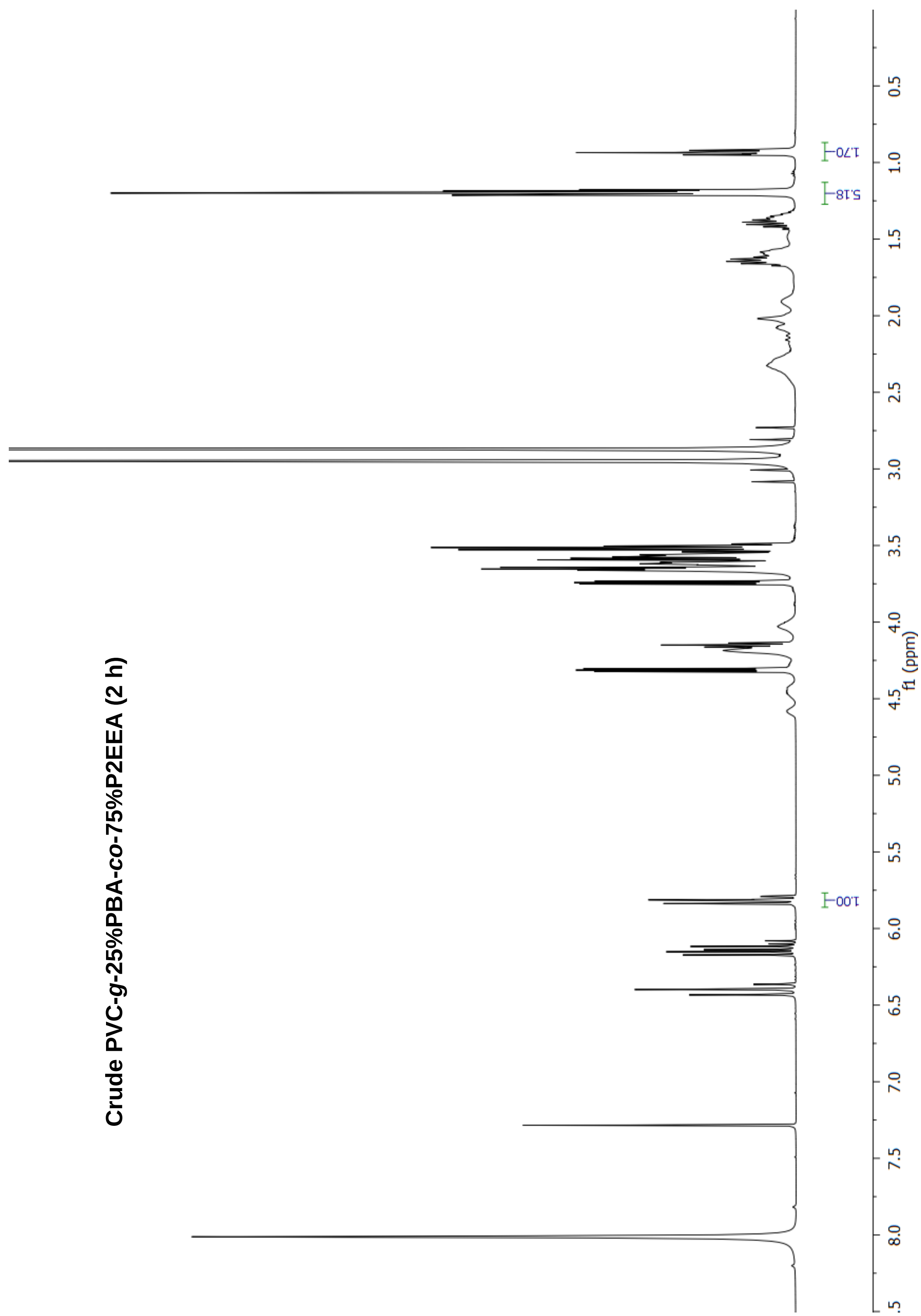
Crude PVC-*g*-25%PBA-*co*-75%P2EEA (2 h)
1.70
5.18
1.00
0.5
1.0
1.5
2.0
2.5
3.0
3.5
4.0
4.5
5.0
5.5
6.0
6.5
7.0
7.5
8.0
f1 (ppm)

PVC-*g*-25%PBA-*co*-75%P2EEA (2 h)

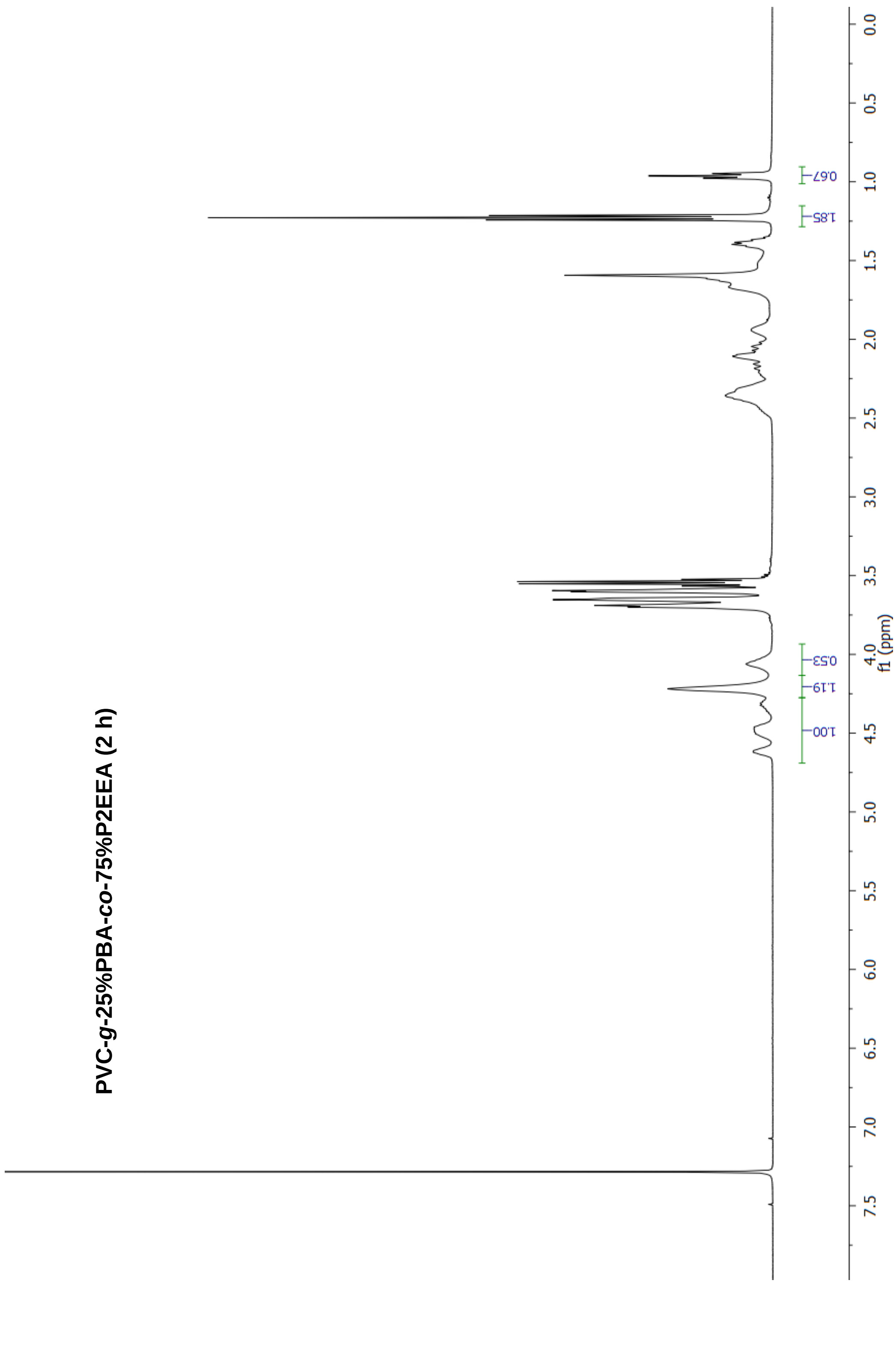

PVC-*g*-25%PBA-*co*-75%P2EEA (2 h)

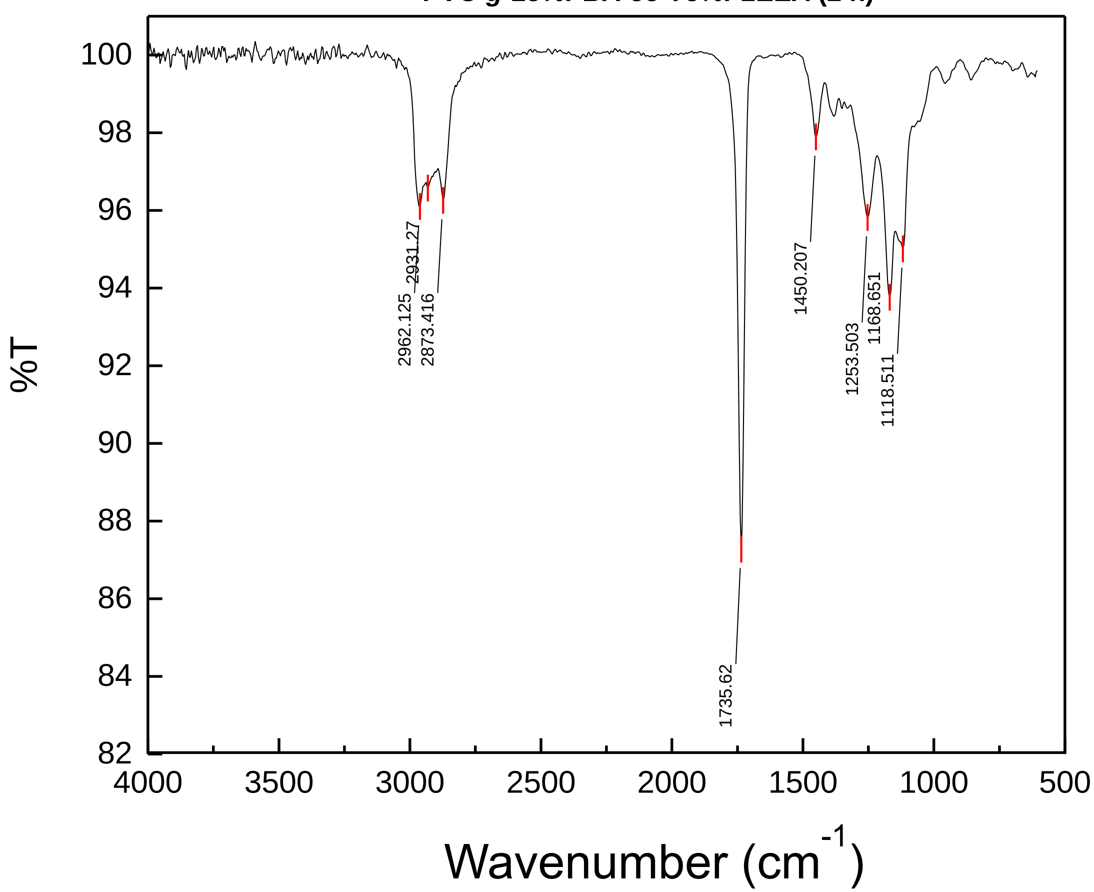

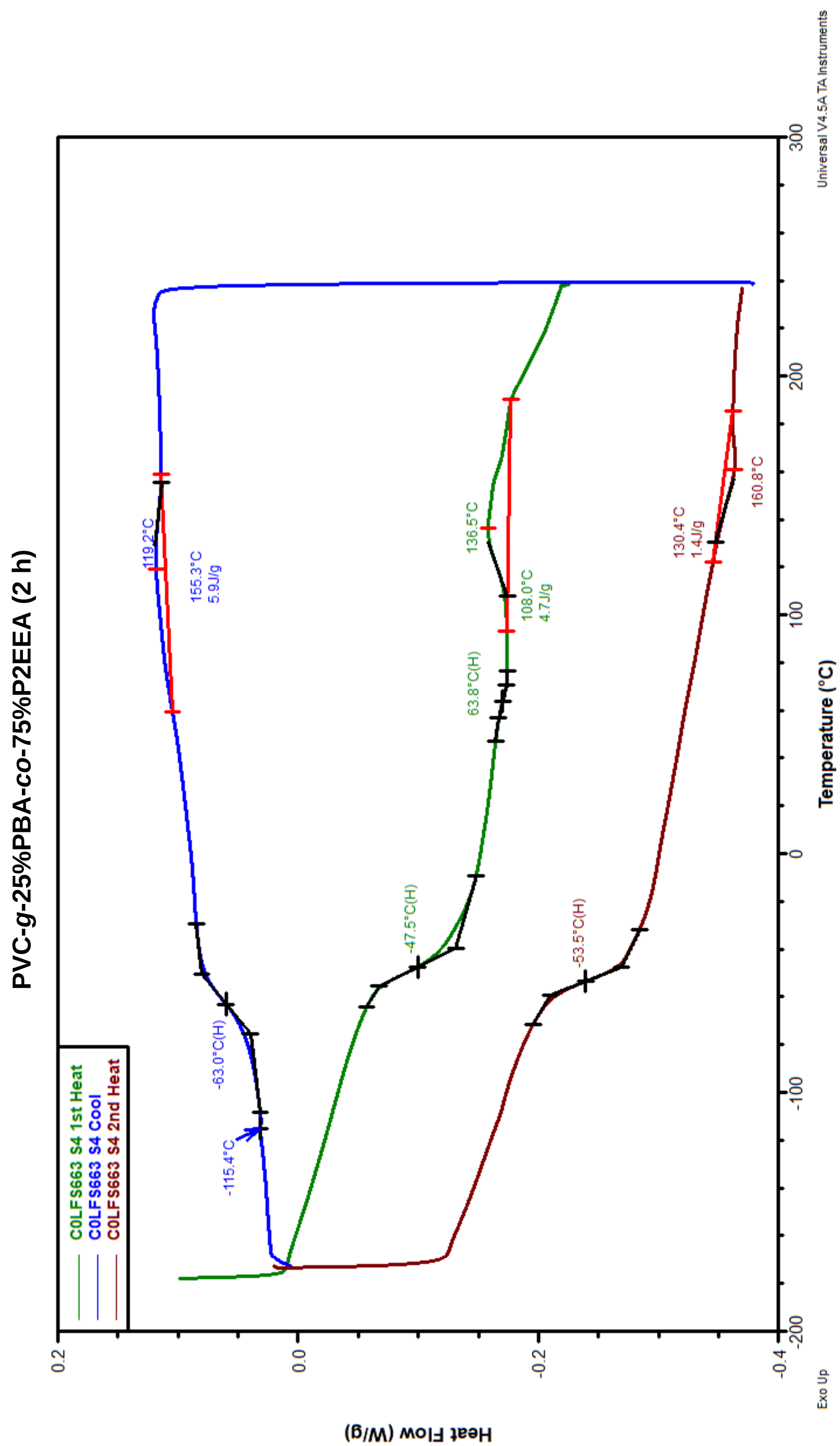

PVC-*g*-25%PBA-*co*-75%P2EEA (2 h)
C0LFS663 S4 1st Heat
C0LFS663 S4 Cool
C0LFS663 S4 2nd Heat
-115.4°C
-63.0°C(H)
119.2°C
155.3°C
5.9J/g
-47.5°C(H)
63.8°C(H)
136.5°C
108.0°C
4.7J/g
-53.5°C(H)
130.4°C
1.4J/g
160.8°C
Heat Flow (W/g)
Exo Up
Temperature (°C)
Universal V4.5A TA Instruments

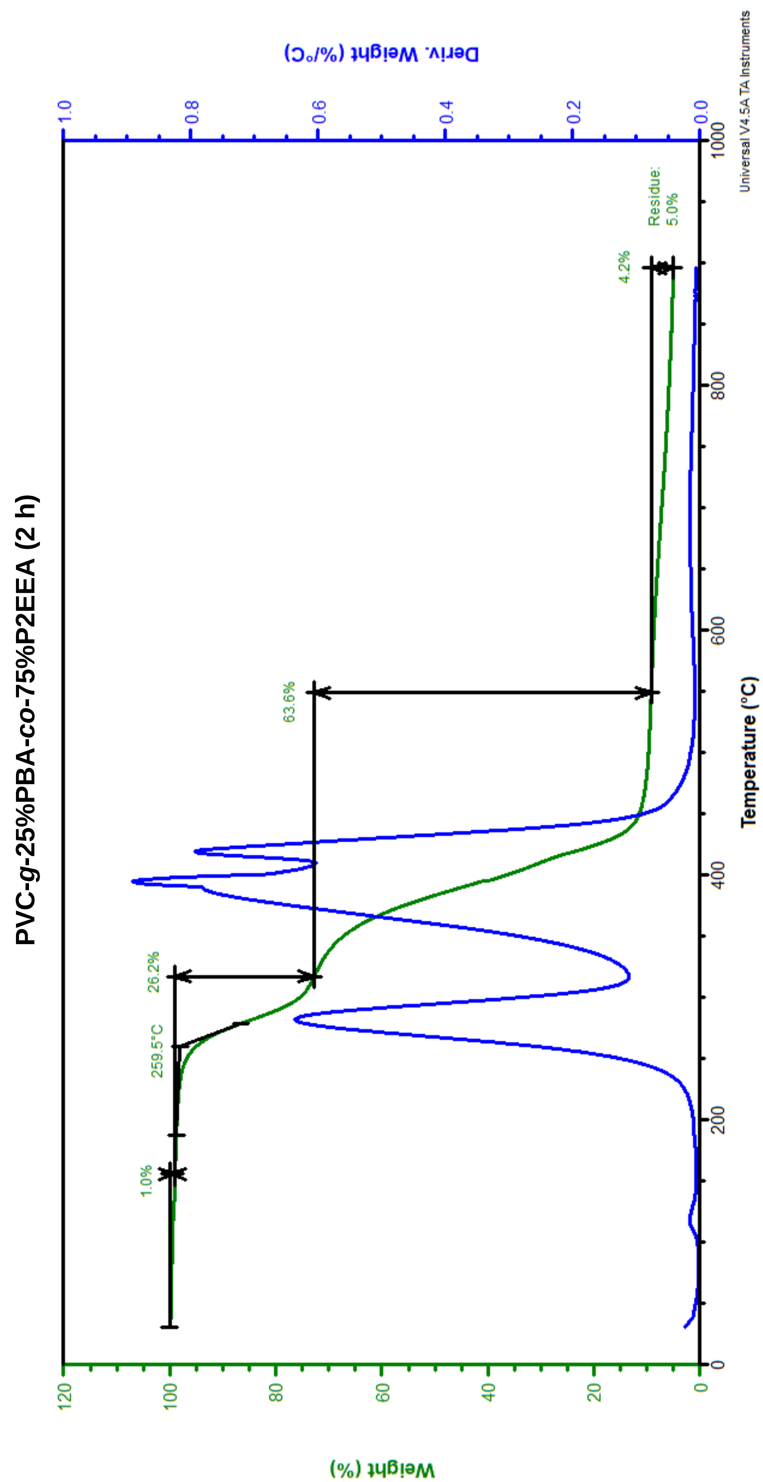
PVC-g-25%PBA-co-75%P2EEA (2 h)
Weight (%)
Deriv. Weight (%/°C)
Temperature (°C)
1.0%
259.5°C
26.2%
63.6%
4.2%
Residue:
5.0%
0
200
400
600
800
1000
0
20
40
60
80
100
120
0.0
0.2
0.4
0.6
0.8
1.0
Universal V4.5A TA Instruments

Crude PVC-*g*-P2EEA-2.5 (2 h)

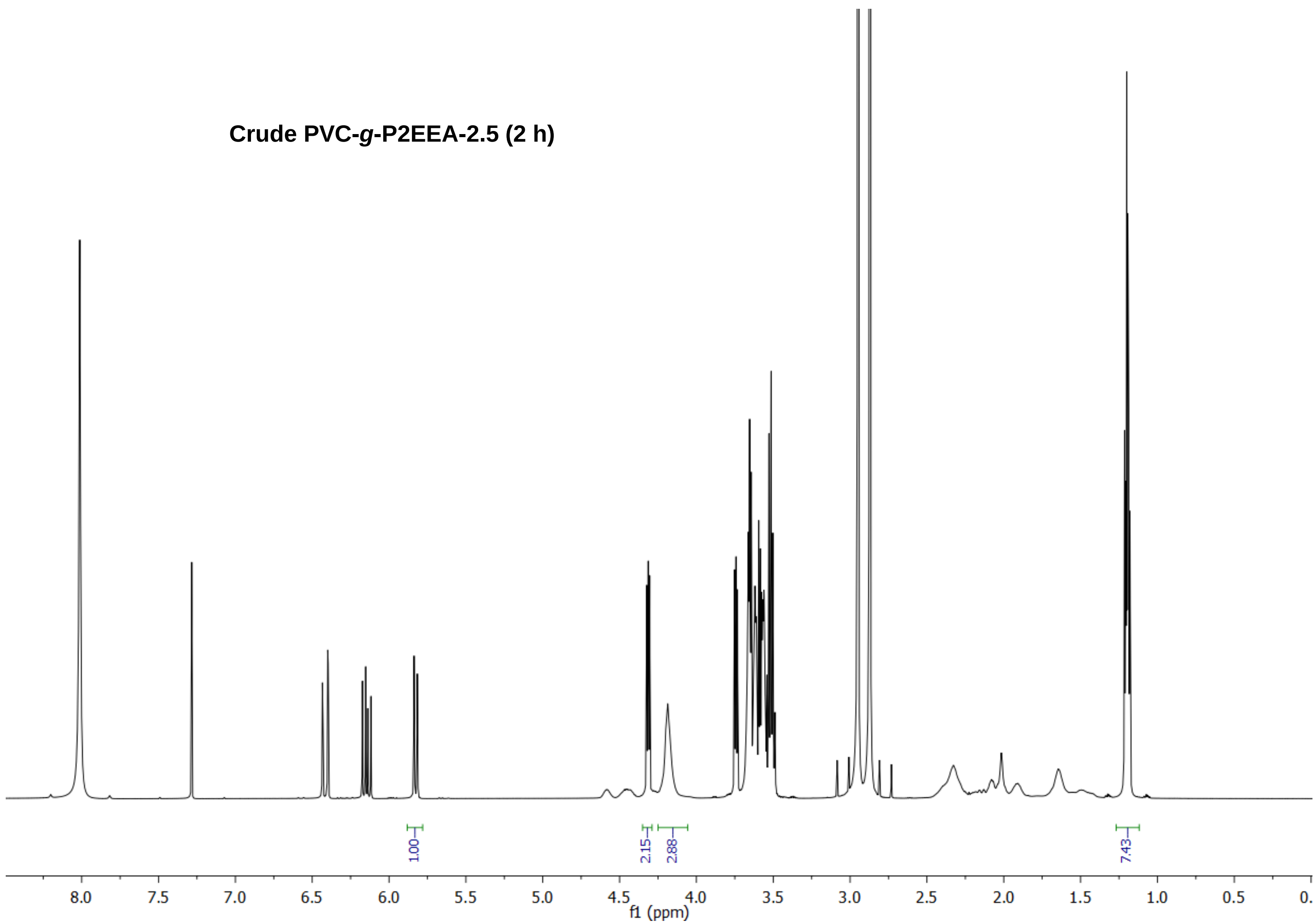

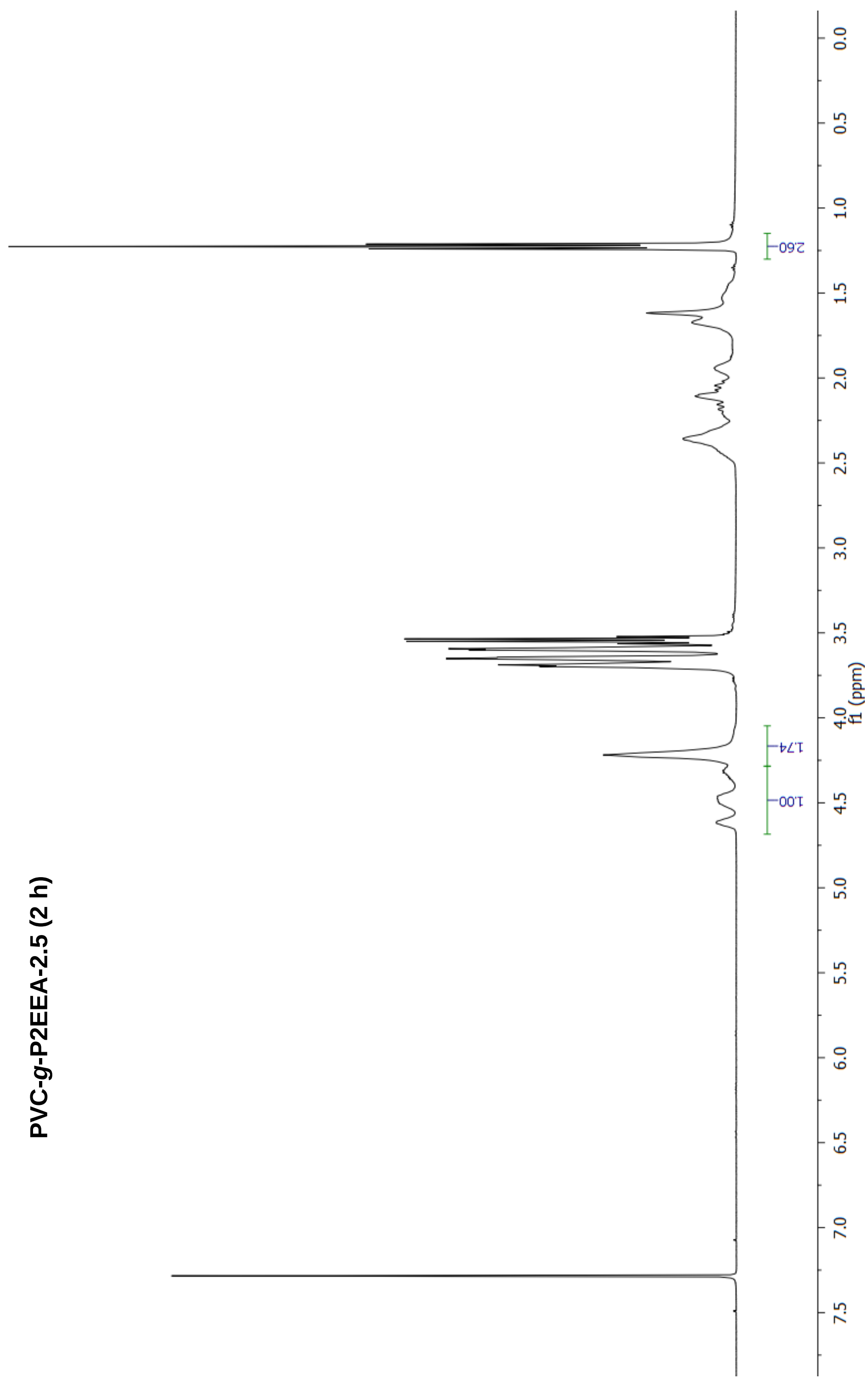

PVC-g-P2EEA-2.5 (2 h)
2.60
1.74
1.00
0.0
0.5
1.0
1.5
2.0
2.5
3.0
3.5
4.0
4.5
5.0
5.5
6.0
6.5
7.0
7.5
f1 (ppm)

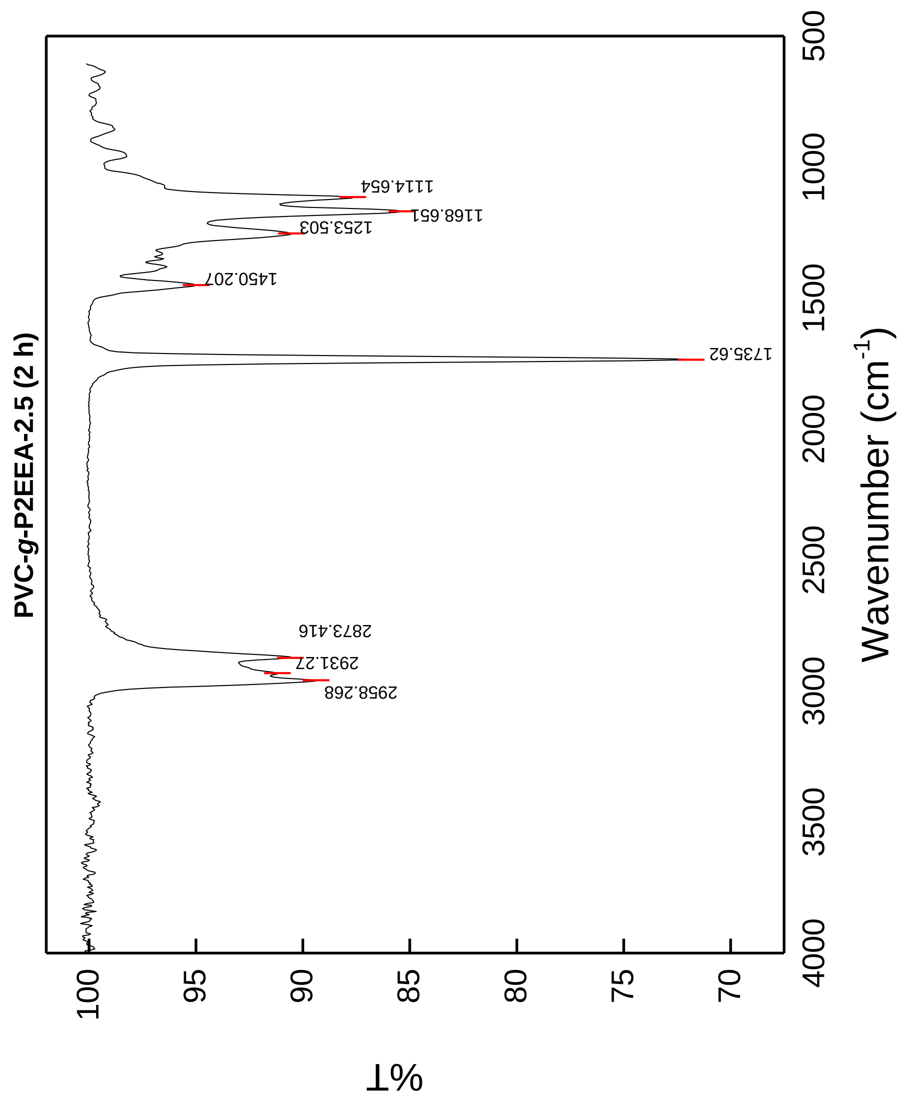
PVC-g-P2EEA-2.5 (2 h)
%T
100
95
90
85
80
75
70
Wavenumber (cm-1)
4000
3500
3000
2500
2000
1500
1000
500
2958.268
2931.27
2873.416
1735.62
1450.207
1253.503
1168.651
1114.654

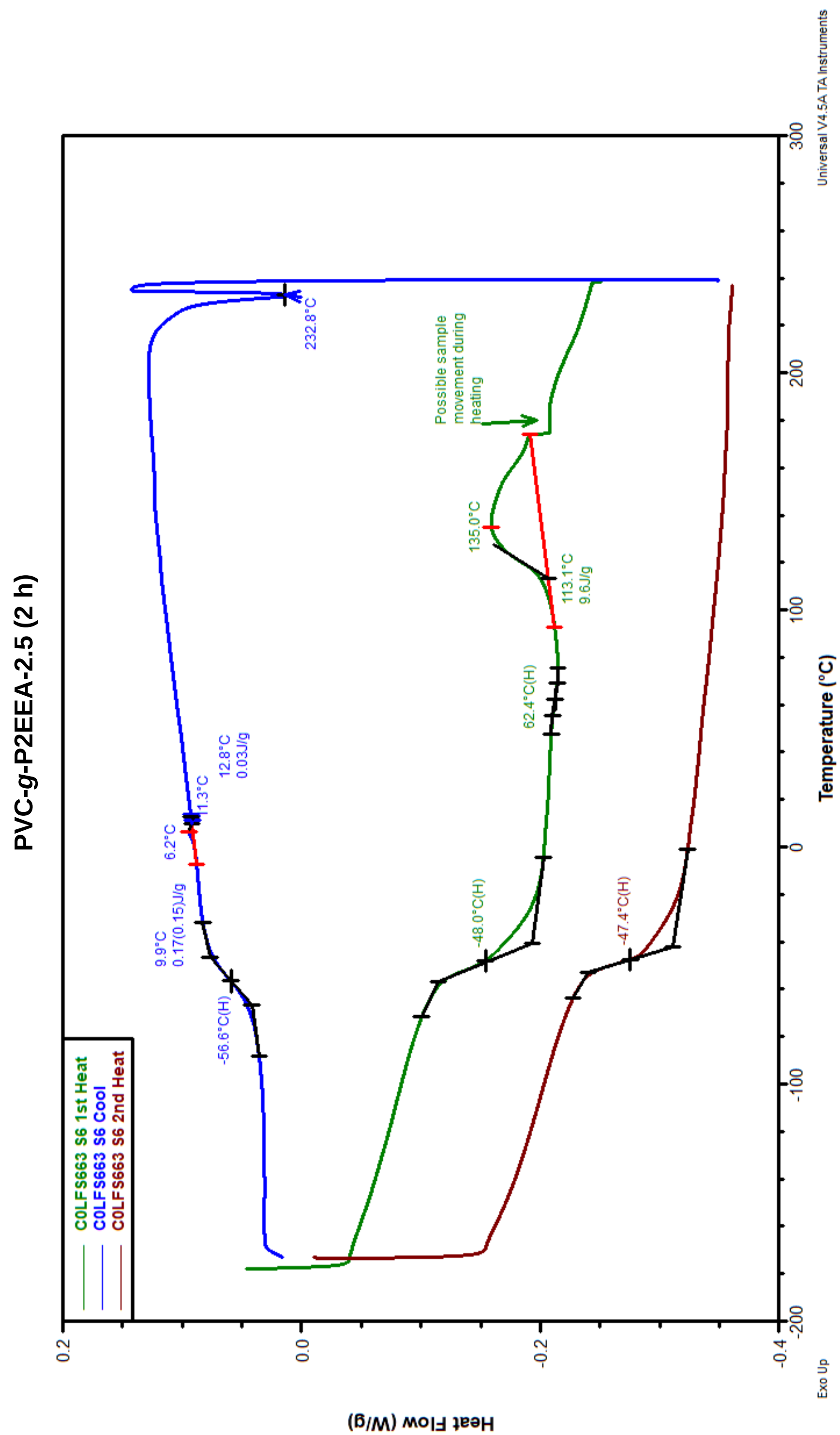
PVC-g-P2EEA-2.5 (2 h)
C0LFS663 S6 1st Heat
C0LFS663 S6 Cool
C0LFS663 S6 2nd Heat
232.8°C
Possible sample movement during heating
135.0°C
113.1°C
9.6J/g
62.4°C(H)
12.8°C
0.03J/g
11.3°C
6.2°C
9.9°C
0.17(0.15)J/g
-56.6°C(H)
-48.0°C(H)
-47.4°C(H)
Heat Flow (W/g)
Temperature (°C)
Exo Up
Universal V4.5A TA Instruments

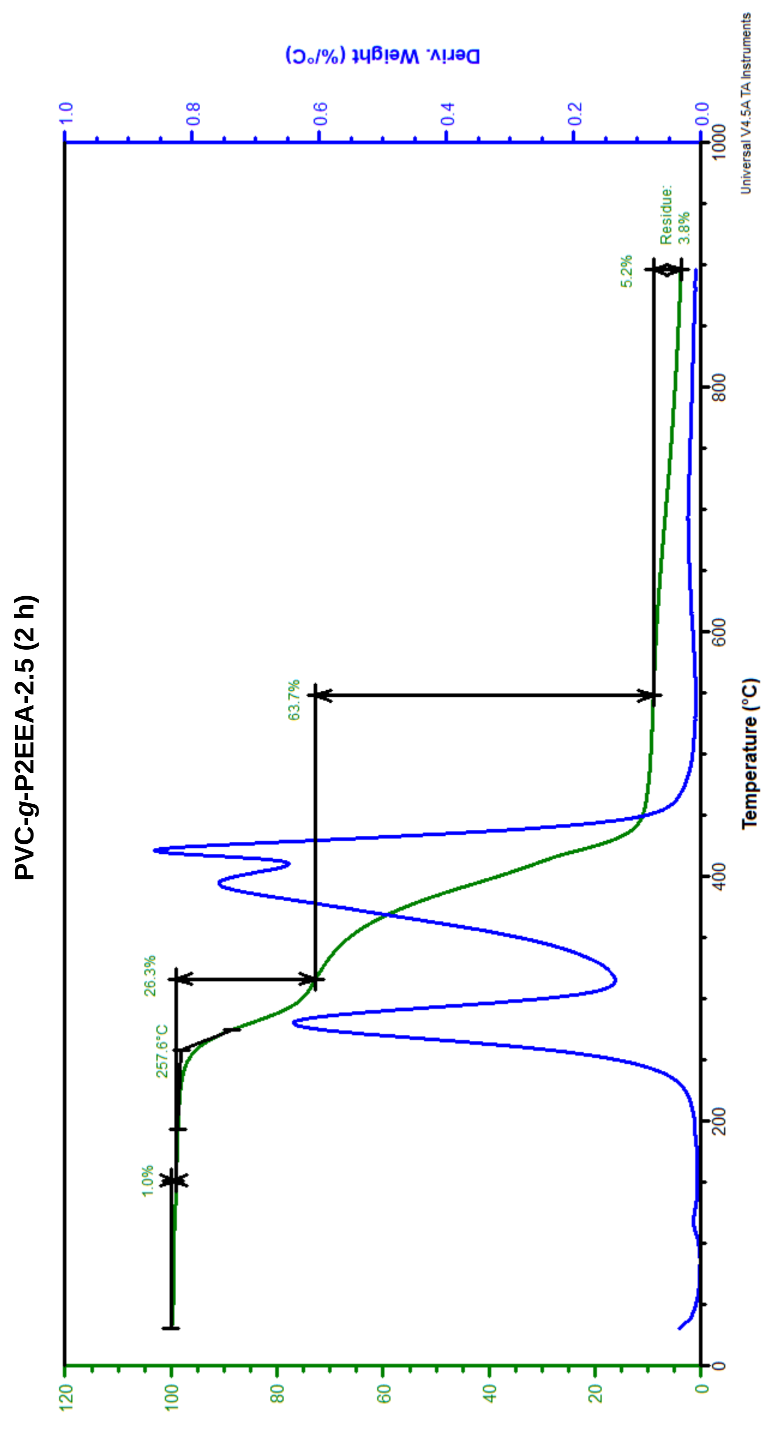
PVC-*g*-P2EEA-2.5 (2 h)
Weight (%)
Deriv. Weight (%/°C)
Temperature (°C)
1.0%
257.6°C
26.3%
63.7%
5.2%
Residue:
3.8%
Universal V4.5A TA Instruments

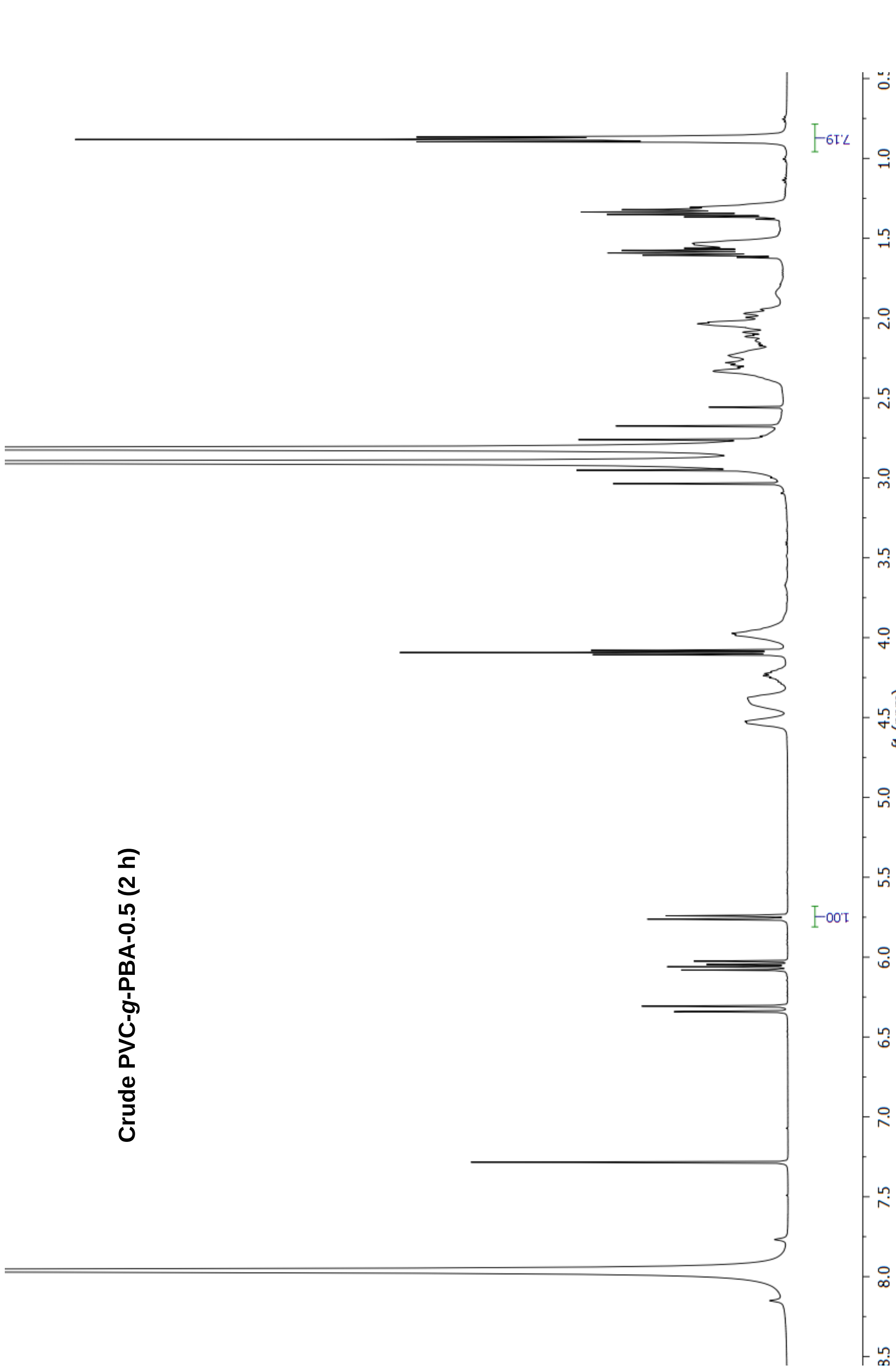

Crude PVC-g-PBA-0.5 (2 h)
7.19
1.00
8.5
8.0
7.5
7.0
6.5
6.0
5.5
5.0
4.5
4.0
3.5
3.0
2.5
2.0
1.5
1.0
0.5
f1 (ppm)

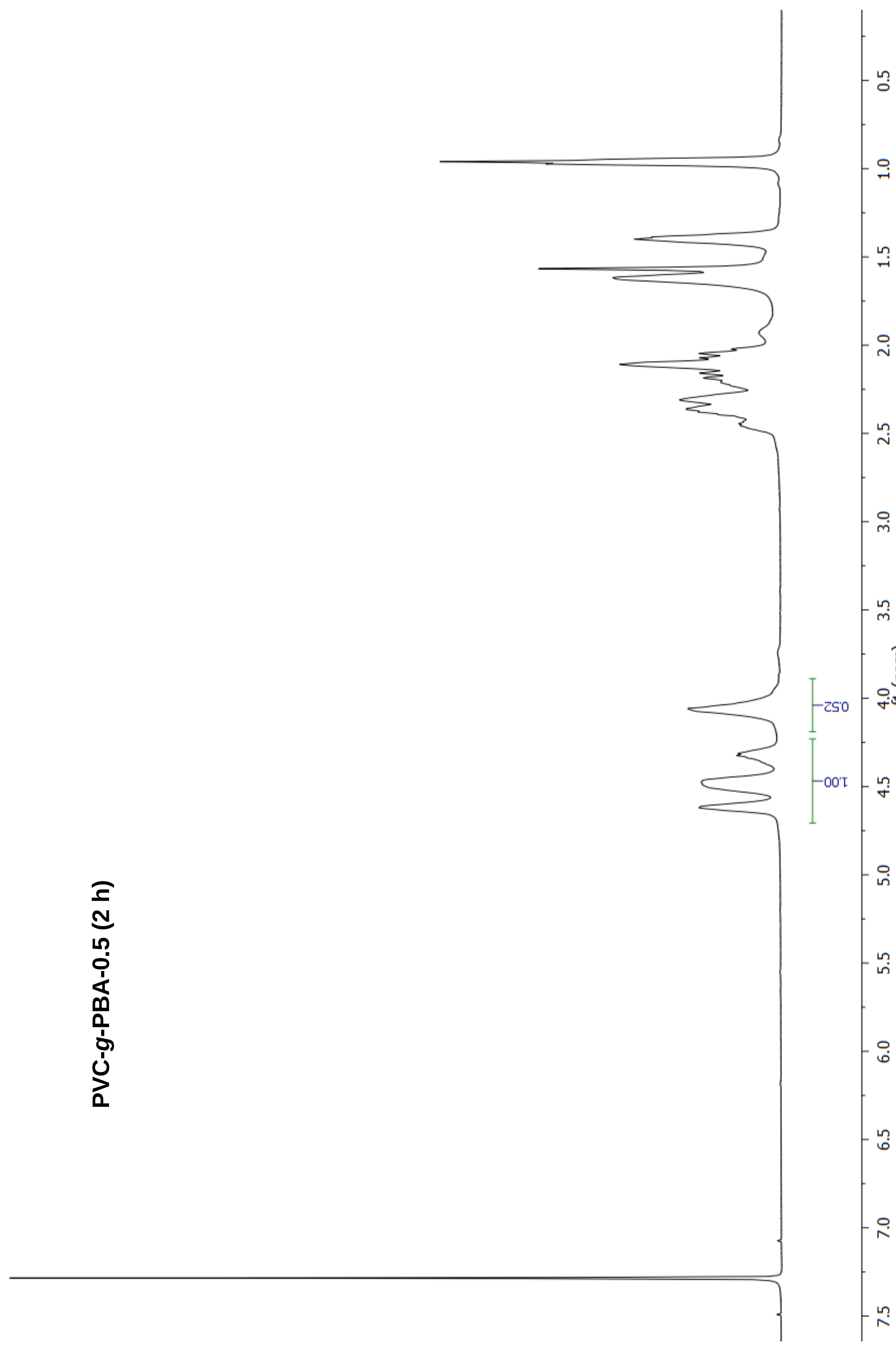

PVC-*g*-PBA-0.5 (2 h)
0.52
1.00
f1 (ppm)
0.5
1.0
1.5
2.0
2.5
3.0
3.5
4.0
4.5
5.0
5.5
6.0
6.5
7.0
7.5

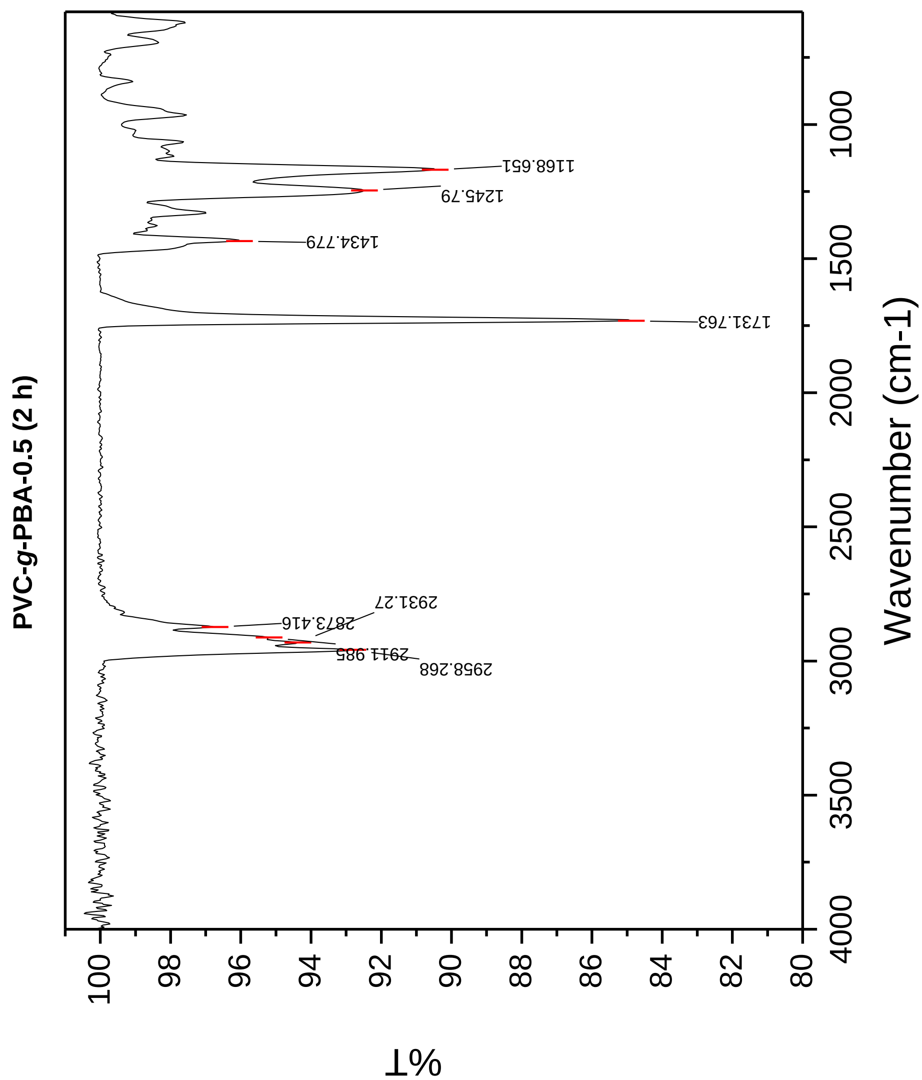
PVC-g-PBA-0.5 (2 h)
%T
Wavenumber (cm-1)
1168.651
1245.79
1434.779
1731.763
2931.27
2873.416
2911.985
2958.268

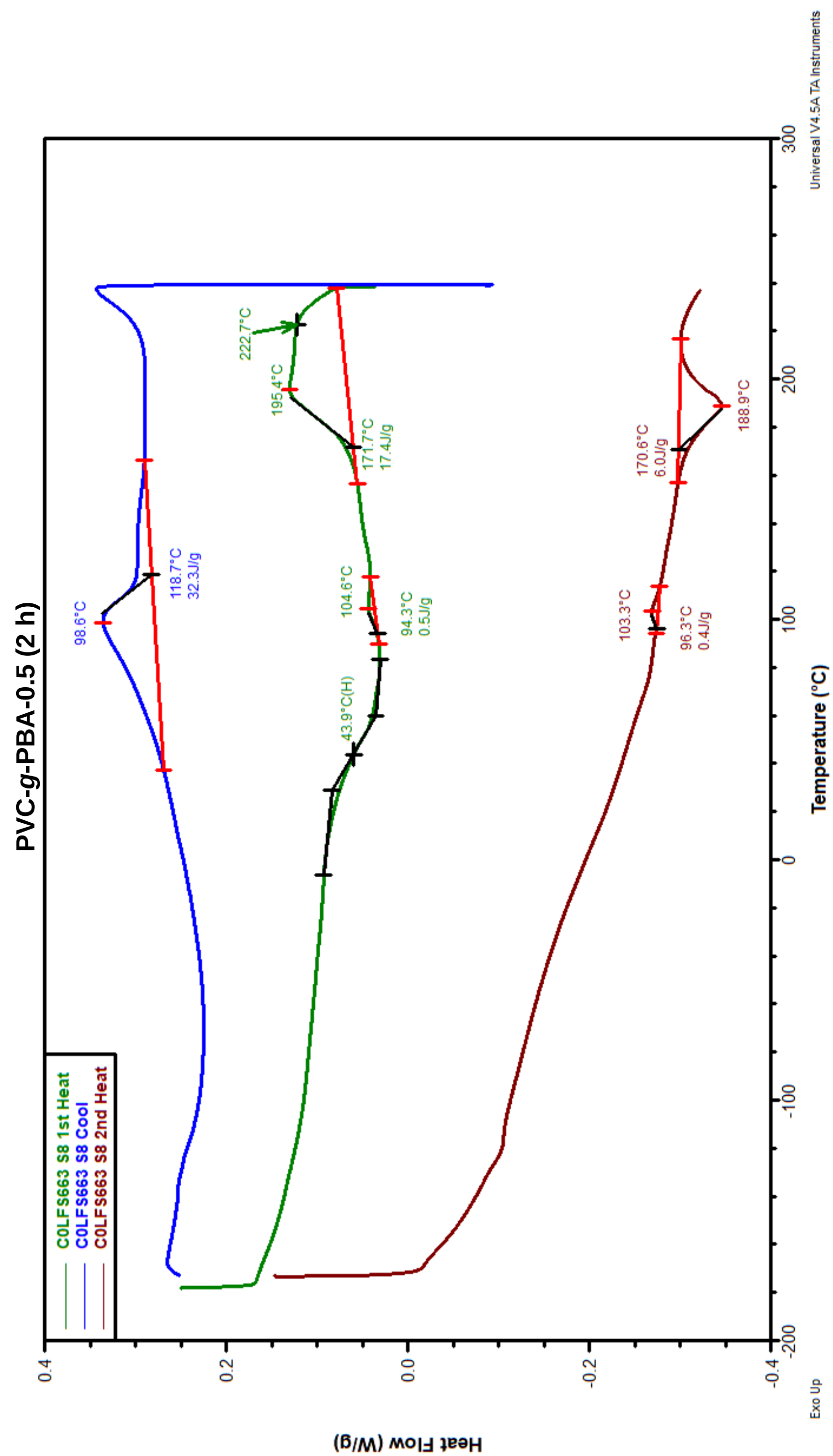
PVC-g-PBA-0.5 (2 h)
C0LFS663 S8 1st Heat
C0LFS663 S8 Cool
C0LFS663 S8 2nd Heat
98.6°C
118.7°C
32.3J/g
222.7°C
195.4°C
171.7°C
17.4J/g
104.6°C
94.3°C
0.5J/g
43.9°C(H)
103.3°C
96.3°C
0.4J/g
170.6°C
6.0J/g
188.9°C
Heat Flow (W/g)
Temperature (°C)
Exo Up
Universal V4.5A TA Instruments

PVC-*g*-PBA-0.5 (2 h)

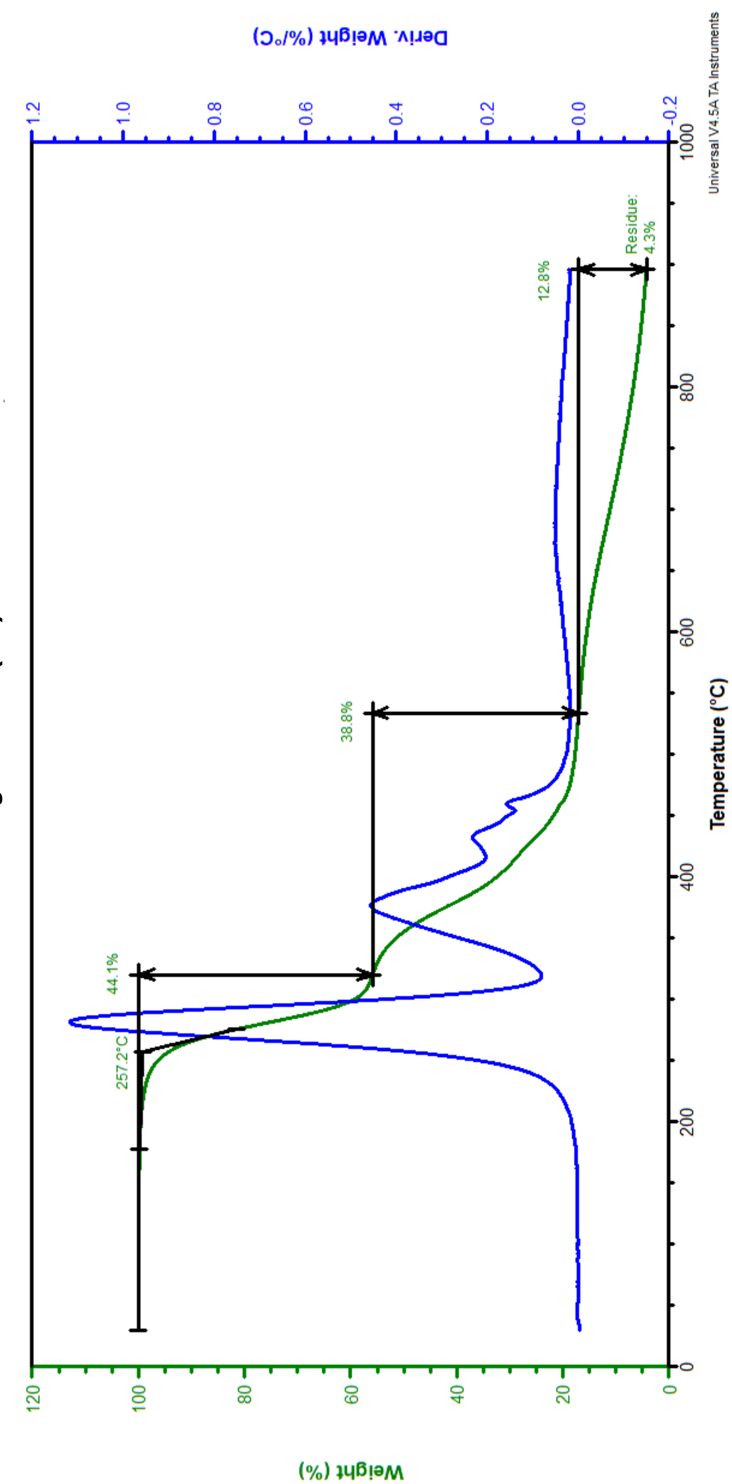

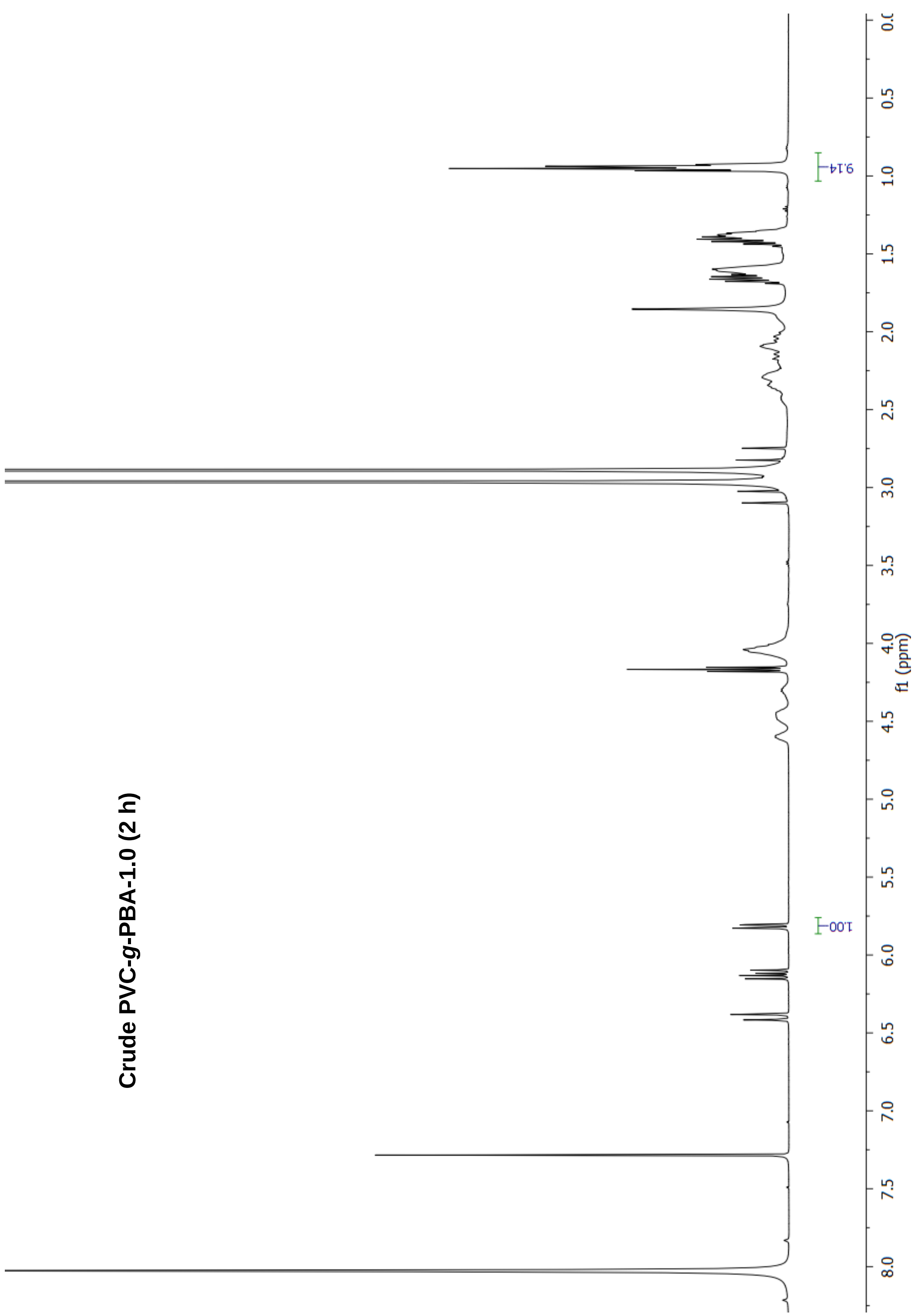
Crude PVC-*g*-PBA-1.0 (2 h)
9.14
1.00
0.0
0.5
1.0
1.5
2.0
2.5
3.0
3.5
4.0
4.5
5.0
5.5
6.0
6.5
7.0
7.5
8.0
f1 (ppm)

PVC-*g*-PBA-1.0 (2 h)

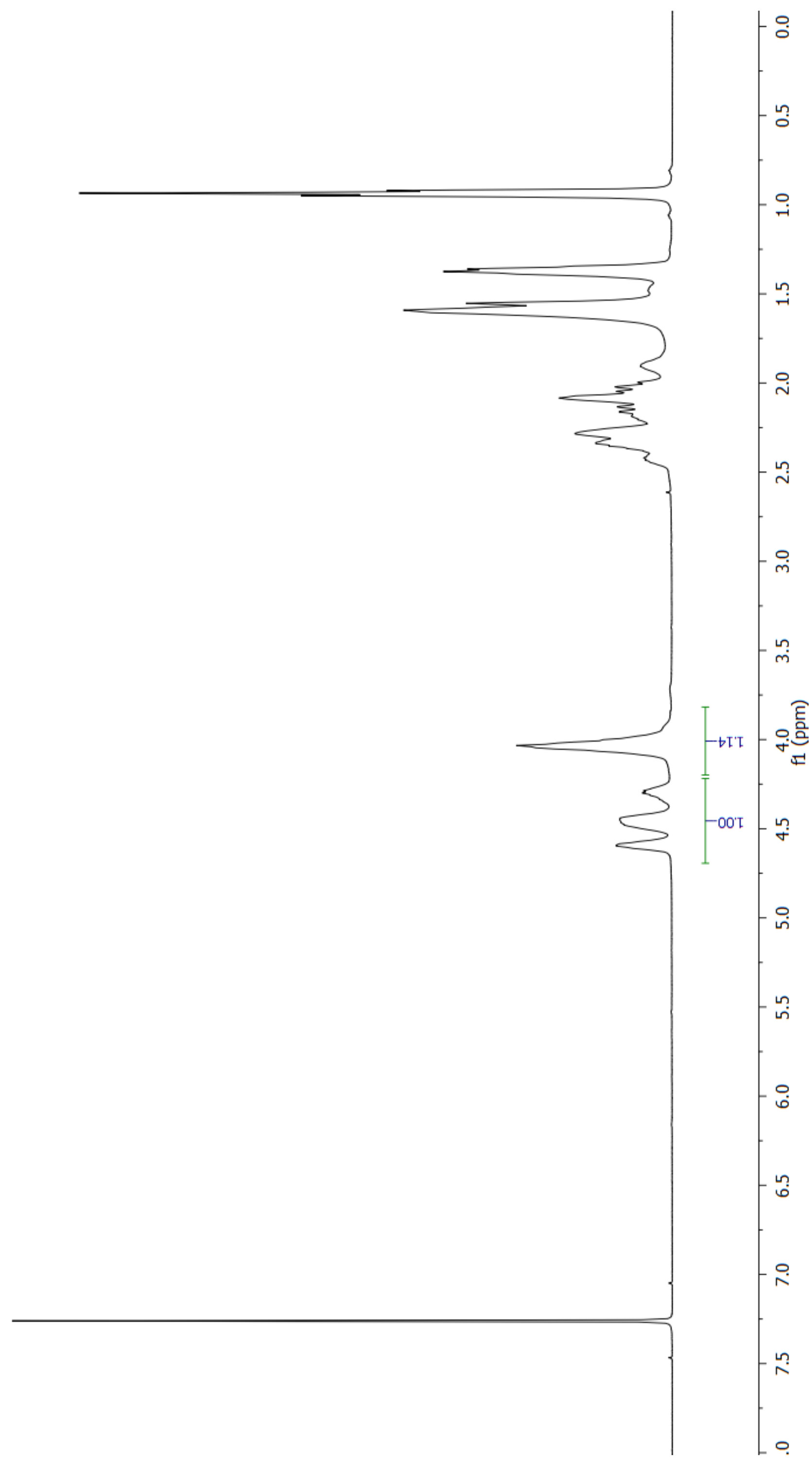

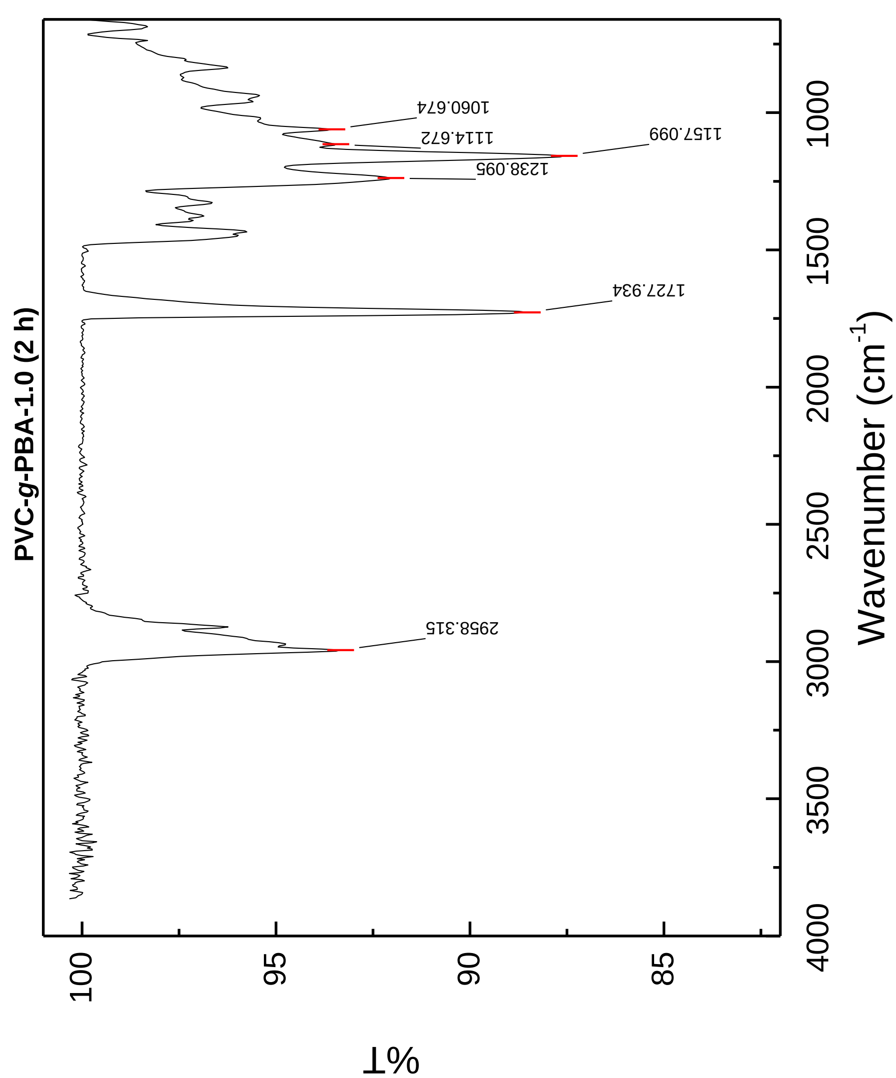
PVC-g-PBA-1.0 (2 h)
%T
Wavenumber (cm-1)
100
95
90
85
4000
3500
3000
2500
2000
1500
1000
2958.315
1727.934
1238.095
1157.099
1114.672
1060.674

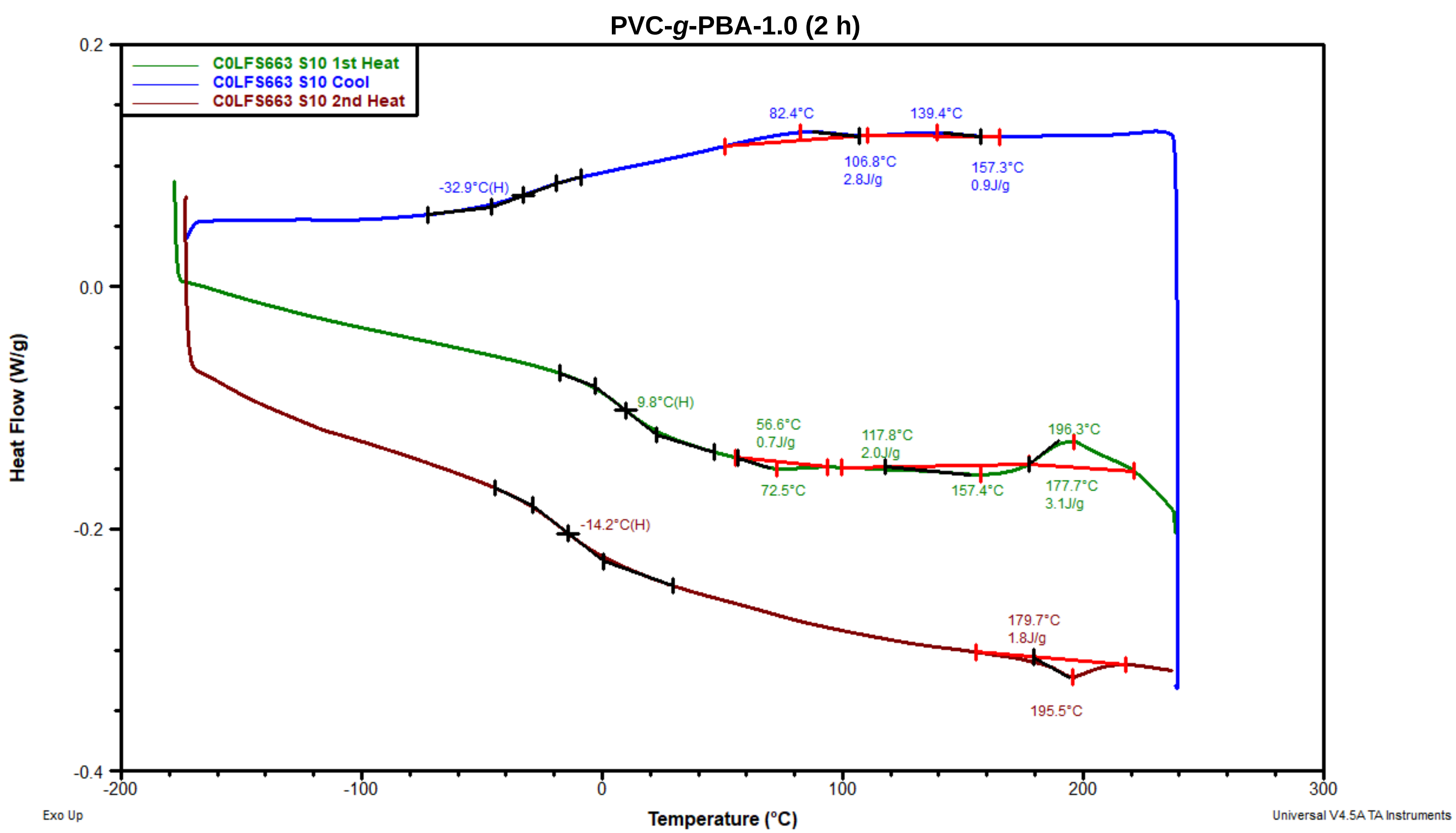

PVC-g-PBA-1.0 (2 h)
C0LFS663 S10 1st Heat
C0LFS663 S10 Cool
C0LFS663 S10 2nd Heat
0.2
0.0
-0.2
-0.4
Heat Flow (W/g)
-200
-100
0
100
200
300
Temperature (°C)
Exo Up
Universal V4.5A TA Instruments
82.4°C
139.4°C
106.8°C
2.8J/g
157.3°C
0.9J/g
-32.9°C(H)
9.8°C(H)
56.6°C
0.7J/g
117.8°C
2.0J/g
196.3°C
72.5°C
157.4°C
177.7°C
3.1J/g
-14.2°C(H)
179.7°C
1.8J/g
195.5°C

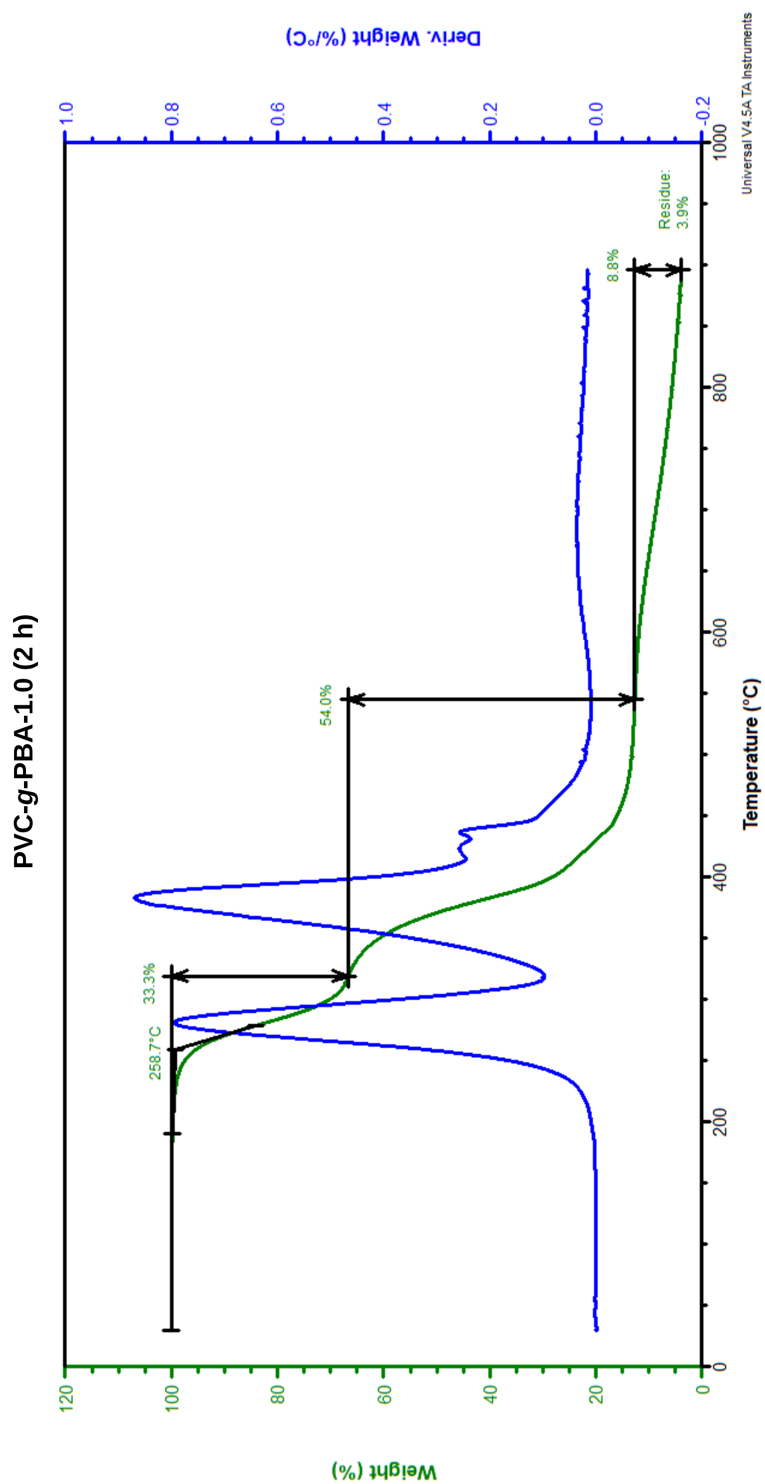

PVC-g-PBA-1.0 (2 h)
Weight (%)
Deriv. Weight (%/°C)
Temperature (°C)
258.7°C
33.3%
54.0%
8.8%
Residue:
3.9%
0
200
400
600
800
1000
0
20
40
60
80
100
120
-0.2
0.0
0.2
0.4
0.6
0.8
1.0
Universal V4.5A TA Instruments

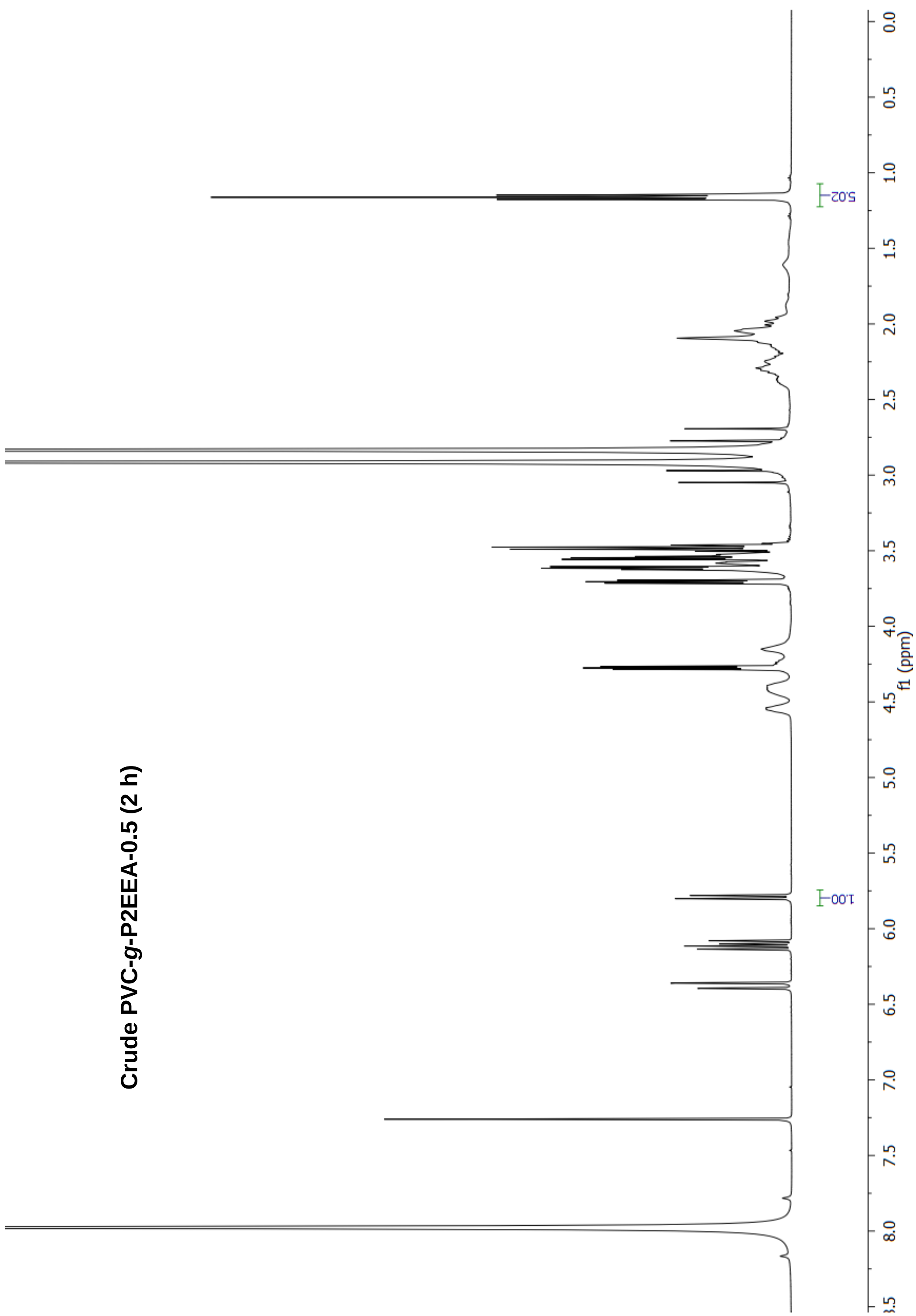
Crude PVC-g-P2EEA-0.5 (2 h)
5.02
1.00
f1 (ppm)
0.0
0.5
1.0
1.5
2.0
2.5
3.0
3.5
4.0
4.5
5.0
5.5
6.0
6.5
7.0
7.5
8.0
8.5

PVC-*g*-P2EEA-0.5 (2 h)

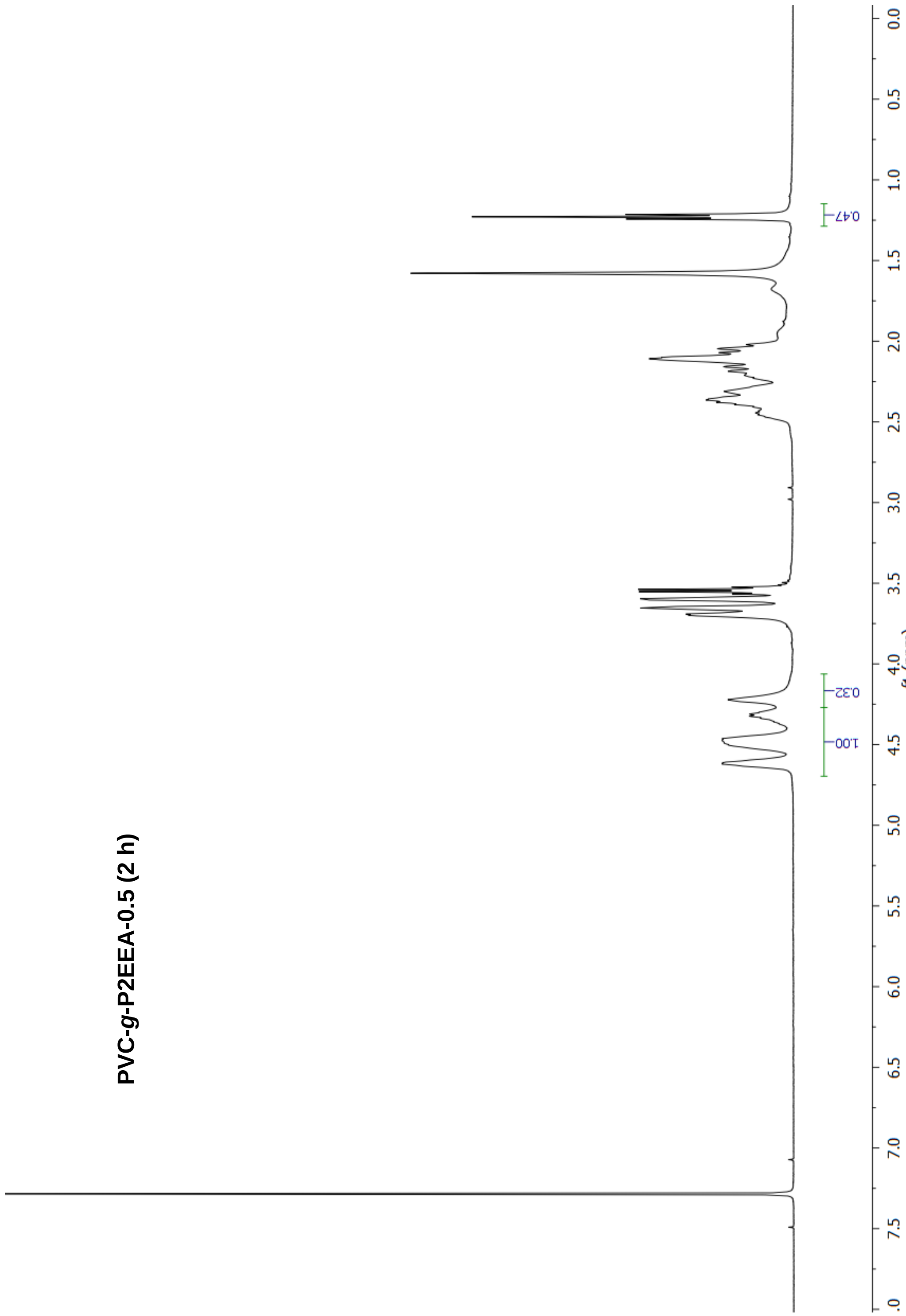

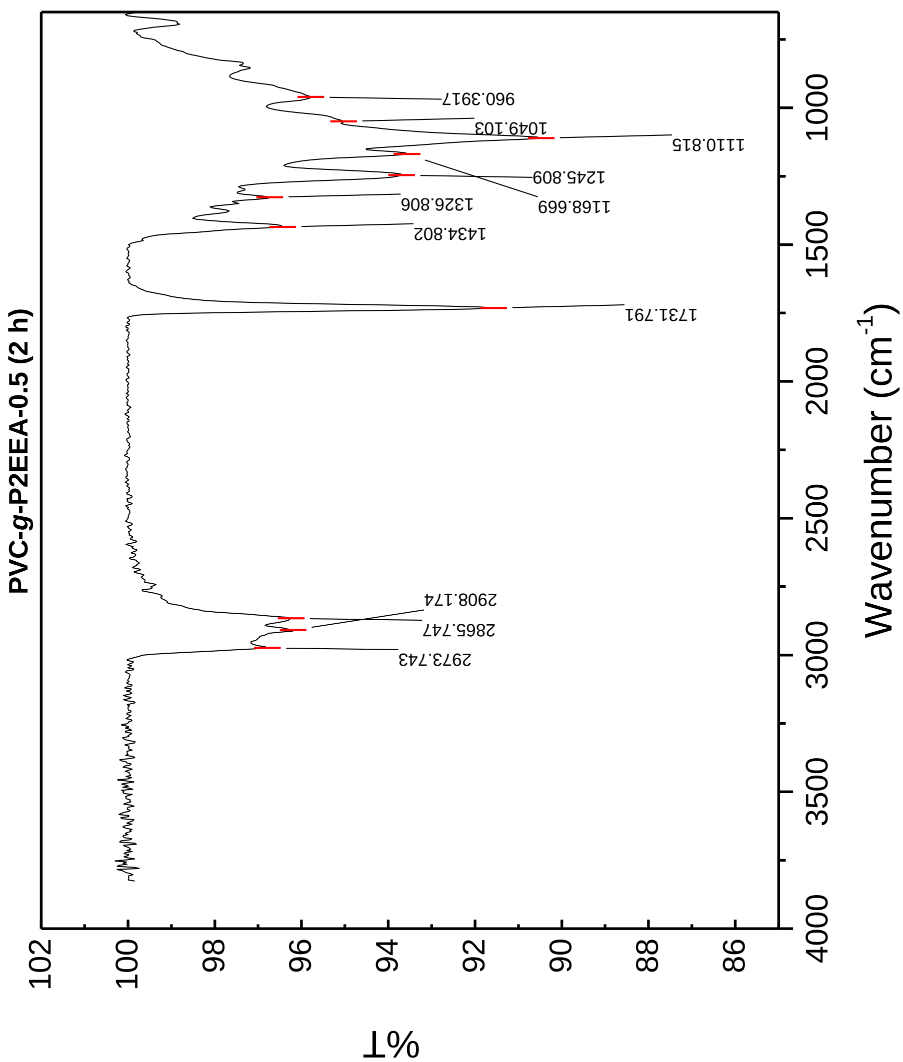
PVC-g-P2EEA-0.5 (2 h)
960.3917
1049.103
1110.815
1245.809
1168.669
1326.806
1434.802
1731.791
2908.174
2865.747
2973.743
Wavenumber (cm-1)
%T

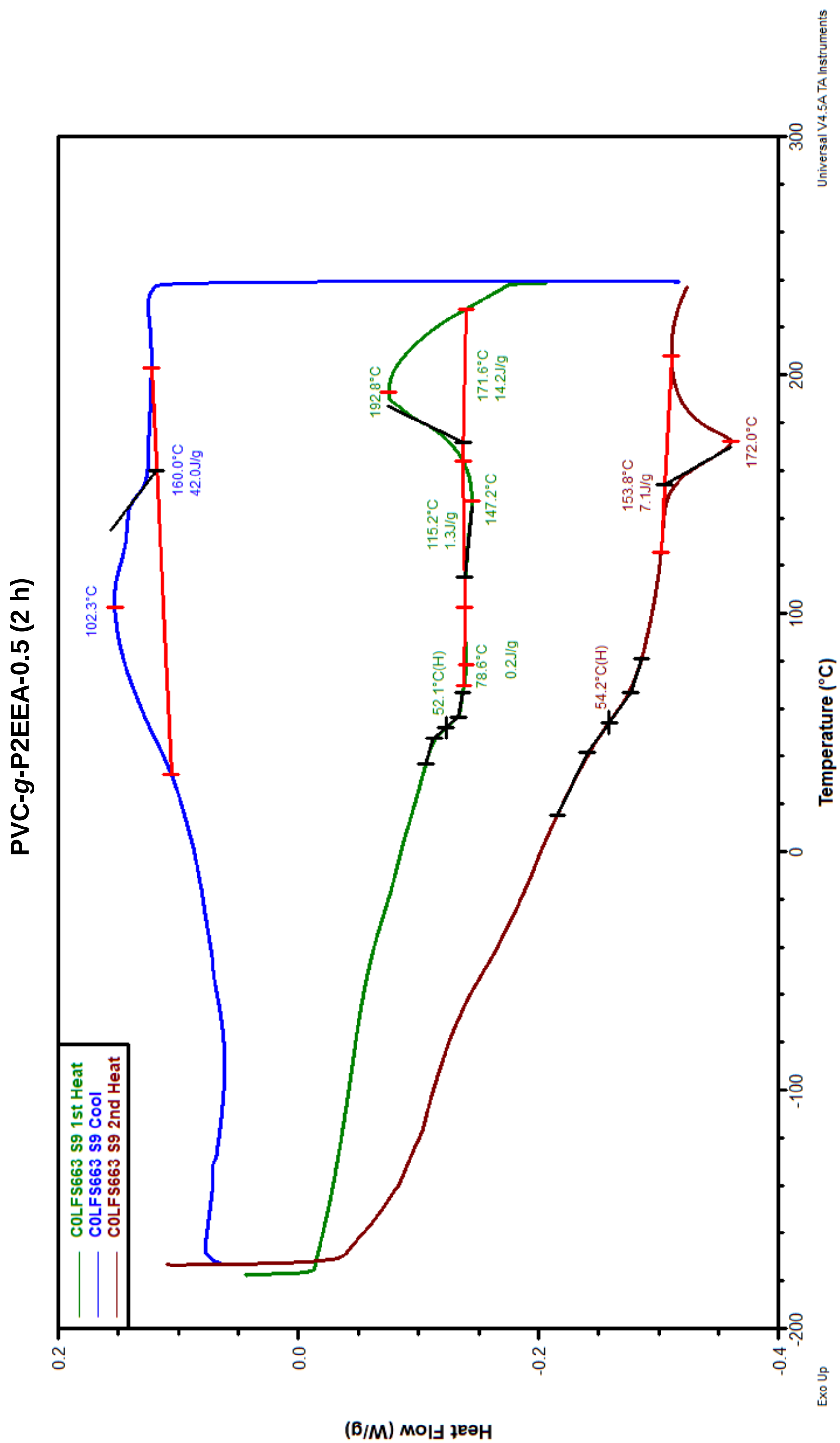
PVC-g-P2EEA-0.5 (2 h)
C0LFS663 S9 1st Heat
C0LFS663 S9 Cool
C0LFS663 S9 2nd Heat
102.3°C
160.0°C
42.0J/g
192.8°C
171.6°C
14.2J/g
115.2°C
1.3J/g
147.2°C
52.1°C(H)
78.6°C
0.2J/g
54.2°C(H)
153.8°C
7.1J/g
172.0°C
Heat Flow (W/g)
Temperature (°C)
Exo Up
Universal V4.5A TA Instruments
0.2
0.0
-0.2
-0.4
-200
-100
0
100
200
300

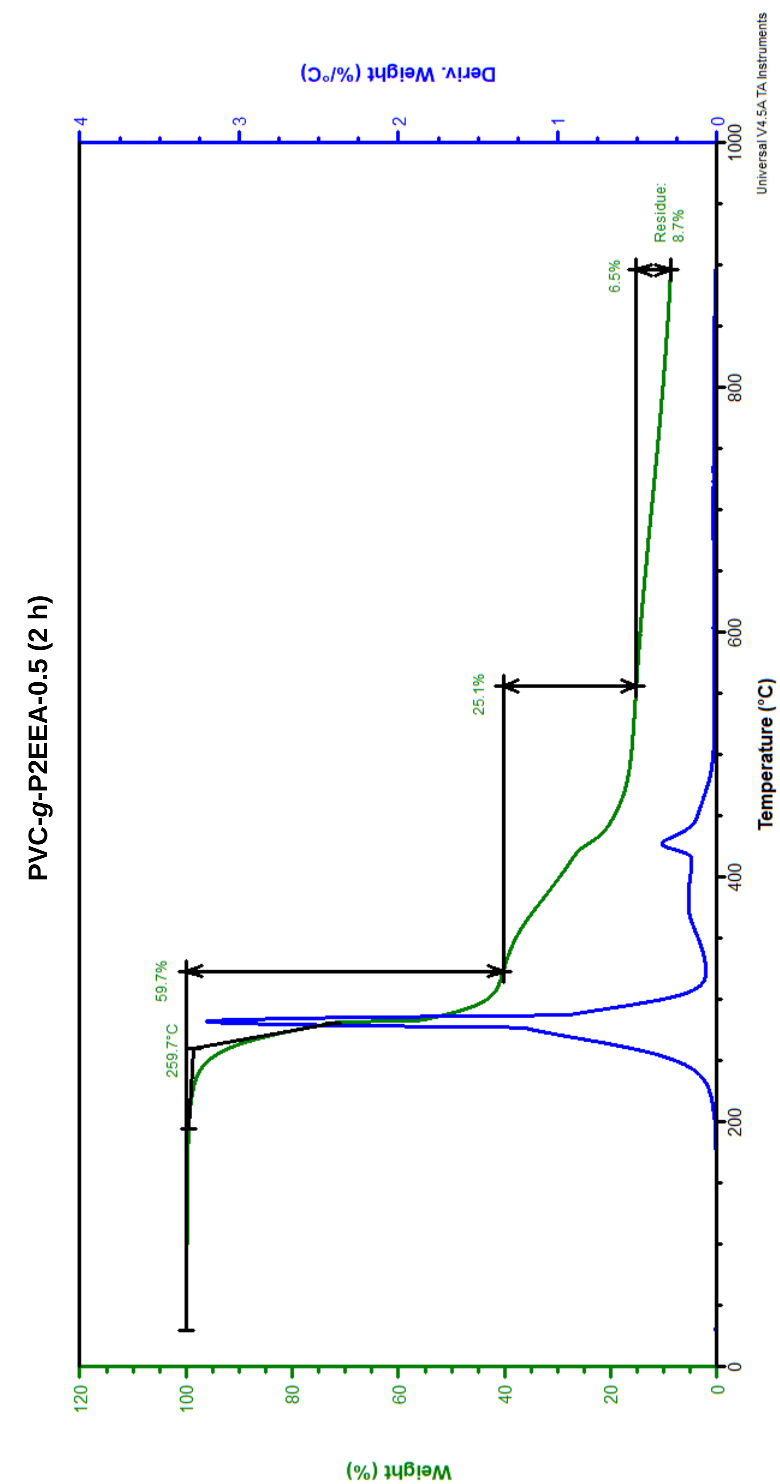

PVC-g-P2EEA-0.5 (2 h)
Weight (%)
Deriv. Weight (%/°C)
Temperature (°C)
259.7°C
59.7%
25.1%
6.5%
Residue:
8.7%
Universal V4.5A TA Instruments

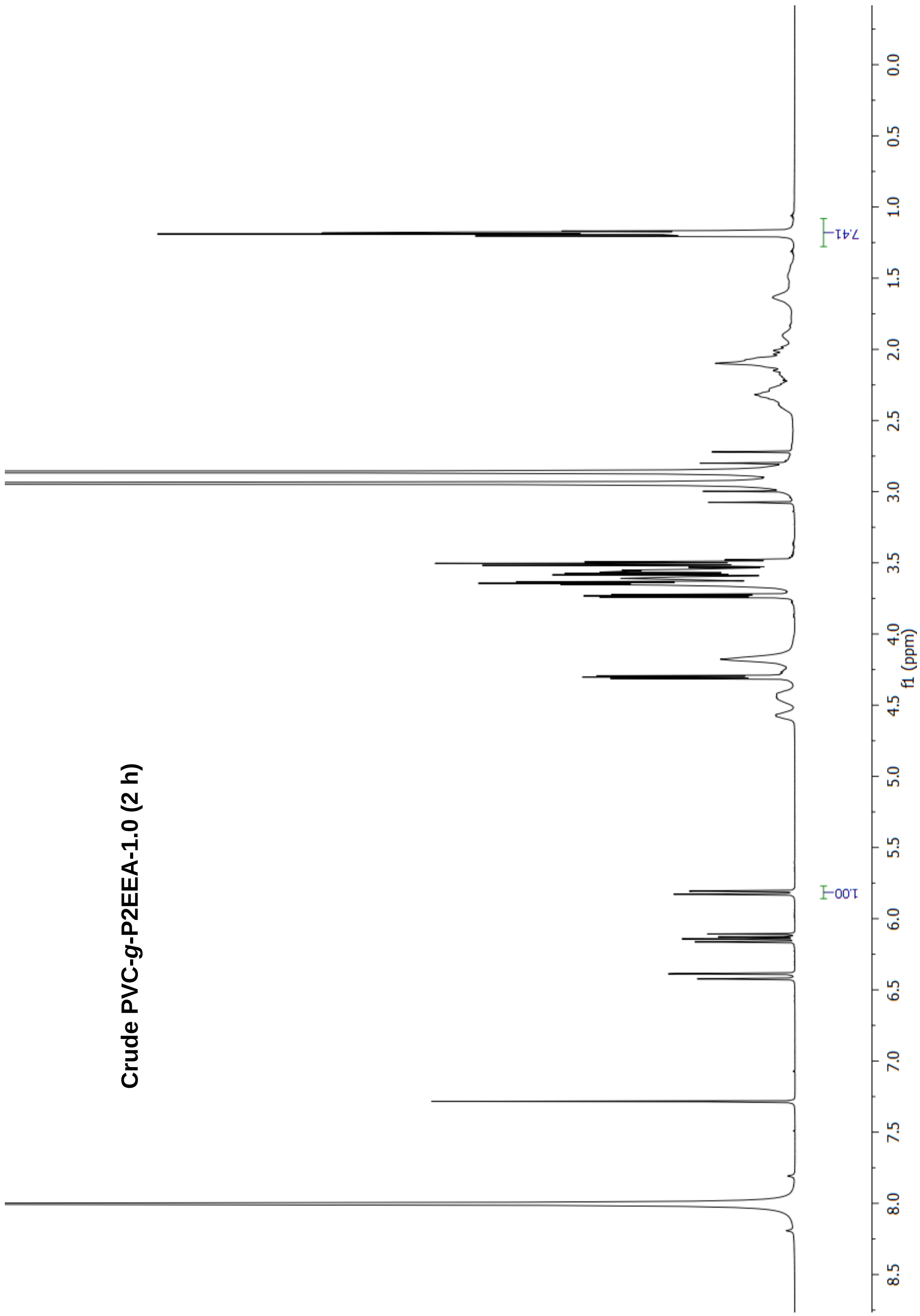
Crude PVC-*g*-P2EEA-1.0 (2 h)
7.41
1.00
8.5
8.0
7.5
7.0
6.5
6.0
5.5
5.0
4.5
4.0
3.5
3.0
2.5
2.0
1.5
1.0
0.5
0.0
f1 (ppm)

PVC-*g*-P2EEA-1.0 (2 h)

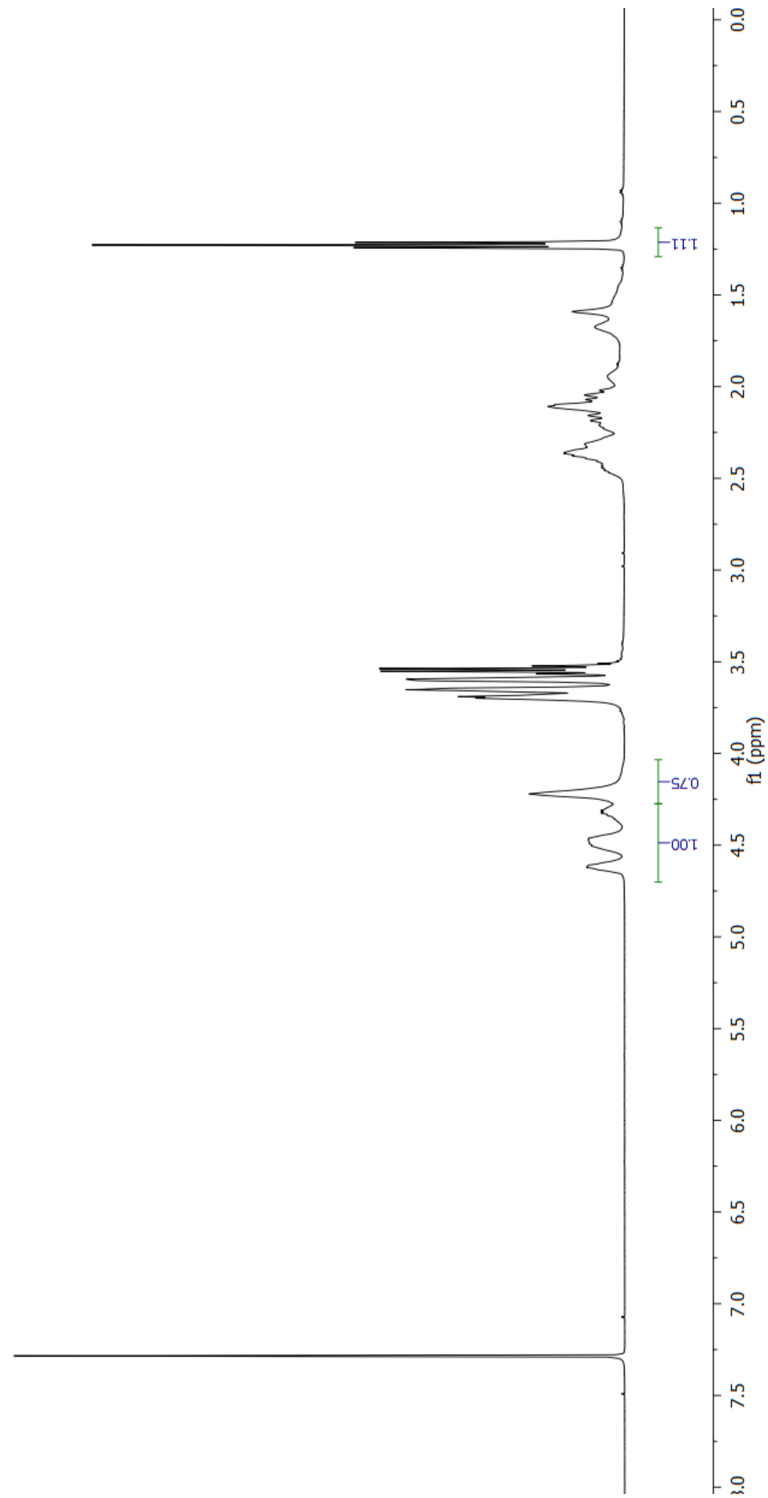

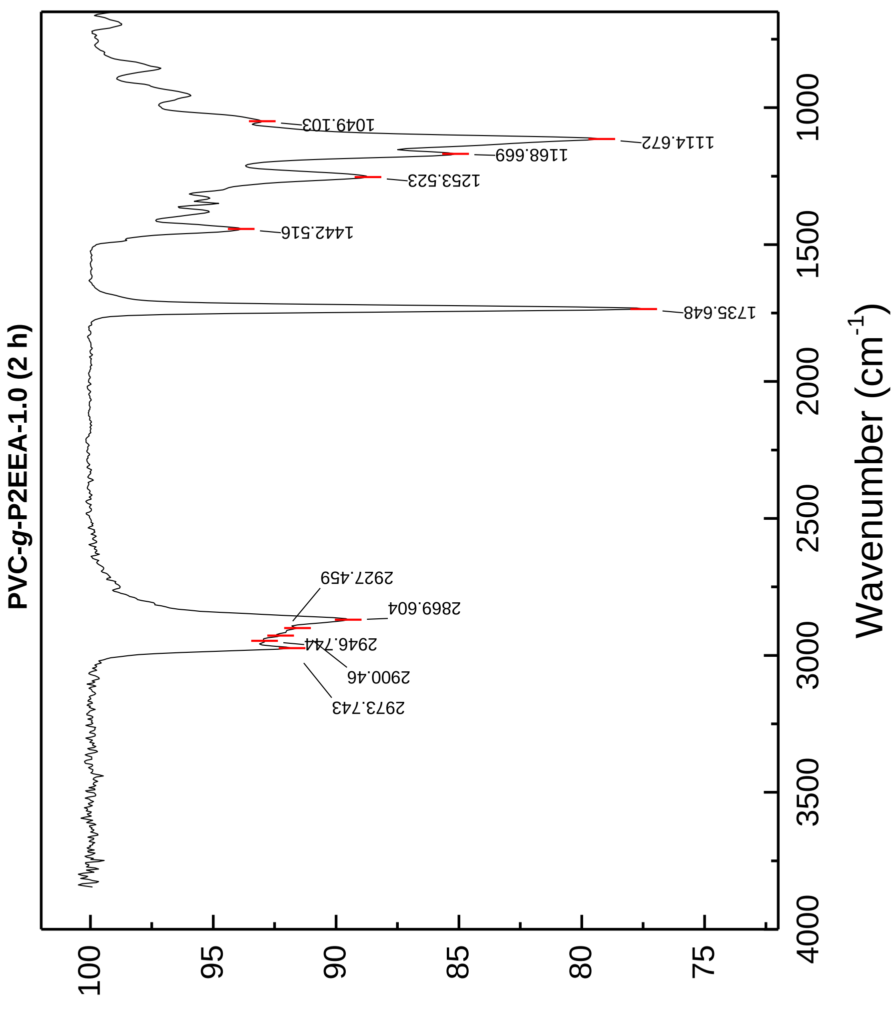
PVC-g-P2EEA-1.0 (2 h)
%T
Wavenumber (cm-1)
100
95
90
85
80
75
4000
3500
3000
2500
2000
1500
1000
1049.103
1114.672
1168.669
1253.523
1442.516
1735.648
2927.459
2869.604
2946.744
2900.46
2973.743

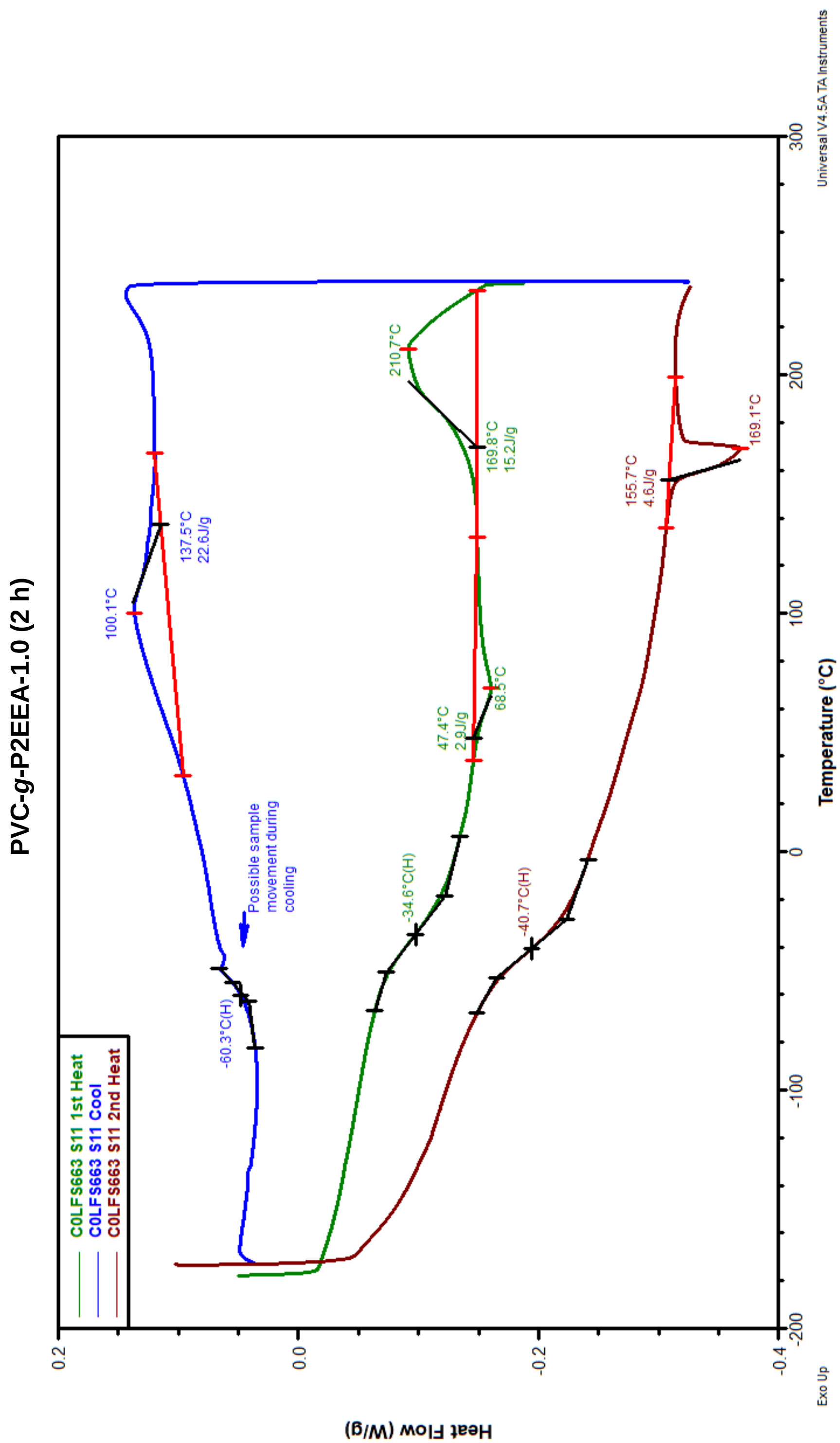
PVC-g-P2EEA-1.0 (2 h)
C0LFS663 S11 1st Heat
C0LFS663 S11 Cool
C0LFS663 S11 2nd Heat
Heat Flow (W/g)
Temperature (°C)
Exo Up
Universal V4.5A TA Instruments
Possible sample movement during cooling
-60.3°C(H)
100.1°C
137.5°C
22.6J/g
-34.6°C(H)
47.4°C
2.9J/g
68.5°C
169.8°C
15.2J/g
210.7°C
-40.7°C(H)
155.7°C
4.6J/g
169.1°C
0.2
0.0
-0.2
-0.4
-200
-100
0
100
200
300

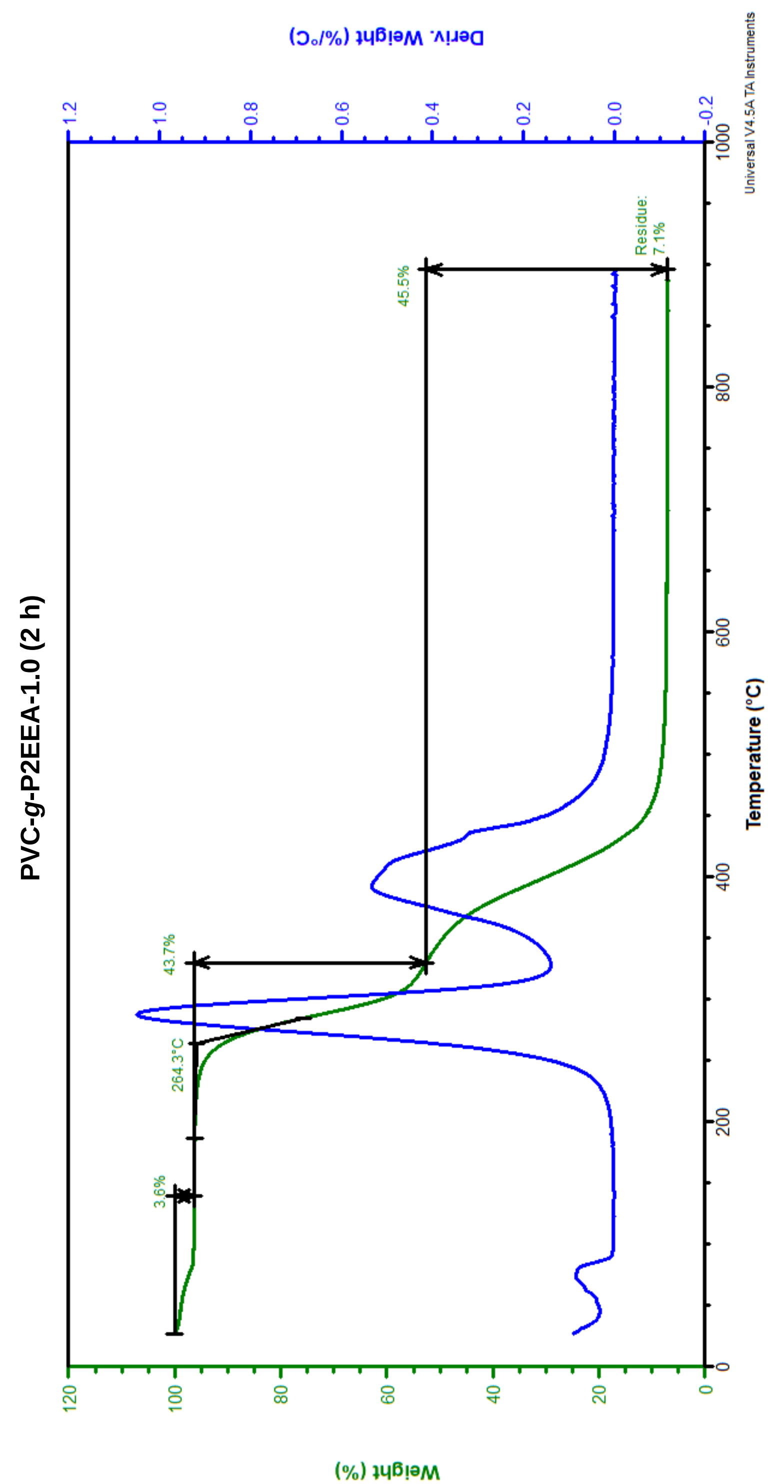
PVC-g-P2EEA-1.0 (2 h)
Deriv. Weight (%/°C)
Weight (%)
Temperature (°C)
3.6%
264.3°C
43.7%
45.5%
Residue:
7.1%
Universal V4.5A TA Instruments

Bibliography

Ahn, S. H., Seo, J. A., Kim, J. H., Ko, Y., & Hong, S. U. (2009). Synthesis and gas permeation properties of amphiphilic graft copolymer membranes. *Journal of Membrane Science*, *345*(1), 128–133. https://doi.org/10.1016/j.memsci.2009.08.037

Aubrey D. Jenkins, Richard G. Jones, & Graeme Moad. (2009). Terminology for reversible-deactivation radical polymerization previously called "controlled" radical or "living" radical polymerization (IUPAC Recommendations 2010). *Pure and Applied Chemistry*, *82*(2), 483–491. https://doi.org/10.1351/PAC-REP-08-04-03

Azzam, T., & Eisenberg, A. (2006). Control of Vesicular Morphologies through Hydrophobic Block Length. *Angewandte Chemie International Edition*, *45*(44), 7443–7447. https://doi.org/10.1002/anie.200602897

Bacaloglu, R., & Fisch, M. (1994a). Degradation and stabilization of poly(vinyl chloride). I. Kinetics of the thermal degradation of poly(vinyl chloride). *Polymer Degradation and Stability*, *45*(3), 301–313. https://doi.org/10.1016/0141-3910(94)90200-3

Bacaloglu, R., & Fisch, M. (1994b). Degradation and stabilization of poly(vinyl chloride). II. Simulation of the poly(vinyl chloride) degradation processes initiated in the polymer backbone. *Polymer Degradation and Stability*, *45*(3), 315–324. https://doi.org/10.1016/0141-3910(94)90201-1

Bacaloglu, R., & Fisch, M. (1994c). Degradation and stabilization of poly(vinyl chloride). III. Correlation of activation enthalpies and entropies for dehydrochlorination of chloroalkanes, chloralkenes and poly(vinyl chloride). *Polymer Degradation and Stability*, *45*(3), 325–338. https://doi.org/10.1016/0141-3910(94)90202-X

Barnard, D., Bateman, L., & Cunneen, J. I. (1961). CHAPTER 21—OXIDATION OF ORGANIC SULFIDES A2—KHARASCH, N. In *Organic Sulfur Compounds* (pp. 229–247). Pergamon. https://doi.org/10.1016/B978-1-4831-9982-5.50024-5

Baumann, E. (1872). Ueber einige Vinylverbindungen. *Annalen Der Chemie Und Pharmacie*, *163*, 308–322. https://doi.org/10.1002/jlac.18721630303

Bellucci, M. C., Marcelli, T., Scaglioni, L., & Volonterio, A. (2011). Synthesis of diverse spiroisoxazolidinohydantoins by totally regio-and diasteroselective 1, 3-dipolar cycloadditions. *RSC Advances*, *1*(7), 1250–1264.

Bernard, L., Cueff, R., Breysse, C., Décaudin, B., & Sautou, V. (2015). Migrability of PVC plasticizers from medical devices into a simulant of infused solutions. *International Journal of Pharmaceutics*, *485*(1), 341–347. https://doi.org/10.1016/j.ijpharm.2015.03.030

Bicak, N., Karagoz, B., & Emre, D. (2006). Atom transfer graft copolymerization of 2-ethyl hexylacrylate from labile chlorines of poly(vinyl chloride) in an aqueous suspension. *Journal of Polymer Science Part A: Polymer Chemistry*, *44*(6), 1900–1907. https://doi.org/10.1002/pola.21298

Bicak, N., & Ozlem, M. (2003). Graft copolymerization of butyl acrylate and 2-ethyl hexyl acrylate from labile chlorines of poly(vinyl chloride) by atom transfer radical polymerization. *Journal of Polymer Science Part A: Polymer Chemistry*, *41*(21), 3457–3462. https://doi.org/10.1002/pola.10944

Breme, F., Buttstaedt, J., & Emig, G. (2000). Coating of polymers with titanium-based layers by a novel plasma-assisted chemical vapor deposition process. *International Conference on Metallurgic Coatings and Thin Films*, *377–378*, 755–759. https://doi.org/10.1016/S0040-6090(00)01329-8

Bui, T. T., Giovanoulis, G., Cousins, A. P., Magnér, J., Cousins, I. T., & de Wit, C. A. (2016). Human exposure, hazard and risk of alternative plasticizers to phthalate esters. *Science of The Total Environment*, *541*(Supplement C), 451–467. https://doi.org/10.1016/j.scitotenv.2015.09.036

Carroll, W. F., Johnson, R. W., Moore, S. S., & Paradis, R. A. (2017). 4—Poly(Vinyl Chloride). In M. Kutz (Ed.), *Applied Plastics Engineering Handbook (Second Edition)* (pp. 73–89). William Andrew Publishing. https://doi.org/10.1016/B978-0-323-39040-8.00004-3

Chang, Y., Pan, M., Yuan, J., Liu, Y., Wang, X., Jiang, P., Wang, Y., Zhong, G.-J., & Li, Z.-M. (2015). Morphology and film performance of phthalate-free plasticized poly(vinyl chloride) composite particles via the graft copolymerization of acrylate swelling flower-like latex particles. *RSC Advances*, *5*(50), 40076–40087. https://doi.org/10.1039/C5RA04747A

Chen, X., Xu, S., Tan, T., Lee, S. T., Cheng, S. H., Lee, F. W. F., Xu, S. J. L., & Ho, K. C. (2014). Toxicity and Estrogenic Endocrine Disrupting Activity of Phthalates and Their Mixtures. *International Journal of Environmental Research and Public Health*, *11*(3), 3156–3168.

Chiellini, F., Ferri, M., Morelli, A., Dipaola, L., & Latini, G. (2013). Perspectives on alternatives to phthalate plasticized poly(vinyl chloride) in medical devices applications. *Progress in Polymer Science*, *38*(7), 1067–1088. https://doi.org/10.1016/j.progpolymsci.2013.03.001

Choi, J., & Kwak, S.-Y. (2007). Hyperbranched Poly(ε-caprolactone) as a Nonmigrating Alternative Plasticizer for Phthalates in Flexible PVC. *Environmental Science & Technology*, *41*(10), 3763–3768. https://doi.org/10.1021/es062715t

Chu, H., & Ma, J. (2018). A strategy to prepare internally plasticized PVC using a castor oil based derivative. *Korean Journal of Chemical Engineering*, *35*(11), 2296–2302. https://doi.org/10.1007/s11814-018-0118-5

Clark, F. W. (1941). Plasticizers. *Chemistry & Industry (London, U. K.)*, 228–230.

Cobellis, L., Latini, G., Felice, C. D., Razzi, S., Paris, I., Ruggieri, F., Mazzeo, P., & Petraglia, F. (2003). High plasma concentrations of di-(2-ethylhexyl)-phthalate in women with endometriosis. *Human Reproduction*, *18*(7), 1512–1515. https://doi.org/10.1093/humrep/deg254

Coelho, J. F. J., Carreira, M., Gonçalves, P. M. O. F., Popov, A. V., & Gil, M. H. (2006). Processability and characterization of poly(vinyl chloride)-b-poly(n-butyl acrylate)-b-poly(vinyl chloride) prepared by living radical polymerization of vinyl chloride. Comparison with a flexible commercial resin formulation prepared with PVC and dioctyl phthalate. *Journal of Vinyl and Additive Technology*, *12*(4), 156–165. https://doi.org/10.1002/vnl.20088

Coelho, J. F. J., Carreira, M., Popov, A. V., Gonçalves, P. M. O. F., & Gil, M. H. (2006). Thermal and mechanical characterization of poly(vinyl chloride)-b-poly(butyl acrylate)-b-poly(vinyl chloride) obtained by single electron transfer – degenerative chain transfer living radical polymerization in water. *European Polymer Journal*, *42*(10), 2313–2319. https://doi.org/10.1016/j.eurpolymj.2006.05.023

Coelho, J. F. J., Silva, A. M. F. P., Popov, A. V., Percec, V., Abreu, M. V., Gonçalves, P. M. O. F., & Gil, M. H. (2006). Single electron transfer–degenerative chain transfer living radical polymerization of N-butyl acrylate catalyzed by $Na_2S_2O_4$ in water media. *Journal of Polymer Science Part A: Polymer Chemistry*, *44*(9), 2809–2825. https://doi.org/10.1002/pola.21389

Coşkun, M., Barim, G., & Demirelli, K. (2007). A Grafting Study on Partially Dehydrochlorinated Poly(vinyl chloride) by Atom Transfer Radical Polymerization. *Journal of Macromolecular Science, Part A*, *44*(5), 475–481. https://doi.org/10.1080/10601320701229068

Crocker, J. F. S., Safe, S. H., & Acott, P. (1988). Effects of chronic phthalate exposure on the kidney. *Journal of Toxicology and Environmental Health*, *23*(4), 433–444. https://doi.org/10.1080/15287398809531126

Dalgaard, M., Nellemann, C., Lam, H. R., Sørensen, I. K., & Ladefoged, O. (2001). The acute effects of mono(2-ethylhexyl)phthalate (MEHP) on testes of prepubertal Wistar rats. *Toxicology Letters*, *122*(1), 69–79. https://doi.org/10.1016/S0378-4274(01)00348-4

David, R. M., Moore, M. R., Finney, D. C., & Guest, D. (2000a). Chronic Toxicity of Di(2-ethylhexyl)phthalate in Rats. *Toxicological Sciences*, *55*(2), 433–443. https://doi.org/10.1093/toxsci/55.2.433

David, R. M., Moore, M. R., Finney, D. C., & Guest, D. (2000b). Chronic Toxicity of Di(2-ethylhexyl)phthalate in Mice. *Toxicological Sciences*, *58*(2), 377–385. https://doi.org/10.1093/toxsci/58.2.377

de Sainte Claire, P. (2009). Degradation of PEO in the Solid State: A Theoretical Kinetic Model. *Macromolecules*, *42*(10), 3469–3482. https://doi.org/10.1021/ma802469u

Dean, L., Dafei, Z., & Deren, Z. (1988). Mechanism and kinetics of thermo-dehydrochlorination of poly(vinyl chloride). *Polymer Degradation and Stability*, *22*(1), 31–41. https://doi.org/10.1016/0141-3910(88)90054-7

Demirci, G., & Tasdelen, M. A. (2015a). Synthesis and characterization of graft copolymers by photoinduced CuAAC click chemistry. *European Polymer Journal*, *66*(Supplement C), 282–289. https://doi.org/10.1016/j.eurpolymj.2015.02.029

Demirci, G., & Tasdelen, M. A. (2015b). Synthesis and characterization of graft copolymers by photoinduced CuAAC click chemistry. *European Polymer Journal*, *66*, 282–289. https://doi.org/10.1016/j.eurpolymj.2015.02.029

Dimarzio, E. A., & Gibbs, J. H. (1963). Molecular interpretation of glass temperature depression by plasticizers. *Journal of Polymer Science Part A: General Papers*, *1*(4), 1417–1428. https://doi.org/10.1002/pol.1963.100010428

Earla, A., & Braslau, R. (2014). Covalently Linked Plasticizers: Triazole Analogues of Phthalate Plasticizers Prepared by Mild Copper-Free “Click” Reactions with Azide-Functionalized

PVC. *Macromolecular Rapid Communications*, *35*(6), 666–671. https://doi.org/10.1002/marc.201300865

Earla, A., Li, L., Costanzo, P., & Braslau, R. (2017). Phthalate plasticizers covalently linked to PVC via copper-free or copper catalyzed azide-alkyne cycloadditions. *Polymer*, *109*, 1–12. https://doi.org/10.1016/j.polymer.2016.12.014

Ess, D. H., & Houk, K. N. (2008). Theory of 1,3-Dipolar Cycloadditions: Distortion/Interaction and Frontier Molecular Orbital Models. *Journal of the American Chemical Society*, *130*(31), 10187–10198. https://doi.org/10.1021/ja800009z

Fang, L.-F., Matsuyama, H., Zhu, B.-K., & Zhao, S. (2018). Development of antifouling poly(vinyl chloride) blend membranes by atom transfer radical polymerization. *Journal of Applied Polymer Science*, *135*(6), 45832. https://doi.org/10.1002/app.45832

Fierens, T., Van Holderbeke, M., Willems, H., De Henauw, S., & Sioen, I. (2013). Transfer of eight phthalates through the milk chain—A case study. *Environment International*, *51*(Supplement C), 1–7. https://doi.org/10.1016/j.envint.2012.10.002

Fisch, M. H., & Bacaloglu, R. (1995). Kinetics and mechanism of the thermal degradation of poly(vinyl chloride). *Journal of Vinyl and Additive Technology*, *1*(4), 233–240. https://doi.org/10.1002/vnl.730010409

Fox, T. G. (1956). Influence of Diluent and of Copolymer Composition on the Glass Temperature of a Polymer System. *Bull. Am. Phs. Soc*, *1*, 123.

Fox, T. G., & Flory, P. J. (1950). Second-Order Transition Temperatures and Related Properties of Polystyrene. I. Influence of Molecular Weight. *Journal of Applied Physics*, *21*(6), 581–591. https://doi.org/10.1063/1.1699711

Fromme, H., Gruber, L., Seckin, E., Raab, U., Zimmermann, S., Kiranoglu, M., Schlummer, M., Schwegler, U., Smolic, S., & Völkel, W. (2011). Phthalates and their metabolites in breast milk—Results from the Bavarian Monitoring of Breast Milk (BAMBI). *Environment International*, *37*(4), 715–722. https://doi.org/10.1016/j.envint.2011.02.008

Golshan, M., Hatef, A., Socha, M., Milla, S., Butts, I. A. E., Carnevali, O., Rodina, M., Sokołowska-Mikołajczyk, M., Fontaine, P., Linhart, O., & Alavi, S. M. H. (2015). Di-(2-ethylhexyl)-phthalate disrupts pituitary and testicular hormonal functions to reduce sperm quality in mature goldfish. *Aquatic Toxicology*, *163*(Supplement C), 16–26. https://doi.org/10.1016/j.aquatox.2015.03.017

Gorobets, N. Yu., Yermolayev, S. A., Gurley, T., Gurinov, A. A., Tolstoy, P. M., Shenderovich, I. G., & Leadbeater, N. E. (2012). Difference between 1H NMR signals of primary amide protons as a simple spectral index of the amide intramolecular hydrogen bond strength. *Journal of Physical Organic Chemistry*, *25*(4), 287–295. https://doi.org/10.1002/poc.1910

Grassie, N., & Speakman, J. G. (1971). Thermal degradation of poly(alkyl acrylates). I. Preliminary investigations. *Journal of Polymer Science Part A-1: Polymer Chemistry*, *9*(4), 919–929. https://doi.org/10.1002/pol.1971.150090408

Gupta, R. K., Singh, J. M., Leslie, T. C., Meachum, S., Flaws, J. A., & Yao, H. H.-C. (2010). Di-(2-ethylhexyl) phthalate and mono-(2-ethylhexyl) phthalate inhibit growth and reduce estradiol levels of antral follicles in vitro. *Toxicology and Applied Pharmacology*, *242*(2), 224–230. https://doi.org/10.1016/j.taap.2009.10.011

Hakkarainen, M. (2008). Migration of Monomeric and Polymeric PVC Plasticizers. In A.-C. Albertsson & M. Hakkarainen (Eds.), *Chromatography for Sustainable Polymeric Materials: Renewable, Degradable and Recyclable* (pp. 159–185). Springer Berlin Heidelberg. https://doi.org/10.1007/12_2008_140

Han, S., Kim, C., & Kwon, D. (1997). Thermal/oxidative degradation and stabilization of polyethylene glycol. *Polymer*, *38*(2), 317–323. https://doi.org/10.1016/S0032-3861(97)88175-X

Hannon, P. R., Brannick, K. E., Wang, W., & Flaws, J. A. (2015). Mono(2-Ethylhexyl) Phthalate Accelerates Early Folliculogenesis and Inhibits Steroidogenesis in Cultured Mouse Whole Ovaries and Antral Follicles1. *Biology of Reproduction*, *92*(120, 1–11). https://doi.org/10.1095/biolreprod.115.129148

Hassner, A., & Stern, M. (1986). Synthesis of alkyl azides with a polymeric reagent. *Angewandte Chemie International Edition in English*, *25*(5), 478–479.

Hein, J. E., & Fokin, V. V. (2010). Copper-catalyzed azide–alkyne cycloaddition (CuAAC) and beyond: New reactivity of copper(i) acetylides. *Chemical Society Reviews*, *39*(4), 1302–1315. https://doi.org/10.1039/B904091A

Henen, A. M., Hamdi, A., Farahat, A. A., & Massoud, A. M. (2017). Understanding Chemistry and Unique NMR Characters of Novel Amide and Ester Leflunomide Analogues. *Magnetochemistry*, *3*(4). https://doi.org/10.3390/magnetochemistry3040041

Heyl, D., & Fessner, W.-D. (2014). Facile Direct Synthesis of Acetylenedicarboxamides. *Synthesis*, 1463–1468.

Higa, C. M. (2018). *Non-Migratory Internal Plasticization of Poly(Vinyl Chloride) via Pendant Triazoles Bearling Alkyl or Polyether Esters*. Ph.D. Dissertation, University of California, Santa Cruz.

Higa, C. M., Tek, A. T., Wojtecki, R. J., & Braslau, R. (2018). Nonmigratory internal plasticization of poly(vinyl chloride) via pendant triazoles bearing alkyl or polyether esters. *Journal of Polymer Science Part A: Polymer Chemistry*, *56*(21), 2397–2411. https://doi.org/10.1002/pola.29205

Hjertberg, T., & Sörvik, E. M. (1983). Formation of anomalous structures in PVC and their influence on the thermal stability: 3. Internal chloroallylic groups. *Polymer*, *24*(6), 685–692. https://doi.org/10.1016/0032-3861(83)90004-6

Houwink, R. (1947). *Proceedings of the XIth International Congress of Pure and Applied Chemistry: London, 17th-24th July, 1947.*

Huang, Z., Feng, C., Guo, H., & Huang, X. (2016). Direct functionalization of poly(vinyl chloride) by photo-mediated ATRP without a deoxygenation procedure. *Polymer Chemistry*, *7*(17), 3034–3045. https://doi.org/10.1039/C6PY00483K

Huisgen, R., Grashey, R., & Sauer, J. (1964). *Chemistry of Alkenes, Interscience*. New York.

Hwang, H.-M., Park, E.-K., Young, T. M., & Hammock, B. D. (2008). Occurrence of endocrine-disrupting chemicals in indoor dust. *Science of The Total Environment*, *404*(1), 26–35. https://doi.org/10.1016/j.scitotenv.2008.05.031

IHS Markit. *Plasticizers https://ihsmarkit.com/products/plasticizers-chemical-economics-handbook.html Accessed 04/26/2020*.

IHS Markit. *Population Growth and Materials Demand Study Prepared for: American Chemistry Council https://plastics.americanchemistry.com/IHS-Economic-Growth-and-Materials-Demand-Executive-Summary.pdf Accessed 04/24/2020*.

Ito, R., Seshimo, F., Haishima, Y., Hasegawa, C., Isama, K., Yagami, T., Nakahashi, K., Yamazaki, H., Inoue, K., Yoshimura, Y., Saito, K., Tsuchiya, T., & Nakazawa, H. (2005). Reducing the migration of di-2-ethylhexyl phthalate from polyvinyl chloride medical devices. *International Journal of Pharmaceutics*, *303*(1), 104–112. https://doi.org/10.1016/j.ijpharm.2005.07.009

Iván, B., Kennedy, J. P., Kelen, T., Tüdõs, F., Nagy, T. T., & Turcsányi, B. (1983). Degradation of PVCs obtained by controlled chemical dehydrochlorination. *Journal of Polymer Science: Polymer Chemistry Edition*, *21*(8), 2177–2188. https://doi.org/10.1002/pol.1983.170210802

Jayakrishnan, A., & Sunny, M. C. (1996). Phase transfer catalysed surface modification of plasticized poly(vinyl chloride) in aqueous media to retard plasticizer migration. *Polymer*, *37*(23), 5213–5218. https://doi.org/10.1016/0032-3861(96)00501-0

Ji, L., Liao, Q., Wu, L., Lv, W., Yang, M., & Wan, L. (2013). Migration of 16 phthalic acid esters from plastic drug packaging to drugs by GC-MS. *Analytical Methods*, *5*(11), 2827–2834. https://doi.org/10.1039/C3AY40234G

Jia, P., Ma, Y., Kong, Q., Xu, L., Hu, Y., Hu, L., & Zhou, Y. (2019). Graft modification of polyvinyl chloride with epoxidized biomass-based monomers for preparing flexible polyvinyl chloride materials without plasticizer migration. *Materials Today Chemistry*, *13*, 49–58. https://doi.org/10.1016/j.mtchem.2019.04.010

Jia, P.-P., Ma, Y.-B., Lu, C.-J., Mirza, Z., Zhang, W., Jia, Y.-F., Li, W.-G., & Pei, D.-S. (2016). The Effects of Disturbance on Hypothalamus-Pituitary-Thyroid (HPT) Axis in Zebrafish Larvae after Exposure to DEHP. *PLOS ONE*, *11*(5), e0155762. https://doi.org/10.1371/journal.pone.0155762

Jia, P., Bo, C., Hu, L., Zhang, M., & Zhou, Y. (2016). Synthesis of a novel polyester plasticizer based on glyceryl monooleate and its application in poly(vinyl chloride). *Journal of Vinyl and Additive Technology*, *22*(4), 514–519. https://doi.org/10.1002/vnl.21468

Jia, P., Hu, L., Feng, G., Bo, C., Zhang, M., & Zhou, Y. (2017). PVC materials without migration obtained by chemical modification of azide-functionalized PVC and triethyl citrate plasticizer. *Materials Chemistry and Physics*, *190*, 25–30. https://doi.org/10.1016/j.matchemphys.2016.12.072

Jia, P., Hu, L., Shang, Q., Wang, R., Zhang, M., & Zhou, Y. (2017). Self-Plasticization of PVC Materials via Chemical Modification of Mannich Base of Cardanol Butyl Ether. *ACS Sustainable Chemistry & Engineering*, *5*(8), 6665–6673. https://doi.org/10.1021/acssuschemeng.7b00900

Jia, P., Hu, L., Yang, X., Zhang, M., Shang, Q., & Zhou, Y. (2017). Internally plasticized PVC materials via covalent attachment of aminated tung oil methyl ester. *RSC Advances*, *7*(48), 30101–30108. https://doi.org/10.1039/C7RA04386D

Jia, P., Wang, R., Hu, L., Zhang, M. & Zhou. Y. (2017). Self-Plasticization of PVC via click reaction of a monooctyl phthalate derivative. *Polish Journal of Chemical Technology*, *19*(3), 16–19. https://doi.org/10.1515/pjct-2017-0042

Jia, P., Ma, Y., Feng, G., Hu, L., & Zhou, Y. (2019). High-value utilization of forest resources: Dehydroabietic acid as a chemical platform for producing non-toxic and environment-friendly polymer materials. *Journal of Cleaner Production*, *227*, 662–674. https://doi.org/10.1016/j.jclepro.2019.04.220

Kelley, F. N., & Bueche, F. (1961). Viscosity and glass temperature relations for polymer-diluent systems. *Journal of Polymer Science*, *50*(154), 549–556. https://doi.org/10.1002/pol.1961.1205015421

Kim, S. H., Cho, S., Ihm, H. J., Oh, Y. S., Heo, S.-H., Chun, S., Im, H., Chae, H. D., Kim, C.-H., & Kang, B. M. (2015). Possible Role of Phthalate in the Pathogenesis of Endometriosis: In Vitro, Animal, and Human Data. *The Journal of Clinical Endocrinology & Metabolism*, *100*(12), E1502–E1511. https://doi.org/10.1210/jc.2015-2478

Kim, S. H., Chun, S., Jang, J. Y., Chae, H. D., Kim, C.-H., & Kang, B. M. (2011). Increased plasma levels of phthalate esters in women with advanced-stage endometriosis: A prospective case-control study. *Fertility and Sterility*, *95*(1), 357–359. https://doi.org/10.1016/j.fertnstert.2010.07.1059

Kirkpatrick, A. (1940). Some Relations Between Molecular Structure and Plasticizing Effect. *Journal of Applied Physics*, *11*(4), 255–261. https://doi.org/10.1063/1.1712768

Koch, H. M., Preuss, R., & Angerer, J. (2006). Di(2-ethylhexyl)phthalate (DEHP): Human metabolism and internal exposure – an update and latest results1. *International Journal of Andrology*, *29*(1), 155–165. https://doi.org/10.1111/j.1365-2605.2005.00607.x

Lakshmi, & Jayakrishnan. (1998). Migration Resistant, Blood-Compatible Plasticized Polyvinyl Chloride for [Medical and Related Applications. *Artificial Organs*, *22*(3), 222–229. https://doi.org/10.1046/j.1525-1594.1998.06124.x

Lakshmi, S., & Jayakrishnan, A. (2002). Synthesis, surface properties and performance of thiosulphate-substituted plasticized poly(vinyl chloride). *Biomaterials*, *23*(24), 4855–4862. https://doi.org/10.1016/S0142-9612(02)00243-0

Lakshmi, S., & Jayakrishnan, A. (2003). Properties and performance of sulfide-substituted plasticized poly(vinyl chloride) as a biomaterial. *Journal of Biomedical Materials Research Part B: Applied Biomaterials*, *65B*(1), 204–210. https://doi.org/10.1002/jbm.b.10562

Lanzalaco, S., Galia, A., Lazzano, F., Mauro, R. R., & Scialdone, O. (2015). Utilization of poly(vinylchloride) and poly(vinylidenefluoride) as macroinitiators for ATRP polymerization of hydroxyethyl methacrylate: Electroanalytical and graft-copolymerization studies. *Journal of Polymer Science Part A: Polymer Chemistry*, *53*(21), 2524–2536. https://doi.org/10.1002/pola.27717

Lee, K. W., Chung, J. W., & Kwak, S.-Y. (2016a). Structurally Enhanced Self-Plasticization of Poly(vinyl chloride) via Click Grafting of Hyperbranched Polyglycerol. *Macromolecular Rapid Communications*, *37*(24), 2045–2051. https://doi.org/10.1002/marc.201600533

Lee, K. W., Chung, J. W., & Kwak, S.-Y. (2016b). Synthesis and characterization of bio-based alkyl terminal hyperbranched polyglycerols: A detailed study of their plasticization effect and migration resistance. *Green Chemistry*, *18*(4), 999–1009. https://doi.org/10.1039/C5GC02402A

Li, L., Tek, A. T., Wojtecki, R. J., & Braslau, R. (2019). Internal plasticization of poly(vinyl) chloride using glutamic acid as a branched linker to incorporate four plasticizers per anchor point. *Journal of Polymer Science Part A: Polymer Chemistry*, *57*(17), 1821–1835. https://doi.org/10.1002/pola.29455

Liu, K., Pan, P., & Bao, Y. (2015). Synthesis, micellization, and thermally-induced macroscopic micelle aggregation of poly(vinyl chloride)-g-poly(N-isopropylacrylamide) amphiphilic copolymer. *RSC Advances*, *5*(115), 94582–94590. https://doi.org/10.1039/C5RA16726D

Liu, T., Li, N., Zhu, J., Yu, G., Guo, K., Zhou, L., Zheng, D., Qu, X., Huang, J., Chen, X., Wang, S., & Ye, L. (2014). Effects of di-(2-ethylhexyl) phthalate on the hypothalamus-pituitary-ovarian axis in adult female rats. *Reproductive Toxicology*, *46*(Supplement C), 141–147. https://doi.org/10.1016/j.reprotox.2014.03.006

Marcelli, T., Olimpieri, F., & Volonterio, A. (2011). Domino synthesis of 1, 3, 5-trisubstituted hydantoins: A DFT study. *Organic & Biomolecular Chemistry*, *9*(14), 5156–5161.

Marcilla, A., & Beltrán, M. (2012). 5—Mechanisms of Plasticizers Action. In G. Wypych (Ed.), *Handbook of Plasticizers (Second Edition)* (pp. 119–133). William Andrew Publishing. https://doi.org/10.1016/B978-1-895198-50-8.50007-2

Marcilla, A., Garcia, S., & Garcia-Quesada, J. C. (2008). Migrability of PVC plasticizers. *Polymer Testing*, *27*(2), 221–233. https://doi.org/10.1016/j.polymertesting.2007.10.007

Marcilla, A., García, S., & García-Quesada, J. C. (2004). Study of the migration of PVC plasticizers. *Journal of Analytical and Applied Pyrolysis*, *71*(2), 457–463. https://doi.org/10.1016/S0165-2370(03)00131-1

Martinez-Arguelles, D. B., Culty, M., Zirkin, B. R., & Papadopoulos, V. (2009). In Utero Exposure to Di-(2-Ethylhexyl) Phthalate Decreases Mineralocorticoid Receptor Expression in the Adult Testis. *Endocrinology*, *150*(12), 5575–5585. https://doi.org/10.1210/en.2009-0847

Martinez-Arguelles, Daniel B., Guichard, T., Culty, M., Zirkin, B. R., & Papadopoulos, V. (2011). In Utero Exposure to the Antiandrogen Di-(2-Ethylhexyl) Phthalate Decreases Adrenal Aldosterone Production in the Adult Rat1. *Biology of Reproduction*, *85*(1), 51–61. https://doi.org/10.1095/biolreprod.110.089920

Matyjaszewski, K. (1996). The importance of exchange reactions in controlled/living radical polymerization in the presence of alkoxyamines and transition metals. *Macromolecular Symposia*, *111*(1), 47–61. https://doi.org/10.1002/masy.19961110107

Matyjaszewski, K. (2012). Atom Transfer Radical Polymerization (ATRP): Current Status and Future Perspectives. *Macromolecules*, *45*(10), 4015–4039. https://doi.org/10.1021/ma3001719

Matyjaszewski, K., & Tsarevsky, N. V. (2014). Macromolecular Engineering by Atom Transfer Radical Polymerization. *Journal of the American Chemical Society*, *136*(18), 6513–6533. https://doi.org/10.1021/ja408069v

Matyjaszewski, K., & Xia, J. (2001). Atom Transfer Radical Polymerization. *Chemical Reviews*, *101*(9), 2921–2990. https://doi.org/10.1021/cr940534g

McGinty, K. M., & Brittain, W. J. (2008). Hydrophilic surface modification of poly(vinyl chloride) film and tubing using physisorbed free radical grafting technique. *Polymer*, *49*(20), 4350–4357. https://doi.org/10.1016/j.polymer.2008.07.063

McNeill, I. C., Memetea, L., & Cole, W. J. (1995). A study of the products of PVC thermal degradation. *Polymer Degradation and Stability*, *49*(1), 181–191. https://doi.org/10.1016/0141-3910(95)00064-S

Messori, M., Toselli, M., Pilati, F., Fabbri, E., Fabbri, P., Pasquali, L., & Nannarone, S. (2004). Prevention of plasticizer leaching from PVC medical devices by using organic–inorganic hybrid coatings. *Polymer*, *45*(3), 805–813. https://doi.org/10.1016/j.polymer.2003.12.006

Michael, A. (1893). Ueber die Einwirkung von Diazobenzolimid auf Acetylendicarbonsäuremethylester. *Journal Für Praktische Chemie*, *48*(1), 94–95. https://doi.org/10.1002/prac.18930480114

Mijangos, C., Martinez, A., & Michel, A. (1986). Fonctionnalisation du polychlorure de vinyle: Greffage de fonctions plastifiantes (type ester d'éthyle-hexyle). *European Polymer Journal*, *22*(5), 417–421. https://doi.org/10.1016/0014-3057(86)90139-4

Moghadam, N., Liu, S., Srinivasan, S., Grady, M. C., Soroush, M., & Rappe, A. M. (2013). Computational Study of Chain Transfer to Monomer Reactions in High-Temperature Polymerization of Alkyl Acrylates. *The Journal of Physical Chemistry A*, *117*(12), 2605–2618. https://doi.org/10.1021/jp3100798

Moorshead T C. (1962). *Advances in PVC Compounding and Processing* (M. Kaufman&Sons, p. Ch. 2). London.

Navarro, R., Gacal, T., Ocakoglu, M., García, C., Elvira, C., Gallardo, A., & Reinecke, H. (2017). Nonmigrating Equivalent Substitutes for PVC/DOP Formulations as Shown by a TG Study of PVC with Covalently Bound PEO–PPO Oligomers. *Macromolecular Rapid Communications*, *38*(6), 1600734-n/a. https://doi.org/10.1002/marc.201600734

Navarro, R., Pérez Perrino, M., García, C., Elvira, C., Gallardo, A., & Reinecke, H. (2016). Highly Flexible PVC Materials without Plasticizer Migration As Obtained by Efficient One-Pot Procedure Using Trichlorotriazine Chemistry. *Macromolecules*, *49*(6), 2224–2227. https://doi.org/10.1021/acs.macromol.6b00214

Navarro, R., Pérez Perrino, M., Gómez Tardajos, M., & Reinecke, H. (2010). Phthalate Plasticizers Covalently Bound to PVC: Plasticization with Suppressed Migration. *Macromolecules*, *43*(5), 2377–2381. https://doi.org/10.1021/ma902740t

Navarro, R., Perrino, P. M., García, C., Elvira, C., Gallardo, A., & Reinecke, H. (2016). Opening New Gates for the Modification of PVC or Other PVC Derivatives: Synthetic Strategies for the Covalent Binding of Molecules to PVC. *Polymers*, *8*(4). https://doi.org/10.3390/polym8040152

Net, S., Delmont, A., Sempéré, R., Paluselli, A., & Ouddane, B. (2015). Reliable quantification of phthalates in environmental matrices (air, water, sludge, sediment and soil): A review. *Science of The Total Environment*, *515–516*, 162–180. https://doi.org/10.1016/j.scitotenv.2015.02.013

Niikura, K., Nambara, K., Okajima, T., Matsuo, Y., & Ijiro, K. (2010). Influence of hydrophobic structures on the plasma membrane permeability of lipidlike molecules. *Langmuir*, *26*(12), 9170–9175.

North, M. L., Takaro, T. K., Diamond, M. L., & Ellis, A. K. (2014). Effects of phthalates on the development and expression of allergic disease and asthma. *Annals of Allergy, Asthma & Immunology*, *112*(6), 496–502. https://doi.org/10.1016/j.anai.2014.03.013

Oriol-Hemmerlin, C., & Pham, Q. T. (2000). Poly 1,3-butylene adipate Reoplex® as high molecular weight plasticizer for PVC-based cling films—Microstructure and number-average molecular weight studied by 1H and 13C NMR. *Polymer*, *41*(12), 4401–4407. https://doi.org/10.1016/S0032-3861(99)00662-X

P. Lattimer, R. (2000). Mass spectral analysis of low-temperature pyrolysis products from poly(ethylene glycol). *Journal of Analytical and Applied Pyrolysis*, *56*(1), 61–78. https://doi.org/10.1016/S0165-2370(00)00074-7

Paik, H., Gaynor, S. G., & Matyjaszewski, K. (1998). Synthesis and characterization of graft copolymers of poly(vinyl chloride) with styrene and (meth)acrylates by atom transfer radical polymerization. *Macromolecular Rapid Communications*, *19*(1), 47–52. https://doi.org/10.1002/(SICI)1521-3927(19980101)19:1<47::AID-MARC47>3.0.CO;2-Q

Pascoal, M., Brook, M. A., Gonzaga, F., & Zepeda-Velazquez, L. (2015). Thermally controlled silicone functionalization using selective Huisgen reactions. *European Polymer Journal*, *69*(Supplement C), 429–437. https://doi.org/10.1016/j.eurpolymj.2015.06.026

Patel, R., Patel, M., Ahn, S. H., Sung, Y. K., Lee, H.-K., Kim, J. H., & Sung, J.-S. (2013). Bioinert membranes prepared from amphiphilic poly(vinyl chloride)-g-poly(oxyethylene methacrylate) graft copolymers. *Materials Science and Engineering: C*, *33*(3), 1662–1670. https://doi.org/10.1016/j.msec.2012.12.097

Penco, M., Sartore, L., Bignotti, F., Rossini, M., D'Amore, A., & Fassio, F. (2002). Binary blends based on poly(vinyl chloride) and multi-block copolymers containing poly(ϵ-caprolactone) and poly(ethylene glycol) segments. *Macromolecular Symposia*, *180*(1), 9–22. https://doi.org/10.1002/1521-3900(200203)180:1<9::AID-MASY9>3.0.CO;2-1

Pepperl, G. (2000). Molecular weight distribution of commercial PVC. *Journal of Vinyl and Additive Technology*, *6*(2), 88–92. https://doi.org/10.1002/vnl.10229

Pepperl, G. (2002). Molecular weight distribution of commercial emulsion grade PVC. *Journal of Vinyl and Additive Technology*, *8*(3), 209–213. https://doi.org/10.1002/vnl.10364

Percec, V., & Asgarzadeh, F. (2001). Metal-catalyzed living radical graft copolymerization of olefins initiated from the structural defects of poly(vinyl chloride). *Journal of Polymer Science Part A: Polymer Chemistry*, *39*(7), 1120–1135. https://doi.org/10.1002/1099-0518(20010401)39:7<1120::AID-POLA1089>3.0.CO;2-Z

Percec, Virgil, Cappotto, A., & Barboiu, B. (2002). Metal-catalyzed living radical graft copolymerization of butyl methacrylate and styrene initiated from the structural Defects of narrow molecular weight distribution poly(vinyl chloride). *Macromolecular Chemistry and Physics*, *203*(10-11), 1674–1683. https://doi.org/10.1002/1521-3935(200207)203:10/11<1674::AID-MACP1674>3.0.CO;2-N

Polyvinyl Chloride (PVC) Properties, Production, Price, Market, and Uses https://www.plasticsinsight.com/resin-intelligence/resin-prices/pvc/#production Accessed 04/25/2020.

Pugh, G., Jr., Isenberg, J. S., Kamendulis, L. M., Ackley, D. C., Clare, L. J., Brown, R., Lington, A. W., Smith, J. H., & Klaunig, J. E. (2000). Effects of Di-isononyl Phthalate, Di-2-ethylhexyl Phthalate, and Clofibrate in Cynomolgus Monkeys. *Toxicological Sciences*, *56*(1), 181–188. https://doi.org/10.1093/toxsci/56.1.181

Reddy, B., Rozati, R., Reddy, B., & Raman, N. (2006). General gynaecology: Association of phthalate esters with endometriosis in Indian women. *BJOG: An International Journal of Obstetrics & Gynaecology*, *113*(5), 515–520. https://doi.org/10.1111/j.1471-0528.2006.00925.x

Reddy, N. N., Mohan, Y. M., Varaprasad, K., Ravindra, S., Vimala, K., & Raju, K. M. (2010). Surface treatment of plasticized poly(vinyl chloride) to prevent plasticizer migration. *Journal of Applied Polymer Science*, *115*(3), 1589–1597. https://doi.org/10.1002/app.31157

Rezende, T. C., Abreu, C. M. R., Fonseca, A. C., Higa, C. M., Li, L., Serra, A. C., Braslau, R., & Coelho, J. F. J. (2020). Efficient internal plasticization of poly(vinyl chloride) via free radical copolymerization of vinyl chloride with an acrylate bearing a triazole phthalate mimic. *Polymer*, *196*, 122473. https://doi.org/10.1016/j.polymer.2020.122473

Rivera-Briso, L. A., & Serrano-Aroca, Á. (2018). Poly(3-Hydroxybutyrate-co-3-Hydroxyvalerate): Enhancement Strategies for Advanced Applications. *Polymers*, *10*(7). https://doi.org/10.3390/polym10070732

Rogestedt, M., & Hjertberg, T. (1993). Structure and degradation of commercial poly(vinyl chloride) obtained at different temperatures. *Macromolecules*, *26*(1), 60–64. https://doi.org/10.1021/ma00053a009

Rostovtsev, V. V., Green, L. G., Fokin, V. V., & Sharpless, K. B. (2002). A Stepwise Huisgen Cycloaddition Process: Copper(I)-Catalyzed Regioselective “Ligation” of Azides and Terminal Alkynes. *Angewandte Chemie International Edition*, *41*(14), 2596–2599. https://doi.org/10.1002/1521-3773(20020715)41:14<2596::AID-ANIE2596>3.0.CO;2-4

Rowdhwal, S. S. S., & Chen, J. (2018). Toxic Effects of Di-2-ethylhexyl Phthalate: An Overview. *BioMed Research International*, *2018*, 1750368. https://doi.org/10.1155/2018/1750368

Sathyanarayana, S., Grady, R., Barrett, E. S., Redmon, B., Nguyen, R. H. N., Barthold, J. S., Bush, N. R., & Swan, S. H. (2016). First trimester phthalate exposure and male newborn genital anomalies. *Environmental Research*, *151*, 777–782. https://doi.org/10.1016/j.envres.2016.07.043

Schaedlich, K., Schmidt, J.-S., Kwong, W. Y., Sinclair, K. D., Kurz, R., Jahnke, H.-G., & Fischer, B. (2015). Impact of di-ethylhexylphthalate exposure on metabolic programming in P19 ECC-derived cardiomyocytes. *Journal of Applied Toxicology*, *35*(7), 861–869. https://doi.org/10.1002/jat.3085

Shapiro, G. D., Dodds, L., Arbuckle, T. E., Ashley-Martin, J., Fraser, W., Fisher, M., Taback, S., Keely, E., Bouchard, M. F., Monnier, P., Dallaire, R., Morisset, AS., & Ettinger, A. S. (2015). Exposure to phthalates, bisphenol A and metals in pregnancy and the association with impaired glucose tolerance and gestational diabetes mellitus: The MIREC study. *Environment International*, *83*(Supplement C), 63–71. https://doi.org/10.1016/j.envint.2015.05.016

Skelly, P. W., Sae-Jew, J., Kitos Vasconcelos, A. P., Tasnim, J., Li, L., Raskatov, J. A., & Braslau, R. (2019). Relative Rates of Metal-Free Azide–Alkyne Cycloadditions: Tunability over 3 Orders of Magnitude. *The Journal of Organic Chemistry*, *84*(21), 13615–13623. https://doi.org/10.1021/acs.joc.9b01887

Srinivasan, S., Kalfas, G., Petkovska, V. I., Bruni, C., Grady, M. C., & Soroush, M. (2010). Experimental study of the spontaneous thermal homopolymerization of methyl and n-butyl acrylate. *Journal of Applied Polymer Science*, *118*(4), 1898–1909. https://doi.org/10.1002/app.32313

Srinivasan, S., Lee, M. W., Grady, M. C., Soroush, M., & Rappe, A. M. (2009). Computational Study of the Self-Initiation Mechanism in Thermal Polymerization of Methyl Acrylate. *The Journal of Physical Chemistry A*, *113*(40), 10787–10794. https://doi.org/10.1021/jp904036k

Starnes, W. H. (2002). Structural and mechanistic aspects of the thermal degradation of poly(vinyl chloride). *Progress in Polymer Science*, *27*(10), 2133–2170. https://doi.org/10.1016/S0079-6700(02)00063-1

Starnes, W. H., Schilling, F. C., Plitz, I. M., Cais, R. E., Freed, D. J., Hartless, R. L., & Bovey, F. A. (1983). Branch structures in poly(vinyl chloride) and the mechanism of chain transfer to monomer during vinyl chloride polymerization. *Macromolecules*, *16*(5), 790–807. https://doi.org/10.1021/ma00239a016

Subotic, U., Hannmann, T., Kiss, M., Brade, J., Breitkopf, K., & Loff, S. (2007). Extraction of the Plasticizers Diethylhexylphthalate and Polyadipate From Polyvinylchloride Nasogastric Tubes Through Gastric Juice and Feeding Solution. *Journal of Pediatric Gastroenterology and Nutrition*, *44*(1), 71–76. https://doi.org/10.1097/01.mpg.0000237939.50791.4b

Sun, Z., Choi, B., Feng, A., Moad, G., & Thang, S. H. (2019). Nonmigratory Poly(vinyl chloride)-block-polycaprolactone Plasticizers and Compatibilizers Prepared by Sequential RAFT and Ring-Opening Polymerization (RAFT-T-ROP). *Macromolecules*, *52*(4), 1746–1756. https://doi.org/10.1021/acs.macromol.8b02146

Sun, Z., Wang, M., Li, Z., Choi, B., Mulder, R. J., Feng, A., Moad, G., & Thang, S. H. (2020). Versatile Approach for Preparing PVC-Based Mikto-Arm Star Additives Based on RAFT Polymerization. *Macromolecules*. https://doi.org/10.1021/acs.macromol.0c00125

Swan, S. H., Sathyanarayana, S., Barrett, E. S., Janssen, S., Liu, F., Nguyen, R. H. N., Redmon, J. B., & the TIDES Study Team. (2015). First trimester phthalate exposure and anogenital distance in newborns. *Human Reproduction*, *30*(4), 963–972. https://doi.org/10.1093/humrep/deu363

Tornøe, C. W., Christensen, C., & Meldal, M. (2002). Peptidotriazoles on Solid Phase: [1,2,3]-Triazoles by Regiospecific Copper(I)-Catalyzed 1,3-Dipolar Cycloadditions of Terminal Alkynes to Azides. *The Journal of Organic Chemistry*, *67*(9), 3057–3064. https://doi.org/10.1021/jo011148j

Troitskii, B. B., & Troitskaya, L. S. (1993). Mathematical models of the initial stage of the thermal degradation of poly(vinyl chloride). II. The thermal degradation of poly(vinyl chloride) with effective removal of HCl. *Journal of Polymer Science Part A: Polymer Chemistry*, *31*(1), 75–81. https://doi.org/10.1002/pola.1993.080310109

Troitskii, B. B., & Troitskaya, L. S. (1999). Degenerated branching of chain in poly(vinyl chloride) thermal degradation. *European Polymer Journal*, *35*(12), 2215–2224. https://doi.org/10.1016/S0014-3057(99)00002-6

Tüzüm Demir, A. P., & Ulutan, S. (2013). Migration of phthalate and non-phthalate plasticizers out of plasticized PVC films into air. *Journal of Applied Polymer Science*, *128*(3), 1948–1961. https://doi.org/10.1002/app.38291

Ueberreiter, K., & Kanig, G. (1952). *7*, 569.

Van Cauter, K., Van Den Bossche, B. J., Van Speybroeck, V., & Waroquier, M. (2007). Ab Initio Study of Free-Radical Polymerization: Defect Structures in Poly(vinyl chloride). *Macromolecules*, *40*(4), 1321–1331. https://doi.org/10.1021/ma062174s

Waldo Semon https://ohiohistorycentral.org/w/Waldo_Semon Accessed 04/25/2020.

Wang, H., Zhou, Y., Tang, C., He, Y., Wu, J., Chen, Y., & Jiang, Q. (2013). Urinary Phthalate Metabolites Are Associated with Body Mass Index and Waist Circumference in Chinese School Children. *PLOS ONE*, *8*(2), e56800. https://doi.org/10.1371/journal.pone.0056800

Wang, J., Chen, G., Christie, P., Zhang, M., Luo, Y., & Teng, Y. (2015). Occurrence and risk assessment of phthalate esters (PAEs) in vegetables and soils of suburban plastic film greenhouses. *Science of The Total Environment*, *523*(Supplement C), 129–137. https://doi.org/10.1016/j.scitotenv.2015.02.101

Wang, Q., & Storm, B. K. (2005). Migration of Additives from Poly(vinyl chloride) (PVC) Tubes into Aqueous Media. *Macromolecular Symposia*, *225*(1), 191–204. https://doi.org/10.1002/masy.200550715

Weiss, B. (2011). Endocrine disruptors as a threat to neurological function. *Journal of the Neurological Sciences*, *305*(1), 11–21. https://doi.org/10.1016/j.jns.2011.03.014

Williams, M. L., Landel, R. F., & Ferry, J. D. (1955). The Temperature Dependence of Relaxation Mechanisms in Amorphous Polymers and Other Glass-forming Liquids. *Journal of the American Chemical Society*, *77*(14), 3701–3707. https://doi.org/10.1021/ja01619a008

Wypych, G. (2015a). 1—Chemical Structure of PVC. In G. Wypych (Ed.), *PVC Degradation and Stabilization (Third Edition)* (pp. 1–23). ChemTec Publishing. https://doi.org/10.1016/B978-1-895198-85-0.50003-0

Wypych, G. (2015b). 2—PVC Manufacture Technology. In G. Wypych (Ed.), *PVC Degradation and Stabilization (Third Edition)* (pp. 25–45). ChemTec Publishing. https://doi.org/10.1016/B978-1-895198-85-0.50004-2

Wypych, G. (2015c). 4—Principles of Thermal Degradation. In G. Wypych (Ed.), *PVC Degradation and Stabilization (Third Edition)* (pp. 79–165). ChemTec Publishing. https://doi.org/10.1016/B978-1-895198-85-0.50006-6

X. Q. Wen, X. H. Liu, & G. S. Liu. (2010). Prevention of Plasticizer Leaching From the Inner Surface of Narrow Polyvinyl Chloride Tube by DC Glow Discharge Plasma. *IEEE Transactions on Plasma Science*, *38*(11), 3152–3155. https://doi.org/10.1109/TPS.2010.2074209

Xie, T. Y., Hamielec, A. E., Rogestedt, M., & Hjertberg, T. (1994). Experimental investigation of vinyl chloride polymerization at high conversion: Polymer microstructure and thermal stability and their relationship to polymerization conditions. *Polymer*, *35*(7), 1526–1534. https://doi.org/10.1016/0032-3861(94)90354-9

Xu, Y., Xiong, Y., & Guo, S. (2015). Issues Caused by Migration of Plasticizers from Flexible PVC and Its Countermeasures. *Progress in Chemistry*, *27*, 286–296. https://doi.org/DOI: 10.7536/PC140826

Yang, P., Yan, J., Sun, H., Fan, H., Chen, Y., Wang, F., & Shi, B. (2015). Novel environmentally sustainable cardanol-based plasticizer covalently bound to PVC via click chemistry: Synthesis and properties. *RSC Advances*, *5*(22), 16980–16985. https://doi.org/10.1039/C4RA15527K

Zhai, W., Huang, Z., Chen, L., Feng, C., Li, B., & Li, T. (2014). Thyroid Endocrine Disruption in Zebrafish Larvae after Exposure to Mono-(2-Ethylhexyl) Phthalate (MEHP). *PLOS ONE*, *9*(3), e92465. https://doi.org/10.1371/journal.pone.0092465

Zhang, X., & Chen, Z. (2014). Observing Phthalate Leaching from Plasticized Polymer Films at the Molecular Level. *Langmuir*, *30*(17), 4933–4944. https://doi.org/10.1021/la500476u

Zhang, X., Li, Y., Hankett, J. M., & Chen, Z. (2015). The molecular interfacial structure and plasticizer migration behavior of “green” plasticized poly(vinyl chloride). *Physical Chemistry Chemical Physics*, *17*(6), 4472–4482. https://doi.org/10.1039/C4CP05287K

Zhao, B., & Brittain, W. (2000). Polymer Brushes: Surface-Immobilized Macromolecules. *Progress in Polymer Science*, *25*, 677–710. https://doi.org/10.1016/S0079-6700(00)00012-5

Ziska, J. J., Barlow, J. W., & Paul, D. R. (1981). Miscibility in PVC-polyester blends. *Polymer*, *22*(7), 918–923. https://doi.org/10.1016/0032-3861(81)90268-8